Fabian Becker

The impact of ancient iron mining and smelting on the landscape balance on Elba Island, Tuscan Archipelago, Italy

Doctoral thesis submitted to the
Department of Earth Sciences, Freie Universität Berlin

Berlin, 2020

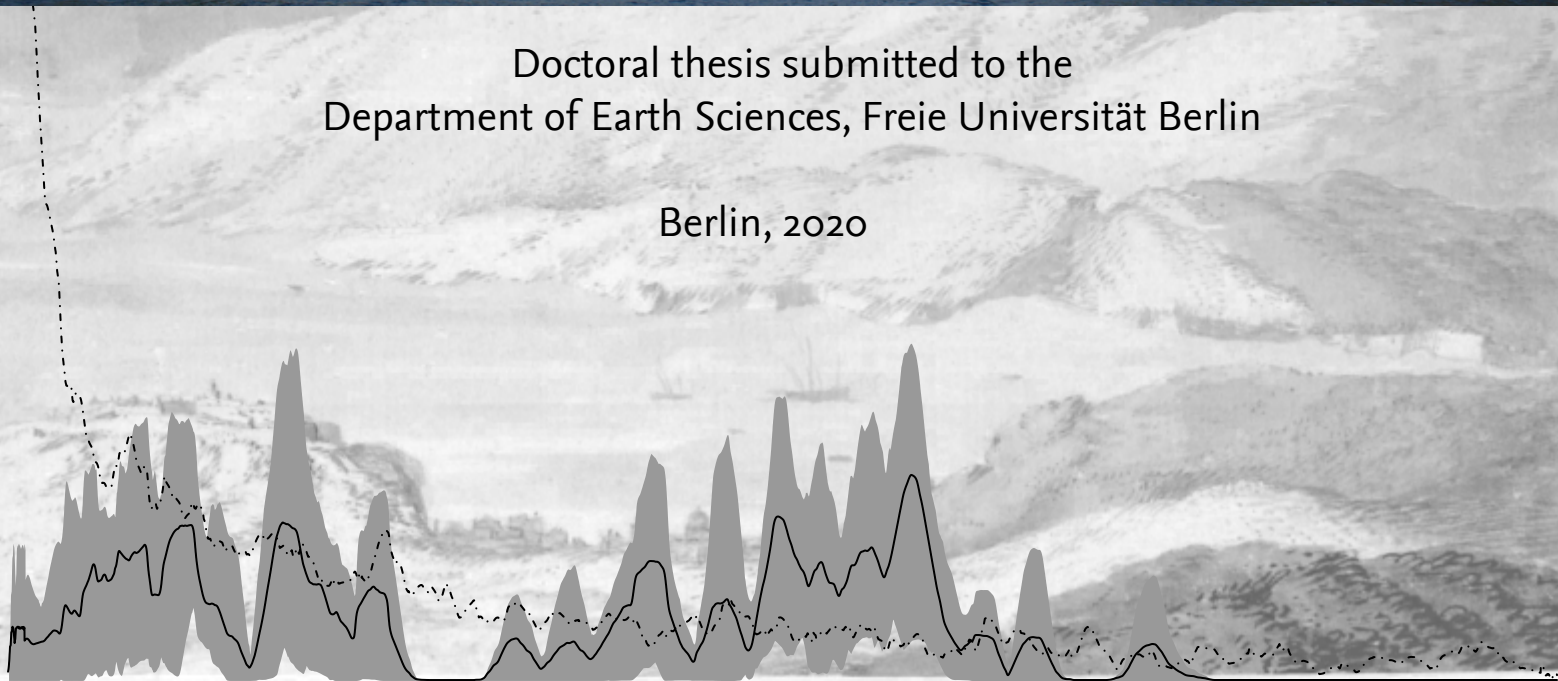

The impact of ancient iron mining and smelting on the landscape balance on Elba Island, Tuscan Archipelago, Italy

Einfluss der Eisenverhüttung und des Eisenabbaus auf den Landschaftshaushalt in der Region Elba und Populonia, Italien.

Dissertation
zur Erlangung des akademischen Grades
Doktor der Naturwissenschaften (Dr. rer. nat.)
am Fachbereich Geowissenschaften
der Freien Universität Berlin

vorgelegt von Fabian Becker

Berlin, 2020

Erstgutacherin:
Univ.-Prof. Dr. Brigitta Schütt
Freie Universität Berlin
Fachbereich Geowissenschaften
Institut für Geographische Wissenschaften
Physische Geographie

Zweitgutachter:
Univ.-Prof. Dr. Stephan G. Schmid
Humboldt-Universität zu Berlin
Kultur-, Sozial- und Bildungswissenschaftliche Fakultät
Institut für Archäologie
Klassische Archäologie / Winckelmann-Institut

Drittgutacherin:
Univ.-Prof. Dr. Wiebke Bebermeier
Freie Universität Berlin
Fachbereich Geowissenschaften
Institut für Geographische Wissenschaften
Physische Geographie

Tag der Disputation: 17. April 2020

Acknowledgements

Throughout field and lab work, analysis, and writing of this dissertation I have received great support.

I have benefited from personal funding (scholarship) and financial support by the Excellence Cluster *Topoi – The Formation and Transportation of Space and Knowledge in Ancient Civilizations* (Deutsche Forschungsgemeinschaft, DFG – EXC 264). The Berlin Graduate School of Ancient studies financially supported the analysis of slag samples by the Deutsches Bergbaumuseum in Bochum.

I owe a very important debt to my first supervisor Prof. Dr. Brigitta SCHÜTT (Freie Universität Berlin). Prof. Schütt share her broad scientific knowledge, her ability for exact observations in the field, her useful pragmatism, and her view on the data with me. Moreover, she encouraged me to observe a phenomenon from different perspectives and consider it from the perspective of various sources. Thank you!

I am also grateful to my second supervisor Prof. Dr. Stephan G. SCHMID (Humboldt-Universität zu Berlin) for developing the idea of the project, his encouragement for an interdisciplinary perspective.

Moreover, special thanks goes to Raphael A. ESER (Humboldt-Universtität zu Berlin), who was my *tandem partner* from Classical Archaeology working on the same topic. Since 2015, we intensively discussed a various hypothesis and ideas on human–environment interactions on Elba Island and learned a lot on the island during four enjoyable and successful collective field trips to Italy. Raphael provided a indispensable contribution to data collection in the field and critically commented all my manuscripts.

I would also like to thank all co-authors of the journal publications which are the core of this dissertation: Nataša DJURDJEVAC CONRAD (Zuse-Institut Berlin, ZIB) , Raphael A. ESER, Luzie HELFMANN (ZIB), Philipp HOELZMANN (Physical Geography, Freie Universität Berlin), Brigitta SCHÜTT, Christof SCHÜTTE (ZIB), and Johannes ZONKER (ZIB).

Percussion drilling and soil sampling on Elba and subsequent analysis of samples in the laboratory would not have been possible without the help of several people:

– Lorella ALDERIGHI (Soprintendenza Archeologia, Belle Arti e Paesaggio per le province di Pisa e Livorno) cooperated and organized official permissions;

– a large number of landowners provided access to their properties on Elba for drilling;
– Alice LEONI (Capoliveri, Livorno) organized the permits for drillings from the landowners;
– Raphael A. Eser, Dr. Daniel KNITTER (Christian-Albrechts-Universität zu Kiel), and Dr. Philipp HOELZMANN were engaged in drilling in Sep. 2015;
– Ole TÖLLE and Annika KIRSCHENEDER, both Freie Universität Berlin, assisted during field work (2016/2017);
– Giuliana BERTOZZI CORRADI and her employees allowed for soil sampling on the *Tenuta La Chiusa* (Loc. Magazzini, Portoferraio, Livorno);
– Manuela ABENDROTH, Michaela SCHOLZ, Frank KUTZ, Robert RETTIG, Sarah MOSSER, and Atossa PANDAZMAPOO (all Freie Universität Berlin) provide valuable assistance in the analysis of soil and sediment samples;
– Lukas WIMMER, Sarah MOSSER, Robert RETTIG, and Atossa PANDAZMAPOO assisted in literature research and digitalisation;
– Michèle DINIES and Dr. Reinder NEEF (German Archeological Institute, Referat Naturwissenschaften – Archäobotanik) identified charcoal samples from sediment sequences.

I express my cordial thank to all of you.

I further would like to acknowledge the discussions in the research group on *Iron as a raw material* within the Excellence Cluster Topoi.

With many (former) colleagues from the Institute of Geographical Sciences, I shared fruitful discussions, coffee in barrels, and nice barbecues. The every-day help was very valuable for the dissertation. My special thanks therefore goes to: Prof. Dr. Wiebke BEBERMEIER, Prof. Dr. Margot BÖSE, Prof. Dr. Karl Tilman ROST, Jun.-Prof. Dr. Julia MEISTER, Dr. Jonas BERKING, Dr. Jan KRAUSE, Dr. Christina MICHEL, Dr. Moritz NYKAMP, Dr. Michael THELEMANN, Dr. Jacob HARDT, Magdalena BARTELS, Ricarda BRAUN, Vincent HABURAJ, Sarah ISSELHORST, Andrew Kudzanayi MARONDEDZE, Shih-Hung LIU, Nicole LÜBKE, Ingo MIDDELHAUFE, Subham MUKHERJEE, Tobias SAUL, Lena SCHIMMEL, Henry SCHUBERT, Johanna SEIDEL, and Xun YANG. Motivation and support my Tilman ROST during my (under)graduate studies and beyond importantly helped me to work on my dissertation.

Norbert ANSELM and I shared office for almost 7 years. Innumerable discussions and jaws meant a lot for me.

I also thank my parents H-W and Susanne BECKER for providing personal support.

This dissertation would not have been possible without the encouragement, affection, and longanimity of my girlfriend Judith BERNBECK.

Fabian Becker, Berlin, January 2020

Abstract

Objectives Elba Island (Tuscan Archipelago, Italy) was one of the hotspots of Etrusco–Roman iron metallurgy. At least since the 6th century BCE, hematite ore was extracted from the deposits on the island. The run-of-mine was at first transported to the 'industrial' area of the major Etruscan city of Populonia. Iron smelting on the Island started most likely in the late 4th century BCE. Production increased after the Roman occupation in the mid-3rd century BCE, peaking around the mid- to late 2nd century BCE. Afterwards, the smelting activities on Elba decreased markedly.

The time lack between the onset of mining and smelting on Elba, and rather the decline in production, are attributed to a lack of fuel on the island after deforestation. A 'deforestation' narrative developed at least since the mid-18th century and is continuously cited until recently. Most scholars rely on the decreases in archaeological material, an ancient observation by Strabo that iron was not processed on the island, and contemporary view on Elba's landscape. Scientific evidence of a lack of fuel, deforestation, or environmental change during the smelting period is sparse.

Besides the use of wood fuel for smelting, also legacy issues are an important aspect of historical human–environment interactions on Elba. The Greek name of Elba—*Aithάleia*, the fuming one—and historical observations point to the emission from furnaces. Some scholars believe that the luxurious *villae maritimae* were constructed on Elba only after the abandonment of most smelting sites, because soot emission would have made the island uninteresting for recreation. Additionally, marine sediments and recent data from the mines suggest that (subrecent) iron production had an environmental impact on Elba. Direct evidence for such an environmental impact caused by *ancient smelting* is, however, not propound.

Approaches In the thesis at hand I use (i) soil chemical data from the ancient smelting site in Magazzini; (ii) geochemical analysis of sediment sequences uncovered from the Campo coastal plain; (iii) a stochastic chronological model of sediment facies sediment accumulation using cumulative probability functions of cal-^{14}C-ages and (iv) Monte-Carlo simulations on the woodlot requirements for iron smelting and the supply of the workforce to reconstruct human-landscape interactions on Elba during the mid- to late Holocene with a clear focus on the ancient smelting period (4th century BCE – 1st century CE).

The body of the thesis comprises four case studies related to the four methodical strategies. The interpretation of the results is embedded in a characterization of the 'metallurgical landscape' on ancient Elba and a conceptual socio-ecological model of iron as a raw material that rests on the ideas of the Vienna School.

Results The main outcomes of the reconstruction of human–environment interactions and the impact of smelting on the landscape balance are as follows.

– A specific signature of ancient iron smelting is still detectable for on-site geochemical data and terrestrial sediment sequences. Soil on the smelting site are increased in As, Fe, Cu, and Ca contents and organic and pyrogenic carbon, magnetic susceptibility, and pH. The spatial variability of these activity marker points to different processes of the smelting procedure; Ca is for instance related to ashes, whereas Cu points to the the deposition of metallurgical remains, and As to run-of-mine. As the data from the smelting site differs from other archives of metallurgy on and around Elba, our record gives a specific chemical impact of *iron smelting*.
– Sedimentological and chronological data suggest that during the ancient smelting period, geomorphic activity on Elba increased clearly. Sediment layers indicating soil erosion and high magnitude floods were deposited in valleys with smelting site in upstream areas; in different sediment archives distributed over several plains and valleys on Elba, sediment accumulation and geomorphic activity increased during Etruscan/Roman times. Sedimentological evidence also imply that the palaeolandscape—especially the accessibility of different land areas limited by the distribution of wetlands—was one location factor for smelting sites.
– Although the impact of smelting on the landscape balance is detectable in different archives using different proxies, Roman metallurgy on Elba did not necessarily cause a lack of fuel. Our Monte-Carlo experiments of the woodlot requirements reveal that it is (very) unlikely that not fuel wood was available during Roman times. This is especially clear when assuming that Elba was autarchic regarding the food supply for metalworkers. The model suggests that the non-technical requirements for smelting importantly contributed to the overall woodland availability on Elba.

Conclusions Sediments and soils prove to be valuable archives of the ancient smelting period. In conclusion, iron smelting on Elba during the antiquity had a remarkable impact on the landscape balance, however, without necessarily causing a lack of fuel. We therefore consider that the 'deforestation narrative' developed under the historical–environmental conditions of the 18th to 21st century and other reasons than deforestation might have triggered the abandonment of smelting sites in the 1st century BCE. Smelting might also have continued after the turn of eras.

Kurzfassung

Die vorliegende Dissertation befasst sich mit den Mensch-Umwelt-Beziehungen auf der Insel Elba (Toskana, Italien) während der klassischen Antike. Im Fokus steht dabei der Einfluss der damaligen Eisenverhüttung auf den Landschaftshaushalt der Insel.

Problemstellung. Die Insel Elba im Tyrrhenischen Meer war ein bedeutender Standort der etruskischen und römischen Eisenproduktion. Beginnend im 6. Jh. v. d. Z. wurde Hämatit-Erz in den Lagerstätten im Nordosten der Insel abgebaut und mit dem Schiff aufs Festland verbracht. Erst gegen Ende des 4. Jh. v. d. Z. wurde dann spätestens auch auf der Insel selbst verhüttet. Die Gründe für das Ausbleiben von Eisenverhüttungsaktivitäten auf der Insel der Lagerstätten für mehr als 200 Jahre ist nicht abschließend diskutiert. Neben der generellen politischen Situation in den Meeren um die Insel wird u. a. das bereits vor der Zeit der Eisenverarbeitung auf dem Festland – in Populonia – existierende industrielle metallurgische Revier angeführt, um die Verzögerung zu erklären. In manchen Beiträgen findet sich auch die (wenig belegte) Hypothese eines Brennstoffmangels auf Elba, sodass eine Notwendigkeit bestand, das Erz zum Verhütten zu verschiffen. An diesen Aspekt anschließend kann auch das Ende der Verhüttung auf Elba diskutiert werden. Während die Etruskische Produktion auf Elba ab dem späten 4. Jh. v. d. Z. nur ein geringes quantitatives Ausmaß erreicht haben dürfte, wuchs die produzierte Menge an Eisen nach der Römischen Besetzung Elbas Mitte des 2. Jh. v. d. Z. stark an, um dann im späten 2. und frühen 1. Jh. v. d. Z. ihren Höhepunkt zu erreichen. Wohl gegen Mitte des 1. Jh. v. d. Z. brach die Produktion ein, wie der starke Rückgang von datierbarem Material aus dieser Zeit andeutet. Die Datierung um das mittlere 1. Jh. v. d. Z. deckt sich mit einer Beobachtung des antiken Geographen Strabo (Str., 5.2.6) aus dieser Zeit. Er beobachtet, dass das Erz nicht auf Elba geschmolzen werden kann, sondern vielmehr zur Verarbeitung auf das

Festland gebracht wird. Zuvor hatte Diodor (Diod. Sic., 5.13.1–2) noch die rauchenden Öfen auf der Insel beschrieben.

Die Ursache für das präsumtive Ende der Verhüttung im 1. Jh. v. d. Z. wird von einigen Autoren und Autorinnen wiederum im Brennstoffmangel gesehen. Zumeist wird als Argument für diese Hypothese einzig auf die Beobachtung Strabos verwiesen, ohne weitere Hinweise anzuführen. An einigen Stellen wird in der Literatur die eigene Charakterisierung der Insel Elba als *waldarm* oder *degradiert* vorgebracht (s. z. B. I. M. B. Wiman in: Turfa, J. M., *The Etruscan World*, 2013, S. 11–28).

Forschungsfragen. Ausgehend von diesem Entwaldungsnarrativ setze ich mich im Rahmen der vorliegenden Arbeit mit einer Rekonstruktion der Mensch-Umwelt-Beziehungen auseinander. Neben dem möglichen Brennstoffmangel steht dabei auch die Frage nach dem beschleunigten Bodenabtrag durch die Entwaldung im Mittelpunkt. Hinzu kommt ein weiterer Aspekt der Mensch-Umwelt-Beziehungen, der sich wiederum aus den historischen Quellen und dem archäologischen Befund ergibt. Durch Diodor ist überliefert, dass der Griechische Name Elbas, *Aithάleia*, die Rauchige bedeute. Diodor beschreibt weiterhin den Rauch aus den Rennöfen, der dick über der Insel liegt. Davon ausgehend, untersuchen wir auch den Einfluss der Eisenverhüttung auf die chemische Zusammensetzung von Böden und Sedimenten.

Methoden und Aufbau der Arbeit. Methodisch stehen dabei in der vorliegenden Dissertation drei Ansätze im Vordergrund, die in insgesamt vier Fallstudien verfolgt werden. Die Fallstudien sind auf unterschiedlichen zeitlichen und räumlichen Skalen angesiedelt und reichen von spezifischen Untersuchungen einer Verhüttungsstätte über einzelne Täler bis hin zur Abdeckung der gesamten Insel. Zeitlich sind die Studien auf die Verhüttungsperiode fokussiert, decken aber teilweise das mittlere bis späte Holozän ab.

(i.) Becker et al. werten in Fallstudie 1 (*J Geochem Explor* **205**, 2019, https://doi.org/10.1016/j.gexplo.2019.04.009) Bodenproben von einem auf einer vermutlich Spätpleistozänen Terrasse gelegenen Verhüttungsplatz aus, um den chemischen Fingerprint der antiken Eisenverhüttung zu charakterisierten. Als Referenz dienen Daten von an die Verhüttungsstätte angrenzenden Flächen, publizierte geochemische Daten von Abraumhalden und Minenböden sowie von archäometallurgischen Resten (v. a. von Schlacken und Erzen). Außerdem werden die Daten von der untersuchten Verhüttungsstätte mit publizierten Proxydaten aus alluvialen und marinen Sedimentarchiven verglichen. Die geochemischen Parameter umfassen die Elementzusammensetzung (portable XRF, ICP-OES), Kohlenstoffgehalte, und pH-Werte. Die Daten wurden mittels Clusteranalyse gruppiert und interferenzstatistisch

bewertet, wobei sich alle Analyseschritte an den Prinzipien der *Compositional Data Analysis* orientieren.

(ii.) In Fallstudie 2 (*Geoarchaeology* **34** (3): S. 336–359, https://doi.org/10.1002/gea.21726) rekonstruieren Becker et al. die Mensch-Umwelt-Beziehungen zur Zeit der etruskisch–römischen Eisenverhüttung anhand von Talverfüllungen aus zwei Transekten in der Küstenebene von Campo. Dazu wurden Sedimentsequenzen mittels Rammkernsondierung aufgeschlossen und physikalisch–chemische Parameter an den Sedimenten bestimmt. Diese umfassen neben der Analyse des Elementgehalts (portable XRF, ICP-OES, Elementanalysator), auch Messungen der Kohlenstoffgehalte, des pH-Wertes, der elektrischen Leitfähigkeit, der magnetischen Suszeptibilität und der Farbe. Ausgehend von einer kompositionsanalytischen Gruppierung der *Chemofazies* wurden die Sedimente auf einen Wechsel des Ablagerungsmilieus, technogenen Eintrag und veränderte geomorphologische Aktivität untersucht. Die Alterseinschätzung der Sedimente basiert auf radiokohlenstoffdatierten organischen Resten und einzelnen archäologischen Funden.

(iii.) Zur Abschätzung des Flächenverbrauchs für die Versorgung der Verhüttungsstätten mit Brennstoff haben Becker et al. in Fallstudie 3 (*PLoS ONE* **15** (11): e0241133, https://doi.org/10.1371/journal.pone.0241133) ein stochastisches Modell der Verhüttungsaktivität aufgesetzt. Ausgangspunkt des Modells sind die Chronologien der einzelnen Verhüttungsstätten und der hauptsächlich mittels Feldbegehung und Archivmaterial rekonstruieren Schlackedeposition auf den Verhüttungsplätzen des antiken Elbas. Mittels technischer Parameter (Ineffizient der Öfen, Produktivität von Kohlenmeilern, etc.) wurde aus der Schlackenmenge der jährliche Bedarf an Holz(-kohle) und damit die benötigte Waldfläche berechnet. Die Unsicherheit in der Parameterschätzung wurde mit Monte-Carlo-Simulationen in das Modell einbezogen. Um die gesamte auf der Insel für die Verhüttung zur Verfügung stehende Waldfläche einschätzen zu können, wurden zu dem eigentlichen technologischen Metabolismus der Verhüttung auch die Verbräuche des biologischen Metabolismus einbezogen, d. h. der Verbrauch der Werktätigen. Letztendlich ist es Ziel der Studie, einen Wahrscheinlichkeitsbereich abstecken zu können, in dem sich eine mögliche Gesamtabholzung der Insel bewegt und somit die Frage zu diskutieren, ob es einen Brennstoffmangel im 1. Jh. v. d. Z. auf Elba gegeben haben könnte.

(iv.) Ausgehend von der Hypothese dass eine mögliche Abholzung der Insel auch Bodenerosion und damit indirekt eine beschleunigte Aggradation zur Folge hatte, wird in Fallstudie 4 (unveröffentlichtes Manuskript) eine Metaanalyse der von Elba zur Verfügung stehenden terrestrischen Sedimentsequenzen durchgeführt. Methodisch basieren die Arbeiten auf einer Auswertung von kumulativen Wahrschein-

lichkeitsfunktionen kalibrierter Radiokohlenstoffalter, den Ablagerungstiefen der Alter und einer Faziesinterpretation der datierten Sedimente. Mittels Monte-Carlo-Simulationen und Bayes'schen Ansätzen können so Zeiträume erhöhter geomorphologischer Aktivität ausgewiesen werden.

Die vier einzelnen Fallstudien sind in das konzeptionelle humanökologische Modell der Wiener Schule eingebunden und werden von einer Beschreibung der metallurgischen Landschaft auf Elba gerahmt.

Diese metallurgische Landschaft auf der Insel ist vor allem durch die teilweise relativ große Distanz zwischen den Minen und den Verhüttungssätten gekennzeichnet. Hierzu wird u. a. von A. Corretti (in Naso, A., *Etruscology*, 2017, S. 445–461) pointiert festgehalten, dass das Standortmuster auf eine vollständige Erschließung der Holzressourcen auf Elba hindeute. Weiterhin sind ein Großteil der etruskisch–römischen Verhüttungsstandorte küstennah gelegen, was auf den maritimen Transport des Eisens hinweist. Die Lage der Minen im Nordosten von Elba, und somit an der zum Festland nächstgelegenen Küste der Insel, kann als Aspekt verstanden werden, der die enge Verknüpfung der Insel mit dem Verhüttungszentrum in Populonia hervorbringt.

Hauptergebnisse. Basierend auf den vier Fallstudien können folgende Aspekte der Mensch-Umwelt-Beziehungen und des Umwelteinflusses der antiken Eisenverhüttung auf der Insel Elba festgehalten werden:

– Die mittel- bis spätholozäne Ablagerung auf Elba ist hauptsächlich durch die Versilianische Transgression geprägt. Vor allem in den höhergelegenen Bereichen der Ebenen wurden bis ca. 5.4 ka BP entsprechende Sedimente abgelagert. An küstennahmen Standorten wurden auch nur Zeit der antiken Eisenverhüttung Sedimente abgelagert, die auf einen paralischen Ablagerungsraum hinweisen. Toponyme und (fossile) Reste des regionaltypischen Bewuches von Feuchtgebieten oder verlandeter Lagunen deuten auf eine (sub)rezente Präsenz von Feuchtgebieten der Küstenebenen auf Elba hin. Teilweise sind die Ebenen akut von Hochwasser bedroht. Eine kombinierte Betrachtung der Paläoumweltrekonstruktion und der archäologischen Daten zu den antiken Standortfaktoren für die Eisenverhüttung deutet an, dass um die Campo-Ebene bewusst solche Standorte zur Verhüttung ausgewählt wurden, die einerseits Zugang zu größeren Waldflächen ermöglichten, andererseits küstenseitig zugänglich waren, ohne die angesprochenen Feuchtgebiete queren zu müssen.
– Der Verhüttungsstandort in Magazzini ist geochemisch durch erhöhte Gehalte an Fe, As, Cu, Ca und pyrogenem und organischem Kohlenstoff sowie hohen pH-Werten klar von den umliegenden Gebieten abzugrenzen. Die geochemische Abgrenzung des Standortes unterscheidet sich nur bedingt von der Interpretation archäologischer Surveydaten. Die

Variabilität der einzelnen chemischen Proxies auf dem Verhüttungsstandort deutet darauf hin, dass in unterschiedlichen Bereichen unterschiedliche Arbeitsschritte vollzogen wurden. So ist beispielsweise der As-Gehalt aufgrund seines volatilen und siderophilen Charakters v. a. in Erzen erhöht, während erhöhte Cu-Gehalt auch in Schlacken zu finden sind. Erhöhte Gehalte an Ca und Kohlenstoff sowie die pH-Werte deuten auf die Ablagerung von Holzkohleresten und Asche hin. Auch in den alluvialen Archiven flußabwärts des antiken Verhüttungsstandortes in Forcioni tritt der technogene Eintrag deutlich hervor. Der Vergleich mit den chemischen Daten aus den Minen(-sedimenten) zeigt klar, dass für die römische Eisenverhüttung nur bestimmte Bereiche der Minen abgebaut wurden. Die in den Minen stark erhöhten Gehalte an z. B. Pb sind nicht auf dem Verhüttungsstandort zu erkennen, da nur in der modernen Abbauperiode auf Elba auch Lagerstätten mit Galenit und entsprechend einem hohen Anteil an (Arseno)-Pyrit abgebaut wurden. Diese Beobachtung deckt sich mit der aus alten Beobachtungen rekonstruierten Verbreitung der römischen Abbaue. Die Ergebnisse aus der Auswertung der terrestrischen Archive des Verhüttungsstandortes machen deutlich, dass Proxydaten aus anderen Sedimentarchiven nur bedingt Aufschluss über den Umwelteinfluss der antiken Eisenverhüttung geben können, da die Signale durch Denudation von nicht-antiken Lagerstätten überprägt sind oder Einträge der schwermetallträchtigeren Kupferverarbeitung aufweisen.

– Die Analyse von Sedimentsequenzen zeigt, dass im Bereich des Verhüttungsstandortes von Forcioni Ablagerungen zu finden sind, die auf erhöhte Hochwasserdynamik hinweisen. Außerdem wurden dort mit der Verhüttung korrelierende Hangsedimente abgelagert. Die Metaanalyse aller verfügbaren Sedimentsequenzen von Elba zeigt außerdem, dass es auf Elba zwei markante und statistisch relativ wahrscheinliche Phasen erhöhter geomorphologischer Aktivität gibt. Während die zeitlich erste Phase in den Zeitraum des Übergangs von transgressiven Bedingungen zum Holozänen Meerespiegelhochstand datiert, ist die zweite Phase in der antiken Verhüttungsperiode zu verorten. Sowohl die hohen kumulativen Wahrscheinlichkeiten der kalibrierten ^{14}C-Alter, als auch aktivitätsanzeigende Fazieswechsel und simulierte Akumulationsraten deuten auf den Einfluss der Verhüttung auf die kontemporäre Morphodynamik hin.
– Auch wenn die antike Eisenverhüttung wie dargelegt einen deutlich erkennbaren Einfluss auf die Umwelt hatte, zeigen die Daten aus der Simulation des Holzbedarfs und Flächenverbrauchs für die Verhüttung und die Werktätigen, dass es nicht wahrscheinlich ist, dass während der Antike kein Wald mehr für die Holzkohleproduktion auf der Insel zur Verfügung stand. Vielmehr zeigt ein Großteil der Monte-Carlo-Simulationen, dass es nicht zu dem für das 1. Jh. v. d. Z. angenommenen Engpass bei der Holzversorgung gekommen sein muss. Nimmt man an, dass die Versorgung der Arbeiter auf Elba

(zumindest teilweise) vom Festland aus erfolgte, ist ein Brennstoffmangel sogar als *sehr unwahrscheinlich* zu bewerten. Die vorliegenden Daten zum Verhüttungsprozess lassen sich vielmehr dahingehend interpretieren, dass die Verhüttung ohne Engpässe durchgeführt werden konnte. Nichtsdestotrotz mussten große Flächen der Insel zumindest zeitweise forstwirtschaftlich genutzt und gepflegt werden, um die Versorgung mit Brennstoff zu gewährleisten. Anhand der (wohlgemerkt spärlichen) anthrakologischen Daten von Elba, dem Wissen über Holzselektion für die Verköhlerung schon zu Etruskischer Zeit und antiken Schriften *(silvae caeduae)* über den Wald gehen wir zurzeit davon aus, dass die Waldnutzung für die Verhüttung aktiv gestaltet wurde.

Übergreifende Schlussfolgerungen. Die vorliegenden Fallstudien und auch die allgemeine Beschreibung von Elba als metallurgische Landschaft zeigen deutlich, dass Mensch-Umwelt-Beziehungen eine wichtige Rolle für die Eisenproduktion auf Elba in der Antike gespielt haben. Der Einfluss der Verhüttung auf die Umwelt ist sowohl kleinräumlich, auf einem Verhüttungsstandort, als auch in den Talverfüllungen standortnah und regional festzustellen, sei es durch erhöhte Morphodynamik oder durch die Ablagerung technogener Sedimente. Auch die räumliche Simulation zeigt, dass einige Flächen auf Elba für die Verhüttung forstwirtschaftlich genutzt wurden, wenn auch nicht zwangsläufig die gesamte Insel abgeholzt werden musste.

Die Beobachtung Strabos, dass auf Elba das Eisen nicht *geschmolzen* wird und das darauf aufbauende Abholzungsnarrativ soll mit Hinblick auf die Ergebnisse der vorliegenden Studien vor allem aus (umwelt-)historischer Sicht neu eingeordnet werden. So ist festzuhalten, dass Strabo nicht zwangsläufig ein Ende der Verhüttung beobachtet, sondern möglicherweise nur sah, dass die Eisen*luppen* auf dem Festland weiterverarbeitet wurden. Außerdem fallen viele neuzeitliche Interpretationen von Strabos Text in eine Zeit, in der Elba von – zumindest im Vergleich zur heutigen Situation – relativ dünnem Waldbestand gekennzeichnet war; in der Reiseliteratur des 18./19. Jh. ist überliefert, dass es zu jener Zeit einen Holzmangel gegeben hat. Der Niedergang der Verhüttung auf Elba im 1. Jh. v. d. Z. fällt weiterhin in etwa in die Zeit eines Dekrets des römischen Senats (Plin., HN, 3.138, 33.78), das möglicherweise den Abbau in ganz *Italia* untersagte. Weiterhin wurden in der Mitte des 1. Jh. v. d. Z. neue bedeutende Eisenerzlagerstätten etwa in Noricum, Gallia, oder Hispania, von den Römern erobert. Auch wenn die Eisenverhüttung insofern als wichtiger Faktor für die Umwelt auf Elba gesehen werden muss, sind letztendlich auch andere, beispielsweise politisch-historische, Aspekte heranzuziehen, um die Entwicklung der Eisenproduktion auf der Insel zu bewerten und zu verstehen.

Table of contents

List of figures

List of tables

List of abbreviations and acronyms

m a.s.l.	meter above (present) sea level
t.a.q.	*terminus ante quem*
BCE	Before Common Era
BP	Before Present (before 1950)
cal BP	calibrated radiocarbon years Before Present
CE	Common Era
CPF	Cumulative Probability Function
CRM	Certified Reference Material
DEM	Digital Elevation Model
DL	Detection Limit
EC	Electric Conductivity
EPSG	European Petroleum Survey Group Geodesy code
FBA	Final Bronze Age
ICP-OES	Inductively Coupled Plasma-Optical Emission Spectroscopy
IQR	Inter Quartile Range
ka	thousand years *(kiloannum)*
LGM	Last Glacial Maximum
LOI	Loss-On-Ignition
Ma	Million years *(Megaanni)*
MAD	Median Absolute Deviation
Mdn.	Median
MGS	Magna Graecia-Sicily (amphorae)
MIS	Marine Isotope Stage
MS	Magnetic Susceptibility
PC	Principal component
PCA	Principal Component Analysis
pXRF	portable energy dispersive X-Ray Fluorescence spectroscopy
PyC	Pyrogenic Carbon
QAQC	Quality Assessment and Quality Control
RSD	Relative Standard Deviation
TC	Total Carbon

TIC	Total Inorganic Carbon
TOC	Total Organic Carbon
TS	Total Sulphur
VC	Variable Cluster

1 Introduction

In the framework of the Excellence Cluster *Topoi. The Formation and Transformation of Space and Knowledge in Ancient Civilizations*, the research group *Iron as a raw material* analyzed the introduction of the iron smelting technology in different parts of the ancient world (see Bebermeier et al., 2016; Figure 1.1). The focus of the research in the group is on the (spatial) organization, technological development, social interaction and spatial effects in the context of early iron smelting (e.g. Thelemann et al., 2015). Researchers in the group deal with ancient texts (e.g. Cordani, 2016), material culture (e.g. Brumlich, 2018b), and aspects of the environment and landscape (Thelemann, 2016; Thelemann et al., 2018), especially resources (Thelemann et al., 2017). The thesis at hand is—together with Raphael A. Eser's dissertation *Insula scoriae ferax – Studien zur Chronologie, Topographie und Ökonomie der antiken Eisenverarbeitung auf Elba* (Humboldt Universität zu Berlin, Faculty of Humanities and Social Sciences, date of defense: 8. Jan. 2021)—integrated in the research group. The focus of the project is on the resources and the environment of the metallurgical landscape on Elba.

Elba is the biggest island of the Tuscan Archipelago and part of the ancient *Etruria Mineraria* mining region (see Camporeale, 1985b; Corretti & Benvenuti, 2001; Neppi Modona et al., 1981; Zifferero, 2017). Notably, the most important oxidic iron ore deposits in Italy are located on Elba. These were intermittently mined since the Etruscan period (Corretti, 2017). According to the *Italian inventory of abandoned mining sites* (1870–2006), 41% of all abandoned hematite mines in Italy were located in Tuscany the most of them on Elba. In 1913, for instance, 603 116 t of iron ore were extracted in Italy, with Elba covering 91% of the nation extraction (Roesler, 1921). Since 1981, all iron mines on Elba are abandoned. Iron ore from Elba was smelted on the island and transported to the Apennines peninsula from the antiquity to the modern era. In the 20th century, ore was also transported to continental Europe, e.g. to smelters in the Rhône valley (Pounds, 1957). The last furnace on Elba was in operation until Word War II.

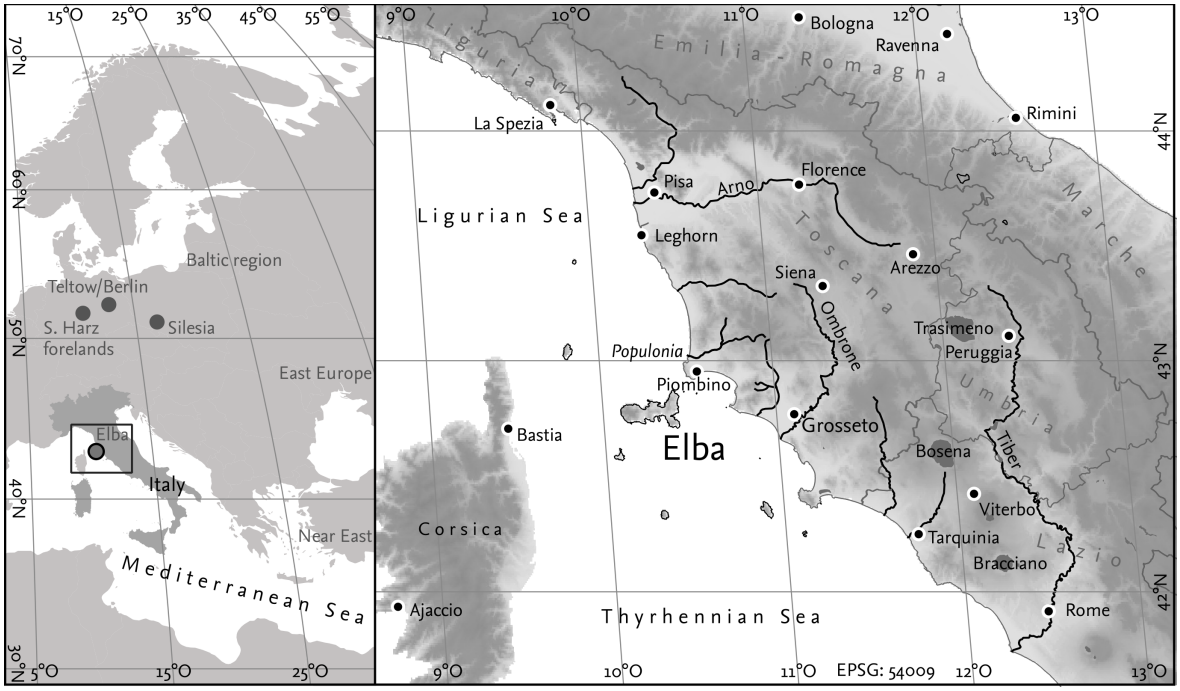

Figure 1.1 Location of Elba island in Central Italy. The study areas of the research group on *Iron as a raw material* are highlighted on the left map (after Bebermeier et al., 2016, completed).

Since archaeological research on ancient iron production on Elba started in the early 19th century (Monaco & Mellini, 1965), several aspects related to the landscape and environment of iron smelting on Elba have been discussed—especially a narrative of a lack of fuel causing the abandonment of (most of the) smelting sites on the island (see Grove & Rackham, 2003)—but not analyzed in full detail. In the following, I will present evidence from geo- and landscape archaeological research on the impact of the introduction of iron smelting on the landscape balance on Elba island in the 4th century BCE. This analysis is embedded in the archaeological and historical knowledge on the 'metallurgical landscape' on Elba and the Etrusco–Roman iron economy between the 7th century BCE and the 2nd century CE. Proceeding from the discussion of the conceptual socio-ecological model of nature–culture interrelations in the research group on early iron, the *socio-ecological model of iron as a raw material* (Bebermeier et al., in press) sets the theoretical scene of the thesis at hand.

1.1 The ores

The initial deposition of notable iron concentrations on Elba is synsedimentary to the middle–late Triassic sedimentary rocks of the Verrucano-formation; iron was possibly preconcentrated during metamorphism of the quartzites (Dünkel, 2002). The subsequent

formation of the ore deposits is strongly connected to the Late Miocene intrusion of the Monte Capanne and the Porto-Azzurro plutons (Dünkel, 2002; Frisch et al., 2008; Tanelli et al., 2001—see Figure 1.2).

During magmatism, iron was metasomatically–hydrothermally mineralized, mobilized by saline, chlorine-rich temperate fluides in the near-contact zone, and deposited in mainly stratiform bodies along north-south striking faults. Host rocks of the iron ore deposits including the quartzites of the Verrucano-group and the adjoining layer (Carbonian–early Permian black phylittes of the Rio Marina Fm., the Triassic–Jurassic dolomitic limestones of the Tuscan nappe, and the late Triassic marbles and dolomitic rocks of the Porto Azzurro unit; see Dünkel, 2002; Frisch et al., 2008; Principi et al., 2015). In the contact zone, iron skarns developed (Frisch et al., 2008). Due to varying composition of the fluids and a temperature-gradient with distance to the plutons, the ore deposits on Elba show a complex pattern; the southern deposits are magnetite-rich, whereas the northern deposits are mainly hematite-rich (±pyrite±limonite; see Tanelli et al., 2001). The main deposits in northeastern Elba (and the Calamita deposit) are allochtonous; hosting rocks slipped off along the Zuccale detachment fault during the intrusion of the Monte Capanne pluton (Dünkel et al., 2003). The Ginvero and Sassi Neri deposits are autochtonous (and located near the Porto Azzurro dyke swarms; see Figure 1.2).

1.2 Mining and smelting history

1.2.1 'Inexhaustibility'

Elba Island was a centre of iron production in *Italia* in antiquity from the 6th century BCE (Corretti, 2017) to the 1st or 2nd century CE. Mainly the hematite-rich deposits in Rio and Rialbano in northeastern Elba were exploited (Tanelli et al., 2001). In the 6th and 5th century BCE, run-of-mine (or crushed ore) was transported to the mainland for smelting and further refining—smelting on Elba started only in the 4th century BCE. Based on the present archaeological record it is relatively clear that early metallurgical activities on Elba were of small scale and increased after the Roman occupation (first half of the 3rd century BCE), especially in the 2nd century BCE. In the 1st century BCE, activities clearly decreased, but mining (and most likely also smelting) continued in the 1st or even 2nd century CE (see Chapter 4).

Estimates of various authors suggest that up to 12 000 000 t of raw iron ore were exploited from the deposits on Elba in pre-modern times, or between 4000 t and 11 000 t annually in antiquity (see Buchwald, 2005; Davies, 1935; Freise, 1907; Haupt, 1888; Piccinini, 1938; Saredo Parodi, 2013; Tanelli, 1985). Estimates of the amount of ferrous slag disposed

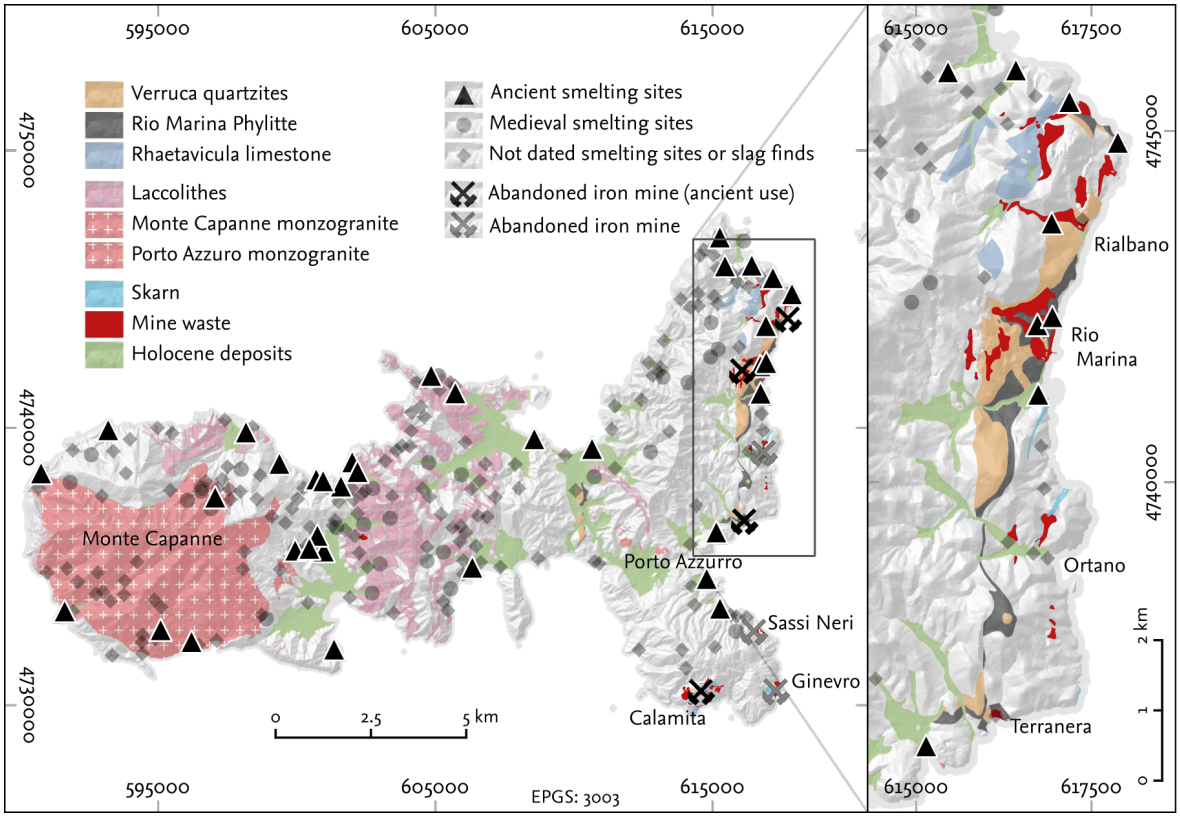

Figure 1.2 Location of smelting sites, ore hosting rocks, and mines on Elba. Database: Regione Toscana, 2014; Adamoli & Rigon, 2013; Capacci, 1911; Corretti, 1988, 1991; Corretti & Firmati, 2011; Nihlén, 1958, 1960; Nihlén & Ejlers, 1958; Pagliantini, 2014; Tanelli et al., 2001; Zecchini, 2001 (database compiled by Raphael A. Eser).

on Elba in pre-industrial times range from 100 000 t to at least 560 000 t (Corretti, 2017; Pistolesi, 2013; Zecchini, 2001—see Case Study 4, Becker et al., submitted.a, Chapter 9, for further details on the estimations). Up to date, more than 252 smelting sites or sites with slag finds are documented (see Figure 1.2); 27 of the sites—including most large ones—are ancient. In antiquity, the ore extracted on Elba was transported mainly to Baratti (the 'industrial' center of the Etruscan/Roman city of Fufluna/Populonia), Follonica-Rondelli and Poggio Butelli in the Gulf of Follonica (i.a. Aranguren et al., 2004, 2009; Benvenuti et al., 2000b; Chiarantini et al., 2007; Corretti & Benvenuti, 2001; Costagliola et al., 2008; Pistolesi, 2013), but also to remote areas along the Tyrrhenian and Ligurian coast (Cambi et al., 2018; Corretti et al., 2018); and maybe also further. The scale of smelting in Populonia might have exceeded the production on Elba, even by an order of magnitude (estimates range between at least 400 000 to 4 000 000 t—see Pistolesi, 2013; Saredo Parodi, 2013; Wertime, 1983). Production around the Gulf of Follonica (especially in Poggio Butelli) was of large scale, too (at least 149 000 to 500 000 t slag—see Costagliola et al., 2008; Pistolesi, 2013). Although smithing slags were found in the fortified hilltop settlement of Castiglione di San Martino (Corretti, 2016), refining

Figure 1.3 The post-mining landscape on Elba at Topinetti. After the end of mining in the second half of the 20th century the former pits were reforested. Note the abandoned mining facilities on the left side of the image and the current use of the beach for tourism. View from the sea in western direction.

on Elba might have been of small scale: raw blooms were transported to the mainland. Archaeological remains and the location of Bronze Age sites in the vicinity of ophiolitic copper deposits on Elba point to early metallurgy on Elba, it was of only minor scale, whereas in Populonia, copper production on notable scale took place (Chiarantini et al., 2018, 2009).

Iron production on Elba is mentioned in ancient texts (see Corretti, 2004; Sherwood et al., 2003). A famous example is Virgil's comment on the 'inexhaustibility' of the iron ore deposits on Elba (*Aeneid*, 10, 173–174): 'ast Ilva trecentos [i]nsula, inexhaustis Chalybum generosa metallis.'—in English: 'But Ilva [i.e. Elba] three hundred, an Island ennobled by unexhausted Mines of Steel' (Davidson, 1790). Also Strabo brings up the *topos* of the inexhaustibility of the mines on Elba (5.2.6): 'However, this is not the only remarkable thing about the island; there is also the fact that the diggings which have been mined are in time filled up again' (Strabo 5.2.6, Jones, 1923, p. 357). In a pseudo-Aristotelian text a description of the metallurgical history of Elba and Populonia is handed down, which is embedded in the metaphoric paradox of iron appearing in an abandoned copper mine (*De mir. Ausc.* 93). In the mid-1st century BCE, the Greek historian Diodorus Sicilus (c early 1st century BCE–30 BCE) described the metallurgical cycle on Elba, including the extraction and crushing of ore, smelting, and trade; and the refining and production of objects on the mainland (Diod. Sic. 5.13.1–2, translation: Loeb III, 1939, p. 131):

Figure 1.4 Abundant slag fragments covering the soil of the Magazzini site. Original photo and redrawing. Image credit: Raphael A. Eser, Aug. 2016.

> Off the city of Tyrrhenia known as Poplonium there is an island which men call Aethaleia [i.e. Elba]. It is about one hundred stades distant from the coast and received the name it bears from the smoke (aithalos) which lies so thick about it. For the island possesses a great amount of iron-rock, which they quarry in order to melt and cast and thus to secure the iron, and they possess a great abundance of this ore. For those who are engaged in the working of this ore crush the rock and burn the lumps which have thus been broken in certain ingenious furnaces; and in these they smelt the lumps by means of a great fire and form them into pieces of moderate size which are in their appearance like large sponges. These are purchased by merchants in exchange either for money or for goods and are then taken to Dicaearchia or the other trading-stations, where there are men who purchase such cargoes and who, with the aid of a multitude of artisans in metal whom they have collected, work it further and manufacture iron objects of every description.

Diodorus refers to the emission of soot from the furnaces on Elba; he mentions emissions from the furnaces and that the Greek name of Elba was *Aithάleia* ('the fuming one'). Additionally, Corretti & Firmati (2011) relate the construction of flourishing *villae maritimae* in the 1st century BCE to the end of iron smelting on Elba. They interpret the issue of the emission of soot (and noise) from the furnaces as (fairly indirect) evidence that smelting activities decreased, as the emissions would have made the island unattractive for recreational issues during the heydays of iron smelting.

1.2.2 *Exhaustibility*

Based on dating material found on ancient smelting sites and text sources (Strabo 5.2.6), most authors date the end of iron smelting on Elba to the 1st century BCE (see, e.g., Corretti, 1988, 2017; Corretti & Firmati, 2011; Pagliantini, 2014). Strabo's description of Elba in his *Geōgraphiká* (second half of the 1st century BCE or early 1st century CE) plays a key role

in the current historical understanding of environmental issues caused by iron smelting on Elba in antiquity (Strabo 5.2.6, translation: Loeb II, 1923, p. 355–7):

> Again, beneath the promontory there is a place for watching the tunny-fish. And in looking down from the city you can see ... the island of Aethalia ... I myself saw these islands when I went up to Poplonium, and also some mines out in the country that had failed. And I also saw the people who work the iron that is brought over from Aethalia; for it cannot be brought into complete coalescence by heating in the furnaces on the island; and it is brought over immediately from the mines to the mainland.

Referring to the observations of Strabo, various authors proposed that smelting on Elba grind to halt due to fuel scarcity (e.g. Casevitz & Jacquemin, 2018; Corretti, 1992; Ettrich, 2006; Groskurd, 1831; Harris, 2013; Hughes, 2014; Jervis, 1860; Köstlin, 1780; Leitch, 2019; Lätsch, 2005; Marzano, 2007, 2015; Meiggs, 1982; Pagliantini, 2014; Perlin, 2005; Piccinini, 1938; Pococke, 1745; Radkau, 2012; Roller, 2018; Schneider, 1992; Simonin, 1858; Sonnabend, 2012; Täckholm, 1937; Toner, 2018; Wikander, 2009; Williams, 2010—see Grove & Rackham, 2003, or Radt, 2003, for critical comments). This 'deforestation narrative' is widely cited or more or less established, not always with reference to Strabo (Camporeale, 1985a; Corretti, 1988, 2004; Corretti & Firmati, 2011; Forbes, 1964; Harris, 2011; Healy, 1978; Lang, 2017; Nihlén, 1960; Penna, 2014; Pini, 1780; Sallares, 2009; Sands, 2013; Schneider, 2016; Schweighardt, 1841; Vanni, 2014; Veal, 2019, 2017a; Williams, 2010; Wiman, 2013).[1] Whereas a decrease in activities in the mid-1st century BCE is evident in the archaeological record (see, e.g., Corretti, 1988, 2017; Corretti & Firmati, 2011; Pagliantini, 2014), sound evidence for a scarcity of fuel is missing. Strabo does not directly relate to wood shortages; to date no study is published that is directly linked to deforestation and subsequent environmental impacts on Elba. The palynological record from Central Elba from Bertini et al. (2014) only shows a decrease in *Quercus* pollen, which started before the iron smelting period, but not a decrease in all fuelwood species.

1.3 Research history

Traces of ancient iron mining and smelting on Elba have been recognized and reported since the 16th century.[2] In Pini's mineralogical record of the mines in Rio (1780), also

[1] A detailed compilation of quotations of the deforestation narrative can be found in Table A.5, Appendix.

[2] A detailed description of the history of archaeological research on pre-industrial metallurgy on Elba is given by Raphael A. Eser (dissertation, Humboldt Universität zu Berlin, Faculty of Humanities and Social Sciences, date of defense: 8. Jan. 2021). See Pagliantini (2014) and Vanagolli (1993) for the periodisation of archaeological research on Elba since the 16th century.

ancient slags are mentioned. Early more or less systematic records are embedded in general descriptions of the island (e.g. Ninci, 1815). Notable descriptions of slag accumulations and smelting sites occurred in the context of mining and contemporary extraction and the re-use of ancient—iron-rich—smelting slag (e.g. Jervis, 1862; Krantz, 1841; Monaco & Mellini, 1965; Nihlén, 1960).

In the second half of the 19th century, V. Mellini conducted the first archaeological research on Elba, describing ancient *fabbrichile* (i.e. smelting sites) and delivering evidence on the distribution and chronology of slag finds on Elba (see Monaco & Mellini, 1965). Further archaeometallurgical analysis were conducted by H. Scott in the the late 19th century (Scott, 1895). A major contribution to the increase of knowledge on smelting on Elba came from the surveys of the philologist Sabbadini from the 1890s to the 1920s (e.g. Sabbadini, 1919). In Sabbadini's writings, environmental aspects of ancient iron smelting were mentioned; he discusses factors for site locations and the use of fuel wood for smelting (see e.g. Coresi del Bruno, 1729, Krantz, 1841, and Jervis, 1862 for earlier notes on site location factors). Since the 1920s, archaeological research on ancient metallurgy in *Etruria Mineraria* focus on Populonia-Baratti (e.g. D'Achiardi, 1929; Minto, 1954; Wrubel, 1929). In the 1950s and 1960s, the Swedish archaeologist John Nihlén visited Elba several times for on-site inspections (Nihlén, 1958, 1960; Nihlén & Ejlers, 1958). Nihlén was the last archaeologist who saw the remains of the main slag heaps (see Figure 1.5) before they were finally re-mined. Being in contact with one of the concessioners for using old slag, Nihlén documented the volume of heaps and the mass of slag removed from sites. He also discusses several environmental aspects of ancient iron smelting on Elba (including e.g.the species composition of the fuel wood used for smelting, for which be commissioned some anthracological analysis).

After reviews and excavations by G. Monaco (i.a. Monaco & Mellini, 1965), further research by M. Zecchini on the history of Elba followed in the 1970s (Zecchini, 1978, 2001), including a discussion of the fuel requirement for smelting on the island. More or less systematic, extensive, surveys were conducted in the 1980s (Corretti, 1988, 1991; Cambi, 2004—see Pagliantini, 2014; and G. Traina, unpubl.). Since then, the current chronology and theories on iron smelting on Elba developed (especially Corretti, 1988, 1991). The analysis of site locations became one focus of attention and the principal antagonism of the location of iron smelting sites on Elba developed, saying that most Roman sites were located on the coast, whereas Medieval sites were located in the inland (Corretti, 1988).

Besides of small excavations of a medieval site by Martin (1994) and the excavation of the San Bennato site in 1999 (Firmati et al., 2006), a major step forward in the understanding of iron smelting on Elba came from the *Aithale*-project (2006–2015), which is—according

Figure 1.5 Detail of John Nihléns field map ('Arbetskarta') from 1960. Mainly the southern side of Western Elba is shown. Accessed from: Lunds Universitetsbiblioteket Arkiv, B:793, *John Nihléns efterlämnade papper, Elba. Kartor och trycksaker*, urn:nbn:se:alvin:portal:record-64946.

to own assessments—focused on 'Men, earth, and sea' on Elba (Corretti et al., 2014; see also Alderighi et al., 2013). Thus, a landscape archaeological view on iron smelting on Elba was put on the agenda, although not directly related to iron metallurgy (e.g. Pagliantini, 2014). In the framework of the *Aithale*-project, prospections and an excavation in San Giovanni and Magazzini were conducted. Besides the landscape-approach, a provenance marker of Elban ore could be identified by archaeometallurgical and experimental studies (Benvenuti et al., 2013, 2016).

So far, the most important environmental data on the impact of ancient iron smelting are available from Vigliotti et al. (2003), who have shown that the deposition of airborne As- and and Pb-rich (magnetic) matter in the Corsica canal peaked during the heydays of iron smelting. Furthermore, Leoni & Sartori (1997) relate increase trace metal(loid) contents in sea-floor sediments obtained next to the ancient metallurgical center in Baratti beach.

Beyond the knowledge on site patterns and ore use, no local (or site-based) geoarchaeological studies were conducted until 2015 that put the emphasis on the two major environmental issues related to ancient iron smelting on Elba, namely emissions and a lack of fuel (or 'deforestation').

1.4 Objectives and Case Studies

In the dissertation at hand, human–environment interactions in the context of iron mining and smelting on Elba island in antiquity are analyzed. The thematic focus is on the effect of ancient iron smelting on the landscape balance.

Table 1.1 Overview on the four case studies.

Case study	Publication	Own contribution
Case study 1	Becker, Fabian, Raphael A. Eser, Philipp Hoelzmann, and Brigitta Schütt (2019): The environmental impact of ancient iron mining and smelting on Elba Island, Italy—a geochemical soil survey of the Magazzini site. *Journal of Geochemical Exploration* **205**:106307. DOI: 10.1016/j.gexplo.2019.04.009	85%
Case study 2	Becker, Fabian, Raphael A. Eser, Philipp Hoelzmann, and Brigitta Schütt (2019): Reconstructing human–landscape interactions in the context of ancient iron smelting on Elba Island, Italy, using sedimentological evidence. *Geoarchaeology* **34** (3): 336–359. DOI: 10.1002/gea.21726.	75%
Case study 3	Becker, Fabian: Meta-analysis of ^{14}C-ages from mid- to late Holocene valley fills on Elba Island, northern Tyrrhennian Sea, Italy.	95%
Case study 4	Becker, Fabian, Nataša Djurdjevac Conrad, Raphael A. Eser, Luzie Helfmann, Brigitta Schütt, Christof Schütte, and Johnnes Zonker (2020): The Furnace and the Goat—A spatio-temporal model of the fuelwood requirement for iron metallurgy on Elba Island, 4th century BCE to 2nd century CE. *PLoS ONE* **15** (11): e0241133. DOI: 10.1371/journal.pone.0241133.	60%

The main objectives are

i. a characterization of a signature and activity marker of ancient iron smelting to analyze the on-site effect of smelting on soil composition and to find traces of pollution that are still visible today;
ii. a reconstruction of morphodynamics related to iron smelting to gain insights on the effects of clearing for fuel production on the landscape balance—embedded in a palaeoenvironmental reconstruction of mid- to late Holocene landscape on Elba to understand the general variance in the record; and

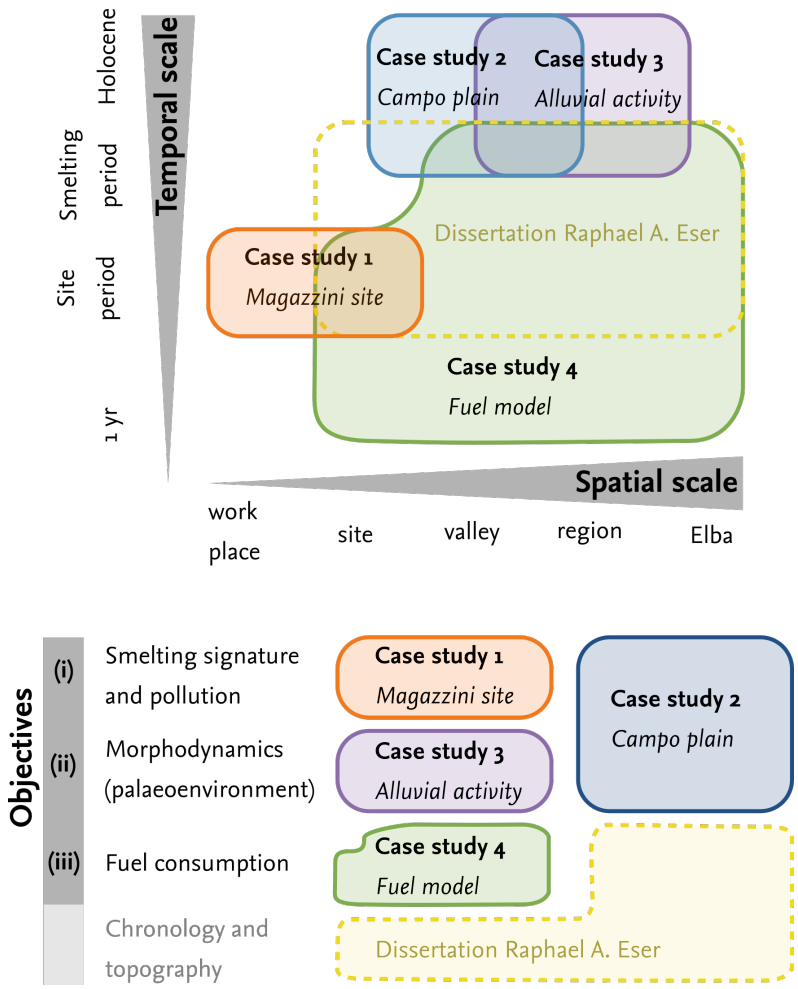

Figure 1.6 Thematic, spatial, and temporal integration of the four case studies and the dissertation of Raphael A. Eser (Humboldt Universität zu Berlin, Faculty of Humanities and Social Sciences, date of defense: 8. Jan. 2021.

iii. a reconstruction of the fuel consumption and the woodlot requirement for iron smelting on Elba to understand if a lack of fuel might have caused the proposed abandonment of smelting sites in the 1st century BCE.

In four case studies (Table 1.1) we try to enhance the understanding of past human–environment interactions and the impact of iron mining and smelting on the landscape balances of Elba island using different approaches from geoarchaeology and landscape archaeology on different temporal and spatial scales (Figure 1.6).

1.5 Socio-ecological model

The socio-ecological perspective on pre-industrial iron smelting formulated by the research group *Iron as a raw material* in the Excellence Cluster 264 *Topoi – The Formation and*

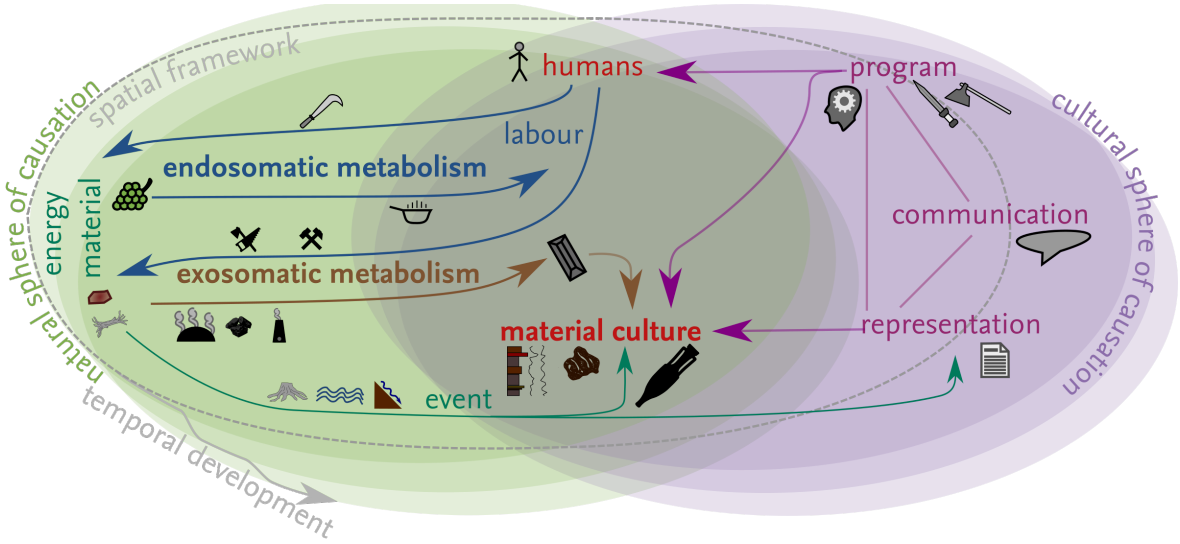

Figure 1.7 The socio-ecological model of the Vienna School, adopted to ferrous metallurgy.

Transformation of Space and Knowledge in Ancient Civilizations builds the theoretical framework of the thesis at hands.[3] The ideas of the *Vienna School of Social Ecology* premise the 'socio-ecological aspects of iron as a raw material' discussed within the group. The terminology used for discussing iron metallurgy on Elba follows the terminology developed in the Topoi-research group.

The socio-ecological model of the Vienna School describes the interaction between 'nature' and 'society' on a macro scale in a general way, making it applicable on various present and past conditions (Fischer-Kowalski & Erb, 2016). The key idea of the concept is operating on 'areas of reality', a hybrid sphere that lies between the classical, dualistic spheres of causation viz. the natural sphere and the cultural sphere. The conceptual socio-ecological model integrates the interaction between culture and nature and describes their co-evolution.

1.5.1 Socio-ecological model of pre-industrial iron metallurgy

The introduction of the iron technology in a spatial entity is part of a *programme*. Under this term, knowledge on iron as a material and on iron ore deposits as well as technological knowledge on the material are subsumed. Furthermore, the demand for iron and ecological strategies on the exploitation and use of primary (iron) and secondary resources (wood, loam, sand, water, refractory stones, wind) are part of a programme.

[3]The socio-ecological model of iron as a raw material is described in a paper submitted for publication and co-authored by the author of the thesis at hand. Details on the research group are available under https://www.topoi.org/group/a-5/.

Therefore, a programme in the context of metallurgy includes instrumental and analytical prerequisites, but also economic and normative instructions.

Within the cultural sphere of interaction, communication describes the link between human agents and cultural conditions relevant for the given spatial and temporal framework.

Human agency is central to the model; humans is the essential part of culture and society and acts within nature, i.a. by interpreting and exploiting it. As the socio-ecological model of iron as a raw material is mainly set up in an archaeological context, material remains ('material culture') of past societies are also a key element of the model and the reconstruction of past human populations. They first and foremost comprise the metallurgical remains of the iron production process, e.g. archaeological ores (run-of-mine and preprocessed ore found in archaeological context), ferrous slags, blooms, remains of smith, or iron objects as well as remains of bloomeries, charcoal, or tools. Material remains may also include written sources or epigraphs, and even data from sediment archives or the distribution of resources and smelting sites. The human agency subsumes individual agents in the model that are engaged in the iron production system.

1.5.2 Metabolisms

Human agents intervene in nature through labor, which includes the intentional modification of the natural prerequisites and actions undertaken to exploit primary and secondary recourses. Labour invested in iron production is part of the *social metabolism* of ferrous metallurgy. The social metabolism comprises the flow of energy (e.g. labour, charcoal) and materials (e.g. ore) between the hybrid societal sphere and the natural sphere. If fundamental parts of the social metabolism are lacking, a metabolism can not be sustained. To better understand energy flows in the social metabolism, we propose to extend the socio-ecological model of iron as a raw material originally proposed by (Bebermeier et al., in press): Referring to Boyden (see Fischer-Kowalski & Weisz, 1998) and Molina & Toledo (2014) in human ecology, we separately analyse an *exosomatic* and an *endosomatic* metabolism. The endosomatic metabolism—also termed biometabolism—covers all flows of energy and material to sustain the human organism. This includes e.g. water and comestible goods, but also wood and charcoal for heating and cooking. The exosomatic metabolism—the technometabolism—includes the flows of energy and material necessary to technological processes; e.g. fuel for charging iron furnaces. Thus, the smelting processes itself is part of the exosomatic metabolism, while labor investment—undoubtedly part of the production process—is included in the endosomatic metabolism. The endosomatic metabolism is marginally effected by the coevolution of the spheres, meaning that e.g. calorific requirements do only slightly change with a changing pro-

gramme of iron production. The exosomatic metabolism, however, is strongly connected to changes within the culture sphere (cf. Molina & Toledo, 2014): changes in silvicultural practices, for example, result in a change in the (local) fuel availability and therefore also the organization of iron production. This may also comprise other changes in technology, ideas on resource use (e.g. species selection for charcoal production; or the use of coal instead of charcoal) and the communication, representation, and coping strategies of resources scarcities. Although the distinction between techno- and biometabolism is e.g. criticized by Fischer-Kowalski & Weisz (1998) for its dualistic implications, we accept the concept for it's analytical capabilities. A separate quantification is not only straightforward, it also claims for the explicit consideration of requirements for labour and charging of furnaces. During the course of the development of human societies, the relative (qualitative) contribution of the exosomatic metabolism to the societal metabolism increased continuously (Casado & Molina, 2017). Accordingly, research addressing aspects of flows of energy and material in the context of pre-industrial iron smelting focus on fuel requirements for furnace operation (Brumlich, 2018a; Cleere, 1981; Eichhorn et al., 2013a,b; Goucher, 1981; Healy, 1978; Iles, 2016; Paysen, 2011; Pleiner, 2000; Rehder, 2000; Saredo Parodi, 2013; Thelemann et al., 2015; Voss, 1988; Wallner, 2013). In contrast, research on non-metallurgical energy requirements focus mainly on the endosomatic metabolism to reconstruct flows of energy, such as the energy consumption of the city of Pompeii or Roman bathes. Both aspects of the metabolism are explicitly analyzed by e.g. Daems et al. (2018)—albeit not in a metallurgical context. Saredo Parodi (2013) reconstructs both labour requirements (so part of the endosomatic metabolism) and fuel requirements (exosomatic metabolism) for iron production in Populonia, however, without explicitly taking the fuel requirements for food production to supply the local work force into account. Although a social metabolism is not entirely bounded to a container space, a differentiation between spatial entities or scales might foster qualitative analysis (see Molina & Toledo, 2014). For instance, the more or less autarkic production in rural areas is characterized by different metabolism when compared to urban centers. Likewise, the metabolism in a specific village is different from the metabolism in a large region.

The perceived effect of physical forces in the natural spheres on humans are included in the conceptual model. They are described with the term *events*. An event is either directly linked to the maintenance of the metabolism of iron smelting—such as the depletion of resources—or events that are perceived to be dedicated to iron production—e.g. accelerated flooding after clearing—but do not directly have an impact on the metallurgical metabolism.

Events can be reflected in e.g. sediment archives or archaeological layers of destruction (e.g. after a flood). They are 'transferred' to the cultural sphere of causation by *representation*.

Representation therefore presupposes that an event is perceived, interpreted or understood, and recorded. Events can be directly represented in material culture (epigraphs, written sources), but also in intangible heritage. The latter can be eventually manifested in the programme and as material remains of the change in programme.

The spatial framework of the socio-ecological model is—as the social metabolism—not spatially bound. This becomes especially clear with regard to the programme. The introduction of the iron smelting technology in a region requires the transfer of knowledge from other regions. Also the demand for iron is not limited to the metallurgical region and its resource catchment. However, for a quantitative perspective, the delineation of a study are is necessary.

1.5.3 Landscape balance

In the context of the socio-ecological model, I understand the term *landscape balance* as a results of the fluxes between the components of a landscape (Volk & Steinhardt, 2001). These components are mainly geology, resources, landforms, soil, vegetation, and land use (human agency); fluxes include the transport of water, material, and energy. The impact on the landscape geo-ecosystem in this context means the change in an equilibrium by land use and and input and output interactions, including changes of the geo-ecosystem, dynamics, adaptation, and feedback effects (Volk & Steinhardt, 2001). Based on the ideas of the socio-ecological model also human perception—so the cultural dimension of human–environment interactions—plays a role in the analysis of the landscape balance, as adaptation and looped feedback effects require any observation and interpretation of the impact on the landscape balance. Human perception is a key aspect in the understanding of *landscape* in landscape ecology (Klink et al., 2002) and in the theoretical framework of *landscape archaeology*. As conceptualized by e.g. Bork et al. (1998) and revisited by Dotterweich (2008), human agency *(destabilization)* effects the ecosystem and the landscape balance, and will lead to restabilization and a system in equilibrium (stability) after human feedbacks to destabilization.

2 State of the art: The environmental impact of iron metallurgy

2.1 Pre-industrial iron production

The production cycle of pre-industrial metallurgy (Figure 2.1) affected the environment in different ways (Figure 2.2). The analysis of the impact of iron smelting on the landscape balance requires a basic understanding of pre-industrial iron production, as different steps of the product's life cycle have different energy (fuel) requirements and caused different types of (potentially) harmful deposits. Modern analyses of the life cycle of metals (e.g. Nuss & Eckelman, 2014) include a cradle-to-grave assessment that comprises all steps of production from resource extraction ('cradle', iron ore, run-of-mine) to the disposal of the end-product ('grave', e.g. a sword).[1] Also cradle-to-gate assessments are common, focusing only on a partial life cycle from extraction to an end product of a particular production step (e.g. a raw iron bloom, a bar, or a nail). The assessment of the impact of iron smelting in the thesis at hand is mainly discussed from resource extraction in the mines to the refining of the blooms, including processing of the raw ore (run-of-mine) and smelting of the dressed ore.

The term *pre-industrial* is here mainly used in a chronological–technological sense, mainly including iron smelting in a charcoal or coal-fueled bloomery furnace; charcoal was the main fuel for iron smelting until the 17th century to 19th century, depending on the development of the iron industry and the availability of resources (cf. Hammersley, 1973; Pleiner, 2000). This transition from charcoal to coal as a main source goes along with the establishment of blast furnaces and is more or less contemporary to the First Industrial

[1] E.g. Blakelock (2013) also included the recycling of an used iron object in the life cycle of medieval iron knives; the scientific assessment of objects or by-products may also be included in an archaeological life cycle assessment.

Revolution. To describe the different steps of the partial life cycle of pre-industrial iron smelting in the thesis at hand (Figure 2.1), the following terminology is used:

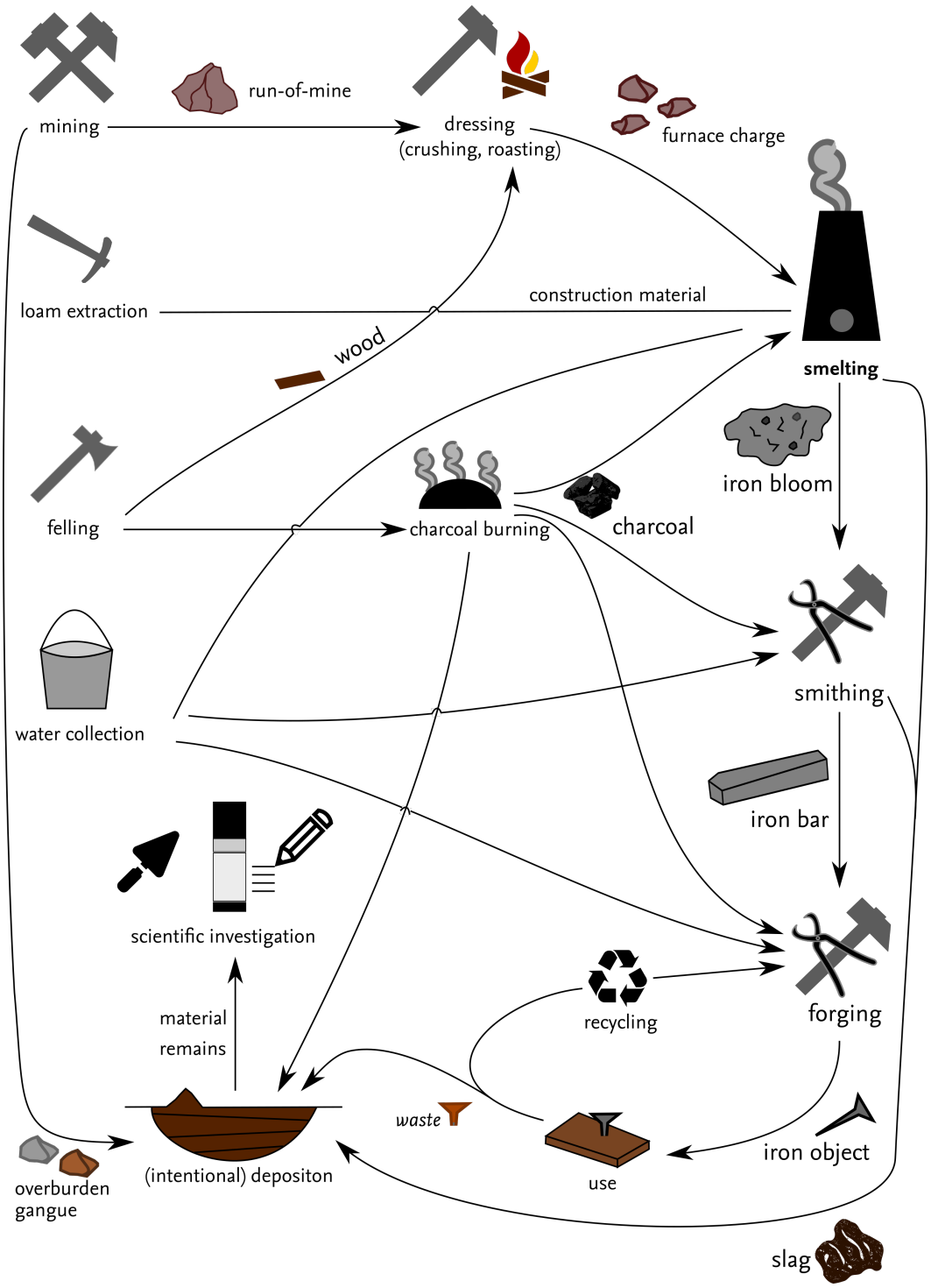

Figure 2.1 Simplified model of a cradle-to-grave life cycle of iron production. Flow of materials/energy is highlighted by arrows. Not all secondary raw products necessary for iron production are included in the depicted life cycle, such as straw or temper required for the construction of the bloomery furnaces or materials used to build tools etc.; not all steps were conducted at the sample place (see Figure 2.3). Illustration adopted from Blakelock (2013) and Baron & Coustures (2015).

Mining. Mining is the extraction of minerals with desired elements (metals) from the ground. These minerals typically occur in rock or sediments and are called *ores* if the concentration of the desired element is economically valuable to be extracted (cf. Lane, 2016).[2] The term iron ore includes several minerals; limonite, goethite, hematite, magnetite, siderite, and pyrites are the most common iron ores (see Pleiner, 2000). A deposit is an accumulation of an ore; ores occur in montan deposits or in sedimentary deposits (e.g. bog iron ores). The minerals containing the desired element are often associated with gangue, i.e. economically unwanted material.[3] The most prominent material remain of mining is overburden; i.e. the material overlying the ore deposits.[4] The product of the mining step is raw ore (sometimes referred to as *run-of-mine*). In pre-industrial times, most iron ore deposits were extracted by opencast mining, although underground works existed (Pleiner, 2000).

Processing of the ore (ore-dressing). The preparation of the raw ore includes some kind of washing, sorting and mechanical crushing. Crushing the ore could have taken place on the mining site to facilitate transport or on the smelting site (Pleiner, 2000). Another step of processing is the roasting of the ore to increase the porosity to facilitate the reduction process and to remove impurities such as sulphur. For roasting, wood could be used as fuel. Unwanted remains of the dressing process are dumped on tailings.

Production of secondary resources. Prior to the smelting (reduction) of the ore in a furnace, several other raw material is required (if ore is roasted, also wood is needed in a preceding step). The processing of the secondary resources may have been contemporary to steps preceding smelting. The most important steps necessary for the provision of secondary resources of the iron production process are felling of wood and the subsequent burning of charcoal[5] in a kiln, the collection of water (e.g. for the construction of the furnace or for fire prevention and cooling), and

[2] In *Webster's new world dictionary of the American language*, the term 'ore' is described as 'an natural combination of minerals, esp. one from which a metal or metals can be profitably extracted.' (Guralnik, 1986). In the *Glossary of Geology*, the description reads, 'The naturally occurring material from which a mineral or minerals of economic value can be extracted at a reasonable profit. Also, the mineral(s) thus extracted' (Jackson, 1997).

[3] In the *Glossary of Geology*, the description of gangue reads, 'The valueless rock or mineral aggregates in an ore; that part of an ore that is not economically desirable but cannot be avoided in mining.' (Jackson, 1997).

[4] In the *Glossary of Geology*, the description of overburden reads, 'Barren rock material, either loose or consolidated, overlying a mineral deposit, which must be removed prior to mining.' (Jackson, 1997).

[5] Charcoal was the main fuel resource for iron smelting until the 18th century (Hammersley, 1973; Sivramkrishna, 2009, cf.). However, examples are known where coal was used for pre-industrial iron smelting (Dodson et al., 2014; Gelegdorj et al., 2007; Park et al., 2008, e.g.). Smith (1997) mentions the use of coal for Roman iron smelting on Great Britain in Roman times. Mattusch (2009) cited Theophrastus (Lap. 16) to show that coal was known as fuel in antiquity.

the extraction of loam that is used for the construction of the furnace. Secondary resources are also required for further steps in the life cycle of iron, e.g. charcoal for smithing of raw blooms. For the production of tools etc., additional resources are required, such as leather for bellows (see e.g. Chirikure et al., 2009 for the use of belows made of animal skins in indigenous metallurgy in sub-Saharan Africa).

Smelting. Pre-industrial iron smelting mainly comprises the reduction of pre-processed iron ore in charcaol-fuelled bloomeries. Although blast furnaces were occasionally used in the medieval ages (e.g. Myrstener et al., 2016), they were mainly introduced in Europe since the 16th century (cf. Hammersley, 1973). In bloomeries, iron is smelted by the direct reduction process with temperatures lower than the melting point of iron. The product is low-carbon iron. In a blast furnace, iron is smelted above the melting point of iron and thus carbon is mixed with the iron (cast iron). Bloomeries and blast furnace also differ in air supply, which is hot and with a higher blowing rate in blast furnaces (see e.g. David et al., 1989). The described output of the bloomery process are blooms (sponge iron), thus a mixture of reduced iron and slag-inclusions. Slag is a by-product of smelting and contains remains of un-reduced iron minerals, gangue, charcoal, and furnace lining (Charlton et al., 2010). If the reduction process is not completed, the processed ore added to the furnace could remain as non-smelted furnace charge.

Post-reduction processing. As an iron bloom could not be readily used for the production of e.g. weapons or tools, refining is needed, which mainly includes heating the bloom and hammering it to remove impurities, e.g. slag-inclusions. The terms refining, *smithing*, and *forging* are used synonymous in the following, although there are some differences. Following Bauvais & Fluzin (2009), refining can be divided in refining directly after the reduction process when the bloom is hot and refining after interruption, which requires reheating. Post-reduction processing as used in the thesis at hand does not necessarily include further processing such as the transformation to semi-products, welding, or shaping of objects (see Bauvais & Fluzin, 2009).

The term *iron production* is used to refer to the partial life-cycle as described here. Not all steps of the (partial) iron production cycle described here were taken in many, but not in all cases. For instance, roasting of high-grade ores containing few impurities was not always necessary. Also some resources, such as animal skins for the production of bellows, was not necessary if natural-draught furnaces were used instead of forced-draught furnaces (e.g. Juleff, 1996).

Further steps may have been part of the iron production cycle, such as exploration and ritual practices. Exploration mainly includes a perceptional perspective and knowledge on the landscape, such as the the location of iron ore deposits and places suitable for the location of e.g. a smelting site. During the introduction of iron production in a region, the exploratory step was an essential part of production. Ritual practices and cultural conceptions may have influenced the (spatial) organization of the pre-industrial iron production process (Chirikure et al., 2009; Iles et al., 2018). Although a ubiquitous resource, the availability of *air* may have also played a role in the iron production, because in the case of the use of natural-draught furnaces, local wind conditions may have made a location more suitable for iron smelting.

2.2 Environmental effects of pre-industrial mining

Important direct impacts of mining are geomorphological changes caused by the creation of extraction structures such as open-pits. *Pinge* (depressions or sink holes caused by mining) are a common anthropogenic landform in pre-industrial mining landscapes, that were either caused by the collapse of underground mine works or by the mining of near surface veins (see, e.g., Swieder, 2014; Wallner, 2013). In addition to the negative landforms of extraction, the deposition of overburden resulted in positive landforms (waste dumps).

In the case that run-of-mine (raw ore) is further processed on the mining site (separation form gangue, cleaning, crushing), other typical landscape features appear, such as tailings or settling/tailing ponds. These ponds were also used to dam up water for water-powered stamp mills (e.g. the Upper Harz Water Regale: Röhling et al., 2010); in the Elbtalschiefergebirge, Central German Uplands, the increasing demand for iron in the Middle Ages involved the need for hydropower and, subsequently, the relocation of ironworks and the construction of watermills (Pflug & Thalheim, 2014). In modern times, failures of tailing dams exposed the risk of floods that potentially transport harmful material (Cambridge & Shaw, 2019; Macklin et al., 2003).

Especially in areas where sulfidic deposits were mined, acid mine drainage from pits or dumps occurs and has an impact on the chemical composition of surface water and groundwater (e.g. Lottermoser, 2013). Additionally, erosion of dumps results in the mobilization of potentially harmful trace metals that are associated to iron and characterize the detrital dump material. This material is transported to downstream locations and deposited there. Thus, the impact of mining appears also off-iste and is not only of local significance (e.g Macklin et al., 2006).

The requirement of (fuel) wood for pre-industrial mining had an environmental impact as well. Wood was necessary for fire-setting in the mines (Ambert, 2002; Weisgerber & Willies, 2000) or for the construction of mining infrastructure, e.g. timbered ground support for adits or shafts in underground mining (Bartels, 1996; Hemker & Lentzsch, 2012).

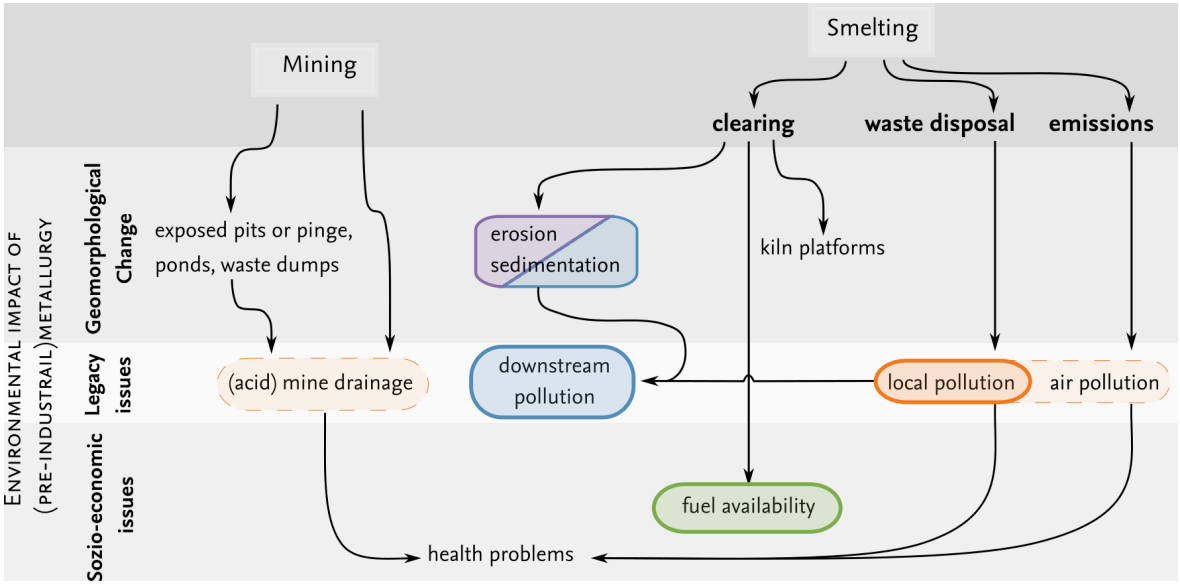

Figure 2.2 The environmental impact of (pre-industrial) metallurgy. Aspects mentioned below are highlighted in bold or italics—the focus of the thesis at hand is emphasized in colour (see Figure 1.6). For references see text (cf. Goldenberg, 1993).

Also the roasting and smelting of ores caused environmental impact. First, the operation of furnaces required fuel, which was nearly exclusively fuel wood (mostly in the form of charcoal) in pre-industrial metallurgy (see above). Clearing for fuel production resulted in soil erosion and reduced the (local) availability of fuel (see, e.g., the examples in Jockenhövel, 1996). Additionally, changes in relief and an alteration of soil characteristics are related to the construction of pits or platforms for charcoal production (Raab et al., 2017, 2015; Rutkiewicz et al., 2019, 2017; Schmidt et al., 2016). Pollution from smelting includes the emission of air pollutants (see Hong et al., 1996; Wagreich & Draganits, 2018) and local legacy issues (Pyatt et al., 2000), mainly the contamination with heavy metals. Pollution from both mining and smelting is also related to health problems and might affect plants by bioaccumulation (e.g. Harrison et al., 2010; Pyatt et al., 2005).

Studies on the environmental impact of pre-industrial *iron* mining and smelting on the landscape balance focus on two major aspects, first and foremost deforestation (and subsequent soil erosion) for fuel production, second, emissions from furnaces. The following summary of the main research approach on the impact of metallurgy on the landscape balance focuses on *pre-industrial iron smelting*. Whereas deforestation for iron smelting may have been more important compared to the processing of other metals (Iles, 2016),

emissions from base metal[6] mining and production might have been much more important than the emission from ferrous metallurgy (see Hong et al., 1996; Wagreich & Draganits, 2018); this is also true for modern production (see Norgate et al., 2007; Nuss & Eckelman, 2014). Although studies on emissions from modern (often coke fired) iron- and steel-making are available, they will not be discussed in detail; scale and heavy metal emission of coke burning is much higher than emissions from pre-industrial charcoal firing (see Bond et al., 2007; Demirbaş, 2003; McConnell & Edwards, 2008).

The description of emissions and waste disposal from iron smelting is mainly restricted to the impact of potentially harmful trace metal(loid)s, because most studies on ancient metallurgy focus on that issue. Nevertheless, also the aerosol emission from pre-industrial furnaces (in combination with deforestation for fuel production) might have had an impact on e.g. climate (Gilgen et al., 2019).

2.3 Deforestation for fuel production

The relationship between pre-industrial (charcoal-fuelled) iron production and deforestation has long been discussed (see Iles, 2016).

The use of charcoal allows for better conditions within the furnaces compared to the use of wood, but requires more woodlot area per unit of iron production (Veal, 2017b). The extent of deforestation and degradation in the ancient Mediterranean region is widely discussed (e.g. Grove & Rackham, 2003; Harris, 2013; Horden & Purcell, 2000; Hughes, 1983, 2011, 2014; Hughes & Thirgood, 1982; Wertime, 1983—see McMahon & Sargent, 2019 for further readings). For instance Harris (2013) argues that metallurgical centres were hotspots of deforestation; he additionally states that 'the amount of wood fuel that was needed across the whole ancient Mediterranean for metallurgy ... was obviously enormous and continuous.' Meiggs (1982) states, however, that wood production (around metallurgical areas) is often underestimated and the demand for fuel wood exaggerated. Mighall et al. (2017) and Mighall & Chambers (1997) report that the impact of Roman metallurgy on the vegetation might be less intensive than often expected or of only local significance (see also Eichhorn et al., 2013a). In addition, Crew & Mighall (2013) emphasize that smelters were self-interested to manage the woodland to maintain metal production. In a review of the impact of past (iron) metallurgy on forests, Iles (2016) states that other factors than metallurgy might have contributed to environmental change

[6]The term *base metal* is used in the sense of a non-ferrous metal of comparatively little value (cf. United States Bureau of Mines & Trush, 1968), in contrast to the definition as a metal that is 'altered by exposure to the air' (Fay, 1920) or definitions including also iron as 'high-volume, low-value' metals' (American Geological Institute, 1997)

in the surroundings of metallurgical production centers (e.g. changes in precipitation, wildfires, population dynamics, or land-use conflicts; see Mighall & Chambers, 1997, or Eichhorn et al., 2013b, for examples). Similarly, Iles (2016) points out that landscapes were not necessarily deforested, but transformed.

Harris (2013) request for definitional sensitivity when discussing ancient deforestation. He distinguishes between 'undisturbed woodland' (Harris, 2013, p. 175), 'anthropogenic disturbance' (*ibd.*, citing Hughes, 2011, p. 49), and 'woodland [that] was cleared away and stayed cleared away' (*ibd.*). Following Williams (1989), in the thesis at hand a *sensu stricto* definition of deforestation is used, understanding it as a process of a long-lasting land cover change from woodland to land without significant tree cover. For instance, neither clearcutting and subsequent regrowth, nor the change from an (old) high forest to a wooded *macchia* shrubland is understood as deforestation.

The latest research history on iron smelting and deforestation can be divided into two distinct periods and approaches, viz. a first period since the 1970s, when evidence is mainly based on calculations of the fuel requirements for production; and a second period (after c 2000), when also geoarchaeological, palynological, and anthracolgoical studies contributed to the knowledge (see especially Iles, 2016, for a comprehensive review on the topic).

2.3.1 Cliometrics—woodlot requirements

Studies on the woodlot requirements for iron smelting are common to assess the economic landscape and ecological impact of ancient smelting. Theses approaches are part of a cliometric approach, thus an attempt to reconstruct past economies by using econometric techniques (see Verboven, 2018, for an overview).

An early example of the calculation of fuelwood requirements for Roman iron production was made by John F. Healey in the late 1970s (Healy, 1978). This orignal estimation reads as follows:

> Experiments have shown that 8 kg . . . of iron can be produced from 50 kg of ore. On this basis, the 2250 tonnes produced per annum in Roman Britain would account for about 13,500 tonnes of ore each year and the Empire would consume annually 495,000 tonnes of ore. It has been estimated that ancient miners removed 11.2×10^6 tonnes of iron ore from the island of Elba. This may have provided around 2,000,000 tonnes of iron, perhaps about 50 years' supply. In addition, each furnace used per annum 24 tonnes of charcoal for smelting alone, excluding subsequent forging or previous roasting of ore. This is equivalent to 96 tonnes of raw wood. It has already been noted that oak predominated among woods for charcoal-making. Thus, taking oak as the example, one furnace consumed 96 tonnes of wood =

> 113 cubic metres (oak is 1.18 cu. m./tonne). For oak, if a Forestry Commission yield class 4, normal age distribution, and an average age of 60 years are assumed, the total yield is 218 m^3/hectare. However, it is important to assume also an overstocking of at least 15% ; the net yield thereby becomes 185 m^3/hectare. Therefore, 113 m^3 of wood consumed annually by one furnace represents the deforestation of an area of about 3/5 of an hectare. Roman Britain would have needed about 240 hectares of wood per annum for smelting alone; and the figure for the Empire would be 5420 hectares (approximately 13,392 acres) deforested annually. *(Healy, 1978, p. 151–2)*

Similar contemporary calculations for Roman Britain and the Etruscan iron production in Populonia are known and are widely reflected (Clark & Yusoff, 2014; Cleere, 1976, 1981; Perlin, 2005; Wertime, 1983) and are also found in e.g. Pleiner (2000) and Rehder (2000). The calculation of the fuel requirement for charging the furnaces are mainly based on archaeological experiments or ethnoarchaeological studies on the productivity of charcoal burning technologies (e.g. Brumlich, 2018a; Horne, 1982; Nikulka, 1995; Thommes, 1997). Other studies use mass balances obtained from the archaeometallurgical analysis of the remains of smelting (especially slag) to estimate production parameter and the woodlot requirements for smelting (e.g. Joosten et al., 1998; Thomas & Young, 1999). A seminal paper on fuel and iron is C. L. Goucher's *Iron is iron 'til it is rust*, where she discusses the ecological aspects in the decline of the West African iron-smelting (Goucher, 1981).

Estimations of the fuel consumption for iron smelting were mainly published as a side kick of archaeological studies in the 2010s (e.g. Brumlich, 2018a; Eichhorn & Robion-Brunner, 2017; Paysen, 2011; Thelemann et al., 2015; Wallner, 2013). Saredo Parodi (2013) includes the estimation of the fuel requirements for smelting in a comprehensive cliometric study on the metallurgical industry in Populonia.

Approaches that include anthracological or palynological analysis in calculations of fuel requirements for iron smelting are i.a. found in Eichhorn et al. (2013a,b) and Mighall & Chambers (1997). Lupo et al. (2015) combines estimations of the fuel requirement with sedimentological analysis. More recent attempts used e.g. archaeological prospection techniques to get further insights in parameter of the calculations to more precisely calculate slag quantities from heap volumes (e.g. Eichhorn & Robion-Brunner, 2017). Although there are many studies on fuel wood consumption in the Roman world and the (ancient) Mediterranean region available, many studies in the last decades focus on West (and Central) African archaeometallurgy and are combined with ethnoarchaeological studies (e.g. Iles, 2017; Thompson & Young, 1999).

2.3.2 Geoarchaeological studies

Sedimentological evidence

The impact of historic metallurgy on fluvial sediments is widely discussed, but most of the studies are not directly related to *iron* smelting. Raab et al. (2010), Brown et al. (2009), Stolz et al. (2013), Stolz et al. (2012), Stolz & Grunert (2008), Schmidt-Wygasch (2011), dos Santos Mendes (2016), and Thelemann et al. (2018) found that the increase in fluvial deposition in different European regions coincides with metallurgical activities.

Records showing increased catchment erosion can not exclusively be related to felling for iron smelting, as an increase in metallurgical production is often also related to population dynamics and agricultural expansion (see Eriksson et al., 2000). The impact of iron smelting on erosion is sometimes evaluated to be relatively small compared to other human activities (Iles et al., 2018; Lane, 2009; Superson et al., 2014). In West Africa, increased soil erosion as evident in fluvial records is contemporaneous to the rise of iron metallurgy (Garnier et al., 2018; Lespez et al., 2011). The (presumed) environmental impact of early iron smelting in West Africa lies within a period of climate change favoring the extinction of forests and falls simultaneously into a period of the advance of farmers (the so-called 'Bantu extension'), thus into a transition period from climate-driven changes to human-and-climate-driven changes. The introduction of iron smelting after the Bantu-expansion to Central Africa in a period of major climatic and floral changes in the 1st millennium BCE is a good example of the (dis)integration of data from archaeology and geoscience. Whereas population dynamics and woodland decrease in the Congo basin are found to be related to early finds of iron furnaces (Marchant et al., 2018; Willis et al., 2004) and related to reconstructed soil erosion intensities (Bayon et al., 2012), others have stated that the archaeological low quantity of material and the vague chronology do not allow to reconstruct a direct relationship or are even contradictory (Maley et al., 2012; Neumann et al., 2012—see also Brncic et al. 2007). Other studies on the late Holocene rainforest crisis combine palynological and palaeohydrological data from lake sediments obtained from western Cameroon with local archaeological data bases to emphasize human triggers (including charcoal burning and iron smelting) of ecosystem changes (Garcin et al., 2018a,b,c). Nevertheless, chronological inconsistencies (i.e. a contradictory time lag) between geoscientific records and archaeological data in Central–Western Africa are observed; additionally, the scale of iron production is assessed as an insignificant driver of forest transition compared to climate changes (see Clist et al., 2018; Giresse et al., 2018; Lézine et al., 2013; Neumann et al., 2012—*contra*: Garcin et al., 2018b,c).

Remains of slag found in alluvial sediments clearly point to the connection between iron smelting and alluviation (e.g. Beckmann, 2007; Verstraeten et al., 2007).

Anthracological evidence

As pointed out by Eichhorn & Robion-Brunner (2017), anthracological studies (e.g. on charcoal found in slag heaps) enable to clarify the link between forest transformations and iron smelting, as they are directly linked to the metallurgical process. Charcoal assemblages from archaeological sites give mainly insights into species selection for smelting (Eichhorn & Robion-Brunner, 2017; Humphris & Eichhorn, 2019; Iles, 2014; Thompson & Young, 1999), e.g. due to the specific gravity, calorific potential, annual increment, ability to withstand coppicing, or even cultural value of some wood species. Charcoal species distributions from smelting can be very uniform, often less-diverse than charcoal assemblages from other, non-metallurgical, contexts (Humphris & Eichhorn, 2019; Thompson & Young, 1999), but can also be composed of various species (Nelle et al., 2013). Assemblages found in contexts related to iron smelting also allow for an assessment of wood availability (e.g. Warren et al., 2012); selection of previously unused species might indicate an overexploitation of the formerly main fuel wood species (Eichhorn et al., 2013a; Humphris & Eichhorn, 2019). Additionally, the use of only one fuel wood species for smelting may indicate continuous supply (Humphris & Eichhorn, 2019). Morphometrics of charcoal samples allow to reconstruct silvicultural practices, e.g. small diameter of wood may indicate coppicing or the use of branches from bigger trees (Nelle et al., 2013; Paradis-Grenouillet, 2012).

From *Etruria Mineraria* few anthracological studies are known. Sadori et al.'s study clearly indicates species selection for iron smelting in Follonica-Rondelli in the 6th and 5th century BCE (Sadori et al., 2010). In the context of an anthracological analysis, Carrari et al. (2017) describe the present forests in the area of *Etruria Mineraria* as 'metallurgical forest', following Paradis-Grenouillet's idea of the *«forêts métallurgiques»* and a *sylvofaciès charbonnés* (Paradis-Grenouillet, 2012, , *passim*).

Palynological evidence

Various authors relate the transition from forest cover to more open (wood) land as evident in pollen records from sediment archives to the onset or intensification of iron smelting (e.g. Lupo et al., 2015). Depending on the scale of the production, the impact may nevertheless be relatively small or of only local significance (Brumlich, 2018b; Crew & Mighall, 2013; Mighall et al., 2017; Mighall & Chambers, 1997). Myrstener et al. (2016) and Bindler et al. (2011) found evidence for increased charcoal fluxes into a lacustrine sediment sequence

after the establishment of an iron blast furnace in their study region, but concluded that the major changes in vegetation as seen in pollen diagrams are mostly related to settlement dynamics and not necessarily to iron processing. On the Tuscan mainland, a decline of arboreal pollen in (archaeo-)sediments and an increase in plants with high calorific value are linked to the use of wood fuel for metallurgy (Drescher-Schneider et al., 2007; Mariotti Lippi et al., 2000; Sadori et al., 2010; Williams, 2009; Wiman, 2013), although not reflected in all archives (Di Pasquale et al., 2014). (Limited) Palynological data from palaeo-lagoonal sediment sequences obtained from the coastal plains at Central Elba indicate that especially the proportion of *Quercus* pollen decreased and *Ericaceae* pollen concentrations increased in antiquity—Bertini et al. (2014) link this transformation to metallurgy. However, the transition to a more open landscape as evident in the published record started much earlier, possibly in the early Bronze Age. Furthermore, also *Ericaceae* spec. are suitable for charcoal burning and were commonly used in (Etruscan) blommeries in Follonica-Rondelli (Sadori et al., 2010).

2.3.3 Spatial organization

The spatial distribution of the smelting sites on Elba is a key aspect of the local *Iron landscape* (cf. Corretti, 1988; see Chapter 4). Whereas the iron ore deposits are located along a N–S stretch at the eastern coast of Elba, ancient (and medieval) smelting sites are distributed allover the island. The location of furnaces close to the coast is occasionally explained by the access to fuel wood (Jones, 1982). The transport of ore/fuel was also a site location factor for industrial iron production (Hartshorne, 1928; Isard, 1948). Hartshorne (1928) mentions a rule of thumb in economic geography that *iron comes to the coal*, because the mass of coal required to smelt one unit of ore is greater than 1; in his conclusions, Hartshorne argues that the rule of thumb is not true and often smelting sites are found in locations that are suitable for the shipping of coal. He additionally observes that a steel plant was build at a lake-side location to avoid trans-shipments from water to land.

Raab et al. (2017) observed that the distribution of charcoal hearths in Brandenburg, Germany, is strongly related to the availability of forests (and in their case also iron ore; cf. Foard, 2001). On Elba, the relationship between smelting sites and sites of charcoal production can be observed, albeit only true for medieval sites (Corretti, 1991; own observations at the Valle Nivera and Martella sites, September 2017). With the availability of high resolution elevation data, several studies focused the spatial distribution of charcoal (mound) kiln sites—and reveal a relationship between a high density of kiln sites and historical iron production sites (Raab et al., 2017, 2015; Rutkiewicz et al., 2019, 2017;

Schmidt et al., 2016), although the chronology of the kilns might not necessary coincide with iron production (Dupin et al., 2017). Using a combination of site densities and site chronology, the distribution of kiln sites near iron production sites may help to evaluate the impact of smelting on the forest cover (Raab et al., 2015). Scholars discussing the pattern of pre-industrial iron production sites also mention the need for hydropower and the change in the ore preference as site location factors (Cleere & Crossley, 1995; Pflug & Thalheim, 2014).

The spatial organization of the partial life cycle of iron smelting is important for fuel wood consumption. The main steps of iron production require fuel, either as wood or as charcoal; as iron ore was mainly extracted in open cast mining, no wood was required for the construction of adits etc. Fire setting for facilitating ore extraction might have been used. Assuming that the fuel production for the main steps of iron production took place in the vicinity of the production location, the spatial organization of the production clearly induced where fuel wood was extracted. If e.g. iron is smelted and further processed at one site, fuel for both production steps was to be extracted and produced in one area, whereas a spatial separation between smelting and post-reduction processing implies that felling of wood took likewise place at different locations. Several scenarios of the spatial organization are theoretically conceivable—see Figure 2.3 for some examples. For instance, Corretti (2017) proposes that the spatial organization of iron smelting on the island of Elba is mainly triggered by exploitation of fuel resources; other scholars argue that the system of transport of ore from Elba to Populonia is triggered by fuel availability (see Chapter 4 for details). This pattern changed through time. Also in other contexts, temporal variability of the spatial organization of smelting is observed (e.g. Bauvais & Fluzin, 2009). For instance, the pre-processing of the raw ore might have taken place at the mining site or at the smelting site, as described by Bauvais & Fluzin (2009) and Iles et al. (2018) for pre-industrial *African* smelting (and also by Hartshorne, 1928, for the modern steel industry).

The importance of the spatial organization of the production process is illustrated by figures on the fuel requirements for the different steps of production, although they are average values of few experimental data (see Case Study 4, Becker et al., submitted.a, Chapter 9, for a more detailed estimation of the fuel consumption for smelting). Pleiner (2000) reports the results of a successful experiment requiring 150 kg of logs to roast 185 kg of raw ore giving 174 kg of prepared ore. Rehder (2000) estimates that the total consumption of c 8 kg of charcal for the smelting and c 4 kg of charcoal for forging of 1 kg of a bloom; he assumes that the productivity of a charcoal kiln is .15 kg of charcoal per 1 kg of wood. According to the experimental data reported by Rehder (2000), the production of an average bloom required a charcoal charge of 3.16 kg (excluding pre-heating). An

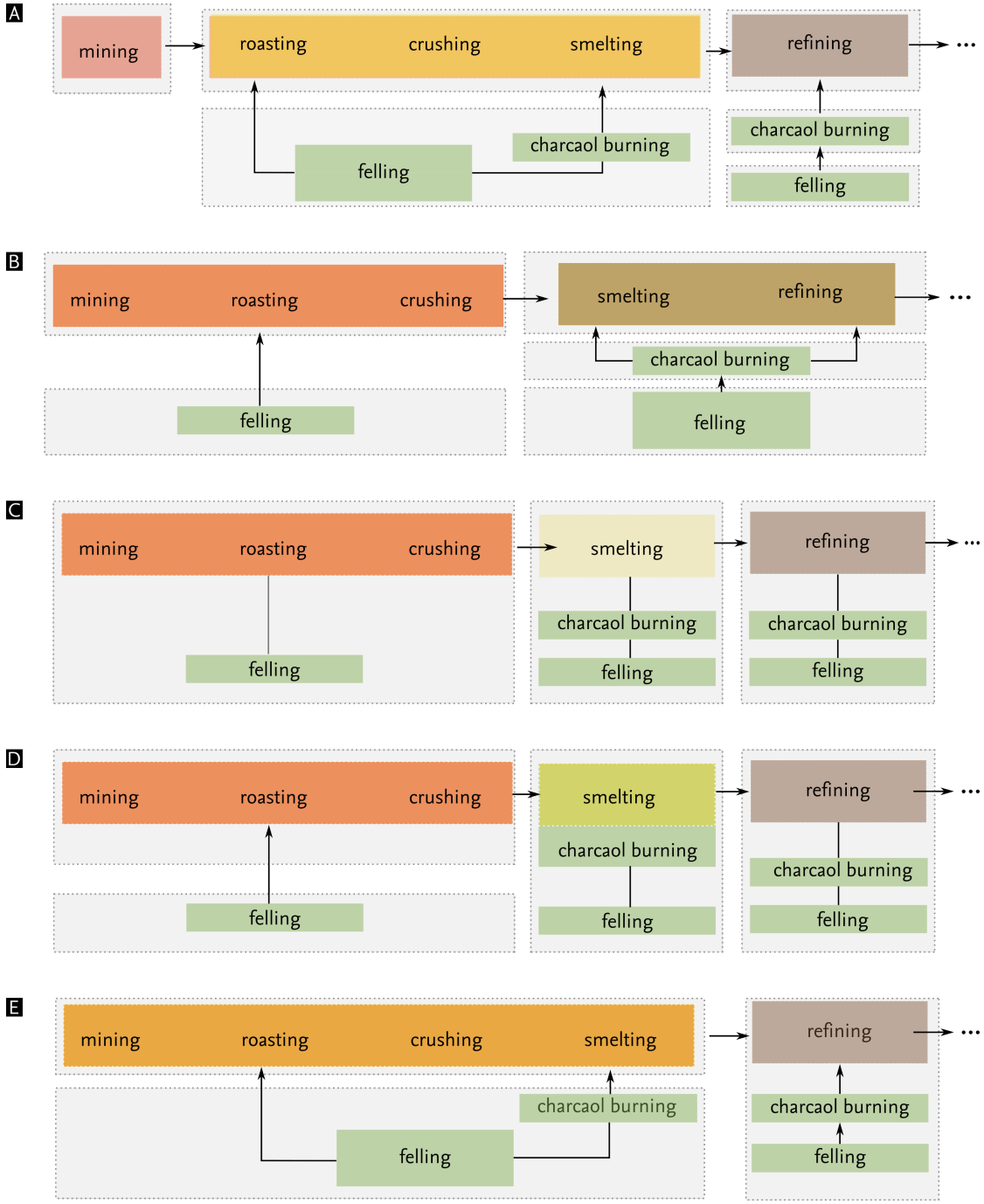

Figure 2.3 Theoretically conceived models of the spatial organization of iron production and the extraction of secondary resources. Dotted rectangles indicate production in close vicinity; arrows indicate transport to another site. In models A, B, C, and E, felling / charcoal burning is conducted in the hinterland of the sites. **A** Roasting and crushing are conducted near the smelting site (e.g. Nihlén, 1958, Campo al'Aia site; see Pleiner, 2000, p. 111). **B** Smelting and refining in the same location (Bauvais & Fluzin, 2009). **C** Extraction and dressing at the mining site, smelting, and refining are spatially separated (Bauvais & Fluzin, 2009). **D** as (C), but smelting and charcoal buring at the same site. **E** Mining, dressing, and smelting at the same site (e.g. the the smelting sites along the northeastern coast of Elba).

ore : charcoal ratio of 1 : 1 for the furnace charge is used in smelting experiments (Pleiner, 2000). Based on these ratios, a general rule of thumb can be formulated:

1 kg bloom →
c 3 kg of wood required for roasting;
c 27 kg of wood for required for smelting; and
c 53 kg of wood required for post-reduction processing
(in total c 83 kg of wood required for producing and processing 1 kg of bloom).

Thus, for fuel consumption, especially the locations of smelting sites and sites of post-reduction processing are important, whereas the requirements for roasting are comparably low.

As known from ethoarchaelogical research the spatial organization of iron smelting might not have been exclusively triggered by the requirement for fuel. Lyaya (2012) for example observed that for iron smelting activities in sub-Sahran Africa, moral considerations are a reason why smelting sites are not located near settlements, but smithing hearths are. For Tanzania, Iles et al. (2018) discuss several reasons for a spatial distinction between upland and lowland sites. The propose that ritual practices and the intensification of agriculture controlled the location of smelting sites there. Guillon et al. (2013) identified different levels of clustering of furnaces in southwestern Niger in the period between the 4th and 9th century CE, viz. complexes, sites, ensemble, batteries, and single furnace. Production on different spatial levels defined by Guillon et al. (2013) was controlled by different factors, including metallurgical traditions, environmental prerequisites, output, and social organization. For modern iron production, Hartshorne (1928) states that the distance to the markets of the products of iron production can also be a site location factor, albeit the location of fuel was a dominant factor also in the 20th century.

2.4 Legacy issues and emissions

The environmental impact of emissions from metal production on soil and sediment composition is studied on a meso- to macroscale in e.g. icecaps, peat bogs, or lake deposits and marine sediments (mainly airborne pollution; e.g. Bränvall et al., 2001; Elbaz-Poulichet et al., 2011; Hong et al., 1996; Renberg et al., 1994; Shotyk et al., 1998) and on a meso- to microscale in soil or allluvial archives (e.g. Brown et al., 2009; Dobler, 2001; Gäbler & Schneider, 2000; Grattan et al., 2013; Hürkamp et al., 2009; Hudson-Edwards et al., 1997; Raab et al., 2010). Most of these studies are related to base metal production. The impact of pre-industrial iron smelting is, however, rarely studied.

2.4.1 Iron smelting sites

In a study on a Roman Iron Age site in Silesia/Poland Thelemann (2016) analyzed soil and sediment samples from an archaeological profile and found some trace elements (Cr, Zn, Cu) to be relatively enriched; nevertheless, absolute values where low. Carey & Moles (2017) used multi-element data as a tool for geochemical prospection of an Iron Age site in Alderly Edge/UK and identified geochemical anomalies related to iron processing; especially Fe and Zn contents were increased. Pettersson et al. (2004) and Karlsson et al. (2016) studied the soil chemistry near Viking Age to medieval iron working sites in Sweden. Peat from a mire site at Åskagsberg did not show any significant enrichments of magnetic matters during the period of iron smelting synsedimentary to smelting activities (Pettersson et al., 2004), whereas soil chemistry at the bloomery site and the chemical composition of the lacustrine sediments at Ängersjö is different compared to the local background (Karlsson et al., 2016). The increase in trace metal contents was only clearly visible in the direct vicinity of the furnace location (distance <40 m). Similar to the case study of Thelemann (2016), the increase in Pb and Zn in soil samples is clearly recognizable, but values are low (< 26 mg/kg in soils). In lake sediments at Ängersjö deposited in the vicinity of a smelting site, Pb values are generally higher and show also a clear increase in Pb and Zn that coincides with a change in vegetation cover and the possible onset of iron production in this region.

2.4.2 Sediments

In samples taken from streambed sediments downstream of a blast furnace in Pennsylvania, increased concentrations of i.a. As, Co, Co, Fe, Pb, Mn, Hg, and Zn, were detected by Sloto & Reif (2011). These studies from Pennsylvania (Piatak & Seal II, 2012; Sloto, 2011; Sloto & Reif, 2011) clearly highlight a difference in the chemical composition of raw material (ore), by-products (slag), soils near the production site, and transported material mixed with 'uncontaminated' material (streambed sediments) (see Figure 2.4).

Several authors discuss legacy issues and emissions (indirectly) related to iron metallurgy on Elba and in Populonia. As stated above, the ancient author Diodorus of Sicily mentions the emission of smoke from the furnaces on Elba and explains that the Greek name of Elba—*Aitháleia*, the fuming one—derives from the smoke lying over the island. Vigliotti et al. (2003) analyzed physical and chemical data from marine sediment sequences obtained in the Corsica chanel. They report that an increase in the concentrations of Pb and As, as well as magnetic susceptibility, coincide with the development of the Etruscan–Roman metallurgy on Elba and in Populonia. Their data show a peak in Pb, Cu, and magnetic susceptibility during the heydays of iron production on Elba; with the

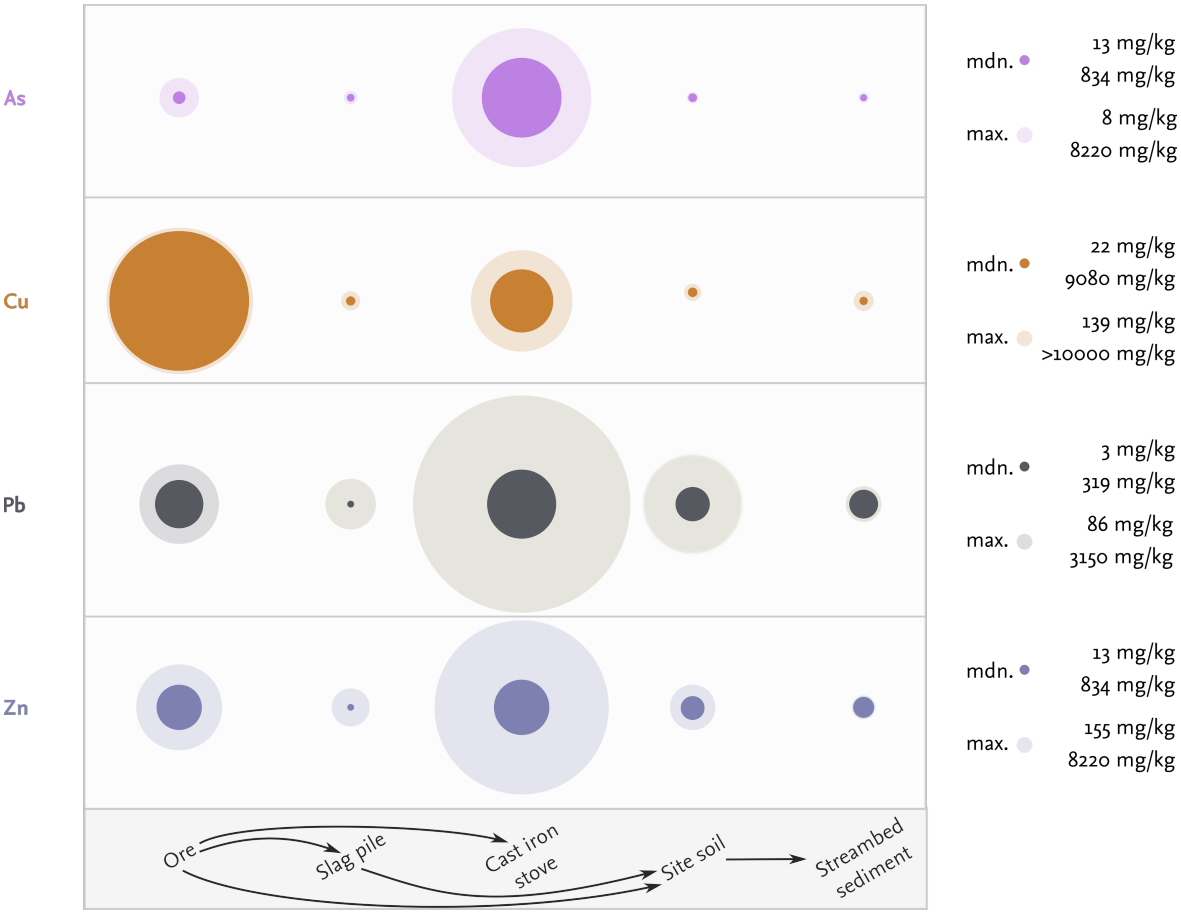

Figure 2.4 Element concentration measured near the Hopewell Blast Furnace in Pennsylvania. The area of the circles is proportional to the concentration; concentrations are scaled to unity graphic size of last lowest concentration per element. Data from Sloto & Reif, 2011.

abandonment of smelting on the island, emissions decreased and the attractiveness for recreation increased. Furthermore, Corretti & Firmati (2011) relate the construction of luxury *villae maritimae* in the 1st century BCE to the abandonment of smelting sites on Elba. They follow the argumentation that the emissions (and the noise) of the furnaces would have made Elba unattractive for recreational issues and that with the decrease of smelting, the attractiveness increased.

Geochemical anomalies in sea floor sediments obtained near Populonia are linked to Etruscan and Roman metallurgy (Leoni et al., 1991; Williams, 2009).[7] Additionally, several authors show that the spatial distribution of heavy metal contents in sea floor sediments around Elba is strongly linked to the ore deposits in eastern Elba (Dall'Aglio et al., 2001; Leoni & Sartori, 1997; Leoni et al., 1991).

Servida et al. (2009) and Servida (2009) document that the content of trace metals (i.a. Pb, Cu, Zn) in soils, waste rock and mine dump from the Valle Giove stope (Rio Mines) are

[7] See Case Study 1, Becker et al., 2019b, Chapter 6, for further discussion.

partly increased compared to reference values and exceed guideline levels. Pistelli et al. (2017) additionally show that As contents of soils in the Rialbano mines clearly exceed values from other parts of Elba; they found trace metal(loid) contents in plants growing in the mining area to be significantly increase, although the bioavailability is relatively low. The mentioned studies are directly related to modern mining; ancient pits were further mined, enlarged and deepened during the modern mining period; pre-industrial overburden—still visible in the 19th century (Krantz, 1841)—was removed. Therefore, traces of ancient and medieval mining on Elba got lost and the environmental impact of mining in the mines cannot be studied anymore.

The environmental impact directly related to (ancient) iron smelting is analyzed in the context of strongly increased As contents in alluvial sediments of the Pecora river located on the Tuscan mainland (see e.g. Costagliola et al., 2008; Donati et al., 2004, 2005). Costagliola et al. (2008) discuss the contribution of iron smelting to the geochemical anomalies and state that the As contents in ancient iron slags are very low; also the emissions from smelting might not explain the increased As contents of topsoils in the Pecora area.

2.4.3 Metallurgical remains

Piatak & Seal II (2012) conclude that slags from the Hopewell furnace contain 'potentially problematic' concentrations of As, Al, Co, Fe, and Mn; additionally Cu-contents (but not As) in leachates from experiments also exceed guideline values. In the magnetite ores sampled from deposits around the Hopewell site, concentrations of As, Cd, Co, Cu, Mn, Ni, Pb, and Zn are significantly enriched. The importance of the type of furnace (bloomery or blast furnace, steel production) for the composition of slag is compiled in a review on the *environmental aspects of slag* (Piatak et al., 2015). Contents of As, Cr, and Mn are evaluated as being of environmental concern in most slag samples, whereas Co and Pb are only partially important. Cr contents are especially enriched in steel-making slag. Although Cu contents of iron slag are not of environmental concern, the review points out that Cu contents are higher in older slags, as it is the case for Pb-contents. Piatak et al. (2015) conclude that the environmental impact of historical iron slag is limited; in contrast, the impact of steel-making slag may be much higher. In leachates from steel-making slags, especially concentrations of Cr and Mn are increased (Piatak et al., 2015).

There is a clear difference between the chemical composition of ore as a primary resource of smelting and slag, (cast) iron, and soils and sediments from the environs of a smelting site (Sloto & Reif, 2011; see Figure 2.4). The chemical differences between metallurgical

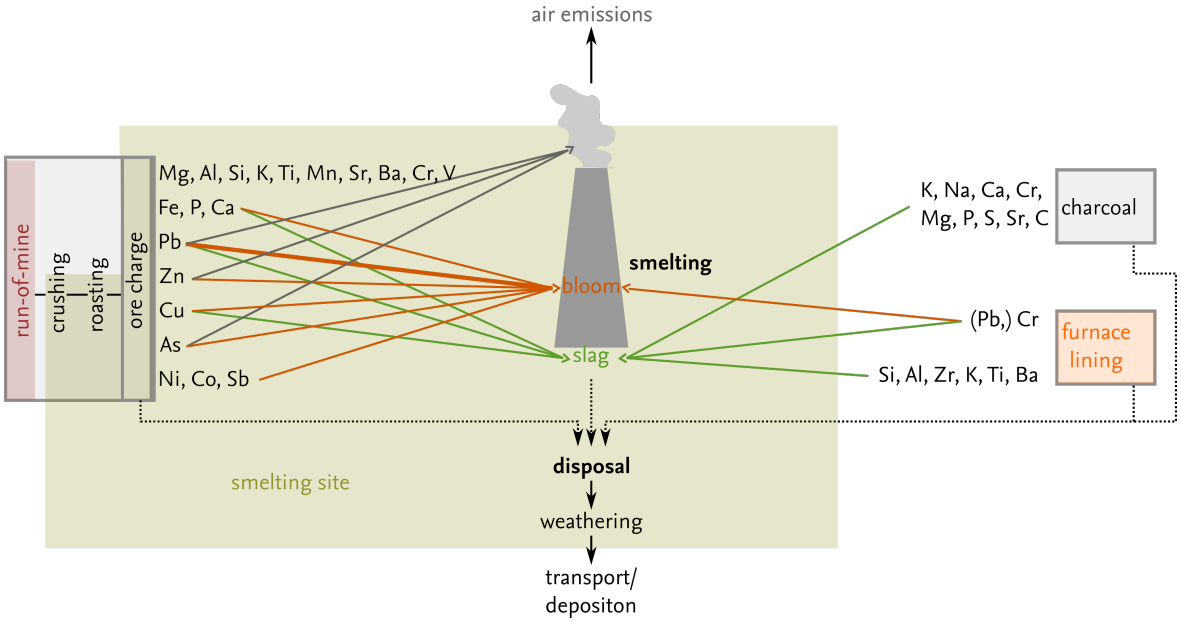

Figure 2.5 Partitioning and of elements during the reduction in a bloomery furnace and the contribution of different materials involved in the bloomery process to the composition of slag. Illustration after data from Benvenuti et al., 2016; Brauns et al., 2013; Charlton et al., 2010; Senn et al., 2010; Serneels & Crew, 1997.

remains and soils/sediments are mainly explained by selective transport and dilution. The difference between the trace element composition of ore and slag is mainly explained by partitioning during the smelting process, as shown in smelting experiments (Benvenuti et al., 2016; Brauns et al., 2013; Senn et al., 2010; Serneels & Crew, 1997). Siderophil elements (Co, Ni, Cu, As and Sb) are partly reduced during the smelting process and tend to be enriched in bloom relative to slag, whereas lithophil elements (e.g. Na, Mg, Al, Si, Ti) are enriched in slag (Figure 2.5). Depending on thermodynamic conditions, some other elements like V, Cr, or Mn are partly reduced and partly segregated to the slag; volatile elements (As, Sb) are additionally volatilized (see also Charlton, 2015).

Besides the difference in the composition of varous archaemetallurgical remains, also the type of ore and the association of iron with mineralization of other metals affect the composition of iron ores. Consequently, the potential emissions from iron smelting depend on the characteristics of the iron ore deposit. As visible in data from Benvenuti et al. (2013), e.g. Pb and Cu contents of goethite-rich ores from Italy and Central–Northern Europe are significantly higher than in hematite-rich ore from the same regions (Pb, goethite: $Mdn. = 127\,\mathrm{mg/kg}$, $IQR = 196 - 22\,\mathrm{mg/kg}$; Pb, hematite: $Mdn. = 1.6\,\mathrm{mg/kg}$, $IQR = 3.75 - 0.5\,\mathrm{mg/kg}$), although some local exceptions are known—such as gossans in Cornwall, U.K., where Pb contents of hematite deposits exceed 200 mg/kg; and in the Schwarzenberg ore bodies (Ore Mountains, Germany), where hematite is found in Fe–Cu–Pb–Zn mineralizations (Benvenuti et al., 2013). The concentrations of e.g. As in slags

from different fuel types (charcoal or anthracite) aslo differs. Higher concentrations in the slags from the charocal-fired furnace compared to a coal-fired furnace may be explained by differences in the ore used and the chemical processes during smelting (Piatak & Seal II, 2012).

3 Study area: Elba Island

Elba Island *(Isola d'Elba)* is the largest island of the Tuscan archipelago and located in the northern Tyrrhenian Sea (Italy, Western basin of the Mediterranean Sea)—between the Apennine peninsula to the east (Canale di Piombino) and the island of Corsica to the west (Canale di Corsica; see Figures 1.1 and 3.1). Pisa (Torre) is c 95 km north of Elba and Rom (Termini) c 193 km south of Elba. The island covers an area of 224 km^2 and stretches c 27 km from west to east (Punta Nera–Capo D'Arco; 42°45'58.6"N, 10°06'08.9"E and 42°46'41.5"N, 10°26'06.8"E, respectively) and c 18 km from north to south (Capo Vita–Punta dei Ripalti; 42°52'22.6"N, 10°24'45.0"E and 42°42'27.3"N, 10°25'11.6"E, respectively). The length of the coastline is c 147 km. The highest peak is Monte Capanne with an elevation of 1019 m a.s.l. (in 3.9 km linear distance from the shoreline at Spiagga di La Cala).

Politically, Elba is part of the region of Tuscany *(Regione Toscana)* and the province of Leghorn/Livorno *(Provinica di Livorno)*. The island is divided into seven municipalities *(Comuni)* and counts a total (permanent) population of slightly above 30 000. The main villages on Elba are Portoferraio (c 8 300 inhabitants), Capoliveri (c 3 700), Marciana Marina (c 2 000), and Rio Marina (c 1 200).

3.1 Geology and geomorphology

Geologically, Elba is part of the Appenin peninsula and Corsica and represents the south-westernmost outcrop of the Northern Apennines (Frisch et al., 2008). The tectonic units found on Elba are part of the Adriatic continental margin (Tuscan Domain) and the (Alpine) Tethys oceanic realm (Ligurian Domain; Carmignani et al., 2013).

The Tuscan Domain constitutes the western margin of the Adriatic microplate (Carmignani et al., 2013), which was still part of the African plate during the Paleozoic. The oldest rocks

on Elba formed during the Precambrian–Paleozoic on the continental margin. They are part of the Monte Calamita Complex, which mainly consists of phyllites with metasandstones and micaschists (Principi et al., 2015). The Monte Calamita Complex was exposed to metamorphism during the Hercynian (Variscan) orogeny (Frisch et al., 2008). After the period of the Hercynian orogeny, layers of terrestrial and marine clastic sediments were deposited in shallow water on top of the basement (Tuscan Domain). From bottom to top, the sedimentary rocks of the (metamorphic) Tuscan Domain include the Late Carbonian–Early Permian Rio Marina graphitic phylittes and Middle–Late Trisassic Monte Serra Quartzites (Frisch et al., 2008; Principi et al., 2015).

From the Late Triassic to the Early Cretaceous, the Tuscan Domain is shaped by pelagic sedimentation on the passive continental margin (Frisch et al., 2008). Bedrock includes crystalline limestones, dolostones, marlstones, calcarenites, and calciutites; Late Cretaceous slates and siltstones of the Cavo Formation; and Cretatceous–Tertiary Porticciolo Phylittes and Metasiltstones (Principi et al., 2015). Occassionally, the sediments are interlayered by Permian magmatites (Ortano porphyroid). The upper part of the Tuscan Domain is made up of Oligocene graded metagrayvakes (*Pseudomacigno*; Principi et al., 2015).

The Ligurian Domain is characterized by ophiolithic sequences (see Bortolotti et al., 2001). The Middle Jurrasic crystalline oceanic basement is formed by the rocks of the lithospheric mantle (Serpentinites and Ohicalcites), plutonic rocks (Gabbro), sheeted dyke complexes, and (pillow lava) basalts (Principi et al., 2015). The gravelly–clayish sea floor sediments of the Ligurian formations were mainly deposited during the middle Jurrassic– early Cretaceous and are over-layered by late Cretaceous and middle Eocene Flysch. The Ligurian sedimentary rocks are mainly early–late Cretaceous Palombini shales overlying early Cretaceous Capionelle Limestones and late Jurassic–early Cretaceous Monte Alpe cherts (red radiolarties).

3.1.1 Tectonic evolution of Elba

The tectonic evolution of Elba is marked by the convergence of the African and European plate since the Late Cretaceous and the development of a subduction zone of the oceanic litosphere under the Corsica–Sardinia continental margin (Bortolotti et al., 2015). During the Alpine orogeny (Apenninic event) in the Late Oligocene and Early Miocene the Ligurian complex obducted the Tuscan units and was subducted under Corsica; the Tuscan units were metamorphosed and nappes formed (Frisch et al., 2008).

The emergence of Elba is mainly caused by compressional events during subduction that led to the collision of the Apulian Plate and Corsica, the subsequent splitting of the

lithospheric upper mantle, the raise of the nappe, and the movement of the lithosphere–asthenosphere boundary (Frisch et al., 2008). This processes led to the melting of the mantle and parts of the crust and finally to the late Miocene magmatism (Bortolotti et al., 2015), which mainly shaped Elba's present occurrence due to folding during the intrusion of the Monte Capanne pluton and subsequent slipping along thrust faults (Frisch et al., 2008). During magmatism, contact metamorphism occurred.

3.1.2 Structural geomorphology

Elba is characterized by a diverse topography that originates from the tecto-stratigraphic structure. Typically, four main geomorphological zones on Elba are identified viz. western Elba dominated by the Monte Capanne massif, central Elba with the major alluvial plains, northeastern Elba, and the Calamita peninsula in the south-east (D'Orefice et al., 2009). The geomorphological zones correspond more or less to the nine tectonic units defined by Bortolotti et al. (2015).

Monte Capanne massif

The mountainous western part of Elba Island is dominated by the Monte Capanne massif that formed during the Late Miocene magmatism when a pluton intruded in the formations of the Ligurian Domain. The pluton has a typical hemispherical dome shape (Bortolotti et al., 2015). The highest peak reaches an elevation of 1018 m a.s.l.(Monte Capanne); other dominant summits are Monte Giove (853 m asl) and Monte Perone (630 m asl). The topographic isolation of Monte Capanne is c 60 km (nearest higher mountain: Monte Stello, Cap Corse).

As a consequence of the intrusion of the Monte Capanne pluton, the Middle Jurassic–Late Cretaceos ophiolithic (pseudo-)sequences slipped of the Procchio Border fault (Frisch et al., 2008). The oliolithic rocks are characterized by basal serpentinites, Palombini shales, and radiolarites (Polveraia-Fetovaia tectonic unit), which crop out at the margin of the Monte Capanne massif, along the coast between Fetovaia and Pomonte, between Chiessi and Punta di Polveraia and along the lower eastern slope of the Monte Capanne massif around the villages of Sant'Ilario and San Piero (see Principi et al., 2015). Basalt is almost exclusively found in the area of Marciana Marina (Frisch et al., 2008). A remarkable gabbro outcrop is found on the Fetovaia peninsula (Frisch et al., 2008).

The coast around the Monte Capanne massif is characterized by steep cliffs, especially on the western coast between Sedia di Napoleone and Punte Nera; rock-fall deposits are common in front of the retreating cliffs (Bortolotti et al., 2015, see also Bowman et al.,

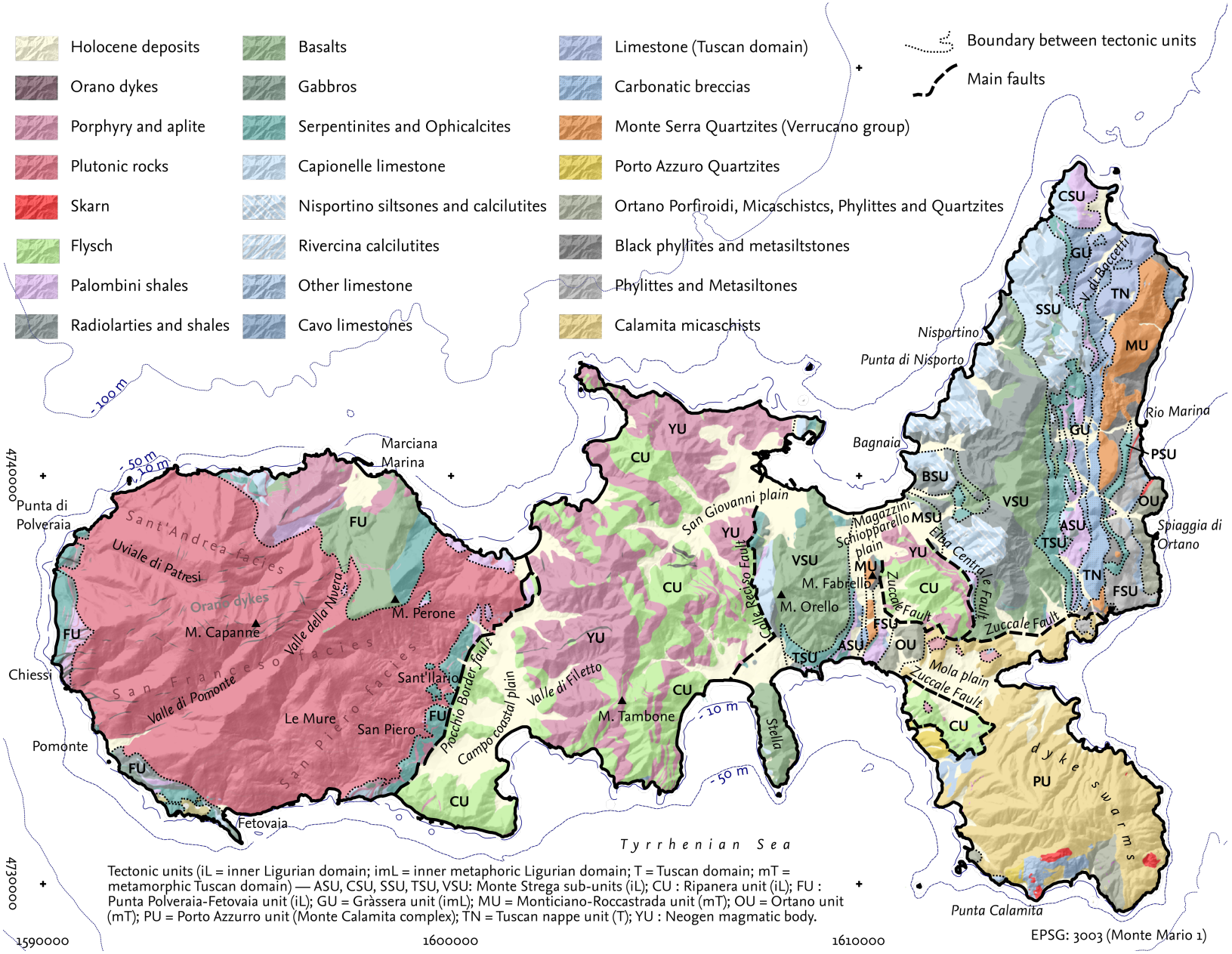

Figure 3.1 Lithology and tectonic units on Elba Island. Bathymetric lines are shown. Capital letters indicate different tectonic units. Database: Regione Toscana, 2014; Principi et al., 2015; Service Hydrographique et Oceanographique de la Marine, 2014 partly summarized.

(a) Western Elba (Marciana Maritima, Marciana, Poggio), Central Elba (Golfi di Biodola and Procchio), and northeastern Elba and the Calamita peninsula. View from Monte Giove in western direction (April 2016).

(b) Bagnaia, the Rada di Portoferraio and the Schiopparello–Magazzini plain, the hills of Central Elba and Portoferraio, and the M. Capanne massif (fore- to background). View from M. Capanello in western direction (August 2015).

(c) Rio Marina, Monte Fico, Ortano valley, and Monte Arco (from left to right); the Italian mainland in the background. View from Cima del Monte in eastern direction (August 2015).

(d) Il Volterraio, Cima del Monte, and Il Sassi Tedeschi (from left to right). The Valle del Frasso in the foreground. View from Monte Capanello in southern direction (August 2015).

Figure 3.2 Landscapes on Elba Island. Please note the transition between the steep rocky outcrops of the Middle Jurassic basalt and radiolarite in the Volterraio subunit (M. Strega unit) in subfigure **(c)**. Image credit (a): Raphael A. Eser.

2014). Sandy beaches mainly occur in the major inlets (e.g. Fetovaia, Seccheto). Gravel beaches are common in small inlets along the cliff coast (e.g. Le Tombe) and at the mouth of the main river valleys (e.g. Redinoce, Pomonte).

The Monte Capanne massif is divided in two regions along the Pomonte–Procchio line (Dini et al., 2008). The southwest–northeastern section of western Elba is characterized by steep slopes and deep straight, fracture-controlled valleys (e.g. the Valle di Pomonte, the Uviale di Patresi valley, or the Fosso della Gneccarin / Fosso di Chiessi valley). The rivers have only a few, mainly first or second order tributaries and are incised along brittle lineations (cooling fractures), dykes (swarms) and secondary thrusts (cf. Aringoli et al., 2009; D'Orefice & Graciotti, 2018). The tributaries are, compared to the main creek, far less pronouncedly incised. The straight river nets are mainly found in the Sant'Andrea and San Francesco facies (Figure 3.1). In the northern section of western Elba, the

same structural–morphological pattern can be observed, although straight, deeply incised valleys are limited to the parts of the rivers flowing through plutonic bedrock (e.g. Valle della Nivera, Figure 3.1).

The difference in river net geometries corresponds to the distribution of different tectonic facies (see Farina, 2008; Principi et al., 2015). The east–southeastern section of western Elba (the plutonic area east of the Pietra Murata ridge and south–east of Mt. Perone) is mainly made up of San Piero facies and a dominantly transverse stream pattern (see Twidale & Romani, 2005). Major rivers follow or cut contour-parallel lineations (see Principi et al., 2015 and Figures 3.1 and 3.3; mainly due to the general slope of the land surface). Valleys are poorly incised; the average terrain slope in the east–southeastern section of western Elba is less steep than the terrain slope in the southwest–northeastern section (Aringoli et al., 2009, cf.). The difference in relief characteristics between the two sections of the Monte Capanne massif may also be due to the differences in weatherability of the inner and outer part of the magmatic bodies (see Dini et al., 2008; Westerman et al., 2004). These differences in weatherability (grussification) and (subsequent) erosion in the facies may be explained by different exposure times (subsequent magma batches), mineral composition (biotite/K-feldspars), and abundance of megacyrsts (see Dini et al., 2008; Farina, 2008; Gagnevin et al., 2008; Pye, 1986; Westerman et al., 2004). Furthermore, laccoliths and pre-intrusive units were detached along the décollement surface of the southeastern part of the Monte Capanne pluton (Dini et al., 2008).

Longitudinal creek profiles (channel slopes) in the south-eastern part of the Monte Capanne massif are characterized by two knick points, which are related to variance in lithology, particularly to the transition from monzogranitic to ophiolitic bedrock to alluvial deposits. One of the two knick points in the longitudinal profiles of the creeks is less prominently developed in the northeastern and western part of West Elba.

Typical small landforms found in western Elba are tors, granitic blocks, tafonis, flat slopes along sheet joints, and exfoliation domes (Aringoli et al., 2009). The development of this small landforms is related to distance from sea (sea spray) and micro-climate (effect on weathering).

Only the lower reaches of the main valleys in West Elba are filled with alluvial sediments, e.g. in Marciana Marina, in Pomonte or Fetovaia. The main portion of the late Pleistocene–Holocene sediment cover in western Elba are slope deposits along the river valleys or on the northern flank of Monte Capanne; and mass-movement deposits that occur mainly in the area between Marciana Marina and Monte Capanne (see D'Orefice & Graciotti, 2018), due to the higher availability of moisture (see Section 3.2). Additionally, the local orientation of fractures and a colder Pleistocene climate might have triggered the formation of debris (Aringoli et al., 2009). The debris bodies are cut by fluvial erosion.

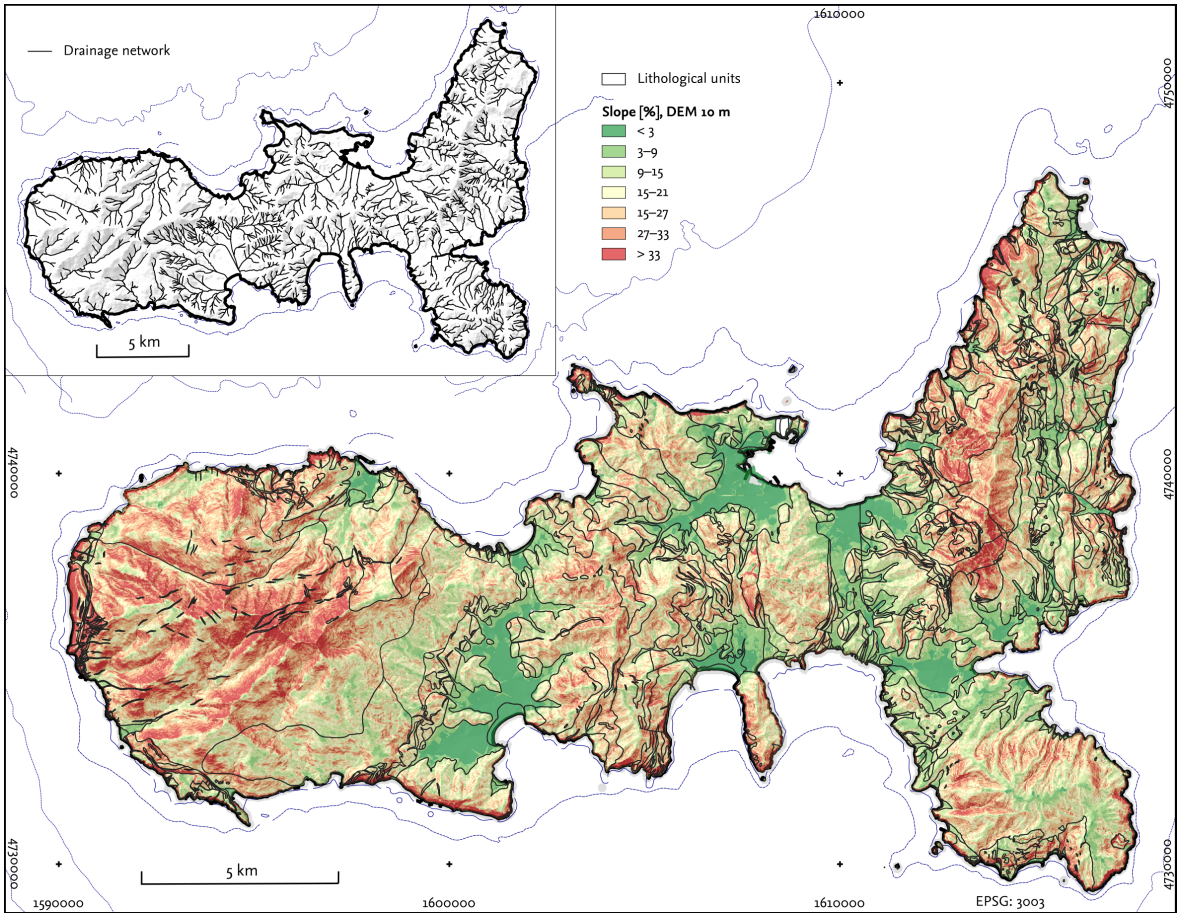

Figure 3.3 Slope inclination and drainage network on Elba island. The boundaries of the lithological units are shown; for details on the units see Figure 3.1. The slope classes are equally spaced and stretched to the histogram of the data set. Database: Regione Toscana, 2014.

Central Elba

Central Elba (i.e. Elba east of the Procchio border fault and west of the Elba Centrale fault, Figure 3.1) is characterized by rolling hills and alluvial plains, viz. the Campo plain, the San Giovanni plain (including the lower reach of the Fosso di Mandonina), and the Schiopparello–Magazzini plain (from west to east). Pleistocene alluvial fans are found on the alluvial plain in the valleys of the large creeks (Valle di Filetto, Valle del Fosso della Madonnina). The highest summit is the Monte Tambone (378 m a.s.l.); several other peaks reach elevations above 300 m a.s.l.The tectonic setting is marked by the Ripanera unit in the western and eastern section of central Elba and several units of the inner and metamorphosed Ligurian Domain.

The alluvial plains are located along the major thrust, detachment, and border faults (Figure 3.1, see Westerman et al., 2004). The mountain ridge in the east (M. Tambone) runs in in south–northern direction (M. S. Martino–M. Pericoli–M. Poppe); it is more pronounced south of Serbatoio (378–255 m a.s.l., Passo di Monumento) compared to the

northern part (up to 256 m asl, Serrone delle Cime). The main pass between west and central Elba is located at Serbatoio (134 m a.s.l.). Another mount range runs from Monte San Martino (368 m a.s.l.) in eastern direction to Monte Moncione (283 m a.s.l.).

The most important tectonic unit is the Monte Serra subunit (M. Strega unit), which is dominated by outcropping basalt that makes up the Monte Orello area (376 m a.s.l.); other ophiolitic rocks found in the area are i.a. Capionelle limestone and serpentinite. Monte Orello is divided from the main west-east running ridge by the Colle Reciso mountain pass (200 m a.s.l.), which intermittently played an important role as a nucleus of human activities since the Eneolithic (see Section 3.5 and Pagliantini, 2014). The ophiolitic (pseudo-) sequence of the M. Strega tectonic units can also be found in northeastern Elba and is divided form Central Elba by the Zuccalle Fault and the Elba Centrale Fault. The Stella peninsula is made up of Middle–Late Jurassic basalts (see Figure 3.1).

The Ripanera unit is characterized by Early-Late Cretaceous Flysch sequences of the Marina di Campo formation (turbiditic limestones, calcarenites and sandstones, see Principi et al., 2015). Flysch is especially found west and south of the Campo coastal plain and south of the San Giovanni and Magazzini–Schiopparello plains. During Miocene magmatism, prior to the intrusion of the Monte Capanne pluton, christmas-tree like laccolithes intruded into the Flysch sequence (Westerman et al., 2004). These crop out alternately with the Flysch units. The older (8 Ma) monzo–sienogranitic Portoferraio Porphyry is mainly found in the northern part of central Elba, whereas the monzogranitic San Martino Porthyry crop out west of the north–south striking ridge of Central Elba. Compared to the valleys in the ophiolitic units in Central Elba, the valleys in the Flysch-Laccolith units are more deeply incised and slopes are steeper. The drainage network in the western Laccolith unit is denser than the drainage network in the Flysch units (see Figures 3.1 and 3.3). In the La Crocetta mine at the Elba Centrale Fault, *Eurite* (i.e. a porphyritic aplite enriched in potassium that is used in the ceramic industry) is extracted (Maineri et al., 2003).

A prominent hill in Central Elba is Monte Fabrello (183 m a.s.l.), that belongs to a north–south running stripe of the Monticiano-Roccastrada tectonic unit and is made up of Quartzites of the Verrucano group and phylittes of the Rio Marina Formation. Monte Fabrello was occasionally occupied by humans since the Bronze Age.

Several occurrences of copper ores are known from Elba (Tanelli et al., 2001). The most important deposits that coincide with Bronze Age–Iron Age hoard finds (Chiarantini et al., 2018) are located in Central Elba. The deposits are located in the ophiolitic host rocks east of the Colle Reciso fault (M. Orello area).

Long sandy beaches (e.g. in Lacona and Marina di Campo) are found in the bays of Central Elba, as well as steep cliff coasts (e.g. Il Sotto Bomba on the northern coast).

Calamita peninsula

The Calamita peninsula (i.e. south eastern Elba south of the Zuccale Fault) is mainly made up of the Monte Calamita Complex (Figure 3.1, Porto Azzurro tectonic unit, metamorphic Tuscan Domain) that is characterized by outcropping Precambrian–Paleozoic (quartzitic) phyllites and metasandstones (Principi et al., 2015). Especially in the southern part of the Calamita peninsular, also metagraywackes occur. The mines at Punta Calamita, Ginevro, and Sassi Neri were extracted for magnetite (Tanelli et al., 2001); iron skarns are known that formed by thermometamorphism during the intrusion of the Porto Azzurro pluton (Frisch et al., 2008).

The Calamita peninsula is more or less single-peaked (the highest elevation is Monte Calamita, 412 m a.s.l.) and characterized by plateau-like higher elevations above 350–300 m a.s.l., that slightly decrease from Monte Calamita to Poggio Fino in eastern direction (307 m a.s.l.).

Geomorphologically, the peninsula is divided in two zones. On the northeastern section, dyke swarms related to the Miocene Porto Azzurro pluton dominate (Principi et al., 2015) and fostered the incision of valleys (cf. Goudie, 2013). Here, the drainage network is characterized by parallel creeks. In the southern and northwestern section, Triassic dolostones and marbles, along with flysch, crop out. Here, the drainage network is rather dentritic and less dense; valleys are wider (Figure 3.3). The monzogranite of the Porto Azzurro pluton crops out in small areas northwest of the Mola plain.

Northeastern Elba

Northeastern Elba is divided in three main parts, which are located west, east, and north of the main ridge, which runs from Monte Castello (389 m a.s.l.) in the south to Monte Serra (421 m a.s.l.) in the north. The highest elevation along the ridge and in northeastern Elba is Cima del Monte (515 m a.s.l.). Hills in the northernmost part of northeastern Elba are rolling, except to Monte Grosso (344 m a.s.l.) close to the shoreline. Morphologically, the area east of Monte Castello belongs also to northeastern Elba, but is tectonically a part of central Elba.

Tectonically and lithologically, northeastern Elba is the most complex part of Elba (see Figure 3.1). The area is characterized by several north–east striking faults and the narrow spatially succession of several (pre-intrusive) tectonic units from both Ligurian ophiolithes and Tuscan Domain (Principi et al., 2015); from west (Punta di Nisporto) to east (Spiaggia di Ortano) this includes

the limestones, radiolarites, basalts, gabbros, and serpentinites of the Monte Strega tectonic unit;

the slates and siltones of the metamorphic Ligurian Domain (Cavo Fromation), tectonic carbonatic breccias and metamorphic rocks (i.a. Verrucano quartzites and Rio Marina phylittes) of the Tuscan Domain;

metamorphic Ligurian phylittes and marbles; and quartzites, phylittes, schists, and porphyroides of the Ortano unit (metamorphic Tuscan domain; see Principi et al., 2015).

The ophiolithic (pseudo-) sequence covers more or less the complete area west of the main ridge in east Elba and also the high elevated parts of the eastern flank of northeastern Elba. The ridge between Cima del Monte and Monte Strega is mainly made up of basalt and radiolarites; whereas the less pronounced northermost (Monte Serra) and southermost (Monte Castello) part of the ridge are mainly made up of Capionelle limestone. The slopes of Monte Serra and Monte Castello are less steep and valleys are more incised compared to the slopes of e.g. Cima del Monte and Monte Serra. The formation of hogbacks at e.g. Monte Castello is related to the resistance of the radiolaritic cherts and the inclination of the structural units.

Valleys west of the ridge are mainly V-shaped with creeks flowing in western direction. Incision, channel slope, and river net density is higher in areas with radiolarite outcropping compared to regions with basaltic bedrock (Figure 3.3). In the lower course of the creeks, the valleys cut into limestone formations and are relatively wide (location of the villages of Nisportino, Nisporto, and Bagnaia). Pocket beaches with pronounced headland developed (see Bowman et al., 2014). The relief linearly falls from the highest elevations above 340 m a.s.l. to the coast. Locally, thick beds of radiolaritic cherts can be observed that exceed the typical sedimentation rate on the sea-floor. The thickness of the bed originate from redepositioning of Radiolaria in turbidity currents (Frisch et al., 2008).

Directly east of the ridge, the relief is relatively steep. In area with radiolaritic (and carbonatic) bedrock, creeks cut a dense net of incised valleys, whereas in basalt the channel network is less dense and less incised. East of the basalt unit, slopes are far less steep. The relief on the eastern side of the main ridge is less constant compared to the western part and several rolling hills interrupt the decrease in elevation from the ridge to the coast. Plateau-like areas between the main ridge and the coastal hills lay around c 160 m a.s.l. and are intensively used for agriculture since the Middle Ages (cf. Foggi et al., 2006a). Here, bedrock is mainly Palomini shale and Cavo siltstones. The hills and crests formed in relation to variation in rock resistability and faults, e.g. a small layer of radiolarite at San Felo (197 m a.s.l.). The peak of the coastal hills (Torre del

Giove, Monte Fico, and Monte Arco; 350, 266, and 277 m a.s.l., respectively) are made up of quartzites and phyllites (and partly of calcicutites) of the Tuscan Domain, whereas the relatively gentle parts between the hills and the northeastern ridge are made up of Palombini shales, serpentinites, and lime and siltstones of the Ligurian Domain. Small crests in the upper Ligurian Domain in the rolling hills east of the ridge are limited to the serpentinitic bedrock and small outcrops of Capionelle limestone and radiolarite. River valleys are less incised compared to the western section (few outcrops of radiolaritic cherts), wide and even less incised in the shale/siltstone units. Channel slope of the Ortano and the Rio is low compared to the other valleys east and west of the main ridge of central Elba in the parts running through the metamorphic Tuscan units (Quartzies, phylittes). Several iron ore deposits are located in northeastern Elba; they are mainly hosted in the quartzite formations of the Verrucano group and the phylittes of the Rio Marina formation (e.g. Tanelli et al., 2001).

The northernmost section of northeastern Elba (north of M. Serra) is mainly made up of Ligurian and Tuscan limestone and occasional Palombini shales. The relief is characterized by rolling hills. The prominent peak of the Monte Grosso is made up of Capionelle limestone of the Ligurian Domain. The main valley in this part of Elba is the Valle di Baccetti, that has a relatively low channel slope, is narrow, and filled with a thick sediment sequence.

3.2 Climate and hydrology

Climate

The climate of Elba Island is hot-dry Mediterranean (*Csa*-climate after the classification of Köppen–Geiger). The annual temperature averages 14.2 °C; annual precipitation totals 679 mm on average with strong seasonality and maximum rainfall amounts during autumn (Monte Calamita, 397 m a.s.l., 1961–1990 normal period, Aeronautica Militare – Servizio Meteorologico). Because Elba is characterized by a pronounced relief, the meso-climate on Elba follows an orographic gradient and is strongly influenced by exposition (Figure 3.4). Following Foggi et al. (2006a), humidity on Elba (mesothermal province; Thronthwaite–Mather classification) ranges from dry sub-humid with negligible winter surplus (e.g. Portoferraio, 20 m a.s.l., 576 mm/a) over dry sub-humid with a normal winter surplus (e.g. San Piero in Campo, 226 m a.s.l., 689 mm/a, 15.,4 °C) to moist sub-humid (Monte Grosso, 348 m a.s.l., 778 mm/a, 14.6 °C) and humid with normal winter surplus (Poggio, m a.s.l., 1010 mm/a, 15.8 °C). Maximum average annual rainfall on Elba occurs on the elevated parts of the northern flanks of the Monte Capanne massif; above c 320 m a.s.l.,

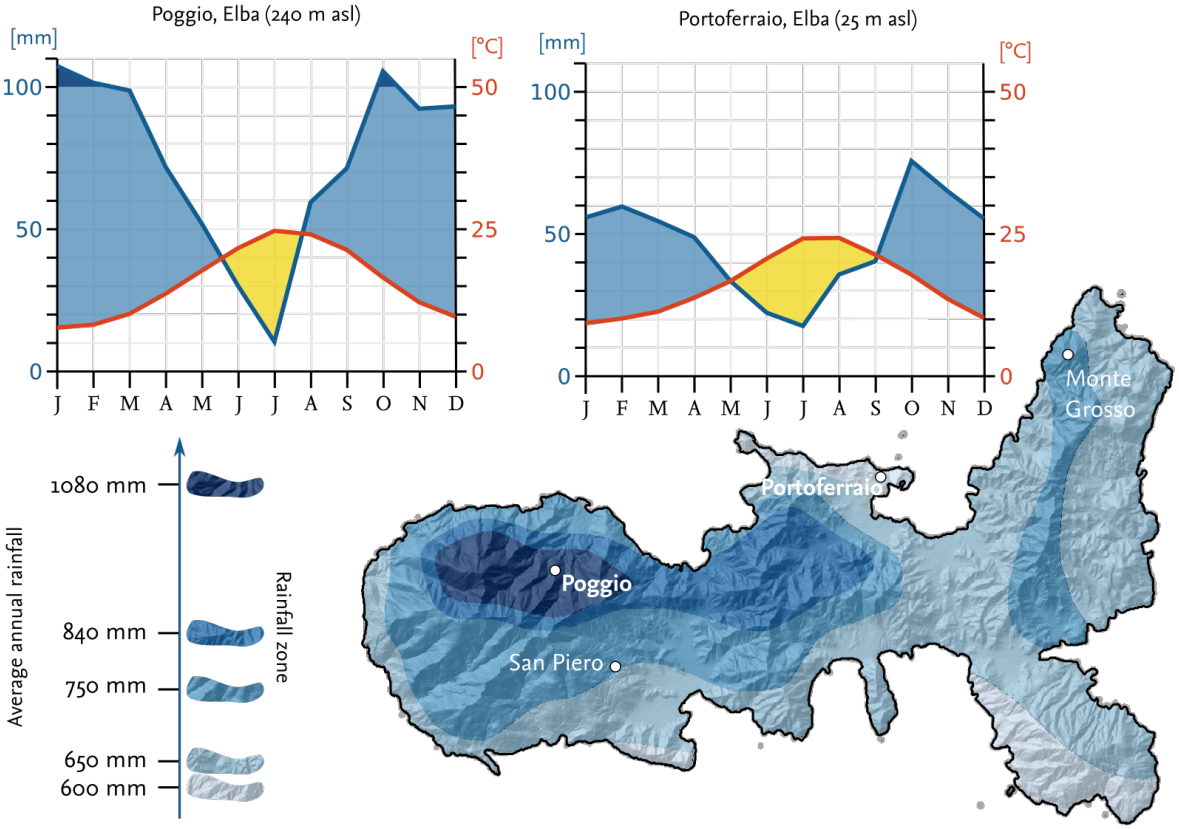

Figure 3.4 Spatial rainfall pattern and temporal distribution of temperature and rainfall. Database: Bencini et al., 1986; Foggi et al., 2006a.

annual precipitation is >1000 mm in average (equations in Foggi et al., 2006a, see Bencini et al., 1986). Most of the area of Elba island (c 70%) receives average annual rainfall between 600 and 800 mm/a (Pinna, 1992). Average annual precipitation is slightly below 600 mm/a in the area of Portoferraio, the southern Calamita peninsula, and the area south-east of the Monte Capanne massif (south of Marina di Campo; see D'Orefice & Graciotti, 2014; Foggi et al., 2006a). This pattern may be explained luv–lee effects. During the main rainfall season in winter, depression systems develop over the northern Tyrrhenian Sea (Alps lee depression). Artic/polar air masses from Europe (coming from the north) warm up over the relatively warm Mediterranean Sea and bring frontal precipitation. The northern side of Monte Capanne is located in the luv of these fronts (cf. Allen, 2001).

Hydrology

Creeks (on Elba usually called *Fosso*) are intermittend. Major flood with exceptionally high discharge after short time rainfall events are documented (2002, 2011), which mainly affected the large plains (Pranzini & Rosas, 2007; Pranzini et al., 2013; Regione Toscana, 2016). On the plains, rivers are for the most parts canalized and embanked (partly since at

least the 19th century, see Catasto Generale della Toscana - Isole, 1841, Archivio di Stato di Livorno and Sistema Informativo Territoriale ed Ambientale Regione Toscana - Direzione Generale Governo del territorio – Regione Toscana: http://www502.regione.toscana.it/geoscopio/servizi/wms/CASTORE.htm). Several check dams were constructed in the middle and lower course of e.g. the Stabbiati river. In historical times, several valleys were occupied with mills, e.g. along the Valle ai Molini or the Rio creek (see Thiébaut de Berneaud, 1814).

3.3 Vegetation and land use

Potential natural vegetation on Elba is deciduous and evergreen oak forest (Blasi et al., 2014). Elba is located in the Central and Northern Tyrrhenian Ecoregional Section which is locally dominated by Mediterranean and Sub-Mediterranean evergreen shrublands of the Italian peninsula with e.g. *Quercus ilex*, *Phillyrea latifolia*, *Arbutus unedo*, *Erica arborea*, and *Pistacia lentiscus* Blasi et al. (2017). Main plants found on Elba are holm oak *(Quercus ilex)*, green olive tree *(Phillyrea latifolia)*, cork oak *(Quercus suber)*, strawberry tree *(Arbutus unedo)*, *Galium scabrum*, spurge *(Euphorbia spinosa)*, tree heath *(Erica arborea)*, spiny broom *(Calicotome spinosa and Calicotome villosa)*, broom *(Genista desoleana)*, Montpellier cistus *(Cistus monspeliensis)*, mastic tree /lentisk *(Pistacia lentiscus)*, rosemary *(Rosmarinus officinalis)*, French lavender *(Lavandula stoechas)*, pitch trefoil *(Bituminaria bituminosa)*, goatgrass *(Triticum ovatum)*, spring sowbread *(Cyclamen repandum)*, etc. (see Foggi et al., 2006b and Foggi et al., 2006a).

Current (semi-) natural vegetation

The present spatial distribution of vegetation on Elba is mainly influenced by relief, rainfall pattern, lithology, and land use history. Based on geomorphological units (see above), exposition, elevation belts, and climatic characteristics, the flora of Elba can be divided in geographic units (Carta et al., 2018a; Foggi et al., 2006b). Three main bioclimatic zones were identified(Foggi et al., 2006b). The zones have different characteristics in West, Central, and Eastern Elba; there is a west–east gradient in the influence of Western-Mediterranean Sardinian–Corsican taxa (Carta et al., 2018a). The three bioclimatic zones are (see Foggi et al., 2006b, Foggi et al., 2006a, and Carta et al., 2018b for the underlying data) :

1. Vegetation of the termomediterranean-dry thermotype is located (1) in the costal (hilly) zones and the alluvial plains, especially near Portoferraio and on the southern slopes of the Calamita peninsula; and (2) in an altitude belt below 550 m a.s.l.. The

zone is dominated by thermophil holm oak woodlands of the *Cyclamino repandi-Quercetum ilicis* assoziation, high *macchia* shrubland (e.g. *Pistacio lentisci-Calicotometum villosae cistetosum monspeliensis*) and low garrique shrubland (e.g. *Lavandulo stoechadis-Cistetum monspeliensis* and *Meliloto elegantis-Triticetum ovati*).

2. The mesomediterranean thermotype–humid obrotype bioclimate dominates on hilly and mountainous areas above 250 m a.s.l. in central , northeastern Elba and the southern section of the Monte Capanne massif; and below 700 m a.s.l. in the northern section of west Elba. This zone is dominated by high macchia (e.g. *Erico aboreae-Arbutetum unedonis*), *Cyclamino repandi-Quercetum ilicis* and *Galio scabri-Quercetum ilicis quercetosum ilicis* holm oak woodlands. Barren rocks are found above 500 m a.s.l., especially on the southern side of the Monte Capanne massif.
3. Locations above 700 m a.s.l.in western Elba are characterized by mesomediterranean and supramediterranean thermotypes. Dominant vegetation associations in these high altitude zone are high macchia shrubland *(Erico aboreae-Arbutetum unedonis)*, holm oak *(Galio scabri-Quercetum ilicis quercetosum ilicis)* and sweet chestnut woodlands *Galio scabri-Quercetum ilicis castanetosum sativae)*.

Especially holm oak woodlands and *macchia* shrubland dominated by *Erica arborea* and *Arbutus unedo* are found in all bioclimatic belts (Foggi et al., 2006b).

Bedrock lithology contributes to the pattern of vegetation distribution. Whereas holm oak woodlands and *garrigue* shrubland are preferably located on calcareous bedrock, high *macchia* shrubland tends to be more frequently found on siliceous soils (Foggi et al., 2006a, see Foggi et al., 2006b and Principi et al., 2015). Especially in central Elba, this pattern appears evident; high macchia dominated by *Erica arborea* and *Arbutus unedo* is abundant on laccolithic bedrock, whereas holm oak woodlands are more frequent on Flysch. Some species typical for *macchia* shrubland on Elba are classified as non-strict calcifuges (i.e. species that prefer soils on siliceous parent material, but tolerate calcareous soils, e.g. *Erica arborea* and *Cistus monspeliensis*; Gastón et al., 2009); *garrique* species like *Rosmarinus officinalis* are in contrast classified as non-strict calcicoles (i.e. plants that tolerate siliceous soils, but are preferably found on calcareous bedrock, Gastón et al., 2009).

On the eastern (leeward) side of the northeastern mountain chain, perennial herbs and *garrique* shrubland are common (especially the *Psoraleo bituminosae-Ampelodesmetum mauritanici* and *Lavandulo stoechadis-Cistetum monspeliensis* associations, respectively). Especially perennial herbs are mainly limited to northeastern Elba, mainly due to a combination of lithological factors, *long duree* agricultural use, and the thermo-mediterranean bioclimate (Foggi et al., 2006a). The mesoscale pattern that the northern and western mountainsides are covered by (denser) mesomediterranean vegetation and eastern and

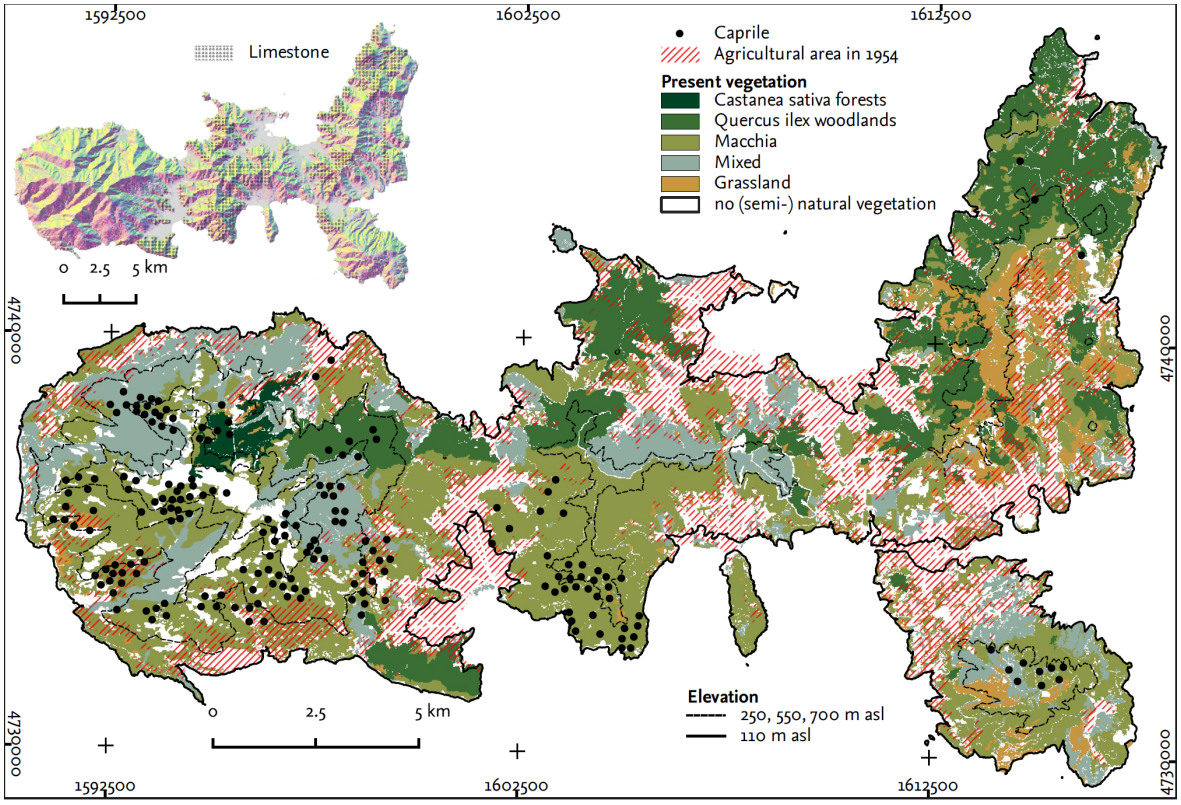

Figure 3.5 Simplified depiction of the main vegetation zones, altitude belts, and past land use on Elba. Black dots indicate the position of *caprili*, i.e. pastoral huts of stone dating to the 18th century–20th century). The red lines show areas which were used for cultivation (cereals, wine) in 1954. The map inlet shows the main slope orientation and areas with limestone. Database: Regione Toscana (2014), Carta et al. (2018b); Foggi et al. (2006a,b).

southern sides by thermomediterranean vegetation can also be observed on a micro-scale (Figures 3.5 and 3.6) because in larger valleys, vegetation differs between north and south exposed slopes (see e.g. Carta et al., 2018b).

Fragmented areas of dune vegetation, lagunal vegetation (e.g. *Zostera nolti*; especially in the area of the former salines in San Giovanni), hydrophil meadow vegetation on former paludal areas (e.g. around the airport in Marina di Campo or in Mola) and vegetation typical for the rocky coast occur. The latter type is mainly found on limestone, especially in areas where bedrock is made up of Flysch formations (e.g. south of Marina di Campo). Here, chasmophytic, sub-halophytic, and aerohaline-lithophytic plants dominate (e.g. *Helichrysum litoreum*, *Anthyllis barba-jovis*, and the endemic *Limonium ilvae*). The riperian zone is dominated by gallery forest with black alder (*Carici Microcarpae-Alnetum Glutinosae* assoziation). On the alluvial plains, the natural vegetation belongs to the *Allio triquetri-Ulmeto minoris* association (Foggi et al., 2006a,b).

Figure 3.6 Vegetation pattern in the Valle dei Mori and the southern slopes of the Monte Capanne. Please note the change in vegetation density with altitude and slope exposition. View from the Monte Orlano area east of Pomonte (c 450 m a.s.l.) in northeastern direction. Image credit: Raphael A. Eser, March 2017.

Human impact

Especially in elevated areas east of Monte Capanne, around Monte Orello in central Elba, north of Porto Azzurro and on the Calamita peninsula, mainly pines, *Erica*, and mastics shrubs were afforested for soil conservation (Foggi et al., 2006b; Friedrich et al., 2000). On the dunes along the shoreline, *Pinus pinea* were planted for logging and the use of non-timber products (Friedrich et al., 2000). Macchia and woodlands were exploited for charcoal production for domestic use purposes until the mid-20th century (see Mazzei-Karl, 1990), as in other parts of Tuscany (cf. Carrari et al., 2017; Mastrolonardo et al., 2018). On the Tuscan mainland, charcoal was used in blast furnaces until the 1960s (Carrari et al., 2017).

In the 2000s, agricultural land use was mainly limited to the alluvial plains (Campo, San Givoanni, Schioparello–Magazzini, Mola, Lacona) and the foot slopes surrounding the villages, and to the eastern and southern section of northeastern Elba (Carta et al., 2018b; Foggi et al., 2006b). Abandoned agricultural terraces that were originally mainly used

Figure 3.7 Terraced slopes in the Gneccarina valley, Monte Capanne massif. La Tabella (881 m a.s.l.) in the background. View from Poggio della Testa (435 m a.s.l.) north of Pomonte in northeastern direction. Image credit: Raphael A. Eser, March 2017.

for viticulture are common on the slopes of the hills and mountains on Elba, especially around the settlement areas (Figure 3.7; see *Carta Tecnica Regionale*, 1:2000 and 1:5000). Vineyards, orchards, and olive cultivation dominate the land use on Elba. In the mid-19th century, around 32 000 000 vine stocks were counted on Elba (Friedrich et al., 2000). Elba is famous for its dessert straw wine, Elba Aleatico Passito. Since the late 19th century, vegetation on Elba changed clearly, mainly due to growing importance of tourism and the decline of agriculture (caused by e.g. emigration and the *Phylloxera* 'plague'; see Bowman et al., 2014; Friedrich et al., 2000). Agricultural area covered c 38% of the surface of Elba in 1954, c 18% in 1978, and c 10% in 2000 (Carta et al., 2018b). In 1954, the agricultural area covered also the slopes and elevated plains around the Monte Capanne massif up to 350 m a.s.l., especially along the southern coast between Fetovaia and Cavoli (La Sughera, Costa dello Svizzero, etc.) and around Pomonte (Vallecchie, Ogliera) as well as the area around the villages of Sant'Ilario and San Piero on the eastern mountainside. On the plains and in the eastern part of northeastern Elba, agricultural land use covered wider areas compared to today's situation. The former agricultural area mainly changed

Figure 3.8 Land use change around the village of Sant'Ilario on the eastern the of the Monte Capanne massif (1954 and 2013). See also Figure 3.6; and Figure A.11, Appendix, for another example; and Carta et al. (2018b) for a quantitative analysis. Database: Regione Toscana, 2014.

to low shrubland and than to high shrubland. This trajectory of land use change from less dense to denser (natural) vegetation is regularly observed on Elba (see Friedrich et al., 2000 for a case study). Between 1954 and 2000, the proportion of area covered by *Quercus* woodlands and high *macchia* changed, whereas the proportion of *garrique* decreased (Carta et al., 2018b).

P astoral land use was common on Elba. As testified by Bronze Age Finds (Zecchini, 2001) and archaeozoological data from hilltop fortresses (Verola & Degl'Innocenti, 2016), *Caprilli*, i.e. small circular pastoral huts made of stone blocks, are abundantly found around the Monte Capanne massif and around Monte Tabonne (south Central Elba) at least since the 18th century (see Cosci, 2001; Ferruzzi & Carpinacci, 2018). Vertical transhumance was common unit the late 19th century; today, pastures are abandoned (Friedrich et al., 2000). Fishery on Elba was dominated by tunny and broadbill fishing.

3.4 Soils

The geographical distribution of different soils on Elba follows more or less the morpho-structural units (Anonymus, *Carta dei suoli in scala 1:250.000 della Toscana, Soil Region 60.7 – Pianure costiere e colline incluse*) and is mainly influenced by bedrock characteristics. Also bioclimatic factors are important for the differentiation of soil units on Elba (Anonymus, *Isola d'Elba. Carta delle Unità di Terre*, 1991).

The following description of the soil geographic regions is based on the soil maps of Tuscany and Elba and the description of the data base of the map of Tuscany given by Vinci & Gardin (n.d.b) and Vinci & Gardin (n.d.a) (see Napoli et al., 2005).

On the Monte Capanne pluton, coarse or skeletal loamy, siliceous, acid, thermic soils with an A-C profil are most common, especially Eutric Regosols and Episkeletic Phaeozems (Vinci & Gardin, n.d.b and Vinci & Gardin, n.d.a). The soils of the Porphyry units of central Elba are similar to those found on the Monte Capanne pluton, although they are less eroded. Therefore, the frequency of soil types differ. In central Elba, the so-called 'Tambone'-soils occure most frequently. They are moderately deep developed, non-calcareous, sandy, acid, well drained soils on intensively weathered siliceous substrate. Also Eutric Regosols (on upper slopes) and Cutanic Luvisols (mainly on foodslopes) can be found (Vinci & Gardin, n.d.b and Vinci & Gardin, n.d.a). On the non-calcareous rocks of the ophiolitic units of western, central and east Elba nonacid, skeletal loamy, thermic Eutri Episkeletic Regosols are frequently found (especially on steeper slopes), but also more developed soils (fine loamy Eutric Cambisols) occur on gentle slopes (Vinci & Gardin, n.d.b and Vinci & Gardin, n.d.a). On the calcareous soils of the upper ophiolitic (pseudo-) sequences and the Flysch units, mainly Chromic Endoleptic Cambisols developed; soils with a less developed profile can be found on eroded abandoned agricultural areas. Fine-loamy Eutric Cambisols occur frequently on the phylittic and quartzitic bedrock in eastern Elba and on the Calamita peninsula. Some soils show a distinct plowing horizon (Vinci & Gardin, n.d.b and Vinci & Gardin, n.d.a).

3.5 Palaeolandscape and occupation history

Late Pleistocene

The landscape evolution on Elba since the Late Pleistocene is mainly driven by transgressive and regressive phases of the Mediterranean. As the Tuscany–Latium shelf is wide and stable, sea level change is mainly eustatic. Sediments of the **Tyrrhenian transgression** (Marine Isotope Stage 5.5, MIS 5.5) were not recorded for Elba, although river terraces

are recorded from 10–15 m a.s.l., e.g. in the Forcioni valley, in Magazzini, and Lacona (Principi et al., 2015; see also D'Orefice & Graciotti, 2014, 2018, and Stocchi et al., 2018). The iron smelting site in Magazzini is located at the edge of such a Pleistocene terrace. The main plains on Elba were flooded during MIS 5.5. The Stella, Enfola, and Calamita peninsulas were separated from the rest of Elba.

During the **regressive phases of MIS 4** (sea level 40 to 80 m below present sea level) and **MIS 2** (last glacial maximum, LGM, c 120 m below present sea level), Elba was connected to the Apennine peninsula mainland (Benjamin et al., 2017; Lambeck et al., 2011; Lambeck & Purcell, 2005); the Elba *peninsula* stretched further north and south along the Elba ridge and included Capraia and the area west of Montecristo (Tortora et al., 2001; c 80 km; see Figure 8.2, p. 163). During this time, marine sands were exposed and dune systems developed along the coast (Aringoli et al., 2009; D'Orefice & Graciotti, 2014); today, they are consolidated and crop out e.g. along the western coast of the Calamite peninsula (Frisch et al., 2008) and the western coast of northeastern Elba (see Principi et al., 2015). Sediment bodies propagated on the shelf south of the Calamita peninsula, that were eroded from the steep Monte Calamite promontory and additionally transported from modern continental rivers that flow on the present shelf during lowstands (Tortora et al., 2001; Bianchi, 1943, cit. in Gerngross, 1959). Present river valleys on the island were incised and palaeosoils developed until 25–22 ka BP; alluvial sedimentation (gravel and sand) in the palaeo-valleys is recorded since the LGM (D'Orefice & Graciotti, 2014).

Holocene

With the onset of the Holocene transgression, fine sediments were deposited on the plains. After 6 ka BP coastal water bodies developed on the plains, when the Holocene transgression ended (D'Orefice & Graciotti, 2014, and therein: Bertini et al., 2014). These water bodies were subject to occasional flooding. Before 6 ka BP the reduction of oak pollen in the palynological record from the Campo plain and the coinciding increase in the deposition of charcoal suggests increased activities of fire (probably during an aridification phase). After 6 ka BP there is an oscillation in oak and *Ericacea* pollen and an increase in pollen of herbaceous plants around 5.3–5.0 ka BP; the microfossil record points to erosive events. *Ericacea* species typically occur in high Mediterranean shrubland. Phases of the reduction of aboreal pollen is recorded for around 4.4 ka BPand around 3.8 ka BP. The later phases is accompanied by a significant increase in *Ericacea* pollen. Also around 2.0 ka BP, the proportion of *Ericacea* pollen increases (Bertini et al., 2014).

Pre-historical settlement history

During the **Neolithic**, human occupation on Elba concentrated on several locations. Archaeological finds point to centers of activities on the southeastern slopes of the Monte Capanne massif in western Elba. Finds of stone tools, axes, and arrowheads of Jasper, quartz or silex are recorded (Zecchini, 2001). Further occupation centers in the Neolithic are the area of Lacona, and on the hilltops of S. Martino and S. Lucia in Central Elba, and around the western section of the Rada di Portoferraio. Only occasional Neolithic finds are known from the northeastern Elba and the Calamita peninsula.

From the **Eneolithic period**, necropoleis in Monte Moncione and the Grotta di S. Giuseppe are known; along with finds from the areas occupied in the neolithic and from Pomonte in the far west. Several authors insinuate a relationship between the location of Eneolithic sites and copper deposits (Chiarantini et al., 2018; Pagliantini, 2014).

Bronze Age activities covered the entire Monte Capanne massif, especially elevated locations. A necropolis dating to the Early Bronze Age was found on the Sughera plain (c 300–400 m a.s.l.). Settlements were located on the ridge of Castiglione di Marina di Campo between two major creeks of the Campo plain, but also on Le Mure (c 600 m a.s.l.) or Monte Giove (c 800 m a.s.l.). Finds of millstones, weaving weights, spine whorls, and ramins of a milk pan point to a pastoral settlements around the Monte Capanne massif (Zecchini, 2001). Activities in Central Elba appear to be less dominated compared to prior periods. Necropolis and settlements in northeastern Elba concentrate on the area around Volterraio and Cima del Monte (see Pagliantini, 2014). The Bronze Age sites in Lacona, Casa del Duca, and Le Trane were located on lower slopes, close to the plains. The settlement pattern observed for the Bronze Age is similar during the Iron Age, also fewer finds were recorded. Some sites, such as Pomonte or Cavoli, are located in lower reaches of valleys (see Pagliantini, 2014).

Etruscans and beyond

During **Etruscan** times, human activities on Elba varied in intensity. Only a few finds from the Orientalising period (675–575 BCE) are known. During the Archaic period (575–480 BCE), several necropolis were located on Elba; mainly on the northern flanks of the Monte Capanne massif, in central Elba and around Volterraio (see Pagliantini, 2014). Coastal sites, such as Bagno, were also occupied, but became more important during the Classical period (480–300 BCE; Zecchini, 1978, 2001). Other Necropolis are known from San Giovanni and Magazzini (see Pagliantini, 2014). The number of finds indicates a decrease in activities with the transition from the Archaic to the Classical period and even an absence of activities in western Elba during the Classical period, mainly due to

political instability; during this time, Syracuse (a main hostile of the Etruscans) gained supremacy over the Tyrrhenian Sea in the 5th century BCE and attacked Elba. This phase coincided with the construction of hilltop fortresses, e.g. at Monte Castello di Procchio and Castiglione di Marina di Campo (Cambi, 2004; Maggiani & Pancrazzi, 1979). These were also inhabited during the Hellenistic period until the Roman occupation (300–260 BCE).

Since the 4th century BCE, Etruria had to counter Roman expansion efforts. No finds from coastal locations were recorded. The occupation of Elba by **Roman**s (c 260 BCE) is strongly connected to the development of iron smelting on Elba Island, although some Etruscan smelting sites were known (see below). Roman settlements are i.a. known from the Piana della Sughera, the Forcioni valley in the upper part of the Campo plain, and elevated position in eastern Elba (Santa Catarian, Cima del Monte; Pagliantini, 2014). Several toponyms (*Marcianus*—Marciana, *Caput Liverum*—Capoliveri, *Rivus*—Rio) may be related to the Roman period (Pagliantini, 2014). With the early Imperial period, *villae maritimae* were constructed on Elba (Corretti & Firmati, 2011). Several wreck finds along the coast of Elba point to activities in the Imperial period. Granite extraction is known from the area of Vallebuia in southwestern Elba; the caves were occasionally exploited since the Eneolithic (Zecchini, 2018). After the 1st century CE, settlement activities on Elba decreased and were mainly concentrated on Portoferraio.

Lombards ruled Elba in the early **Middle Ages**; the island and was later handed over to the Papacy and became part of the Holy Roman Empire (Gerngross, 1959; Mancuso & Pasquali, 2016). Upland villages on Elba (e.g. San Piero, Sant'Ilario, Rio *Alta*, Marciana *Alta*) were founded in the Early and High Medieval Period, although it is believed that for instance Marciana is Roman foundation (from the Roman name *Marcianus*, Gerngross, 1959; Pagliantini, 2014). Under Pisan/Appianian rule, iron was (again) smelted on Elba (between the 11th century and 14th century; see Corretti, 1991). During this time, the hilltop fortress of Volterraio (early 11th century) and the Tower of S. Giovanni (c 1000 CE) were constructed (Baldi & Pucci, 2016; Mancuso & Pasquali, 2016). In the 16th century, Elba was raided by Barbary pirates (Pacchiarini, 2016); later, the area around Portoferraio became part of the Grad Duky of Tuscany, while Elba partly was reigned by the Principado de Piombino, whose accessors controlled Elba since the mid-15th century . Porto Longone (Porto Azzurro) was occupied by the Spanish in the 16th century (Baldi & Pucci, 2016; Mancuso & Pasquali, 2016). During the War of the First Coalition (1792–1797), British troops landed on Elba. The island became French after the Treaty of Amiens in 1802. In 1814, Napoleon was exiled to Elba and formally reigned over the island for 300 day. After the Napoleonic 'era' Elba became again part of the Grand Duchy of Tuscany and later of the Kingdom of Italy (1860). During World War II, Elba was occupied by Nazi Germany

and liberated during ‘Operation Brassard’ by France on June 19, 1944. The blast furnace in Portoferraio was bombed during World War II.

Since the 1960s, Elba increasingly became a touristic destination. Whereas in the past, the settlement activities were mainly focused on the upland villages, key settlement areas shifted towards the coast. Lots of agricultural areas were abandoned and the coastal settlements spread (Carta et al., 2018b) by building holiday homes and hotels. Employment shifted from the agricultural to the tertiary sector (29% and 34% in 1951, and 4% and 77% in 2001, respectively; Cipriani et al., 2011).

4 The ancient metallurgical landscape on Elba

The 'fall and decline' of ancient iron mining and smelting on Elba is linked to the regional to sub-continental economic and political development. Moreover, the specific environmental setting and the *'metallurgical landscape'* of the island strongly triggered the development of the iron metallurgy on Elba. The iron metallurgy on Elba is strongly linked to the overall economic development in *Etruria* and the Roman Republic and Empire. Especially the tide political connections to Populonia influenced the iron production on Elba.

The following description of the mining landscape on Elba is based on the *Determinative factors of mining production in early societies* proposed by Stöllner (2003, 2008).[1] The terminology is adopted to both mining and smelting (thus, the *metallurgical* landscape). With this chapter, I intend to summarize the state of the art on iron smelting on Elba—with a clear focus on the landscape, far more than on e.g. technological aspects. In addition, the chapter is a description of the study area that is focused on resources for the iron metallurgy—see Chapter 3 for a more general description of the landscape on Elba.

4.1 Phases of the ancient iron metallurgy on Elba

The ancient period of mining and smelting on Elba can be divided into seven phases (Figure 4.1). During these phases, the specific metallurgical landscape on Elba developed; the aspects defining the metallurgical landscape on Elba changed during the phases. The

[1] A first conceptualization of the mining landscape on Elba was presented by Raphael A. Eser in a talk given at the *19th International Congress of Classical Archaeology (Cologne/Bonn, 22–26 May 2018)* in Session 4.2 *Mining Landscapes* (Panel 4, *System of extraction: mining, pollution, technology*). A manuscript was submitted to the session conveners to be published in the conference proceedings: Eser, R. A. and F. Becker: *New insights into an old iron mining landscape: Elba Island.*

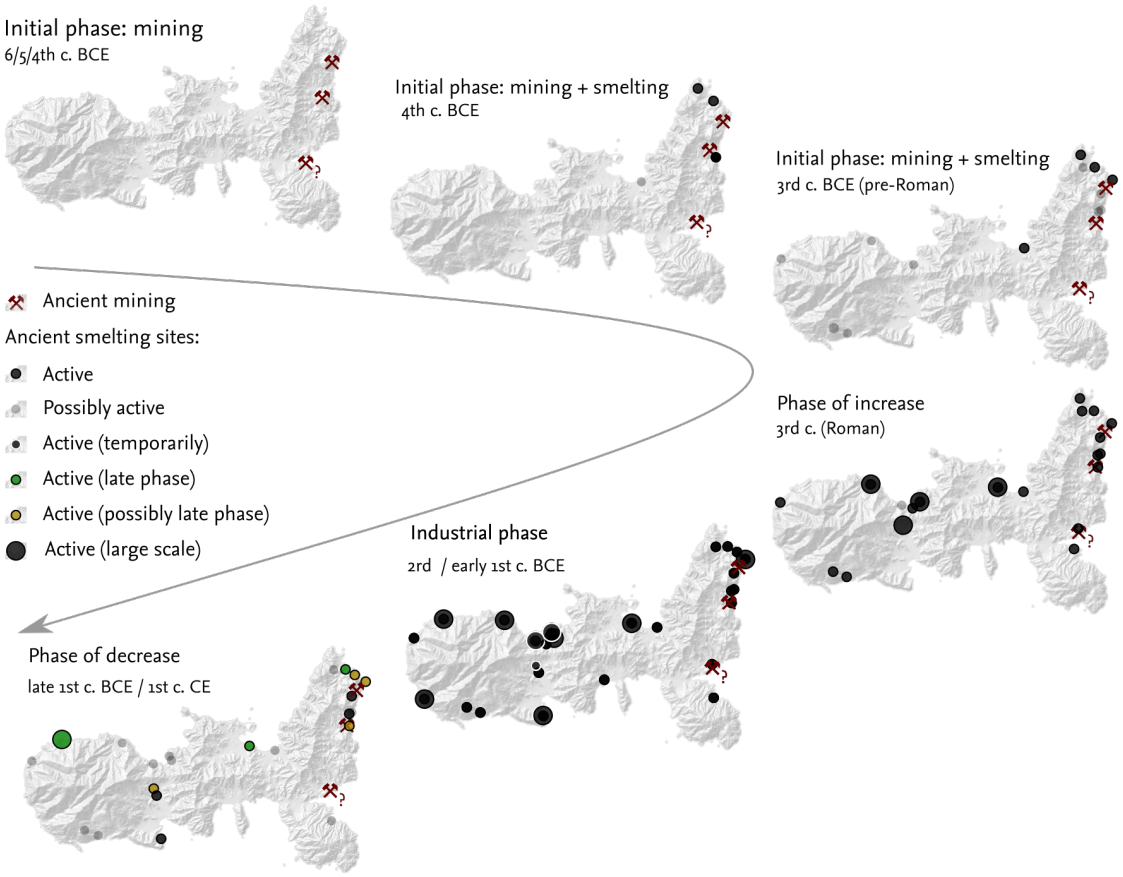

Figure 4.1 Smelting activity during the different metallurgical phases on Elba. Please note that it is not always clear if sites were active during the phase. The size of the points marks the relative slag deposition at each site (large points: 1st quartile of relative disposal). For references see text; chronology and quantity of slag as in Case Study 4, Becker et al., submitted.a, Chapter 9 (certain chronology and minimum slag estimation).

following description of the phases of iron smelting refers to the general idea of the coming of iron in Europe as e.g. discussed in Meyer (2017).[2]

Anterior phase. At least since the late Eneolithic, copper objects were used on Elba (hoard of Grotta San Giuseppe; Cremonesi 2001). From the Final Bronze Age to the

[2]A detailed discussion of the chronology of the smelting sites on Elba and different phases of iron production on the island will be available from Raphael A. Eser's dissertation (*Insula scoriae ferax – Studien zu Chronologie, Topographie und Ökonomie der antiken Eisenverarbeitung auf Elba*, Humboldt Universität zu Berlin, Faculty of Humanities and Social Sciences, date of defense: 8. Jan. 2021). Preliminary ideas on the chronology of smelting on Elba in the context of fuel consumption are discussed in the proceedings of the conference *The Coming of Iron – Anfänge der Eisenverhüttung in Mitteleuropa*, Berlin, 2017-10-19 to 2017-10-21; Fabian Becker, Raphael A. Eser, Stephan G. Schmid, and Brigitta Schütt, *Framing the Chronology and Fuel Consumption of Ancient Iron Smelting on Elba Island* In: M. Brumlich, E. Lehnhardt and M. Meyer: *The Coming of Iron – The Beginnings of Iron Smelting in Central Europe* [Berliner Archäologische Forschungen; 18]. Marie Leidorf, Rahden/Westf., 2020. A generalized stochastic model of slag disposal on Elba is given in Case Study 4, Becker et al., submitted.a, Chapter 9.

Early Iron Age, copper hoards are e.g. known from Pomonte, central Elba (Santa Lucia, San Martino, Colle Reciso) and northeastern Elba (Cima del Monte), which are located near othiolithic copper deposits (Chiarantini et al., 2018). However, copper production in *Etruria Mineraria* during that time took mainly place in the Colline Metallifere area on the Apennine peninsula mainland, i.a. in Populonia (Chiarantini et al., 2018, 2009; Zifferero, 2017). Shepherd (1993) states that iron processing in northern Etruria started around the 10th century BCE, but only scare traces of iron objects are known from this time (Delpino, 1989; Giardino, 2005; see specially Corretti & Benvenuti, 2001, for details on the discussion of early iron production in *Etruria Mineraria*). Evidence for the extraction of iron ore on Elba prior to the 6th century BCE is dubious. The dating of the onset of mining on Elba is mainly indirect, as most traces of mining on the island got lost during modern mining operations. Buchner (1969), Buchner (1985) , Ridgway (1992), Snodgrass (1980), and Turfa (2018) proposed that iron mining on Elba started in the 8th century BCE. Other scholars proposed an even earlier onset (Berveglieri & Valentini, 2001). The presumably 'oldest' (8th century BCE) ore find that is proposed to have been extracted from the mines on Elba is a piece of hematite found on Pithekoussai, the modern Ischia (Buchner, 1969, 1985). The origin from Elba has been under discussion (Corretti & Benvenuti, 2001), but results of geochemical proveniencing presented in 2018 (Cambi et al., 2018; Corretti et al., 2018) show that it is hematite from Elba (see Benvenuti et al., 2013, 2016, for the unique W–Sn signature of ore from Elba). Nevertheless, the contexts of the finds are disrupted and contain dating material from the Late Bronze Age to the 2nd century BCE.[3] Sperl (1993) argues that it is reasonable to assume that the piece of hematite was used as jewelery, not for iron production.

Initial phase (1): Mining. From the 6th to the 4th century BCE, iron from the deposits in northeastern island was extracted (cf. Corretti, 2017). Simultaneously, smelting took place in i.a. Follonica-Rondelli and Populonia-Baratti on the mainland. The stratigraphy and chronology of a beach profile near the smelting site at Baratti beach indicates smelting in Populonia at least since the 5th century BCE, possible peaking in the the 4th and 3rd century BCE (Cartocci et al., 2007; Chiarantini et al., 2007). Ore for the iron production in Populonia came from Elba (e.g. Benvenuti et al., 2013). Finds of potentially Elban ore from other locations such as Aleria, Pisa, Velia, or Genova might indicate mining in the 6th/5th century BCE or later (Cambi et al., 2018; Corretti et al., 2018, , V. Gassner, pers. com., 2018). Few traces of Roman mining on Elba are document, which date only to a *terminus post quem* in the 3rd century BCE (Capacci, 1911; Krantz, 1841).

[3]manuscript submitted by Eser and Becker, see fn. on p. 61

Initial phase (2): Mining and smelting. Although it is previously stated that early iron smelting activities on Elba started in the 5th century BCE (or even the 6th century BCE), it is reasonable to assume that furnaces were operated on Elba in the 4th century BCE (cf. Corretti, 2017; Pagliantini, 2014). Berveglieri & Valentini (2001) and Hartmann (1982) proposed that smelting on Elba could have started around 1000 BCE, however, without any clear evidence. It was previously proposed that furnaces in San Bennato may date to the 5th century BCE (Firmati et al., 2006, archaeomagnetic dating, 450 ± 100 BCE). The data was later reassessed with a higher uncertainty range (6th to 1st century BCE, Principe et al., 2011) and may be obscured by the vicinity to iron deposits and a sea cable. Moreover, recalibration with more recent and more spatially specific palaeosecular variations curves (see Malfatti et al., 2011; Pavón-Carrasco et al., 2009; Tema et al., 2006) might show a later chronology of the site. The earliest evidence for smelting on Elba originates from the sites in the vicinity of the mines in northeastern Elba. Several sites were presumably occupied in the late 4th century BCE.[4] The chronologies of other sites like Magazzini remain unclear, but activities may date to the late 4th century BCE (cf. Corretti et al., 2014) .

Phase of increase. The abundance of dating material and the number of active sites points to a clear increase of smelting activity on Elba in the 3rd century BCE. The increase is most evident for the period after the Roman occupation in the first half of the 3rd century BCE (see Pagliantini, 2014). Also sites distant from the mines in West Elba were in operation during that phase, e.g. in Campo all'Aia, Marciana Marina, and Gnacchera.

Industrial phase. The peak in iron production on Elba dates to the mid-2nd century BCE (Case Study 4, Becker et al., submitted.a, Chapter 9). Activities on sites with high output—some of them located in West Elba (Figure 4.1)—started most likely in the 2nd century BCE, e.g. Pomonte, La Guardiola, Scoglio della Paolina, or Sant'Andrea. Also activities in small sites (Forcioni, La Pila) date to the 2nd/1st century BCE.

Phase of decline. Most authors date the decline of iron smelting activities on Elba to the 1st century BCE. The abundance of ceramic finds dating to this time decreases clearly. Most of the sites with notable output in the West and along the Golfo di Procchio, e.g. Pomonte, Scoglio della Paolina, Marciana Marina, and Campo all'Aia were abandoned in

[4] chronology from Raphael A. Eser's catalogue, pers. comm., 2019-03-29 and 2020-01-15: Lentiso-Martella (finds of Will 1A and MGS IV/V amphorae, late 4th to early 3rd century BCE, Sabbadini, 1919, cf. Corretti, 1991), San Bennato (stratigraphic context and finds of MGS VI amphorae, mid-3rd century BCE , *t.a.q.*, Corretti & Firmati 2011; Firmati et al. 2006), Gli Spiazzi (Rio Marina; Monaco & Mellini 1965, seal emitted in the 4th century BCE and ceramics dating to the second half of the 4th century BCE, possibly Morel Series 4242 or 6210/6220).

the mid-1st century BCE. It is, however, relatively clear that smelting activities continued in the1st century BCE, as indicated by several finds indicate activities on smelting sites in the 1st century CE (e.g. the coin finds from Fornacelle and San Bennato, Sabbadini, 1919). Other chronological data allow for the possibility that activities continued after the turn of the eras, but are unclear.[5]. Most of the sites active in the phase of decline were located in central–northeastern Elba.

The abandonment of Roman smelting. Ceramic evidence from the sites in San Giovanni, Sant'Andrea, and Gli Spiazzi (and coins from northeastern Elba) indicate that the end of iron smelting at least dates to the 1st century CE.[6] No evidence for smelting after the mid-2nd century CE is known, but mining might have continued. A Roman ship wreck found in the Golfo di Procchio sunk with notable hematite load (G. Brambilla and V. Serneels, pers. comm., 2017-10-19). Finds from the wreck and radiocarbon ages from parts of the ship at the load suggest an operation of the ship somewhen between 140 and 350 CE (see Alessio et al., 1973, 1971).

4.2 Characteristics of the metallurgical landscape

4.2.1 Topography of the mines and ore quality

The topography of the ore deposits on Elba is—in addition to the high quality of the ore—the most important 'natural prerequisite' (Stöllner, 2003, 2008) of the metallurgical landscape on Elba.

Quality of the ore

The quality of the ore is of special importance for ancient societies, which had less developed technology of processing (roasting of sulphide ores, recovery of iron in bloomeries);

[5]Raphael A. Eser's catalogue (dissertation, Humboldt Universität zu Berlin, Faculty of Humanities and Social Sciences, date of defense: 8. Jan. 2021), pers. comm, 2019-03-29 and 2020-01-15. Finds includes ^{14}C-ages from slag layer in the beach profile exposed in Capo Pero (unpublished), Dressel 2/4 amphorae from Forcioni and Capo Pero (Maggiani, 1981), and frequent finds of *terra sigillata italica* from Forcioni, Magazzini, Paolina, San Giovanni, and San Bennato (cf. Corretti, 1988; Corretti et al., 2014; Firmati et al., 2006; Pagliantini, 2014)

[6]Raphael A. Eser's catalogue (Humboldt Universität zu Berlin, Faculty of Humanities and Social Sciences, date of defense: 8. Jan. 2021), pers. comm, 2019-03-29 and 2020-01-15: The coin finds of Sabbadini (1919) further dates to 54 CE and 138/9 CE (Claudian *sestertius* and a Antoninian *as*) find in the context of slag heaps indicate occasional activities even in the 2nd century BCE near the mines. San Giovanni (*terra sigilata italica* with a *C.MA* stamp, 15–100 CE, Corretti 1988), a find of late *terra sigilata italica* from Sant'Andrea (Nihlén & Ejlers, 1958), and a lamp fragment from Gli Spiazzi (Monaco & Mellini, 1965).

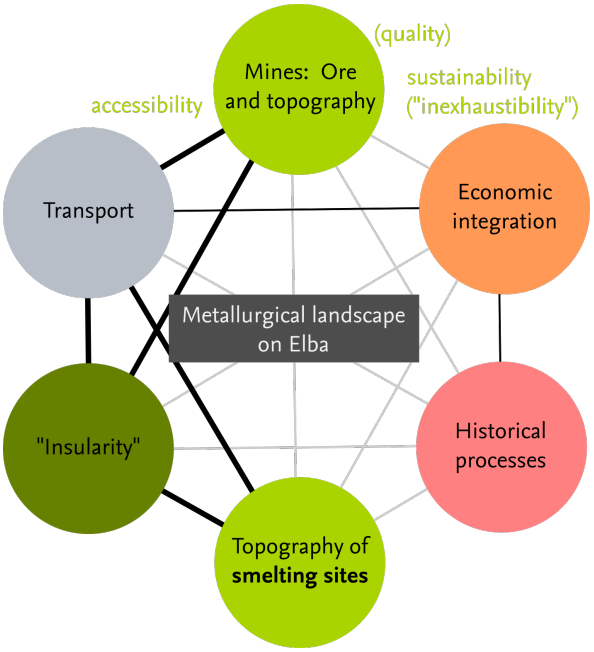

Figure 4.2 The metallurgical landscape on Elba Island: The determinant factors of metallurgical activities on the island and in *Etruria Mineraria*. Adopted from Stöllner (2003).

the re-smelting of Fe-rich ancient slags on Elba in the first half of the 20th century (Corretti, 2017; Nihlén, 1958; Pistolesi, 2013) reveals that ancient production was relatively uneffi-cient and ore with a high Fe-content was necessary for worthwhile production in antiquity. Pleiner (2000) assumes that ores containing more than 55–60 % Fe were extracted by early iron producing societies. Hematite (usually 60–70 % Fe) and magnetite (>70 % Fe) are considered as very good oxide ores; limonite (up to 60 %; gossan, bog iron ore, pea-ores) was also regularly extracted (Pleiner, 2000). Siderite (up to 50 % Fe) was occasionally used after roasting; pyrite could not be used by early smelter due to high phosphorous content.

The ore extracted and smelted on Elba Island in antiquity was of high quality. Hematite-rich ore from Elba (mainly from Rio Marina and Terranera) contains between 55 % and 67 % Fe (data in Benvenuti et al., 2016; Saredo Parodi, 2013, recalculated from Fe_2O_3). Archaeological ore (i.e. ore find in the context of a pre-industrial smelting site, mineral charge) from Follonica contained in average 64,2 % Fe (data from Benvenuti et al., 2000b; Saredo Parodi, 2013, gross average, $n = 15$). Chemical analysis made available by the Comitato Tecnico per l'esame dell'utilizzo dei minerali elbani in siderurgia (1980) show that the hematite-rich ores from Rio Marina (and partially from Rialbano) contain more Fe than ores from e.g. Ginevro. The pyrite-rich ores from Ortano, although rich in iron, were not mined in antiquity (Tanelli et al., 2001); they were either not known or technologically not processible due high sulphur contents.

Sustainability

A reconstruction of the amount of ore extracted in ancient times (and the Medieval period) is—due to intensive open-pit mining in the modern period—only a rough guess (cf. Corretti, 2017). However, Haupt (1888) estimates that around 11 000 000 t ore were mined from the deposits on Elba in pre-industrial times, of these between 4 000 and 10 000 t by the Etruscans (see also Davies, 1935; Freise, 1907). Buchwald (2005) estimates that around 200 BCE, 1 000 t of ore were extracted annually (Piccinini, 1938; Saredo Parodi, 2013; Tanelli, 1985). Albeit ore from Elba was shipped to distant locations, a lower limit of the ore mined in Elba can be estimated based on the amount of slag found on sites in Elba, Populonia, and Poggio Butelli. Depending on the quantitative estimations of slag disposal (Corretti, 2017; Costagliola et al., 2008; Crew, 1991; Pistolesi, 2013; Saredo Parodi, 2013; Voss, 1988; Wertime, 1983), between c 900 000 t and 3,700 000 t ore were at least necessary for the production on the three sites (ore:slag ratio 1.35, see Nikulka, 1995), thus at least between c 1250 t and 5300 t *per annum* in average. Taking the numbers of the production intensity assumed by Saredo Parodi (2013), at least c 2 400 t/a to 12 500 t/a were extracted in the 2nd century BCE.

Although the metallurgical activities on Elba ceased in the 1st/2nd century CE, iron ores were extracted in the Middle Ages (11th to 14th century) and the modern period (especially since the mid-19th century). Considering the scale of iron mining after the Roman period, it seems likely that ancient mining was sustainable and large quantities of ore were available when extraction decreased. In the early 20th century, the extraction of ore on Elba increased from 200 000 t/a around the fin de siècle to a maximum of 800 000 t/a during World War I. In the post-World-War-II era around 400 000 t were extracted annually, before extraction dropped to 180 000 t/a and finally ceased in 1981. According to the Comitato Tecnico per l'esame dell'utilizzo dei minerali elbani in siderurgia (1980) 16 000 000 t of iron ore remain on Elba; around 60 000 000 t of ore were extracted on Elba since the Etruscan period.

Accessibility

Due to the processes of ore formation and the tectonic setting, iron ore deposits on the island are located exclusively along the eastern coast of Elba. As described above, the iron ore concentrations on Elba are synsedimentary to the desert deposits of the Verrucano Formation (quartzites) and were potentially preconcentrated during metamorphosis. During Miocene magmatism, the preconcentrated iron was metasomatically–hydrothermally mineralized and precipitated in the quartzites and the stratigraphically adjacent units (i.a. phylittes of the Rio Marina formation and the Rhaetavicula Contorta limestone; Dünkel

2002; Frisch et al. 2008; Principi et al. 2015). As a consequence of the intrusion of the Monte Capanne plution, the host rocks slipped along border faults, bringing them in the present location (Dünkel, 2002; Dünkel et al., 2003; Frisch et al., 2008; Tanelli et al., 2001). In locations where limonite-rich layers are eroded, hematite-rich ore crops out at the surface or at shallow depth. Seven main iron ore deposits on Elba are known (Figure 4.3) viz., Rialbano, Rio Marina, Ortano, Terranera, Sassi Neri, Ginevro, and Calamita (cf. Tanelli et al., 2001). The massive bodies of the Rialbano (hematite + limonite ± pyrite) and Rio Marina deposits (massive bodies, lenses, and veins of hematite ± limonite ± pyrite, Tanelli et al. 2001) in northeast Elba were exploited intermittently since the 6th century BCE in open-pit mines and small galleries. Although occasional finds dating to the Roman period (Capacci, 1911) are from the Calamita mine (pod-like and massive bodies of magnetite ± limonite; Tanelli et al. 2001), it remains unclear weather the deposits were actually exploited. The magnitude is presumably not comparable to the aforementioned deposits. Tanelli et al. (2001) states that mining in Terranera as well as Calamita started not earlier than the 17th century and 19th century, respectively. Open-pit mining and underground extraction in Ginevro (magnetite and skarn lenses) and Sassi Neri (magnetite lenses) on the Calamita peninsula and in Ortano (northeastern Elba, mainly pyrite) took place in the 20th century (Tanelli et al., 2001). Considering the location close to the coast and and the near-surface ore bodies, the deposits extracted in ancient times on Elba can regarded as readily accessible. The topographic position in eastern Elba, thus close to the Italian peninsula, increased the accessibility of the ore deposits.

4.2.2 Transport

It is widely accepted that the extraction of ore from the mines on Elba started in the 6th century BCE (cf. Corretti, 2017; Corretti & Benvenuti, 2001). Until the 3rd century BCE, the ore was mainly transported to Populonia–Baratti, where archaeological evidence point to production at least since the 5th century BCE (Cartocci et al., 2007; Chiarantini et al., 2007, 2009). Production in Follonica-Rondelli started in the late 6th century BCE (Aranguren et al., 2004, 2009). Data from remote locations (e.g. Aleria, Genova) also indicate the import of iron ore from Elba (see Cambi et al., 2018; Corretti et al., 2018). Thus, the transport of ore from Elba to other locations for smelting (and forging) is key feature of the islands metallurgical landscape. Capo Pero in northeastern Elba is located in c 11 km linear distance to the mainland. The estimated travel distance between the Vigneria stope (Rio Marina deposits) and the ancient smelting site at Baratti beach

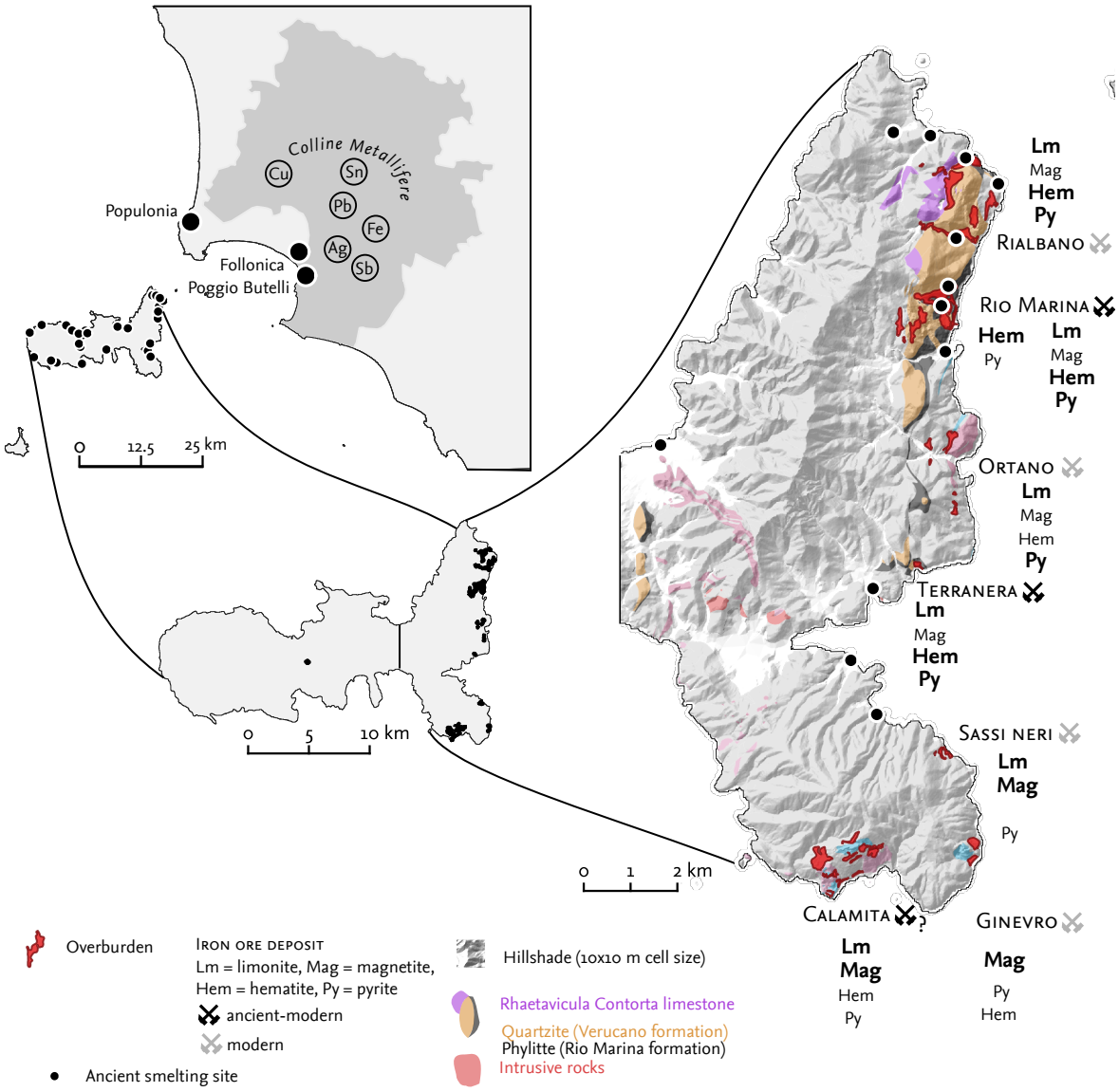

Figure 4.3 Ore deposits and ancient smelting sites on Elba and in the Colline Metallifere. Database: Camporeale, 1985a; Corretti, 1988; Luppi & Salvati, 1987; Pagliantini, 2014; Tanelli, 1985; Tanelli et al., 2001; Regione Toscana, 2014.

(Populonia) is c 22 km; the distance between Vigneria and Follonica or Poggio Butelli is 33–38 km.

In ancient texts (e.g. Strabo 5.2.6) the transport of ore to the mainland is described; in modern times, in the 19th century, raw ore from Elba was not only processed in the blast furnaces in Portoferraio, but also transported to Piombino, Corsica, Genua, etc. on the Italian peninsula for smelting (Swinburne, 1814; Thiébaut de Berneaud, 1814).

The vicinity of the iron deposits on Elba to the mainland is also more important when regarding the topography of Elba (see Section 4.2.1). Several ancient smelting sites were uncovered near the ancient mines in Rio Marina and Rialbano, such as Capo Pero, Fegatella,

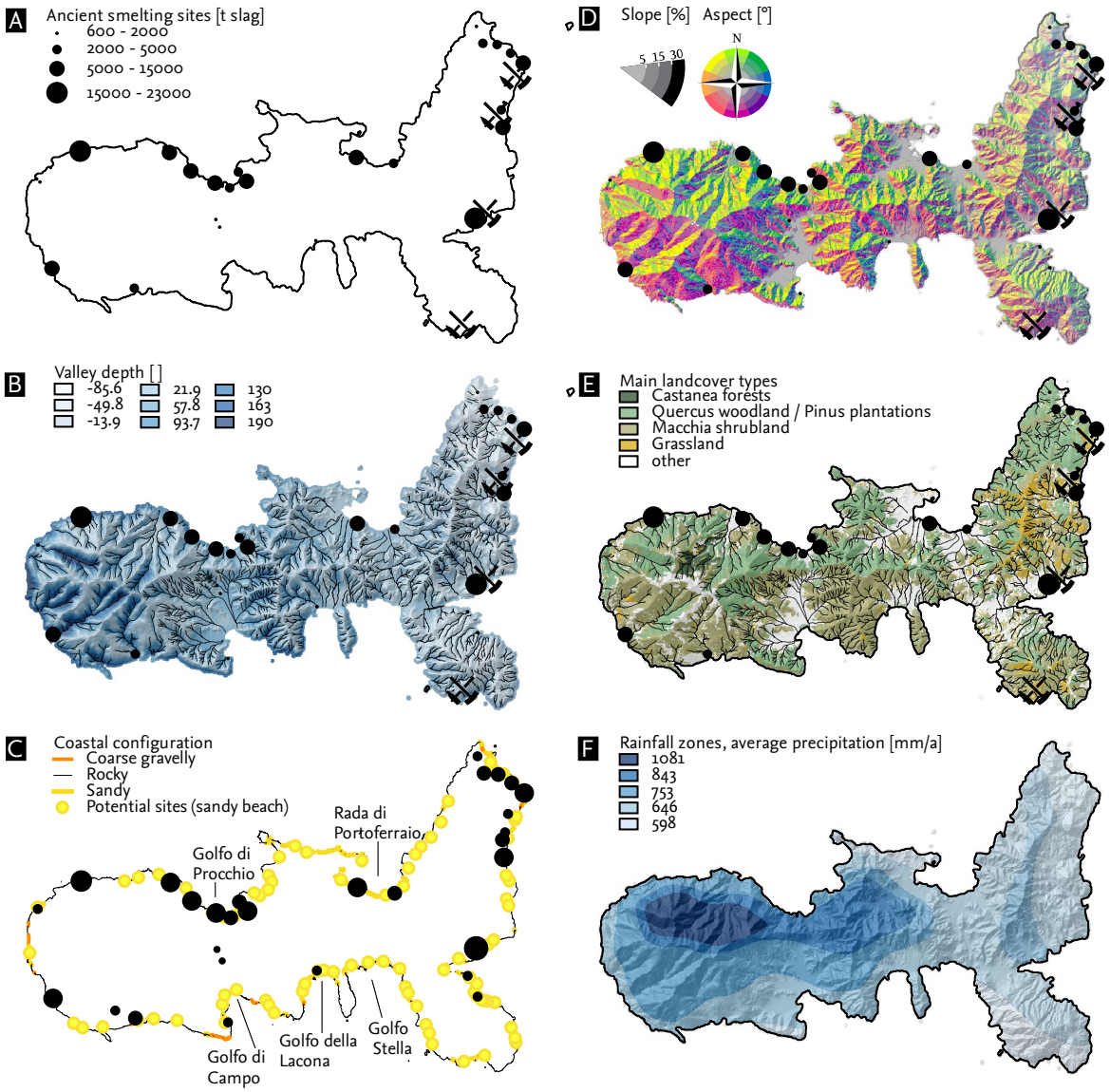

Figure 4.4 Topographical features of the metallurgical landscape on Elba; the left column shows aspects related to the transport and accessibility; maps shown in the right column are related to availability of fuel wood resources. **(A)** Distribution of smelting sites, approximated quantification of slag disposal on sites, an location of ancient mines. **(B)** Relief, drainage network, and morphometric valley depth. **(C)** Location of actual smelting sites and 'potential' sites, i.e. location on a sandy/gravelly beach with a creek in the hinterland. **(D)** Slope inclination and exposition. **(E)** Main vegetation types on Elba. **(F)** Rainfall zones on Elba (see Figure 3.4). Database: Regione Toscana, 2014. The different maps where created as follows: (A) Chronological site classification, site location, and amount of slag disposed on the site as given in Case study 4; (B) Slope and aspect calculated using the default setting of the SAGA *Slope, aspect, curvature* function (Terrain Analysis- Morphometry). based on a 10 m cell size raster from Regione Toscana, 2014. The classification of slope and aspect as well as the colour scheme is taken from Jon Reades' blog: https://kingsgeocomputation.org/2016/03/16/aspect-slope-maps-in-qgis/ (last visit: 2019-05-22).

Gli Spiazzi, San Bennato, or Valle del Giove. The hinterland of these sites is restricted by the main crest in northeastern Elba; therefore, accessible fuel resources in the vicinity of these sites are limited. It was necessary to transport either the fuel to the smelting sites near the mines or to transport the ores from the mines to locations were abundant fuel resources were available. Transport over the main crest appear difficult, taking the high elevation and the short distance to the coast of the most important mountain pass (Le Panche, 327 m asl, 2.8 km linear distance from the coast): The transport distance by sea from the mines to Populonia is shorter than the distance to most of Western and Central Elba; Vigneria–Populonia: c 22 km — Vigneria–Rada di Portoferraio: c 18 km, Vigneria–Gulfo di Procchio: c 28 km, Vigneria–Sant'Andrea: c 37 km, Vigneria–Pomonte: c 46 km (see Figure 4.3). The linear distance from Vigneria to Sant'Andrea and Pomonte (23.7 and 26.5 km, respectively) is even higher than the transport distance to Populonia (c 22 km).[7] Ore was mostly transported by ship. The interpretation of Diocletian's *Edict on Maximum Prices* (although from late antiquity and only valid for a short period of time) shows that land transport was much more expensive than transport by ship. Calculations from Saredo Parodi (2013) suggest that large quantities of ore could be transported by ship to Populonia without requiring an excess of people involved in the transport.

4.2.3 Insularity

The insularity—i.e. the condition of being an island different from *non-islands*—of Elba is another feature of its metallurgical landscape. This becomes especially apparent in the possibility of cost-effective sea transport (see above) and the limited space on the island. Elba covers an area of 224 km^2. Having the scale of iron smelting on Elba in mind—more than 100 000 t of slag were disposed on the island in antiquity (Corretti, 2017; Pistolesi, 2013)—is might appear clear that charcoal production for smelting required a significant portion of the woodland on Elba. Today >140 km^2 of Elba are covered with woodland (mainly *Quercus ilex* and *macchia* woodlands and *Pinus pinaster* plantations; see Carta et al., 2018b). As discussed in Case Study 4, Becker et al., submitted.a, Chapter 9, a significant portion of this area was necessary for the fuel wood requirements of the iron industry on Elba. Also the discussion on the deforestation hypothesis (Case Study 4, Becker et al., submitted.a, Chapter 9; see Section 10.2.3, p. 235) shows the important of the limited resources on Elba. Thus, the limited availability of fuel wood resources is a special feature of Elba as an island; in Populonia, more fuel wood could have been available. The scale of production in Populonia clearly exceed the amount of slag smelted

[7] The Vigneria is the location of the Rio Marina mines most proximal to the coast; it remains unclear if ore was extracted in Vigneria during antiquity (cf. Tanelli et al., 2001 and Pagliantini, 2014).

on Elba (see Section 4.2.1). Also the space for settlements and concomitant agricultural production is a factor of limited resources on the island.

The issue of the foundation of *villae maritimae* and associated *pars rusticae* (agricultural estates) after the abandonment of smelting—i.a. Corretti & Firmati (2011) discuss that noise and emissions from the furnaces would have made Elba unattractive for recreational issues during the heydays of iron smelting—elucidates that space is limited on the island. An aspect connected to this is the *economic monostructure* of Elba island. As mentioned above, in contrast to Populonia, Elbas metallurgical production was limited to iron in antiquity. The foundation of agricultural estates only appeared after the abandonment of most smelting sites (some small *farms* are known, e.g. from the Campo area; Pagliantini, 2014).

4.2.4 Topography of the smelting sites

The topic of the limited space on Elba island is strongly connected to the current understanding of the pattern of smelting sites[8] on the island.

The following aspects characterize the topography of the ancient smelting sites:

Macroscale

1. Most ancient slag accumulations were located in considerable distance to the mines (Figure 4.4: A). The remote sites include some of those with the highest estimate output viz. the sites along the wider Golfo di Procchio (five sites, c 19 800–45 800 t of slag), Marciana Marina (c 9 000–10 500 t), Sant'Andrea (c 10 000–23 000 t), and Pomonte (c 4 800–14 700 t) in western Elba; and San Giovanni in central Elba (see Case Study 4, Becker et al., submitted.a, Chapter 9 for an estimation of the slag disposal of each site—there are also some sites with high output known from eastern Elba, viz. Capo Pero and Barbarossa).
2. Smelting sites are not equally distributed over Elba. More sites are located along the northern coast (and in the vicinity of the mines). Especially larger sites are located along the northern coast, e.g. around the Golfo di Procchio and the Rada di Portoferraio; in the wide bays of the southern coast (Golfo di Campo, Golfo della Lacona, Golfo Stella) only one (presumably small) ancient smelting site is known (Figure 4.4; not-dated sites are reported).

Mesoscale

[8]The term *smelting site* refers to archaeological sites where different types of archaeometallurgical remains were found, typically including slag and technical ceramics (remains of furnace linings or tuyères), archaeological (raw ore processed), or charcoal remains (see Humphris & Carey, 2016). Sites where only slag is found, thus lacking any evidence for smelting *in situ* are classified as 'slag accumulations'.

3. A clear majority of the ancient smelting sites (24 out of 27) were situated in coastal locations notwithstanding they are located close to the mines or in remote locations. The Sughera, Forcioni, Santa Lucia alla Pila, and Lentisco-Martella sites are notable exceptions. However, these sites were relatively small (estimated amount of slag disposed is <1800 t each); in addition, the scale of ancient production in Lentisco-Martella remains unclear, as mainly medieval remains were uncovered form the site. The Sughera site is not a typical iron smelting location, as it was mainly used as settlement, especially before the onset of the smelting period (Pagliantini, 2014). The distance from the site in Campo all'Aia to the coast is up to c 350 m; Ombria and Fegatella lie in about 400–500 m distance from the coast in the lower course of medium sized creeks. The site in Valle del Giove and Vigneria are located between major ore deposits in Rio Marina and the coast. Other sites are located even closer to the (present) coast line, e.g. Ferrato (c 15 m), Patresi (c 20 m), Capo Pero (c 35 m), San Benatto, Magazzini (c 50 m), San Giovanni (less than c 70 m), and Pomonte (c 90 m).
4. Most of the smelting sites are located in the (flat to gently sloping) lower course of relatively wide valleys (Figure 4.4), except the sites near the iron ore deposits in northeastern Elba (i.a. Lentisco-Martella, Capo Pero, Fornacelle, Valle Giove). This becomes particularly clear in western Elba (around Monte Capanne pluton), where the sites in Marciana Marina (Uviale Marciana and Fosso del Lavaccio), Patresi (Uviale di Patresi), Pomonte (Fosso di Pomonte), and Seccheto (Fosso di Vallebuia) are located in major catchments; especially the valley of the Fosso di Pomonte and the Uviale di Patresi are deeply incised. Also the Sant'Andrea site is located close to (local) major streams (Fosso dei Marconi, Fosso della Noce), although the valleys are not deeply incised.

Microscale

5. An important salient characteristic of smelting sites on Elba is that they are located *close to* a creek; the Lentisco-Martella site (as it appears today) cut by the upper course of a (small) creek. The Valle Giove and the Sughera sites are exceptions. However, ancient smelting sites were not directly located *at* the creeks, but in slightly elevated positions. This becomes apparent when looking at the Maggazini sites. Ancient metallurgical remains were found on the part of the alluvial plain that was not subject to flooding, at least since Roman times (Case Study 1, Becker et al., 2019b, Chapter 6). No remains of iron smelting were found on the the (sub-) recent floodplain; the Fosso di Val di Piano, which drains the area of the site, was channelized in the 19th century. Also the sites in e.g. Campo all'Aia, San Giovanni, and San Bennato are located in slightly elevated positions.

6. The coast of Elba is intended. Coastal smelting sites are all located on mostly sandy or partly fine gravelly beaches, albeit most of the coast on Elba is rocky (cliff) coast (Bowman et al., 2014: 131 of 142 km). The location of sandy beaches is connected to sufficient sediment supply by creeks and thus its catchment area. Pocket beaches (i.e. small beaches between two headland with minimal sediment exchange between the adjacent shoreline) are commonly found on Elba. Some of the ancient smelting sites are located near a pocket beach, albeit some exceptions are known, e.g. sites close to the Rio/Rialbano mines, Bagno and Pomonte. Pocket beaches with smelting sites that were analyzed for their planview geometry are (semi-) closed (Barbarossa, Naregno, Procchio, Sant'Andrea, Seccheto; see Bowman et al., 2014).
7. Smelting sites that are located more or less directly at the beach (distance to the present shore line <100 m) tend to be located on the edges of a pocket beach (e.g. Gnacchera, Marciana Marina, Galenzana, Ferrato, Barbarosa) or in elevated positions (>3 m above present sea level: La Guardiola, Patresi, Pomonte, Seccheto).

The characteristic topography of the ancient smelting sites on Elba points to several aspects of the metallurgical landscape. First and foremost, the distance of the smelting sites to the ore resources can be interpreted as evidence for a system of the use of secondary—forest—resources on the island, as implied by i.a. Corretti (2017). The vicinity of the sites to the coast facilitated the transport of the iron ore from the mines to the smelting sites. The texture of the mostly sandy beaches allowed for the landing/beaching of the boats. The geometry of the bays were some smelting sites were located may indicate that locations for smelting sites were chosen that are protected. Albeit plenty of the sandy beaches are embayed pocket beaches (Bowman et al., 2009, 2014), it is a least not implausibly that protection from waves played a role in the selection of the site locations. Therefore, accessibility for transport is a key feature of the smelting sites. This interpretation is supported by the bias of the smelting locations to the northern flanks of the main crests, because main sailing routes around Elba operated counter-clockwise; also the route from the mainland to Corsica got past Elba on its northern coast. There is also a coincidence between the location of the smelting sites and the location of *old* anchorages. Besides the absence of sandy beaches for landing, the west coast of Elba (especially between Pomonte and Patresi), is classified as difficult to sail in modern literature.

The contribution of the suitability for landing might not be overemphasized, because their are competing factors, as illustrated by the Pomonte site. The shoreline in Pomonte is relatively less intended, but the hinterland of the smelting site is wide. One slope of the valley is exposed to north (Figure 4.2 D), with relatively dense vegetation cover (Figure 4.2 E; mainly associations of the meso–suparamediterranean, subhumid–humid vegetation belt, i.a. *Galio scabri-Quercetum ilicis* holm oak woodland and *Galio scabri-*

Quercetum ilicis castanetosum sativae woodlands with sweet chestnut; Foggi et al., 2006b). The fact that sites were preferably located along the northern coast is also explained by bioclimatic factors. Wind is mainly blowing from north-northeastern and northeastern direction; north exposed part of Elba receive significantly more rainfall than south exposed parts (Figure 4.4). In addition, the insulation on northern slopes is less than on south-exposed slopes. Therefore, vegetation zones on the north and south side of Elba differ; on the northern side, larger and denser woodlands grow. *Castanea sativa* forest were only found in north exposed slopes, where also woodlands dominated by *Quercus ilex* occur more frequently on north-exposed slopes; *macchia* shrubland and *garrique* is more often found on south-exposed slopes (cf. Carta et al., 2018b; Foggi et al., 2006a,b). This is also true on a micro-scale. In the valley of the Fosso di Pomonte, were a large smelting site is located, the north–south contrast is very clear, albeit the valley is not located on the northern part. Thus, the availability of denser woodland may also have played a role in locating smelting sites along the coast of Elba. Additionally, the forest in the hinterland of the smelting sites are well accessible, due to their wide valleys and relatively large catchment areas.

Not only forests, but also water, e.g. for ore washing, may have been an important secondary resource for the smelting, as smelting sites were located near creeks. (The vicinity to creeks may nevertheless also be explained by the fact that paths in the hinterland can easily be established along the creek; also today, hiking paths go along creeks.)

4.2.5 Economic integration and historical circumstances

Different explanations for the time lag between the onset of mining and smelting on Elba are possible. The accessibility of the ore deposits facilitates the transport to the mainland; either run-of-mines, iron blooms, or bars had to be transported to the mainland, as the local demand for iron on Elba was of only little importance, taking the low number of settlements on the island (Pagliantini, 2014). Forges are known from Populonia (Chiarantini et al., 2007), while current evidence from Elba point only to a rather small scale smithing on the island (cf. Corretti, 2016). Additionally, political dangers in the Tyrrhenian Sea between the 6th and 4th century BCE by i.a. Greeks coming from the south(west) might have made the production on Elba insecure (see Corretti, 2017; Zecchini, 2001). Chiarantini et al. (2018) states that a lack of fuel supply in the 6th century BCE *(sic!)* restricted the production on Elba, although it seems implausible that the woodland of the island was exhausted before the actual smelting period on Elba started. The most plausible explanation for the lagged onset of smelting activities on Elba is existence of an established 'industrial' quarter in Barrati, where copper was produced at least since the 9th century BCE (Chiarantini

et al., 2018, 2009). Important base metal deposits are known from the hinterland of Populonia in the Colline Metallifere (see Figure 4.3). In pre-industrial times (Eneolithic period to Middle Ages), sphalerite, galena, chalcopyrite, cassiterite, and limonite were extracted in the Colline Metallifere grossetane (Zifferero, 2017). From the Campiliga area deposits of polymetallic sulphides (Cu + Fe ± Zn, Pb, Ag, Bi) and iron–zinn oxides are known (Mascaro et al., 1995). As the mines on Elba, also Baratti beach is well accessible by boat; the beach is protected by the promontory of Populonia and headlands and offers good conditions for beaching.

A historical process linked to the development of the iron industry on Elba was the transition from Etruscan to Roman dominance on Elba, when the number of smelting sites most likely increased, especially after the sea around Elba was secured.[9]. Under Roman rule, iron metallurgy became more important on Elba and the production in Populonia decreased. The demand for iron for warfare in the Roman republic, e.g. during the Second Punic war (218 to 201 BCE), contributed to the development of the iron production on Elba. Livy reports that the people of Populonia delivered weapons for Scipio's invasion of Africa; the iron for the weapons might have come from Elba (Forbes, 1964).

Also the decrease of iron smelting on Elba is (partly) linked to the integration of metallurgy on Elba in the Roman economy (cf. Corretti, 2004). As proposed by Corretti (2004), the fear of slaves made the metallurgical business dangerous. The abandonment of smelting sites on Elba coincides with the integration of new provinces in the Roman territory—from were important iron ore mines are known—in the 1st century BCE, viz. Gallia between 58 and 51 BCE, Noricum in 15 BCE, and Hispania Tarraconensis in 27 BCE. Additionally, a *senatus consultum* (senate's decree) to save the resources in Italy (Plinius) may have affected the iron industry on Elba.[10]

[9] manuscript submitted by Eser and Becker, see fn. on p. 61

[10] The relationship of the *senatus consultum* and the iron metallurgy on Elba is in detailed discussed in Raphael A. Eser's dissertation (Humboldt Universität zu Berlin, Faculty of Humanities and Social Sciences, date of defense: 8. Jan. 2021).

5 Methodology

This chapter comprises the methodological approach of the four case studies is described. The sedimentological–geochemical approach is described in more detail, the modelling approaches based on Monte-Carlo experiments are only summarized, details can be found in the respective chapters. Additionally, geodata and archaeological data used in the thesis are briefly described. Finally, a statement on the computational reproducibility of the four case studies is given.

5.1 Methods and materials

Methodically, the case studies (Chapters 6, 7, 8, and 9) are based on data from sediment sequences obtained by percussion drilling (Case Study 2, Becker et al., 2019a, Chapter 7 and Study 3, Chapter 8) and topsoil samples (Case Study 1, Becker et al., 2019b, Chapter 6) and archaeological site data (Case Study 4, Becker et al., submitted.a, Chapter 9). Statistical analysis of chemical and physical laboratory data (Case studies 1 and 2); analysis and simulation of radiocarbon ages (Case study 3) and stochastic modelling of fuel wood requirements (Case study 4). A overview on the methods can be found in Figure 5.1.

The text in this *Methods and materials* section is based on the texts of the published case studies (1, 2, and 4) and was partly reworked and extended.

5.1.1 Field work

During four field campaigns (April 2015, August 2015, August 2016, September/Oktober 2017) several ancient smelting sites and the Rio, Rialbano, Calamita, and Ginevro mines were inspected. Additionally, geomorphological features around the drilling locations

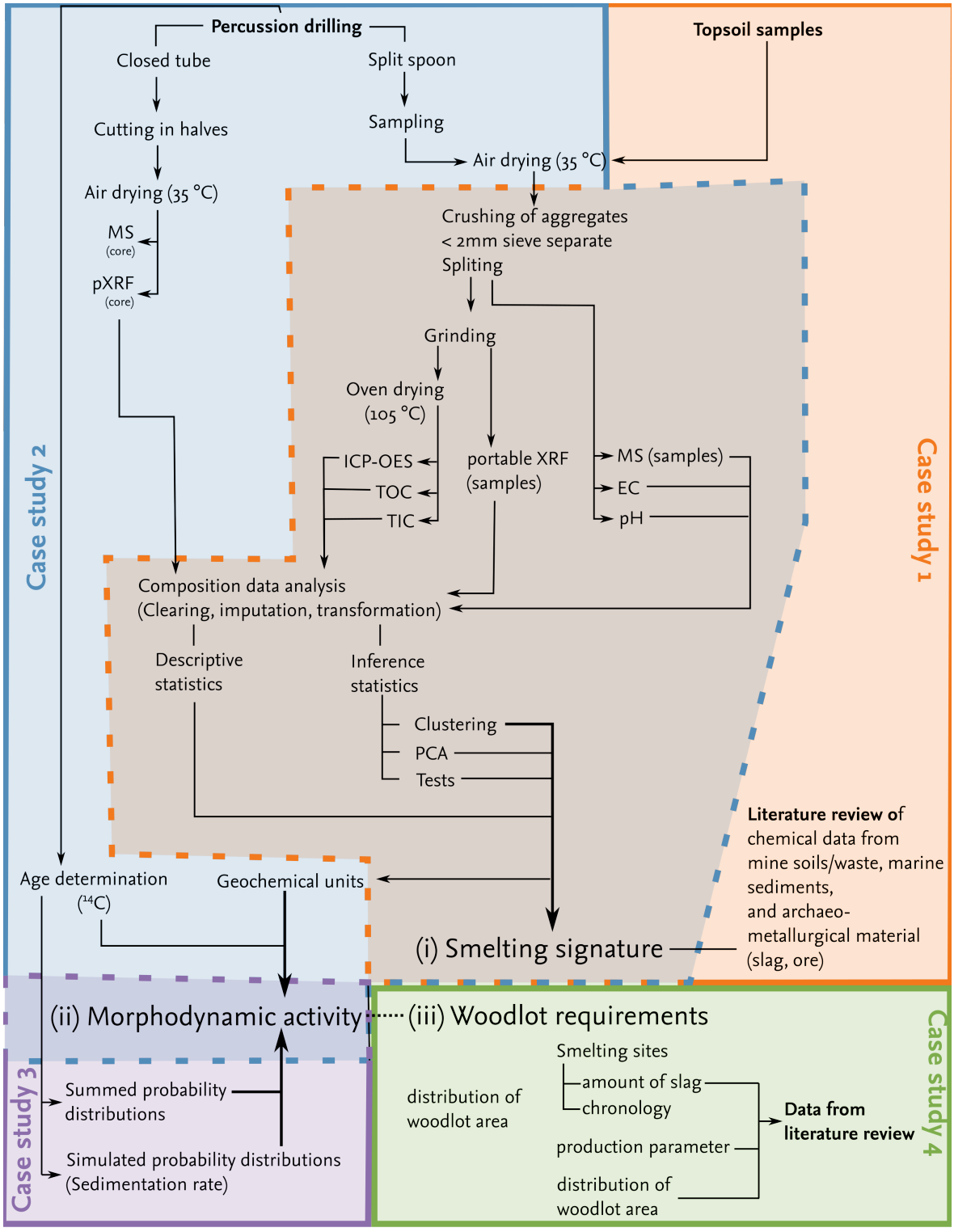

Figure 5.1 Overview on the methods used in the thesis at hand.

were recorded and geological outcrops observed and partly sampled. Geomorphological mapping followed the guidelines in Barsch & Liedtke (1985).

In April 2015, sediment archives were mapped and visited; in September 2015, sediment sequences were obtained along five transects on Elba by percussion drilling using a Cobra motor driven vibracoring device and a Wacker hammer on alluvial plains and in infilled valleys (see Table 5.1 for meta data and Table 5.1 for details on the analysis). Sediments were either exposed in split spoons and described and sampled in-loco or cored in 1 m sections in closed tubes. The closed tubes were split into halves in the Laboratory for Physical Geography (Freie Universität Berlin). The macroscopic description follows the guidelines of Ad-hoc-AG Boden (2005). Samples were taken in 10 cm intervals; additional samples were taken at specific depths, related to stratigraphic layers. Sediment sequences from two transects (Forcioni, Stabbiati) are published in Becker et al. (2019a); data from cores of two transects were used in Case study 3 (Baccetti, Ortano).

Table 5.1 Metadata of sediment cores obtained for the thesis at hand. Elevation in m a.s.l.(meters above sea level, Genova height), obtained from Topographic maps (1 :10 000 and 1 : 2 000). Relief (see Jasiewicz & Stepinski, 2013 for the terminology): VL = valley, FL = flat (plain), FS = footslope, AF = alluvial fan. Analysis: ∘ = only description; ∗ = some analyses, unpublished; ∗∗ = published analyses (see Table 5.2 for details). Publications: *a* = Case Study 2, Becker et al., 2019a, Chapter 7; *b* = Study 3, Chapter 8; *c* = Becker et al., 2018. Coring: sps = split spoon, ct = closed tube. Depth in meter below ground level. ^{14}C = samples dated with the radiocarbon method. *N.b.*Dùe to logistical resons, we did not core at location B-I.

Transect	Core	Northing	Easting	Elevation	Relief	Coring	Depth	Analyses	^{14}C	Publications
Forcioni	F-I	42° 46′ 03.39″	10° 14′ 13.49″	11 m	VL(–FL)	sps	1000 cm	∗∗	$n = 5$	*a*, *c*
	F-II	42° 46′ 09.66″	10° 14′ 04.41″	16 m	VL	ct	500 cm	∗∗	—	*a*, *c*
	F-III	42° 46′ 15.16″	10° 13′ 56.89″	20 m	VL	ct	500 cm	∗∗	$n = 4$	*a*, *c*
Stabbiati	S-I	42° 44′ 32.40″	10° 13′ 47.69″	5 m	FL	sps	1100 cm	∗∗	$n = 4$	*a*, *c*
	S-II	42° 44′ 28.18″	10° 12′ 59.97″	12 m	FL	sps	500 cm	∗∗	$n = 2$	*a*, *c*
Baccetti	B-II	42° 51′ 15.02″	10° 25′ 21.21″	8 m	VL	sps	810 cm	∗	$n = 5$	*b*
	B-III	42° 51′ 09.08″	10° 25′ 11.21″	10 m	AF(–VL)	ct	600 cm	∗	$n = 3$	*b*
	B-IV	42° 51′ 05.40″	10° 25′ 09.12″	15 m	VL(–AF)	ct	500 cm	—	—	—
Ortano	O-I	42° 47′ 48.84″	10° 25′ 16.32″	15 m	VL	sps	1100 cm	∗	$n = 3$	*b*
	O-II	42° 47′ 52.80″	10° 25′ 10.92″	19 m	VL	sps	900 cm	∗	—	—
	O-III	42° 48′ 02.88″	10° 24′ 53.64″	30 m	VL	sps	850 cm	∗	—	—
Aqua Bona	AB-I	42° 47′ 46.32″	10° 20′ 58.20″	1 m	FL	sps	700 cm	—	—	—
	AB-II	42° 47′ 32.64″	10° 21′ 03.60″	5 m	FL	ct	500 cm	—	—	—
	AB-III	42° 47′ 23.28″	10° 21′ 03.60″	7 m	FL(–VL)	ct	500 cm	—	—	—
	AB-IV	42° 47′ 18.96″	10° 21′ 08.28″	11 m	FL(–VL)	ct	500 cm	—	—	—

Table 5.2 Overview on the laboratory analysis of sediment sequences (Case Study 2, Becker et al., 2019a, Chapter 7) and topsoil samples (Case Study 1, Becker et al., 2019b, Chapter 6). ×-marks indicate for which samples the parameter were obtained, parenthesis indicate that a parameter was obtained for a subset of all samples. Data obtained for the five sediment sequences are available in an online repository (Becker et al., 2018, https://doi.org/10.1594/PANGAEA.891242). EC = electric conductivity; MS = magnetic susceptibility, κ = volume-specific MS, χ = mass-specific MS, χ_{fd} = frequency-dependent MS; TC = total carbon; TIC = total inorganic carbon; PyC = pyrogenic carbon; LOI = loss-on-ignition at 360 °C, 560 °C, and 900 °C; TS = total sulphur; pXRF = portable energy dispersive X-ray fluorescence spectroscopy; ICP-OES = inductively coupled plasma-optical emission spectroscopy.

	Sediment sequences					Topsoil samples
	F-I[a]	F-II[b]	F-III[b]	S-I[a]	S-II[b]	
pH	×	×	×	×	×	×
EC	×	×	×	×	×	
MS (κ)	×	×	×	×	×	×
MS (χ)	×		×			×
MS (χ_{fd})	×		×			
Colorimetry	×		×	×		
TC	(×)		(×)	(×)		×
TIC	(×)		(×)	(×)		(×)
PyC						(×)
LOI_{360}						(×)
LOI_{560}	×		×	×		(×)
LOI_{900}	×		×	×		
TS				×		
pXRF	×	×	×	×	×	×
ICP-OES	×		×			(×)

[a] Split spoon [b] Closed tube

In August 2016, we took soil samples from the ancient smelting site in Magazzini and the adjacent area along four transects with 10–20 m distance. In total 134 samples were collected at two depth (0–15 cm and 15–30 cm). Additionally, we took samples in the catchment of the Fosso del Molinaccio upstream the Magazzini site to evaluate background variability.

5.1.2 Laboratory analysis

Sample preparation. Samples from sediment sequences and topsoils were analyzed in the laboratory following the same procedure. All samples were air-dried at c 35 °C for c 24 hr, and stored in plastic bags prior to analysis. After crushing of aggregates and obtaining the < 2 mm sieve separate, we split the samples for further analysis using a

bisection sample divider. One aliquot was homogenized in a cobalt-cemented tungsten carbide grinding bowl (Widia; Kennametal Widia Produktions GmbH & Co. KG, Essen, Germany) and partly oven-dried at 105 °C.

Electrical conductivity and pH. Electrical conductivity of sediments' water solubles was measured in a solution of 5 g of air-dried sediment in 12.5 ml ddH2O (<1 µS/cm) with a Dissolved Solids Tester EC/Temperature checker (Hanna Instruments, Inc., Woonsocket, RI). We measured soil pH in a 1 mol KCl solution with a 1:2.5 soil:solution ratio (air-dried samples) using a hand held tester with 0.01–0.1 pH resolution (Hanna Instruments, Inc., Woonsocket, RI). Average values of 2–3 non-consecutive measurements of pH and electrical conductivity are reported.

Magnetic susceptibility. The sediment's volume-specific magnetic susceptibility (κ) at low (0.465 kHz) and high frequency (4.65 kHz) was measured in brimmed 10 cm^3 sample containers at the 0.1 range (MS2B sensor, Bartington Instruments, Witney, United Kingdom). The containers were weighted before measurement. In cases were undisturbed samples were available, measurements were conducted along the closed tubes at 2.5 cm intervals applying the MS2C sensor (Bartington Instruments, Witney, United Kingdom). The measurement protocols followed Dearing (1999). Instrument stability and accuracy was tested by measuring sample sells filled with water, a standard devliered by the manufacturer of the device, and in-house reference material. Calculation of mass-specific susceptibility (χ) and frequency-dependent susceptibility (χ_{fd}) followed the procedure of Dearing (1999). Measurements in sample containers were repeated 5–10 times to increase the reliability of the results, especially for the calculation of χ_{fd}, which is highly sensitive to uncertainties (Dearing, 1999); means are reported. In addition, the standard error of the mean is estimated by applying a Monte Carlo simulation in R (*propagate*-package; Spiess, 2018) to account for error propagation.

Colorimetric analysis. Colorimetric analysis of the sediments was conducted using the portable spectrophotometer CM-2500d providing data in the L*a*b* color space (Konica Minolta, Marunouchi, Japan).

Carbon contents. Total carbon contents (**TC**, in % m/m) were measured in a TruSpec CHN elemental analyzer (Leco Corporation, Saint Joseph, MI) by infrared spectroscopy of C-fluxes after combustion of 0.1 g sediment in an oxygen stream at 950 °C.

Total inorganic carbon (**TIC**, in % m/m) contents were determined by conductometric titration using a Carmhograph C-16 (H. Wösthoff Messtechnik GmbH, Bochum, Germany).

0.2 g of homogenized and oven-dried sample material is treated with tempered 42.5% H_3PO_4 acid (70–80 °C), a 0.05 mol NaOH solution is titrated with the evolving CO_2-fluxes and the change in the conductivity of the solution is recorded. Certified reference material is occasionally measured and used for the calibration of the sample data; blank samples were measured to determine the instrumental detection limit.

Total organic carbon (**TOC**, in % m/m) was calculated as the difference between total carbon (TC) and and total inorganic carbon (TIC).

Pyrogenic carbon contents (**PyC**, *i.e.* the fraction of organic carbon resistant to wet oxidation) of selected samples were estimated by measuring TC contents after treatment of 1 g sample material with 40 mm 30% H_2O_2 and 20 mm 1 mol HNO_3 in a temperate shaking water bath at 80 °C according to the procedure described by Kurth et al. (2006); in contrast to the original version of Kurth et al. (2006) we avoided heating to 100 °C on a hot plate to reduce foaming and evaporation of the sample. Obtained values were compared to different mixtures of acid purified quartz sand and anthropogenic charcoal or pine needles for quality control (cf. Maestrini & Miesel, 2017).

Loss-on-ignition. Loss-on-ignition (LOI) of homogenized samples was determined after oven-drying of c 4 g material and combustion at 360 °C, 560 °C, and 900 °C (Dean, 1974); the calculation is based on the equations given in Heiri et al. (2001). The samples were filled in crucibles, weighted, and heated in a muffle furnace for 4 hr. After removing from the furnace samples were cooled to room temperature in a desiccator. In-house standards were used for quality control. Values of LOI_{560} were calibrated ($n = 38$, $R^2 = 0.91$) using measured total organic carbon contents (TOC) to get approximated organic carbon contents for samples not analyzed by applying the TruSpec CHN analyzer and the Carmhograph C-16 Case Study 2, Becker et al., 2019a, Chapter 7.

Total sulphur. Sulfur contents of core S-I were obtained using the sulfur module of the Truspec CHN S-Add-On analyzer (quantification of SO_2 by infrared-detection after combustion at 1450 °C in an oxygen atmosphere).

ICP-OES. Element concentrations were measured using an Optima 2100 DV ICP-OES (inductively coupled plasma-optical emission spectroscopy; PerkinElmer, Inc., Waltham, MA) after microwave-assisted aqua regia digestion of 1–3 g powdered and oven-dried sediment (Vogel et al., 2016).

Portable XRF. For the analysis of the elemental composition 10 cm^3 sample cells were filled to >2 mm height with air-dried and grinded samples and covered with a 0.4 µm

polyethylene terephthalate film (BoPET; Mylar, DuPont, Wilmington, DE). The samples were analyzed by portable energy dispersive X-ray fluorescence spectroscopy (pXRF) using a NITON XL3t-900 GOLDD+ device (Thermo Fisher Scientific Inc., Waltham, MA) with an Ag anode tube ((6–50 kV, 0–200 μA max) without He purification under standardized conditions in a sample chamber (lab-based test stand). Sediment samples were measured in the manufacturer's "mining Cu/Zn" mode with main, high, low, and light filters (50, 50, 15/20, and 8 kV, respectively) with a total measurement duration of 120 s. The analytical range of the device is between atomic numbers $Z = 12$ and $Z = 92$ (Mg to U). In addition, air-dried core halves were logged semi-continuously in an arranged unit (Hoelzmann et al., 2017) with 13 mm spot size every 2 cm without a thin film using the same device and settings. Our results were compared with certified reference material (LKSD-4; Lynch, 1990) and an acid-purified silica sand during operation to ensure measurement quality. The quality assessment and quality control procedure applied in Case study 1 follows Kalnicky & Singhvi (2001). Elements were excluded from further analysis in case the proportion of samples with values below the detection limit (*i.e.* the 3-fold standard deviation of the measurement error) exceeded 10%. Precision (repeatability) was determined by 5–10 times repeated non-consecutive measurements of selected samples at a rate of 14.7%, ($n = 21$); 'field' duplicates of 2.1% of the samples were independently prepared and measured to check for reproducibility ($n = 3$; Becker et al., 2019c). Instrument stability was monitored with the in-device *System Check* and an in-house standard. Accuracy of the data was evaluated by measuring certified reference material (see above). We additionally compared the composition of confirmation samples obtained by pXRF to independent laboratory data (ICP-OES). Accuracy is assessed based on regression analysis of centered log-ratio transformed pXRF and ICP-OES data and evaluated based on the quality criteria given in (Kilbride et al., 2006). Further analysis of the pXRF-data set only include those elements which were at least evaluated as 'quantitative' (*i.e.* $r^2 > .7$, $RSD < 20\%$, and $y = ax + 0$ or $y = mx + b$).

5.1.3 Statistical analysis of sediment data

All statistics were performed in R (R Core Team, 2016, 2018). Packages used are described in the respective case studies.

The statistical analysis of the sediment data is mainly focused on a chemostratigraphic grouping of element data (Figure 5.2), albeit inference statistics and techniques of dimension reduction are also implied to other parameters

The analysis follow the **principles of compositional data analysis** to account for the unity sum constraint, the fact that all components of a composition are strictly positive real

numbers and carry only relative information (Weltje & Tjallingii, 2008). Compositional data (e.g. element concentrations or carbon contents) are relative quantitative description of the part of a whole and are usually expressed as proportions (e.g. mg/kg), percentages, or parts per million; composition data are closed—all parts of a composition sum to a constant sum κ (often unity, $\kappa = 1$; see Van den Boogaart & Tolosana-Delgado, 2013). The sum of measured components of a composition is irrelevant, as being an artifact of the sampling procedure. A single part of a composition can not be analysis isolated, as e.g. the concentration of one part decreases if the concentration of another part increases. We use the general term *part* when referring to an element (measured in several samples) and *observation* when referring to the measurement of a single sample; these terms a commons used in literature on compositional data analysis. As described by Aitchison (1986) statistical analysis of compositional data must fulfill several conditions.

Because compositional data are not in the Euclidean space, **transformations** are necessary to conduct common statistical analysis. Ratios of parts of a composition are sufficient to account for the characteristics of compositional data, as numerator and denominator are not interchangeable. Therefore, log-ratio transformations are required for statistical analysis. In the case studies, we used two common log-ratio transformation viz., the centered log-ratio transformation (clr) and the isometric log-ratio transformation (e.g. Filzmoser et al., 2009).

$$clr(x) = \left[ln\frac{x_1}{g(x)}; \ldots ; ln\frac{x_D}{g(x)} \right] \tag{5.1}$$

where the geometirc mean $g(x) = \sqrt[D]{x_1 \cdots x_D}$ is calculated as the nth root of the product of all D components of the D-part composition $x = [x1, \ldots, x_D]$.

The ilr-transformation (Egozcue et al., 2003) maps the D-part composition isometrically to a Euclidean matrix of D rows and $D - 1$ columns . Although the ilr-transformation is mathematically preferred for classical multivariate analysis, the interpretation of the results are difficult, as the lower-dimension transformed variables are not in a direct relationship to the original parts and can thus not easily be interpreted e.g. geochemically (see Aitchison & Egozcue, 2005). Therefore, the ilr-transformation is only used for analysis of the entire composition (e.g. MANOVA) and the clr-transformation is used if values of parts are interpreted separately (e.g. in a principal component analysis where the knowledge on the loading of each part is of interest). Correlation analysis and clustering of element data obtained by portable XRF are additionally based on symmetric balances (Kynclová et al., 2017; Reimann et al., 2017; Templ et al., 2011).

Because the geometric mean—and so the product of all parts—is used for transformation, **missing values** (rounded zeros, non-detects) are a major issue regarding the analysis of elemental composition obtained by pXRF from our sediment sequences and

soil samples (Aitchison & Egozcue, 2005; Martín-Fernández et al., 2000, 2003; Palarea-Albaladejo & Martín-Fernández, 2013, 2015). Missing values in our data sets are values below the instrumental detection limit. Thus, they are missing not at random; the reason why the values are missing is related to the value (they are too low to be detected by the applied method). As the geometric mean of a composition containing rounded zeros is zero, the clr-transformation can not be calculated; division by zero is not possible. There are three main strategies to cope with non-detects. First, parts containing zeros can be excluded from further analysis. Second, observations (e.g. elements) can be excluded from further analysis. Or, third, missing values can be imputed, i.e. replaced by an non-zero value. The first and second approach are prejudical to the understanding of the composition due to loss of information. Often very low values are essential for the understanding of a composition. When leaving samples with zero components out of the analysis, the information of all other components is lost. Likewise, some observations (elements) may contain frequent non-detects in most of the layers, but carry important information that are specific for a single facies, e.g. highly increased sulphur contents in salt marsh deposits. We applied a mixed-approach on our data set. All elements measured with pXRF with a high contribution of samples with values below the detection limit (DL) were excluded from further analysis. The maximal allowed percentage of values below the detection limit is set to 10% <DL (Case Study 1, Becker et al., 2019b, Chapter 6) or to 50% <DL (Case Study 2, Becker et al., 2019a, Chapter 7). Occasionally, elements with high percentage of the values below the detection limite were not excluded from the data set as the non-zero values are of special interest, e.g. high contents of a trace metal enriched in a thin layer related to iron smelting. Non-detects in the subcomputation are then imputed using a (parametric) model-based approach (log-ratio Expectation-Maximisation algorithm or multiplicative lognormal replacement; Palarea-Albaladejo & Martín-Fernández, 2015; Palarea-Albaladejo et al., 2007) to avoid spurious correlations when using a single-value imputation (Palarea-Albaladejo & Martín-Fernández, 2013). We used a value-by-value imputation, as the detection limits calculated from the measurement error of our pXRF-device are specific for each observation and each part.

Grouping of sediment element data (Case Study 2) and soil chemical data (Case Study 1) is the main tool applied for the thesis at hand to facilitate the interpretation of chemical sediment characteristics. Compositional analysis of specially distributed data can e.g. found in Reimann et al. (2012) or Templ et al. (2008); our respective analysis follows McKinley et al. (2016). The sediment chemical data are used to identify *chemofacies* (Montero-Serrano et al., 2010). A detailed example of the entire procedure for the chemofacies grouping is given by some of the (co-)authors of Case Studies 1 and 2 in Schmidt et al. (2018) (see Schmidt et al., 2019). Chemofacies models are used in the different sedimentological

studies. This includes research on deposition processes, studies on the application of geochemistry as a proxy for biostratigraphic information (Ferriday & Montenari, 2016), and applications that are aiming on resolution data (Craigie, 2018). Chemofacies models are also used to identify changes in sediment characteristics that are not detectable by visual lithological description (Rowe et al., 2017) and, more generally, for palaeoenvironmental reconstructions (Duarte et al., 2019). Different technieques to group chemofacies data can be found in Duarte et al. (2019). Observations (samples) were grouped applying a hierarchical cluster analysis (Ward's method; (Murtagh & Legendre, 2014)) to the element data after standardization (centering to median, Mdn, and scaling to median absolute deviation, MAD), isometric log-ratio (ilr) transformation, and calculation of a distance matrix using the Manhattan method (see Templ et al., 2008). The number of clusters was chosen based on the number of archaeological–geomorphological units obtained in the field (topsoil samples) or estimated based on a broken-stick model (sediment sequences; Bennett, 1996). Sediment sequences were grouped using a depth-constrained hierarchical clustering (Gill et al., 1993; Montero-Serrano et al., 2010) by applying the *coniss*-method (Grimm, 1987).

Univariate descriptive parameters of geochemical units were obtained after isometric log-ratio (ilr) transformation. Values were back-transformed to obtain measures of central tendency (Filzmoser et al., 2009). **Inference statistics** follow the procedure proposed by Martín-Fernández et al. (2015). As the data do not strictly follow a multivariate normal distribution (M Box test), we applied a rank-based non-parametric MANOVA and follow-up MANOVA of isometric log-ratio (ilr) transformed parameters; test statistics are based on 'Erdfelder's extension' of Pillai's trace (Ellis et al., 2017; Finch & French, 2013). Wilcoxon rank sum tests were applied to evaluate the between-group differences between centered log-ratio (clr) transformed element contents. 95%-confidence intervals in data visualizations are based on percentile bootstrapping. Between-group differences in carbon composition and pH were tested applying Kruskal-Wallis and Dunn tests. Significance levels are Bonferroni corrected. The central tendency composition of each group is additionally compared to the central tendency of an entire core by visualization in geometric-mean bar plots or a log-ratio difference plot (Martín-Fernández et al., 2015). The bars show the log-ratio of the group center and the core center for each element; the center is here defined as the geometric mean of a part (i.e. an element) after closure of the composition. Confidence intervals of the center are estimated by simple quantile bootstrapping ($\alpha = .05 \times 6 \times 15 = 1.25 \times 10^{-5}$, Bonferroni correction; $B = 1000$). Absolute concentrations were calculated by predicting clr-transformed compositions using the coefficients of the regression analysis and back transforming to the original space following Weltje et al. (2015).

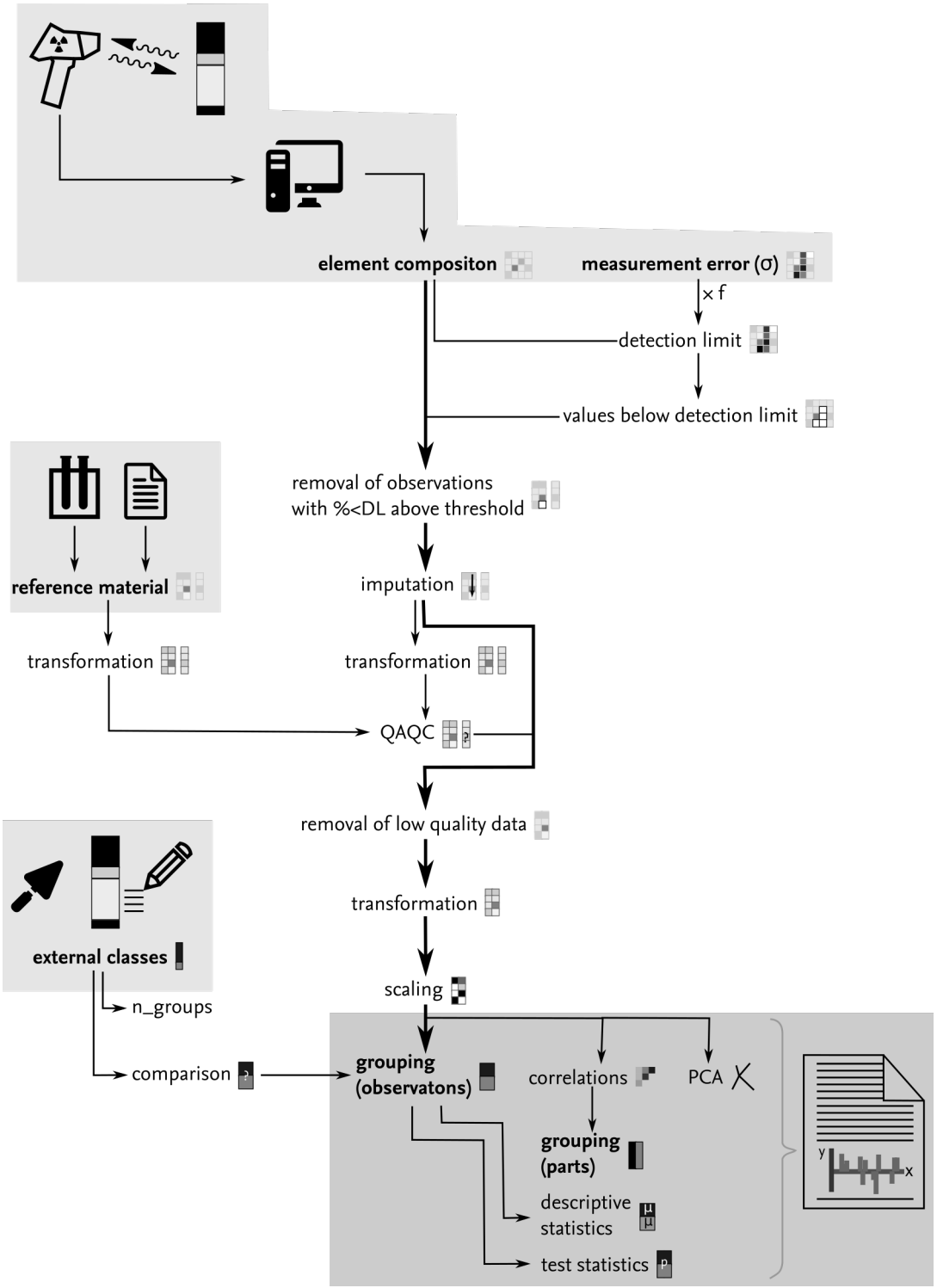

Figure 5.2 Work flow of the statistical analysis to identifiy groups in sediment sequences (and spatially distributed soil samples). QAQC = quality assessment and quality control, PCA = principal component analysis.

5.1.4 Age control

The sediment sequences obtained from the coastal plains and alluvial valleys on Elba Island were dated using the radiocarbon method (^{14}C-method). Samples of charcoal and macroscopic plant remains were send to the Poznan Radiocarbon Laboratory, Poland, for accelerator mass spectometry (AMS) dating; cal-^{14}C-ages ages published in Case Study 2, Becker et al., 2019a, Chapter 7 were calibrated in OxCal, v4.2 (Bronk Ramsey, 2009) and where recalibrated with other samples for the meta-analysis in Study 3, Chapter 8, using the *radiocarbon*-package, v1.2.0 (Bevan & Crema, 2018) in R, v3.5.1 (2018-07-02, R Core Team, 2018). We applied the IntCal13 reference curve (Reimer, 2013) in both cases.

5.1.5 Monte-Carlo-experiments

The description of the models used for the meta-analysis of sediment sequences and the woodlot requirement for iron smelting are described in Study 3, Chapter 8 and Case Study 4, Becker et al., submitted.a, Chapter 9 in detail. A preliminary, simple, version of the woodlot model is submitted for publication in the conference proceedings of the conference *The Coming of Iron - Anfänge der Eisenverhüttung in Mitteleuropa*, Berlin, 2017-10-19 to 2017-10-21.[1] The principles of the model were also discussed at the *19th International Congress of Classical Archaeology*, Cologne/Bonn, 2018-05-22 to 2018-05-26;[2] and a very brief summary of the procedure is given in the respective proceeding (submitted). A short description of the main principles is given below.

Fuel model

Based on theoretical considerations of the endo- and exosomatic metabolism of iron metallurgy, we estimated the area requirement for both, the furnace charge and the supply of the working people. The model is based on chronology of the sites and the amount of the slag disposed on the sites. By using parameters of the fluxes of material and energy during the smelting process, we calculated the wood requirement for smelting. This is then compared to the available woodland on Elba and for each year under consideration, the woodland area is reduced according to the requirements. After felling, the woodland

[1] Presentation: Fabian Becker and Raphael A. Eser, *Scales and Dimensions of Iron Production in Etruria Mineraria – Landscape Archaeological Perspectives* — Manuscript published as:Fabian Becker, Raphael A. Eser, Stephan G. Schmid, and Brigitta Schütt, *Framing the Chronology and Fuel Consumption of Ancient Iron Smelting on Elba Island* In: M. Brumlich, E. Lehnhardt and M. Meyer: *The Coming of Iron – The Beginnings of Iron Smelting in Central Europe* [Berliner Archäologische Forschungen; 18]. Marie Leidorf, Rahden/Westf., 2020.

[2] Presentation/Manuscript, accepted: Fabian Becker, Raphael A. Eser, and Brigitta Schütt, *Elba deforested? New perspectives on the ancient bloomery smelting landscape of Elba Island (Tuscany, Italy)*

regrows and is available for repeated cutting after a given period of time. The number of workers for each of the production steps is estimated and used to estimate an reducion of the available woodland area; the reduction is modelled from thethe area required for farming and the impact of browsing on woodland recovery.

The main input data were obtained from the archaological records on Elba Island. Based on a literature review, a list of dating material for each site was compiled and used to estimate the duration of the operation period of each of the sites. The quantity of slag from each site is estimated based on archive data from the re-smelting period, the spatial extend of the smelting site or simple estimations. The parameters of the smelting process were taken from literature and are mainly based on experimental archaeology or ethnographic records.

The uncertainty of the data is taken into account by using Monte-Carlo experiments and random sampling from a given distribution of possible input data. The outcome of the model is thus a probability function of a specific woodlot area that is required for smelting.

Meta-analysis of sediment sequences

Radiocarbon ages, the depth of the ages, and the facies association of the respective sediment sequences were used to conduct a meta-analysis of the sediment accumulation on Elba during the Holocene.

The basic step of the approach is the calculation of cumulative probability functions, i.e. summing the probability function of all calibrated ^{14}C-ages. The cummlative probability function is understood as an indicator for fluvial activity following the assumption that an increase in fluvial actvity would result in an increase in deposition of datable material. Additionally, the deposition rate implied by the age and the depth of a sample is calculated. Furthermore, the age of a randomly chosen point in a sediment sequence is simulated as a function of depth and the over- and underlying age. A simulated cumulative probability function of the random ages was then calculated to estimate the rate of sediment accumulation for a time interval. Additionally, the age of the simulated random samples and the facies description of the respective sediment layer were taken to model the probability that a facies type occurred during a point in time. The facies therefore attributed with indicating ‘geomorphic activity’ or ‘quiescence’.

As these models are biased due to the nature of the sediment archives and the sampling procedure, we compared the obtained (empirical) probability functions with theoretical functions following assumptions on the taphonomy of sediment layers, the maximum thickness of sediment sequence in the data set and an gross average deposition rate of all radiocarbon ages and the respective depths.

5.2 Geodata

During field work, the *KOMPASS Wanderkarte Isola d' Elba: Wander-, Rad- und Seekarte mit Aktiv Guide. 1:25000 [KOMPASS Wanderkarten; 2468]* was used for guidance. The *Carta Tecnica Regionale scala 1:10000 continuum territoriale* (rt_ctr.10k) was used as basis for mapping. The map is available as a Web Map Service from the Sistema Informativo Territoriale ed Ambientale (Regione Toscana – Direzione Generale Governo del territorio): http://www502.regione.toscana.it/wmsraster/com.rt.wms.RTmap/wms?map%3Dwmsctr%26version%3D1.3.0%26map_resolution%3D91%26map_mnt%3Dfotogram.

The *Carta Tecnica Regionale* in scales of 1 :5 000 and 1 : 2000 available under the given URL was used to obtain detailed information on e.g. elevation and for the localisation of smelting sites.

The database for the maps shown in the thesis at hand is the *DataBase Topografico in scala 1 : 10 000 della Regione Toscana* ('Geoscopio'; `DBG_REGIONE_TOSCANA_NOVEMBRE_2014`) from 2014 (Regione Toscana – Direzione Generale Governo del Territorio – Sistema Informativo Territorial ed Ambietala). The geodata are published under the *Creative Commons Attribution-ShareAlike 4.0 International Public License*. Vector data on geological information were obtained from the *Continuum Geologico della Regione Toscana alla scala 1:10.000* (`SHP_ContinuumGeoRT_20131115`) from 2013 (data from 2009–2011; Regione Toscana – Direzione Generale Governo del Territorio – Sistema Informativo Territoriale ed Ambientale) under the *Attribution 3.0 Italy (CC BY 3.0 IT)* license.

Elevation data used in the thesis are from the *Modello Digitale del Terreno Orografico* digital elevation model (DEM) with 10 m horizontal resolution obtained from *Regione Toscana - Direzione Urbanistica e Politiche Abitative - Settore Sistema Informativo Territoriale e Ambientale*. The DEM is based on contour lines and elevation points as shown in the *Carta Tecnica Regionale 1:10.000* (data from 1995).

The *Carta Geologica dell'Isola d'Elba alla scala 1:25,000* (Geological Map of Elba Island, Principi et al. 2015) and the *Carta della vegetazione dell'Isola d'Elba (Arcipelago Toscano). Scala 1:25.000* (Vegetation map of Elba Island, Foggi et al. 2006b) are the main sources for the description and interpretation of the geological and phytogeographic characteristics on Elba, respectively (see *Study area*, Sections 3.1 and 3.3). Additionall, the accompanying guides were studied (Bortolotti et al., 2015; Foggi et al., 2006a). Data on vegetation used for spatial analysis and visualization were obtained from the *Geoscopio* database.

Bathymetric data were digitalized from the French marine map *Cote ouest d'Italy – Ile d'Elbe* published by the Service Hydrographique et Oceanographique de la Marine (scale 1 : 40 000; 1987–2014, 3rd edition, last updated in 2014). The map is based on the 2011 version of map nr. 117 of the *Instituto Idrografico della Marina (Marina Militare)*.

Unless otherwise indicated, all original data and the map derivatives are given in the Gauss–Boaga projection (western zone) that uses the Hayford ellipsoid and the Roma 1940 datum (Monte Mario / Italy zone 1, EPSG: 3003).

5.3 Archaeological data

General archaeological data on the distribution and chronology of finds on Elba were obtained from the catalog of L. Pagliantini's dissertation, which is available online (Pagliantini, 2014). These data are used for visualisation and the kernel density estimates in Study 3, Chapter 8.

Data used for the description and interpretation of the spatial distribution of the smelting sites on Elba is taken from the most recent data set provided by Raphael A. Eser (Humboldt Universität zu Berlin, Faculty of Humanities and Social Sciences, date of defense: 8. Jan. 2021). The chronology of ancient sites is mainly based on publications of A. Corretti (i.a. Corretti, 1988; Corretti et al., 2014; Corretti & Firmati, 2011). Raphael A. Eser took the geographic location of most of the sites from the original description of the authors and the (rough) approximation from Pagliantini (2014). The author of the thesis at hand and Raphael A. Eser visited a majority of the sites between 2015 and 2018. Thus, for some sites, exact coordinates are available, while for others, the location was estimated by the description or digitalized from (coarse) maps.

A list of ancient smelting sites and their estimated chronology is available as an appendix to Case Study 4, Becker et al., submitted.a, Chapter 9.

5.4 Data availability and reproducibility

The outcomes of the four case studies presented in the thesis at hand are to a different degree reproducible. Data for all case studies are available in an digital online repository or in the Appendix of the thesis; Partially, also the computational code for scripted analyses or even a dynamic report is available (Table 5.3). The Case Study 1, Becker et al., 2019b, Chapter 6, is highly reproducible.

Table 5.3 Evaluation of the degree of computational reproducibility of the four case studies following the scheme proposed by (Marwick, 2017).

Case Study	Reproducibility	Data	Analysis	Manuscript
Case Study 1, Becker et al., 2019b, Chapter 6	High	plain text, open online repository[a]	scripted, available[a]	reproducible, available[a]
Case Study 2, Becker et al., 2019a, Chapter 7	Low–moderate	plain text, open online repository[b]	–[c]	–
Case Study 4, Becker et al., submitted.a, Chapter 9	Moderate–high	plain text, open online repository[d]	scripted, key parts available	–
Study 3, Chapter 8	High	plain text[e]	scripted, available[e]	–

[a] http://dx.doi.org/10.17632/k4cgsps4hk.1
[b] https://doi.org/10.1594/PANGAEA.891242
[b] modified version of the script used available from Schmidt et al. (2018) [d] submitted
[e] currently unpublished, see https://box.fu-berlin.de/s/AEDH5TASKxZfjQ5

6

Case Study 1: The environmental impact of ancient iron mining and smelting on Elba Island, Italy – a geochemical soil survey of the Magazzini site

Published manuscript Becker, Fabian, Raphael A. Eser, Philipp Hoelzmann, and Brigitta Schütt (2019): The environmental impact of ancient iron mining and smelting on Elba Island, Italy – A geochemical soil survey of the Magazzini site. *Journal of Geochemical Exploration* **205**: 106307. DOI: 10.1016/j.gexplo.2019.04.009.

Keywords: *Roman metallurgy, Bloomery smelting, Compositional data analysis, Archaeometallurgy,Pollution*

Highlights

1. Iron smelting on an ancient site clearly changed soil element composition and pH.
2. The alteration matches the composition of ferrous slag or ore, charcoal and fuel ash.
3. Trace metal(loid) contents partly exceed guideline levels, but only negligibly.
4. Compared to (ancient) base metal processing, values are of secondary importance.
5. Deposits showing high contents of trace metal(loid)s were only mined in modern times.

Supplementary materials For supplementary tables and figures see Appendix (due to lincence restrictions only included in the print version of the present thesis) or the webpage of the publisher of the journal article.

Research data, code of analysis, and dynamic report Becker, Fabian, Raphael A. Eser, Philipp Hoelzmann, and Brigitta Schütt (2019): Data for: The environmental impact of

ancient iron mining and smelting on Elba Island, Italy —a geochemical soil survey of the Magazzini site, *Mendeley Data*, **v1**. DOI: 10.17632/k4cgsps4hk.1.

Access note (online version of this dissertation) Due to lincence restrictions, the published article is not include in the present document, but can be accesed from the publishers webpage.

Abstract Elba Island was a hotspot of iron mining and smelting in Italy since Etruscan times (6th century BCE). Whereas the environmental burden of *modern* (base) metal mining in Tuscany is well studied, the impact of both *ancient* iron mining and smelting on soils in the region is poorly understood. Therefore, we took soil samples from an ancient smelting site and adjacent areas to evaluate the release of trace metal(loid)s from smelting. Additionally, we evaluated 'metallurgical activity markers' on the site, i.e. the chemical signature of the production process. The evaluation is based on the soils' element composition, total and pyrogenic carbon contents, pH, and magnetic susceptibility. Statistical analysis include clustering, principal component analysis, and inference tests. Our results indicate that (i) Fe, As, Cu, Ca, total organic, and pyrogenic carbon contents and pH are increased on the smelting site. (ii) This increase corresponds to relatively high contents in these parameters in slag, ore, charcoal, and ash compared to values from background soils. (iii) Metal(loid) contents partly exceed guideline values, but appear negligible compared to (modern) mining – mostly hematite was mined in antiquity, whereas limonite (associated with galena) was only extracted in modern times.

7

Case study 2: Reconstructing human–landscape interactions in the context of ancient iron smelting on Elba Island, Italy, using sedimentological evidence

Published manuscript Becker, Fabian, Raphael A. Eser, Philipp Hoelzmann, and Brigitta Schütt (2019): Reconstructing human–landscape interactions in the context of ancient iron smelting on Elba Island, Italy, using sedimentological evidence. *Geoarchaeology. An International Journal* **34** (3): pp. 336–359. DOI: 10.1002/gea.21726

Keywords: *fluvial activity, geochemistry, multivariate methods, palaeoenvironment, pre-industrial metallurgy*

Supplementary materials For a supplementary table see Appendix. *N.b.* This table was originally published as an in-text table.

Research data Becker, Fabian, Raphael A. Eser, Philipp Hoelzmann, and Brigitta Schütt (2018): Geochemistry of five sediment sequences obtained in the Campo coastal plain on Elba Island (Tuscany, Italy). *PANGAEA*. DOI: 10.1594/PANGAEA.891242.

Publication note In the following, you can find the accepted version of the manuscript. The published (typeset) version is accessible from the journal as stated above.

Abstract We reconstruct human–landscape interactions in the context of ancient bloomery smelting on Elba Island, Tyrrhenian Sea, based on sedimentological evidence. Elba was, together with Populonia, the center of iron production in antiquity (mid-6th century BCE to 1st century CE). The sediment sequences obtained by vibracoring in the Campo plain reveal

that the Holocene transgression triggered aggradation during the Early–Middle Holocene (>5.4 ka BP). Nevertheless, wetland conditions prevailed in low-lying areas during Roman times. Correspondingly, ancient smelting sites are found only on elevated areas along the edge of the plain. The palaeolandscape thus plays a key role in understanding location factors for smelting sites in antiquity. Our sediment sequences indicate that during Etrusco–Roman times (2.4–2.0 ka BP) morphodynamics on the island increased, as is evident from the alteration of slope deposits and slack water deposits in upstream positions, and the change from lacustrine to alluvial deposition in downstream areas. The charcoal record shows that fire dynamics increased simultaneously. The sediments that are synsedimentary to the ancient smelting period show significantly increased arsenic contents and high sediment magnetic susceptibility, whereas overall concentrations of heavy metals remain in the range of the geogenic background signal.

7.1 Introduction

Elba Island was, together with Populonia, the center of iron mining and bloomery smelting in Italia during antiquity. Smelting sites were distributed all over the island (Figure 7.1). In his *Bibliotheca historica* Diodorus of Sicily (first half of the 1st century BCE) describes iron smelting on Elba (the Greek *Aitháleia*): '[the island] received the name it bears from the smoke (*aíthalos*), which lies so thick about it. For the island possesses a great amount of iron rock, which they quarry to melt ... in certain ingenious furnaces' (5.13.1, Loeb Vol. III: 131). Half a century later Strabo (c 63 BCE to 23 CE) paints a contrasting picture in his *Geographica*: Elba is characterized as an island where iron 'cannot be brought into complete coalescence by heating in the furnaces on the island'; the ore had to be 'brought over immediately from the mines to the mainland' (5.2.6, Loeb Vol. III: 355–357). The archeological chronology of iron smelting on Elba provides corresponding evidence of an abandonment of most smelting sites in the second half of the 1st century BCE (Corretti, 1988; Corretti & Firmati, 2011).

The reasons for the abandonment of the smelting sites are under discussion (cf. Corretti, 2004). A common hypothesis is that smelting on Elba could not be pursued due to a lack of fuel after deforestation of the island (Corretti, 2004, 2017; Corretti et al., 2014; Harris, 2013; Hughes, 2014; Nihlén, 1960; Pococke, 1745; Williams, 2009; Wiman, 2013—contra: Grove & Rackham, 2003). Authors refer to the ancient texts or their own observations of a degraded landscape on Elba (Penna, 2014; Wiman, 2013). In travel narratives from the 18th and 19th century, Swinburne (1814), Thiébaut de Berneaud (1814), Barker (1815), and Schweighardt (1841) described a contemporary lack of wood fuel. Furthermore, in contemporary landscape drawings Elba is depicted as a treeless island (e.g., A. Cozens'

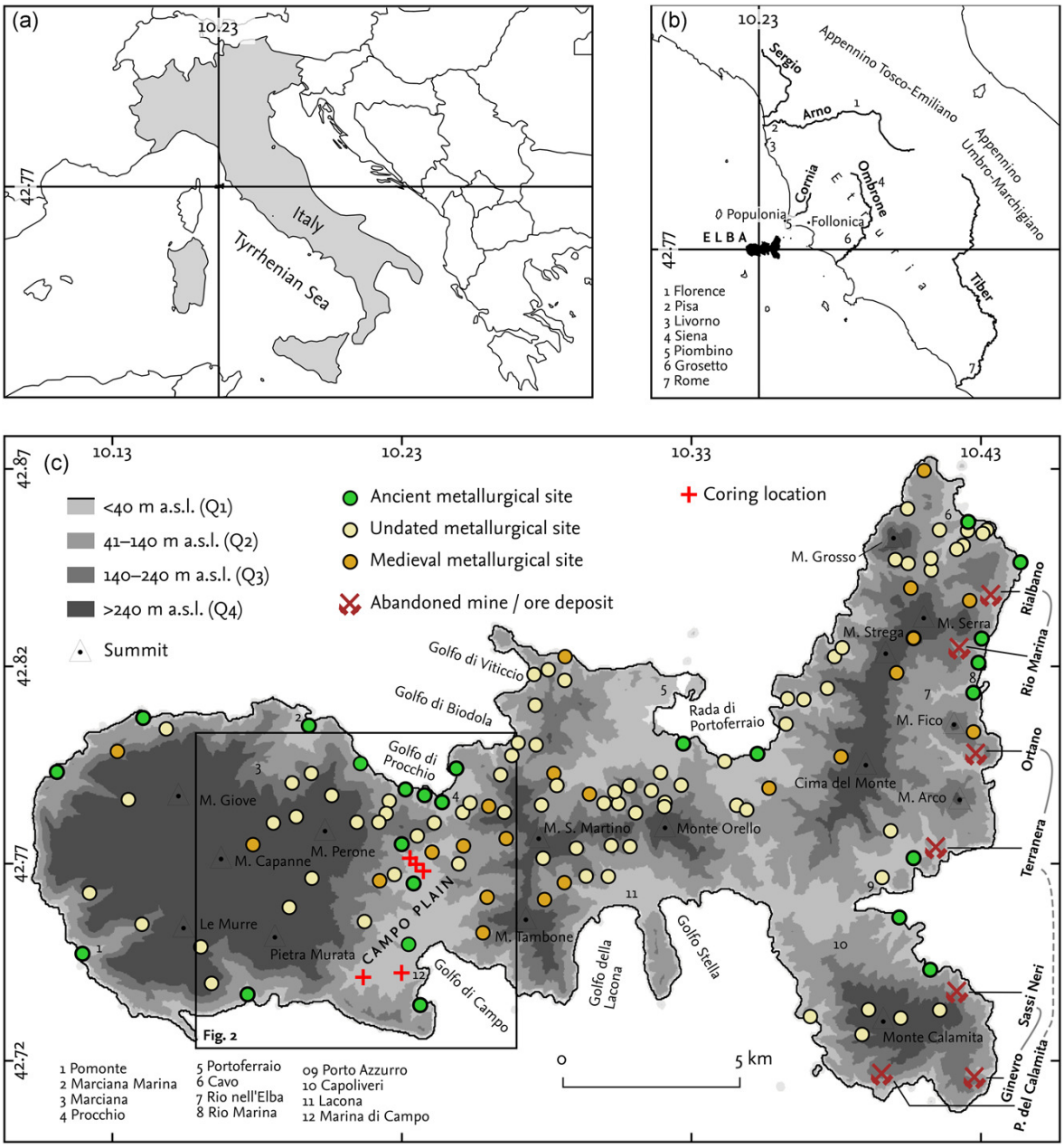

Figure 7.1 Location of Elba Island in the Tyrrhenian Sea (a), off the coast of ancient Etruria (b); and pre-industrial smelting sites and ore deposits (c) on Elba. Database: Corretti, 1988; Pagliantini, 2014; Regione Toscana, 2014.

untitled view of Porto Longona, 1746, The British Museum: 1867, 1012.35), contrasting with present-day views of the landscape (Cyffka, 2006). The ancient comment by Strabo gives no reason for the abandonment of smelting on Elba, although it is believed that he perceived deforestation elsewhere (Hughes, 1983; Hughes & Thirgood, 1982).

The extent of deforestation and degradation in the ancient Mediterranean region is a widely discussed issue (Grove & Rackham, 2003; Harris, 2013; Horden & Purcell, 2000; Hughes, 1983, 2011; Wertime, 1983), although metallurgical centers are often found to be hotspots of deforestation. Meiggs (1982), nevertheless, states that wood production around metallurgical areas might have been higher than the demand for fuelwood. Mighall & Chambers (1997), Mighall et al. (2017), and Eichhorn et al. (2013a) report that the impact of metallurgy on the vegetation might be less intensive than often expected (or of only local significance). In addition, Crew & Mighall (2013) emphasize that it was in the interests of the smelters to manage the woodland to maintain production. In a review of the impact of past (iron) metallurgy on forests, Iles (2016) states that factors other than metallurgy might have contributed to environmental change in the surroundings of production centers (e.g., changes in precipitation, wildfires, population dynamics, or land-use conflicts; see Eichhorn et al., 2013a; Mighall & Chambers, 1997, for examples) and that landscapes were not necessarily degraded/deforested, but transformed.

On the Tuscan mainland, a decline of arboreal pollen in (archaeo-)sediments and an increase in plants with high calorific value are linked to the use of wood fuel for metallurgy (Drescher-Schneider et al., 2007; Mariotti Lippi et al., 2000; Sadori et al., 2010; Williams, 2009; Wiman, 2013), although not mirrored in all archives (Di Pasquale et al., 2014). Palynological investigations from Elba indicate an according decline in arboreal pollen and an increase in microcharcoal content in lagoonal sediments around 2500 BP (Bertini et al., 2014; Toti et al., 2014)—both findings underline the intense use of wood with the onset of iron metallurgy. A complete disappearance of arboreal pollen is not indicated in these archives and the increase in Ericacae-pollen indicates that fuel might have continued to be available on Roman Elba; *Erica arborea* and *Arbutus unedo* were used as firewood.

In addition to forest degradation, emissions—deduced from the quote from Diodorus of Sicily (Elba = *aithaleia* = gr. 'the Smoky')—are described as being an environmental issue for ancient Elba. Emissions from ancient metallurgy are documented globally, i.a. in Greenland ice cores (Hong et al., 1996), peat bogs and mires (e.g. Mariet et al., 2016; Martínez Cortizas et al., 2013; Shotyk et al., 1998), and lacustrine or lagoonal sediment archives (e.g. Elbaz-Poulichet et al., 2011; Renberg et al., 1994). (Air) Emissions from metallurgy on Elba are evident in marine sediments (Leoni & Sartori, 1997; Leoni et al., 1991; Vigliotti et al., 2003). In addition, environmental pollution because of acid mine drainage is an issue related to subrecent mining on Elba (Pistelli et al., 2017; Servida

et al., 2009). Indirect evidence for air pollution on Elba might be provided by the fact that the construction of luxury *villa maritimae* on the island (Le Grotte and Cavo; Pancrazzi & Ducci, 1996) took place after the abandonment of (most) smelting sites. These observations suggest that during antiquity the constant emission of soot from the furnaces during the heyday of smelting made the island unattractive for recreational pursuits (Corretti & Firmati, 2011—*contra:*: Marzano, 2015). Analysis of floodplain sediments of the receiving streams allows the environmental effect of pre-industrial metallurgy to be reconstructed (cf. Brown et al., 2009; Hudson-Edwards et al., 1997; Macklin et al., 1994; Raab et al., 2010; Stolz & Grunert, 2008); evidence given by alluvial deposits provide information on increased fluvial activity after deforestation as well as changed metal fluxes. For Elba Island, there is a lack of such research.

Therefore, the overall aim of this study is to assess the impact of ancient iron smelting on the local landscape balance on Elba—based on sedimentological evidence from the Campo coastal plain (Figure 7.2). This includes the characterization of (a) morphodynamics and (b) geochemical material fluxes during the ancient smelting period. As a starting point, we aim to provide (c) an evaluation of presmelting sediment history; the palaeoenvironmental reconstruction might help to set the variability of the sedimentological record in context and facilitates discussion of triggering processes other than human activity. An understanding of the palaeolandscape might also give further insights into potential location factors (Corretti, 1988).

7.2 Study area: The Campo plain, central Elba

The Campo plain (Figure 7.2) is one of the six main coastal alluvial plains on Elba Island. The plain is located in Central Elba east of the Monte-Capanne massif and covers an area of c 28 km^2 (13% of the island's surface). To the east, the plain is bound by the central Elban hills, the south(eastern) boundary is marked by the Tyrrhenian Sea (Golfo di Campo). To the north, the saddle of the Colle di Procchio divides the Campo plain and the Procchio area.

The Campo area is composed of four geomorphological zones: (a) the coastal plain, dissected by (b) pronounced interfluves, (c) the plutonic Monte-Capanne massive with its steep slopes in the West and (d) the rolling hills of the flysch/laccolith complex in the East (Figure 7.2).

Bedrock is characterized by an intrusion into the ophiolites of the Ligurian-Piedmontese basin causing a thermal metamorphose (Figures 7.2 and 7.3). During the late Miocene magmatism (c 6.8 Ma), Christmas-tree laccoliths, sills, and dykes (San Martino porphyry)

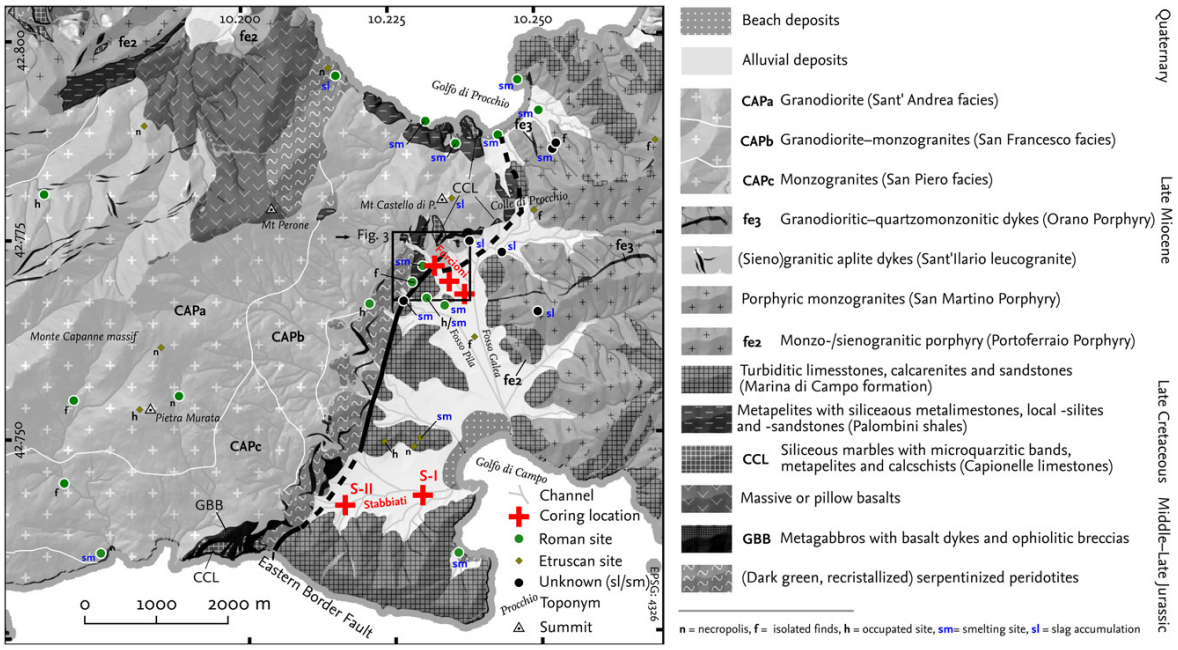

Figure 7.2 Geological map of the Campo plain and the surrounding mountainous areas, including ancient archeological sites. Database: Regione Toscana, 2014; Pagliantini, 2014.

injected into the Middle Jurassic–Late Cretaceous ophiolitic units (Dini et al., 2004; Principi et al., 2015), followed by the intrusion of the Monte-Capanne granodiorites–monzogranites and the coeval Sant'Ilario leucogranite dykes (Pandeli et al., 2013). The flysch units slipped off eastwards on the Eastern-(Procchio) border-fault after the intrusion (Frisch et al., 2008).

The climate of Elba Island is hot-dry Mediterranean (Csa climate after Köppen–Geiger). The annual temperature averages 14.2 °C; precipitation totals 679 mm/a on average with strong seasonality and maximum rainfall amounts during autumn (Monte Calamita, 397 m a.s.l., 1961–1990 normal period, Aeronautica Militare – Servizio Meteorologico). On the eastern slopes of Monte-Capanne, precipitation underlies an orographic effect, increasing from c 600 at the foot to c 850 mm/a in the upslope areas (1922–1981, Bencini et al., 1986). Creeks and rivers flow periodically and are in parts embanked. Flood barriers were constructed in the middle course of the Stabbiati River, where vast floods occurred in the last decades (especially in 2011).

The coastal plain is cultivated and used as semi-natural pasture; settlements have grown with the increase of tourism since the 1950s. Small areas along the Stabbiati River floodplain and the Pila River floodplain are captured by wetlands (Foggi et al., 2006b). Macchia shrubland, afforested *pinus*, and semi-natural forests dominate the slopes of the neighboring hills. Along the floors of the incised valleys, (riparian) forest is abundant (Foggi et al., 2006b). The lower slopes in the Forcioni valley are characterized by agricultural terraces (Figure 7.3).

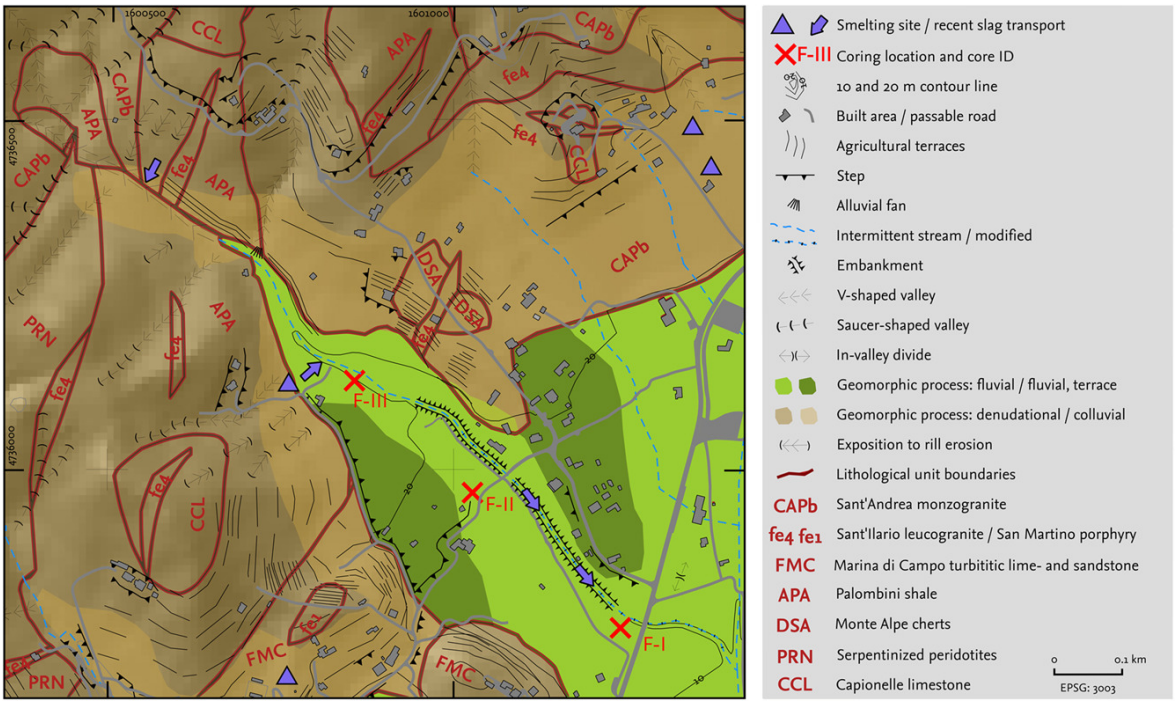

Figure 7.3 Geomorphological-geological map of the Forcioni valley (coring transect 1). Recent slag finds in slope deposits and channel beds are highlighted by arrows; known finds (Corretti, 1988; Pagliantini, 2014) are highlighted by triangles. Database: Regione Toscana, 2014

7.3 Archaeological context

7.3.1 Mining and smelting history

The onset of mining on Elba most likely occurred in the mid-6th century BCE, as indicated by several hematite fragments from Elba found at the ancient smelting sites in Populonia and Follonica/Rondelli (Corretti & Benvenuti, 2001). Ancient mines on Elba were in the north-east (mainly hematite) and on the Calamita peninsula (magnetite; Capacci, 1911; Mori, 1960; Tanelli et al., 2001; Figure 7.1.

First iron smelting may have taken place in north-eastern Elba at San Bennato (430–68 BCE, archaeomagnetic dating, Principe et al., 2011; cf. Firmati et al., 2006) and definitively from the 3rd century BCE (Corretti & Benvenuti, 2001). Iron production increased in Populonia in the 4th to 3rd century BCE (Camporeale, 1985b), and on Elba Island after the Roman occupation (First Punic War, 264–241 BCE) and throughout the 2nd century BCE; smelting on Elba (and Populonia) seems then to have continued until the late 1st century CE, as indicated by Roman material found in some slag heaps (cf. Chiarantini et al., 2007, 2018; Corretti et al., 2014; Sabbadini, 1919). A wreck with abundant ore fragments found in front of the Procchio smelting sites, dating to the late 2nd century CE (cf. Brambilla, 2003), is the latest evidence of ancient iron mining on Elba.

The medieval metallurgical period on Elba dates between the late 11th and the 14th century (Corretti, 1991). Several short phases of iron production occurred from the Renaissance to the Napoleonic era. Industrial iron production started in the late 19th century (Mori, 1960) and continued until 1981 (Tanelli et al., 2001). During this phase, historical mines were reactivated, and pre-industrial slags were resmelted (Pistolesi, 2013; Wrubel, 1929; Zecchini, 2001).

According to Corretti (1988), there are several factors influencing the preferred location of smelting sites during antiquity, (a) accessibility from the sea, (b) the vicinity of streams for washing of the ore, and (c) a hinterland with accessible forests. Deviating from this, two ancient smelting sites in the Campo plain were located at a considerable distance from the coast, this may be explained by an ancient coastline located further inland than today (Corretti, 1988). Medieval smelting sites were in contrast located primarily in the interior along streams and tracks (Corretti, 1991; Figure 7.1).

7.3.2 Settlement history (Campo plain)

Palaeolithic and Neolithic sites with a high concentration of stone tools, axes, and arrowheads of Jasper, quartz or silex appear mostly on the Monte-Capanne massif (Grifoni Cremonesi, 2004; Pagliantini, 2014). Bronze Age sites (13th to 10th century BCE) are located in the southern part of the Campo area in elevated locations (Pagliantini, 2014) and consist of circular structures of megalithic stones; millstones, weaving weights, spindle whorls, and a ceramic lid of a milk pan suggest pastoral settlements (Zecchini, 2001). The production of bronze is indicated by a mold for axes (Pagliantini, 2014). Late Bronze Age/Early Iron Age sites (9th to mid-8th century BCE) are rare in the Campo area (Pagliantini, 2014), comprising only a necropolis and a hoard with weapons, brooches, and weaving weights (Delpino, 1981). The hoard shows highly developed bronze metallurgy related to the copper deposits at Monte Perone (Corretti & Benvenuti, 2001; Pagliantini, 2014—cf. Chiarantini et al., 2018); as yet, no copper processing sites have been identified in the Campo area.

The dominant elements of the Campo plain are the Etruscan hilltop settlement of Monte Castello di Procchio (late 5th to early 3rd century BCE and mid-1st century BCE) and Castiglione di Marina di Campo (second half of 4th to second half of 2rd century BCE). They are located in strategic positions overlooking the plain, at landing sites, and on paths (Cambi, 2004; Maggiani & Pancrazzi, 1979; Pagliantini, 2014). Necropoles have been found at Massa alla Quata in about 745 m a.s.l. and close to the sea at Fosso del Bagno (Zecchini, 1978, 2001).

Nearly all find spots of the Roman era (mid-3rd century BCE to 3rd century CE) are slag heaps or iron smelting sites (Pagliantini, 2014; Figure 7.2). Finds of slags, amphoras and roof tiles in Forcioni valley, Capannili and Santa Lucia della Pila (Figures 7.2 and 7.2) indicate metallurgical and agricultural uses (Cambi, 2004). Widespread iron slags around the bay of Procchio in the North show evidence for large scale smelting (Zecchini, 2001). Another nucleus of Roman structures, possibly remains of a villa maritima, is located at Spartaia close to a deposit of Cipollino marble (Zecchini, 2001; Figure 7.2).

According to current understanding, there is an occupation gap on the Campo plain from the 3rd century CE until Medieval times. The villages of San Piero in Campo and Sant'Ilario in Campo (c. 200 m a.s.l.) have been inhabited since the 11th century. (Monaco & Tabanelli, 1976). Pastoralism was established on the high plains, as indicated by several pastoral huts (Cosci, 2001). Activities in the granite quarries and agriculture in the Campo area are evident.

7.4 Materials and methods

7.4.1 Sampling strategy and coring

Vibracoring along two longitudinal transects (Figure 7.2; Table 7.1) provided sediment sequences of 5 cm in diameter (Cobra motor driven vibracoring device, Atlas Copco). Cores were obtained from the Forcioni valley, a location with ancient smelting in the hinterland (Figures 7.1, 7.2, and 7.3; Corretti, 1988). Additional sediment sequences were extracted from the Stabbiati valley, where smelting locations have not been reported (cf.

Table 7.1 Metadata of the five obtained cores; cores F-I and F-III are our key-profiles. Note. m a.s.l. = meters above sea level.

Transect	Core	Northing	Easting	Elevation (m a.s.l.)	Coring	Depth (cm)
Forcioni	F-I	42°46′3.39″	10°14′13.49″	11	split spoon	1000
	F-II	42°46′9.66″	10°14′4.41″	16	closed tube	500
	F-III	42°46′15.16″	10°13′56.89″	20	closed tube	500
Stabbiati	S-I	42°44′32.40″	10°13′47.69″	5	split spoon	1100
	S-II	42°44′28.18″	10°12′59.97″	12	closed tube	500

Corretti, 1991; Pagliantini, 2014). Sediments were macroscopically described following the guidelines of Ad-hoc-AG Boden (2005) and sampled at 10 cm intervals; additional samples were taken at specific depths, related to stratigraphic layers. Geomorphological mapping of the study site was conducted following the guidelines in Barsch & Liedtke (1985).

7.4.2 Sediment analyses (Table 7.2)

Samples were dried at 40 °C for c 24 hr, sieved to the <2 mm separate after the crushing of aggregates. Electrical conductivity of the sediments' water solubles was measured in a solution of 5 g of sediment in 12.5 ml ddH_2O (<1 µS/cm) with a Dissolved Solids Tester EC/Temperature checker (Hanna Instruments, Inc., Woonsocket, RI). Sediments' pH-values were measured in a solution of 5 g of sediment in 12.5 ml 0.01 mol KCl using a 0.1-pH-resolution handheld checker (Hanna). The sediment's volume-specific magnetic susceptibility κ at low (0.465 kHz) and high frequency (4.65 kHz) was measured along the closed tubes at 2.5 cm intervals applying the MS2C sensor (Bartington Instruments, Witney, United Kingdom). In case of disturbed samples—as available from the split spoon corings—measurements were conducted in 10 cm^3 sample containers at the 0.1 range (MS2B sensor, Bartington Instruments, Witney, United Kingdom) up to ten times per sample (Dearing, 1999).Calculation of mass-specific susceptibility (χ) and frequency-dependent susceptibility (χ_{fd}) followed the procedure of (Dearing, 1999). The standard error of the mean is estimated by applying a Monte Carlo simulation in R (*propagate*-package; Spiess, 2018) to account for error propagation. Colorimetric analysis of the sediments was conducted using the portable spectrophotometer cm-2500d providing data in the L*a*b* color space (Konica Minolta, Marunouchi, Japan).

For further analyses, samples were homogenized in a cobalt-cemented tungsten carbide grinding bowl (Widia; Kennametal Widia Produktions GmbH & Co. KG, Essen, Germany). Loss-on-ignition (LOI) of homogenized samples was calculated after oven-drying (105 °C) of c 4 g material and combustion at 560 °C and 900 °C for 4 hr (Dean, 1974; Heiri et al., 2001). Total carbon content was measured by a TruSpec CHN elemental analyzer (Leco Corporation, Saint Joseph, MI) by infrared spectroscopy of C-fluxes after combustion of 0.1 g sediment at 950 °C. Total inorganic carbon (TIC) content was determined conductometrically using a Carmhograph C-16 (H. Wösthoff Messtechnik GmbH, Bochum, Germany) after treatment of 0.2 g of homogenized and oven-dried sample material with a tempered 42.5% H_3PO_4 acid (70–80 °C); the evolving CO_2 was transferred into a 0.05 mol NaOH solution. Total organic carbon was calculated as the difference between total carbon (TC) and TIC. Values of LOI_{560} were calibrated ($n = 38$, $R^2 = 0.91$) using measured total

organic carbon (TOC) to get approximated organic carbon contents for samples not analyzed by applying the TruSpec CHN analyzer and the Carmhograph C-16.

7.4.3 Elemental composition

The elemental composition of the sediments was obtained using a NITON XL3t-900 GOLDD+ portable energy dispersive X-ray fluorescence spectroscope (pXRF, analytical range between $Z = 12$ and $Z = 92$, Thermo Fisher Scientific Inc., Waltham, MA) with an Ag anode tube (6–50 kV, 0–200 µA max). Homogenized and air-dried samples were transferred to a sample cell and covered with a 0.4 µm polyethylene terephthalate film (BoPET; Mylar, DuPont, Wilmington, DE) and measured under standardized conditions in a sample chamber. In addition, in situ measurements of air-dried core halves were logged semi-continuously in an arranged unit (Hoelzmann et al., 2017) with 13 mm spot size every 2 cm without a thin film. Sediment samples were measured in the standard 'mining Cu/Zn' mode with main, high, low, and light filters (50, 50, 15/20, and 8 kV, respectively) with a total measurement duration of 120 s. Our results were compared with certified reference material (LKSD-4; Lynch, 1990) and an acid-purified silica sand during operation to ensure measurement quality; recoveries of major oxides range between 75% and 125% except for K (135%). Contents of Pb were overestimated by a factor of 1.5; we failed to measure reliable Cu contents with pXRF, which is overestimated by a factor of 4.5. All measurements were performed with the in-device calibration as the interpretation is based on element ratios. The 3.3-fold in-device error is used as the detection limit (cf. Niton XL3t User's Guide). Element concentrations of cores F-I and F-III were, in addition, measured using an Optima 2100 DV ICP-OES (inductively coupled plasma-optical emission spectroscopy; PerkinElmer, Inc., Waltham, MA) after microwave-assisted aqua regia digestion of 1–3 g powdered and oven-dried sediment (Vogel et al., 2016). Reported heavy metal concentrations (Cu, Cd, Pb, Ni, Zn, and Cr) were obtained by ICP-OES except where otherwise specified. Sulfur contents of core S-I were obtained using the sulfur module of the Truspec CHN S-Add-On analyzer (quantification of SO_2 by IR-detection after combustion at 1450 °C in an oxygen atmosphere).

Table 7.2 Proxies used in the current study and their proposed interpretation. LOI: loss-on-ignition; ICP-OES: inductively coupled plasma atomic emission spectroscopy; pXRF: portable X-ray fluorescence fluorescence spectrometry; TIC: total inorganic carbon; TOC: total organic carbon.

		Proxy value		
Method/ parameter	**Parameter**	**Landscape reconstruction (green lines in Figs 6, 9, 10)**	**Anthropogenic Impact (purple)**	**Morphodynamics (orange)**
LOI/Carbon analysis	LOI_{560}, TOC	Enriched in palustrine sediments	May increase with increasing charcoal content [mobility of trace metal(loid)s]	
	LOI_{990}, TIC	Indicates i.a. calcite precipitation in lacustrine sediments		
Bulk parameter	Color	Facies/layer change (alluvial, palustrine, lacustrine)		
	Gravel content	Facies/layer change		Indicates slope/channel bed sedimentation
	pH	Decreases in palustrine layers (marine influence)	[Mobility of trace metal(loid)s]	
	EC	Increases with increasing marine influence		
	Low-frequency MS		deposition of iron artefacts	
	Frequency-dependent MS			Surface stability (soil formation, catchment erosion)
pXRF	All elements	Variation depends on deposition environment(‘chemofacies,’ geochemical units)		
	Al, Fe, Rb, Ti	Variability of texture (lacustrine deposits)		
	Al, Fe, K	Deposition of glauconitic sand (high marine influence)		
	Ti, Rb, Zr			Weathering resistant elements (increased surface stability)
	Zr/Rb			Variation of fine and coarse layers (varying flood magnitudes)
	Si/Ti			Sediment source (catchment vs slope input)
	Fe/Mn		[Mobility of trace metal(loid)s]	
	Sr/K	Marine vs terrestrial influence		
	As		Enriched in iron ore	[May vary with sediment source]
ICP-OES	S	Sulfur precipitation in palustrine sediments (marine influence)		
	Heavy metals (Pb, Zn, Cr, Ni, Cd, Cu)		Elemental sediment smelting signature? (elements are enriched iron ore/slag)	

7.4.4 Semi-automated geochemical grouping and statistics

Delineation of core units based on geochemical sediment characteristics (pXRF-measured elemental composition) were obtained using a clustering approach based on the principles of compositional data analysis in R (R Core Team, 2016—packages: *zoo*, Zeileis & Grothendieck, 2005; *car*, Fox & Weisberg, 2011; *EnvStats*, Millard, 2013; *compositions*, Van den Boogaart et al., 2014; *rioja*, Juggins, 2015; *vegan*, Oksanen et al., 2015; *zCompositions*, Palarea-Albaladejo & Martín-Fernández, 2015). All elements measured with pXRF with a high number of nondetects (more than 50% values below instrumental detection limits) were excluded from further analysis; remaining nondetects were imputed (i.e., estimated) using the parametric lrEM-algorithm (Palarea-Albaladejo & Martín-Fernández, 2015; cf. Palarea-Albaladejo et al., 2007); non-detects of arsenic and sulfur were additionally imputed. All components were closed, that is, normalized to a constant sum, before statistical analysis. Semi-automatic unit delineation of scaled and centered log-ratio (clr) transformed element compositions is based on a depth-constrained hierarchical clustering (Gill et al., 1993; Montero-Serrano et al., 2010) using the *coniss*-method (Grimm, 1987); a suitable number of clusters is estimated based on a broken-stick model (Bennett, 1996). Descriptive and test statistics of geochemical units were obtained after isometric log-ratio (ilr) transformation. Values were back-transformed to obtain measures of central tendency (Filzmoser et al., 2009). The ilr-approach is necessary to consider the remaining parts of the composition and to account for the constant-sum constraint. The central tendency composition of each geochemical unit is compared to the central tendency of an entire core by visualization in geometric-mean bar plots (Martín-Fernández et al., 2015). The bars show the log-ratio of the group center and the core center for each element; the center is here defined as the geometric mean of a part (i.e., an element) after closure of the composition. The confidence intervals of the center are estimated by simple quantile bootstrapping ($\alpha = .05 \times 6 \times 15 = 1.25 \times 10^{-5}$, Bonferroni correction; $B = 1000$). The clr-transformation of trace metal(loid) contents was performed on a subcomposition of the elements and LOI_{560} (organic matter) and Fe, Mn, and Al (clay) contents to take factors affecting mobility into account (Figure 7.4).

7.4.5 Access to data

All relevant raw and processed data of the core analysis are available as a data publication in a Pangaea repository: https://doi.org/10.1594/PANGAEA.891242 (Becker et al., 2018).

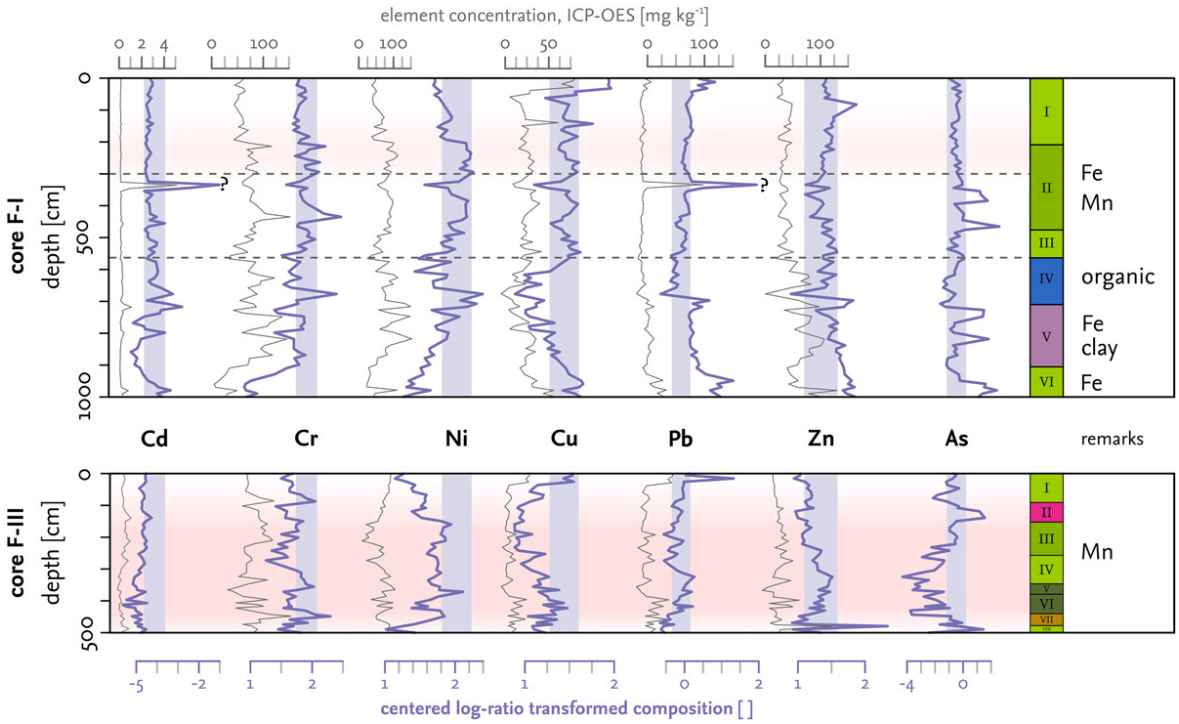

Figure 7.4 Heavy metal concentrations (gray lines) and centered log-ratio (clr) transformed trace metal(loid) composition (purple lines) of cores F-I (top) and F-III (bottom). The purple shadow highlights pre-metallurgical background values of alluvial sediments in core F-I (between dashed horizontal lines). Simplified unit-specific remarks are taken from core descriptions. The red background color marks the layers dating approximately to the ancient smelting period on Elba; for the key to the unit colors see Figure 7.7.

7.4.6 Core chronology

Core chronology is based on AMS radiocarbon dating of ten charcoal and five plant remains, conducted at the Poznan Radiocarbon Laboratory (Table A.4). Common ^{14}C-ages were calibrated in OxCal 4.2 (Bronk Ramsey, 2009) using the IntCal13 calibration curve (Reimer, 2013).

7.5 Results

Analysis of geochemical sediment characteristics and facies interpretation focuses on the two key-profiles of cores F-I and F-III from transect 1, as they cover mid- to late Holocene landscape development and human impact on the Campo plain. The analysis of core F-II and transect 2 (cores S-I and S-II) is undertaken to support the interpretation.

7.5.1 Core F-I

Core F-I has a total length of 10 m and was obtained from the alluvial plain near the confluence of Forcioni River and Galea River.

The element composition obtained by portable XRF was used to group core F-I in six geochemical units (cluster; Figure 7.5). Unit VI is characterized by low values of Sr, Mn, Cr, and Ca compared to some of the overlying units; the confidence interval of the normalized group geometric mean of these elements do not importantly overlap in the groups mentioned (Figure 7.5). Values of Rb, Zn, and Al are high in unit VI (and in unit V). (Fe,) Cr, and Ti contents increase between unit VI and V, whereas K contents decrease; Si-contents in unit V are low compared to the overlying units. Unit IV is characterized by an increase in Sr, Ca, and S-contents and a decrease in Rb and Fe. Except for a sharp decrease in S with decreasing depth, there is no difference between units III and IV; values of Sr and Ca in unit IV are low compared to unit II. There is no clear difference in the element composition between unit III, unit II, and unit I apart from high Mn-values in unit II.

Sediments are carbonate-free, show a varying texture from sandy clay to gravel, and are moist below 229 cm depth. Some important geochemical proxies of core F-I are given in Figure 7.6.

Basal sediments (unit VI, 1000–910 cm depth) consist of gravel in clayish matrix interlayered with yellowish brown loams. There is a marked peak in TOC and frequency-dependent magnetic susceptibility at 982–977 cm depth, which is accompanied by a change in color (Figure 7.6).

Above 910 cm depth (unit V) sediments are composed of greyish–brownish clay with abundant redox characteristics (iron mottles), occasional plant remains, and coarse sand or gravel interbedded (846–840 cm, 790–780 cm, and 760–743 cm depth).

A sand layer between 708 and 696 cm depth (subunit IV3) marks the distinct boundary between the clayish sediments and the overlaying layers, which mainly consist of black, soft gravel-free sandy loams (unit IV, 708–544 cm depth). The transition from unit V to IV is characterized by a recognizable decrease in sediment lightness (L*), pH-value (pH 3.6 at 700 cm depth), and the Fe/Mn-logratio; electrical conductivity (1,296 µS/cm at 700 cm depth), TOC (4.2 mass-% in 690 cm depth), S-contents ($mean\text{-}ilr = 726$ mg/kg, $SD\text{-}ilr = 0.2$, unit IV; $mean\text{-}ilr = 89$ mg/kg, $SD\text{-}ilr = 0.26$, core F-I, $n = 69$), Ca/Fe and Sr/K log-ratios strongly increase.

Between 544 cm depth and surface level, sediments are characterized by repeated normal grading from sandy layers to loam, and a brownish color. Manganese and iron mottles are abundant especially between 475 and 205 cm depth (unit II); Fe/Mn-log-ratios correspond.

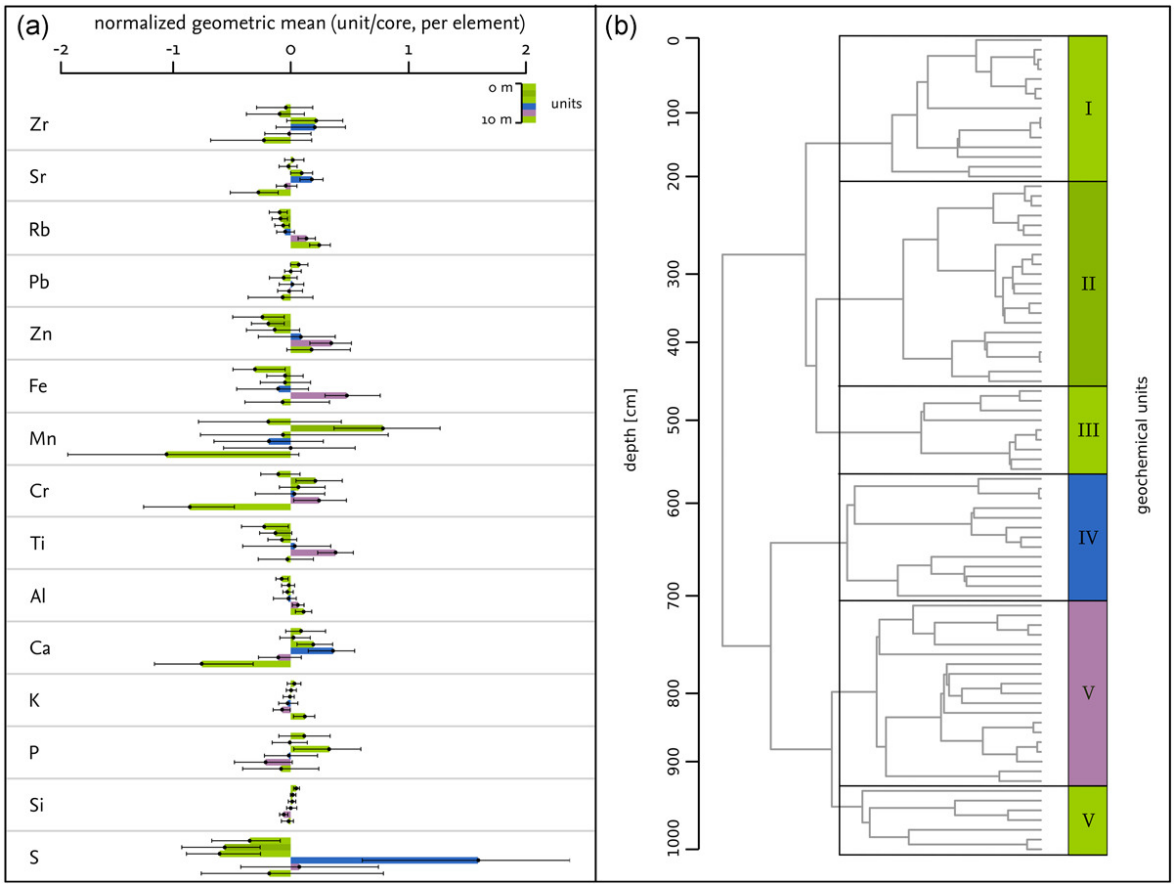

Figure 7.5 Geometric mean bar plot and clustering dendrogram of core F-I. Please note that the depth scale is not equidistant due to irregularly spaced sampling. For the key to the unit colors see Figure 7.7.

Charcoal and brick fragments were found between 229 cm depth and surface level; frequency-dependent magnetic susceptibility increases between 400 and 375 cm depth.

In the basal sediments, heavy metals and arsenic peak in the lowermost fine layer (980 cm depth); Cu and Pb also peak at 950 cm depth. In the clayish sediments between 907 and 708 cm depth, trace metal(loid) contents (except of Cu) are increased; in the organic-rich deposits between 708 and 557 cm depth, concentrations of Ni, Cr, and Zn are increased, whereas values of Cu decrease with depth. In the overlying sediments, two major peaks of As-values occur, which correspond to iron mottles (470/460 and 390–360 cm depth). Concentrations of Ni and Cr are increased between 475 and 205 cm depth, especially in layers with manganese mottles. Pb and Cd concentrations are strongly enriched at 350–340 cm depth (97 mg/kg and 5.1 mg/kg, respectively). A Cu-peak at c.130 cm depth corresponds to the occurrence of brick fragments. Concentrations of Pb and Cu are increased in the uppermost layers of core F-I. In Figure 7.4, contents of trace metal(loid)s are centered log-ratio transformed to facilitate a comparison with core F-III.

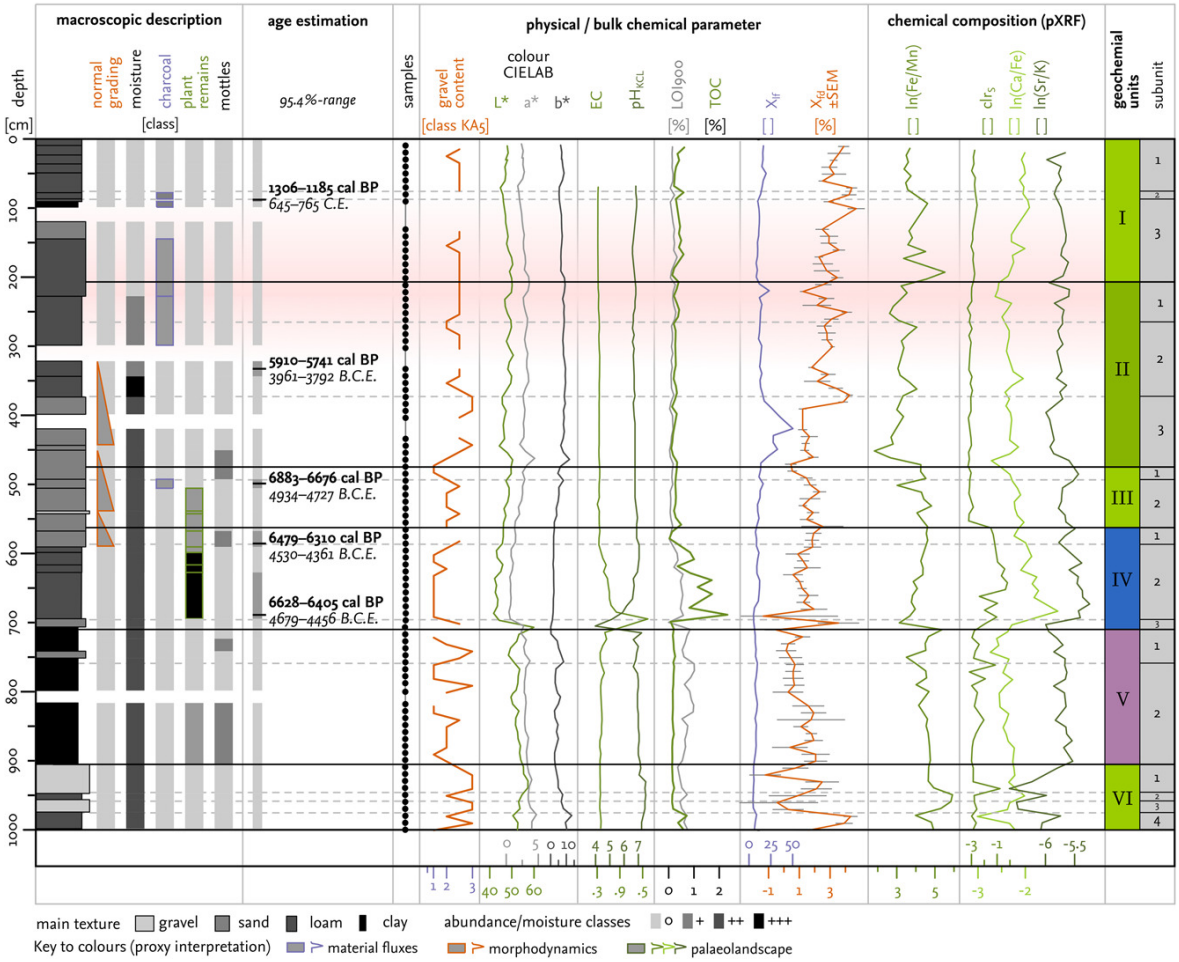

Figure 7.6 Macroscopic description, bulk chemistry, and elemental composition of core F-I. Gravel content and texture according to the classification of Ad-hoc-AG Boden (2005). Calibrated radiocarbon ages are given at the 95% confidence level. The red background color marks the layers dating approximately to the ancient smelting period on Elba; for the key to the unit colors, see Figure 7.7. EC: electrical conductivity; LOI: Loss-on-ignition; TOC: Total organic carbon content; X: Mass-specific magnetic susceptibility; %fd: frequency-dependent susceptibility; SEM: standard error of the mean; clr: centered log-ratio transformed

7.5.2 Core F-II

Sediments exposed in core F-II (Figure 7.7) were divided into two units based on element composition. Sediments in unit II (500–248 cm depth) are marked by alternating layers of fines (dark gray silt loam) and coarse layers (yellowish-greyish brown loamy sand). The basal layer of core F-II (500–418 cm depth) consists of silt loam rich in charcoal fragments. Contents of arsenic in unit II are characterized by several peaks at 492–378 and 292–242 cm depth, corresponding to the occurrence of iron mottles. Sediments in unit II (248–0 cm depth) consist of an organic-rich, dark gray silt loam with abundant plant remains (248–172 cm depth) and an overlying sand–sandy loam layer (172–110 cm depth); the upper layers in unit II (110–0 cm depth) consist of light brown loamy sand

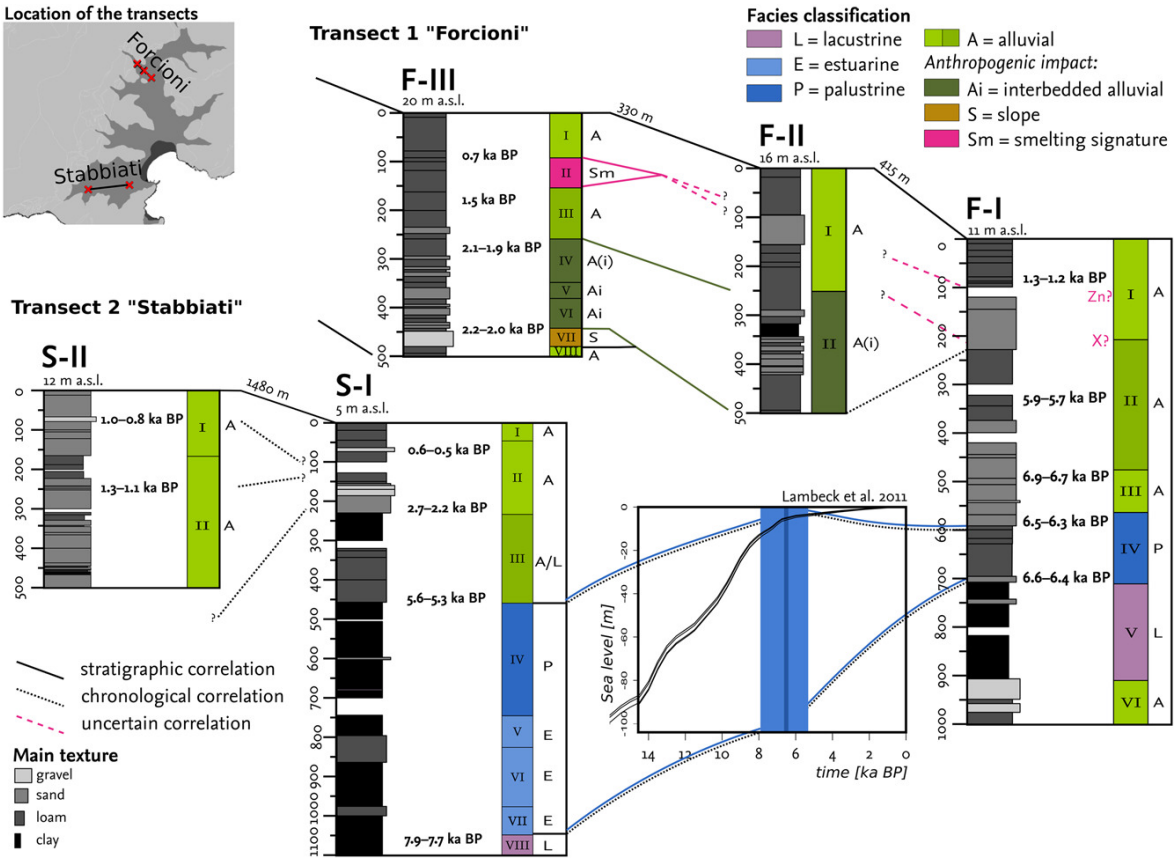

Figure 7.7 Overview of cores in the two analyzed transects. Correlation according to radiocarbon dates and corresponding facies. Layers showing marine influence (paludal and palustrine facies) are correlated to Holocene sea level rise (Database: Lambeck et al., 2011, data from northern Tyrrhenian Sea)

containing plant remains and a distinctive root structure. In addition, As contents peak between 248 and 192 cm depth, corresponding to the occurrence of iron mottles.

7.5.3 Core F-III

Based on clustering of the sediments' element composition, the sediment sequence obtained by core F-III is grouped into eight units (Figure 7.8) that correspond to the lithological differences. The element composition of units VIII, VI, and V is not clearly different, whereas the interlayered unit VII is characterized by increased contents of Sr, Rb, As, Zn, Fe, Mn, Ti, Ba, Ca, and decreased contents of Al and Si. Units IV, III, and I also show no clearly different composition between elements except for partly decreased contents of Mn (unit IV) and increased contents of Cr (unit III). Compared to units VIII–V, sediments in these units are (partly) increased in Zr, Sr, As, Zn, Fe, Mn, Ti, and Ca. Sediments grouped in unit II are characterized by increased values of As and Fe compared to the over-/underlying unit. At the base of core F-III bedrock fragments are exposed, overlain by

sandy loams with low LOI_{560}. Between 459 and 440 cm depth (unit VII) sediments consist of moist angular to sub-angular gravel in a loamy matrix, Ti/Si log-ratios are low compared to over- and underlying units (Figure 7.9). Between 440 and 258 cm depth, sediments consist of sand or sandy loam alternating with dark gray (sandy clay) loam. There are few charcoal fragments in the loamy layers below and abundant fragments above 347 cm depth; peaks in TOC contents correspond to charcoal concentrations. Zr/Rb log-ratios show high variability in unit VI (440–380 cm depth) and unit IV (348–254 cm depth)—and are generally high in unit V (380–348 cm depth; Figure 7.9). Gravel contents, Zr/Rb log-ratios, and texture descriptions vary in parallel. Unit IV contains non-dating sherds (326–321 cm depth). Sediments between 258 and 154 cm depth consist of slightly moist sandy (clay) loam high in charcoal and organic matter contents. Manganese mottles are recorded within moist layers at 234–197 cm depth. Fe/Mn log-ratios widely correspond to the pattern of Fe- and Mn-mottle occurrence (Figure 7.8). Values of pH are high in the lower layers, but decrease constantly below 170 cm depth. Brick fragments are abundant in 234–206 cm depth and sherds below 200 cm depth. A *ceramica d'impasto* fragment (c 166 cm depth) dates to the 3rd or 2rd century BCE. Below 155 cm sediments contain slag and hematite fragments up to 2 cm in diameter. The abundance of slag fragments coincides with a distinct increase in magnetic susceptibility from 150 to 110 cm depth. The surface layers (92–0 cm depth) consist of sandy clay loam rich in plant remains and root fragments; charcoal fragments are almost absent. Mn mottles are recorded at 112–92 cm depth at the present boundary between moist and dry sediments. The electrical conductivity of the sediments' easy solubles increases strongly in the upper part of unit I, where pH-values are relatively low (Figure 7.9).

7.5.4 Core S-I

Two sediment cores were extracted from the Stabbiati valley; core S-I was extracted close to the present coastline (c 0.5 km linear distance; 5 m a.s.l.), core S-II was extracted from the higher parts of the plain (c 1.6 km linear distance to the present coastline; 12 m a.s.l.).

Sediments in core S-I consist of greyish–blackish (sandy) clay with distinct Fe-mottles in layers below 1045 cm depth, plant or charcoal remains were not observed. Between 1045 and 825 cm depth sediments are more bluish and less clayish; a distinct increase in electrical conductivity, S-contents, S/K and Fe/Ca log-ratios and a decrease in pH-values (Figure 7.10), coinciding with a change from clayish to loamy texture, is observed. There is a small interbedded layer with high gravel contents at c 930 cm depth. Below 825 cm depth sediments consists of a brownish–blackish gray (sandy) clay to loam; plant remains were not observed. Sediment pH-values and log-ratios of Fe/Ca and Sr/K decrease with

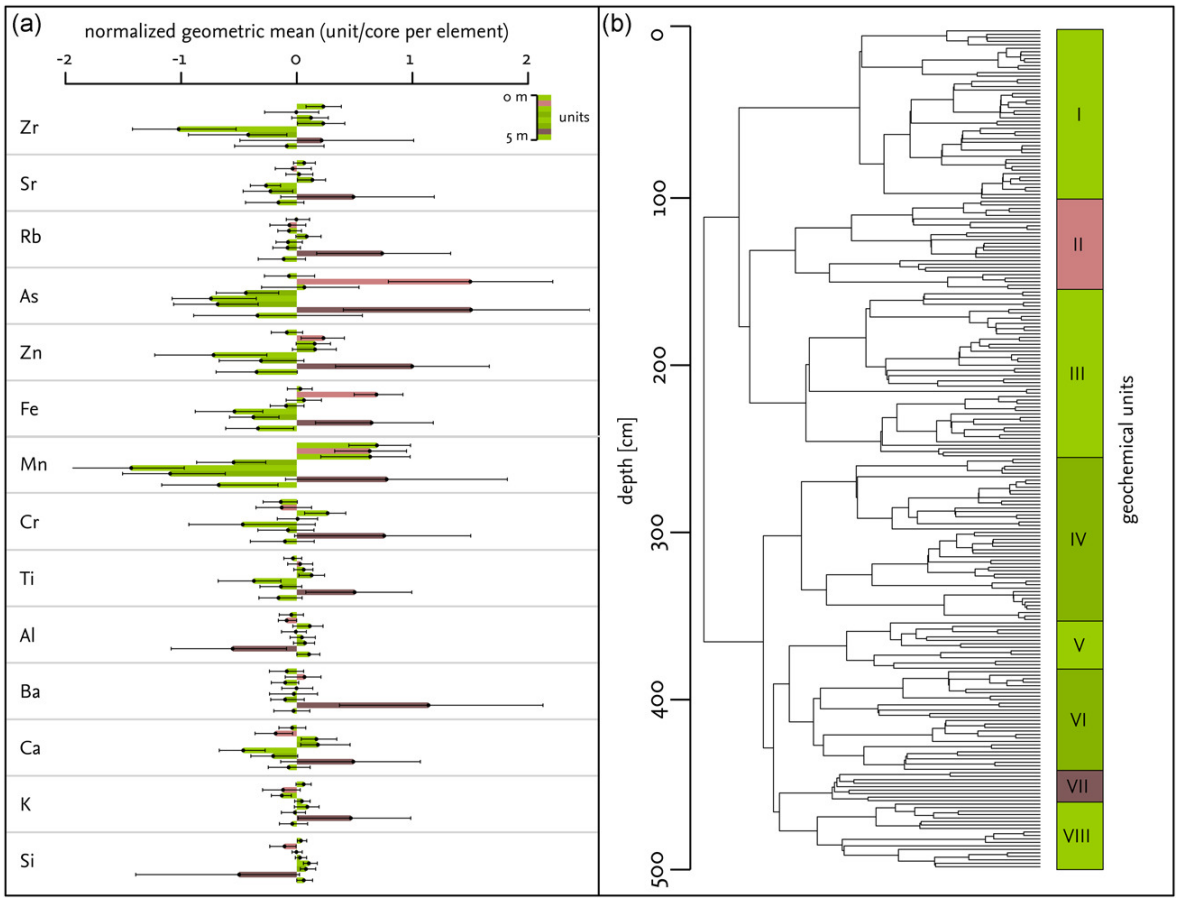

Figure 7.8 Geometric mean bar plot and clustering dendrogram of core F-III. For the key to the unit colors, see Figure 7.7.

increasing depth. Sediments in the overlaying layers (720–457 cm depth) consist of a blackish gray wet, soft-ductile sandy clay interbedded by a mottled greenish loamy sand layer at 603–597 cm depth and a gravelly sandy clay at 540 cm depth. Contents of Fe, Al, K, Zr, and Cr, and electrical conductivity peak around the greenish layer, whereas pH-values are low. Values of TOC contents peak parallel to an abundance of visible plant remains (Figure7.10). S contents show distinct peaks. At 427 cm depth a distinct layer boundary occurs, which is documented by changes in color, bulk chemistry, texture, and elemental composition. Sediments consist mainly of (sandy) loam, interlayered by a clay layer with abundant iron mottles and plant remains and a peak in K/Sr log-ratios between 300 and 230 cm depth; gravel contents increase above 280 cm depth. Between 230 and 42 cm depth layers are characterized by fining upward cycles; coarse charcoal detritals and stones are abundant in the lower section of the unit (Figure 7.10). Sediments show distinct hydromorphic characteristics (iron mottles) above the water table during sediment exposure (c 186 cm depth), which is also visible by a change in sediment color (Figure 7.10). The surface layer consists of a brownish, slightly gravelly (silt) loam with a dense root structure and undecomposed plant remains. TOC contents decrease from top

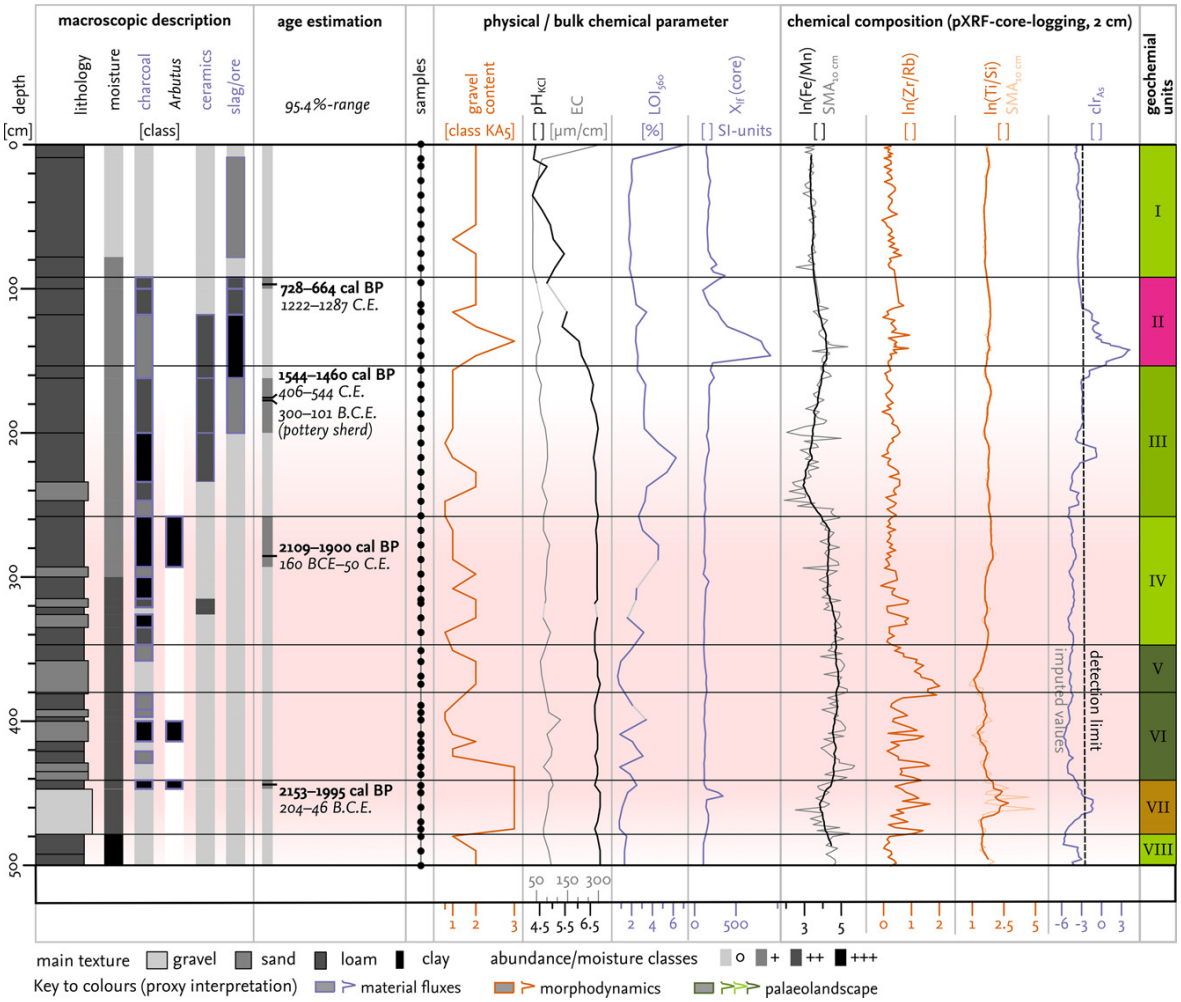

Figure 7.9 Macroscopic description, bulk chemistry, and elemental composition of core F-III. Gravel content and texture according to the classification of Ad-hoc-AG Boden 2005. The red zone marks the ancient smelting period. For the key to colors, see Figure 7.7. EC: electrical conductivity; LOI: Loss-On-Ignition; X: Mass-specific magnetic susceptibility (core logging); SMA: simple moving average; clr: centered log-ratio transformed; *Arbutus*: typologically characterized charcoal samples are *Arbutus*.

to bottom. The pH values are relatively low and electrical conductivity reaches minimum values (Figure 7.10). Values of As concentration show distinct peaks at 450 cm depth and 350 cm depth, corresponding to the occurrence of iron mottles.

7.5.5 Core S-II

The sediment sequence exposed in core S-II is subdivided into two major units, mainly driven by variation in texture. The underlying unit II is marked by alternating layers of gravelly coarse sand (432–400 cm depth and 248–223 cm depth), loamy sand, and silt loams (500–437 cm depth and 400–248 cm depth). Between 400 and 248 cm depth, iron mottles are abundant. A thin layer with high yields of charcoal fragments is embedded

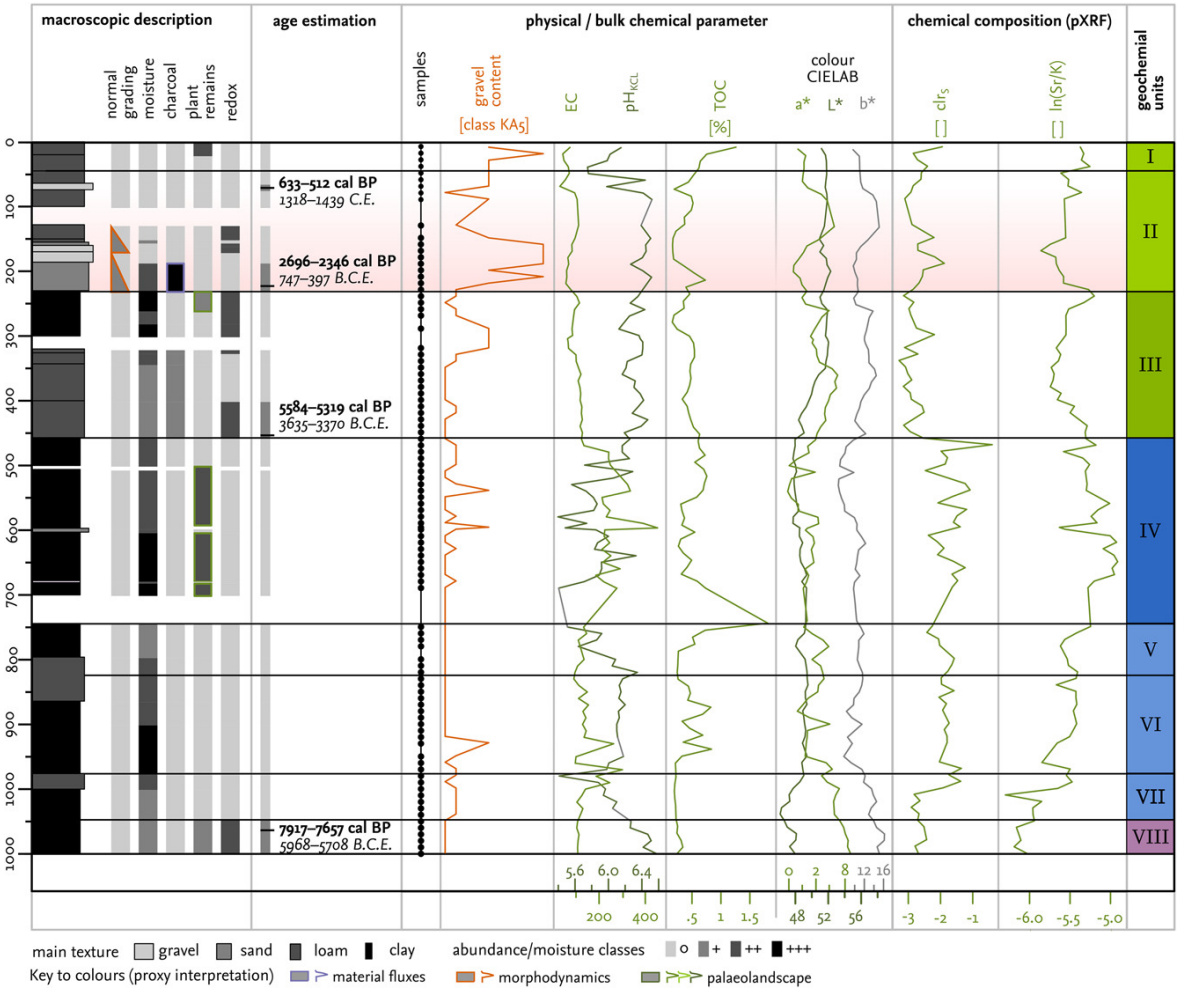

Figure 7.10 Macroscopic description, bulk chemistry, and elemental composition of core S-I. Gravel content and texture according to the classification of Ad-hoc-AG Boden (2005). The red background color marks the layers dating approximately to the ancient smelting period on Elba; for the color key to the unit colors, see Figure 7.7. EC: electrical conductivity; TOC: Total organic carbon content; clr: centered log-ratio transformed.

in 252–248 cm depth; beyond this, unit II is free of macroscopically visible charcoal fragments. Sediments in unit I consist of sandy–silt loam interbedded with a loamy sand layer and densely rooted in the topsoil layer (64–0 cm depth). Distinct hydromorphic characteristics occur between 188 and 79 cm depth. Charcoal content is high and peaks between 188 and 79 cm depth.

7.6 Discussion

We provide an overview of mid- to early late Holocene sedimentation dynamics in the Campo area before we discuss the direct imprint of iron smelting on the sediment history on Elba. The aim is to, first, assess the development of site location factors, and, second,

to grasp the landscape dynamics before the onset of the iron metallurgical period in the 4th/3rd century BCE. The contextualization is especially important for understanding the background variability of trace metal(loid)-contents and morphodynamics.

7.6.1 Mid- to early late holocene sediment history

Holocene sea level rise

Geochemical proxies (Table 3) show a marine imprint on the sediment sequences of cores F-I (unit IV) and S-I (units VII–IV); the radiocarbon ages of the sediments allow a correlation to the post-LGM sea level rise in the Tyrrhenian Sea (Figure 7.7). Sediments exposed in cores F-II and F-III do not indicate any marine influence on the depositional processes because the upstream section of the Forcioni valley was not affected by Holocene marine inundation. Core S-II with a total depth of 5 m was presumably not deep enough to reach littoral deposits (cf. Bertini et al., 2014). The initial, late- to postglacial valley infills (>6.5 ka BP) deposited under early transgressive conditions are marked by gravel deposits in core F-I (unit VI; cf. Breda et al., 2016); the dominance of conservative (i.e., weathering-resistant) elements in the fines of these deposits (Ti, Rb, and Zr contents; Figure 7.6) indicates pre- or synsedimentary intensive weathering. A thin fossil soil layer (subunit VI2) is interlayered into the gravels, as indicated by an increased TOC content, peaking frequency-dependent magnetic susceptibility (cf. Alekseeva et al., 2007), and a darker–reddish color indicating pedogenic iron (Jarmer & Schütt, 1998). This soil layer corresponds to early transgressive palaeosoils dating to the Pleistocene–Holocene boundary, known from the Tuscan coast (Amorosi et al., 2014a).

Sediments in unit V (core F-I) and in the basal unit of core S-I are interpreted as low-energy, lacustrine still water deposits, as indicated by the clayish texture and occasional plant remains; relatively increased values of Fe, Al, Rb, and Ti in the elemental composition of unit V support this interpretation (cf. Cuven et al., 2010; Loring, 1991; Turner et al., 2015). The gray color and a distinct Fe-pattern (Figure 7.6) indicate reducing conditions as present in an oxygen-poor environment (Klein et al., 2016). A gravel layer interbeds the lacustrine deposits (subunit V2). Coarse layers indicate (increased) riverine inflow (Schillereff et al., 2014). Slightly increased values of electrical conductivity and of S contents emphasize a terrestrial to a brackish environment (cf. Chagué-Goff, 2010).

The transgressive boundary dates to c 6.5 ka BP in core F-I (unit IV) and between 7.7 and 5.4 ka BP in core S-I (units VII to IV), corresponding to late transgressive conditions around meltwater pulse (MWP) 1C (Blanchon & Shaw, 1995; Figure 7.7). Transgressive boundaries obtained on the Tuscan mainland date to MWP 1A or MWP 1B (Amorosi

et al., 2013b; Breda et al., 2016). Sediments in unit IV (F-I) show the textural and chemical characteristics of a brackish, palustrine, microtidal (<0.4 m), low-energy coastal environment (Edwards, 2007). Increased values of S and peaking Sr/K log-ratios point to a distinct influence of seawater on the depositional environment (Chagué-Goff, 2010). Other characteristics indicating a marine environment such as increased B, Br, and Cl contents (Chagué-Goff et al., 2017; López-Buendía et al., 1999) remain below the instrumental detection limit of the pXRF-device, but peaking values of electrical conductivity and TOC/plant remains and low pH values confirm a marine to brackish depositional environment. This interpretation is underlined by the strongly increased sulfur contents, which are related to the sulfur cycle of a coastal environment (cf. Jørgensen, 1977). Comparison of these proxies indicating littoral facies deposited under the marine influence between units IV and V suggests that the marine influence on the sediments of the underlying unit V is relatively low. For the sediments in unit IV the intrusion of salty groundwater (see, for the case of the Campo plain, Giardi et al., 1983; Giménez-Forcada et al., 2010) has to be considered to have influenced sediment characteristics post-depositionally; secondary salt precipitation in the sediment pores might dissemble a primary marine depositional environment. Nevertheless, the intrusions did not influence the abundance of plant remains and TOC contents.

The maximum flooding surface in core F-I corresponds to the coarse sand layer (probably a beach deposit) at the base of the palustrine unit, where proxies for marine influence are most pronounced; this layer dates to 6.6–6.4 ka BP.

In core S-I, palustrine–estuarine deposits (units VII to IV) reflect varying marine influence. Increased S contents in these units as well as the high Sr/K log-ratios, high pH values, increased electrical conductivity and increased TOC support this deduction (Chagué-Goff, 2010). Oscillating values and interlayered gravelly sands point on occasional river inflow, indicating a fluvio-lacustrine environment as typical for river mouths. This discontinuity corresponds to phases of fluvial activity or quiescence observed in the Mediterranean region (Benito et al., 2015b; Piccarreta et al., 2011) and to oscillations in sea level rise during the Holocene (Figure 7.7).

The maximum flooding surface in core S-I is marked by coarse detrital input and greenish mottles (c 600 cm depth), interpreted as glauconitic sands, which reflects inland transport of shelf sediments (Williams & Meisburger, 1987). Concurrent relative maxima of Al, K, and Fe contents in the geochemical record (along with high Si contents) support this interpretation. This minimum depth of marine inundation dates between 7.7 and 5.4 ka BP; a period that corresponds to the turning point from late transgressive to early high-stand conditions in the Tyrrhenian Sea (Lambeck et al., 2011; Figure 7.7).

Early high-stand morphodynamics

Lacustrine–palustrine deposits in core F-I and S-I are overlain by alluvial facies associations. S contents and electrical conductivity are low in unit III (F-I) compared to unit IV (F-I), indicating a transition from marine–brackish to terrestrial conditions. The transition is marked by a continuous change in color from blackish (unit IV) to brownish (unit III; Figure 7.6); increased Sr contents of unit III in core F-I also underline a littoral depositional influence (Chagué-Goff, 2010).

In core F-I (units III and II) the lower alluvial deposits are characterized by several fining-upwards cycles. Gravelly sand layers indicate channel-associated sedimentation (Schneider et al., 2014) in braided river systems; estimated aggradation rates during early high-stand conditions (6.5–6.4 ka BP: 12 mm/a; 6.4–5.8 ka BP: c 5 mm/a) exceed later aggradation (<5.8 ka BP: <2 mm/a). The frequency-dependent magnetic susceptibility record may indicate a lower variability after the early alluvial phase. The change from channel-associated or (near-channel) coarse flood sedimentation in the lower alluvial succession to non-grading alluvial fines in the upper alluvial deposits corresponds to changing aggradation rates and is typical for early high-stand conditions in the Tyrrhenian Sea (cf. Amorosi et al., 2013b; Breda et al., 2016). The period of high aggradation does not necessarily correspond to known superregional (Benito et al., 2015a; Macklin et al., 2006) or regional (Borrelli et al., 2013; Piccarreta et al., 2011; Vincenzo et al., 2013) flood-prone phases. Thus, the post-transgressive valley architecture explains the decrease in aggradation (Brückner, 1983). Trends in the aggradation rate deduced for core F-I are similar in core S-I (Figure 7.7). However, normal grading is limited to the upper alluvial sections in core S-I. The difference in normal grading between the cores is related to different valley morphologies coinciding with differences in channel width and channel gradient (Figure 7.2).

7.6.2 Sediments deposited in the context of iron smelting (since c 2.4 ka BP)

Palaeolandscape

From c 6.9–6.3 ka BP alluvial conditions prevailed in the Forcioni valley. Marine influence in the lower part of the Campo plain (core S-I) diminished around 5.6–5.3 ka BP, but lacustrine deposition occurred until c 2.7–2.3 ka BP. At other locations in the Campo coastal plain, wetland conditions prevailed. (a) The microfaunal assemblage characterization of sediments obtained from the Campo plain display brackish-lagoonal conditions between 3.8 ka BP and 1.4 ka BP and an onset of palustrine conditions after 2.2 ka BP (Bertini et al.,

2014; Toti et al., 2014). (b) The toponyms *Lo stagno* (it. pond) and *La Maremma del Elba* (Ferruzzi, 2010; Pagliantini, 2014) indicate original swampy conditions in the southern Campo plain. (c) Hydrophilic vegetation occurs in small patches in palaeo-palustrine areas (Foggi et al., 2006b). Therefore, in the south(west) of the Campo plain wetland conditions prevailed also during the ancient smelting period; this might explain why smelting sites are unknown in the area, both in the coastal strip and the inland. The results from the Forcioni valley show that no wetlands were present in the upper part of the plain during the smelting period, so that better accessibility can be assumed.

Morphodynamics

The changes in the depositional environment from lacustrine to alluvial in core S-I (around c 2.4 ka BP) correspond to the proposed beginning of ancient iron smelting around the Campo plain (4th/3rd century BCE) and might indicate a change in morphodynamics.

Also cores F-II, F-III, and S-II show a distinct pattern of changing morphodynamics, such as the deposition of high magnitude flood layers and an interbedded succession of coarse and fine sediments. The geochemical pattern of Zr/Ti and Zr/Rb log-ratios supports the interpretation as high magnitude flood deposits, because Rb, Ti, and Zr are associated to different grain-size fractions (Turner et al., 2015). In core F-III these layers date between 2.1 and 2.0 ka BP.

The phases of intense morphodynamics in the Campo area (c 2.4–2.0 ka BP) overlap with Mediterranean-wide flooding phases (2.3–2.1 ka BP; Benito et al., 2015a) including south and central Italian phases of high fluvial activity (2.35–1.85 ka BP; Piccarreta et al., 2011, 2.2-2.0 ka BP, Borrelli et al., 2014). In contrast, contemporary lake level low stands of Lago dell'Accesa (Magny et al., 2007) and lower propagation of the Tiber delta (Bellotti et al., 1995) point to warm and dry conditions ('Roman climatic optimum') during the flood-prone phases; it, therefore, appears unlikely that increased fluvial activity was caused by a regional climatic trigger alone. Furthermore, local flood-prone phases coinciding with phases of human occupation are typically an indicator for a human-induced acceleration of fluvial activity (for Italy, see, e.g., Ayala & French, 2005; Boenzi et al., 2008; Borrelli et al., 2014; Brückner, 1983). On Elba Island, human pressure is said to have increased during the period of Roman iron smelting (especially in the 2nd century BCE) and to a smaller extent in the medieval period due to the demand for wood fuel (see Section 7.1).

In addition to flood layers, the sub-angular gravel deposits in core F-III (unit VII, c 2.2 ka BP) indicate soil erosion processes on the slopes during the period of ancient smelting. The interpretation as slope deposits interlayering the alluvial sediment sequence is supported by the distinct overall geochemical pattern of the sediments: Zn values of the sediments

are increased corresponding to those of the slope bedrock (Palombini shale; $z = 1.66$, $p = 0.048$; Dunn test). Decreased Si/Ti log-ratios in the gravel layers support this interpretation: a Kruskal–Wallis test indicates a difference in Si and Ti contents between the lithological units in the Forcioni catchments (Si: $\chi^2 = 50.92$, $p < 0.001$; Ti: $\chi^2 = 51.42$, $p < 0.001$); Si/Ti ratios of Palombini shale on the slopes ($mean = 41$, $SD = 14.4$, $n = 4$) are lower than the granitic bedrock in the wider catchment ($mean = 101$, $SD = 72.8$, $n = 8$).

The clear imprint of increased morphodynamics in the upper Forcioni floodplain is related to the location of the Forcioni valley in a cluster of smelting sites (Figure 7.2). Also in the Stabbiati valley, intensified morphodynamics are indicated by the change from palustrine to alluvial conditions, although the density of smelting sites is lower here. High magnitude flood layers in core S-II cannot be directly related to the ancient smelting period (radiocarbon dates only reveal a *terminus ante quem* of 1.2 ka BP).

A layer of initial soil formation in core F-I dates to c 1.3 ka BP and corresponds to a stability phase in the western Mediterranean region (Benito et al., 2015a; Piccarreta et al., 2011). This stability phase is not concurrent with the medieval smelting phase (11th to 14th century) and predates the onset of the documented foundations of the villages in the Campo area (from 11th century).

Charcoal record

In core F-I, macroscopic charcoal content increases around 2.3 ka BP. Also in the Stabbiati transect covered by S-I, an increase in the charcoal content occurs corresponding to the onset of the period of iron smelting. Large charcoal fragments with diameters up to 10 mm are abundant in core F-III (450–280 cm depth, 2.2–1.9 ka BP). Their uniform typological distribution (14/14 samples are classified as *Arbutus*, Dinies, DAI Berlin, personal communication, 2016) suggests an origin by charcoal production. *Arbutus unedo* is a common Mediterranean species for coppicing and charcoal production (Carrari et al., 2017), although *Erica arborea* was possibly preferred (Mariotti Lippi et al., 2000). Subassociations of *Erico arboreae-Arbutetum unedonis Allier & Lacoste 1980 ex Foggi in Foggi & Grigioni 1999* (high macchia shrubland dominated by tree heath and strawberry tree) are typical for the recent vegetation on the slopes around the Campo plain (Foggi et al., 2006b). Low species variability in the anthracological record has been shown for a smelting site on the Tuscan mainland (Rondelli, 6th–5th century BCE, Sadori et al., 2010). and for Roman imperial charcoal production (Veal, 2017b).

Sedimentary smelting signatures

Ancient iron smelting has been found for the Forcioni catchment (Corretti, 1988; Figures 7.1 and 7.2). Direct sedimentary evidence of smelting by ore and slag fragments is macroscopically evident in core F-III and to a lower extent in core F-II.

Heavy metal (Pb, Zn, Cr, Ni, Cd, and Cu) and arsenic concentrations show a distinct pattern of variation in core F-I (Figure 7.4). This pattern is mainly explained by natural background noise. Increased concentrations of Ni and Cr in the alluvial facies (unit II) correspond to the occurrence of Ni- and Cr-bearing Serpentinite in the study area (Figure 7.2) and the adsorption of Ni and Cr in manganese mottles (see Figures 7.5 and 7.6; cf. Kierczak et al., 2007; Rinklebe et al., 2016). Concentrations of Pb and Zn are increased in the fine-grained lacustrine facies exposed in core F-I (unit V; grain-size effect, Ackermann, 1980). Pb, Zn, and Ni are additionally accumulated in the organic-rich palustrine facies (unit IV). Increased concentrations of As in the sediments directly correspond to the occurrence of iron mottles because As gets adsorbed by sesquioxides (Matschullat, 2000).

Several distinct peaks in trace metal(loid) concentrations in core F-I exceed the pre-metallurgical background values of the alluvial sediments (units III and II; Figure 7.4, purple shadows). (a) Peaking concentrations of Pb and Cu in the topsoil unit are linked to atmospheric deposition after the onset of the Industrial Revolution (Shotyk et al., 1998) or the beginning of the combustion of leaded petrol (Renberg et al., 2001). (b) A second Cu-peak at c 160 cm depth, dated to a *terminus post quem* of 2.3 ka BP, may be caused by the presence of brick fragments in the respective layer, although an impact caused by iron smelting cannot be ruled out as Cu is slightly enriched in historical ferrous slags (Costagliola et al., 2008; Piatak et al., 2015).

Trace metal concentrations in core F-III are widely below pre-metallurgical background values as obtained in core F-I (Figure 7.4). The slight enrichment of Ni, Cr, Cd, As, Cu, and Zn between 500 and 380 cm depth is linked to slope deposits from Palombini shale and the occurrence of serpentinite in the catchment, because trace metal(loid) concentrations are typically increased in shale and ultramafic rocks compared to granitic bedrock (Salminen et al., 2005). Peaking Cu and Pb concentrations in the topsoil correspond to (sub)recent atmospheric deposition.

The most striking features in core F-III are increased values of arsenic (Figures 7.8 and 7.9, 166–144 cm depth). We assume that pXRF-measured As values are not subject to an As-Kα/Pb-Lα interference as As-Kα and As-Lα peaks are included in in-device calibrations (Parsons et al., 2013). Furthermore, ICP-OES measurements document that there is no correlation between $Pb_{ICP\text{-}OES}$ and As_{pXRF} (core F-I, $\rho = 0.26$), The As-rich layer contains slag and ore fragments—arsenic is enriched in slag relative to bedrock (Dunn test, $z = -2.66$,

$p = .004$)—and shows a distinct pattern of high magnetic susceptibility (Figure 7.9, values are up to 600×10^{-5} SI-units higher in the slag layer), exceeding values of pre-metallurgical sediments (core F-I, Figure 7.6).

A rise of mass-specific magnetic susceptibility to values larger than 20×10^{-8} m^3/kg ($K = 20 \times 10^{-6}$, SI-units) might indicate a possible anthropogenic imprint (cf. Hanesch & Scholger, 2005)—a marked peak in magnetic susceptibility recorded in core F-I ($K = 50 \times 10^{-6}$, SI-units; c 6.9–5.7 ka BP) predates the Roman smelting period; a second smaller peak may date to the Roman period. Vigliotti et al. (2003) show that magnetic susceptibility, as well as other magnetic properties of marine sediment west of Elba Island, are enriched in layers dating to the ancient smelting period on Elba. Mighall et al. (2009) conclude that magnetic susceptibility helps to detect ore remains and furnace dust (at least in peat records); i.a., Powell et al. (2002) and Birch et al. (2015) state that a magnetic susceptibility is a valuable tool for identifying iron smelting activities on sites. Because of the more pronounced pattern of As in core-logging data compared to homogenized samples of the <2 mm sieve separate, we assume that the enrichment of arsenic is mainly related to the presence of (coarse) slag fragments (cf. Raab et al., 2010). Simultaneously increased pre-metallurgical background values of As and Fe are likely related to adsorption of As(III) on (pedogenic) Fe-oxides (cf. Matera et al., 2003; Matschullat, 2000).

Arsenic enrichments are documented for surficial marine sediments obtained from the Elba-Argentario basin off-shore Elban iron deposits and modern blast furnaces in Piombino (Leoni & Sartori, 1997; Leoni et al., 1991); in addition, the results of Leoni et al. (1991) may indicate the weathering of ancient waste heaps in the metallurgical center of Populonia. Vigliotti et al. (2003) show a strong relation between metallurgy on Elba and airborne As-deposition in marine sediments from the Corsica channel west of Elba. In contrast, arsenic anomalies in the Pecora valley sediments (Tuscan mainland) are related to natural As-sources, although ferrous and non-ferrous smelting took place in the catchment (Costagliola et al., 2008). Low As-concentrations in the ferrous slags found in the area is nevertheless higher than the natural background value in the Campo plain, corresponding to the enrichment of arsenic in historical ferrous slags (Piatak et al., 2015). In hematite ore, the arsenic content is higher than in slags, mainly because of contamination with pyrite. Besides, dissolute (natural) As(III) might also be bound to metallogenic Fe-oxides in slags (cf. Mohan & Pittman, 2007). Corrected heavy metals are not enriched in the slag layer (core F-III, Figure 7.4, purple lines), although increased values of Pb and Cu compared to the pre-occupational sedimentary background values (core F-I) are known from some Tuscan ores, slags, and mining areas (Benvenuti et al., 2013, 2000b, 2016; Costagliola et al., 2008; Servida et al., 2009). Nonetheless, heavy metal contents of pre-industrial slags and ores are often only slightly increased (Piatak et al., 2015; seeBenvenuti et al.,

2013, 2000b, 2016; Costagliola et al., 2008 for example from Tuscany). The mobility of heavy metals in the slag-containing layer may be increased, as pH-values decrease in the respective depth (Figure 7.9), although not below pH 5.4. Thus, the increase in mobility may not be important (cf. Bradl, 2004; Martínez & Motto, 2000). Relatively constant LOI_{560}-values and the constant texture in the units over-/underlying the slag layer indeed indicate that mobilization of heavy metals might not have been important. Zn-peaks in cores F-I and F-III are possibly caused by human impact as Zn, like Cu, occurs enriched in slags (Benvenuti et al., 2013). The radiocarbon chronology of the cores indicates that these peaks might date to c 1.3–1.2 ka BP (7th/8th century CE century; F-I) and to >2.2–2.0 ka BP (3rd–1st century BCE; F-III); the latter date corresponds to the ancient iron smelting period. Corresponding values of As are not increased at the same depth, and magnetic susceptibility is low. A resilient interpretation of Zn-peaks is hence suggestive.

Charcoal samples from core F-III date the smelting signature roughly between the 5th and the 13th century CE (at 95% confidence, Figure 7.9). The stratigraphic order of cal-^{14}C-ages in core F-III is without any age-inversions. Nevertheless, an ancient sherd fragment in the slag layer dates to the 3rd to 2nd century BCE, indicating metallurgical remains of Roman age. The smelting sites in the Forcioni valley are accordingly dated to the 2nd to 1st century BCE (Corretti, 1988; Pagliantini, 2014)—in the Forcioni valley, no archeological traces of medieval smelting are reported (Corretti, 1991; Corretti & Firmati, 2011). Thus, metallurgical fragments in core F-III might have been subject to postdepositional reworking and secondary deposition after catchment storage in for example, slope deposits (de Moor & Verstraeten, 2008; Lang & Hönscheidt, 1999) or temporally lacking sediment connectivity (Bracken & Croke, 2007). A survey in 2016 showed that slag fragments frequently occur in reworked slope deposits (Figure 7.3), slag fragments were in addition recovered from the recent channel bed down- and upstream of coring location F-III.

In summary, the clear identification of a sedimentary smelting signature in the present cores is possible, combining both arsenic contents and magnetic susceptibility. The lack of a smelting signature in core F-I is explained by the location of the core in a wider floodplain and resulting alluvial architecture; metallurgical remains or impacted sediments may not have been deposited in a regular vertical distribution (Brewer & Taylor, 1997; Hürkamp et al., 2009; Macklin et al., 1994). In addition, core F-III is located in close proximity to slag deposition sites (Figure 7.3). Nevertheless, a small peak in magnetic susceptibility in F-I might be related to iron smelting, also no increase in As and slag/ore fragments were recorded.

7.7 Conclusions

Human–landscape interactions are hypothesized to play an important role in understandings of pre-industrial iron smelting on Elba Island. Deforestation, and resulting changes in morphodynamics, are regularly cited as explaining the supposed abandonment of smelting sites on the island (i.a. Meiggs, 1982). The Greek name of Elba, *Aithάleia*, is related to emissions from bloomeries (Diodorus of Sicily 5.13.1). The smelting site pattern on Elba is described as being linked to coast–inland interactions (landing possibilities and access to secondary resources).

Sediment sequences from the Campo coastal plain offer new evidence to supplement the existing perspectives on human–landscape interactions during the ancient period of iron smelting on Elba Island.

1. The palaeolandscape of the Campo plain is strongly influenced by the Holocene transgression. During the subsequent period of ancient smelting, marine influence was low in the vicinity of the smelting sites at the northern boundary of the plain; in the Forcioni valley wetland conditions prevailed only until 6.4 ka BP. In the low-lying parts of the Stabbiati valley, where no smelting sites are known, wetland conditions dominated until subrecent times. Thus, the accessibility of the Forcioni valley (Cambi, 2004) and the idea of coastal configuration as a site location factor (Corretti, 1988) are evident in the sedimentary record.

2. Aggradation in the Forcioni valley is triggered by (a) high dynamics caused by sea-level rise during early high-stand conditions (channel-associated deposition), and (b) human impact since the 4th century BCE: Slope deposits, high-magnitude flood layers, and a change from palustrine to alluvial deposition indicate increased morphodynamics during the period of Roman iron smelting (3rd to 1st century BCE). Accelerated aggradation during the period of medieval iron smelting is not evident in our sediment sequences but is at least preceded by a phase of relative stability. Intensified morphodynamics are most likely caused by local wood consumption; the impact of smelting on the forest cover is evident from the deposition of abundant charcoal during the period of ancient iron smelting and a uniform species composition *(Arbutus)*.

3. Matrix effects (absorption, source area, grain-size, and organic matter content) strongly affect the geochemical record of the sediments in the Campo plain. Nevertheless, an enrichment of arsenic in combination with strongly increased values of magnetic susceptibility is inherently characteristic of a sedimentary smelting

signature. Heavy metals (Pb, Cr, Cd, Cu, Zn, and Ni) are, in contrast, not enriched in sediments impacted by ancient smelting.

In summary, evidence on local human–landscape interactions in the context of pre-industrial iron smelting on Elba Island is provided by (a) the relation between coastal palaeoenvironments and the location of Roman smelting sites, (b) the deposition of high-magnitude flood layers and slope deposits in the vicinity of smelting sites during Roman times, possibly affected by logging for the production of fuel charcoal to operate the smelting furnaces, and (c) a sedimentary signature of iron smelting.

Acknowledgements

The present study is funded by the Excellence Cluster *Topoi – The Formation and Transformation of Space and Knowledge in Ancient Civilizations* (EXC 264). We are grateful to Lorella Alderighi (Soprintendenza Archeologia, Belle Arti e Paesaggio per le province di Pisa e Livorno) for cooperation and permissions, to Alice Leoni (Capoliveri, Livorno) who organized the permits for drilling from the landowners, and to Daniel Knitter (Christian-Albrechts-Universität zu Kiel) for his help during fieldwork. We thank Michel Dinies and Reinder Neef (German Archeological Institute, Referat Naturwissenschaften) for the identification of charcoal samples. We are also grateful to two anonymous reviewers and K. Thomas, Kempen (copy editing), who helped to significantly improve the quality of the article.

8

Case Study 3: Meta-analysis of ^{14}C-ages from mid- to late Holocene valley fills on Elba Island

Unpublished report

Keywords: *fluvial activity, Bayesian simulations, human impact, transgression*

Abstract The filling of late Pleistocene palaeo-valleys in Central Italy during the mid- to late Holocene is mainly driven by the Versilian transgression, climate variability, and human impact. Scholars believe that fuel production for iron smelting was the most important human impact on Elba Island. To evaluate the hypothesis of accelerated soil erosion after deforestation on Elba, we use cal-^{14}C-ages from mid- to late Holocene sediment sequences from coastal plains and filled valleys to reconstruct past geomorphic activity on the island. Our data set includes 56 ages from 14 sequences. We calculated cumulative probability functions from the cal-^{14}C-ages and simulated cal-^{14}C-ages from random depth. To account for researcher and taphonomic biases, we tested the empirical against theoretical functions. Additionally, we used a stochastic chronological model of facies associations as a proxy to reconstruct geomorphic activities. The data indicate that there were two main periods of sediment accumulation. Statistical tests show that the increase in these periods is likely not caused by biases in the data. The cumulative probability of the cal-^{14}C-ages, sediment accumulation, and geomorphic activities increased during these periods. During the first main phase of sediment accumulation in the mid Holocene, mainly coarse alluvial sediments where deposited. Geomorphic activities during that phase is mainly triggered by the transition from Holocene marine trangressive to early high stand conditions. After sea level rise decelerated, relative geomorphic quiescence is recorded for Elba. The second phase of activity and accumlation coincides with the Roman occupation of Elba. Therefore, we conclude that ancient iron smelting had a significant impact on morphodynamics on Elba.

8.1 Introduction

Scholars have frequently proposed that deforestation on Elba during the main ancient smelting period in *Etruria Mineraria* (6th century BCE to (1st century CE) caused the abandonment of smelting sites because of a lack of fuel to charge the furnaces (Bebermeier et al., 2016; Corretti, 1991; Forbes, 1964; Harris, 2013; Hughes, 2014; Meiggs, 1982; Penna, 2014; Perlin, 2005; Pococke, 1745; Sands, 2013; Schweighardt, 1841; Simonin, 1858; Williams, 2010; Wiman, 2013, see Chiarantini et al., 2018; Corretti, 2009; Di Pasquale et al., 2014; Veal, 2017a — *contra:* Becker et al., submitted.a; Grove & Rackham, 2003; Radt, 2003). The presumed deforestation event is related to soil erosion and degradation (e.g. Wiman, 2013). Moreover, authors often propose that ancient metallurgy in general was a driver of environmental change (e.g. Harris, 2013; Hughes, 2011). Near an an ancient smelting site in the Forcioni valley (2nd to 1st century BCE/CE?), Becker et al. (2019a) uncovered sediment sequences indicating the deposition of high magnitude floods and slope deposits contemporary to smelting activities. These results point to a relationship between accelerated geomorphic activities and iron metallurgy at least on a local scale. An extended view on the Holocene geomorphic activities on the island is, however, missing. Therefore, the overall objective of the following study is to extent the view from the Forcioni valley to other parts of Elba by using data from several sediment sequences obtained on Elba.

Scholars have shown that the Versilian transgression triggered the aggradation of late Pleistocene palaeovalleys in Central Italy during the early and mid-Holocene. Human impacts are, however, a main cause of accelerated geomorphic activities in the late Holocene, especially since Roman times (see Section 8.2). One approach used to evaluate geomorphic activities in Italy is the meta-analysis of cal-^{14}C-ages (Borrelli et al., 2014, 2013; Piccarreta et al., 2011; Rossato et al., 2015; Rossato & Mozzi, 2016; Vincenzo et al., 2013; see Benito et al., 2015a; Walsh et al., 2019).

Meta-analysis of cal-^{14}C-ages

The meta-analysis of valley fills based on summed assemblages of probability distributions of calibrated ^{14}C-ages (cumulative probability functions, CPFs)—especially from alluvial sequences— is a valuable tool to reconstruct geomorphic activities related to climate fluctuations, changes in base level, and human impact (Jones et al., 2015). Since the first published database in the mid-2000s (Johnstone et al., 2006), methodologies of the meta-analysis of dating probabilities developed. Where first approaches were based of frequencies in bins with a given range (e.g. Macklin & Lewin, 1993), later studies used CPFs (see Jones et al., 2015). The method was improved including information

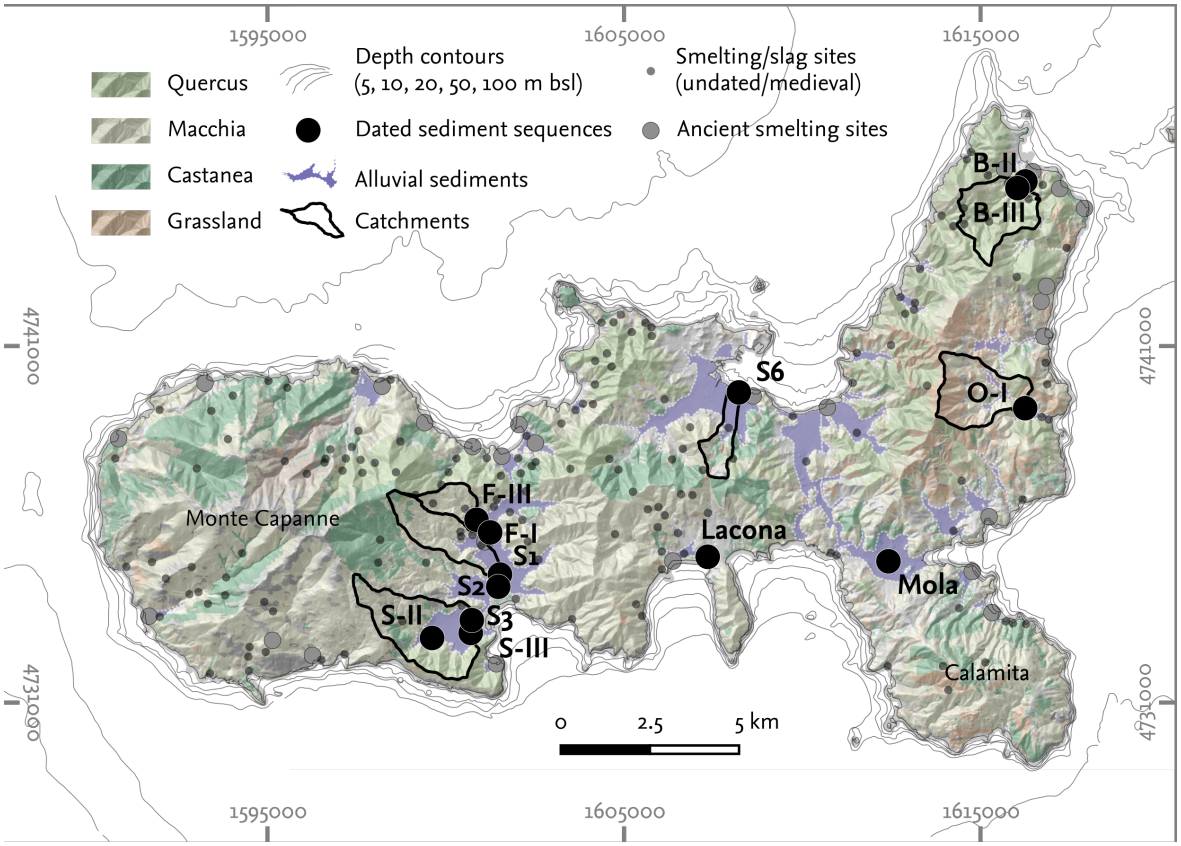

Figure 8.1 Sediment sequences used for meta-analysis of cal-^{14}C-ages in their geographical setting. Database: Regione Toscana, 2014; Corretti, 1988, 1991; Corretti et al., 2012; Corretti & Firmati, 2011; Nihlén, 1958, 1960; Pagliantini, 2014; Zecchini, 1978; Case Study 2, Becker et al., 2019a, Chapter 7; D'Orefice & Graciotti, 2014.

on the depositional environment, the differentiation between dates indicating geomorphic instability or quiescence, and the introduction of 'change' and 'change after' dates (Lewin & Macklin, 2003; Macklin et al., 2010a). The latter approach accounts for major changes in sedimentation rate or pattern. Furthermore, attempts were made to correct for the calibration-curve bias in the probability functions (Hoffmann et al., 2008). Sedimentation rates were calculated on the basis of cal-^{14}C-ages and CPFs (Dusar et al., 2012). Some critical aspects of the CPF-approach were discussed by Chiverrell et al. (2011a,b) and Macklin et al. (2011), stressing i.a. the issue of divergence between a age given by the radiocarbon method and the actual date of the deposition of a sample; and the indicative meaning of peaks in the CPF of the data. The discussion on the use of CPFs as an archaeological population proxy provides further insights in potential biases in the meta-analysis, such as research intensity, sample procedure, and size of the database (Contreras & Meadows, 2014; Orton et al., 2017).

Some scholars used a small data base of cal-^{14}C-ages from a specific catchments for their meta-analysis (e.g. Borrelli et al., 2014, 2013; Vincenzo et al., 2013). Other meta-analysis

cover a river catchments or are on supra-regional scale; they are, thu,s often based on a larger number of samples (e.g. Benito et al., 2015b; Hoffmann et al., 2009, 2008; Panin & Matlakhova, 2015; Zielhofer & Faust, 2008; Zielhofer et al., 2008). Some studies cover large areas where only a relatively low number of cal-^{14}C-ages are available (Kale, 2007; Turner et al., 2010). For some small catchments, a relatively high number of data is available (Dusar et al., 2012) . During the c last 20 years, the numbers of dates in data bases increased (cf. Jones et al., 2015; Macklin et al., 2010a; Thorndycraft & Benito, 2006)

8.2 Palaeoenvironment in Central Italy: Sea-level changes and human impact

The Holocene transgression, climate variance as well as human activities triggered the filling of coastal valleys around the (northern) Tyrhenian Sea during in the late Pleistocene, particularly in Central Italy.

Until the Last Glacial Maximum (LGM, c 18 ka BP), when the global sea level was up to 130 m lower than today (Lambeck et al., 2011), incised valleys were exposed around the central Italian coast. The coastline moved c 10–30 km seawards compared to the modern situation (see Figure 8.2 and e.g. Antonioli et al. 2011; Tortora et al. 2001). Under late low stand conditions of the marine sea level, thick (coarse) floodplain sediment sequences were deposited in the palaeovalleys (cf. Marra et al., 2013). During the transgression after the LGM, beach-barrier systems moved landwards (Aguzzi et al., 2007). The alluvial sediments are typically overlayered by swamp, inner and outer estuarine and lagoonal sediments of the transgressive sequence; the maximum flooding surface dates between 9.2 and 7.8 ka BP (Amorosi et al., 2014b; Breda et al., 2016; Rossi et al., 2011). Within the palustrine deposits, salinity may have varied due to e.g. variability of riverine input (Breda et al., 2016; Mazzini et al., 1999). The dominance of esturaine backfilling successions indicate a initial dominance of eustatic sedimentation over sediment supply by rivers in valleys along the Central Italian coast (Amorosi et al., 2014b; Breda et al., 2016). However, e.g. palaeotopography or sediment supply controlled local variation of sediment fills (Breda et al., 2016; Rossi et al., 2011). Since the Sub-Boreal (ca. 7 ka BP), alluvial successions occurred in the palaeovalley fills (Bellini et al., 2009; Breda et al., 2016). Marine influence locally imprinted the sediments until historic times (c 3 ka BP), when deltas propagated due to changing climate conditions and human impact, especially since the late Middle Ages (see Bellotti et al., 2011, 2004; Giraudi, 2011; Pranzini, 2001; Salomon et al., 2018). Palustrine environments in the coastal plains also occurred during

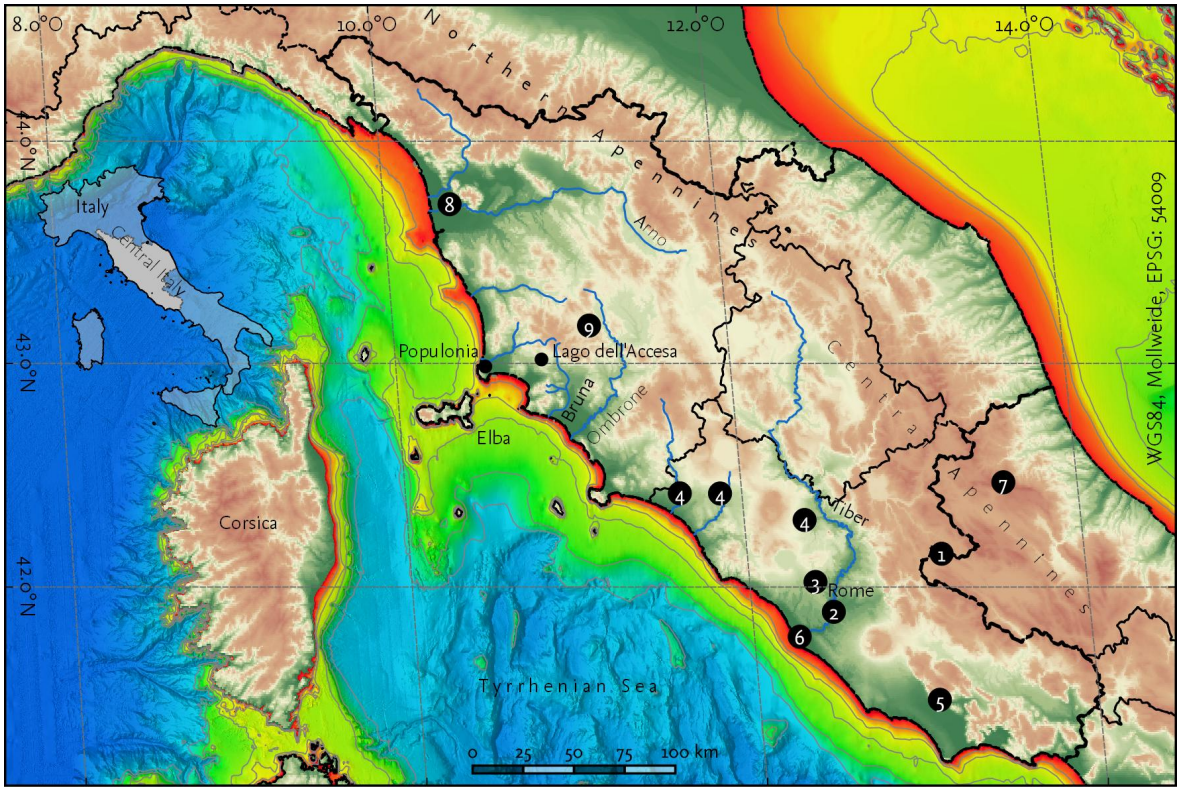

Figure 8.2 Location of Elba in the northern Tyrrhenian Sea. Major locations in Central Italy mentioned in the text are indicated—1: Borrelli et al. (2013), 2: Marra et al. (2018), 3: Brown & Ellis (1995); Judson (1963), 4: Brown & Ellis (1995), 5: Attema & Delvigne (2000), 6: Salomon et al. (2018), 7: Giraudi (2005a,b), 8: Amorosi et al. (2013a) 9: Hunt & Gilbertson (1995). Database: EMODnet Bathymetry Consortium (2018), bathmetry; Earth Resources Observation and Science Center/U S. Geological Survey/U S. Department of the Interior (1997), elevation.

Roman and prevailed modern times, e.g. the Lago di Castilinoe or *Aquae Populoniae* (Giroldini, 2012).

Human activities e.g. in the coastal areas of Central Italy were strongly liked to the development of the coastal plains and the (artificial) drainage of wetlands (i.e. *La bonifica della Maremma*, c 1830–1930). During sea level high stand in the late Holocene, the propagation of the major rivers in Central Italy (such as the Tiber, the Arno, the Ombrone, and the Bruno) buried important lacustrine and riverine harbours in Ostia, Pisa, Rosellae, and presumably Vetulonia, respectively (Arnoldus-Huyzendveld, 2011; Benvenuti et al., 2006; Ceccarelli & Niccolucci, 2003; Colombi, 2018; Kaniewski et al., 2018; Luti, 2000; Michetti, 2017; Rossi et al., 2012). The sediment delivery from the catchments of these rivers vary greatly due to differences in morphological configuration, size, bedrock wheaterability, and human impact (i.a. Bellotti et al., 2004).

Human disturbances in the Mediterranean region had a great environmental impact; historic deforestation and subsequent soil erosion in the area are of major concern—not only for rivermouth propagation. In an early study from central Italy, near Rome and

Veii, Judson (1963) found late Roman sites in alluvial valleys buried by meter-thick layers of sediments. Other studies also proposed late–post Roman (medieval) flooding phases in the Abbruzzi mountains in upstream areas and an early late-Holocene onset of valley alluviation in middle reaches (Borrelli et al., 2014, 2013; Vincenzo et al., 2013). Amorosi et al. (2013a) found evidence for increased sedimentation rates in coastal plains since the Bronze age due to human impact. In the Appenine region near Rome, sedimentation might have been increased during Roman occupation and the Middle Ages (Borrelli et al., 2013). Flooding at *Portus Romae*/Rome dates to the Roman Imperial period (Salomon et al., 2018). Historically testified floods of the Tiber in Rome peaked in Roman times, during Carolingian times, and after the Middle Ages (Aldrete, 2007; Alessandroni et al., 2002). Buried soil horizons in the northern and central Appenines indicate the deposition of alluvial sediments in the early Iron Age–Roman times, the early Middle Ages, and the modern period (Giraudi, 2005a,b). Sediment sequences in the area analyzed by Brown & Ellis (1995) indicate a post-Roman change in facies characteristics and high accumulation rates since late-Medieval times; Attema & Delvigne (2000) did not found a clear coincidence between alluviation and settlement dynamics in the Pontine plain. Results from Mensing et al. (2015) propose an increase in erosion in the early Middle Ages, after Roman sites were abandoned, coinciding with data from Borrelli et al. (2014). In the Tiber valley in ancient Rome, three main phases of non-eustatic valley aggradation in the mid- to late Holocene were linked to fault displacement and increased human activities (Marra et al., 2018).

Holocene valley fills and badland formation in Basilicata, southern Italy, indicate a late Neolithic, a Greek–Roman and an early medieval accumulation phase (Boenzi et al., 2008; Piccarreta et al., 2012); Piccarreta et al. (2011) propose also a mid-Holocene phase of aggradation in the region. Whereas early Holocene aggradation phases in Basilicata and central Italy are believed to be triggered by climate variability, later phases coincide with increased human pressure on the landscape.

Calanchi and *biancane* are typical badland formations found in Central Italy (Phillips, 1998). They occur frequently in cropland areas between the Ombrone and Tiber rivers, especially in areas with clay or marly clay bedrock (Del Monte, 2017; Della Seta et al., 2009; Vergari et al., 2013). Buccolini et al. (2014) propose that erosion rates in this areas increased after early Holocene biostasy, potentially due to human impact. Besides in southern Tuscany and northern Latium, Italian badlands are common in southern Italy, especially in the Basilicata region. Here, scholars conduced intensive research on the pheonomena (e.g. Phillips, 1998). Human impact (deforestation) also plays an important role in the explanation of the formation of the badlands (Phillips, 1998; see also Brückner, 1986).

The discussion on climate vs human driven (i.e. soil erosion and flooding after land clearance) aggradation of Mediterranean valleys was mainly stimulated by Vita-Finzi's contributions on the 'older fill' (late Pleistocene) and the 'younger fill' (little ice age) (Vita-Finzi, 1969—Goudie & Viles, 2016; Macklin & Woodward, 2009). Whereas Vita-Finzi proposed climate-driven aggradation, others, e.g. Van Andel et al. (1986); van Andel et al. (1990) and Butzer (1980) favor a anthropoic trigger of erosion in upstream areas. More recent contributions, such as the above mentioned, and notably Bintliff (2002), stress the varying impact of both, climate and humans (in contrast: Bintliff, 1975). Several case studies focus on the differenciation between climatic and human triggers of environmental change (see e.g. studies in an issue of Galop et al., 2009, and references therein, or Brown & Ellis, 1995; Finsinger et al., 2010; Peyron et al., 2011; Vannière et al., 2008). Besides the actual trigger, the sensitivity of the landscape to climate variability and human impact explains the occurrence of degradation phenomena in the region (e.g. Brückner, 1986, 1990). In the literature on the environmental impact of ancient societies around the Mediterranean, deforestation—and subsequent geomorphological impacts on soil and fluvial systems—are extensively discussed (Hughes, 2014; Hughes & Thirgood, 1982).

8.3 Methods and material

8.3.1 Study area

The climate of Elba Island is typcial Mediterranean with hot and dry summers (*Csa* after the Köppen–Geiger classification); depending on altitude, average annual temperatures vary around 13–17 °C and average annual rainfall is approximately 550–950 mm (Bencini et al., 1986; Foggi et al., 2006b). Present vegetation cover depends mainly on meso-climate (slope exposition, altitude, mountain side), lithology (siliceours or calcarous soils), and vegetation dynamics (succession status, land-use history). Thermomediterraean vegetation (coastal macchia, e.g. *Arbutus unedo* and *Erica arborea*) dominates on south-exposed slopes (Figure 6.1). The more humid mesomediterraean *Querus ilex* and *Castanea sativa* woodlands occur on north-exposed slopes up to 700 m asl. On elevations above c 700 m asl along the Monte Capanne massif, mainly supramediterranean garrique is found (Carta et al., 2018b; Foggi et al., 2006a,b). During the second half of the 20th century vegetation on Elba changed significantly; successively, agricultural land was abandoned or used as settlement area; garrique turned into macchia, macchia into *Quercus* woodlands (Carta et al., 2018b).

Based on mesoclimate, lithology, and (structural) geomorphology, Elba can be divided in four regions:

(i) The **western region** is mainly made up of Tuscan magmatic rocks dominated by the early Messinian (6.9 Ma) monzogranitic Monte Capanne pluton (1108 m asl) and the Orano porphyry and dykes. On the margins of the pluton, especially in the north, the middle Jurassic–late Cretaceos ophiolithic sequence crops out, which is characterized by basal Serpentinites and Palombini shales on top. The southwest-to-northeastern part of the Monte Capanne massif is characterized by long valleys deeply incised along brittle lineations, dyke (swarms) and secondary thrusts in the Sant'Andrea–San Franesco tetconic facies. In contrast, the east–southeastern subregion is mainly made up of the San Piero facies; major river valleys flow contour-parallel to lineations and valleys are less deeply incised. Petrovariance (grussification) and difference in (subsequent) erosion between the tectonic facies may be explained by different exposure times (subsequent magma batches), chemical composition (biotite/K-feldspars), and abundance of megacrysts. Longitudinal creek profiles (channel slope) in the southeast are characterized by two knick points, which are related to variance in lithology, particularly to the transition from monzogranitic to ophiolitic bedrock and from ophiolitic bedrock to alluvial deposits, respectively.

(ii) The boundary between the western part of the island and **central Elba** is marked by the Colle Palombaia–Procchio Fault, where mainly Eocene flysch and christmas-tree laccoliths slipped eastwards during Miocene magatism. These units are deposited in central Elba east of the Central Elba fault along thrusted units of the Tuscan oceanic basement.

(iii) **North-eastern Elba** is characterized by a complex pattern of pre-intrusiv units. The eastern sub-region is dominated by tectonic units of the inner Ligurian domain (basalts, serpentintits, and mainly radiolarits) and v-shaped valleys; in the eastern sub-region also bedrock of the metamorphic Tuscan domain (mainly quartzite, tectonic breccias, and black phylittes) crops out. Hills are rolling and crests formed in relation to variation in rock resistability and faults. Limestone dominates in the northern sub-region.

(iv) The Calamita peninsula in southeastern Elba consists of Precambrian–Palaozoic phylitts with metasandstones. On the northeastern part of the Calamtia peninsula, dyke swarms related to the the Porto Azzuro pluton are dominant and fostered the incision of valleys (see Goudie, 2013). In the southern and northwestern part of the area, Triassic dolostones and marbles, coming along with flysch, crop out.

The four regions are divided by distinct alluvial plains (Marina di Campo–Procchio, Lacona–San Giovanni, and Mola–Magazzini), which developed along the Colle Palombaia–

Proccio Fault and the Central Elba fault and are, thus, related to Miocene magmatism (Monte Capanne und Porto Azuro pluton). The coastal plains differ by slope gradient and degree of channel incision. In Lacona, alluvial sediments are mainly Pleistocene terraces. Relatively wide, steep, and coarse alluvial fills are found near Marciana and Pomonte in the northwest and near Porto Azzuro in the (north)east and in the western sub-region of Northeastern Elba (e.g. Nisporto); they are partly overlain by Pleistocene–Holocene landslide deposits. Differences in alluviation between sub-regions in western Elba are due to valley slope and structural setting (tectonic facies and the presence of ophilolites and flysch); along the main faults, slope gradients of the alluvial plains are lower. Gentle, narrow, filled valleys are mainly found in the eastern sub-region of northeast Elba (e.g. Baccetti, Rio Marina, Ortano, Reale). No significant (subaerial) valley fills occur in other (incised) valleys, e.g on the Calamita peninsula.

8.3.2 Data set

We collected $n = 56$ ^{14}C-ages from $s = 14$ dated sediment sequences from Elba Island, which were obtained from six different plains or valleys. Data are available mostly from percussion drillings published in D'Orefice & Graciotti (2014) and Becker et al. (2019a), additionally, three unpublished sequences are included. Along with the uncalibrated ages, we obtained metadata of the sequences (location, elevation, coring depth), the stratigraphy/facies of the cores, the dated material, and the depth of the samples. We took information on texture and facies for each layer from the original publication and the core description if available. Homogenization of the data was necessary (Table 8.1). Alluvial facies were divided in 'coarse' if it consists mainly of gravel or sand and is related to channel-deposition and in 'fine' in all other cases. Sediments were classified as 'palustrine' if fine and as 'paludal' if relatively coarse and organic- or sulphur-rich (Becker et al., 2019a). 'Marine' sediments subsumes all layers related to sub-aerial deposition in a marine or littoral environmental. Facies interpretation in the original publication of D'Orefice & Graciotti (2014) is based on bioindiactors. Furthermore 'palaeosoil' layers and 'colluvial' layers occur. In addition to the facies classification, we categorized all layers with available facies information to phases of relative geomorphic instability or quiescence (see Figure 8.3).

8.3.3 Chronological models

We calculated three different types of stochastic chronological models, including

(i) a cumulative probability function (CPFs) of all calibrated ^{14}C-ages;

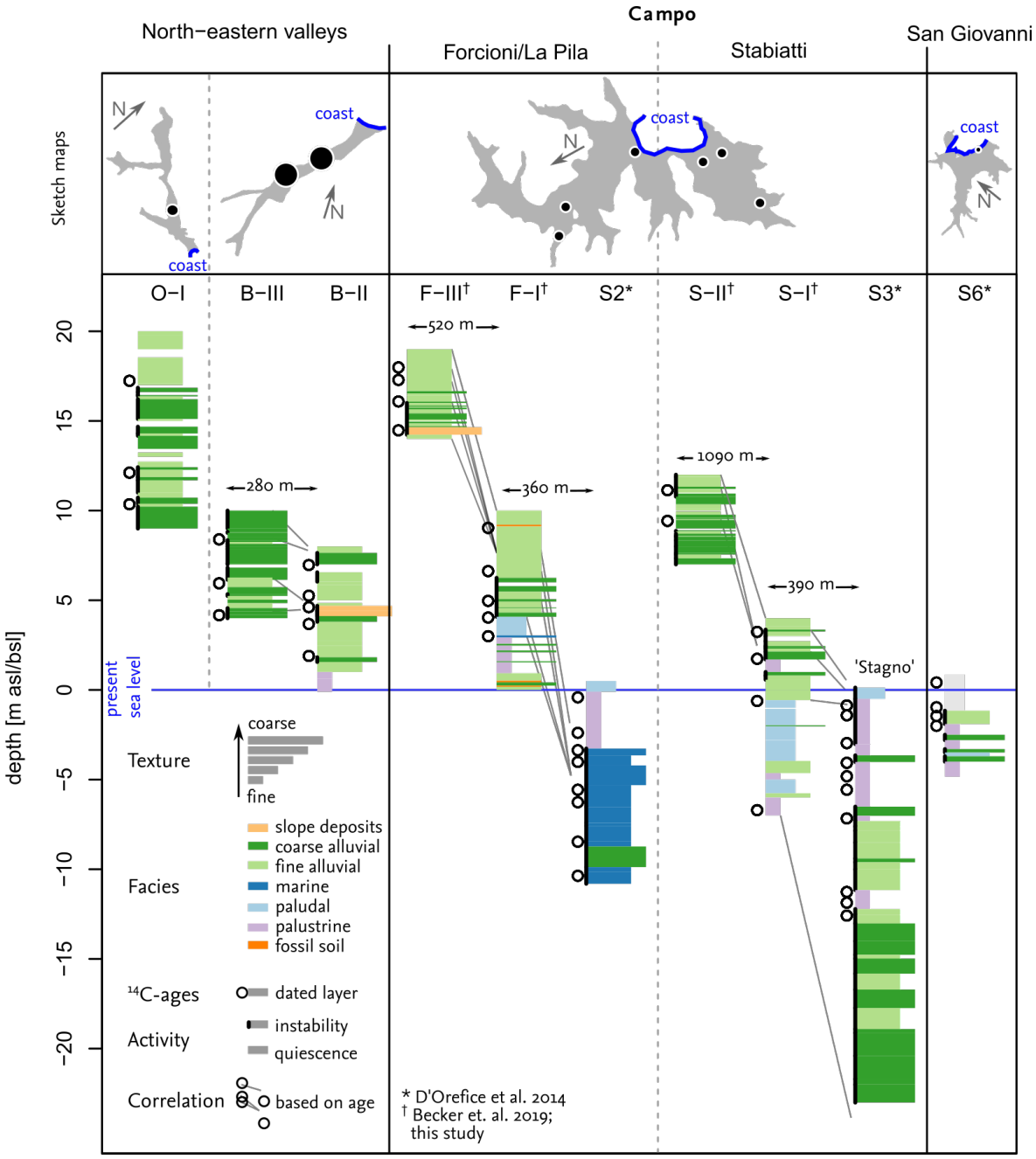

Figure 8.3 Sediment sequences used for the meta-analysis of the cal-^{14}C-ages. The sketch maps depict the Late Pleistocene/Holocene valley fills and the coring locations; maps are not oriented towards the North. We estimated correlation between sediment sequences based on ages of the samples.

(ii) CPFs of randomly sampled, simulated ^{14}C-ages in all sediment sequences (Bayesian model); and
(iii) the probability distributions of the facies related to the random samples and their interpretation as markers of geomorphic activity or stability.

We used the *rcarbon*-package (v1.2.0, Bevan & Crema, 2018) in R v3.5.1 (2018-07-02) for calibration (*IntCal13*, Reimer, 2013), summing, and the simulation of cal-^{14}C-ages for given calender dates.

Cumulative probability functions (i)

The first model follows the basic principles outlined by i.a. Jones et al. (2015). The CPF is calculated by calibrating and summing the conventional ^{14}C-ages and normalizing to unity (500 simulations, 250 yr window, Bevan & Crema, 2018). To account for the effect of the irregular shape of the calibration curve on peaks in the CPF, we calculated a simulated CPF of calibrated, even spaced dates ($0, 0.001, 0.002, \cdots, 11.699, 11.700$ ka BP) (Hoffmann et al., 2008). Phases of high activity are identified where the CPF of at least three cal-^{14}C-ages is higher than the median of the CPF (cf. Jones et al., 2015)

We compared the empirical CPF with CPFs calculated from random samples with the same number of dates as the empirical data set (Bevan & Crema, 2018). This approach allows to estimate the likelihood that peaks in the empirical CPF are not-random, i.e. not importantly influenced by the number of available cal-^{14}C-ages or a sampling bias. The probability that a year between 0 ka BP and 11.7 ka BP is sampled follows the theoretical distribution. We conducted 1000 Monte-Carlo simulations with 56 random samples each to calculate the theoretical CPF. Additionally, we bootstrapped the empirical data set by sampling with replacement from the cal-^{14}C-ages and calculating a CPF. During each simulation run, it is assessed wheater the difference between the simulated CPF_i and the bootstrapped CPF is smaller or larger than zero. After i runs we calculated the likelihood that peaks and depressions in the empirical CPF derivate from the simulated CPF.

Simulated cumulative probability functions (ii)

The procedure developed for the empirical CPF is also applied to simulated age distributions. We generated simulated age distributions by repeatedly ($i = 100$) estimating the age of a randomly chosen depth in a randomly selected sediment sequence ($i = 15\,000$) as a function of the stratigraphical upper and lower age, assuming no change in aggradation pattern between both ages.

As the overall density of dated sediment units is biased by sample selection (and the implicit agenda of the researchers), taphonomy, and even more by the overall depth of the exposed sediment sequences, we compared the simulated CPFs with theoretical CPFs to minimize these biases. Therefore, we calculated the proportion of all sediment sequences covering an age x ($x = [0, \cdots, 11.7]$ ka BP); the date range of each sequence spans from 0 BP to the median date of the lowest calibrated age of the sequence. Additionally, we used the grand median average deposition rate of the calibrated ages $median(DR_{a,1}, \ldots, DR_{a,n})$ to estimate a possible age of the lowest point of each sediment sequences assuming equal, average, depositon rates in each sequence. We than used the estimated age of the lower end of each sediment sequence to estimate the probability that an age x could have been covered with the given sediment sequences. The average deposition rate ($DR_{a,n}$) of an individual calibrated cal-^{14}C-ages is calculated applying the formula given by Dusar et al. (2012):

$$DR_{a,n} = \frac{t_i}{d_i} \tag{8.1}$$

where t_n is the calibrated age and d_n is the depth of sample n.

We calculated a third theoretical distribution function of ages assuming that the preservation potential of a sediment layer in year x follows a power function (cf. Bridge & Mackey, 2009; $e = 0.6^{-1}$).

We compared the simulated CPFs ($n = 56$) with the empirical CPF ($n = 56$). This Bayesian model takes both information age and depth of the samples into account. This model is therefore less sensitive to sampling biases.

Facies association (iii)

From each simulated age, we additionally took the age and the depth as well as the facies associated with the layer at the depth. After 2 500 experiments we calculated uniform 125-yr-kernel densities of ages for each facies and normalized these by the kernel density of all ages. For the final facies probability distribution, we sampled from 100 ages for each facies layer (with replacement) to avoid underrepresentation of thin layers.

8.3.4 Availability of data and code

The data set collected for the meta-analysis as well as the model code is available from the Compact Disk attached to the thesis at hand.

Table 8.1 Facies interpretation as a proxy for morphodynamic activity. . x = indicating quiescene/activiy; cells marked with (x) are interpreted either as indicating quiescence or activiy, depending on the characteristics of the sediment sequences, see Figure 8.3.

Facies	Typical characteristics	Quiescence	Activity
Alluvial fine	loamy sand to silty texture, occasionally gravel	(x)	(x)
Alluvial coarse	sand and gravel layers, indicate channel-related deposition or fan-deposits		x
Palustrine	clayish texture, includes lacustrine deposits (low conductivity) and lagoonal deposits	x	...
Paludal	clayish to loamy texture, marsh fauna, high sulphur content, includes peat	(x)	(x)
Palaeosoil	dark, organic rich layer, increase in frequency-dependent magnetic susceptibility	x	
Marine	Fossils, chemical properties	(x)	
Colluvial	Chemical composition, shape of pebbles		x

8.4 Results

8.4.1 Cumulative probability functions

A cumulative probability functions (CPF) is obtained for the 56 calibrated ^{14}C-ages from the available sediment sequences (Figure 8.4). The CPF shows seven phases of increased cumulative probability (Table 8.2; Figure 8.4a). No dated layers where recorded for three phases (3.2–3.5 ka BP, 8.1–8.3 ka BP; and 9.1–11.7 ka BP).

Table 8.2 Phases of increased geomorphic activity on Elba. Symbols indicate presence, likelihood, or relative high/low values. CPF = cumulative probability function. > 0 = 95%-confidence interval does not include 0. Likelihoods of simulations (8.5: a = power function, b = average aggregation, c = length of sequence.

Phase	CPF			Simulation			Facies
ID	Chronology	> 0	> random	a	b	c	(In)stability
I	0.8–1.6	x	++	+	++	-	-
II	1.9–2.3	x	++	++	+	+	+
III	2.5–2.7	x	++	o	(-)	-	o
IV	4.6–5.0	x	++	+	–	-	-
V	5.3	x	++	+	o	-	o
VI	5.7–7.1	x	++	+++	+++	+++	++

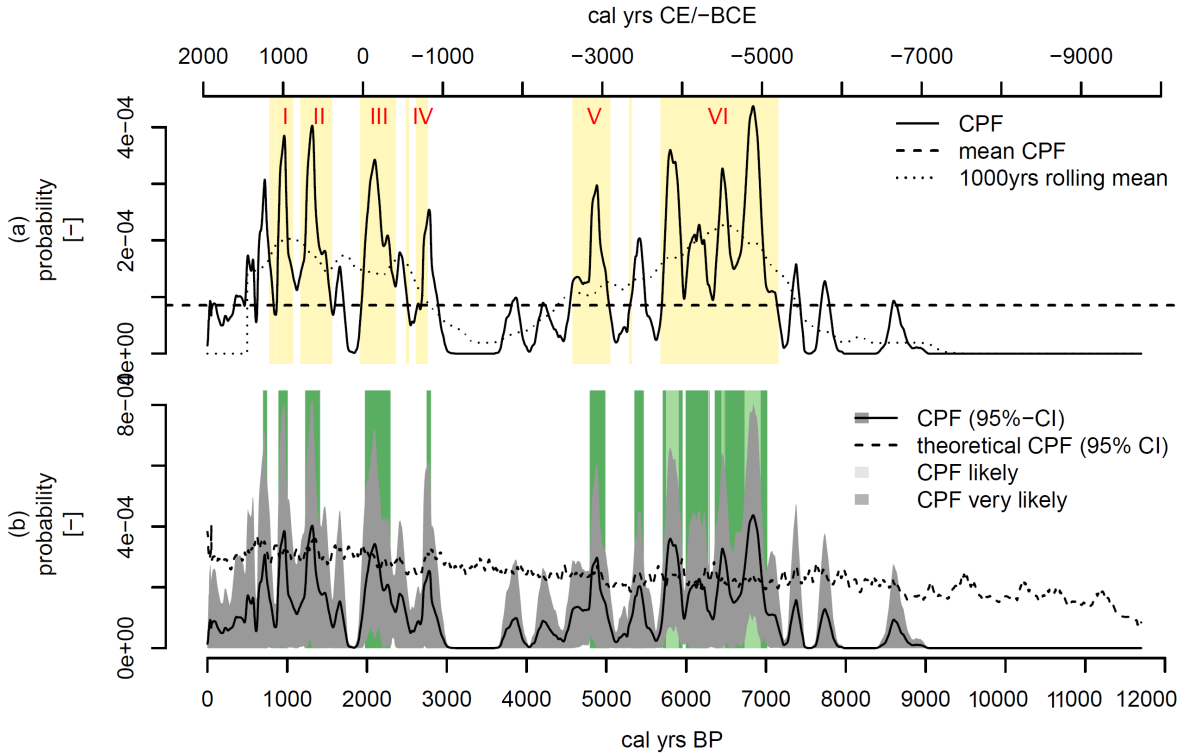

Figure 8.4 Cumulative probability function (CPF) of cal-^{14}C-ages from Elba. (a) Running mean: 250 yrs, solid line, and 1000 yrs, dashed line. Phases of high cumulative probability are highlithed in yellow. **(b)** CPF (solid line) and it's bootstrapped confidence interval (grey envelope, 95% likelihood, B = 1000) of CPFs. The upper 95%-confidence limit of 1000 random CPFs is shown (dot-dash line; 56 ages cal-^{14}C-ages each CPF) drawn from a theoretical power distribution. Green bars indicate the likelihood that a bootstrapped empirical CPF exceeds the theoretical CPF.

The bootstrapped confidence interval (CI) of the CPF (Figure 8.4b, grey envelope) exceeds zero in several phases at 95%-confidence (phases I-II, III, V, and VII). The CI of the CPF also exceeds the theoretical CPF of randomly distributed samples (dot-dash line) in all seven phases. It is likely for most phases (II, III, IV, and V) and very likely for one phase (VI) that a bootstrapped CPF is (at least in parts of the phase) higher than the theoretical random CPF. There is a clear divergence between the theoretical CPF and the decreasing probability of dating a layer after ca. 1 ka BP.

8.4.2 Simulated cumulative probability functions—Sediment accumulation

Based on the depth information and the calibrated cal-^{14}C-ages of the samples, we estimated probability density functions of the age of 'samples' randomly distributed over the available sediment sequences; each of the $i = 2\,500$ simulations covers 56 random samples (i.e. the number of samples in the original data set). The simulated CPF (Figure 8.5)

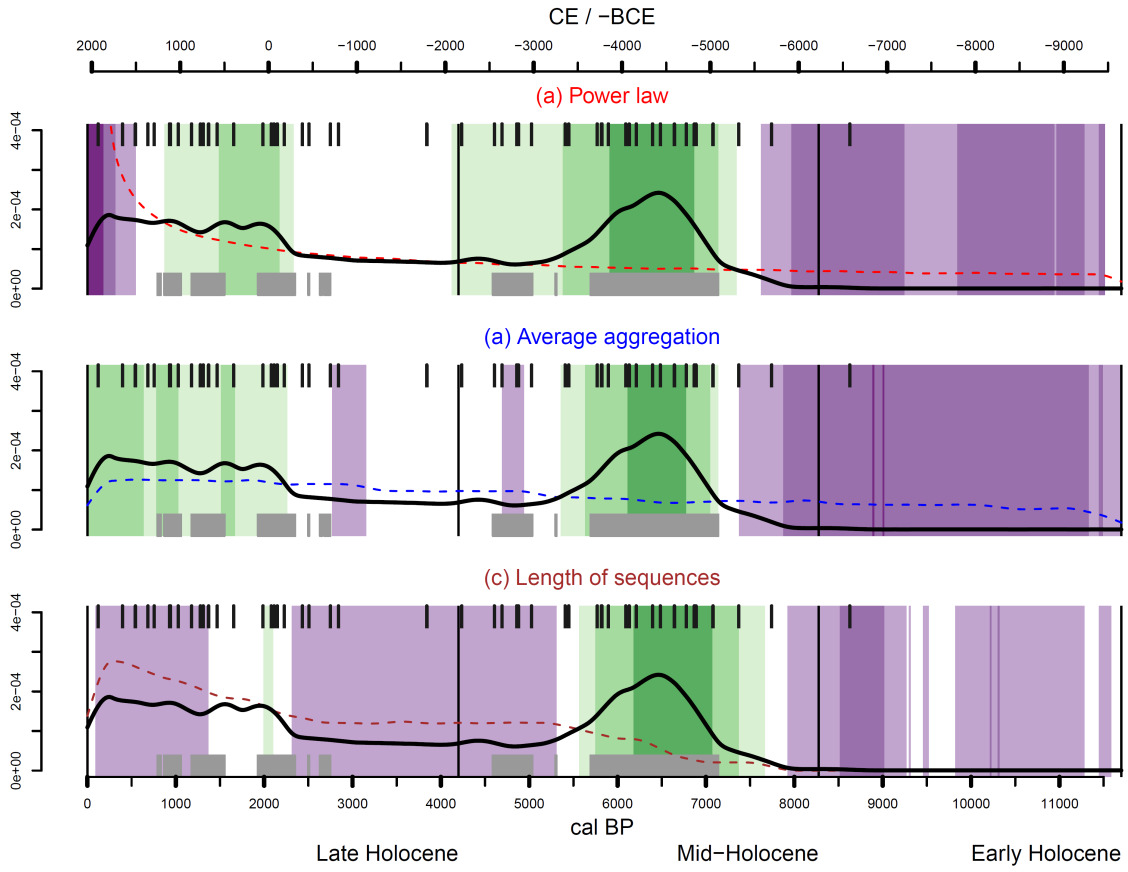

Figure 8.5 Simulated and theoretical cumulative probability functions (CPF). Bold lines show the simulated CPF ($i = 2500$), dashed lines the theoretical CPF. The likelihood that the CPF of 56 simulated ages is greater than CPF of 56 random ages is indicated (green and purple backgrounds. **(a)** Power-distributed ($e = 0.6^{-1}$) theoretical distribution of random samples taken from all sediment sequences. **(b)** Theoretical distribution estimated from average aggregation rate of all cal-^{14}C-ages. **(c)** Theoretical distribution obtained from chronological coverage of the sediment sequences.

exceeds the theoretical distribution of random samples in several phases, depending on the theoretical model (Figure 8.5). Peaks in the simulate CPF that exeed the theoretical distributions are indicative for increased sediment accumulation during a phase (see Section 8.3.3). The oldest phase of increased sediment accumulation dates to 7.6–5.4 ka BP; the likelihood that the empirical CPF exceeds the theoretical CPF is especially high between 7.0 and 5.9 ka BP (classified as *likely*). The younger phase of increased sediment accumulation dates to 2.2–1.9 ka BP (classified as *as likely as not*).

8.4.3 Facies associations

Based on the given age–depth data and the classification of the facies associations of the sediment sequences, we calculated an chronological model of the development of

depositional environments. Layers indicating deposition of marine sediments date to the period before 9.0 ka BP. As only few dates for the period prior to the middle Holocene are available from our data set, the uncertainty of the chronology is high. The youngest sediments related to marine impact are deposited between 5.0 and 4.0 ka BP. Paludal and palustrine sediments were deposited between c 9.0 ka BP and c 5.0 ka BP, peaking between 8.0 and 7.0 ka BP. During the late Holocene, wetland sediments do not dominate the deposition record. A marked decrease of the proportion of sediments indicating a wetland depositional environment is observed around 2.3 ka BP. Dated coarse alluvial sediments occurred after 9.0 ka BP. However, chronology is uncertain. Fine alluvial units occurred after 8.0 ka BP, when the relative contribution of paludal/palustrine and coarse alluvial sediments decreased. Between 6.0 and 5.0 ka BP, coarse alluvial layers became again more important than alluvial fines. The proportion of fines increases after 5.0 ka BP until 1.6 ka BP. There was a distinct decrease of coarse sediments and a remarkable increase of fines recorded for the time around 1.6 ka BP. Slope deposits were recorded since c 6.2 ka BP; their contribution tends to increase more or less constantly. A clear increase in the proportion of slope deposits is recorded for the period between 2.4 and 1.8 ka BP. Dated layers indicating soil formation were only recorded for the period after 1.6 ka BP.

Grouping of facies suggests changes in the facies associations. The sediments deposited after and prior to c 7.0 ka BP show the clearest difference. In descending order of importance, changes occurred around 2.2, 5.4, 0.9, 6.2, 1.9, and 7.5 ka BP.

The interpretation of the facies data in terms of geomorphic activity revealed several phases of activity and stability. We modeled an increase in activity around 7.2 ka BP, peaking around 6.7 ka BP, and followed by a decrease in activities until c 5.5 ka BP. Between 5.5. and c 2.4 ka BP, modeled activity remains relatively stable. The modeled activity clearly peaks between 2.4 and 1.9 ka BP. Another peak dates to 1.2 to 0.4 ka BP.

8.5 Discussion

8.5.1 Palaeolandscape and geomorphic activity

The overall pattern of the sediment's facies succession from Elba Island shows the typical deposition sequence of the coastal plains of the northern Tyrrhenian Sea and corresponds to phases of accelerated and decelerated sea level rise during the Versilian/Holocene transgression (cf. Amorosi et al., 2004, 2013b; Breda et al., 2016; Rossi et al., 2011, 2012; Sarti et al., 2012). Moreover, the data set from the sediment sequences from Elba mirrors major Holocene climate changes and increasing human impact since the late Holocene.

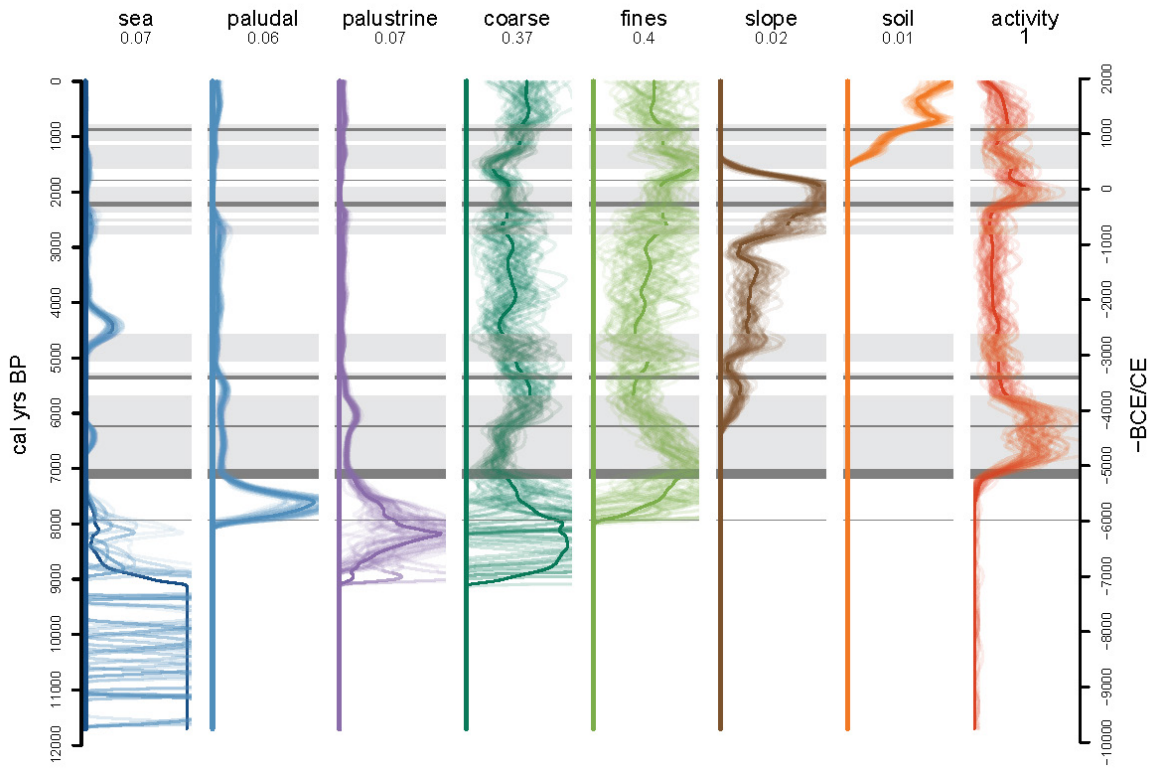

Figure 8.6 Chronological model of the facies associations in the alluvial plains and valleys on Elba. Each column represents the contribution of each depositional environment to the contemporary overall facies record. The bold dark lines mark an average value of all simulation runs, whereas the thine light lines mark results of a single simulation run. Horizontal grey bars show the results of a cluster analysis of the facies associations; the width of the lines represents the cutting of the clustering dendrogram. The grey shadow shows the phases of increased cumulative probability of cal-^{14}C-ages. The numbers below the facies headings highlight the relative proportion of the facies association to the overall record.

Transgressive propagation and progradation (>9 to 7.6 ka BP)

The cumulative probability function (CPF) of cal-^{14}C-ages indicates that the sediment accumulation before c 9 ka BP was low. Marine layers were deposited in the dated early Holocene sequences (Figure 8.7, e). The deposition of the marine layers coincides with well- known melt water pulses (MWPs 1b and 1c) and an acceleration of sea level rise in the northern Tyrrhenian Sea (Figure 8.7, e). Shoreline propagation dominated (see Posamentier, 2009).

Between c 9 and 7.1 ka BP sediments indicating a wetland environment were deposited in the valleys (between 5 m above and 11 m below present sea level, see Figure 8.3). During this time, sea level rise in the northern Tyrrhenian Sea decelerated from a Holocene maximum of 1.8 cm a^{-1} in c 9.5 ka BP to c 0.67–0.79 cm a^{-1} around 7.1 ka BP.[1] After the late

[1]predicted data for the Ligurian and Tyrrhenian sea from Lambeck et al. (2011), sites nr. 1–15, 36, 39, 40. Reported values are the mean of these sites. The relative standard deviation of the Holocene sea level rise

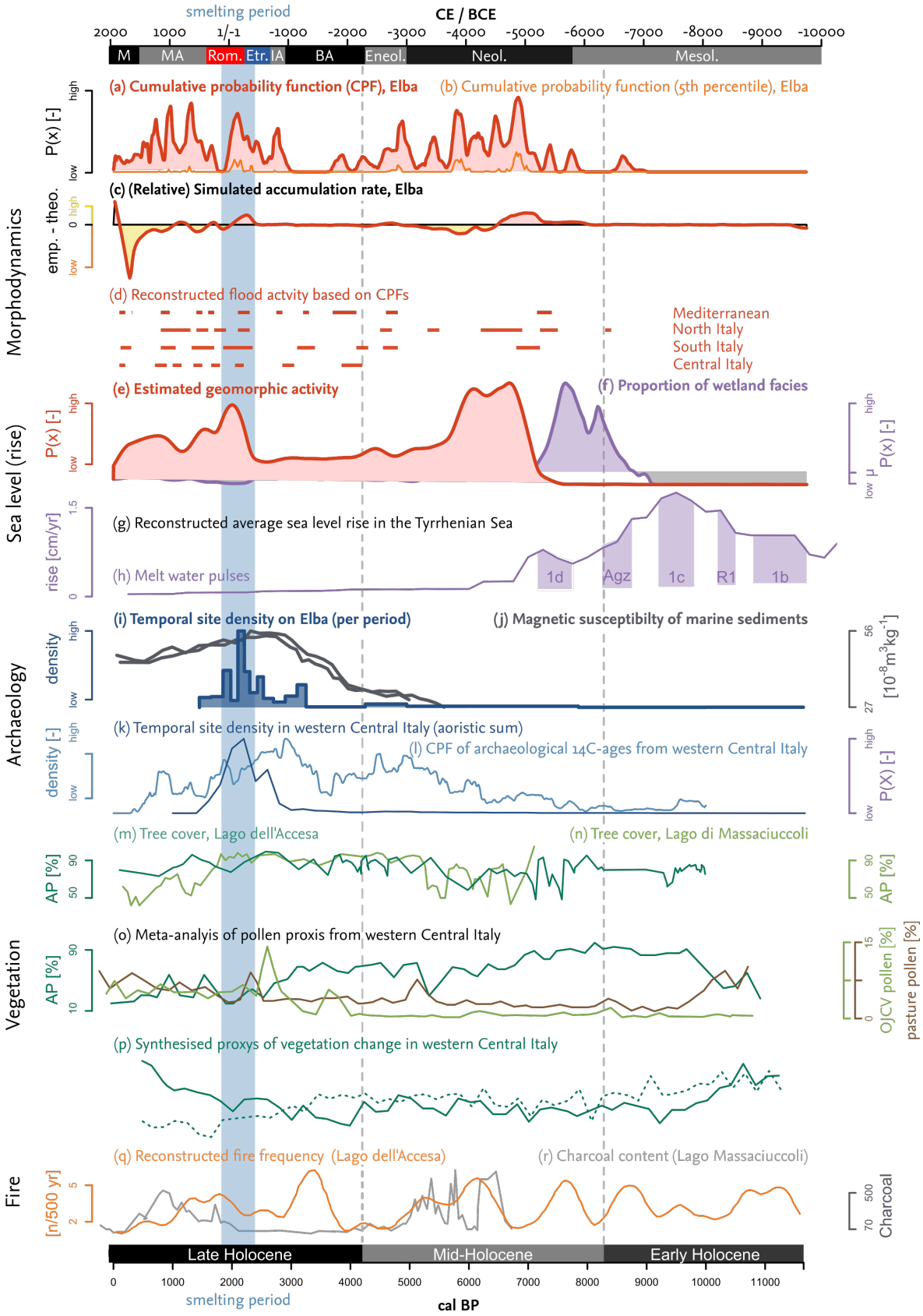

Figure 8.7 Outcomes of the meta-analysis of and sediment sequences on Elba in comparison with other proxies from Elba, (Central Italy), and the Mediterranean region.

continued on next page . . .

. . . Figure 8.7, continued. Remarks: **(a)** and **(b)** *this study*, see Figure 8.4; **(c)** *this study*, see Figure 8.5; **(d)** major flood phases (CPF) in catchments in the entire Mediterranean region and in different regions of Italy (Benito et al., 2015b; Borrelli et al., 2014; Piccarreta et al., 2011; Rossato et al., 2015); **(e)**, **(f)** *this study*, see Figure 8.6; **(g)** Lambeck et al., 2011; **(h)** Smith et al., 2011; **(i)** summed probability of archaeological finds on Elba, 250-yr bins, data from Pagliantini, 2014; **(j)** Magnetic susceptibility of sea sediment sequences obtained from the Corsica channel, interpreted as proxy for metallurgical activity (Vigliotti et al., 2003, see Case Study 1, Becker et al., 2019b, Chapter 6); **(k)** site density in Central Italy and **(l)** CPF of cal-^{14}C-ages from archaeological sites Palmisano et al., 2017, 2018; **(m)**, **(n)** aboreal pollen in the record from Lago dell'Accesa (Peyron et al., 2011) and Lago di Massaciuccoli (Colombaroli et al., 2007), respectively (mediterranean and sub-mediterranean trees); **(o)**, summarized record of pollen from western Central Italy indicating forests (AP), pastures, and anthropogenic impact, OJCV: *Olea*, *Juglans*, *Castanea*, *Vitis* (Stoddart et al., 2019); **(p)** summarized pollen proxies indicating dissimilarity between composition of the pollen record from 143 sites around the Mediterranean Sea, average nonmetric multidimensional scaling (Woodbridge et al., 2018); and **(q)** fire frequency, Lago dell'Accesa Vannière et al., 2008 and **(r)** charcoal influx, Lago di Massaciuccoli Colombaroli et al., 2007 — Periodisation (acc. to Palmisano et al., 2018, adopted to development on Elba, see Section 3.5): M = Modern period, MA = Middle Ages, Rom. = Roman period, Etr. = Etruscan period, IA = Iron Age, BA = Bronze Age, Eneol. = Eneolithic, Neol. = Neolithic, Mesol. = Mesolithic. Subdivision of the Holocene acc. to the *The ICS international chronostratigraphic chart*, v2019/05 (Cohen et al., 2013).

Pleistocene lowstand of the sea-level at the end of the Late Glacial Maximum (c 125 m below present sea level; c 19 ka BP), sea level rise in the Tyrrhenian Sea reached its maximum rate around 14 ka BP (3.4 cm a^{-1}) (Benjamin et al., 2017; Lambeck et al., 2011). Occasional deposition of coarse alluvial sediments indicate riverine inflow and progradation.

Sedimentation began to change after c 7.9 ka BP, when sea level rise decelerated to a local minimum (Figure 8.7). Paludal sediments were more frequently deposited and the earliest dated layers of alluvial fines occur, indicating early aggregation.

After 7.6 ka BP, valley aggradation set on; (fine) alluvial sediments dominated the valley-fills on Elba. The early alluvial deposits in phase VI mainly consist of sand and gravel ('coarse' in Figure 8.6) and are indicative for channel-related deposits (Schneider et al., 2014); after 7.9 ka BP, the proportion of overbank fines increased. We interpret this pattern as an indicator for early valley consolidation and the geomorphological change from a close-delta, unincised braided-river system to a (meandering) incised system, as seen today in the plains on Elba.

The maximum flooding surface record at different locations of the central Italian peninsula dates to 9.2—7.8 ka BP (Amorosi et al., 2014b; Breda et al., 2016; Rossi et al., 2011).

between the sites varies from 3.5–8.9% prior to 7000 ka BP and 14.3–28.0% after 7000 ka BP. Variance is greater for the post-LGM transgression (Lambeck et al., 2011). The northern Tyrrhenian coast north of Orbetello and along Sardinia; and the eastern Ligurian coast is tectonically stable, with Holocene and last glacial absolute vertical displacement rates < 0.15 mm a^{-1} (Antonioli et al., 2007, 2011; Lambeck et al., 2011).

Late transgressive–early high stand aggradation (7.1 to 5.4 ka BP)

The change in facies associations from palustrine/paludal deposits to alluvial sedimentation amplifies around 7.1 ka BP and coincides with an increase in the cumulative probability of cal-^{14}C-ages (phase VI, 7.1–5.7 ka BP). Moreover, the rate of simulated sediment accumulation increases clearly. The interpretation of the facies pattern suggests a change from geomorphic quiescence to geomorphic activity. This change in sedimentation pattern roughly corresponds to MWP 1d (the so-called '7.6-ka-event'; Smith et al., 2011; Yu et al., 2007). The deceleration of the sea level rise resulted in a stagnant base level and the increasing relative contribution of alluvial input by flooding.

Additionally, accelerated geomorphic activity and sediment accumulation around 7.1–5.7 ka BP (phase IV) falls within the Holocene climate optimum (c 9 to 4 ka BP; Zanchetta et al., 2013).

After c 6.2–5.4 ka BP, only minor layers of palustrine sediments were deposited in the low-lying portion of the valleys (Figure 8.7). The record is dominated by alluvial sediments and slope deposits. After 5.7 ka BP, valley aggradation (phase VI) and fluvial activity on Elba Island decreased. This pattern corresponds to the transition from late transgressive to early high stand conditions (Figure 8.7); sea level change dropped from 0.79 cm a^{-1} after the last MWP (1d, c 7.5–7.0 ka BP) to 0.13 cm a^{-1} round 6.0 ka BP, only slightly increasing until recent times (0.04 cm a^{-1}, Lambeck et al., 2011).

In the (central) Mediterranean, the period between 7.1 and 5.4 ka BP is characterized by warm and wet conditions; an aridisation trend started around 5.5 ka BP reaching maximum dryness in Italy around 4.0 ka BP (see e.g. Jalut et al., 2009). Lake level high stands occurred between 9.2 and 4.2 ka BP at Lago Trasimeno or between 7.6 and 6.2 ka BP at Largo dell'Accesa. The phase of maximum precipitation recorded by flowstone accumulation dates to 8.2–7.1 ka BP (Zhornyak et al., 2011). Moreover, tree cover between 8.0 and 7.0 ka BP and around 5.5 ka BP decreased in Central Italy and charcoal accumulation or fire frequency record in lake sediments increased (see Figure 8.7). Contemporary increasing geomorphic activities suggest an interpretation of increasing human activities on the Apennine peninsula mainland. Therefore, increased rainfall and human disturbance may have also contributed to sediment accumulation; beyond, the Versilian transgression appears to be the dominant factor: Highest sediment accumulation on Elba Island during the mid-Holocene doe not coincide with the wet period between the 8.2-cold-event and maximum precipitation. Additionally, sediment facies records do not show simultaneously increased geomorphic activity (Figure 8.7, presumably because not all sequences were obtained from low lying areas). The frequency of archaeological finds from Elba Island in the phase between 7.1 and 5.4 ka BP does not increase markedly.

Mid- to Late Holocene stabilization (5.3 to 4.5 ka BP)?

CPF of cal-^{14}C-ages indicate phases of higher deposition around 5.3 ka BP and between 5.0 and 4.5 ka BP (phases V and IV). The simulated sediment accumulation for this period gives an ambivalent picture; depending on the theoretical model selected, increased accumulation is either classified as 'more likely than not' or 'unlikely'. As both phases are characterized by relative quiescence as indicated by the facies pattern, the overall pattern from the sediment sequences might be indicative for a gradual stabilization between 5.3 and 4.5 ka BP.

This late mid-Holocene phase of possible geomorphic stability coincides with a period of increasing aridisation between 5.5 and c 4.0 ka BP (Jalut et al., 2009). Records from Lago dell'Accesa indicate increasing summer precipitation, summer cooling, and decreasing winter precipitation (Peyron et al. 2011; see also Magny et al. 2007). However, the peak in the CPF of cal-^{14}C-agesroughly coincides with a pronounced phase of flooding in the Mediterranean, and especially in southern and southern Italy (Figure 8.7).

From the data at hand, it is at the moment difficult to estimate the change in Human activity during the phases between 5.3 and 4.4 ka BP. The frequency of archaeological finds from Elba increased slightly with the Eneolithic (c 5.5 ka BP), mostly originating fro the Campo area (Figure 8.8); cal-^{14}C-ages are biased towards the Campo plain(Figure 8.8; see Section 8.5.2). The the rate of finds per year is, however, low compared to other archaeological periods (Figure 8.7).

Late Holocene quiescence (4.5 to c 3.0 ka BP)

After 4.5 ka BP (end of phase IV) relative geomorphic stability occurred on Elba, continuing until ca. 3 ka BP. This is evident in the low CPF, facies associations, and a low likelihood that sediment accumulation exceeded the theoretically expected sedimentation rates. This transition coincides with major climate changes observed—not only—in the Mediterranean region (see Figure 8.7p). The so-called '4.2'-event is characterized by a phase or phases of prominent, global, multi-decadal to centennial scale cooling and drying (Di Rita & Magri, 2009; Magny et al., 2009). The actual dating of the event ranges from 4.3 to 3.8 ka BP (Bini et al., 2019). The record from Basilicata, Southern Italy, shows phases of increased and clearly decreased activity between 4.2 and 3. ka BP. Moreover, on Crete, the interval between 4.2 and 3.4 ka BP is marked by incision and fluvial erosion (Macklin et al., 2010b). In other studies focussing on fluvial activity in the Mediterranean region, the 4.2-event is—in contrast to the record from Elba—associated with phases of increased fluvial activity (Zielhofer et al., 2008). In contrast to our study, Borrelli et al. (2014) observed ephemeral aggradation prior to 4.3 ka BP in alluvial plainstributary to the Turano river in the Appenine

mountains; they explain the absence of mid-Holocene sediments with limited sediment supply in a phase of stability and biostasys during the climate optimum. Based on a review of lake records, also Walsh et al. (2019) propose relative stability between 8.0 and c 4.2 ka BP and an increase in erosion between 4.2 and c 3.0 ka BP, which they attribute to climate variability and increasing human pressure. Piccarreta et al. (2011) identified two phases of increased geomorphic activities between 4.2 and 3.0 ka BP (4.3–4.1 ka BP and 3.4–3.1 ka BP) in Basilicata, southern Italy, while for c 3.0 ka BP and 2.4 ka BP, they did observe increased geomorphic activity. They associate phases of increased geomorphic activity with climate variability coinciding with increased humidity (lake level high stands); a major cold phase might explain the decrease in aggregation prior to 4.3 ka BP. In a synthesis of multi-proxy data of continental archives from Central Italy, Giraudi et al. (2011) state that the 4.2-event went along with pronounced and frequent environmental variability.

Vigliotti et al. (2003) proposed increased metallurgical activity during the period of late Holocene quiescence (4.5–3.0 ka BP) on Elba (Figure 8.7), which is not confirmed the the data on geomorphic activity on Elba and the relative slight increase of archaeological finds from the period (Figure 8.7). Instead, the data of Vigliotti et al. (2003) correspond to human activity on the mainland, where the increase in human activity is more pronounced (Figure 8.7, l). Furthermore, palynological and antracological proxies indicate peaks in human disturbance during the Eneolithic in western Central Italy (Figure 8.7). The frequency of archaeological material from Elba dating to the proposed phase of late Holocene quiescence increased during the Late Bronze Age, as it is the case for human activity on the mainland (Figure 8.7, l). Fire frequency and charcoal accumulation point to increased or low human activity, respectively (Figure 8.7, q, r). The palynological proxy record from central Italy reveals human environmental disturbance during the Bronze Age (Figure 8.7, o, p).

Three reasons may explain this contradiction between the different records from Italy. First, the absence of any cal-^{14}C-ages from Elba dating to the interval between early late Holocene fits to a general trend in drier and warmer conditions; the transition from a major pattern of aggradation prior to 4.2 ka BP to less aggradation after 4.2 ka BP coincides with the major 4.2-event (e.g. Zanchetta et al., 2012) that triggered a clear change in vegetation pattern (Peyron et al., 2011). Second, Elba is located in the transition zone between north and south Mediterranean conditions (typically placed between 41°and 43°N). Scholars observed a low impact of the 4.2-event in the north Mediterranean north of 43° N and a clear impact in the southern Mediterranean (Marchegiano et al., 2019; Peyron et al., 2013). Magny et al. (2009) show that after 4.2 ka BP, the climatic oscillations had a complex spatial pattern. Di Rita & Magri (2009) observe a distinct opening of the landscape around

4.0 ka BP, which they explain by repeated droughts caused by regional circulation pattern. Thus, the climatic impact of the 4.2-event and subsequent environmental changes might not have had a marked impact on the morphdynamics on Elba Island. Third, although the vegetation composition in central Italy changed after 4.2 ka BP, the total tree coverage might not have been significantly reduced, so that soil erosion might have potentially remained stable. On the other hand, incision and fluvial erosion might have affected our sediment record.

As shown by Borrelli et al. (2013), valley aggradation in the Appenine 'propagated' from lower reaches to higher reaches. Taking this view, the coupling of archives also explains the decrease in sediment accumulation Elba during the early late Holocene. While progradational sediments (that are triggered by transgression) are deposited below present sea level (Figure 8.3), aggradation, e.g. in the upper sediment sequence from Forcioni valley, start much later, probably around 2.2 ka BP. Also Fontana et al. (2008) observe a tendency of coastal propagation and a scarcity in river deposition in lower reaches of the Po valley after the Holocene transgression (mid-Holocene until ca. 3.5 ka BP).

Etrusco–Roman human and geomorphic activity (2.7 to 1.9 ka BP)

The phase of relative geomorphic stability and low sediment accumulation since 4.5 ka BP is followed by a moderate increase in geomorphic activities observed from c 3.0 ka BP onwards (phase IV, 2.7–2.5 ka BP), culminating in accelerated activities between 2.3 ka BP and 1.9 ka BP (phase III). Further phases of increased geomorphic activity are recorded between 0.8 and 1.6 ka BP (phase I–II). The statistical analysis indicates that the empirical cumulative probability during these phases significantly exceeds the theoretical CPF as expected from the location of the cal-^{14}C-ages in the sediment sequence. The modeled rate of sediment accumlation reveales a major phase of aggradation around 2.0 ka BP, although the likelihood of the result is based on the selection of a theoretical distribution of sedimentation (Figure 8.5). Based on our data set, it is not clear wether the increase in the CPF after 1.0 ka BP is a sampling artifact. Our facies record (Figure 8.6) clearly supports the interpretation of the empirical and simulated CPFs. Around 2.2 ka BP, the pattern of the facies associations cleary changed. The data from the facies record additionally show that the probability of the deposition of layers indicating geomorphic activity increased during phase III. Moreover, the facies pattern indicates a further decrease in palustrine layers.

The increase in valley aggragation and geomorphic activities in phase III are strongly linked to the Roman occupation of Elba Island and the subsequent economic changes on the island (see Case Study 4, Becker et al., submitted.a, Chapter 9, for details and references).

For this phase the number of archaeological finds from Elba clearly increased (Figure 8.7). Etruscans exploited iron mines on Elba Island from the 6th to the 3rd century BCE; and smelted the ore on the mainland until the late 4th or 3rd century BCE. The Romans established a large-scale iron industry on the island in the late 2nd and 1st century BCE and also increased felling for fuel production. Scholars asserted that fuel run short on Elba due to intensive clearing in the 1st century BCE and smelting sites were abandoned. Thus, deforestation plays a key role in the understanding of human activities on Elba in the second half of the first millennium BCE. Also the increase in the quantity of archaeological finds dating to the Roman period reflects the increase in metallurgical activities on Elba (Figure 8.7). The abandonment of most smelting sites in the mid-1st century BCE and a decline of human activities in the 1st and 2nd century CE is synchronous to the decrease in fluvial aggradation and geomorphic activities after 1.9 ka BP (phase III).

Data from the sparse pollen records from Elba suggest a change in species composition that coincides with the increase in aggradation and geomorphic activity on Elba (phase III). From 4.4–4.1 ka BP to around 2.3–2.0 ka BP, the proportion of pollen from *Quercus pubescens*, *Quercus suber* and *Quercus ilex* decreased, as it is the case for other boreal pollen. Concentrations of major herbal pollen show a variable picture; while the proportion of pollen from *Asteracea/Cichorioideae* and *Chenopodiaceae* decreased. The proportion of *Ericaceae* pollen increased (Bertini et al., 2014). Bertini et al. (2014) interpret this pattern as a palynological proxy for the impact of ancient metallurgy on the landscape. As discussed in context of the debate on the fuel scarcity on Elba Island during the phase of Roman iron smelting (Case Study 4, Becker et al., submitted.a, Chapter 9), the palynological records are ambiguous, especially because of the use of *Ericacea* species (*Erica arborea*, *Arbutus unedo*) as fuel species and the variability of the proportion of Quercus pollen prior to the smelting period. A woodland transition from a dominance of oak to Erica shrubland might not necessarily induce increased susceptibility to erosion and therefore an increase of gemorphic activites. Nevertheless, both an increase in gemorphic activities and the transformation of woodland cover point to human impact (see e.g. the change in *Quercus ilex* and *Ericaceae* in the Lago dell'Accesa record, Drescher-Schneider et al. 2007). Likewise, the co-instantaneous decrease in the proportion of different Quercus species points to human felling, as the different species are normally present in associations reflecting different bioclimatic belts. Data from a meta-analysis conducted by Woodbridge et al. (2018) show that both phases of increased sedimentation and geomorphic activities on Elba Island occurring between 3.0 and 1.9 ka BP correspond to changes in the overall vegetation composition in central Italy. Moreover, increased human impact on vegetation composition on the mainland is also evident in a higher relative contribution of anthropic

indicator species to the palynological records (Figure 8.7). Mercuri et al. (2013) observed a sharp increase in cultivated trees *(Olea, Junglas, Castanea)* during Roman times.

Reconstructed accelerated geomorphic activities triggerd by human impact during Roman occupation obtained from sediment archives on Elba fit to the geomorphological, archaeological, and palynological findings from the Apennine peninsula, especially from central Italy. CPF of cal-^{14}C-ages from archaeological sites in central Italy do not show an increase in geomorphic activities during Etruscan–Roman times. However, a research bias affects the archaeological CPF-records, as the relative-chronological dating is favored over absolut-chronolgoical methods in Roman archaeology.

The Roman smelting period falls into a transition period from 'natural to anthropogenic-dominated environmental change in Italy' (Zanchetta et al., 2013, p. 1). Other studies on CPF from different regions in Italy and the entire Mediterranean region have observed a phase of increased geomorphic activity around 2.0 ka BP. Several studies from the Apennine Peninsua, including those from Central Italy, show the importance of the human impact as a trigger for increased geomorphic activities (see overview in Section 8.2). Although Romano et al. (2013) propose that especially a decrease in human activities might result in geomorphic instability—e.g. due to the abandonment of terrace systems—, the phase of increased geomorphic activity on Elba Island during Roman times is followed by quiescence; maybe agriculture, especially with cropping terraces, was not important on Elba as the economic focus was on iron smelting (see Chapter 4; most terraces found on the island today were build after the 17th century; see Chapter 3).

Notwithstanding the observation that mainly human activities triggered environmental change during and after the Roman times, other examples are known. For instance, the record from Lago dell'Accesa in Central Italy mainly indicates climatic triggered lake level changes (Magny et al., 2007). Heading towards the same direction, Ramrath et al. (2000) identified a coincidental change in sediment pattern and climate, albeit they also observed that the sedimentological record allows to distinguish between different phases of human occupation by presence of turbidites and charcoal.

Post-roman variance

Phase II/I (1.6–0.8 ka BP) falls within a period of reduced human activities on Elba (Figure 8.7, f) and coincides with the onset of high medieval human dynamics and a second historical phase of iron production on the island. Nevertheless, inference tests indicate that our data is not sufficient enough to clearly state that this phase is non-random. Activities clearly peak after 1.1 ka BP. During the early Middle Ages less evidence for human

settlement activities were found on the Elba Island (compared to the Roman period); only after the 9th century CE, so during Pisan times, new settlements were founded.

A relatively high sequence of fluvial activity phases is recorded from allover Italy and the Mediterranean after antiquity (Figure 8.7, d). Palynological and anthracological data suggest human disturbance (e.g. a clear decrease in arboreal pollen) in central Italy from c 2.0 ka BP to present (Figure 8.7, j–p).

8.5.2 Methodical biases

The data set at hand is biased by several factors. These biases are introduced by the nature of the sampling process and the representativeness of the uncovered sediment archives on Elba. (See Contreras & Meadows, 2014; Hinz et al., 2012; Williams, 2012 for bias in archaeological methods using CPF of cal-^{14}C-ages in reconstruction of demographics.) Moreover, the relatively small number of samples in our data set might reduced the reliability of the results (cf. Jones et al., 2015). We nevertheless argue that it is reasonable that the 56 samples in our data set reflect a trend in geomorphic activities and sediment accumulation on Elba: It has to be considered that the source area of our

Table 8.3 Biases of the meta-analysis of cal-^{14}C-ages. The last column shows the approaches used to reduce the bias; 'quantitative' = discussed, but not modeled.

Bias	Description	Approach
Archive bias		
Accessibility	The coastal plains offer the most accessible archives; the geographical distributions of the plains is limited to Central Elba; few accessible archives are found in the Northwest	–
Researcher bias		
Location	Most sampled sediment sequences were obtained from the Campo coastal plain	Qualitative
Drilling	Drilling depth does not always reach the base of the sediments, overprepresentation of younger sediments	Theoretical CPF
Sampling	Selection of samples for radiocarbon dating (research agenda)	Simulated ages
Sample bias		
Production	Charcoal burning increases availability of dating material	Simulated ages
Taphonomoy	Likelihood that younger samples and layers are preserved is higher (fragmentation and erosion); better conditions of preservation in anoxic milieu	Theoretical CPF

sediment sequences is from relatively small catchments with an area between 1.5 km^2 (San Giovanni) and 5.4 km^2 (Stabiatti/Campo; see Figure 8.1). In total, the sediment sequences represent a catchment area of c 18.4 km^2. Consequently, compared to other studies on cumulative probability functions, this is an intermediate–high relative number of samples (see Section 8.1). Second, the Bayesian approach using age–depth models and test statistics applied to the CPF show that the empirical data are likely different from randomly distributed samples with the same number of samples (bootstrapping approach, Figure 8.4, and Figure 8.5). We propose that a smaller number than the data density proposed by Michczynska & Pazdur (2004) and Williams (2012) also covers environmental dynamics.

Archive biases

The alluvial archives on Elba are not equally distributed over the different morphological regions of the island (Figure 8.1; see also Section 3.1.2). In consequence, the cal-^{14}C-ages in our data set were obtained from the coastal plains in Central Elba and valleys in northeastern Elba, where alluvial archives are available. Valley fills in the western island consist mainly of stony–blocky gravitational deposits. Beyond, the potential sediment archives on the island do not equally cover environmental dynamics in the different ecological–geomorphological regions on the island (Figure 8.1; cf. Hoffmann et al., 2009). The cal-^{14}C-ages in the current data set were sampled from sediment sequences that were uncovered by percussion drillings or hand auger corings. Therefore, the very coarse deposits were not accessed and no cal-^{14}C-ages are available for these archives. In other regions, such as the Calamita peninsuala, alluvial fills are very limited, as valleys are deeply incised and valley slopes are steep. Additionally, some sediment archives are not accessible the plains in parts densely build-up areas. The regions underrepresented due to the limited accessibility of sediment archives are, however, areas of important past human activity that might have triggered Holocene geomorphic activities (Figure 8.8).

Researcher bias

Sediment sequences available do not equally represent the available archives. Our data set is strongly controlled by sediments from the Pianura di Marina di Campo. Especially valleys that are draining the eastern flank of Monte Capanne dominate the present record (Figure 8.1); we collected 50% of all sequences and 61% of all ages from this area (7 sequences and 34 ages), albeit only 17% of the the alluvial plains and valleys on Elba are filled with sediments originating from the eastern side of the Monte Capanne (< 10% of the island's surface area). The Magazzini/Schiopparello plain is not represented in our

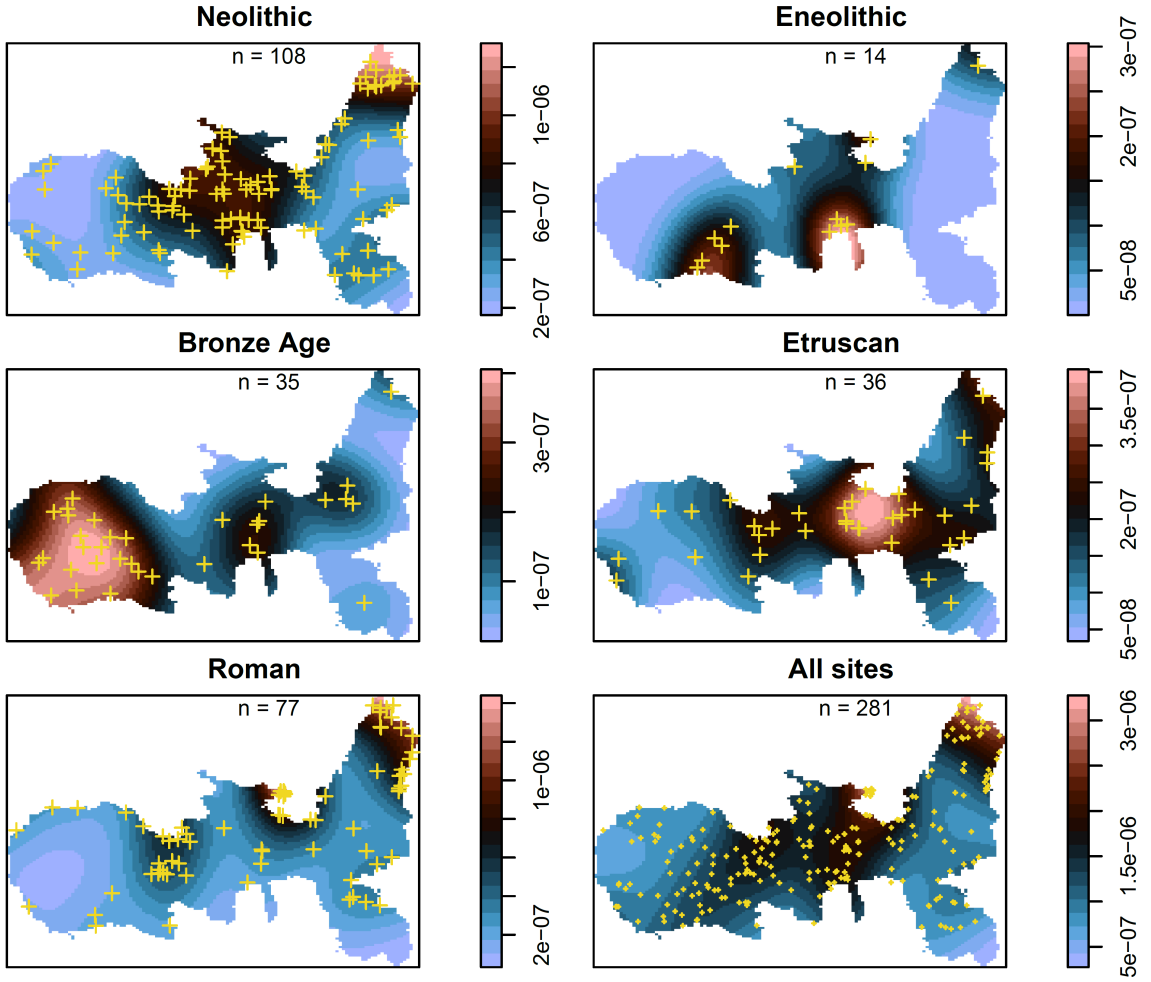

Figure 8.8 Kernal Density Estimate of archaeological finds on Elba during different archaeological periods. Data were taken from Pagliantini (2014). Please note the different duration of the periods and the number of finds per period. The categorization of the colour palette for the phases is not equally spaced.

data set; Mola, Lacona, and San Giovanni are only represented by one sequence each (in total 3 sequences and 11 ages). Sediments sequences in our data set obtained from alluvial valleys are limited to the Ortano and Baccetti valley in the northwest of the island (also 3 sequences and 11 ages). All watershed under consideration experienced intensive land use in the mid-20th century, and are (except of the Ortano and Stabbiatti catchment) today relatively covered by relatively dense woodland vegetation.

Although our data set is quantitatively biases towards the Campo area, it nevertheless represents different regions on Elba (western, central, and northeastern Elba). The data set includes sediments from different relief positions (plains and valleys; low-lying parts and middle reaches). Additionally, the regions mirrored in the sediment archive cover different intensities of human activities with time; e.g. the eastern slopes of Monte

Capanne that are a key area of human activities used during the Eneolithic, the Neolithic, and the (final) Bronze Age (Figure 8.8).

Sample bias

Not only the availability of sediment archives suitable for palaeoenvironmental reconstructions, also the availability of datable material may introduce bias to the data set for the meta analysis of cal-^{14}C-ages. Most of the samples dated applying the radiocarbon method in our data set were charcoal or plant remains. The availability of these materials for dating is biased by production and taphonomic phenomena. Macroscopic plant remains in the sediment sequences from Elba Island are mostly limited to palustrine deposits. Plants were abundant in these depositional environment and were preserved under subaquatic, anoxic conditions. Therefore, ages from palustrine environments may be overrepresented in a data set of cal-^{14}C-ages.

Human-induced fires and (natural) wild fires are the main sources of charcoal in the environment. Both are common in Elba's eco-region. Human-induced fires may led to a greater abundance in charcoal fragments from alluvial archives. Becker et al. (2019a) show that charcoal fragments from layers dating to periods of smelting in antiquity are more abundant and often larger compared to other pre- or post-dating layers. Thus, an increase in the relative frequency of cal-^{14}C-ages is merely a proxy for increased charcoal production (charcoal burning) than an indicator for increased geomorphic activities. In addition, charcoal-samples may be damage during transport and frequently got fragmented (Figueiral & Mosbrugger, 2000). Charcoal fragments are thus underrepresented in coarse layers. In our data set, the increase in CPF of cal-^{14}C-ages in the mid-Holocene is related to the deposition of plant remains and Holocene transgression. Nevertheless, it is reasonable that also increased geomorphic activities were contemporary due to increasing stability of the erosion basis. The effect of the production bias and morphodynamic processes are inter-fingering. Charcoal burning results in a greater abundance of charcoal production, but also triggers soil erosion and therefore also deposition. The vertical and horizontal reworking of charcoal fragments may introduce bias to the record, which is especially important for possible age-inversions in the sediments (Carcaillet, 2001; Schroedter et al., 2013).

Using not only the CPF of cal-^{14}C-ages, but also modelling of age–depth information in the Bayesian approach attenuates the this effect. Our models based on sediment accumulation and facies change are less sensitive to the effect and may better reflect geomorphic activities.

The sampling of dating material from sediment sequences is strongly affected by a researcher bias, i.e. the behavior of the person taking the samples and his or her overall research agenda (Orton et al., 2017). Often, samples were taken from sediment layers that indicate a change in the sedimentation pattern. Therefore, researcher often sample sediments from the transition from transgressive to early high stand conditions. Additionally, the prior aim of Becker et al. (2019a) was to reconstruct the environmental impact of ancient iron smelting. Thus, their emphasis was to cover the Etrusco–Roman period with their samples.

The most important bias when analysing CPFs of cal-^{14}C-ages from (alluvial) sediment sequences obtained by coring—and also from trenches—is the overrepresentation of younger sediments compared to older layers. Older layers are more likely to be eroded and reworked. This taphonomic effect is amplified by coring depth. If the sampled layers do not cover the whole sequence from the sediment basis at the bedrock to the topsoil layer, only the younger parts of the sediments are dated. In our data set, for instance, a great majority of the dated sediment sequences cover the last 2000 years. Only few dated sequences cover the last 7000 years. However, this phenomenon mainly effects the results of the conventional CPF-analysis. Testing the actual CPF of the dated sediment layers against a theoretical CPF, the drilling bias does not importantly corrupt the results. Models of the taphonomic bias are common in approaches using CPF of cal-^{14}C-ages (e.g. Bluhm & Surovell, 2019; Surovell & Brantingham, 2007; Williams, 2012; cf. Hoffmann et al., 2008).

8.6 Conclusions

We conducted a meta-analysis of cal-^{14}C-ages from sediment sequences to reconstruction sediment accumulation and geomorphic activities on Elba Island during the mid and late Holocene. The sequences were obtained by hand auger and percussion drilling from four coastal plains and two filled valleys on Elba (Becker et al. 2019a; D'Orefice & Graciotti 2014, and unpublished data). We based our methodical approach on the traditional procedure of cumulative probability functions of cal-^{14}C-ages to reconstruct fluvial activities, but included a stochastic component. Additionally, we applied Bayesian statistics on the data set, thus including the stratigraphic information and the depth of the samples as *prior* information in our models, giving a proxy for geomorphic activities.

We identified several phases of increased sediment accumulation in the coastal plains on Elba Island based on cumulative probability functions: 0.8–1.6 ka BP; 1.9–2.3 ka BP; 2.5–2.7 ka BP; 4.6–5.0 ka BP; 5.3 ka BP; 5.7–7.1 ka BP. A chronological model of the facies associations and simulated cumulative probability functions reveals that during the phases

from 1.9 to 2.3 ka BP and from 5.7 to 7.1 ka BP likely correspond to increased sediment accumulation and geomorphic activity; major quiescence is recorded for the interval between 4.6 and c 3.0 ka BP; no dated layers are older than c 9.0 ka BP.

Three major triggers of a change in geomorphic activity and sediment accumulation can be observed:

Holocene transgression. The record prior to c 9 ka BP shows the occasional deposition of layers indicating marine flooding and propagation. Between 9 and 5.7 ka BP the changing dominance of sediments typical for wetland environments and coarse to fine alluvial sediments indicate progradation and increasing aggradation at base level when sea level rise decelerated. During high stand conditions, wetland sediments were only occasionally deposited in low lying areas.

Climate. The phase of increased sediment accumulation during the late transgressive and early high stand conditions partially coincided with wetter conditions during the Holocene and may have contributed to increased accumulation and geomorphic activities. However, the contribution of sea level rise is more important. A change of sediment accumulation around 4.6 ka BP and a long phase of observed geomorphic quiescence is more or less contemporary to the major climatic event at the transition between the mid and late Holocene.

Human impact. The clearly increased gemorphic activities, the increased sediment accumulation, and peaking cumulative probability of cal-^{14}C-ages points to marked environmental change between 2.3 and 2.0 ka BP. This period is strongly connected to the iron smelting activities on Elba, which started in the 4th century BCE and increased in the 2nd century BCE. Strong human impact on the environment during this time is a common *topos*; a strongly increasing number of archaeological find counts during this time coincides.

The pattern of geomorphic activity is similar to a general trend observed for (central) Italy, although especially the long phase of geomorphic quiescence in the early late Holocene is not mirrored in all archives. Proxy data from various archives from the Appenine peninsula show that human impact as record on Elba comes visible relatively late. Nothwithstanding, especially the Roman period is not only a phase of major environmental changes on Elba Island, but also in other regions (Section 8.2).

Iron smelting on Elba had a clear impact on the geomorphic activity and sediment accumulation on Elba.

9

The Furnace *and* the Goat— A spatio-temporal model of the fuelwood requirement for iron metallurgy on Elba Island, 4th century BCE to 2nd century CE

Submitted version of a manuscript now published as: Becker, Fabian, Nataša Djurdjevac Conrad, Raphael A. Eser, Luzie Helfmann, Brigitta Schütt, Christof Schütte, and Johannes Zonker: The Furnace *and* the Goat—A spatio-temporal model of the fuelwood requirement for iron metallurgy on Elba Island, 4th century BCE to 2nd century CE. *PLoS ONE* 15(11): e0241133. **https://doi.org/10.1371/journal.pone.0241133**.

Supplementary materials. For a supplementary materials see Appendix of this dissertation and the following link to the supplementary materials available on the publishers webpage: https://journals.plos.org/plosone/article?id=10.1371/journal.pone.0241133#sec035.

Research data. Code, input data of the main model, and intermediate and basic final results are available from the publishers webpage (see link above).

Abstract. Scholars frequently cite fuel scarcity after deforestation as a reason for the abandonment of most of the Roman iron smelting sites on Elba Island (Tuscan Archipelago, Italy) in the 1st century BCE. Whereas the archaeological record clearly indicates the decrease in smelting activities, evidence confirming the 'deforestation narrative' is ambiguous. Therefore, we employed a stochastic, spatio-temporal model of the wood required and consumed for iron smelting on Elba Island in order to assess the availability of fuelwood on the island. We used Monte Carlo simulations to cope with the limited knowledge available on the past conditions on Elba Island and the related uncertainties in the input

parameters. The model includes both, wood required for the furnaces and to supply the workforce employed in smelting. Although subject to high uncertainties, the outcomes of our model clearly indicate that it is unlikely that all woodlands on the island were cleared in the 1st century BCE. A lack of fuel seems only likely if a relatively ineffective production process is assumed. Therefore, we propose taking a closer look at other reasons for the abandonment of smelting sites, e.g. the occupation of new Roman provinces with important iron ore deposits; or a resource-saving strategy in *Italia*. Additionally, we propose to read the development of the 'deforestation narrative' originating from the 18th/19th century in its historical context.

9.1 Introduction

In his seminal paper *The Furnace versus the Goat* published in 1983, Theodor A. Wertime put forward that 'pyrotechnological industries'—including metallurgy—were the main cause for deforestation in the Mediterranean region during antiquity (Wertime, 1983). Citing the case of Etruscan Populonia at the coast of Tuscany, Italy, Wertime follows two lines of arguments. First, he identifies economic strategies of the Etruscans to cope with fuelwood scarcity. This strategy includes the transport of raw ore to locations with available forest resources and the transition from energy-inefficient copper production to the more efficient iron smelting process (Rehder, 2000; Wertime, 1983). Second, Wertime estimates 'energy costs'—i.e. the demand of woodlot—of iron smelting in Populonia based on the quantity of slag found there and a factor to estimate fuelwood requirements from the quantity of slag. The latter approach is common in studies on the resource consumption for pre-industrial (charcoal-fuelled) iron metallurgy (Brumlich, 2018a; Cleere, 1981; Goucher, 1981; Healy, 1978; Iles, 2016; Paysen, 2011; Pleiner, 2000; Rehder, 2000; Saredo Parodi, 2013; Thelemann et al., 2015; Voss, 1988; Wallner, 2013); recent approaches focus on anthracological or palynological analysis (Eichhorn et al., 2013a,b; Mighall & Chambers, 1997).

Romans and Etruscans exploited most of the iron that was processed in Populonia from the ore deposits on Elba Island (Figure 9.1). Historical texts and archaeological and archaeometallurgical records suggest that Elba Island played a key role in the supply of raw iron ore and iron bloom for the Etruscan and Roman economy (e.g. Diod. Sic. 5.13.1; Str. 5.2.6; Verg. Aen. 10.170; Ps.-Aristot. Mir. 93; Benvenuti et al., 2013, 2016; Corretti, 2004; Tanelli et al., 2001).

Ancient metallurgical centres are often regarded as hotspots of deforestation and subsequent fuel scarcity (Harris, 2013; Hughes, 2011). Therefore, the reconstruction of past human–environment interactions plays a key role in the current understanding

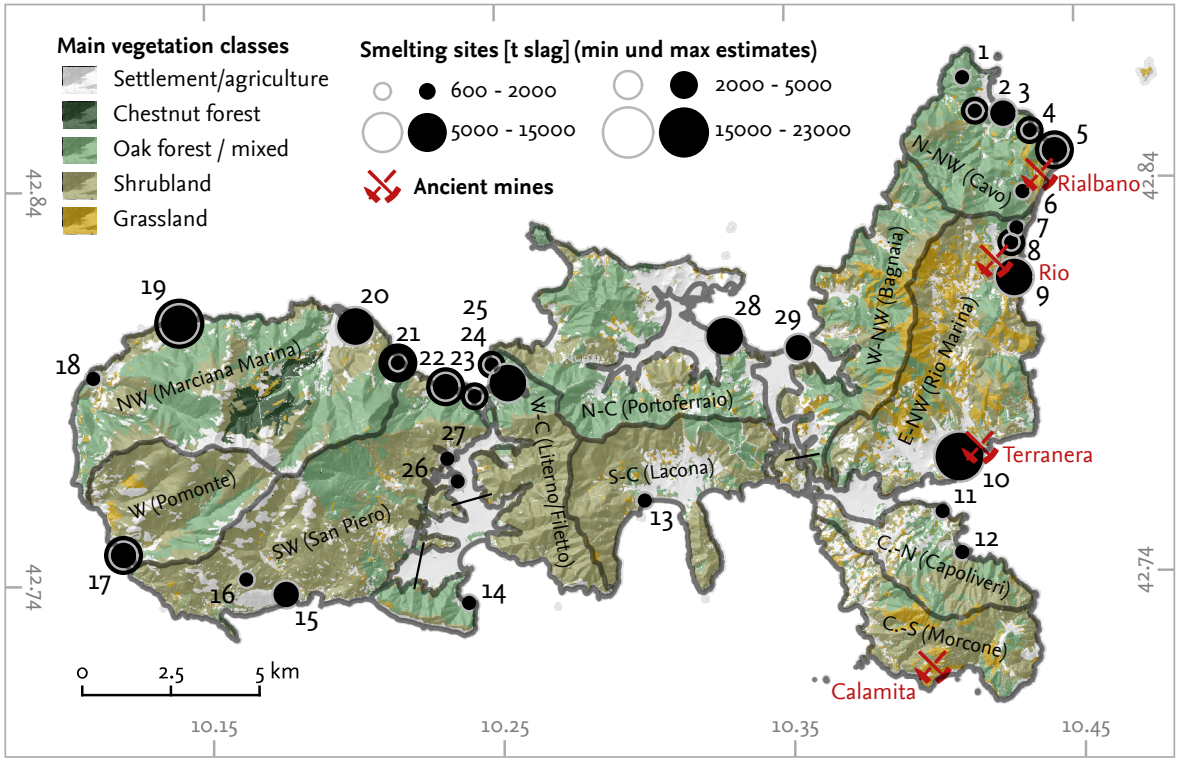

Figure 9.1 Ancient smelting sites, ancient mines, and main vegetation types on Elba Island. The size of the dots for each site is a function of the estimated quantity of slag disposed on each site during antiquity; black dots indicate upper estimates, whereas grey circles indicate lower estimates (see Table 9.2). The regions that were used for the model analysis in the *Results* section are shown (grey borders). IDs of the sites corresponds to those given in Table 9.2.

of the development of the iron metallurgy on Elba and Populonia. While the onset of iron smelting in Populonia dates to the 7th or 6th century BCE (Chiarantini et al., 2009; Corretti & Benvenuti, 2001), first smelting activities on Elba most likely date to the 4th century BCE (Becker et al., submitted.b; Corretti & Firmati, 2011; Eser & Becker, submitted; Firmati et al., 2006). Scholars invoke several reasons for the time lag between the first smelting operations in Populonia and on Elba Island. First, an 'industrial quarter' for copper metallurgy in Populonia existed before the onset of iron production. Copper production on Elba Island, on the contrary, took place only on a small scale between the 9th and 7th century BCE (Chiarantini et al., 2018). Thus, the proximity of the deposits on Elba Island to Populonia and the accessibility from the coast might have made the transport of the ore directly from the mines to Populonia an obvious choice. Moreover, political threats in the Tyrrhenian Sea (see Corretti, 2017; Zecchini, 2001) made Elba Island an unsecure place during that time. Chiarantini et al. and Wiman (Chiarantini et al., 2018; Wiman, 2013) rose the issue of a lack of fuel supply on Elba in the 6th century BCE BCE *(sic!)*. Also Veal and Lang (Lang, 2017; Veal, 2017a) believe that the reason for the transport of ore from Elba to Populonia in Etruscan or early Roman times was deforestation.

Iron production on Elba Island increased after the Roman occupation (mid-3rd century BCE, Corretti, 2017). Ancient authors took notice from smelting activities on the island during Roman time (e.g. Diod. Sic. 5.13.1; see Corretti, 2004; Sherwood et al., 2003). Smelting sites dating to the Roman period were located all over the island, although iron mines on Elba are only located along the eastern coast (Tanelli et al., 2001; see Figure 9.1). Scholars explain this pattern by rational use of the fuelwood resources on the entire island (Corretti, 1988, 2017). Occasional finds of forging slags in a contemporary hilltop settlement point to small scale refining on Elba Island for domestic use (Corretti, 2016); from Populonia, large forges are known (Chiarantini et al., 2007). Corretti (2017) proposes that the location of smithing activities on the mainland also transferred parts of the fuel requirement to the Apennine peninsula. Smithing—like smelting—required significant amounts of wood or charcoal. This fact, along with the location of the smelting sites on Elba, may therefore imply a strategy of rational fuel consumption. Crew & Mighall (2013) proposed that bloomery smelters were interested in a rational use of resources to maintain production.

In the mid-1st century BCE, most of the smelting sites on Elba Island were abandoned (Corretti, 1988, 2017; Corretti & Firmati, 2011; Pagliantini, 2014). It is widely cited that a lack of fuel caused the abandonment of smelting on the island in the mid-1st c. BCE (Bebermeier et al., 2016; Corretti, 1991; Forbes, 1964; Harris, 2013; Hughes, 2014; Meiggs, 1982; Penna, 2014; Perlin, 2005; Pococke, 1745; Sands, 2013; Schweighardt, 1841; Simonin, 1858; Veal, 2017a; Williams, 2010; Wiman, 2013). Other authors mention the role of deforestation and the scarcity of resources for the decline of metallurgy on Elba Island as well as in Populonia (Corretti, 2009; Di Pasquale et al., 2014). These scholars mainly cite historical evidence to argue for a lack of fuel as the (main) driver of the decline of iron industries on Elba Island during antiquity: According to a report by the ancient Greek geographer Strabo dating to the late 1st century BCE, the Romans did not produce iron directly on Elba, but they transported the raw ore to the mainland.

> I myself saw these islands [i.e. Elba, Sardinia, and Corsica] when I went up to Poplonium, and also some mines out in the country that had failed. And I also saw the people who work the iron that is brought over from Aethalia [i.e. Elba]; for it cannot be brought into complete coalescence by heating in the furnaces on the island; and it is brought over immediately from the mines to the mainland.—*Strabo 5.2.6; (Jones, 1923), pp. 355–356.*

Scientific evidence for deforestation or a lack of fuel on Elba Island during the 1st century BCE is sparse. Although data from palynological records indicate a decline in oak pollen (Bertini et al., 2014), they do not indicate the disappearance of arboreal species, as it is e.g. shown for (palm) trees on Easter Island (Horrocks et al., 2017; Rull et al., 2015, 2010).

Sedimentological data from alluvial deposits—surely only a limited direct indicator of deforestation—at least show that morphodynamics increased during the period of Roman iron smelting on Elba (Becker et al., 2019a). However, inconsistency in evidence for the 'deforestation narrative' point out the need for additional data.

9.1.1 Aims

Our main aim is to reconstruct the woodlot required for iron smelting on Elba Island in antiquity—guided by the question whether the available wood resources were sufficient to supply the smelting sites with wood fuel. More specifically, we are aiming at

1. the setup of a stochastic spatio-temporal model of energy and material flows and the land area required for fuelwood supply for iron smelting;
2. an assessment of the variation of the model output related to the uncertainty of reconstructing past metallurgical processes and model parameters; and
3. the development of a model including both the fuelwood consumption to run the furnaces and the land area required for the supply of the labour force employed in smelting activities.

The focus of our analysis is the model setup and the uncertainty in the parameter specification. Concerning Wertime's antagonism—*The Furnace* versus *the Goat*—we propose to take the contribution of both furnace *and* goat (i.e. the food and fuel supply for workers) into account when estimating the extend of 'deforestation' in a metallurgical hotspot. Browsing of leaves and young shoots by livestock—goat in particular—is regarded as causative for forest degradation and reduced regeneration in antiquity (Hughes & Thirgood, 1982; Sands, 2005; Williams, 2000). Ancient authors observed the destructive force of goats (Theophr. Caus. pl. 5.17.6; Pl. Leg. 1.639a; Macrob. Sat. 7.5.8–9). *Erica arborea*—a common wood species on Elba that was preferred by smelters (Becker et al., 2019a; Sadori et al., 2010)—is more palatable than other macchia species (Allen, 2014; Meurer, 1986), due to the high tannine demand of goats.

9.1.2 Theoretical framework

The theoretical framework of our study is a socio-ecological perspective on past iron metallurgy (Bebermeier et al., in press) that developed from the concept of *societal metabolism* (Fischer-Kowalski & Haberl, 1997; Fischer-Kowalski & Weisz, 2005; Wardenga & Weichhart, 2006). The application of the socio-ecological model to iron smelting

on Elba Island is illustrative for the current knowledge on the 'deforestation narrative' and shows major research gaps. Moreover, the concept allows for a formalisation of human–environment interactions on a material basis (Molina & Toledo, 2014) and forms the basis of a numeric analysis of material and energy flows between a society and its physical environment (e.g. Erb, 2012). The model builds an appropriate framework for the understanding of dynamics in the area required for human consumption.

The socio-ecological model on iron metallurgy is based on the interactions between a natural and a cultural sphere of causation (Figure 9.2, Fischer-Kowalski & Weisz, 2005). The initial point of the model's cultural sphere is the metallurgical *program*. This includes, for instance, the transition from copper to iron production, the development of the smelting technology, and the changing demand for iron. *Communication* between humans is crucial for the transfer of knowledge on iron production and the development of a strategy for the exploitation of resources. In addition, events related to metallurgical activities are communicated. *representation* in the model is the record of recognized events or other aspects within the model. This includes e.g. written texts, epigraphs, or toponyms. The basis of the model is—from an archaeological perspective—*material culture* (i.e. the remains of iron production, slag in particular). Material culture is indicative for past activities, but also allows for conclusions on human agency.

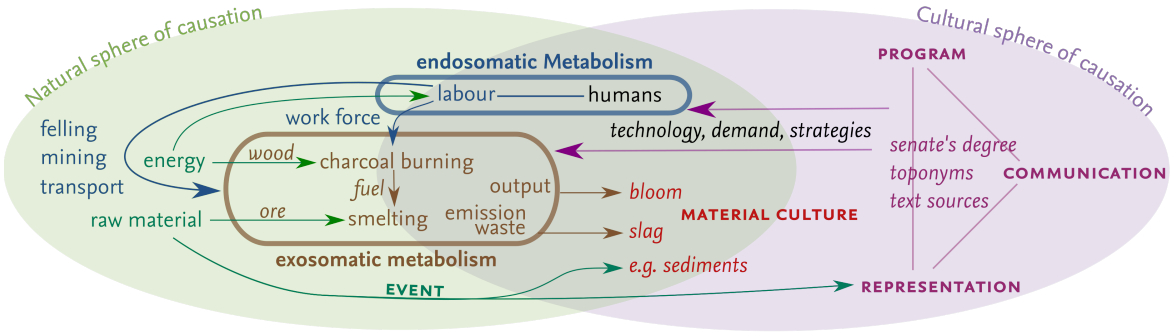

Figure 9.2 The socio-ecological model of iron metallurgy on Elba.

The natural sphere is the physical space in which humans are able to conduct the activities set in the program, including the availability and accessibility of (primary and secondary) resources. In the natural sphere, effect of human interactions with nature are included in the model as *events* (*e.g.* flooding after clear-cutting, wood shortage, or the emission of soot).

The interaction between nature and culture is described by the societal metabolism (Fischer-Kowalski & Haberl, 1997). This concept from ecology includes the flow of energy and raw material, the conversion to a desired product, and the disposal of by-products (waste). The metabolism of iron metallurgy can be separated in an exosomatic (techno-)metabolism and an endosomatic (bio-)metabolism (Fischer-Kowalski & Weisz, 1998; Molina & Toledo,

2014). The exosomatic metabolism includes not only the fluxes necessary for iron smelting (raw iron ore and charcoal in particular), but also the disposal of by-products (e.g. furnace remains, slag, and charcoal fragments) and the emission of soot. The endosomatic metabolism comprises the energy necessary for nutrition of humans involved in all operations of the metallurgical production processes, supervision, and supply. Material culture in the model is often a product of both, endo- and exosomatic metabolism.

Most models of the fuel requirement for iron smelting do not take the endosomatic metabolism into account and are centered on the exosomatic metabolism. Models on the energy requirement for e.g. life in cities, in contrast, focus on the endosomatic metabolism (e.g. Janssen et al., 2017; Veal, 2012). Recently, some authors have considered the entire societal metabolism (Daems et al., 2018; Hughes et al., 2018)—these studies are nevertheless not conducted in areas with dominant metallurgical production. Saredo Parodi (2013) and Cleere (1981) analyse aspects of both endosomatic and exosomatic metabolism in the context of iron smelting—however, without combining both. For Elba Island, the cultural sphere of causation, material remains, and events are relatively well analysed, whereas (formalised) knowledge on the socio-ecological metabolism is limited.

9.2 Model description

Our modelling approach focuses on a reconstruction in space and time of the woodlot area required for the metabolism of iron smelting on Elba Island between 360 BCE and 139 CE. The model is composed of three sub-models including (i) a sub-model of fuel demand for iron smelting (the exosomatic metabolism); (ii) a sub-model of the fuel demand and non-wood land use for supplying the workers employed in activities related to iron smelting (the endosomatic metabolism); and (iii) a sub-model of the requirements for workers employed in ore extraction on Elba Island (additional endosomatic requirements). Fuelwood availability is included in the model. The woodland area is reduced by cutting for fuelwood, clearing for food production, and animal browsing (see Figure 9.3; Table 9.1). Annual regrowth is also modelled.

9.2.1 Uncertainty analysis

For modelling in the archaeological context, it is of special interest to include the uncertainty of the input parameters, because data is mostly sparse and validation against known data is often not possible. Historical data, for instance, only allows for a rough qualitative assessment of the model outcome. Exact data on the operation conditions and inefficiencies of ancient smelting operations are missing; only experimental data is

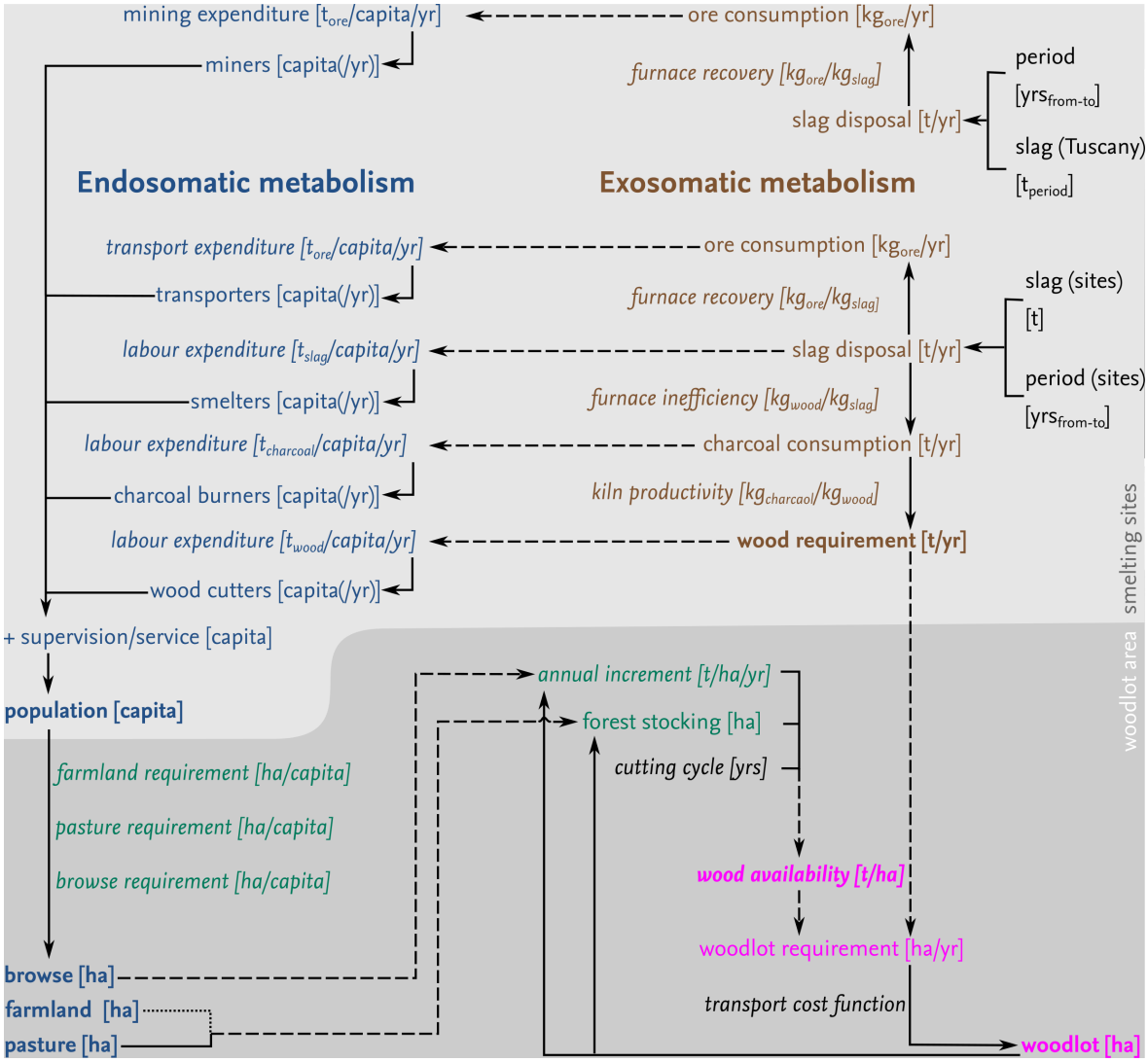

Figure 9.3 Sketch of the stochastic model of the wootlot requirement on Elba.

available, which is based on the reconstruction of ancient techniques. Therefore, it is necessary to include uncertainty of the parameter estimates into the model. We use a data-centred approach to quantify uncertainty, thus focusing on the input data as a source of uncertainty. Other sources of uncertainty such as the choice of model parameter or model mechanisms (see Brouwer Burg et al., 2016; Gardner & O'Neill, 1983) are not part of our stochastic model; we evaluate them qualitatively in the *Discussion* section. Uncertainty in our case is not to be confused with variability. Whereas uncertainty is related to a lack of current knowledge on production conditions, it is reasonably clear that iron production in antiquity was (highly) variable. This variability may be related to random differences in a single batch, but also due to inter-subject differences, and technological development. We did not explicitly take this into account.

We did Monte-Carlo simulations, i.e. we did repeated simulations for different sets of parameters that are drawn randomly from a given distribution (see e.g. Bevan et al., 2013; Brown, 2015; Crema, 2012; Kennedy et al., 2017; Orton et al., 2017 for probabilistic models of uncertainty in archaeological dating). The distributions for each parameter are estimated from the archaeological findings (Table 9.1, last column). Since we have no detailed information on the *true* values valid for ancient Elba, we followed Laplace's *Principle of insufficient reason*. We assumed a Gaussian distribution of the parameter values centred around the mean between the estimated possible extreme values, with variances according to the interval length.

Given the simulation results, we then evaluated the likelihood (i.e the percentage of simulation runs) that no wood was available for smelting on Elba based on the scheme proposed for the IPCC report (Stocker et al., 2013).

9.2.2 Exosomatic requirements

The basic units of the model are the ancient smelting sites on Elba (Figure 9.1). We used the estimated slag disposal and the chronology of each site (Table 9.2) to calculate the site-specific annual slag disposal during the period of interest. Based on a furnace inefficiency factor obtained from smelting experiments (Nikulka, 1995), we calculated the amount of charcoal necessary for the smelting activities on each site in each year. We defined the inefficiency factor as the ratio of slag removed from the furnace after smelting to charcoal charge. Using a productivity factor of charcoal kilns obtained from literature review, we obtained the fuelwood demand of a site in each year. Kiln productivity is the quantity of wood necessary to produce one unit of charcoal.

Smelting sites

We compiled a list of ancient smelting sites on Elba ($n = 29$) which contains all finds of material dating to the Etrusco–Roman smelting period ($n = 96$), *viz.* ceramics, coins, ^{14}C-ages, and stratigraphic position. The date density per site ranges from a single isolated find (e.g the Naregno site, Corretti, 1988; Pagliantini, 2014) to well dated excavated sites (the San Bennato site, Firmati et al., 2006; Pagliantini, 2014). In case that dating material clearly predates the general chronology of smelting on Elba (4$^{\text{th}}$ or 3$^{\text{rd}}$ century BCE to 2$^{\text{rd}}$ century CE), the material was excluded from our data set; some sites were not exclusively used for smelting.

The absolute date of the deposition for most of the dating material is not known. For instance, the production of Dressel 1A amphorae conventionally date to the pre-Caesarian

period (prior to 50 BCE), starting in the mid-2nd century BCE (ca. 140–50 BCE) (Tchernia, 1983; Williams et al., 2014); *Terra sigillata italica* was mainly produced between ca. 60 BCE and60 CE (Pucci, 1985). The dating material thus only indicates a possible time span of the *true* moment of deposition and, so, the operation phase of a site. In order to deal with this issue, we used a probabilistic approach to incorporate the uncertainty of dating into our model input.

We assume that the activity for a single site is monophasic. For each site and each simulation run, we draw the initial point t_s and the end point t_e of the activity time span from normal distributions. From the data of each site we can estimate possible time frames[1] $t_\alpha \leq t_s \leq t_\beta$ of starting dates and $t_\gamma \leq t_e \leq t_\delta$ of end dates with $t_\gamma > t_\beta$. We choose the mean μ of each time frame as the centre of the distributions and $\frac{1}{6}$ of the interval length as the standard deviation σ for the distributions resulting in

$$t_s \sim \mathcal{N}\left(\frac{t_\beta + t_\alpha}{2}, \left(\frac{t_\beta - t_\alpha}{6}\right)^2\right)$$
$$t_e \sim \mathcal{N}\left(\frac{t_\delta + t_\gamma}{2}, \left(\frac{t_\gamma - t_\delta}{6}\right)^2\right)$$

We then set the activity period for a site to be the interval $[\tilde{t}_s, \tilde{t}_e]$, where $\tilde{t}_s, \tilde{t}_e$ are the drawn random numbers rounded to the next integer. The times for the boundary values of the intervals are estimated from the archaeological findings of the site (see supplementary material). Each finding i is dated with a time interval $[a_i, b_i]$. We choose $t_\alpha = \min_i\{a_i\}$, $t_\delta = \max_i\{b_i\}$ and the time interval $[t_\beta, t_\gamma]$ is chosen as the smallest interval such that it intersects with all $[a_i, b_i]$ in at least one time point. For our data also $t_\beta = \min_i\{b_i\}$ and $t_\gamma = \max_i\{a_i\}$ holds for all sites with multiple findings. In the case of only one finding at a site we choose $t_\beta = a_1 + \frac{b_1 - a_1}{4}$ and $t_\gamma = b_1 - \frac{b_1 - a_1}{4}$ in all simulations.

Amount of slag

Ancient slag from Elba contains high amounts of iron, which could be reduced in modern blast furnaces. Therefore, old slag heaps were mined and slags re-smelted in the first half of the 20th century (Pistolesi, 2013). The amount of slag removed from ancient heaps was well documented by the slag mining concessionaires (John Nihlén's records: Nihlén, 1958; $n = 6$). Figures range from 1 000 t (Straccoligno site) to 20 500 t (Barbarossa site). For some slag accumulations that were excavated by the concessionaires, no exact figures are documented. The concessionaires described the slag heaps as 'of small quantity which

[1] Since we want the start and end date to lie inside of the chosen time frames, we redraw the random variable whenever values that lie outside are drawn.

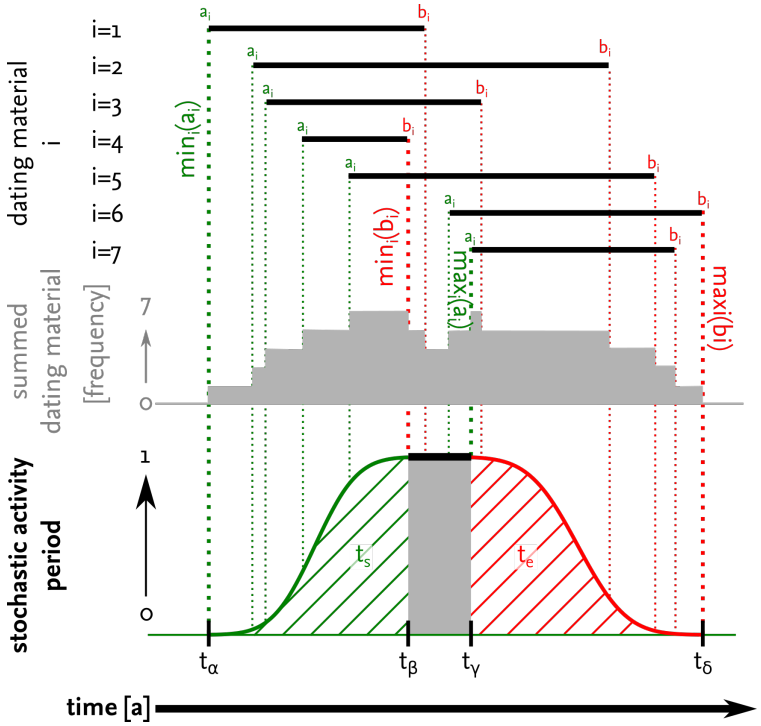

Figure 9.4 Estimation of the activity period for an example smelting site.

is still to be excavated' (Nihlén, 1958). This description is in other cases used for slag accumulation of between 600 and 1,200 t. As Nihlén's data is mainly based on figures from Italo Sapere, who worked on Elba between 1938 and 1943 (Pistolesi, 2013), some slag heaps were removed prior to documentation; these numbers are not included in our data set. We used the documented areal extent and depth of the slag heaps/accumulations to estimate the quantity of slag deposited on sites were no figures from concessionaires are available (Arnaldi, n.d.; Corretti, 1988; Corretti et al., 2014; Nihlén, 1958; Pagliantini, 2014; Zecchini, 2001; and own data). To calculate the slag weight W_i of a site from the areal extent and the average height when accessible, we used the following approach (cf. (Bachmann, 1982; Crew, 1991)):

$$W_i = ((h \times \delta) \times a \times b) \times Q \times \rho$$

where $a \times b$ is the area of the slag accumulation, h is the height/depth of the accumulation, $\delta = (.41, .75)$ is a topographical correction factor for irregular shaped underground and surface of the accumulation, $Q = (.24, .4, .5)$ is the ratio of slag to debris in an accumulation, and $\rho = (2.0, 2.2)\,\mathrm{t/m^3}$ is the density of slag. Values of constants were taken from the literature (Crew, 1991; Florsch et al., 2011; Humphris & Carey, 2016). The depth correction obtained from Humphris & Carey (2016) is calculated as the average of the ratio between the topographically obtained volume of the accumulation and the

volume obtained by resistivity measurements or excavations. For the estimation of the slag amounts of all other sites, for which no areal extent of the slag accumulation is available, we used the data estimated by Zecchini (Zecchini, 2001).

The uncertainty assessment of the slag amount is based on minimum and maximum values of the calculations applying the equation for W_i and the range of published estimations. For sites where the extent of the slag accumulations and data from slag mining concessionaires are available, we used the numbers of both data sets. Following Laplace's *principle of insufficient reason*, we assume a normal distribution of the *true* slag amount between the extreme values estimated for each site i:

$$\hat{W}_i \sim \mathcal{N}\left(\frac{W_{max}+W_{min}}{2}, \left(\frac{W_{max}-W_{min}}{6}\right)^2\right)$$

9.2.3 Endosomatic requirements

The labour requirement is calculated separately for the main steps of the metallurgical processes, including mining, furnace operation, charcoal burning, and wood felling. In addition, labour investment is necessary to transport material from the site of extraction (mines, forests) to the site of production (kilns, smelting sites) and for security and supply of these workers. Estimates of the work force base on the quantities estimated for the different production steps (see Figure 9.3). The ore charge is calculated as the ratio of ore to slag for each furnace; the number of furnaces is calculated from the number of workers typically necessary to handle one furnace with a defined charge. The estimate of the work force for mining bases on estimated quantities of slag found around the Gulf of Follonica (including Populonia–Baratti and Poggio Butelli, which were the most important known production centres on the mainland, and Elba). For each labour group, we applied a specific factor of the annual *per capita* productivity (Table 9.1). From the number of workers required in each year, we obtained the total amount of fuelwood necessary for heating and cooking. These requirements contribute to the total fuelwood demand for the entire metabolism of iron smelting.

9.2.4 Woodlot area and wood availability

Woodlot requirements are calculated as a function of the demand on each smelting site in each year and the available wood in the lands around it. The pattern of available wood is initially based on the current distribution of the main vegetation classes on Elba (oak forest, Mediterranean *macchia* shrubland, and sweet chestnut forest, see Figure 9.1). We assume that the current vegetation cover roughly corresponds to the pattern at the onset

of the smelting period, as also the potential natural vegetation is deciduous and evergreen oak forest (Blasi et al., 2014). Elba is located in the *Central and Northern Tyrrhenian Ecoregional Section* which is locally dominated by Mediterranean and Sub-Mediterranean evergreen shrublands of the Italian peninsula (Blasi et al., 2017). Dominant species are e.g. *Quercus ilex*, *Phillyrea latifolia*, *Arbutus unedo*, *Erica arborea*, and *Pistacia lentiscus*. Palynological data suggest that during the Etrusco–Roman period, as today, vegetation was dominated by *Ericaceae* shrubland and oak forests (Bertini et al., 2014). Since the 1950s forests regenerated following a typical succession (Carta et al., 2018b), mainly because the primary sector lost its importance on the island and tourism became the main source of income. For our model, we assume that today's grasslands were covered with *macchia* shrubland at the beginning of the smelting period. We fitted a sigmoid function to average values of the (age-specific) annual increment in each of the vegetation classes to calculate the standing volume (at a tree age of 42 yrs; Castellani, 1970, 1972); we applied a constant specific gravity of wood to obtain dry mass from the standing volume. The felling area is selected based on the Pandolf least-cost function for positive and the Pandolf-Santee equation for negative slopes (walking speed is calculated using Tobler's hiking function; Herzog, 2014); areas with the lowest transport cost are preferably felled. The available woodland area was reduced by the area necessary for agricultural and horticultural production (field cultivation and animal grazing). We modelled the regrowth of the woodland for each year after harvest using the sigmoid function. The minimum age for harvesting is set to 5 yrs, which fits to ages for coppicing reported in ancient literature; Plin. HN 17.35.147–159 reports rotation periods for *Castanea sativa* (7 years) and *Quercus* (10 years); Columella (Meiggs, 1982) reports similar cycles (*Castanea*, 5 years; *Quercus*, 7 years). We define the moment of a lack of fuelwood as the year when the fuelwood requirement exceeds the available wood biomass on Elba.

Table 9.1 Model parameter. Parameter emphasised in **bold** are specific for Elba; other parameter are estimated for past conditions. For a detailed description of the parameter see Supplementary Materials (unspecific parameter) and the main text (specific parameter).

Parameter		Values	Distribution
Smelting	**Chronology**	site-specific, see Table 9.2	normal
	Slag	site-specific, see Table 9.2	normal
	Furnace inefficiency	2.0 to 8.5; mean 5.25 ± 1.75 kg/kg (charcoal : slag)	lognormal
	Kiln productivity	Pit: .05 to .17; $\bar{x} = .11 \pm .04$ kg/kg (charcoal : dry wood)	normal
		Mound: .135 to .28; $\bar{x} = .21 \pm .07$ kg/kg (charcoal : dry wood)	normal
Mining	Ore extraction	0.97 to 3.67 Mt × 1.35 kg/kg (slag : ore)	uniform
	Mine chronology	varying intensity between 600 BCE and 200 CE	*const.(ant)*
Labour	Mineworker	23 t/capita/yr (ore)	*const.*
	Charburner	Pit: 3.5 t/batch, 12.5 person-days/batch	*const.*
		Mound: 45 t/batch, 25 person-days/batch	normal
	Woodcutter	13 ha/capita/yr (woodlot)	*const.*
	Smelter	2.5 t/capita/year (slag)	*const.*
	Transport	Animals: 187.5 t/capita/yr	*const.*
		Driver: 1 /5 animals	*const.*
		Seafarers: 300 tcapita/yr = 1 t/capita/day (ore)	*const.*
	Supervision/Service	+30% (each)	*const.*
Food supply	agricultural land	2 ha/capita	*const.*
	Pasture	transport animals: 0.8 to 1.1 ha/animal	*const.*
		Food supply: 0.72 ha/capita	
	Forest browse	0.69 ha/capita	*const.*
	Household fuel	0.5 to 2.0 t/capita/yr (charcoal)	*const.*
Wood supply	**Vegetation types**	spatially specific	–
	Rotation period	5 to 10 yrs	uniform
	Increment (10 yr mean)	age-dependent, 10 yr mean: Oak: 2.2, Macchia: 3.6, Chestnut: 5.7 m^3/ha/yr	*const.*
	Specific gravity	0.69 t/m^3 (dry wood)	*const.*
	Browse biting	40–60% increment reduction	uniform

Table 9.2 Chronology and slag disposal of ancient smelting sites on Elba Island. Uncertainties as outlined in the main text and related references are given. Details on the dating material used to define the dating range can be found in the Supplementary Materials (references: Adamoli & Rigon, 2013; Camporeale, 1989; Corretti, 1988; Corretti et al., 2014; Firmati et al., 2006; Maggiani, 1981; Monaco & Mellini, 1965; Nihlén, 1958; Pagliantini, 2014; Sabbadini, 1919; Zecchini, 2001). Age estimation: t_α = lower bound, t_β = lower start, t_γ = lower end, t_δ = upper bound. Methods to estimate quantity of slags: *a* Characterisation by re-smelting concessionaires as economic or as 'significant but low quantity', i.e. ca. 600–1200 t; *b* area extent /volume given in literature (slag not removed); *c* own measurements of slag accumulation; *d* data from re-smelting concessionaires; *e* (own) classification as small site; *f* estimation of locals, area with small density of slags; *g* published estimation. References for slag estimation: [1]: Nihlén, 1958; [2]: Zecchini, 2001; [3]: Firmati et al., 2006; [4]: Corretti, 1988; [5]: Pagliantini, 2014; [6]: Nihlén, 1958; [7]: Monaco & Mellini, 1965; [8]: Corretti, 1991; [9]: Arnaldi, n.d.; [10]: Corretti et al., 2014.

Site		**Chronology [-BCE/CE]**				**Slag [t]**			
ID	**Name**	t_α	t_β	t_γ	t_δ	**min**	**max**	**Meth.**	**Ref.**
1	Martella ant.	-360	-280	-211	-180	400	1400	*a;c*	[1]
2	Ombria	-300	-232	-93	-25	1000	5000	*e,g*	[2]
3	San Bennato	-300	-180	138	139	100	5000	*b; e,g*	[2, 3]
4	Fornacelle	-140	-10	73	73	1000	5000	*e,g*	[2, 4]
5	Capo Pero	-300	-201	-47	100	4400	13500	*b*	[2, 5]
6	Fegatella	-300	-300	-25	-25	600	1900	*a; b*	[6, 7, 8]
7	Valle del Giove	-300	-140	-25	-10	600	1200	*a*	[6]
8	Vigneria	-300	-226	-75	-1	1000	5000	*e,g*	[2]
9	Rio Marina	-225	-145	1	50	100	15000	*b; e*	[2, 4, 5, 7]
10	Barbarossa	-260	-210	-120	-50	20500	20500	*d*	[6]
11	Naregno	-260	-248	-222	-210	1200	1200	*d*	[6]
12	Straccoligno	-260	-210	-200	-120	1000	1000	*d*	[6]
13	Lacona	-140	-140	-10	-10	600	1200	*a*	[6]
14	Galenzana	-130	-123	-107	-100	600	1200	*e*	[6]
15	Seccheto	-280	-217	-88	-25	2600	4300	f	n/a
16	Sughera	-280	-217	-88	-25	100	1000	c	n/a
17	Pomonte	-130	-100	-100	-50	4800	14700	*f,c; b,c*	[4, 5, 9]
18	Patresi	-260	-140	-120	-10	1000	2000	*c*	n/a
19	Sant'Andrea	-200	-120	-101	-10	10000	23000	*d; b*	[6]
20	Marciana M.	-290	-240	-60	-10	9000	10500	*b*	[2]
21	Bagno	-220	-175	-85	-40	2000	10000	*g*	[2]
22	Paolina	-200	-135	-60	60	5000	15000	*g*	[2]
23	Gnacchera	-300	-232	-93	-25	1000	5000	*g*	[2]
24	Guardiola	-204	-140	-120	-10	1000	5000	*g*	[2]
25	Campo all'Aia	-130	-100	-60	-20	10800	10800	*d*	[6]
26	La Pila	-140	-108	-42	-10	300	600	*b*	[4]
27	Forcioni	-140	-50	-10	100	400	1800	*c*	[4, 5]
28	San Giovanni	-200	-120	15	100	10500	14500	*d; b*	[5, 6, 10]
29	Magazzini	-300	-165	-60	60	200	4000	*b*	[10]

9.2.5 Simulation details

We constructed a grid from the vegetation increment data with a $10m \times 10m$-resolution. All cells with woodland vegetation have a variable for the tree type and age. From these data we can determine the estimated available woodland through the previously described sigmoid function approach and whether the rotation period for felling has finished or forest browse is possible. For each site a distance measure is constructed that determines the distance to nearby cells in terms of transport costs using the average slope and distance of the direct path as input.

The first step of each simulation was drawing the parameters as described in the previous section and determining from them the number of time steps, the activity periods and woodlot requirements of each site according to the model description. The time step size was chosen as one year and we assume that the woodlot requirement of a site is the same for all time steps.

For each time step of one simulation, all active sites were determined and according to their woodlot requirements the nearest (with respect to the previously constructed site-specific measure) cells with tree ages older than the respective rotation period were used for wood collection. For all cells that were chosen for wood collection or forest browse, the tree age variable was set to zero. After saving the current state the regrowth step was initiated and for each cell the tree age was increased by one year (to a maximum of 42 yrs). The simulation stops either because of complete deforestation (i.e. when there is no cell with a tree age older than the rotation period is reached, while the required woodlot is not yet met) or when the end of all site activity periods.

9.2.6 Results

9.2.7 Overall model outcomes

We did 11,479 simulations with parameters chosen as described in the model description section. From these we can estimate the metallurgical activities and the availability and distribution of woodland on Elba Island. The estimated amount of slag disposed on Elba Island during antiquity ranges between 122,770 t and 173,500 t with an average of 146,170 t±6,464 t (Mdn±MAD). The minimum availability of woodland area (trees $>$ 5 yrs) in the simulation runs ranges between 0% and 62.9% of the undisturbed woodland area (41.1% ± 11.0pp); the minimum availability of mature woodland area (trees $>$ 42 yrs) ranges between 0% and 58.9% (23.4%±17.5pp). Between 4×10^{-4}% and 30.4% (5.5%±2.2pp) of the original woodland area are estimated to be cleared within one year of operation.

9.2.8 Likelihoods

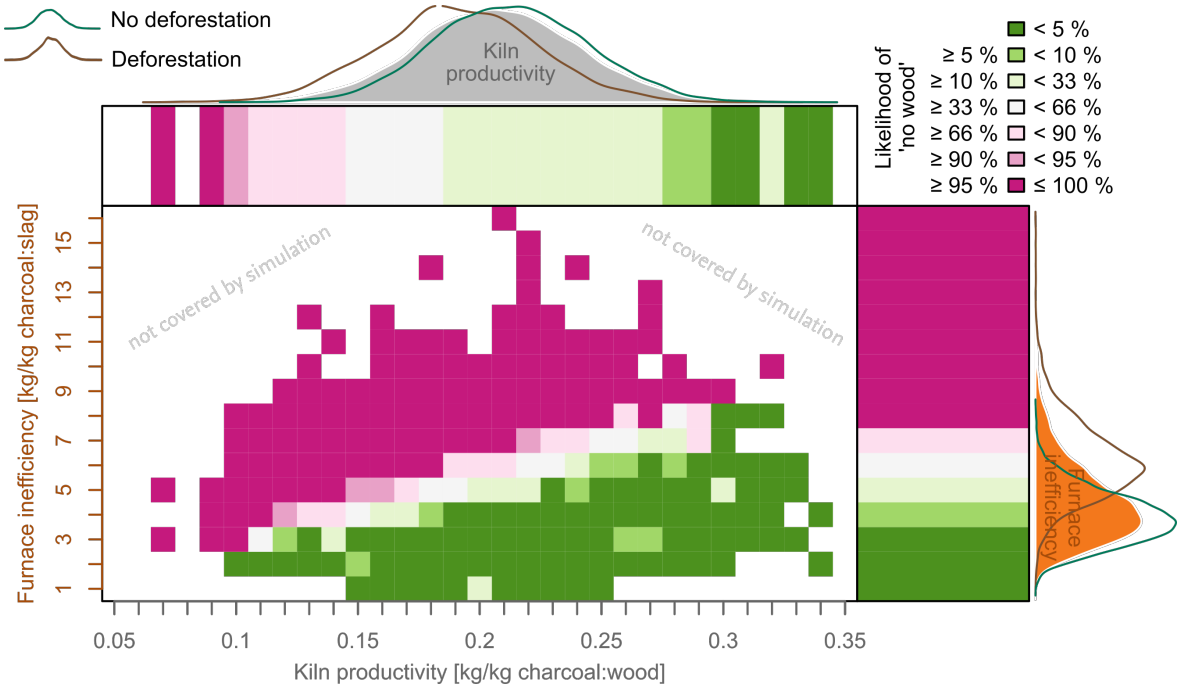

Figure 9.5 The likelihood that a lack of fuel for smelting on Elba occurred between the 4th century BCE and the 2nd century CE in relationship to the main technical input parameter of the woodlot model. The density plots show probability distribution of the kiln and the furnace parameter for all simulations (grey), for simulations where no sufficient wood is available for smelting (brown) and where no lack occurred (green). The bars below the density plots show the likelihood of a lack of fuel for the furnace or the kiln parameter; the raster for a combination of both parameter.

Table 9.3 Uncertainty of the parameter and model outcomes and likelihoods of the availability of woodland (trees older 5 yrs) for given parameter values. %RMAD = relative median absolute deviation (percent MAD divided by median), %RD = relative difference (percent range divided by median).

Parameter	%RMAD	%RD
Slag	6.1	1.1
Furnace inefficiency	35.4	3.7
Charcoal	37.4	4.7
Kiln productivity	16.8	1.3
Wood	40.1	5.0
%Trees (>40 yrs)	74.7	2.4

Table 9.4 Likelihoods of the continuous availability of woodland (trees >5 yrs) during the smelting period for given parameter values. Furnace inefficiency in kg/kg charcoal : slag and kiln productivity in kg/kg charcoal : dry wood. See also Figure 9.5.

Likelihood		Furnace inefficiency		Kiln productivity	
Term	Outcome	labour	no labour	labour	no labour
virtually certain	> 99%	< 2.6	< 2.6	> 0.31	> 0.28
extremely likely	> 95%	< 3.7	< 4.7	> 0.29	> 0.27
very likely	> 90%	< 4.1	< 5.0	> 0.27	> 0.22
likely	> 66%	< 4.9	< 6.2	> 0.19	> 0.15
unlikely	< 33%	> 6.0	> 8.0	< 0.14	< 0.12

9.2.9 Distributed model outcomes

The period of smelting activities on Elba started in our model after 360 BCE and ended before 139 CE (Table 9.2). The modelled point of the strongest increase in felling dates between 146 BCE and 98 BCE (67%; between 237 BCE and 79 BCE at 95% likelihood) with a median at 117 BCE ± 22 yrs. The strongest modelled decrease of the felling activity most likely dates between 95 BCE and 51 BCE (67%; 130 BCE and 36 BCE with 95% likelihood; median 75 BCE ± 22 yrs). The point in time of maximum felling is simulated to be between 125 BCE and 64 BCE at a 95%-likelihood and between 100 BCE and 75 BCE at 67%-likelihood (86 BCE ± 13 yrs). Our data show a relatively smooth increase of the fuel consumption between 360 BCE and 117 BCE ± 22 yrs. In contrary, the decrease of smelting activities around 75 BCE ± 22 yrs is modelled to be relatively rapid. The time lag between the strongest increase of felling activities and the point of maximum felling activities is around 30 ± 22 yrs (1–140 yrs at 95%-likelihood), whereas the the time lag is only 5.0 ± 7.4 yrs (0–53 yrs at 95%-likelihood) between the maximum and the strongest decrease of felling activities.

If modelled, a lack of fuel on Elba might have most likely occurred between 124 BCE and 85 BCE with 67% likelihood (between 237 BCE and 73 BCE with 95% likelihood). The likelihood that smelting ended in the 2nd century BCE or the first half of the 1st century BCE is 6.6% each. In 0.7% of the simulations, all woodland area was cleared before 200 BCE.

In addition to the general trend on Elba Island, we also analysed the fuel consumption for twelve geographical regions on Elba separately (Figure 9.1). The onset and the increase of felling in these regions—as well as the decrease and end—differ clearly (Figures 9.6 and 9.7); the earliest onset is simulated for northeastern Elba (Cavo region) and the latest for central Elba (Lacona region). Our data indicate that felling activities first increased in northwestern Elba and the northern Calamita peninsula (Cavo and Rio Marina regions; Capoliveri region). The increase pursued in western and central Elba (Figure 9.7). There

is a general trend of later increase of felling activities from east to west and central Elba. Felling around Pomonte in the far west is modelled to have increased relatively early compared to the general trend, whereas felling around Lacona in south-central Elba started relatively late. The point in time of maximum felling activities around Capoliveri, Cavo and Rio Marina (median between 201 BCE and 94 BCE) dates to an early period. Maximum felling in western and central Elba is modelled to have taken place later than in eastern Elba (median between 86 BCE and 66 BCE; see Figure 9.7). Latest potential activities are recorded for northeastern Elba (Cavo and Rio Marina regions, mid-1st century BCE, Figure 9.7), whereas in the other regions, felling decreases in the very late 1st century BCE. The latest modelled felling activities took place in the northwestern region (Cavo and Rio Marina regions). Felling intensities around Morcone, Lacona, and Bagnaia is modelled to have been low compared to the other regions. For the regions around Morcone and Bagnaia, no ancient smelting sites are recorded. A single, small, smelting site was found in the Lacona-region (Figure 9.1). The highest average and maximum felling intensities were modelled for the San Piero–Procchio region in western Elba, the region around Cavo in the northwest, and around Marciana and Pomonte in the west (in order of decreasing intensity; see Figure 9.7).

9.2.10 Labour

We estimated that during the heydays of iron production on Elba Island, between 1,321 and 3,296 capita were required for the different steps of iron smelting (95%-likelihood; range between 514 and 9,615 capita; 1842±350 capita, $Mdn \pm MAD$). In increasing order of their relative contribution to the total amount of worker, the most important occupational groups were smelters (48.6–57.8% at 95%-likelihood), service staff (37.5%), charcoal burners (3.6–12.1%); and fellers, and transport operators (< 1% each).

9.3 Discussion

Our results show that the likelihood that no woodland area was available for smelting on Elba Island is 14% when taking only the exosomatic metabolism of smelting into account; the likelihood is 27% when taking both endo- and exosomatic metabolism into account. Therefore, we state that it is *unlikely* that a lack of fuel is the reason for the abandonment—or decline—of smelting on Elba during antiquity. In only 6.2% of our simulations, a lack of fuel is simulated for the 1st century BCE, which corresponds to the accepted period of the abandonment or decline of smelting on Elba Island (e.g. Corretti,

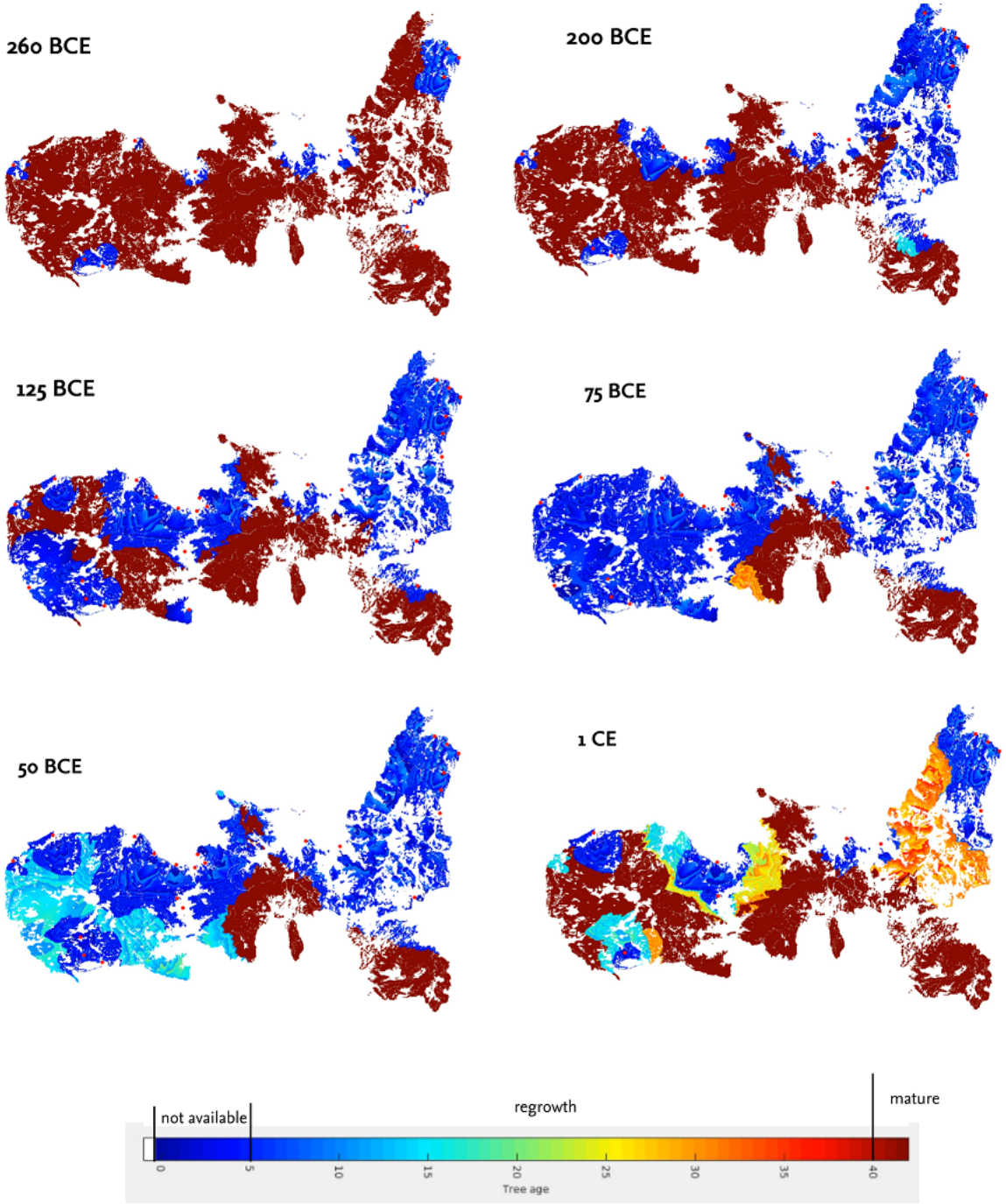

Figure 9.6 The modelled distribution of woodlot area on Elba in different time slices. Data is from a simulation using the mean values of the parameter distributions as input. Dark blue colour indicates that trees on the area were not available for harvesting (< 5 yrs), light blue to orange colour indicates that the trees in the area are regrowing. Mature trees (> 40 yrs) are indicated in reddish brown.

2017). Non of our simulations resulted in a lack of available woodland area on Elba Island in the 1st century CE or later, as production decreased in the 1st century BCE.

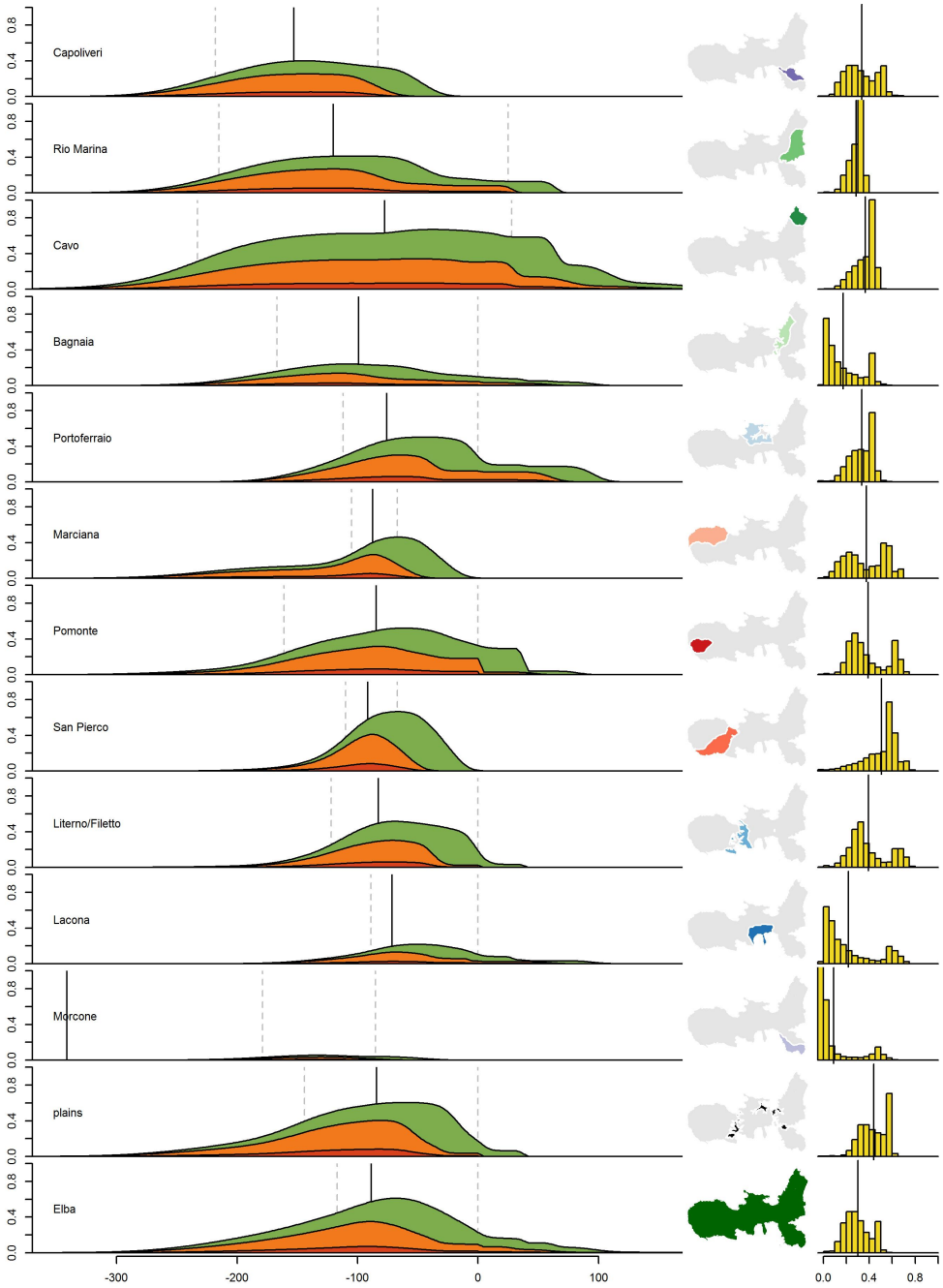

Figure 9.7 Model outcome for geographical regions on Elba. Order of the regions counter-clockwise starting from the northern Calamita-peninsula. **(a)** Average woodlot cover in the regions, red = cleared area, orange = area covered with young woodland not available for cutting (≤ 5 yrs), and green = woodland available for cutting, but not mature (≤ 42 yrs, the dashed lines indicate the point in time of maximal growth/decline in woodland use, the solid line indicates the point in time of maximal woodland use; **b** Location of the regions on Elba; **c** Relative area of the regions covered with woodland not available for cutting ($age \leq 5$ yrs) in each of the 11400 simulations, the horizontal line indicates the mean coverage in all simulations.

Table 9.5 Main parameters of our model in comparison to other estimates of the resource consumption of early iron smelting. Studies are ordered from low to high. Furnace efficiency in brackets is without preheating and reheating. Notes mark the data source of the respective studies. For studies where range of values is given, medians were estimated.

Reference	**Furnace inefficiency [kg/kg]**		**Kiln productivity [kg/kg]**		**Specific gravity [kg/kg]**
	median	range	median	range	
Wertime, 1983[b]	0.75		.29		–
Voss, 1988[b]	0.75		.29		–
Pleiner, 2000[b]	[1.40]		.25		–
Healy, 1978[b]	[1.5]		.25		?
Brumlich, 2018a[c]	1.65		.25		.70
Paysen, 2011[a]	1.27		.25		.70
Joosten et al., 1998[d]	[1.8]	[1.1–2.5]	?		–
Wallner, 2013[b]	[1.9]		.20		?
Williams, 2010[b]	1.13		.06		?
Eichhorn et al., 2013a[b]	3.00		.23	.20–.25	.67
This study[a]	4.2±1.5	1.0–15.6	.21±0.04	.07-.34	.69
Goucher, 1981[b]	4.00		.10		?
Cleere, 1981[b]	4.00		.14		.60
Saredo Parodi, 2013[a]	18.09		.29		–

Table notes: [a] literature review [b] literature [c] experimental mass-balance [d] chemical mass-balance

9.3.1 Production parameter—the endosomatic metabolism

Slag

The modelled number of around 150 000 t of slag that were disposed on Elba between the 4th century BCE and the 2nd century CE is similar to common assumptions on the scale of the ancient iron production on Elba (Corretti, 2017), which are also based on data from resmelting concessionaires. Zecchini (2001) estimates that between ca. 550 000 and 1 015 000 t slag were disposed in pre-industrial times (a large amount of them ancient), thus proposing a much higher number than our figures or the figures of Corretti (2017). However, Zecchini's numbers appear to be rough guess; numbers known from resmelting concessionaires differ importantly from his numbers.

Smelting process

Values of furnace efficiency we used in our model are in accordance with values reported from experiments (Paysen, 2011; Senn et al., 2010) and other studies on the resource consumption of pre-industrial metallurgy outside the Italian peninsula (Table 9.5). In smelting experiments conducted on Elba Island, Benvenuti et al. (Benvenuti et al., 2016) obtained a furnace inefficiency of 2.5 kg/kg and Brambilla (2003) a furnace inefficiency of 6.17 kg/kg. Taking the experiment of Benvenuti et al. (2016) and an average kiln productivity of .21 kg/kg, our model shows that it would have been *very unlikely* that no woodland area on Elba was available for smelting during antiquity. When taking Brambilla's experiment (Brambilla, 2003) as a basis, a lack of fuel during antiquity is, however, evaluated as *as likely as not* (Figure 9.5). Values of kiln productivity we used in our model are relatively low compared to studies conducted for Populonia, but are in the range of other studies on resource consumption (Table 9.5). Additionally, some studies do not account for the specific gravity of wood (i.e. difference in weight between fresh wood and dry wood used in kilns). Taking parameters used in the other studies, it would be even less likely that iron production on the island suffered from fuel shortage. However, taking the relatively low kiln productivity used by Goucher (1981) or Cleere (1981) (or even Saredo Parodi's exceptionally high—unrealistic—furnaces inefficiencies (Saredo Parodi, 2013)), complete deforestation of Elba Island in antiquity seems more likely (see Figure 9.5 and Table 9.5).

Although we principally understand our data as a likelihood of a lack of fuel due to smelting on Elba, the results can also be interpreted with regard to the suitability of the production parameter for iron smelting on Elba. Thus, a simulation run with a given set of parameter that results in a lack of fuel prior to the (presumed) abandonment of

smelting sites in the 1st century BCE indicates that the applied parameters are unrealistic. This is true for more than half of the simulation runs.

Charcoal production

Regarding charcoal production, major issues in the modelling of fuel consumption are the kiln type used and the qualitative requirements on charcoal for metallurgical use. As proposed by Veal (Veal, 2012, 2013, 2017b), the ratio of wood to charcoal could have even been higher for the production of high quality charcoal. She assumes that for metallurgical purposes, high quality charcoal is required to achieve higher and constant temperatures. Veal proposes a productivity of .05–.10 kg/kg for high quality charcoal. Taking this values, it is at least *more likely than not* that all woodlands on Elba were cleared for charcoal production. Thus, further knowledge on the quality of charcoal used for smelting is needed. There were no ancient kilns were uncovered on the island; consequently, we cannot clearly state if e.g. earth kilns or mound kilns were used during the ancient smelting period. Both mound kiln and pit kiln were known during antiquity, as testified by Theophrastos (*Hist. pl.* 5.9.4; *Hist. pl.* 9.3.1–3; cf. Donati & Aminti, 2006; Nenninger, 2001; Olson, 2012). The outcomes of our models are quite different for typical values of pit and mound kilns (0.07–0.17 and 0.13–0.28 kg/kg, respectively; cf. Thommes, 1997); taking values for mound kilns the likelihood that no fuelwood was available on Elba is 13.9% and 34.8% for pit kilns. Given the sheer amount of charcoal necessary for iron smelting on Elba Island during antiquity ($Mdn = 3.1$ Mt, between 1.4 and 7.0 Mt at 95% confidence) and the high required kiln density (3 batches/ha assuming a high kiln volume of 45 t; cf. Raab et al., 2017; Schmidt et al., 2016), some productions sites may be found in future. Several charcoal kiln platforms were found near medieval smelting sites.

Site chronology

For our model, we used dating material found on smelting sites to define the operation period of the site; we considered the uncertainty in the chronology by defining certain and uncertain periods of use based on the dating material. Based on the uncertainty in dating some material, the end of the smelting period in our model is recognized for a later period than commonly assumed, i.e. later than the mid-1st century BCE. However, other finds may allow for the conclusion that smelting continued throughout the 1st century BCE. For instance, a ship wreck dating to the 2nd century CE which carried abundant haematite blocks and sunk in front of known smelting sites (Brambilla, 2003; Zecchini, 2001) documents the use of raw iron ore after the commonly assumed end of the smelting period on Elba Island. Also coin finds from slag accumulations (Sabbadini, 1919), Roman imperial amphorae or

so called *Warzenlampen* (Eser & Becker, submitted) indicate smelting activities in the 1st century CE.

Most authors assume that iron smelting on Elba was abandoned (or declined) in the 1st century BCE. The simulation runs in our model resulting in a lack of fuel (14% of the simulations taking only exosomatic metabolism into account) date the abandonment between the mid-3rd and the first half of the 1st century BCE. Dated material clearly indicates that activities at least continued in the 1st century BCE. The likelihood of a lack of fuel in the 1st century BCE is 6.2% in our simulations.

9.3.2 Labour—the endosomatic metabolism

We estimated the contribution of the supply of workers for ancient iron processing and service to wood availability on Elba Island (the endosomatic metabolism). The fuel consumption for supply and the impact of browsing goats and grazing sheep/cattle reduces the availability of woodland by between 3 and 100% compared to simulations where only the demand for charging the furnaces is modelled; The likelihood that no woodland was available for smelting increases from 14% (only exosomatic metabolism modelled) to 28% (exo- and endosomatic metabolism modelled). Thus, the likelihood of a lack of fuelwood for smelting during antiquity doubles, although the area required for both exo- and endosomatic metabolism is only 1.19 times higher than the requirements for the exosomatic metabolism only. Therefore,—although it is according to our simulations still *unlikely* that there was a phase where no forest was available on Elba during the ancient smelting period—the contribution of food and fuel supply for work force is an important factor when calculating the availability of secondary resources for iron smelting.

According to our simulations, around 1850 capita were employed in iron smelting and services in a phase of highest iron production during Roman times (95%-confidence interval between 1300 and 3300 capita). This does not include the work force necessary for mining, although in northeastern Elba, a significant amount of iron ore were extracted.

Mining

As stated by Corretti (Corretti, 2017) figures on the amount of ore extracted on Elba Island are wild guess. Numbers of ore extraction on Elba Island and iron smelting around the Gulf of Follonica vary widely (Buchwald, 2005; Costagliola et al., 2008; Davies, 1935; Freise, 1907; Haupt, 1888; Piccinini, 1938; Pistolesi, 2013; Saredo Parodi, 2013; Tanelli, 1985; Voss, 1988; Wertime, 1983; see Supplementary Materials). It needs to be noted that our rough estimate takes only the production in the centres around the Gulf of Follonica

into account, although it is known that ore from Elba Island was transported to distant locations around the Tyrrhenian Sea (Cambi et al., 2018; Corretti et al., 2018). What renders the estimation of persons involved in mining difficult is the fact that we have no data at hand that gives information on the intensity of extraction during the centuries. The intensities given by Saredo Parodi (2013) may represent an overall trend, but are speculative. With the available data, it seems that the number of workers could have been increased by around 500 capita for extraction in a phase of maximum extraction.

The estimated number of workers for iron metallurgy on Elba appears to be on an intermediate level compared to numbers estimated for other important *ancient* mining districts (cf. Andreau, 1990; Harrison, 1931; Healy, 1978; Shaw, 1998, and Strabo, 3.2.10, Xen. Poroi 4.23 f., Diodor 34.2.19). We are aware that the estimation of the number of workers exploited in extractions is difficult. The wide range of estimations of the number of workers employed in the ancient silver mines in Laureion (Attika) illustrates the problem. Here, figures for the 4th century BCE vary by more then one order of magnitude (between 5 000 and 60 000 capita, cf. Freise, 1907; Lauffer, 1979; Shepherd, 1993). However, our rough estimations help to understand the scale of requirements for workforce and potential impact on area requirements for the supply. We additionally argue that a parameterized estimation of the labour required for all the different steps of iron production on Elba is rewarding to obtain useful figures of the workforce.

9.3.3 Assumptions

Due to limited knowledge on several historical conditions on Elba, the uncertainty in the parameter estimate for our model is partially high. Some simplifications are necessary for the model setup as well. Nevertheless, we assume that our model sufficiently covers the main factors of the (fuel) wood consumption on Elba from the 4th century BCE to the 2nd century CE.

Smelting

For the production on Elba and in Populonia, different furnace reconstructions are proposed (Benvenuti et al., 2003; Nihlén, 1958, 1960; Sperl, 1981), but at the moment the record is restricted due to disturbed contexts of the finds. We therefore assume that during the ancient smelting period, smelting and charcoal burning technologies—and thus furnace inefficiency and kiln productivity—did not change importantly. The data on smelting experiments reported by Nikulka (1995) suggest that there is only a relatively small difference between the inefficiencies of different furnace types. However, variability during each furnace batch and between subjects is also reasonable (e.g. experimental

data in (Nikulka, 1995)). Therefore, the outcomes of each Monte Carlo experiment reflect an average production parameter during the period of smelting activity.

We assume that the production intensity at each smelting site did not change over time. An overall change of the output of iron production on Elba is nevertheless included in our model. It is assumed that during an early phase, few (small) sites were in operation and a high number of (larger) sites operated during an intensive phase (see Table 9.2). The overall trend of modelled production as shown in Figure 9.7—an increase in the 2nd century BCE and a decrease in the 1st century BCE—is commonly found in the literature (Corretti, 2017). The varying intensities in the iron production on Elba Island coincide with major political events in the Roman period, such as the Second Punic War, the beginning of Rome's civil wars, the occupation of new provinces such as *Gallia*, or the transition from the Republic to the Empire.

Fuelwood production

In our model, felling preference is a function of transport *cost*. We did not model species selection, albeit it is known that some *macchia* species were preferably used at the Follonica–Rondelli site (Sadori et al., 2010). Nevertheless, *e.g. Quercus* species were also suitable as fuel (Nihlén, 1958). We additionally presume that coppicing was the common practice for fuelwood production on Elba Island, because only small branches of wood are necessary for charcoal production. Coppiced woodlands (*silvae caeduae*, (Visser, 2010)) with various species (e.g. sweet chestnut or oak) are mentioned by several ancient authors (e.g. Theoph. Hist. pl. 4.8.11). High *macchia* coppices were also common due to the high calorific value and its suitability for coppicing (presence of a lignotuber, resprouting after disturbances) of some species (especially *Erica* spec. Durand et al., 2009; Poggiali et al., 2017; Voulgaridis & Passialis, 1995). Meiggs (1982)states that coppicing was common in silviculture to produce fuel for metallurgy.

We think that it is reasonable to assume that no fuelwood or charcoal was transported from the mainland to Elba Island. The shipping of fuelwood is mentioned only in one ancient text from the 4th century CE, that focuses on the use of wood for heating baths in Rome (Meiggs, 1982). The volume of ore required to produce one unit of iron is much lower than the volume of charcoal required to produce the same amount of iron. Therefore, it appears more reasonable that in case of fuel shortage, ore was transported from Elba Island to the mainland than that charcoal (or even fuelwood) was transported to Elba Island. It is archaeologically and historically assured that also in times of sufficient fuelwood supply, ore was transported to the mainland. As some of the smelting sites on Elba Island are located in great distance from the mines (Figure 9.1), we assume that

the raw ore was transported to these sites by sea. As concluded from interpretations of Diocletian's *Edict on Maximum Prices* (early 4th century CE), over longer distances, the transport by sea is more rational than the land-transport (Greene, 1986)

We assume that the woodland cover on Elba Island in antiquity was similar to the present cover building on the assumption that (1) the woodland was only importantly changed after smelting operations on Elba Island occurred; that (2) the present vegetation is relatively dense as regrowth started after the primary sector lost its important on Elba since the 1950s (Carta et al., 2018b); and that (3) the present land cover (especially on the slopes) is controlled by major ecological factors, mesoclimate (exposition) in particular. North-exposed slopes are more densely covered than south-exposed slopes (see Figure 9.1). Further modelling approaches on fuelwood consumption could also implement a climate-driven change in vegetation regrowth or the impact of succession or accelerated soil erosion after felling on vegetation regrowth and stand. Degradation of vegetation (or even soil) is not incorporated in our model; only the impact of forest browse is considered as a factor reducing the regrowth of woodland.

Our model has a 1-yr-resolution. Thus, seasonality is not considered in our model, although it might have played an important role in the ancient iron production cycle. From medieval–modern times it is reported that especially the felling of wood is a seasonal task (e.g. Corretti, 1991; Mazzei-Karl, 1990).

Other fuelwood consumers

Our model takes mainly the wood consumption for smelting operations and the supply of the workers employed in the metallurgical production metabolism into account. We did not model the wood demand for fire setting in the mines. We assume that fire setting was not important for mining on Elba Island. During Roman times, mainly near-surface ores where extracted that were relatively easy recoverable. Other pyrotechnical industries on Elba than iron smelting (e.g. copper production, iron forging, or glass, brick, and pottery production) contemporary to the smelting period are not archaeologically recorded. During the middle to late Imperial Age—so after the smelting period—, lime-slaking might have taken place on Elba Island (Principe et al., 2011). Forging of raw blooms on Elba Island took place only on a very small scale (Corretti, 2016, 2017); further processing is known from Populonia-Baratti on the mainland (Chiarantini et al., 2007). It appears unreasonable that shipbuilding took place on Elba Island, though small scale overhaul work might have been carried out. The activities in the *villae maritimae* and their *partes rusticae* (mid-1st century BCE to 1st century CE) might have had significant influence on the land cover. Orcharding is known from Le Grotte (Milanesi et al., 2016). Agricultural

production or fuelwood consumption for baths might also have been important in the context of the main city of *Fabricia* (Portoferraio). Scholars considered bathes as important consumers of fuel (Janssen et al., 2017). Nevertheless, the heydays of documented food production and bathing post-date the phase of intensive iron production on Elba Island.

9.3.4 Elba as a case study

The question whether the decline of the smelting economy on Elba Island was triggered by ecological factors is important for the understanding of Elba's history and the metallurgical landscape in *Etruria Mineraria*. Besides, we think that the conditions on Elba island present a test case for a model with a high uncertainty of input parameters. Several factors facilitate the application of the proposed stochastic model on Elba Island. (i) Given the fact that Elba is an island, surrounded by sea, the boundaries of the model are well defined. Although sea-borne transport appears to be much cheaper than land transport (for longer distances in particular), the transport of raw ore from Elba Island to the mainland might have been more economic than the transport of charcoal fuel from the mainland to Elba Island. Hence, fuel production for smelting on Elba Island was presumably local; the assumption of a closed system is reasonable. (ii) Additionally, the amount of slag disposed on Elba Island during antiquity is well documented. Between the 1910s and 1950s—especially in the interwar period—old slag heaps in Tuscany were removed and the slag was re-used in modern blast furnaces throughout Europe. The exploitation of the slag heaps was documented by concessionaires (Nihlén, 1958; Pistolesi, 2013). (iii) Furthermore, scholars documented (ancient) smelting sites since the 18th century (e.g. Lambardi, 1791; Mellini, 1879; Ninci, 1815; Sabbadini, 1919). Especially since the late 1950s, huge parts of the island were surveyed. These surveys provide a comprehensive data set on ancient and medieval smelting sites (Corretti, 1988, 1991; Corretti et al., 2014; Nihlén, 1958; Pagliantini, 2014; Zecchini, 2001). Although not all sites are dated, Corretti (Corretti, 1991) expects that most non-dated sites located in the interior of Elba are medieval—few exceptions are known (Corretti, 1988). Most sites with large quantities of slag uncovered are Roman. Therefore, we expect that a large portion of slag 'produced' in antiquity is known. (iv) Considering the archaeological documentation of the ancient smelting sites, historical interrelations, and ancient texts, the chronology of iron smelting and phases of production intensity are well known (see above).

9.3.5 'Deforestation hypothesis'—revisited

Our results clearly indicate that it is at least *unlikely* that Elba Island was deforested during the ancient smelting period. With the set of parameters at hand, it appears possible that iron smelting on Elba could have been conducted without a lack of fuel. It appears worth to revise the 'deforestation hypothesis' indicating that the smelting sites on Elba Island were abandoned in the 1st century BCE due to a lack of fuel.

Several scholars that argue for a lack of fuel cite Strabo's observation that iron was not processed on Elba, but only on the mainland. Strabo does, however, not provide any reasons why ore was not smelted on Elba Island during the time of his observation (Grove & Rackham, 2003; Pococke, 1745). In contrast, the relationship between human agency and deforestation (or forest use) was observed by Strabo on the Apennine peninsula (Hughes, 1983; Hughes & Thirgood, 1982; Williams, 2000). Moreover, the transport of raw ore from the Elban mines to the metallurgical centre in Populonia-Baratti was part of the production system since the 6th century BCE, long before iron was smelted on Elba (cf. Grove & Rackham, 2003). Additionally, Strabo's note that '[the iron] cannot be brought into complete coalescence by heating in the furnaces on the island' may not only be interpreted as indicating the absence of smelting on the island. It may also indicate that the blooms from Elba were impure—what is typical for bloomery smelting—and had to be refined in the forges in Populonia. Sometimes, Strabo's text is also translated with ' cannot reduce it into bars in the furnaces on the island'—see Grove & Rackham (2003) or Radt (2003) for comments on the interpretation of Strabo's text. The near absence of evidence for smithing on Elba Island, but remains of large forges in Populonia (Chiarantini et al., 2007), support this interpretation. Second, information from (limited) pollen data indicates rather a shift in the species composition—from deciduous oak to woody shrubland species *(Ericaceae)*—than a loss of woodland cover. *Erica arborea* and *Arbutus* spec. were common fuelwood species in Etruscan and Roman metallurgy (Becker et al., 2019a; Sadori et al., 2010). Sedimentological analysis of alluvial sediments have shown that morphodynamics—i.e. the deposition of high-magnitude flood layers, slope deposits, and gravel—in the Campo plain (central Elba) increased during the Roman smelting period. Nevertheless, there is no distinct evidence for an island-wide clear-cutting (Becker et al., 2019a). Other reasons than fuelwood scarcity—such as upheaval in the Roman world between the Republic and the Empire—might have fostered the abandonment of smelting sites. In the 1st century BCE, the Roman Republic conquered new provinces with important iron ore deposits. A senate's decree *(senatus consultum)* (Plin. HN, 3.138, 33.78) to save the resources in *Italia* is contemporary to the decline in iron production on Elba Island. The decree emphasizes a general trend of resource conservation (either to prevent or cope with scarcities or to focus on resource exploration in the provinces). Last, smelting

activities on the island continued also in the 1st or even 2nd century CE, albeit on a small scale.

The 'deforestation narrative' may have developed when Strabo's text was read in the light of a contemporary impression on the landscape from the 18th to the mid-20th century (Schweighardt, 1841; Täckholm, 1937). In 1814, Schweighardt refers to the situation in antiquity and states that 'even now, due to a lack of firewood, the ore is not processed on Elba, but on the mainland' (Schweighardt, 1841). Most recently, Wiman mentions that deforestation was the reason for the shift of iron production from Elba to Populonia and adds that 'Elba Island today is still heavily marked by erosion and barren hills.' (Wiman, 2013, p. 17). That 'actualistic' view on the ancient environment on Elba is similar to Grove and Rackham's 'ruined landscapes' theory (Grove & Rackham, 2003). Additionally, in the 18th–early 20th c. the perspectives on forests changed clearly. The idea of sustainability popped up (von Carlowitz, 1713). The *problem* of deforestation reached the political agenda and measures against (actual or feigned) overexploitation of forest became an instrument of power (see e.g. Radkau, 1986; Schenk, 2006 for the *Holznotdebatte*, the debate on wood shortage in 18th century Germany, or (Davis, 2004) for the myths of desertification in colonial northern Africa). Historic documents (Giovannelli, 1771) indicate an expansion of agriculture in the 18th century on Elba Island. Also in this time, a lack of fuel for iron works is deplored (Campbell & MacLachlan, 1869; Swinburne, 1814; Thiébaut de Berneaud, 1814). In the 1950s—when tourism on Elba Island was in its early development and the local economy mainly relied on the primary sector—forest cover was far less than today. Agriculture use characterized the plains and the adjacent slopes during that time (Bowman et al., 2014; Carta et al., 2018b; Rosas et al., 2011). With the growing importance of tourism, also the land cover and the perception of the island changed. Elba Island was marked as 'green island' (A. Natan: *Grüne Insel Elba – Hohe Grantifelsen, weite Kastanienwälder*, Die Zeit, 09/1968). Today, only some hills on northeastern Elba Island are covered with grassland vegetation, while wide areas of the island are covered by forests (Cyffka, 2006; Foggi et al., 2006b) (see Figures 9.1 and 9.8).

9.4 Conclusions

Our simulations of the woodland requirement for iron smelting on Elba during antiquity indicate that it is unlikely that a lack of fuel occurred in antiquity; iron production could have been possible without overexploiting the woodlands. Thus, other reasons have to be taken into account to explain the abandonment of most iron smelting sites on Elba in the 1st century BCE, e.g. the access to new iron ore deposits in the Roman provinces. The 'deforestation narrative' that is commonly cited in the literature at least since the

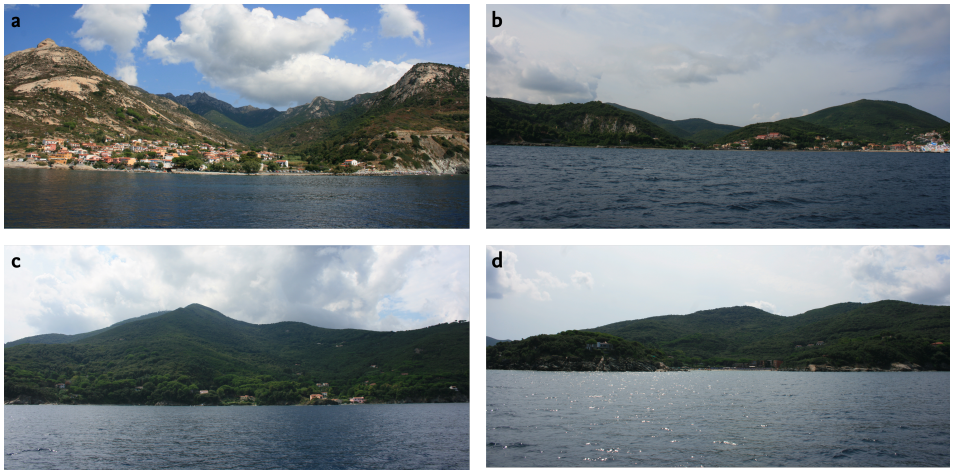

Figure 9.8 Impressions of valleys on Elba island where important ancient iron smelting sites were located. (**a**) Pomonte, west Elba; (**b**) San Bennato, northeast Elba; (**c**) Procchio, central Elba; (**d**) Isola della Paolina, northwestern Elba.

18th century therefore needs to be reinterpreted. The narrative may rather build on the perception of the modern landscape on Elba than on a sensitive reconstruction of the ancient conditions. However, the scale of the fuelwood requirement on Elba shows that smelting might have importantly contributed to changes in the landscape, as shown for morphodynamics by Becker et al. (2019a).

In terms of the socio-ecological model of iron production (Figure 9.2), the current study shows the importance of considering both the natural and the cultural sphere of causation to better understand ancient iron production. Not only the metabolism of iron production itself, but also the program of smelting (e.g. the demand for iron or the access to new ore deposits) and the representation of smelting in modern texts are crucial to understand human–environment interactions on Elba in antiquity.

Besides the evaluation of the 'deforestation narrative', our modelling approach has shown that although we have abundant data on the size and chronology of the smelting sites on Elba at hand, uncertainties are high. An estimation of the likelihood of a lack of fuel is nevertheless possible, especially because of the insularity of Elba. Our model outcomes clearly show the need to take both the endosomatic and the exosomatic metabolism of iron smelting into account when discussing the woodland requirements of production. Although still unlikely, the likelihood that no fuel on Elba was available for iron smelting in the 1st century BCE increased when taking the entire metabolism of iron production into account.

Referring to Theodore Wertime's antagonism 'The furnace versus the goat' (Wertime, 1983), we propose that based on our model results, both furnaces *and* goats (in the sense of food production) importantly contributed to the availability of woodlot on Elba.

Supporting information

S1 Appendix. Description of model parameter. Description of the procedure to estimate the parameter used for the model, viz. furnace inefficiency; kiln productivity; ore extraction; labour demand: felling, charcoal burning, and smelting, transport, supervision, and service; required farmland, woodland, and rangeland area.

S2 Table. Dating material. Overview on dating material used to define the chronology of the smelting sites. Data from literature review, own finds, ^{14}C-ages and archive material.

S3 Computer code. Computer code of the model. Matlab code of the main settings of the model and the outcomes of an average simulation.

Acknowledgments

We are grateful to the Deutsche Forschungsgemeinschaft (DFG, German Research Foundation) for funding under Germany's Excellence Strategy – *The Berlin Mathematics Research Center MATH+* (EXC 2046/1, project ID: 390685689) and *Topoi. The Formation and Transformation of Space and Knowledge in Ancient Civilizations* (EXC 264); F.B. and R.A.E. hold a scholarship from Topoi. Preliminary results of our research were presented at a conference in Berlin (*The Coming of Iron – Anfänge der Eisenverhüttung in Mitteleuropa*; 19.–21.10.2017) and in the session *System of extraction: mining, pollution, technology* during AIAC 2018 in Cologne and Bonn (22.–26.05.2018); our manuscript benefited from the discussions. F.B., R.A.E. and B.S. submitted a contribution to the conference proceedings of the *Coming of iron*-conference describing a preliminary simplified version of the current model.

10 Synthesis: The impact of iron smelting on Elba on the landscape balance

10.1 Palaeoenv*iron*ment

Topography is a main environmental prerequisite for metallurgy on Elba (Section 4.2.1). This includes the island status along with the short distance to the Apennine peninsula mainland and the location of the mines along the northeastern coast of Elba. Another site location factor is the configuration of the coast, which is characterized by mainly a rocky cliffs that are occasionally interrupted by fine–medium grained beaches (Figure 4.4, p. 70; e.g. Bowman et al., 2014). The mainly hilly to mountainous relief of the island, dissected by several coastal plains, is also a site location factor. Both coastal setting and relief control the accessibility of the hinterland and facilitated sea transport to locations with beaches suitable for landing. The variance between the ecoclimate of different mountainsides and slopes with different exposition is another site location factor. Biomass production on the generally wetter north–northwest exposed slopes is higher. On a macro-scale, the topography of Elba therefore determines the access and the availability of wood resources for smelting and prevails the characterization of the 'metallurgical landscape' on Elba.

On a meso- to micro-scale, the local (palaeo-)environmental conditions might have played a role in the selection of locations for iron smelting. Ancient smelting sites were located in protected position along the coast, i.e. in the sheltered, embayed part of the coast and on landforms that are slightly elevated compared to the near water course (Section 4.2.1).

In Case Study 4, Becker et al., submitted.a, Chapter 9, we have shown that the fuel requirement for iron smelting was high; the data show that large parts of western Elba have been used for forestry. Therefore, accessibility of large parts of Elba was necessary to satisfy the need for fuel for smelting and locate sites in the vicinity of all forest resources. The palaeoenvironmental situation gives also insights in location factors for ancient

smelting sites (Case Study 2, Becker et al., 2019a, Chapter 7). Especially (palaeo)wetlands and flood-prone areas limited the accessibility of some parts of the island.

[1] The palaeoenvironmental setting was one factor that influenced locating smelting sites on Elba during antiquity.

- Some Roman smelting sites in the northern *Campo* area are—non-typically—located in inland position.
- The sites are part of a nucleus of Roman metallurgical and agricultural activities around the Monte Castello di Procchio.
- Sediment sequences uncovered from the locations in the northern plain indicate the existence of a palustrine depositional environment only prior to the Roman smelting period.
- The low lying parts of the plain were covered with wetlands during the smelting period, as indicated by sedimentological evidence, toponomstatic interpretations, and recent vegetation; the area is flood-prone.
- The southern part of the Campo plain was less accessible during historic times.

Wetlands

It is a common conception that Roman smelting sites are located along the coast of Elba, while medieval sites are preferably located in inland positions (Corretti, 1988, 1991, 1992, 1997, 2012, 2017; Corretti et al., 2014; Corretti & Firmati, 2011; Corretti & Taddei, 2001; Pagliantini, 2014). According to Corretti (e.g. 2017), there are two exceptions. The Roman sites in La Pila and Forcioni on the border of the northern, more elevated, part of the Campo plain are located in considerable distance from the coast.[1] Several other slag finds were recorded by F. Cambi in the 1980s here (Pagliantini, 2014). Furthermore, by reinterpretation of archival material (see Nihlén, 1958, 1960; Nihlén & Ejlers, 1958) and the existing literature (Corretti, 1991; Monaco & Mellini, 1965; Pagliantini, 2014), Raphael A. Eser shows that other sites in the area are potentially ancient (Fosso di Campotondo, La Calcinaia; see also Corretti, 1997; Corretti & Taddei, 2001). The area was intensively used during Roman times. Raphael A. Eser points to the fact that there is, however, not necessarily a coexistence between e.g. the hilltop settlement on Monte Castello and the smelting site in its vicinity (unpublished Master's thesis, Humboldt-Universität zu Berlin, 2015: see Cambi, 2004; cf. Corretti, 2012). Several other human activities than

[1] Corretti, 1988, 1991, 2012, 2017; Corretti et al., 2014; Corretti & Firmati, 2011; Corretti & Taddei, 2001—interestingly, Corretti sometimes left these sites aside when discussing Roman iron metallurgy on Elba, see Corretti, 1992, 1997.

smelting are evident in the area, including agriculture (Cambi, 2004; Pagliantini, 2014). The sites in the northern Campo area are part of a cluster of (potentially) ancient sites on both sites of the Monte Castello di Procchio (along the wider bay of Procchio and on the northern part of the Campo plain). The location of other smelting sites along the Golfo di Procchio may have fostered economies of agglomeration. It is reasonable to assume that the access to the eastern slopes of the Monte Capanne massif was mainly possible from the north, not through the low lying parts of the plain in the south. In the southern part of the Campo area, the only ancient smelting site at Galenzana is not located along the plain, but on embayment of the headlands of the main Golfo di Campo (Corretti, 1988). The presence of small scale—and maybe insignificant—deposits of limonitic iron ore at Monte Perone, just <c 3 km north east of the smelting sites along the Campo plain, may have also played a role in the development of the smelting activities in this area. There has as yet been no credible evidence for the exploitation of the deposit in antiquity, although Nihlén (1958) attests that limonite was found at some Roman-dating smelting sites in the area (Case Study 1, Becker et al., 2019b, Chapter 6). This being the case, palaeoenvironmental conditions are worth to get attention when discussing the metallurgical landscape on Elba.

The uncharacteristic position of the sites in the northern part of the Campo plain may be strongly related to the paludal environment prevailing in at least lowlying position in the area during the Late Holocene. The Campo plain is the largest of the coastal plains on Elba, which developed along the main border faults on Elba that are associated with the Late Miocene Magmatism on Elba (Monte Capanne and Porto Azzurro plutons; Section 3.1.2).

As shown by D'Orefice & Graciotti (2014) and in Case Study 2, Becker et al., 2019a, Chapter 7, and Study 3, Chapter 8, the Holocene palaeoenvironmental development on Elba is mainly triggered by sea level oscillations. Sea level high stands during MIS 5 are recorded on Elba by occasional Pleistocene alluvial terraces (D'Orefice & Graciotti, 2014; Principi et al., 2015). During the regressive/low stand conditions, the subaerial palaeo-valleys along the present plains were exposed to incision; these valleys extent below the present sea level (Bianchi, 1943, in Gerngross, 1959). The incised palaeo-valleys were subsequently filled with sediments during the Holocene transgression. The main phase of the deposition of sediments indicated marine–paludal environments ended with the transition from late transgressive to early highstand conditions around 7.1 ka BP and is followed by a phase of fast aggradation until c 5.4 ka BP. This development of the coastal plains is in line with the *typical* development of the coast of western Central Italy after the Late Glacial Maximum (e.g. Amorosi et al., 2013b; Breda et al., 2016; see Study 3, Chapter 8).

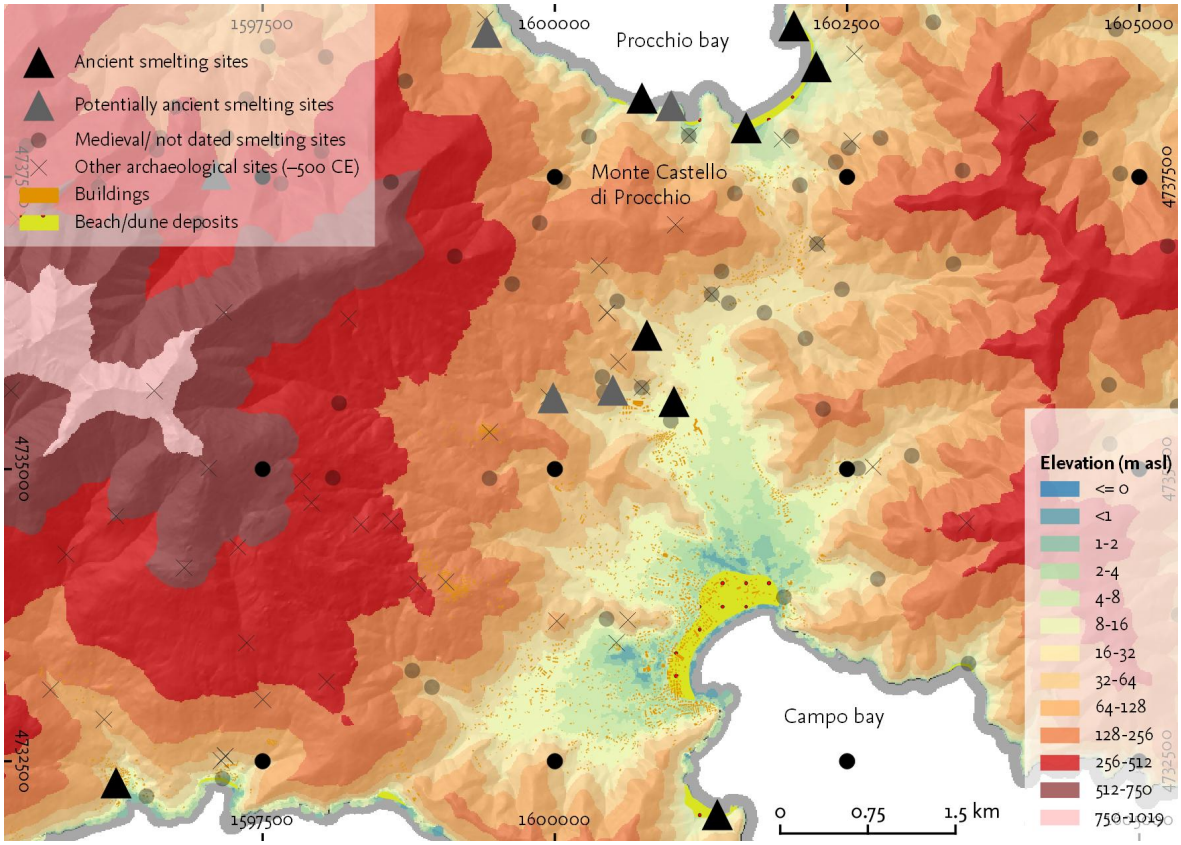

Figure 10.1 Elevation, archaeological sites, and buildings in the Campo plain. Archaeological sites cover the period from the Palaeolithic to the late antiquity. Database: Pagliantini, 2014, Carta tecnica regionale, 1:2000, 2013 (Regione Toscana). DEM (<32 m a.s.l.interpolated from elevation point data, 1:2000 (Inverse distance weighted, 25 m radius, nearest 10 points); DEM (>32 m a.s.l., Regione Toscana, 2014, DEM 1:10000)

As reconstructed based on sediments from the Valle di Forcioni—and also insinuated by the record of the Stabbiati valley—, the elevated parts of the plain (around >10 m asl) were not covered by wetlands during the period of ancient iron smelting. The outcomes of Case Study 2, Becker et al., 2019a, Chapter 7, shows that in parts of the lower Stabbiati valley, palustrine deposition environments disappeared only in Roman times, while in other parts of the plain, wetlands prevailed during antiquity (Bertini et al., 2014).

The sedimentological data is in line with historical evidence. The foundation of the upland villages of Sant'Ilario and San Piero in Campo in the High Middle Ages may also be related to the wetlands in the plain; the villages are located in elevated position, where area for agricultural production was available (cf. Carta et al., 2018b). From the Tuscan mainland, it is known that Malaria was an important issue since antiquity (see e.g. Sallares & Sallares, 2002 and Wiman, 2013). As handed down in travel narratives, swamps and malaria were common in the plains of Elba in the 19th century (Thiébaut de Berneaud, 1814; Williams, 1820). Since the 18th century, the expression 'Maremma dell'Elba' is used when

referring to the Campo plain (Ferruzzi, 2010). The byname alludes to the expansive coastal wetlands of the Maremma region in southern Tuscany. Toponyms in the Campo area refer to wetland conditions (e.g. 'Lo Stagno' in Marina di Campo, see Ferruzzi, 2010; Pagliantini, 2014); fragmented patches of hydrophilic meadow vegetation are still found in the Stabbiati valley and along the Marina di Campo Airport (Foggi et al., 2006a,b). Today, the plains on Elba and on the mainland are used for farming; the area is mainly drained since the *bonificatio* in the mid-19th century, which was introduced by the grand-duke Leopold of Tuscany. The present settlement pattern in the plain mainly developed with the boom in the tourism sector on Elba since the 1950s (Carta et al., 2018b; Cyffka, 2006; Friedrich et al., 2000). Several holiday homes and hotels were constructed in the area, as well as the Marina di Campo Airport.

The importance of the Last Glacial regression and the Holocene transgression and the subsequent propagation of river valleys up to the bonification in the 19th century plays an important role in the understanding of settlement and economic development in Tuscany, especially in the Maremma region. For instance, the history of the ancient *Lacus Prilius* (Fiume Bruna, Castiglione della Pescaia) is strongly connected to the Etruscan city of Vetulonia. A lagoon or coastal lake extended for several kilometer inland during Etruscan times, which provided access from Vetulonia to the sea; the location of the city around 300 m a.s.l.was protective against malaria. The subsequent propagation of the Bruna/Sovato delta caused the development of settlements along the new plain and e.g. the development of salt production during the Middle Ages (Colombi, 2018; Vaccaro, 2008). Although the distribution of archaeological finds along the former lagoon of Piombino is strongly connected to the sedimentation of the lagoon (Di Paola, 2018; Giroldini, 2012).

The Stabbiati valley (i.e. the southwestern part of the Campo plain) is today exposed to floods; e.g. in November 2011 (Trambusti et al., 2014; see also Jackson et al., 2013). Several torrent controls were installed in the course of the Stabiatti in the aftermath.

Floods

A location near a stream is an important characteristic of the metallurgical landscape on Elba (see Chapter 4). However, smelting sites are often located in (slightly) elevated positions. This position in relation to local landforms may be interpreted as a protected location, where the risk of floods is relatively low. In Campo all'Aia at the bay of Procchio, slag finds were mainly found on elevated positions, although Nihlén (1958) found evidence for roasting at the mouth of the Fosso del Campo all'Aia directly at the coast (Figure A.10). The Magazzini site is another example. The local microtopography and

especially geochemical data (Case Study 1, Becker et al., 2019b, Chapter 6) suggest that the smelting site is located on small fluvial terrace that was not flooded recently. The soils from the active floodplain are characterized by lower contents of less weathering resistant elements (e.g. Ca), whereas in the soils of the smelting site and the adjacent terrace, contents of conservative elements are higher. This interpretation is supported by the decreased TIC contents of the terrace soils compared to the floodplain soil; the recent floodplain is covered with sediments originating from calcareous bedrock abundantly found in the catchment area draining the area of the Magazzini site (Figure 7.2, p. 132).

Some finds of slag from recent floodplains (e.g. Corretti 1984/85, cit. in Pagliantini, 2014: S. 085, 'Fosso Baccetti') may not point to smelting activities *in situ*, but to reworking of material from upstream sites. The age determination of a sediment sequence published in Case Study 2, Becker et al., 2019a, Chapter 7, points to the reworking of material, as the age of archaeometallurgical remains in the sediments and cal-^{14}C-ages show age inversions; additionally, slag remains are found in recently reworked slope deposits and channel-bed sediments. Also in the coring location B-II in the Baccetti valley (data used in Study 3, Chapter 8), the surface of the floodplain is covered with slag (Figure A.9, Appendix). These slag finds may be reworked from upstream smelting sites that are of presumably medieval age (see Corretti, 1991; Corretti & Firmati, 2011; Figure 1.2, p. 4). Sediment data from the percussion drilling at these locations indicate that the upper 100 cm of the sediment sequence were deposited after the medieval period (B-II; 1521–1296 BP, 95 cm depth; see Study 3, Chapter 8); no slag finds were uncovered from the sediments. A sediment sequence from the fan of the Fosso della Fonte alla Pergola in the Baccetti valley indicates that slag was deposited during or prior to the medieval smelting period (c 230 cm depth, see Study 3, Chapter 8). Although it is possible that slags finds from the floodplain are reworked, other interpretations are proposed. Corretti 1984/1985 interprets the slag finds as evidence for smelting on the valley floor (cit. in Pagliantini, 2014). Also evidence from aerial photo interpretation points to smelting in-situ (Appendix: Figure A.9). The age of the presumed smelting site is however unknown.

10.2 Fuel consumption and morphodynamics

[2] Geomorphic activities on Elba increased during the ancient smelting period, most likely due to widespread woodland cover reduction for charcoal production.

- Detailed sedimentological analysis, grouping of sediments in chemofazies, and age control suggest that morphodynamics increased in the Forcioni valley during antiquity (slope deposits and layers indicated high magnitude floods).
- A phase of increased geomorphic activities coinciding with the ancient smelting period is indicated by cumulative probability functions of cal-^{14}C-ages from several sediment sequences distributed over Elba.
- Sediment accumulation during the ancient smelting period is relatively high compared to a pre-metallurgical or post-smelting periods.
- The facies pattern of the available sediment sequences from Elba points to increased geomorphic activities during the smelting period.
- Besides smelting, the main trigger of sediment accumulation on Elba during the Holocene is the deceleration of the sea level rise at the end of the Versilian transgression.
- The modeled woodlot requirement for smelting and the supply of the metallurgical work force indicates that significant areas of woodland had to be felled during Roman times, supporting the interpretation of smelting as a trigger of increased geomorphic activities on Elba (reduction of vegetation cover and subsequent soil erosion).

10.2.1 Morphodynamics

Based on detailed analysis of sediment sequences uncovered in the vicinity of a smelting site (Case Study 2, Becker et al., 2019a, Chapter 7) and the meta-analysis of chronological and facies data of dated sediment layers from various archives on Elba (Study 3, Chapter 8), we reconstructed past morphodynamics related to iron smelting on Elba. Both studies reveal that sediment accumulation and geomorphic activities increased during the antiquity. There is a strict temporal simultaneity of smelting and accelerated morphodynamics. Additionally, the frequency of finds dating to the Roman smelting period on Elba is much higher compared to the Etruscan period and late antiquity (Study 3, Chapter 8). Besides coincidence, there is also a causal relation between iron production and environmental dynamics. There is a good case to assume that iron smelting had significant negative impact on land cover and therefore soil erosion; in Case Study 4, Becker et al., submitted.a,

Chapter 9, we have shown that large woodlot areas were required on Elba to produce the charcoal necessary for charging the bloomeries on Elba.

The following observations from the sedimentological data point to changes in morphodynamics during the Etruscan–Roman smelting period:

- The morphodynamic impact of iron smelting is clearly visible in a sediment sequence (F-III) obtained from the Valle di Forcioni in the transition zone between the Campo plain and the Monte Capanne massif. We interpret angular to sub-angular, partly brittle gravel in loamy matrix that dates to 2.0–2.2 ka BP(c 200–50 BCE) as slope deposits overlaying floodplain sediments. This interpretation is supported by the element composition of the sequence. The Ti/Si log-ratio of slope and alluvial deposits, for instance, differs clearly. The slope deposits originate from bedrock of the slopes adjacent to the smelting site, which is mainly Palombini shale, whereas most of the bedrock in the catchment area of the Fosso di Forcioni is made up of sienogranite (Figure 7.3, p. 133). The geochemical composition of the parent material differs.
- Additionally, increased variability in e.g. Zr/Ti or Zr/Rb log-ratios from sequence F-III (2.2–1.9 ka BP, 200 BCE to 50 CE) points to the deposition of higher magnitude flood layers. The element rations are related to variability in grain size and thus transport capacity of floods (Turner et al., 2015).
- The thickness of the sediment layers between dated samples in the F-III sequence points to the highest aggradation rate during the period of Roman iron smelting in that specific area.
- A significant change in the chemostratigraphy of a sediment sequence obtained from a low-lying part of the Stabbiati valley dates to c 2.4 ka BP, thus to the onset of the iron smelting period on Elba. We interpret this chemical change as a transition from a lacustrine depositional environment to (coarse) alluvial sedimentation in that area, which might indicate siltation due to increased detrital input.
- Cumulative probability functions of cal-^{14}C-ages from different locations on Elba clearly show a peak of 'geomorphic activities' during the ancient smelting period.
- The stochastic model of sediment data and cal-^{14}C-ages shows that sediment accumulation clearly increased during the Roman smelting period compared to prior periods.
- The facies-based model of instability and quiescence indicate an increase in geomorphic activities during the Roman smelting period.

In synopsis of all these points, we argue that felling for charcoal production to charge the bloomery furnaces and subsequent soil erosion resulted in the deposition of facies

indicating geomorphic activity (e.g. slope deposits and high magnitude flood layers); and an increase in the rate of sediment accumulation.

Our observations from Elba fit well to previous interpretations of the impact of iron smelting and the late Holocene landscape development in Central Italy. Various scholars have shown that an increase in geomorphic activities as recorded in sediment archives is contemporary to local metallurgical activities (Bayon et al., 2012; Brown et al., 2009; dos Santos Mendes, 2016; Raab et al., 2010; Schmidt-Wygasch, 2011; Stolz et al., 2012; Stolz & Grunert, 2008; Stolz et al., 2013; Thelemann et al., 2018).

Archaeological data shows that smelting was the most important economic sector on Elba (cf. Pagliantini, 2014). As shown in Case Study 4, Becker et al., submitted.a, Chapter 9, the woodlot area required to produce charcoal for the furnace charge (exosomatic metabolism) is much higher than the area required for the supply of the work force for smelting (endosomatic metabolism). Studies in other regions have, however, emphasized that smelting might not have been the most important trigger of environment change, as e.g. population dynamics coincide with increased metallurgical production (Eriksson et al., 2000; Marchant et al., 2018; Willis et al., 2004; see Iles et al., 2018; Lane, 2009; Superson et al., 2014). This is especially important when metal production is for local needs—on Elba, however, the production during the 'industrial' phase (see Section 4.1, p. 61) was export-oriented. Although scholars have proposed that metallurgical centers—such as Elba—are centers of deforestation and erosion, the increase in geomorphic activities on Elba is not unique compared to the development in (Central) Italy (Study 3, Chapter 8, Figure 61 i, j), although evidence for accelerated morphodynamics on Elba during Roman times is very clear. Especially the Roman expansion in Etruria triggered change in land use intensity and population dynamics (Study 3, Chapter 8, Figure 8.7, p. 176). In both meta-analysis (Figure 8.7, p. 176) and sedimentological case studies (see Section 8.2, p. 162), an increase in sediment accumulation and geomorphic activities is observed during the Roman times, although peaks in morphodynamics triggered by human activities were also recorded during the Bronze Age and the post-Roman period.

10.2.2 Fuel consumption

The increase of geomorphic activities on Elba during the ancient smelting period fits to the hypothesis of an extreme requirement of woodlot for smelting on Elba (e.g. Corretti, 1991; Forbes, 1964; Harris, 2013; Healy, 1978; Hughes, 2014; Meiggs, 1982; Penna, 2014; Pococke, 1745; Sands, 2013; Veal, 2017a; Wiman, 2013) and the subsequent positive impact on erosion dynamics. Our model of the fuel consumption for iron smelting clearly shows that it is likely that large woodlot areas were required to supply the iron

industries (Case Study 4, Becker et al., submitted.a, Chapter 9). This observation fits to the assumption that metallurgy in Etruria Mineraria and also iron smelting in general importantly contributed to deforestation, although in some regions, iron smelting was not the hugest consumer of woodland and most important trigger of deforestation (cf. Iles, 2016; Mighall et al., 2017). Elba, however, was the center of iron mining and smelting on the Apennine peninsula and even of the whole Roman area until the mid-1st century BCE.

Although the input parameter of the model are subject to uncertainty, our Monte-Carlo experiments show that especially woodlands in northeastern Elba—so the area around the ancient mines—but also in remote areas of western Elba were probably intensively used for ancient iron smelting. However, it is *not likely* that the entire island was cleared for ferrous metallurgy. We simulated with a likelihood of 28% that no woodland on Elba was available for felling; complete deforestation in the 1st century—as often expected—is less likely. When assuming that the vessels that transported raw ore from Elba to the Appenine peninsula mainland transported food for workers employed in iron production, the competing land consumption for forestry and food production would have been reduced. Then, it is even *very unlikely* that no fuel was available on Elba during the Roman smelting period (6%).

When comparing the results of our model with various other attempts to quantify the fuel wood consumption for ferrous metallurgy and production parameters assumed therein, our estimation appears 'conservative' (Table 9.5, p. 212), i.e. tending to result in relatively low modeled woodland cover. Taking the parameter of the most successful smelting experiments (Nikulka, 1995)—and a smelting experiment with hematite ore from the Rio Marina mines (Benvenuti et al., 2016)—, it was possible to sustain smelting activities on Elba even during the phase of intensive production (Case Study 4, Becker et al., submitted.a, Chapter 9). Thus, it is reasonable to assume that smelting on Elba not necessarily ceased in the 1st century BCE due to a lack of fuel. Crew & Mighall (2013) proposed that it was the self-interest of pre-industrial smelters to save as many wood as possible to allow production to be continued.

[3] Although if the use of wood resources for smelting had a clear impact on the vegetation cover on Elba, our evidence does not support the hypothesis that a lack of fuel caused the abandonment of smelting sites in the 1st century BCE.

– The outcomes of the woodlot model imply that it would have at least been possible to smelt iron on Elba in the reconstructed scale without causing the deforestation of the entire island.

- The woodlot model suggests that it is not likely that the entire available woodland on Elba was cleared for smelting and the supply of the work force.
- The integration of the supply for the workforce in the calculation of the fuel requirement for the entire metabolism of smelting clearly changes the likelihood of deforestation, although it is not high.
- When assuming that the supply for the workers (partially) came from the mainland, it is even less likely that a lack of fuel occurred due to smelting.
- The sparse palynological data from Elba does not support the deforestation hypothesis, but supports the interpretation that smelting caused clear environmental change.
- We recommend to reconsider the 'deforestation narrative' taking other (political–economical) reasons for the abandonment of some smelting sites on Elba into account.
- The resurface of the 'deforestation narrative' in the last c 200 years is strongly connected to a contemporary view on the landscape of Elba.

10.2.3 The 'deforestation narrative'

The outcomes of the fuel model (Case Study 4, Becker et al., submitted.a, Chapter 9) contradict the popular narrative that a *lack of fuel*[2] on Elba occurred in the 1st century BCE and resulted in the abandonment of smelting on the island (see Chapter 1 and Appendix 11 for references); it is *likely* that the woodlot area required for smelting did not exceed the available woodland area. Some scholars at least cite a lack of fuel as one reason for the abandonment among others (Corretti, 1988, 1992, 2004; Corretti & Firmati, 2011; Pagliantini, 2014). Although a decline in smelting activities is evident in the archaeological record (Section 4.1, p. 61, Case Study 4, Becker et al., submitted.a, Chapter 9; and e.g. Corretti, 2017; Corretti & Firmati, 2011) equivocal evidence for the 'deforestation' narrative has been discussed. The outcomes of the fuel model suggests to re-interpret the evidence for the 'deforestation narrative'.

First, various authors cite the ancient Greek writer Strabo (5.2.6) to underpin their deforestation hypothesis (Casevitz & Jacquemin, 2018; Corretti, 1992; Ettrich, 2006; Groskurd, 1831; Harris, 2013; Hughes, 2014; Jervis, 1860; Köstlin, 1780; Lätsch, 2005; Marzano, 2007, 2015; Meiggs, 1982; Pagliantini, 2014; Perlin, 2005; Piccinini, 1938; Pococke, 1745; Radkau, 2012; Roller, 2018; Schneider, 1992; Simonin, 1858; Sonnabend, 2012; Täckholm, 1937; Toner, 2018; Wikander, 2009; Williams, 2010). There is a good case to dispute the conclusion that Strabo witnessed deforestation and a lack of fuel on Elba. Strabo described that the ore ' cannot be brought into complete coalescence by

[2]for simplicity and harmonization, we used the terms *lack of fuel*, *shortage of fuel*, and *scarcity of fuel* interchangeably; other expressions used in the cited literature are i.a. 'not the conveniency of wood'.

heating in the furnaces on the island' (Jones, 1923), without explaining why the ore could not be 'smelted' there. Grove & Rackham (2003) point to the idea that Strabo observed the typical production system of iron in Etruria Mineraia, which included the transport of blooms from Elba to Populonia for refining ('could not be brought into complete coalescence' = containing impurities). Alternative translations of the phrase in Englisch (and German) by e.g. Hamilton (1903: ' cannot reduce it into bars in the furnaces on the island', cf. Gossellin et al., 1809) and Radt (2003) support this interpretation. Also in a note to the Loeb-translation of Strabo's text, the editor evokes that 'Strabo speaks of "iron," not "iron ore" and [that] he does not mean to say that *iron-ore* was not *smelted* at all on the island' (emphasis in original). Thus, there is a different understanding—or even an unprecise translation—of the original text, concluding that either raw iron or iron blooms were transported to Populonia on the mainland. Interestingly enough, the editor's note does, however, also rise the issue of fuel scarcity.[3] In a German translation, the relevant sentence from Strabo 5.2.6 reads as follows: 'Ich sah auch die Bearbeiter des von Aethalia [herüber] gebrachten *Eisens*; denn dieses kann nicht in *Schmelzöfen* auf der Insel selbst ausgeschmolzen werden sondern wird *sogleich aus den Gruben* nach dem Festlande geschafft. Sowohl diese Sonderbarkeit enthält die Insel …' (Forbiger, 1857 (emphasis by FB); similar : 'Wir sahen auch die Bearbeitung des von Aithalia gebrachten Eisens; denn Dieses kann nicht in Schmelzöfen auf der Insel selbst ausgeschmolzen werden, sondern wird sofort aus den Gruben aufs Festland gebracht.' Also Groskurd (1831) approaches the issue of the specificity of the translation, but states that Strabo speaks of smelting of the raw ore, not of casting and hammering of iron; Groskurd (1831) supports the hypothesis of a lack of fuel in the 1st century BCE.[4] Remains of smithing are rarely found on Elba (see Corretti, 2016 for an exceptional find of smithing slag), whereas smithing hearth were recovered for Populonia (Chiarantini et al., 2007).

The differentiation between the transport of run-of-mine, dressed ore, and iron blooms is important for the fuelwood requirement, as all steps of the production process, viz. roasting, smelting, and refining, require fuel wood (see Section 2.3.3, p. 28). Thus, the location of the different steps is an important location factor in iron metallurgy (see also Chapter 4).

Second, in Strabo's text, the *iron* is immediately brought from the mines to the mainland. Therefore, the interpretation of the transport of run-of-mines rather than processed

[3] 'Strabo is thinking primarily of the high temperature necessary to bring the iron from a brittle and spongy to a soft and tough texture; but for the lack of wood on the island … any further working of the iron there was wholly impracticable.'

[4] in German: 'Freilich gehört das Giessen und Hämmern des Eisens in Stangen und Platten und Bleche zu seiner Bearbeitung, aber das Ausschmelzen der rohen Erze ist doch das erste und wichtigste Geschäft, ohne welches das andere nicht statt findet. …Beides aber war zu Strabons Zeit auf der Insel Aithalia nicht mehr möglich, weil es der Insel an Holz fehlt' Groskurd, 1831, p. 386, note 3., transl. FB

iron (blooms?) is not far to seek; however, also to the time of Strabo's observation (mid-1st century BCE), ore was smelted near the mines, after some other smelting sites were abandoned (see Section 4.1, esp. Figure 4.1, p. 62).

Third, Strabo observed the impact of the felling of trees in other locations (Hughes, 1983; Hughes & Thirgood, 1982; Williams, 2000)—referring to deforestation in the context of metallurgy on Cyprus (Corretti, 2004)—, but does not mention with any word the forests on Elba. Interestingly, Wikander (2009) cites Strabo's comments on Cyprus (14.6.5) and Elba (5.2.6) to illustrate the fuel requirement for metallurgy in antiquity (see also Schneider, 1992).

Evidence for deforestation on Elba from other archives than historical accounts are also sparse. *Fourth,* palynological data from Bertini et al. (2014) show a decrease of oak species and the increase of *Ericaceae* species that is more or less contemporary to the ancient smelting period. However, the evidence does neither point to complete deforestation nor to a lack of fuel. *Ericacea* species were common fuelwood species in the region of Etruria Mineraria. In the sediments from the Forcioni valley, the concentration of (large) charcoal fragments is relatively high in layers dating to the Roman smelting period; all of the samples determined by anthracological techniques are classified as *Arbutus* ($n = 14$, see Case Study 2, Becker et al., 2019a, Chapter 7). Anthracological data from the Follonica-Rondelli smelting site from the 6th/5th century BCE reveal that more than 90% of the charcoal used there was from *Erica*, Sadori et al., 2010). *Ericacea* species are common fuel wood in the Mediterranean region. Thus, an increase in *Ericacea* pollen may reflect an impact of smelting on vegetation cover, but does not mean that there was no fuel wood.

Fifth, the scale of the decline of smelting on Elba is not entirely clear. Also it is reasonable to assume that production decreased, some smelting sites—potentially those around the mines and in central Elba—were still active in the 1st century CE (see Chapter 4, esp. Figure 4.1, p. 62; Raphael A. Eser, diss. in prep.). For instance, the wreck found at the Bay of Procchio (around the 2nd century CE) carried abundant hematite lumps (Brambilla, 2003, V. Serneels, pers. comm., 2017-10-20)—which is at least points to mining on Elba during that time.

Sixth, other reasons for the abandonment of most smelting sites on Elba should be taken into account to understand the decline of iron production on Elba in the 1st century BCE, such as the availability of new important deposits in the provinces. The Roman conquest of *Noricum*, *Gallia*, and *Hispanica* is contemporary due to the decline of the iron production on Elba. The *senatus consultum* reported by Pliny that forbid extraction in *Italia* may also be contemporary to the decline in production or may predate (e.g. Benvenuti et al., 2013; see Sherwood et al., 2003 for a contrary chronology of the decree). Scholars

also proposed that upheavals in the Roman world could also have contributed to the decline of ferrous metallurgy on Elba. Edmondson (1989) discusses the 'decline of large mining districts'—having also smelting in mind. Corretti (1997) points out that the construction of the *villae maritimae* on Elba could have contributed to the abandonment of smelting, not only because of the emission of soot (cf. Corretti & Firmati, 2011), but also because of agricultural use and *'sfruttamento . . . naturalistico'* (p. 75; *sensu* nature-related experiencing).

10.2.4 The 'deforestation narrative' in context

The type of source in which the 'deforestation narrative' is taken up is a substantial point of a source-critical analysis. In historical (pre-1950s) and archaeological texts on Elba, the hypothesis of a lack of fuel is cited, mainly in the context of other hypothesis on the development of the iron production on Elba, and commentated (Corretti, 2004, esp. fn. 46). Furthermore, the 'deforestation narrative' is told in more general literature on (global) forest history, (environmental) crisis, and (ancient) Mediterranean environments. Especially in the later texts, the authors have—by nature of the kind of publication—no specific focus on the regional context on Elba. Furthermore, the 'deforestation narrative' fits well to a present-day perspective on forestry and the general topic of the publications; e.g. Williams's *Deforesting the Earth: From Prehistory to Global Crisis, An Abridgment* or Radkau, 2012, *Kapitel 1 – Holzwege in der Geschichte* = 'barking up the wrong tree throughout history').

Another type of sources are the travel narratives for mineralogical descriptions of Elba from the 18–20th century. As outlined in Case Study 4, Becker et al., submitted.a, Chapter 9, we propose to read the coming of the 'deforestation' narrative in the light of situation on Elba during that period. Change in land use and land cover in the three centuries before present may also have contributed to the emergence of the 'deforestation' narrative.

We know from geography of vegetation (Friedrich et al., 2000) and the interpretation of orthophotos (Carta et al., 2018b) that the present view of Elba as an island with relatively dense woodland cover (see Cyffka, 2006; Foggi et al., 2006b) is a new phenomenon. The travel journalistic labeling of Elba as a 'green island' came up in the 1960s (A. Natan: *Grüne Insel Elba – Hohe Granitfelsen, weite Kastanienwälder*, Die Zeit, 09/1968). (Interestingly, e.g. Wiman, 2013 still characterizes Elba as of 'barren hills'.) As described by GIOVANELLI, expansion of agriculture and viticulture triggered deforestation in the 18th century. Just with the crisis in wine production during the plaque in the late 19th century and the expansion of tourism since the 1950s, agricultural area decreased and forests recovered (see Section 3.3, Bowman et al., 2014; Carta et al., 2018b; Cipriani

et al., 2011; Friedrich et al., 2000). Old images of Elba visualize a sparse forest cover (see illustrations in e.g., Swinburne, 1814 or Seewald, 1921; or A. Cozens *View of Porto Longono with our settea ye Castle & ye Town from ye top of Mount Andrea*, c 1746, British Museum, inv. nr. 1867,1012.35), also not true in all cases (see, e.g. Figure 10.4). Pini (1780) saw many woodlands on Elba, while the cover is continuously reduced due to the shipping of wood. Whereas some authors of the 19th century describe the woodland on Elba (e.g. Anonymous, 1814, p. 7, saw 'lush woodlands') the sparse tree cover is frequently cited: Weir (1799) states that the trees are only of low size; F. F. (1814) remarks a scarcity of woodland. Although witnessing a lack of trees in parts of Elba, Brunner (1828) raves of dark forest with venerable chestnut trees (similar Gregorovius, 1864). Different reasons for the sparse vegetation cover on Elba are proposed; scholars cite e.g. shallow soils (Weir, 1799) or clear-cutting (Brunner, 1828: 'significant parts [of the Campo area] are still occupied by tree stumps of eradicated woodlands', in German, see Appendix 11). Hall (1837) observed a sparse wood cover of only small trees, but also the intensive transport of wood from rural areas to Portoferraio.

Several 19th-century-writers state that a lack of fuel or spare woodland cover contributes to the absence of smelting activities during their times (Barker, 1815; Brunner, 1828; Campbell & MacLachlan, 1869; F. F., 1814; Gregorovius, 1864; Hall, 1837; Krantz, 1841; Swinburne, 1814; Wolff, 1855). A well known description of 19th-century Elba is from the French military and agronomist A. Thiebaut de Berneaud, who brings together fuel wood scarcity, the abandonment of the iron industry—and, remarkably similar to Strabo's account, the transport of ore to the Italian mainland (Thiébaut de Berneaud, 1814, p. 23*ff.*):

> Wood for fuel is still more rare. The island affords nothing beyond a meagre underwood, the chief plantations of which are at Monte-Giove, the valley of Tre-Acque, and Mont de Fonza . . . The oak, though endowed with the hardiest formation, does not arrive at that pitch of peculiar beauty, or at that majestic height which made it the earliest object of the religious worship by which it was consecrated . . . Its branches do not display the stamp of ages; it is not in Elba, the patriarch of the vegetable world . . . In a word, forest-trees are wanted throughout the island . . . Diodorus (n) speaks of its iron works. It still contained them at the era of the Republic of Pisa; and in the thirteenth century it was covered with wood. The last of these works was that which, about the year 1589, was still in existence . . . At the present, all the iron works in the island are destroyed; they have no wood, and they are obligate to transport the ore to Corsica, the coast of Genua, and the shores of Tuscany, in order to have it manufactured.

Groskurd (1831) even mentions a contemporary lack of fuel in his notes to the translation of Strabo 5.2.6, stating that '[smelting] on Aithalia was not possible during Strabo's times,

because the island lacked wood, and still lacks, wherefore the raw ore is still brought to the mainland' (pp. 386–7, fn. 3; see Appendix 11, nr. 11, transl. FB). Similar accounts with reference to Strabo and a link between an ancient and contemporary lack of fuel can be found in Jervis (1860) and Köstlin (1780, Appendix 11, nrs 3, 15; see also Corretti, 1991). Pini (1780) does not directly link Strabo's observation to fuel shortage, but links the transport of ore to and Populonia with his own observation that iron is not smelted on Elba (Appendix 11, nr. 2). Schweighardt (1841) cites Diodor and states 'even now, due to a lack of firewood, the ore is not processed on Elba, but on the mainland' (p. 23, see Appendix 11, nr. 12). Meiggs (1982)—which is one of the most cited reference for the 'deforestation narrative' (see Appendix)—draws connection between the fuel consumption on Elba and more recent history, citing two examples of a lack of fuel in 17th-century- U.S. and in Anatolia. The reference to a contemporary lack of fuel is cited to explain the situation in antiquity.

The description of a lack of fuel on Elba in the 18th century and during Strabo's times corresponds to issues of iron production in general. The negative impact of iron smelting on woodland cover was a topic of importance in modern literature on smelting, e.g. in the 16th to 18th century in Britain (Hammersley, 1973), which fostered the transition from charcaol iron production to coal-fired smelting. In other countries, such as the U.S. and Italy, charcoal remained the most important fuel in the 19th century and was still in use until the mid-20th century (Straka, 2017; Williams, 2005). Iron smelting on Elba during the modern period was absent until the early 20th century. The construction of blast furnaces on Elba began in 1899 with the foundation of the *Società Anonima Elba di Miniere e di Altoforni*. Between 1902 and 1909, three coal-fired blast furnaces were opened in Portoferraio (Anonymus, 1912; Gentini, 2014), when also in Piombino, production was transposed from charcaol- to coal firing. During operation Brazzard (World War II), the blast furnaces in Portoferraio were bombed, implying the end of iron smelting on Elba.

Wiman (2013) provides another example of a more recent linkage between ancient smelting and contemporary landscapes: 'Both the extraction of and the processing of the ores were believed to have taken place near the sources on Elba. It has been shown by recent excavation in the ancient port areas that from the mid-fifth *[sic!]* century BC large-scale production was transferred to or concentrated in Populonia. Most scholars believe that this shift took place after the island had become totally deforested. Elba today is still heavily marked by erosion and barren hills' (p. 17).

Most references to a lack of fuel on Elba agree that smelting declined in the 1st century BCE. Some scholars, however, propose that even in the 6th century BCE, smelting was not possible on Elba because of a lack of fuel (Chiarantini et al., 2018; Veal, 2017a). This lack of fuel is used to explain why early iron smelting in *Etruria Mineraria* took place only

in Populonia, not on Elba (see Chapter 4). However, the reasons for a lack of fuel on Elba during the early period of ferrous metallurgy remain unclear and are unlikely.

Albeit there is no direct connection to the specific situation on Elba it is worth to mention that the emergence of the 'deforestation' hypothesis is more or less contemporary to the *'Holznot'* (wood shortage) in the late 18th century in Germany (Radkau, 1986; Schenk, 2006) and the development of the concept of *Nachhaltigkeit* (sustainability) in the aftermath of H. von Carlowitz's *Sylvicultura oeconomica* (von Carlowitz, 1713). The concept of the 'ruined landscape' theory as i.a. discussed by Grove & Rackham (2003)

Table 10.1 Evidence on the 'deforestation narrative' from different research methodologies of different disciplines. Structure of the table based on Haldon et al., 2018 (see Haldon et al., 2019).

	Historical	Archaeological	Palaeoenvironmental
Subject	Ancient observations (Strabo, Diodor) *and* contextualization of previous interpretations	Quantitative estimation of output	Assessment of geomorphic impact during smelting period
Data	ancient texts *and* modern travel narratives and environmental literature	survey finds of slag and dating material *and* old reports of re-smelting concessionairs	sediment sequences
Data preparation	source criticism	dating, uncertainty assessment, stochastic modelling	chemical and statistical analysis
Precision	annual to decadal	decadal to centennial (uncertainty)	±smelting period
Interpretation	evaluation in historical context and context of development of the 'deforestation narrative'	identification of phases of production intensity	identification of increase/decrease of geomorphic activities
Causality	not mentioned in ancient text, but lack of fuel seen in the 19th century due to contemporary lack, other triggers for abandonment of sites (new deposits in provinces, *senatus consultum*)	model results show lack of fuel is unlikely or not necessary	coincidence of smelting period and increased geomorphic activities and sediment accumulation (erosion after deforestation)

Figure 10.2 Drawing of 'Porto Longona [i.e. Porto Azzurro] in ye Island Elbe' by A. Cozens, c 1746. British Museum, 117×185 mm, reg.-nr. 1867,1012.33. Image courtesy of the ©Trustees of the British Museum, 2019, CC BY-NC-SA 4.0 license.

provides—even the other way around—good link for the superimposition of contemporary views on the landscape and the palaeoenvironment. Interestingly, Wiman (2013) and Penna (2014) even link the modern 'barren hills' and 'environmental damage' to the ancient smelting (albeit most *barren* hills, especially in east-northeastern Elba are most likely linked to modern agriculture, cf. Carta et al., 2018b).

Seizing on the lack of fuel on ancient Elba and the inevitable consequences on iron smelting in recent literature mark a specific element of the 'deforestation narrative'. Narratives are not only simplified self-evident common knowledge—or rather viewpoints—(Kumar, 2004), they are likewise political issues. Albeit this is not directly true for the case of Elba as presumed deforestation took place more than two millenia before, other narratives on more recent deforestation always guiding policy making (Klein, 2002; Knudsen, 2011; Kumar, 2004; McCann, 1997). Elba's 'deforestation narrative' is nonetheless part of a debate on *global* deforestation (Penna, 2014; Perlin, 2005; Radkau, 2012; Sands, 2013; Williams, 2010). In the context of narratives on deforestation in the last centuries in (Western) Africa (e.g. Fairhead & Leach, 1995), the interrelation between the political nature of environmental narratives, (colonial) political interests, and the understanding of (traditional, charcoal-fuelled) iron smelting (Goucher, 1981; see Section 2.3, p. 23).

Figure 10.3 San Benatto and the Baccetti valley as seen from the sea. Former location of the ancient San Bennato site at the coast and several medieval/undated sites in the inland. Sep. 2017, view from the sea in western direction.

Taking the data from the fuel model (Case Study 4, Becker et al., submitted.a, Chapter 9), evidence on increased sediment accumulation and geomorphic activities during the Etruscan–Roman smelting period, and the critical evaluation of the 'deforestation narrative', the socio-ecological model offers valuable perspectives on iron as a raw material (on Elba). The model especially fosters the integration of archaeological, geoscientific, historical views (so textual chronological evidence) to understand the development of the iron industry on Elba.

10.3 Smelting signature and pollution

Using data from soil samples obtained from the ancient Magazzini smelting site in Central Elba Case Study 1, Becker et al., 2019b, Chapter 6, and sediment sequences from the Forcioni Valley at the northern border of the Campo coastal plain Case Study 2, Becker et al., 2019a, Chapter 7, we were able to reconstruct the geochemical signature of ancient iron smelting. Soils and sediments are thus a valuable archive of pre-industrial metallurgy on Elba.

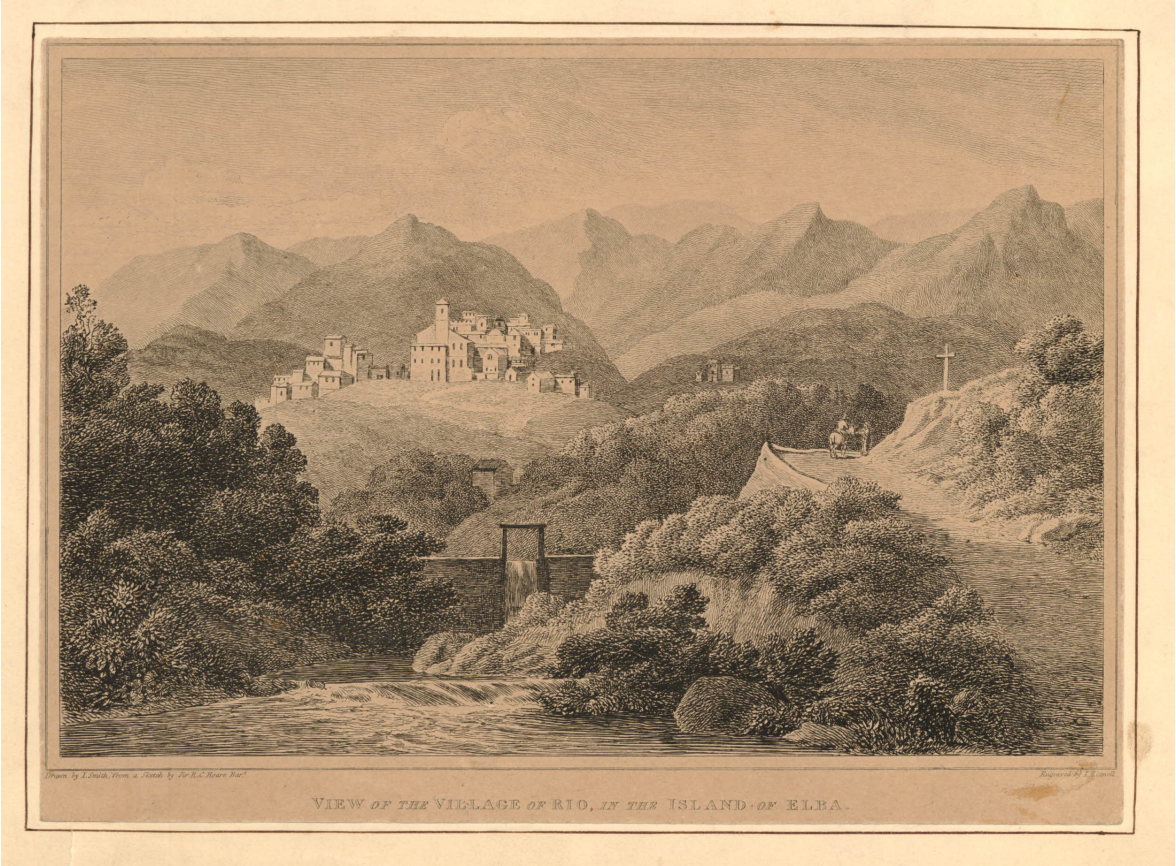

Figure 10.4 Book illustration *View of the Village of Rio, on the Island of Elba*. Drawn by I. Smith from a sketch by R. Colt Hoare, c 1807–1867, travel narrative by Colt Hoare (1814), British Museum, 172×238 mm, reg.-nr. 1867,1214.323. Image credit: © Trustees of the British Museum, 2019, CC BY-NC-SA 4.0 license.

[4] Iron smelting on Elba clearly changed the composition of soils and sediments by the deposition of *technogenic* sediments; the (terrestrial) smelting signature clearly differs from other records of mining and smelting.

- Geochemical data from the Magazzini site allows for a clear delineation of the smelting site.
- Several element contents and other proxies are increased on the smelting site (Cu, Fe, As, pH, carbon contents) and in sediments downstream the Forcioni site and characterize the smelting signature.
- Different spatial manifestations of the smelting signature on the site indicate that the production steps of iron smelting were conducted in specific areas.
- A comparison with other archives of metallurgy on and around Elba suggests that the signature of smelting is unique, as other archives are affected by processing of other metals than iron; or iron deposits that were not extracted by the ancients.

- Smelting may also be indicated by the composition of the (alluvial) charcoal record, as *Erica* species were preferably used by the ancient smelters.
- Also potentially harmful trace metal(loid)s were emitted by smelting on Elba, the impact is relatively low or even negligible.

10.3.1 Characterization

Soil chemical data from the Magazzini site and its surroundings allows for the delineation of the ancient smelting similar to the results of an archaeological survey by Corretti et al. (2014) (see Case Study 1, Becker et al., 2019b, Chapter 6). Differences between archaeological data and chemical data are mainly due to differences in the size of remains under consideration (soil laboratory analysis: <2 mm, survey: >3 cm) and therefore different material composition; e.g. ore dust, ashes, and microscopic charcoal remains may be overrepresented in soil samples compared to survey remains.

The smelting signature is characterized by an increase in Fe, Cu, As, magnetic susceptibility, Ca, total organic carbon and pyrogenic carbon and a clear relative decrease in Ti, Cr, and V compared to adjacent soils. This pattern fits to the chemical composition of metallurgical remains (run-of-mine, charcoal, slag, and ashes). We interpret the difference in the spatial distribution of the composition of chemical proxies as evidence for 'metallurgical' activity marker, i.e. data pointing to different steps of the production system of iron (crushing/roasting, smelting, disposal of by-products; cf. Birch et al., 2015; Carey et al., 2014). Also slag and ore remains found in sediment sequences (core F-III; Case Study 2, Becker et al., 2019a, Chapter 7) clearly point to smelting activities in the upland area of the drilling location. The geochemical record shows that contents of Fe and As, and magnetic susceptibility are enriched in layers related to iron smelting. In contrast to the on-site data from the Magazzini site, in the off-site record from Forcioni, contents of Cu are not increased. Loss-on-ignition at 560 °C is only slightly increased and highly varying. We found slag fragments in unpublished sediment sequences obtained from the Ortano valley and the Baccetti valley in Northeastern Elba (Study 3, Chapter 8). In all of these valleys, smelting sites are known from upland locations. At a coring location in direct vicinity to a pre-industrial (un-dated) smelting site (Appendix 11) no archaeometallurgical remains were detected, which may be due to an uneven distribution of remains in soil or to a relatively stable ground level on the floodplain after the medieval smelting period (core B-II in Study 3, Chapter 8).

In the Forcioni valley, the deposition of the slag remains in the alluvial sediments occurred after the reworking of slope deposits directly below ancient smelting sites. Although the

sequence of dated radiocarbon samples from the F-III is in chronological order, metallurgical remains from the smelting site in the core date to the Middle Ages. We explain this by progressive erosion on the ancient smelting site and the reworking of the slope deposits near the smelting site. No remains of medieval smelting are known from the Forcioni valley. Finds of sherds in the layer containing the metallurgical remains could clearly be identified as Roman *ceramica d'impasto*. This ceramics are also reported for other archaeological sites on Elba. In the sediment sequences in the lower Forcioni valley (core F-I), the sediment signature from further downstream the ancient site could not be identified, a peak in the Cu-content might point to metallurgical activities, but could not be directly linked to the ancient smelting period due to dating uncertainty.

Abundant charcoal remains were found in core F-III directly downstream the Forcioni smelting site (Figure 7.9). They are partly clearly larger than remains from sediment sequences from other locations in the Campo plain (Forcioni and Stabbiati). The typological analysis of $n = 14$ charcoal samples revealed that the record is dominated by *Arbutus*. Contrary to the element smelting signature, the deposition of the charcaol-containing layers dates to the Roman smelting period (c 204 BCE to 50 CE at 95% confidence). Also in the Baccetti valley, abundant (relatively large) charcoal finds were found in stratigraphic context of metallurgical remains.

Therefore, our data allow to identify an imprint of iron smelting activities during antiquity in soil and sediment archives that are still detectable today. With this, our results are in line with other studies that were able to identify the chemical record of pre-industrial iron smelting (Carey & Moles, 2017; Costagliola et al., 2008; Karlsson et al., 2016; Pettersson et al., 2004; Sloto, 2011; Sloto & Reif, 2011; Thelemann, 2016) and to reconstruct it experimentally (Birch et al., 2015). However, there is no unique smelting signature.

10.3.2 Differentiation

The environmental record of iron smelting in various archives or materials reveals major difference in the chemical signature of smelting due to the nature of the deposits and the metallurgical processes mirrored (see Case Study 1, Becker et al., 2019b, Chapter 6, and Section 2).

Mines

Analyses of the elemental composition from the Valle Giove, Rosetto, and Falcacci stopes (Rio Marina) by Servida (2009) and from Rialbano by Pistelli et al. (2017) have shown that contents of Zn, Pb, Cu, and As are increased in (waste) rocks and soils. Partly, trace

metal(loids) accumulate in plants growing on the former mining sites (Pistelli et al., 2017). This data are in agreement with analysis from seafloor sediments onshore Elba (Figure 6.1, p. 97), where an increase in a similar set of elements could be observed. However, it appears difficult to infer an environmental impact of *ancient* iron mining from this data (Case Study 1, Becker et al., 2019b, Chapter 6.) For one thing, the high values of especially Pb and Cu in the Rosetto stope are related to deposits of hematite + limonite ± galena (lead(II) sulfide) with related weathering products, such as anglesite (lead sulfate) and cerussite (lead carbonate) (cf. Luppi & Salvati, 1987). Old reports and maps from the early industrial mining period in the 19th century (Héron De Villefosse, 1819; Krantz, 1841) suggest that in the Rio Marine mines mainly the hematite ± pyrite deposits of the Bacino and Falcacci stopes were exploited during Roman times. The mineralogy of archaeological ore from smelting sites on Elba supports this interpretation. Although reports occasional limonite finds from the (ancient) Pomonte, Campo all'Aia, and Sant'Andreas sites, the vast majority of finds are hematite-rich ore (own observation from a majority of the ancient sites; cf. Benvenuti et al., 2013, 2016; Corretti, 1988; Corretti et al., 2014; Corretti & Firmati, 2011). Infrequent finds of magnetite ore are also known, that might originate from the Calamita mines (see Capacci, 1911; Scott, 1895; Tanelli et al., 2001 for a discussion of the early exploration of the deposits). For another thing, the very high accumulation of As in seafloor sediments (especially near the Terranera iron deposits, see Figure 6.1, p. 97) is not necessarily due to iron mining. Drainage from the Capo Bianco Mine (limonite + Mn-oxide and -hydroxide, see Luppi & Salvati, 1987) may have importantly contributed to high As-concentrations, as rocks contained >1000 mg/kg As (own measurements at the DBM Bochum, see Case Study 1, Becker et al., 2019b, Chapter 6).

Impact

The (chemical) environmental impact of ancient iron mining and smelting is considerably lower than the impact of modern iron mining on Elba (Case Study 1, Becker et al., 2019b, Chapter 6); trace metal contents of the soils from the ancient Magazzini site are much lower than values reached in remains of the modern mining period and the present mine soils (Pistelli et al., 2017; Servida, 2009). For instance, Co-contents of the Magazzini site are in average 142±44 mg/kg (median±MAD), but 552.6 ± 380.5 mg/kg in mine soils (mean±standard deviation); average values of mine waste (including waste rocks) are lower (47 ± 37 mg/kg, median±MAD). Maximum Cu-contents are higher in mining remains (6169 mg/kg) and mine soils (1337 mg/kg) than in soils from the ancient smelting site (245 mg/kg). When compared to the (sub-recent) impact of non-ferrous mining and smelting in *Etruria Mineraria* on the Apennine peninsula mainland, the impact is even

less distinct. Cu-contents of mine waste from e.g. Boccheggiano are in average 390 mg/kg (gross average; Benvenuti et al., 1997); around the polymetallic Fenice Capanne deposits, average Cu-contents of mining remains are 1226 mg/kg (gross average). Also some of these deposits were exploited in pre-industrial times, the impact of the mines on the environment is—as on Elba—not clear, as traces of ancient mining got lost during modern extraction.

The results from Elba are with some reservations comparable to the findings from other studies on the environmental impact of pre-industrial iron smelting. For instance, Thelemann (2016) found only minor increases of trace elements in pits related to iron smelting. However, Carey & Moles (2017); Carey et al. (2014) were able to identify an iron smelting signature in the U.K. Major differences in the different characteristics of local smelting signatures are related to the mineralogy of the ore used. Limonite-rich (often bog or bean iron ore) has a different trace element composition than hematite-rich montane ore; trace element contents tend to be lower in hematite ore (see Section 2, p. 17, and data in Benvenuti et al., 2013), as used in ancient Elba.

Activity marker

Notwithstanding there is no straightforward connection between modern chemical data and ancient pollution, it is worth to distinguish between the impact of mining and smelting. As shown by the chemical data from the Magazzini site Case Study 1, Becker et al., 2019b, Chapter 6 and metallurgical remains, different metallurgical material and processes contribute to the smelting signature of a site—including charcoal combustion (pyrogenic carbon, Ca), ore processing and disposal (Fe, As, Cu), and slag disposal (Fe, Cu). The difference between slag and ore are mainly related to partitioning during the smelting process (see Section 2, especially Figure 2.5, p. 35). Therefore, some 'pollutants' are limited to the mining district; high As-contents may be detected in the mining area, but due to volatilziation and the siderophilic character, they are typically not found in the abundant slag remains on a smelting site (see Costagliola et al., 2008, 2010). The deposition of fuel ashes and the related increase of the Ca-content and subsequently lower soil acidity Case Study 1, Becker et al., 2019b, Chapter 6, may also contribute to different environmental issues on smelting sites and mines, where acid mine drainage might occur (cf. Servida et al., 2009).

Emissions

The hypothesis by Vigliotti et al. that '[a] complete history of metallurgy on Elba can be read in the magnetic record of our sediments [i.e. sediment sequences obtained from

the Corsica channel, c 17–26 km southwest of Elba]' (Vigliotti et al., 2003, p. 812) needs further discussion. Although their data clearly show a decisive correspondence between a peak in iron production (cf. Case Study 4, Becker et al., submitted.a, Chapter 9) and the accumulation of magnetic matter and an increase in sediment's Pb and As content, there is no clear relationship between the history and emissions of iron smelting—or even metallurgy on Elba in general. As shown in Figure 8.7, the increase in magnetic susceptibility in the marine sediment sequences is not exclusively linked to (Etruscan or Roman) iron production on Elba or in Populonia. Additionally, our findings from the alluvial sediments in the Valle di Forcioni (Case Study 2, Becker et al., 2019a, Chapter 7) and the soil chemical data from Magazzini (Case Study 1, Becker et al., 2019b, Chapter 6) suggest that high Pb contents are not necessarily linked to iron smelting. Although Pb and As are volatilized during the iron smelting process (see Section 2.5, p. 35), copper processing is more likely accountable for Vigliotti et al.'s record; Pb contents of metallurgical remains and in soils and sediments related to iron smelting are low (see Table 6.2, p. 120). Copper was processed in Populonia much earlier than iron (Cartocci et al., 2007; Chiarantini et al., 2007) and thus clearly earlier than iron on Elba (see Section 4.1). On Elba, traces of copper processing are rare, albeit the location of Bronze Age sites near Cu-deposits suggests production (see Chiarantini et al., 2018; Pagliantini, 2014); scatter evidence for metal processing in *Etruria Mineraria* from the Bronze Age are known, but are most likely orders of magnitude lower than the Etrusco–Roman production. In other case studies on emissions from metallurgy by sedimentological evidence, the temporal consistency between increase of proxies and metallurgical history is much more coupled than on Elba (Figure 8.7). Vigliotti et al.'s record does not correspond to human activities on Elba or in Central Italy or global emission patterns; and may be generally influenced by emissions from fire (Figure 8.7). The interference between the emissions/deposition from iron and copper smelting is also apparent in the seafloor data from onshore the metallurgical site in Populonia (Baratti beach); here, copper and iron production took place wherefore the weathering of both remains contributed to the geochemical record.

Emissions from iron smelting on Elba are *represented* in the ancient Greek name of the Island, *Aithálеia*—'the fuming one' (Diodorus Siculus, 5.13.1, see, e.g., Corretti & Firmati, 2011). As proposed by Corretti & Firmati (2011), the construction of luxurious *villae maritimae* in the 1st century BCE more or less contemporary to the decline of iron smelting points to the end of emission of smoke from the furnaces, as emission would have made Elba uninteresting for recreation. This *topos* is part of the *representation* of the emission-*event*. However, a temporal overlap of smelting and activities in the *villae* is reasonable

(see Chapter 4) and *villae* may have been involved in (small scale?) iron production (Raphael A. Eser, pers. comm., June 25, 2019).

Secondary record

The smelting signatures obtained from sediment sequences Case Study 2, Becker et al., 2019a, Chapter 7 and soil chemical data Case Study 1, Becker et al., 2019b, Chapter 6 also differ. This may be explained by, first, different sampling techniques. Whereas only a small amout of material was sampled from 'smelting' layers from vibracores (40 cm thickness, 6 samples), the smelting site was extensively sampled ($n = 134$). Because also visually similar slag remains may vary significantly in (trace) element composition (Veldhuijzen, 2003), a small sample containing only a few archaeometallurgical remains may have a different composition. Additionally, not all types of archaeometallurgical remains might be contained in small amount samples. Second, the alluvial archives are secondary deposits. Contaminants from iron smelting found in the fluvial system— mainly dispersed as particulate pattern (cf. Beckmann, 2007; Leenaers, 1989)—were initially disposed and stored on smelting sites. The size of the metallurgical remains ranges from ore dust to slag blocks, hence hydraulic sorting occurred during erosion and transport (Brown et al., 2016). Moreover, technogenic sediments from a smelting site were diluted with un-contaminated sediments during transport. Based on the idea of 'passive dispersal' (Lewin & Macklin, 1987) (i.e. transport of metallurgical remains together with natural sediments), a capacity threshold had to be passed for erosion and transport of relatively coarse remains. Intermediate deposition in slope deposits and reworking affect the alluvial record (see e.g. Bracken et al., 2015; Fryirs, 2013; Fryirs et al., 2007) and is evident in the field record. Slag finds are abundantly found in slope deposits in the Forcioni valley, in natural exposures of the bankside (see also Bradley & Cox, 1990) and in recent stream-bed sediments of the Fosso Forcioni. The reworking is directly evident in the inversions in sediment sequence F-III. Slag remains from most likely ancient smelting were deposited in layers dated to medieval times (by radiocarbon dating of charcoal remains), whereas the abundance of charcoal fragments in the sediment layers dates to the smelting period (see e.g. Brown et al., 2016 for *archaeology and human artefacts* in fluvial geomorphology.).

We interpret the absence of a sedimentary smelting signature in sediment sequences further downstream as influenced by a increasing valley width—and thus higher dispersion of sediments of the floodplain (Dobler, 2001; Lewin & Macklin, 1987)—and lower transport capacity of sediments; sediments deposited in upstream locations are finer than in downstream locations (cf. Section 7.6, p. 143 and Section 7.9, p. 147). Generally, there is a variability of the chemical characteristics of floodplains affected by mining (e.g. Taylor, 1996).

Transport of slag remains can also be observed in other areas, especially in the Baccetti valley in northeastern Elba, were slags are linearly distributed along the course of creeks (Appendix 11). Finds of slag, technical ceramics, and less frequently ore fragments are abundant in recent stream bed sediments and on the surface of the floodplain (field observation in Aug. 2015 and 2016 and Corretti, 1988; Pagliantini, 2014; see Figure 10.5). Technogenic sediments of iron smelting can also be found in other locations, as e.g. observed by Kleßen (1993) in the Bode valley (Harz mountains, German Central Uplands) or described by Brown et al. (2016). Finds of slag in stream-bed sediments provide a 'survey tool' (Raphael A. Eser, pers. comm., passim); several recent examples were documented where slag finds in stream beds may point to hitherto unknown smelting sites (somewhere in an upstream location; e.g. in the Stabbiati valley and the Ortano valley, see Figure 4.3). Metallurgical remains were additionally removed from the smelting sites (for decoration purposes, as construction material, and especially for re-smelting) and may have reached the fluvial system (cf. Kleßen & Chrobok, 1989). The smelting site in Magazzini is less affected by erosion after abandonment than most other sites (including Forcioni), although the site was partly cut by rivers moving their course (Case Study 1, Becker et al., 2019b, Chapter 6). For instance, the Patresi, Capo Pero, and Ferrato sites are exposed to coastal erosion, while other pre-industrial smelting sites are subject to soil erosion and mass wasting (e.g. Forcioni; see Martin, 1994; Sperl, 1993 for the example of the M. Serra sites on Elba). Additionally, mining and re-smelting of ancient slags in the 20th century might have less affected the Magazzini site; no re-working is documented so far (see Nihlén, 1958; Pistolesi, 2013). The record from the site is mainly disrupted by tillage, although there is no statistically significant difference between the chemical composition of samples from below and above the plowing depth (Case Study 1, Becker et al., 2019b, Chapter 6). Therefore, the Magazzini site is of specific value as an archive of ancient iron smelting compared to the other (ancient) iron smelting sites on Elba.

Charcoal

This becomes especially evident when looking at the species selection for charcoal production. Although sparse in absolute numbers, the unique anthracological species distribution from the Forcioni sediment sequences (dominance of *Arbutus*) points to species selection (Case Study 2, Becker et al., 2019a, Chapter 7). As shown by Sadori et al. (2010) for the Etruscan iron smelting site at Follonica-Rondelli, *Erica arborea* was mainly used for furnace charge, whereas other species dominate the archaeobotanic record from other types of sites and the pollen record from lacustrine sediments in the region (e.g. Drescher-Schneider et al., 2007). Species selection for metallurgical purposes is also known from other areas (see Section 2.3.2, p. 27). The knowledge on species selection also contributes

Figure 10.5 Slags on the channel bed of the Uviale di Patresi. Image credit: Raphael A. Eser, Aug. 2016.

to the understanding of the metabolism of iron smelting and the interpretation of the presumed 'deforestation' event on Elba in the 1st century BCE; the palynological record from Bertini et al. (2014) shows a decrease in *Quercus* pollen during the smelting period; a contemporary increase in *Ericaceae* pollen, however, shows that fuel might have been available for smelting.

10.4 Prospects for development

For future research on the metallurgical landscape on Elba, in our point of view, several aspects may be payed special attention to.

Further geochemical surveys. A detailed study on geochemical on-site data and the distribution of different metallurgical remains might provide further in metallurgical activity marker (cf. Carey et al., 2014). Although the Magazzini site analysis in this study is relatively less affected by post-abandonment degradation, other non-dated and medieval sites are better preserved. The differentiation between areas with different metallurgical remains on the Magazzini site was not possible by soil chemical survey (Case Study 1, Becker et al., 2019b, Chapter 6). Other sites may allow for a differentiation into different production areas, such as crushing places, roasting places, storage places for ore or places for slag disposal (cf. Carey & Moles, 2017). Field observation on the sites in Valle di Nivera or Case Colli showed that a differentiation into places with different concentrations of ore, tapped slag, or furnace slag.[5] For Campo all'Aia, Nihlén (1958) reported slag accumulation and a roasting place nearby (see Appendix, Figure A.10).

Unknown smelting sites? Surveys in areas where metallurgical remains were recorded in sediment sequences (Fosso di Ortano) and stream bed sediments (Fosso di Ortano, Fosso di Forcioni, Fosso Stabbiati) might provide further insights in the distribution of smelting sites on Elba. Interestingly enough, finds of slag in a channel in the upper part of the Valle Forcioni (southeast of Pietra Acuta) were located downstream the toponym 'Fornello' (Toponomastica catasto Agenzia delle Entrate, Regione Toscana – Repertorio Toponomastico Regionale, 2019-06-27, and *Catasto Generale della Toscana – Isole* , Sezione F, Foglio 2, 1840, Turchi Angelo).

Smelting in the Ortano valley. Having in mind the overall distribution of slag finds from the pre-industrial era on Elba (Figure 4.3), the Ortano valley appears to be one of the districts with a low density of sites. Therefore, slag finds from sediment sequences might help to complete the image of the distribution of smelting sites on Elba. However, the *gap* in the Ortano valley coincides with a lack of local wood availability as seen on modern maps (Figure 3.5, p. 51); at the moment, it remains unclear if the dominance of grassland in the Ortano valley is a result of intensive land use in the last centuries and related to lower stage in the vegetation succession (cf. Carta et al., 2018b; the area is today characterized by a high density of abandoned agricultural terraces, see 1.:2000 topographic map of the Regione Toscana, 2014) or related to unfavorable natural conditions for forest growth (relief, lithology and exposition, see Section 3.3).

Undated smelting sites. The data base on ancient smelting sites is of special importance for the modelling of the fuel wood consumption of ancient metallurgy on Elba.

[5] N.b.: The Valle di Nivera site is heavily disturbed by the excavation of old slag in modern times.

Although we argue that we have a suitable data set at hand (Case Study 4, Becker et al., submitted.a, Chapter 9), further research on the chronology and topography of smelting sites is required. The upcoming dissertation of Raphael A. Eser (Humboldt Universität zu Berlin, Faculty of Humanities and Social Sciences, date of defense: 8. Jan. 2021) will provide a comprehensive revision of the state of the art of the chronology and topography of smelting sites on Elba. Up to now, 252 sites with finds of slag are known, 27 of them ancient; 8 potentially ancient or multi-phased smelting sites; and 31 medieval sites (Raphael A. Eser, pers. comm., 2019-06-21). Thus, a majority of sites is undated. Although the topographical dichotomy proposed by A. Corretti (cf. Corretti, 1988, 1991)—ancient sites located along the shore, medieval sites in the inland—tends to be true for most sites, several exceptions are known.

Anthracology. The setting up of the fuel consumption model has also constrained by the fact that the current knowledge on fuel production on Elba (i.e. charcoal burning) is sparse. Although data from the Apennines peninsula mainland (Sadori et al., 2010) and data from the sediment sequences from the Valle di Forcioni (Case Study 2, Becker et al., 2019a, Chapter 7) provides insights in fuel selection for iron smelting, direct evidence from an ancient kiln is missing. The archaeological record of charcoal remains is generally sparse, as remains were often not sampled during excavation or survey (Graham & Dam, 2019; Thompson & Young, 1999). To our knowledge, currently no ancient charcoal production site from Elba is known. Albeit not studied anthracologically, at least the spatial relationship between potentially medieval smelting sites and kiln platforms (e.g. in Valle Nivera and Lentisco-Martella, cf. Corretti, 1991) is documented. The lack of knowledge on ancient charcoal production becomes especially relevant—and is important for the understanding of fuel wood consumption—when taking the hypothesis of R. Veal (Veal, 2012, 2013, 2017b) in to account that iron smelting required high quality charcoal that, in turn, required much more wood for burning than *customary* charcoal for e.g. domestic use. Further discussions of this topic as well as a quality analysis of ancient charcoal is necessary to judge on this point. The uncertainty in the modelling the fuel requirement for smelting is mainly to a large part due to a lack of knowledge on the charcoal production process; therefore, further research would also enable to simulate more precisely the woodlot requirement for smelting.

Kiln sites. Also for Elba high resolution elevation data is available. In a trial study, we tested the suitability of the data to map known kiln sites near pre-industrial smelting sites. Although located in relatively steep relief, which might facilitate the detection of kiln platforms, we were not able to detect the known sites. This may be explained by noise

in the elevation data, a step-like relief in the test region (due to e.g. forest paths), and the size of the kiln platforms. Additionally, the forests on Elba under consideration are relatively densely stocked and the canopy cove is high compared to other studies (e.g. Carrari et al., 2017; Due Trier et al., 2016; Raab et al., 2017, 2015).

Population dynamics. The social history of Elba island during antiquity is sparsely written. Although much is known on iron smelting, the human dimension is not equivalently studied. Further modelling of especially the endosomatic metabolism of iron smelting would benefit on demographic information on Elba and aspects of daily life. Additionally, information from archaeology of economics could contribute with a reconstruction of autarky of Elba and the import of goods for daily consumption.[6]

Morphodynamics around Populonia. Based on the estimation of the slag disposal in Elba and Populonia discussed in Case Study 4, Becker et al., submitted.a, Chapter 9, it seems worse to evaluate the impact of iron smelting on the morphodynamics around the Populonia. Taking the data published by Saredo Parodi (2013), the wootlot requirement for smelting on the mainland could have been higher than on Elba. Thus, also in the sediment archives in the area, the impact of smelting could be visible.

[6] A work report by A. Kirschender (Freie Universität Berlin, Institute of Classical Archaeology) on the wrecks of Elba gives some hints on the transport of goods from and to Elba.

11

Conclusions

The iron oxide ore deposits on Elba Island have been intermittently exploited since at least the 6th century BCE; during antiquity, iron was smelted on Elba between the 4th century BCE and the 1st century CE. The archaeometallurgical remains of ancient iron smelting—slag, ore, and fragments of technical ceramics—attract the interest of scholars since the 19th century (V. Mellini, c 1879–1881, Monaco & Mellini, 1965). The focus of research was at first mainly on localization, dating, and a technological description. Later, scholars turned attention to archaeometallurgical questions of provenance and distribution (e.g. Benvenuti et al., 2016) and landscape archaeological issues (e.g. Alderighi et al., 2013; Corretti et al., 2014; Pagliantini, 2014).

The thesis at hand is in line with this development; different approaches from landscape archaeology and geoarchaeology are applied to reconstruct human–environment interactions in the context of ancient iron mining and smelting on Elba. The focus is here on the impact of iron smelting on the landscape balance.

Whereas the chemical environmental impact of ancient iron smelting ('smelting signature') was previously rarely studied, charcoal-fueled smelting is often regarded as a trigger of *deforestation* (see, e.g., Hammersley, 1973; Harris, 2013; Iles, 2016; Wertime, 1983).

The applied methods range from the chemical/sedimentological analysis of on-site soil samples and alluvial sediments to a stochastic meta-analysis of sedimentary cal-^{14}C-ages and a model of the woodlot requirement for iron smelting.

Being integrated in a research group on different aspects of early iron in Europe, the theoretical framework of the thesis is build on a socio-economic model of iron as a raw material developed by the members of the group (Bebermeier et al., in press).

The programme. The exploitation of primary and secondary resources for iron production on Elba—mainly ore and fuel—in the antiquity followed a distinct programme. Due

to the accessibility of the mines and their topographic configuration close to the coast facing the preexisting metallurgical centre in Populonia-Baratti and because of tension in the northern Tyrrhenian Sea, the Etruscans exploited the deposits on Elba, but smelted the ores on the mainland. Besides the mentioned political and economic explanations for the time lag, there is also a hypothesis that shortage of fuel on Elba was an important factor that caused the time lag between the onset of smelting in Populonia and the onset of smelting on Elba (e.g. Chiarantini et al., 2018). However, the archaeological data, the existing palynological record, and the data from the resource modelling indicate that this hypothesis can be abandoned. It has to be discussed in further studies if the demand for iron in Etruscan times could have been covered by a production on Elba.

A programme to use the fuel resources on Elba became important since the Roman occupation (mid-3rd century BCE)—splendidly described by Corretti (2017, p. 446): 'The location of the workshops aims at the fullest exploitation of wood resources'. The location of the mines, the topography of the island, and the economic-political integration in *Etruria Mineraria* are the main constituents of the metallurgical landscape on Elba. The development of the landscape is mainly driven by the fuel requirement for smelting. The location of smelting sites distant to mines, on shoreline positions well accessible by vessels, and at the lower reach of relatively wide valleys with mainly north-exposed slopes points to the availability of fuel wood resources as a main location factor; north exposed slopes tend to provide more biomass, because they receive less solar irradiation and more rainfall. The near absence of remains of smithing on Elba insinuated a translocation of fuel-intensive step of iron production to the mainland.

The palaeoenvironment might also have played a role as site location factor, especially in the production *nucleus* around Monte Castello di Procchio. Taking together data from sediment archives, toponyms, old travel reports, and present relics of past vegetation, it is evident that the northern part of the Campo plain (south of Monte Castello di Procchio) was covered by wetlands in antiquity. In contrast, but low-lying areas were covered by wetlands during that time. Thus, the southern parts of the Campo area were not well accessible from the coast. The forest resources of the eastern Monte Capanne massif could be best exploited from the north, were the accessibility is not reduced by the presence of wetlands. Consequently, no ancient smelting sites are located along the eastern coast of the Campo plain, whereas some smelting sites, including the Forcioni and La Pila sites—-and presumably others (see the dissertation of Raphael A. Eser, Humboldt Universität zu Berlin, Faculty of Humanities and Social Sciences, date of defense: 8. Jan. 2021)—are located along the northern edge of the Campo plain. These are the only ancient smelting sites on Elba that are not located at the coast, but in the inland—on the northern, elevated

part of the Campo plain (slag was only found on the Sughera site, but this site was used as a settlement before).

The abundance of charcoal remains from *Ericaceae* species in the sedimentological record (Case Study 2, Becker et al., 2019a, Chapter 7)—in line with the archaeoantracological records from the mainland (Sadori et al., 2010)—points to a *programme* of species selection.

As evident in the difference between the chemical signature of smelting sites and mines; the mineralogy of archaeological ore; the few traces of archaeological remains in the mining districts; and the location of old overburden mapped in 19th century prior to the intensive modern mining period, predominately hematite deposits were exploited in ancient times (Case Study 1, Becker et al., 2019b, Chapter 6). Thus, hematite rich deposits were preferably exploited by the ancient miners; i.a. due to the better accessibility and due to the higher Fe content.

Based on the quantity of slag finds from ancient sites on Elba and their chronology, it appears evident that the iron production on Elba increased, especially in the 2nd century BCE. This increase is linked to increased requirements for warfare and agricultural production in the Roman empire.

Smelting activities on Elba declined in the 1st century BCE because of several reasons, maybe including a *programme* to save resources in *Italia*; a *senatus consultum* prohibiting mining in *Italia* from the first half of the 1st century BCE and the occupation of new iron ore deposits in the provinces in the 1st century BCE.

Metabolism. Although persistently suggested in literature during the last three centuries, it is (very) unlikely that a lack of fuel occurred during the Roman period of iron smelting, as shown by Monte-Carlo-experiments of the woodland area required for iron production on Elba (Case Study 4, Becker et al., submitted.a, Chapter 9). We therefore suggest that fuel scarcity was not the main driver of the abandonment of smelting sites on Elba in the 1st century BCE. The exosomatic metabolism of iron smelting on Elba, i.e. the area required for food production and heating, may have nevertheless importantly contributed to the risk of fuel scarcity. However, food imports from the mainland would have made it less likely that the iron industry lacked fuel. With the given set of parameter uncertainties, we argue that it was possible to smelt iron on Elba without running the risk of fuel scarcity. However, especially in northeastern Elba, around the mines, woodlands were most likely intensively used. Wide areas on the island were under management for fuel wood extraction.

Event. Iron smelting on Elba had a clear impact on the landscape balance of the island. The (even temporally) clear-felling of some woodlands on Elba involved increased morphodynamics. The geochemical–statistical analysis of a sediment sequence downstream an ancient smelting site showed that the deposition of slope layers, high-magnitude flood layers, and a relatively thick sediment packages coincides with the Roman smelting period. The abundance of large charcoal remains of *Arbutus* supports the interpretation that the layers directly correspond to human-induced charcoal production or use that was related to iron smelting (Case Study 2, Becker et al., 2019a, Chapter 7).

The reconstruction of morphodynamics by different cumulative probability functions of cal-^{14}C-ages from coastal plains and filled valleys also reveals that sediment accumulation and geomorphic activities on Elba clearly increased during the ancient smelting period—and decreased after the abandonment of most of the smelting sites on the island (Study 3, Chapter 8).

Both chemical data from sediment sequences that were uncovered in locations downstream of an ancient smelting sites (Case Study 2, Becker et al., 2019a, Chapter 7) and soil chemical data from an ancient smelting site (Case Study 1, Becker et al., 2019b, Chapter 6) show that the reconstruction of a smelting signature is still possible today. Whereas the alluvial record is altered by processes of sediment transport, the on-site record allows for the identification of metallurgical activity marker. Different chemical proxies point to different production steps on the site. Change in the chemical composition of soils (increased Ca, total organic carbon, and pyrogenic carbon; and decreased acidity) are indicative for the use of charcoal and the deposition ash residues on a smelting site. A relative increase in Fe and Cu in soils from a smelting site compared to adjacent soils points to the disposal of slag remains, whereas increase contents of As are related to ore processing. Being a volatile and siderophile element, As is emitted during the reduction process and attached to the bloom; therefore, the As content of slag is much lower than the As content of ore. The iron smelting signature obtained from the terrestrial off- and on site-record is not in line with data obtained from marine sediment archives. We emphasize that the terrestrial records is less affected by overprinting from e.g. copper production (at i.a. Baratti), human-induced fires that are not ignited for iron production, and discharge from non-ferrous deposits that were supposedly not extracted in antiquity (e.g. the Capo Bianco mine or galena deposits in the Rosseto stope/Rio Marina mine). Nevertheless, the record from Vigliotti et al. (2003) shows some coincidence with intensity of iron production on Elba and thus the emission of volatile elements from bloomeries. (Technogen) sediments deposed downstream smelting sites are part of the *material culture* of iron smelting. They do not only point to socio-ecological *events*, but are also a valuable

archive of past activities, as metallurgical remains in sediment sequences were uncovered in catchments where hitherto no smelting activities are evident.

Representation. Emissions from the furnaces are represented in ancient texts and toponyms. Diodorus Siculus mentioned the 'smoke that lies to thick over the island ' (Diod. Sic. 5.13.1) and the Greek toponym of Elba: *Aithάleia*—the fuming one. Although there is a chronological overlap between iron production and the activities in luxury *villae maritimae* on Elba, the presumed construction of the estates after the decline of iron production on Elba can as indirectly evidence for the emission of sooth from the furnaces—although small scale iron production might haven been part of the economy of the *villae maritimae*. In line with this argumentation, the emissions of soot from furnaces made the island unattractive for recreational issues. Also aspects of the programme of iron smelting on Elba—the demand for iron—are represented in texts, such as Titus Livius' description in his *Ab urbe condita* that the Populonia delivered iron for warfare to Scipio *(Africanus)* during the Second Punic War ('Populonenses ferrum', Liv. 28.45.15). The increased demand of iron (for warfare) is also evident in our modeled production intensity on Elba. The mines and production steps of iron on Elba were also described in ancient texts (e.g. Diod. Sic. 5.13.1). The (exosomatic) metabolism of iron smelting and a possible event of a lack of fuel on Elba, is quite often thought to be presented in Strabo's report on Elba (5.2.6). However, we argue that neither Strabo's text give any evidence that a lack of fuel triggered the abandonment of smelting sites on Elba, nor available palynological reconstructions or our fuel model. Instead, we advance the opinion that Strabo's text is misconstrued since the 18th century, when woodland cover on Elba was clearly reduced because of agriculture, viticulture and pastoralism. Moreover, a lack of fuel affected the contemporary iron industries, as suggested in travel narratives from the early and mid-19th century. The proposed history of the coming of the deforestation narrative in the 18th and 19th century (Section 10.2.3) further asks to integrate the history controversy on fuel scarcity as part of the representation of iron as a raw material in the socio-ecological model.

The iron landscape

The key findings of the thesis is the idea that human–environment interactions play a key role in the understanding of ferrous metallurgy on Elba Island and it's iron landscape. Both human activities and the human understanding of the natural situation on Elba, as well as the impact of smelting on the landscape balance and the human response to the impact are constitutive for the iron landscape on the island. The iron landscape on Elba island was and is—from an socio-ecological perspective—characterized by the programme

for iron production, the establishment of an exo- and endosomatic metabolism, events related to the impact of iron smelting on the landscape balance, and the representation of iron production in ancient *and* modern texts. With the conceptual model, findings from physical geography (or geoarchaeology) and archaeology can be productively thought together to understand the iron landscape.

Bibliography

Ackermann, F. (1980). A procedure for correcting the grain size effect in heavy metal analyses of estuarine and coastal sediments. *Environmental Technology Letters*, *1*(11), 518–527.
DOI/URL: https://doi.org/10.1080/09593338009384008

Ad-hoc-AG Boden (2005). *Bodenkundliche Kartieranleitung, KA5*. Stuttgart: Schweizerbart Science Publishers.

Adamoli, R., & Rigon, D. (2013). *Meloa: Preistoria e storia di una terra elbana*. Pontedera: Bandecchi & Vivaldi.

Aguzzi, M., Amorosi, A., Colalongo, M. L., Lucchi, M. R., Rossi, V., Sarti, G., & Vaiani, S. C. (2007). Late Quaternary climatic evolution of the Arno coastal plain (Western Tuscany, Italy) from subsurface data. *Sedimentary Geology*, *202*(1-2), 211–229.
DOI/URL: https://doi.org/10.1016/j.sedgeo.2007.03.004

Aitchison, J. (1986). *The Statistical Analysis of Compositional Data*. London, UK: Chapman & Hall.

Aitchison, J., & Egozcue, J. (2005). Compositional Data Analysis: Where Are We and Where Should We Be Heading? *Mathematical Geology*, *37*(7), 829–850.
DOI/URL: https://doi.org/10.1007/s11004-005-7383-7

Alderighi, L., Benvenuti, M., Cambi, F., Chiarantini, L., Chiesa, C. X. H., Corretti, A., Dini, A., Firmati, M., Pagliantini, L., Principe, C., Quaglia, L., & Zito, L. (2013). Aithale. Ricerche e scavi all'Isola d'Elba: Produzione siderurgica e territorio insulare nell'antichità. *Annali della Scuola Normale Superiore di Pisa*, *5*(2), 169–188.

Aldrete, G. S. (2007). *Floods of the Tiber in Ancient Rome*. Ancient society and history. Baltimore: Johns Hopkins University Press.
DOI/URL: https://doi.org/10.1353/book.3303

Alekseeva, T., Alekseev, A., Maher, B. A., & Demkin, V. (2007). Late Holocene climate reconstructions for the Russian steppe, based on mineralogical and magnetic properties of buried palaeosols. *Palaeogeography, Palaeoclimatology, Palaeoecology*, *249*(1), 103–127.
DOI/URL: https://doi.org/10.1016/j.palaeo.2007.01.006

Alessandroni, M. G., Remedia, G., Snorrason, r., Finnsdóttir, H. P., & Moss, M. E. (2002). The most severe floods of the Tiber River in Rome. In *The Extremes of the Extremes: Extraordinary Floods. Proceedings of an international symposium on extraordinary floods held at Reykjavik, Iceland, in July 2000*, vol. 271 of *IAHS Series of Proceedings and Reports*, (pp. 129–132). IAHS Press.

Alessio, M., Bella, F., Improta, S., Belluomini, G., Calderoni, G., Cortesi, C., & Turi, B. (1973). University of Rome Carbon-14 Dates X. *Radiocarbon*, *15*(1), 165–178.
DOI/URL: https://doi.org/10.1017/S0033822200058677

Alessio, M., Bella, F., Improta, S., Belluomini, G., Cortesi, C., & Turi, B. (1971). University of Rome Carbon-14 Dates IX. *Radiocarbon*, *13*(2), 395–411.
DOI/URL: https://doi.org/10.1017/S0033822200008511

Allen, H. (2014). *Mediterranean Ecogeography*. Routledge. Google-Books-ID: fUKg-BAAAQBAJ.

Allen, H. D. (2001). *Mediterranean Ecogeography*. Ecogeography series. Harlow, Munich, et al.: Prentice-Hal.

Ambert, P. (2002). Utilisation préhistorique de la technique minière d'abattage au feu dans le district cuprifère de Cabrières (Hérault). *Comptes Rendus Palevol*, *1*(8), 711–716.
DOI/URL: https://doi.org/10.1016/S1631-0683(02)00078-7

American Geological Institute (1997). *Dictionary of Mining, Mineral, and Related Terms*. Alexandria, VA: American Geological Institute, 2nd ed.

Amorosi, A., Bini, M., Giacomelli, S., Pappalardo, M., Ribecai, C., Rossi, V., Sammartino, I., & Sarti, G. (2013a). Middle to late Holocene environmental evolution of the Pisa coastal plain (Tuscany, Italy) and early human settlements. *Quaternary International*, *303*, 93–106.
DOI/URL: https://doi.org/10.1016/j.quaint.2013.03.030

Amorosi, A., Bruno, L., Rossi, V., Severi, P., & Hajdas, I. (2014a). Paleosol architecture of a late Quaternary basin–margin sequence and its implications for high-resolution, non-marine sequence stratigraphy. *Global and Planetary Change*, *112*, 12–25.
DOI/URL: https://doi.org/10.1016/j.gloplacha.2013.10.007

Amorosi, A., Ricci Lucchi, M., Sarti, G., Vaiani, S. C., Prandin, S., & Muti, A. (2004). Late Quaternary sedimentary evolution of the Piombino alluvial plain (western Tuscany) as revealed by subsurface data. *GeoActa*, *3*, 97–106.

Amorosi, A., Rossi, V., Sarti, G., & Mattei, R. (2013b). Coalescent valley fills from the late Quaternary record of Tuscany (Italy). *Quaternary International*, *288*, 129–138.
DOI/URL: https://doi.org/10.1016/j.quaint.2011.10.015

Amorosi, A., Rossi, V., Scarponi, D., Vaiani, S., & Ghosh, A. (2014b). Biosedimentary record of postglacial coastal dynamics: High-resolution sequence stratigraphy from the northern Tuscan coast (Italy). *Boreas*, *43*(4), 939–954.
DOI/URL: https://doi.org/10.1111/bor.12077

Andreau, J. (1990). Recherches récentes sur les mines à l'époque romaine, 2: Nature de la main d'ø euvre. Histoire des techniques et de la production. *Revue numismatique*, *32*, 85–108.
DOI/URL: https://doi.org/10.3406/numi.1990.2021

Anonymous (1814). *Neueste Kunde von der Insel Elba und ihren Umgebungen : in Briefen an einen Freund*. s.l.: s.n.
DOI/URL: http://mdz-nbn-resolving.de/urn:nbn:de:bvb:12-bsb10717816-1

Anonymus (1912). Erzverladeanlagen der Societa anonima di Miniere e dix [sic!] Alti Forni „Elba“ auf der Insel Elba. *Polytechnischen Journals*, *327*, 261–265.
DOI/URL: http://dingler.culture.hu-berlin.de/article/pj327/ar327082

Antonioli, F., Anzidei, M., Lambeck, K., Auriemma, R., Gaddi, D., Furlani, S., Orrù, P., Solinas, E., Gaspari, A., Karinja, S., Kovačić, V., & Surace, L. (2007). Sea-level change during the Holocene in Sardinia and in the northeastern Adriatic (central Mediterranean Sea) from archaeological and geomorphological data. *Quaternary Science Reviews*, *26*(19), 2463–2486.
DOI/URL: https://doi.org/10.1016/j.quascirev.2007.06.022

Antonioli, F., D'Orefice, M., Ducci, S., Firmati, M., Foresi, L. M., Graciotti, R., Pantaloni, M., Perazzi, P., & Principe, C. (2011). Palaeogeographic reconstruction of northern Tyrrhenian coast using archaeological and geomorphological markers at Pianosa island (Italy). *Quaternary International*, *232*(1), 31–44.
DOI/URL: https://doi.org/10.1016/j.quaint.2010.03.017

Aranguren, B., Ciampoltrini, G., Rendini, P., Firmati, M., Giachi, G., Cortesi, L., Pallecchi, P., & Tesi, P. (2004). Attività metallurgica negli insediamenti costieri dell'Etruria centrale fra VI e V secolo a. C. Nuovi dati di scavo. In A. Lehoërff (Ed.) *L'artisanat métallurgique dans les sociétés anciennes en Méditerranée occidentale: Actes du colloque*, Collection de l'École Française de Rome, (pp. 323–339). Roma: École Française de Rome.

Aranguren, B., Giachi, G., & Pallecchi, P. (2009). L'area siderurgica di Rondelli ed il contesto produttivo etrusco nel Golfo di Follonica e al Puntone di Scarlino. In F. Cambi, F. Cavari, & C. Mascione (Eds.) *Materiali da costruzione e produzione del ferro*, Bibliotheca archaeologica, (pp. 159–162). Bari: Edipuglia.

Ardaillon, d. (1897). *Les mines du Laurion dans l'antiquité*, vol. 77 of *Bibliothèque des Écoles françaises d'Athènes et de Rome*. Paris: Thorin et fils.

Aringoli, D., Coltorti, M., D'Orefice, M., Dramis, F., Federici, P., Foresi, L., Graciotti, R., Iotti, A., Molin, P., & Moretti, S. (2009). *Carta Geomorfologica dell'Arcipelago Toscano*. No. 86 in Memorie descrittive della Carta Geologico d'Italia. Roma: Istituto Superiore per la Protezione e la Ricerca Ambientale / Servizio Geologico d'Italia.

Arnaldi, I. (n.d.). *La memoria di Pomonte*. s.n.: s.n.

Arnoldus-Huyzendveld, A. (2011). Landscape development of the coastal plains of Rome and Grosseto between 20.000 and 3.000 years ago. In M. van Leusen, G. Pizziolo, & L. Sarti (Eds.) *Hidden Landscapes of Mediterranean Europe. Cultural and Methodological Biases in Pre- and Protohistoric Landscape Studies: Proceedings of the International Meeting Siena, Italy, May 25-27, 2007*, no. 2320 in British Archaeological Reports, Internat. Ser., (pp. 161–169). Oxford: Archaeopress.

Attema, P., & Delvigne, J. (2000). Settlement dynamics and alluvial sedimentation in the Pontine Region, central Italy: a complex relationship. In F. Vermeulen, & M. De Dapper (Eds.) *Geoarchaeology of the landscapes of classical antiquity = international colloquium Ghent, 23-24 October 1998 = Géoarchéologie des paysages de l'antiquité classique : colloque international Gand, 23-24 octobre 1998*, vol. 5 of *Bulletin antieke beschaving. Supplement*, (pp. 35–47). Leiden: Stichting BABESCH.

Ayala, G., & French, C. (2005). Erosion modeling of past land-use practices in the Fiume di Sotto di Troina river valley, north-central Sicily. *Geoarchaeology*, *20*(2), 149–167. DOI/URL: https://doi.org/10.1002/gea.20041

Bachmann, H.-G. (1982). *The identification of slags from archaeological sites*. No. 6 in Occasional publication (University of London. Institute of Archaeology). London: Institute of Archaeology.

Bailis, R. (2009). Modeling climate change mitigation from alternative methods of charcoal production in Kenya. *Biomass and Bioenergy*, *33*(11), 1491–1502. DOI/URL: https://doi.org/10.1016/j.biombioe.2009.07.001

Baldi, G., & Pucci, M. (2016). *The Volterraio castle: digital tools for documentation, survey and promotion*. Florence.

Banducci, L. M. (2013). *Foodways and Cultural Identity in Roman Republican Italy*. PhD thesis, University of Michigan.

Bargagli, R., Baldi, F., & Leonzio, C. (1985). Trace metal assessment in sediment, molluscs and reed leaves in the Bay of Follonica (Italy). *Marine Environmental Research*, *16*(4), 281–300. DOI/URL: https://doi.org/10.1016/0141-1136(85)90024-8

Barghigiani, C., Ristori, T., & Lopez Arenas, J. (1996). Mercury in marine sediment from a contaminated area of the northern Tyrrhenian Sea: less than 20 micron grain-size fraction and total sample analysis. *Science of The Total Environment*, *192*(1), 63–73. DOI/URL: https://doi.org/10.1016/0048-9697(96)05292-8

Barker, H. A. (1815). *A Short Description of the Island of Elba, and Town of Porto-Ferrajo: Illustrative of the View now exhibiting in Henry Aston Barker's Panorama, Leicester Square*. London: J. Adlard, printer.

Baron, S., & Coustures, M.-P. (2015). Apports et limites des méthodes isotopiques pour restituer la circulation des métaux aux périodes anciennes. *Les nouvelles de l'archéologie*, *138*, 35–39. DOI/URL: https://journals.openedition.org/nda/2743

Baroni, F., Boscagli, A., Di Lella, L. A., Protano, G., & Riccobono, F. (2004). Arsenic in soil and vegetation of contaminated areas in southern Tuscany (Italy). *Journal of Geochemical Exploration*, *81*(1), 1–14. DOI/URL: https://doi.org/10.1016/S0375-6742(03)00208-5

Baroni, F., Boscagli, A., Protano, G., & Riccobono, F. (2000). Antimony accumulation in Achillea ageratum, Plantago lanceolata and Silene vulgaris growing in an old Sb-mining area. *Environmental Pollution*, *109*(2), 347–352. DOI/URL: https://doi.org/10.1016/S0269-7491(99)00240-7

Barsch, D., & Liedtke, H. (1985). *Geomorphological mapping in the Federal Republic of Germany*. Selbstverl. des Inst. für Phys. Geographie der Freien Univ. Berlin, Berlin. DOI/URL: https://e-docs.geo-leo.de/handle/11858/7219

Bartels, C. (1996). Mittelalterlicher und frühneuzeitlicher Bergbau im Harz und seine Einflüsse auf die Umwelt. *Naturwissenschaften*, *83*(11), 483–491. DOI/URL: https://doi.org/10.1007/BF01141950

Bauvais, S., & Fluzin, P. a. (2009). Archaeological and archaeometrical approaches of the chaîne opératoirein iron and steelmaking: Methodology for a regional evolutionary study. In S. A. Rosen, & V. Roux (Eds.) *Techniques and people: anthropological perspectives on technology in the archaeology of the proto-historic and early historic periods in the southern Levant*, no. 9 in Mémoires et travaux du Centre de recherche français à Jérusalem, (pp. 159–180). Paris: De Boccard.

Bayon, G., Dennielou, B., Etoubleau, J., Ponzevera, E., Toucanne, S., & Bermell, S. (2012). Intensifying Weathering and Land Use in Iron Age Central Africa. *Science*, *335*(6073), 1219–1222.
DOI/URL: https://dx.doi.org/10.1126/science.1215400

Bebermeier, W., Becker, F., Eser, R. A., Knitter, D., Cordani, V., Eilbracht, H., Kaiser, E., Klinger, J., Lehnhardt, E., Meyer, M., Schmid, S. G., Schütt, B., & Michael Thelemann (in press). Socio-ecological aspects of iron as a new raw material. Berlin: Edition Topoi.

Bebermeier, W., Brumlich, M., Cordani, V., Vincenzo, S. d., Eilbracht, H., Klinger, J., Lehnhardt, E., Meyer, M., Schmid, S. G., Schütt, B., Thelemann, M., & Wemhoff, M. (2016). The Coming of Iron in a Comparative Perspective. *eTopoi. Journal for Ancient Studies*, *6*(0).
DOI/URL: http://journal.topoi.org/index.php/etopoi/article/view/254

Becker, F., Djurdjevac Conrad, N., Eser, R. A., Helfmann, L., Schütt, B., Schütte, C., & Zonker, J. (submitted.a). The furnace *and* the goat—a spatio-temporal model of the fuelwood requirement for iron metallurgy on elba island, 4th century BCE to 2nd century CE. *Plos ONE*.

Becker, F., Eser, R., Hoelzmann, P., & Schütt, B. (2018). Geochemistry of five sediment sequences obtained in the Campo coastal plain on Elba Island (Tuscany, Italy). *Supplement to: Becker, F et al. (submitted): Reconstructing human-landscape interactions in the context of ancient iron smelting on Elba Island (northern Tyrrhenian Sea, Italy) by sedimentological evidences. Geoarchaeology-An International Journal*.
DOI/URL: https://doi.pangaea.de/10.1594/PANGAEA.891242

Becker, F., Eser, R., Hoelzmann, P., & Schütt, B. (2019a). Reconstructing human–landscape interactions in the context of ancient iron smelting on Elba Island, Italy, using sedimentological evidence. *Geoarchaeology*, *34*(3), 336–359.
DOI/URL: https://dx.doi.org/10.1002/gea.21726

Becker, F., Eser, R. A., Hoelzmann, P., & Schütt, B. (2019b). The environmental impact of ancient iron mining and smelting on Elba Island, Italy – A geochemical soil survey of the Magazzini site. *Journal of Geochemical Exploration*, *106307*.
DOI/URL: https://doi.org/10.1016/j.gexplo.2019.04.009

Becker, F., Eser, R. A., Schmid, S.G., & Schütt, B. (submitted.b). Framing the Chronology and Fuel Consumption of Ancient Iron Smelting on Elba Island. In *The Coming of Iron - Anfänge der Eisenverhüttung in Mitteleuropa*. Berlin.

Becker, F., Hoelzmann, P., Eser, R. A., & Schütt, B. (2019c). Data for: The environmental impact of ancient iron mining and smelting on Elba Island, Italy —a geochemical soil survey of the Magazzini site. *1*.
DOI/URL: http://dx.doi.org/10.17632/k4cgsps4hk.1

Beckmann, S. (2007). *Kolluvien und Auensedimente als Geoarchive im Umfeld der historischen Hammerwerke Leidersdorf und Wolfsbach (Vils/Opf.)*. No. 12 in Regensburger Beiträge zur Bodenkunde, Landschaftsökologie und Quartärforschung. Regensburg: Schriftenreihe der Universität Regensburg.
DOI/URL: https://nbn-resolving.org/urn:nbn:de:bvb:355-opus-7529

Bellini, C., Mariotti-Lippi, M., & Montanari, C. (2009). The Holocene landscape history of the NW Italian coasts. *The Holocene*, *19*(8), 1161–1172.
DOI/URL: https://doi.org/10.1177/0959683609345077

Bellotti, P., Calderoni, G., Di Rita, F., D'Orefice, M., D'Amico, C., Esu, D., Magri, D., Martinez, M. P., Tortora, P., & Valeri, P. (2011). The Tiber river delta plain (central Italy): Coastal evolution and implications for the ancient Ostia Roman settlement. *The Holocene*, *21*(7), 1105–1116.
DOI/URL: https://doi.org/10.1177/0959683611400464

Bellotti, P., Caputo, C., Davoli, L., Evangelista, S., Garzanti, E., Pugliese, F., & Valeri, P. (2004). Morpho-sedimentary characteristics and Holocene evolution of the emergent part of the Ombrone River delta (southern Tuscany). *Geomorphology*, *61*(1-2), 71–90.
DOI/URL: https://doi.org/10.1016/j.geomorph.2003.11.007

Bellotti, P., Milli, S., Tortora, P., & Valeri, P. (1995). Physical stratigraphy and sedimentology of the Late Pleistocene-Holocene Tiber Delta depositional sequence. *Sedimentology*, *42*(4), 617–634.
DOI/URL: http://dx.doi.org/10.1111/j.1365-3091.1995.tb00396.x

Bencini, A., Giardi, M., Pranzini, G., & Tacconi, B. M. (1986). *Le risorse idriche dell'Isola d'Elba*, vol. 2 of *Quaderni sull'assetto del territorio. N.S.*. Pisa: Tacchi Editore.

Benito, G., Macklin, M. G., Panin, A., Rossato, S., Fontana, A., Jones, A. F., Machado, M. J., Matlakhova, E., Mozzi, P., & Zielhofer, C. (2015a). Recurring flood distribution patterns related to short-term Holocene climatic variability. *Scientific Reports*, *5*, 16398.
DOI/URL: http://dx.doi.org/10.1038/srep16398

Benito, G., Macklin, M. G., Zielhofer, C., Jones, A. F., & Machado, M. J. (2015b). Holocene flooding and climate change in the Mediterranean. *CATENA*, *130*, 13–33.
DOI/URL: https://doi.org/10.1016/j.catena.2014.11.014

Benjamin, J., Rovere, A., Fontana, A., Furlani, S., Vacchi, M., Inglis, R. H., Galili, E., Antonioli, F., Sivan, D., Miko, S., Mourtzas, N., Felja, I., Meredith-Williams, M., Goodman-Tchernov, B., Kolaiti, E., Anzidei, M., & Gehrels, R. (2017). Late Quaternary sea-level changes and early human societies in the central and eastern Mediterranean Basin: An interdisciplinary review. *Quaternary International*, *449*, 29–57.
DOI/URL: https://doi.org/10.1016/j.quaint.2017.06.025

Bennett, K. D. (1996). Determination of the number of zones in a biostratigraphical sequence. *New Phytologist*, *132*(1), 155–170.
DOI/URL: https://doi.org/10.1111/j.1469-8137.1996.tb04521.x

Benvenuti, M., Dini, A., D'Orazio, M., Chiarantini, L., Corretti, A., & Costagliola, P. (2013). The tungsten and tin signature of iron ores from Elba Island (Italy): A tool for provenance studies of iron production in the Mediterranean region. *Archaeometry*, *55*(3), 479–506.
DOI/URL: http://onlinelibrary.wiley.com/doi/10.1111/j.1475-4754.2012.00692.x/abstract

Benvenuti, M., Isabella, M., Fernando, C., Costagliola, P., Pierluigi, P., Lattanzi, P., & Tanelli, G. (1999). Environmental problems related to sulfide mining in Tuscany. *Chronique de la Recherche Minière*, *534*, 29–46.

Benvenuti, M., Mariotti-Lippi, M., Pallecchi, P., & Sagri, M. (2006). Late-Holocene catastrophic floods in the terminal Arno River (Pisa, Central Italy) from the story of a Roman riverine harbour. *The Holocene*, *16*(6), 863–876.
DOI/URL: https://doi.org/10.1191%2F0959683606hl978rp

Benvenuti, M., Mascaro, I., Corsini, F., Ferrari, M., Lattanzi, P., Parrini, P., Costagliola, P., & Tanelli, G. (2000a). Environmental mineralogy and geochemistry of waste dumps at the Pb(Zn)-Ag Bottino mine, Apuane Alps, Italy. *European Journal of Mineralogy*, *12*, 441–453.
DOI/URL: https://doi.org/10.1127%2F0935-1221%2F2000%2F0012-0441

Benvenuti, M., Mascaro, I., Corsini, F., Lattanzi, P., Parrini, P., & Tanelli, G. (1997). Mine waste dumps and heavy metal pollution in abandoned mining district of Boccheggiano (Southern Tuscany, Italy). *Environmental Geology*, *30*(3), 238–243.
DOI/URL: https://doi.org/10.1191%2F0959683606hl978rp

Benvenuti, M., Mascaro, I., Costagliola, P., Tanelli, G., & Romualdi, A. (2000b). Iron, copper and tin at Baratti (Populonia): smelting processes and metal provenances. *Historical Metallurgy*, *34 (2)*, 67–76.
DOI/URL: http://hdl.handle.net/2158/201837

Benvenuti, M., Orlando, A., Borrini, D., Chiarantini, L., Costagliola, P., Mazzotta, C., & Rimondi, V. (2016). Experimental smelting of iron ores from Elba Island (Tuscany, Italy): Results and implications for the reconstruction of ancient metallurgical processes and iron provenance. *Journal of Archaeological Science*, *70*, 1–14.
DOI/URL: https://doi.org/10.1016%2Fj.jas.2016.04.008

Benvenuti, M., Pecchioni, E., Chiarantini, L., Mariani, A., Mascaro, I., Di Pierro, S., Serneels, V., & Maggetti, M. (2003). An investigation on the "Etruscan" iron furnaces from Baratti-Populonia (Tuscany, Italy). In *Ceramic in the society: proceedings of the 6th European Meeting on Ancient Ceramics, Fribourg, Switzerland 3–6 October 2001*, (pp. 1–18). Fribourg, Switzerland: Department of Geosciences, Mineralogy and Petrography, University of Fribourg.

Bertini, A., Ricci, M., & Toti, F. (2014). Analisi Palinologiche. In M. D'Orefice, & R. Graciotti (Eds.) *Note illustrative della carta geomorphologica d'italia alla scala 1:50.000 – foglio 316-317-328-329 – Isola d'Elba*. Roma: Istituto Superiore per la Protezione e la Ricerca Ambientale / Servizio Geologico d'Italia.

Bertoldi, T. (2012). *Guida alle anfore romane di età imperiale: forme, impasti e distribuzione*. Roma: Editoria e Servizi Archeologi.

Berveglieri, A., & Valentini, R. (2001). Le miniere di ferro dell'Elba e i forni fusori etruschi, antenati dell'altoforno. *La Metallurgia Italiana*, *93*(6), 49–56.

Bevan, A., Conolly, J., Hennig, C., Johnston, A., Quercia, A., Spencer, L., & Vroom, J. (2013). Measuring Chronological Uncertainty in Intensive Survey Finds: A Case Study from Antikythera, Greece*. *Archaeometry*, *55*(2), 312–328.
DOI/URL: https://onlinelibrary.wiley.com/doi/abs/10.1111/j.1475-4754.2012.00674.x

Bevan, A., & Crema, E. R. (2018). *rcarbon: Methods for calibrating and analysing radiocarbon dates [R package]*.
DOI/URL: https://github.com/ahb108/rcarbon

Bianchi, E. (1943). Alcuni effetti delle oscillazione eustatiche del livello marino sulla morfologia dell'Elba orientale (n.v.). *Atti della Società toscana di scienze naturali, residente in Pisa. Memorie.*, *52*, 23–26.

Bindler, R., Segerström, U., Pettersson-Jensen, I.-M., Berg, A., Hansson, S., Holmström, H., Olsson, K., & Renberg, I. (2011). Early medieval origins of iron mining and settlement in central Sweden: multiproxy analysis of sediment and peat records from the Norberg mining district. *Journal of Archaeological Science*, *38*(2), 291–300.
DOI/URL: https://doi.org/10.1016%2Fj.jas.2010.09.004

Bini, C. (Ed.) (2011). *Environmental Impact of Abandoned Mine Waste: A Review*. New York: Nova Science Pub Inc.

Bini, M., Zanchetta, G., Perşoiu, A., Cartier, R., Català, A., Cacho, I., Dean, J. R., Rita, F. D., Drysdale, R. N., Finnè, M., Isola, I., Jalali, B., Lirer, F., Magri, D., Masi, A., Marks, L., Mercuri, A. M., Peyron, O., Sadori, L., Sicre, M.-A., Welc, F., Zielhofer, C., & Brisset, E. (2019). The 4.2 ka BP Event in the Mediterranean region: an overview. *Climate of the Past*, *15*(2), 555–577.
DOI/URL: https://doi.org/10.5194/cp-15-555-2019

Bintliff, J. (2002). Time, process and catastrophism in the study of Mediterranean alluvial history: A review. *World Archaeology*, *33*(3), 417–435.
DOI/URL: https://doi.org/10.1080/00438240120107459

Bintliff, J. L. (1975). Mediterranean Alluviation: New Evidence from Archaeology. *Proceedings of the Prehistoric Society*, *41*, 78–84.
DOI/URL: https://doi.org/10.1017%2FS0079497X00010914

Birch, T., Scholger, R., Walach, G., Stremke, F., & Cech, B. (2015). Finding the invisible smelt: using experimental archaeology to critically evaluate fieldwork methods applied to bloomery iron production remains. *Archaeological and Anthropological Sciences*, *7*(1), 73–87.
DOI/URL: https://doi.org/10.1007%2Fs12520-013-0141-8

Blakelock, E. S. (2013). *The Early Medieval Cutting Edge of Technology: An archaeometallurgical, technological and social study of the manufacture and use of Anglo-Saxon and Viking iron knives, and their contribution to the early medieval iron economy.*. PhD thesis, University of Bradford, Division of Archaeological, Geographical and Environmental Sciences. Bradford, U.K.: University of Bradford eTheses.
DOI/URL: http://hdl.handle.net/10454/5517

Blanc, L. G. (1846). *Die skandinavischen Reiche. Die Schweiz. Deutschland. Italien. Griechenland (die europäische Türkei, das Königreich Griechenland) und die Jonischen Inseln*. Dr. L.G. Blanc's Handbuch des Wissenswürdigsten aus der Natur und Geschichte der Erde und ihrer Bewohner : zum Gebrauch beim Unterricht in Schulen und Familien, vorzüglich für Hauslehrer auf dem Lande, sowie zum Selbstunterricht. Halle: C.A. Schwetschke und Sohn, 5th ed.
DOI/URL: https://doi.org/10.3931/e-rara-70855

Blanchon, P., & Shaw, J. (1995). Reef drowning during the last deglaciation: Evidence for catastrophic sea-level rise and ice-sheet collapse. *Geology*, *23*(1), 4–8. DOI/URL: https://doi.org/10.1130%2F0091-7613(1995)023%3C0004%3ARDDTLD%3E2.3.CO%3B2

Blasi, C., Capotorti, G., Alós Ortí, M. M., Anzellotti, I., Attorre, F., Azzella, M. M., Carli, E., Copiz, R., Garfì, V., Manes, F., Marando, F., Marchetti, M., Mollo, B., & Zavattero, L. (2017). Ecosystem mapping for the implementation of the European Biodiversity Strategy at the national level: The case of Italy. *Environmental Science & Policy*, *78*, 173–184. DOI/URL: https://doi.org/10.1016%2Fj.envsci.2017.09.002

Blasi, C., Capotorti, G., Copiz, R., Guida, D., Mollo, B., Smiraglia, D., & Zavattero, L. (2014). Classification and mapping of the ecoregions of Italy. *Plant Biosystems - An International Journal Dealing with all Aspects of Plant Biology*, *148*(6), 1255–1345. DOI/URL: https://doi.org/10.1080/11263504.2014.985756

Bluhm, L. E., & Surovell, T. A. (2019). Validation of a global model of taphonomic bias using geologic radiocarbon ages. *Quaternary Research*, *91*(1), 325–328. DOI/URL: https://doi.org/10.1017%2Fqua.2018.78

Boenzi, F., Caldara, M., Capolongo, D., Dellino, P., Piccarreta, M., & Simone, O. (2008). Late Pleistocene–Holocene landscape evolution in Fossa Bradanica, Basilicata (southern Italy). *Geomorphology*, *102*(3), 297–306. DOI/URL: https://doi.org/10.1016%2Fj.geomorph.2008.03.013

Bond, T. C., Bhardwaj, E., Dong, R., Jogani, R., Jung, S., Roden, C., Streets, D. G., & Trautmann, N. M. (2007). Historical emissions of black and organic carbon aerosol from energy-related combustion, 1850–2000. *Global Biogeochemical Cycles*, *21*(2). DOI/URL: https://doi.org/10.1029%2F2006GB002840

Boogaart, K. G. v. d., Tolosana-Delgado, R., & Bren, M. (2018). *compositions: Compositional Data Analysis [R package, v1.40-3]*. DOI/URL: https://CRAN.R-project.org/package=compositions

Bork, H. R., Bork, H., Dalchow, C., Piorr, H. P., Schatz, T., & Faust, B. (1998). *Landschaftsentwicklung in Mitteleuropa: Wirkungen des Menschen auf Landschaften*. Perthes GeographieKolleg. Gotha, Stuttgart: Klett-Perthes.

Borrelli, P., Domdey, C., Hoelzmann, P., Knitter, D., Panagos, P., & Schütt, B. (2014). Geoarchaeological and historical implications of late Holocene landscape development in the Carseolani Mountains, central Apennines, Italy. *Geomorphology*, *216*, 26–39. DOI/URL: https://doi.org/10.1016%2Fj.geomorph.2014.03.032

Borrelli, P., Hoelzmann, P., Knitter, D., & Schütt, B. (2013). Late Quaternary soil erosion and landscape development in the Apennine region (central Italy). *Quaternary International*, *312*, 96–108. DOI/URL: https://doi.org/10.1016%2Fj.quaint.2012.12.007

Bortolotti, V., Pandeli, E., & Principi, G. (2015). *Geological Map of Elba Island, 1:25,000 Scale (Sheet 316, 317, 328 e 329 from the Geological map of Italy scale 1:50,000)*. Note Illustrative della Carta Geologica d'Italia alla scala 1:50.000. Pratovecchio Stia, Pistoia: D.R.E.Am. Italia.

Bortolotti, V., Principi, G., & Treves, B. (2001). Ophiolites, Ligurides and the tectonic evolution from spreading to convergence of a Mesozoic Western Tethys segment. In G. B. Vai, & I. P. Martini (Eds.) *Anatomy of an Orogen: the Apennines and Adjacent Mediterranean Basins*, (pp. 151–164). Dordrecht: Springer Netherlands.
DOI/URL: https://doi.org/10.1007/978-94-015-9829-3_11

Bowman, D., Guillén, J., López, L., & Pellegrino, V. (2009). Planview Geometry and Morphological Characteristics of Pocket Beaches on the Catalan Coast (Spain). *Geomorphology*, *108*(3-4), 191–199.
DOI/URL: https://doi.org/10.1016%2Fj.geomorph.2009.01.005

Bowman, D., Rosas, V., & Pranzini, E. (2014). Pocket beaches of Elba Island (Italy) – Planview geometry, depth of closure and sediment dispersal. *Estuarine, Coastal and Shelf Science*, *138*, 37–46.
DOI/URL: https://doi.org/10.1016/j.ecss.2013.12.005

Bracken, L. J., & Croke, J. (2007). The concept of hydrological connectivity and its contribution to understanding runoff-dominated geomorphic systems. *Hydrological Processes*, *21*(13), 1749–1763.
DOI/URL: https://doi.org/10.1002/hyp.6313

Bracken, L. J., Turnbull, L., Wainwright, J., & Bogaart, P. (2015). Sediment connectivity: a framework for understanding sediment transfer at multiple scales. *Earth Surface Processes and Landforms*, *40*(2), 177–188.
DOI/URL: https://doi.org/10.1002/esp.3635

Bradl, H. B. (2004). Adsorption of heavy metal ions on soils and soils constituents. *Journal of Colloid and Interface Science*, *277*(1), 1–18.
DOI/URL: https://doi.org/10.1016%2Fj.jcis.2004.04.005

Bradley, S. B., & Cox, J. J. (1990). The significance of the floodplain to the cycling of metals in the river Derwent Catchment, U.K. *Science of The Total Environment*, *97-98*, 441–454.
DOI/URL: https://doi.org/10.1016/0048-9697(90)90255-S

Brambilla, G. (2003). *Le Impronte degli Antichi Abitatori dell'Isola d'Elba dalla Preistoria agli Etruschi*. No. 1 in Argomenti di Archeologia. Pavia: Gianni Iuculano editore.

Brauns, M., Schwab, R., Gassmann, G., Wieland, G., & Pernicka, E. (2013). Provenance of Iron Age iron in southern Germany: a new approach. *Journal of Archaeological Science*, *40*(2), 841–849.
DOI/URL: https://doi.org/10.1016%2Fj.jas.2012.08.044

Brückner, H. (1983). Holozäne Bodenbildungen in den Alluvionen süditalienischer Flüsse. *Zeitschrift f. Geomorphologie N. F., Suppl,*, *48*, 99–116.

Brückner, H. (1986). Man's impact on the evolution of the physical environment in the Mediterranean region in historical times. *GeoJournal*, *13*(1), 7–17.
DOI/URL: https://doi.org/10.1007/BF00190684

Brückner, H. (1990). Changes in the Mediterranean ecosystem druing antiquity – A geomorphological approach as seen in two examples. In S. Bottema, G. Entjes-Nieborg, & W. Van Zeist (Eds.) *Man's role in the shaping of the Eastern Mediterranean landscape : proceedings of the INQUA/BAI Symposium on the Impact of Ancient Man on the Landscape*

of the Eastern Mediterranean Region and the Near East, Groningen, Netherlands, 6 - 9 March 1989, (pp. 127–137). Rotterdam: Balkema.

Breda, A., Amorosi, A., Rossi, V., & Fusco, F. (2016). Late-glacial to Holocene depositional architecture of the Ombrone palaeovalley system (Southern Tuscany, Italy): Sea-level, climate and local control in valley-fill variability. *Sedimentology*, *63*(5), 1124–1148. DOI/URL: https://doi.org/10.1111%2Fsed.12253

Brewer, P. A., & Taylor, M. P. (1997). The spatial distribution of heavy metal contaminated sediment across terraced floodplains. *CATENA*, *30*(2), 229–249. DOI/URL: https://doi.org/10.1016%2FS0341-8162(97)00017-9

Bridge, J. S., & Mackey, S. D. (2009). A revised alluvial stratigraphy model. In *Alluvial Sedimentation*, (pp. 317–336). John Wiley & Sons, Ltd. DOI/URL: https://doi.org/10.1002/9781444303995.ch22

Brncic, T. M., Willis, K., Harris, D. J., & Washington, R. (2007). Culture or climate? The relative influences of past processes on the composition of the lowland Congo rainforest. *Philosophical Transactions of the Royal Society B: Biological Sciences*, *362*(1478), 229–242.
DOI/URL: https://doi.org/10.1098%2Frstb.2006.1982

Bränvall, M.-L., Bindler, R., Emteryd, O., & Renberg, I. (2001). Four thousand years of atmospheric lead pollution in northern Europe: a summary from Swedish lake sediments. *Journal of Paleolimnology*, *25*(4), 421–435. DOI/URL: https://doi.org/10.1023/A:1011186100081

Bronk Ramsey, C. (2009). Bayesian analysis of radiocarbon dates. *Radiocarbon*, *51*(1), 337–360.
DOI/URL: https://doi.org/10.1017/S0033822200033865

Brouwer Burg, M., Peeters, H., & Lovis, W. A. (2016). Introduction to Uncertainty and Sensitivity Analysis in Archaeological Computational Modeling. In M. Brouwer Burg, H. Peeters, & W. A. Lovis (Eds.) *Uncertainty and Sensitivity Analysis in Archaeological Computational Modeling*, Interdisciplinary Contributions to Archaeology, (pp. 1–20). Cham: Springer International Publishing. DOI/URL: https://doi.org/10.1007/978-3-319-27833-9_1

Brown, A., Bennett, J., & Rhodes, E. (2009). Roman mining on Exmoor: a geomorphological approach at Anstey's Combe, Dulverton. *Environmental Archaeology*, *14*(1), 50–61. DOI/URL: https://doi.org/10.1179/174963109X400673

Brown, A. G., & Ellis, C. (1995). People, climate and alluviation: theory, research design and new sedimentological and stratigraphic data from Etruria. *Papers of the British School at Rome*, *63*, 45–73.
DOI/URL: https://doi.org/10.1017%2FS0068246200010199

Brown, A. G., Petit, F., & James, L. A. (2016). Archaeology and human artefacts. In *Tools in Fluvial Geomorphology*, (pp. 40–55). John Wiley & Sons, Ltd. DOI/URL: https://doi.org/10.1002/9781118648551.ch3

Brown, W. A. (2015). Through a filter, darkly: population size estimation, systematic error, and random error in radiocarbon-supported demographic temporal frequency analysis. *Journal of Archaeological Science*, *53*, 133–147.
DOI/URL: http://www.sciencedirect.com/science/article/pii/S0305440314003835

Brumlich, M. (2018a). Die Siedlung Glienick 14. Eine Studie zur eisenzeitlichen Besiedlung des Teltows unter besonderer Berücksichtigung der Eisenverhüttung und -verarbeitung. In M. Brumlich (Ed.) *Frühe Eisenverhüttung bei Glienick. Siedlungs- und wirtschaftsarchäologische Forschungen zur vorrömischen Eisen- und römischen Kaiserzeit in Brandenburg.*, vol. 1 of *Berliner Archäologische Forschungen*, (pp. 15–544). Rahden, Westf.: Verlag Marie Leidorf GmbH.

Brumlich, M. (2018b). *Frühe Eisenverhüttung bei Glienick: Siedlungs- und witschaftsarchäologische Forschungen zur vorrömischen Eisen- und römischen Kaisereit in Brandenburg*, vol. Band 17 of *Berliner Archäologische Forschungen*. Rahden, Westf.: Verlag Marie Leidorf GmbH.

Brunner, S. (1828). *Streifzug durch das östliche Ligurien, Elba, die Ostküste Siciliens, und Malta, zunächst in Bezug auf Pflanzenkunde im Sommer 1826 unternommen*. Winterthur: Steinerischen Buchhandlung.
DOI/URL: https://doi.org/10.3931/e-rara-28606

Buccolini, M., Materazzi, M., Aringoli, D., Gentili, B., Pambianchi, G., & Scarciglia, F. (2014). Late Quaternary catchment evolution and erosion rates in the Tyrrhenian side of central Italy. *Geomorphology*, *204*, 21–30.
DOI/URL: https://doi.org/10.1016%2Fj.geomorph.2013.07.023

Buchner, G. (1969). Mostra degli scavi di Pithecusa. *Dialoghi di Archeologia*, *3*(1-2), 85–101.

Buchner, G. (1985). Isola d'Ischia, Lacco Ameno, Monte di Vico (scarico Gosetti): Minerale di Ferro. In G. Camporeale (Ed.) *L'Etruria mineraria*, Progetto Etruschi, (p. 46). Milano: Electa.

Buchwald, V. F. (2005). *Iron and Steel in Ancient Times*, vol. 29 of *Historisk-filosofiske skrifter*. København: Kong. Danske Videnskab. Selskab.

Butzer, K. W. (1980). Holocene alluvial sequences: problems of dating and correlation. *Timescales in geomorphology*, (pp. 131–142).

Cambi, F. (2004). Populonia e l'isola d'Elba: Territorio e viabilità delle fortezze d'altura. In M. L. Gualandi (Ed.) *Materiali per Populonia 3*, Quaderni del Dipartimento di Archeologia e Storia delle Arti, Sezione Archeologia, Università di Siena, (pp. 291–307). Firenze.

Cambi, F., Pagliantini, L., Vanni, E., Longo, C., Manca, R., Milanesi, C., Paratico, F., Scapolaro, S., Graziano, A., & Corretti, A. (2018). Isola d'Elba. Archeologia e storia nella rada di Portoferraio: la villa repubblicana di San Giovanni. *Annali della Scuola Normale Superiore di Pisa. Classe di Lettere e Filosofia*, *10*(2), 147–183.
DOI/URL: http://hdl.handle.net/11365/1069373

Cambridge, M., & Shaw, D. (2019). Preliminary reflections on the failure of the Brumadinho tailings dam in January 2019. *Dams and Reservoirs*, *29*(3), 113–123.
DOI/URL: https://doi.org/10.1680/jdare.19.00004

Campanella, B., Onor, M., D'Ulivo, A., Giannecchini, R., D'Orazio, M., Petrini, R., & Bramanti, E. (2016). Human exposure to thallium through tap water: A study from Valdicastello Carducci and Pietrasanta (northern Tuscany, Italy). *Science of The Total Environment*, *548-549*, 33–42.
DOI/URL: https://doi.org/10.1016%2Fj.scitotenv.2016.01.010

Campbell, N., & MacLachlan, A. N. C. (1869). *Napoleon at Fontainebleau and Elba, being a journal of occurrences in 1814 - 1815 with notes of conversations by the late Major-General Sir Neil Campbell. With a memoir of the life and services of that officer by his nephew A. N. Campbell Maclachlan. With a portrait*. London: John Murray, Albemarle Street. DOI/URL: https://hdl.handle.net/2027/uc2.ark:/13960/t9m32s202

Camporeale, G. (1985a). Introduzione. In P. Etruschi, & G. Camporeale (Eds.) *L'Etruria mineraria: exhibition catalogue: Portoferraio, Massa Marittima, Populonia, 25 Maggio - 20 Ottobre, 1985*, (pp. 21–35). Milano: Electa for the Regione Toscano.

Camporeale, G. (Ed.) (1985b). *L'Etruria mineraria: [catologo della mostra, Portoferraio, fortezza della Linguella, Massa Marittima, area archeologica del lago dell'Acessa, palazzo del Podestà Populonia, ex Frantoio, 25 maggio - 20 ott. 1985]*. Progetto Etruschi. Milano: Electa.

Camporeale, G. (1989). Gli Etruschi e le risorse minerarie. Aspetti e problemi. In C. Domergue (Ed.) *Minería y metalurgía en las antiguas civilizaciones mediterráneas y europeas 1*, vol. 1, (pp. 205–212). Madrid: Dirección General de Bellas Artes y Archivos and Ministero de Cultura.

Canti, M. G. (2003). Aspects of the chemical and microscopic characteristics of plant ashes found in archaeological soils. *CATENA*, *54*(3), 339–361. DOI/URL: https://doi.org/10.1016%2FS0341-8162(03)00127-9

Capacci, C. (1911). The Iron Mines of the Island of Elba. *The Journal of the Iron and Steel Institute*, *84*(2), 412–450.

Carcaillet, C. (2001). Are Holocene wood-charcoal fragments stratified in alpine and subalpine soils? Evidence from the Alps based on AMS 14c dates. *The Holocene*, *11*(2), 231–242. DOI/URL: https://doi.org/10.1191/095968301674071040

Carey, C. J., & Moles, N. R. (2017). Geochemical Survey and Evaluation Excavations at Alderley Edge: Recognizing Anthropogenic Signatures within a Mining Site-scape. *Archaeological Prospection*, *24*(3), 225–244. DOI/URL: https://doi.org/10.1002%2Farp.1566

Carey, C. J., Wickstead, H. J., Juleff, G., Anderson, J. C., & Barber, M. J. (2014). Geochemical survey and metalworking: analysis of chemical residues derived from experimental non-ferrous metallurgical processes in a reconstructed roundhouse. *Journal of Archaeological Science*, *49*, 383–397. DOI/URL: https://doi.org/10.1016%2Fj.jas.2014.05.017

Carlon, C., D'Alessandro, M., Swartjes, F., & for Environment {and} Sustainability (Joint Research Centre), I. (2007). Derivation methods of soil screening values in Europe : a review of national procedures towards harmonisation. Tech. rep., Office for Official Publications of the European Communities, Brüssel. DOI/URL: https://publications.europa.eu/en/publication-detail/-/publication/206489ef-386d-4bcb-8b39-25b41d4d3c45

Carmignani, L., Conti, P., Cornamusini, G., & Pirro, A. (2013). Geological map of Tuscany (Italy). *Journal of Maps*, *9*(4), 487–497. DOI/URL: https://doi.org/10.1080/17445647.2013.820154

Carrari, E., Ampoorter, E., Bottalico, F., Chirici, G., Coppi, A., Travaglini, D., Verheyen, K., & Selvi, F. (2017). The Old Charcoal Kiln Sites in Central Italian Forest Landscapes. *Quaternary International*, *458*, 214–223.
DOI/URL: https://doi.org/10.1016%2Fj.quaint.2016.10.027

Carreras Monfort, C. (2003). Carreras Monfort, César: Haltern 70: a review. *Journal of Roman Pottery Studies*, *10*, 85–91.

Carta, A., Forbicioni, L., Frangini, G., Pierini, B., & Peruzzi, L. (2018a). An updated inventory of the vascular flora of Elba island (Tuscan Archipelago, Italy). *Italian Botanist*, *6*, 1–22.
DOI/URL: https://doi.org/10.3897%2Fitalianbotanist.6.26568

Carta, A., Taboada, T., & Müller, J. V. (2018b). Diachronic analysis using aerial photographs across fifty years reveals significant land use and vegetation changes on a Mediterranean island. *Applied Geography*, *98*, 78–86.
DOI/URL: https://doi.org/10.1016/j.apgeog.2018.07.010

Cartocci, A., Fedi, M. E., Taccetti, F., Benvenuti, M., Chiarantini, L., & Guideri, S. (2007). Study of a Metallurgical Site in Tuscany (Italy) by Radiocarbon Dating. *Nuclear Instruments and Methods in Physics Research Section B: Beam Interactions with Materials and Atoms*, *259*(1), 384–387.
DOI/URL: https://doi.org/10.1016%2Fj.nimb.2007.01.183

Casado, G. I. G., & Molina, M. G. d. (2017). *Energy in Agroecosystems: A Tool for Assessing Sustainability*. Boca Raton, FL: CRC Press.

Casevitz, M., & Jacquemin, A. (2018). *Bibliothèque historique. Tome 5, livre 5. Livre des Îles / Diodore de Sicile; texte établi par Michel Casevitz ; présenté et commenté par Anne Jacquemin*. No. 516 in Collection des universités de France / Série grecque. Paris: Les Belles Lettres, 2nd ed.

Casson, L. (1986). *Ships and Seamanship in the Ancient World*. Princeton: Princeton U. P.

Castellani, C. (1970). *Tavole stereometriche ed alsometriche costruite per i boschi italiani*, vol. 1. Trento: Istituto sperimentale per l'assestamento forestale e per l'alpicoltura.

Castellani, C. (1972). *Tavole stereometriche ed alsometriche costruite per i boschi italiani*, vol. 2. Trento: Istituto sperimentale per l'assestamento forestale e per l'alpicoltura.

Ceccarelli, L., & Niccolucci, F. (2003). Modelling time through GIS technology: the ancient Prile lake (Tuscany, Italy). In M. Doerr, & A. Sarris (Eds.) *CAA 2002 : the digital heritage of archaeology : computer applications and quantitative methods in archaeology : proceedings of the 30th Conference, Heraklion, Crete, April 2002*, (pp. 133–138). Athens: Hellenic Ministry of Culture, Directorate of the Archive of Monuments and Publications.

Chagué-Goff, C. (2010). Chemical signatures of palaeotsunamis: A forgotten proxy? *Marine Geology*, *271*(1), 67–71.
DOI/URL: https://doi.org/10.1016%2Fj.margeo.2010.01.010

Chagué-Goff, C., Szczucinski, W., & Shinozaki, T. (2017). Applications of geochemistry in tsunami research: A review. *Earth-Science Reviews*, *165*, 203–244.
DOI/URL: https://doi.org/10.1016%2Fj.earscirev.2016.12.003

Charlton, M. F. (2015). The last frontier in 'sourcing': the hopes, constraints and future for iron provenance research. *Journal of Archaeological Science*, *56*, 210–220. DOI/URL: https://doi.org/10.1016%2Fj.jas.2015.02.017

Charlton, M. F., Crew, P., Rehren, T., & Shennan, S. J. (2010). Explaining the evolution of ironmaking recipes – An example from northwest Wales. *Journal of Anthropological Archaeology*, *29*(3), 352–367. DOI/URL: https://doi.org/10.1016%2Fj.jaa.2010.05.001

Chiarantini, L., Benvenuti, M., Costagliola, P., Cartocci, A., Fedi, M. E., & Guideri, S. (2007). Iron production in the Etruscan site of Populonia: New data. In Associazione Italiana di Metallurgia (Ed.) *Proceedings of the Second International Conference on "Archaeometallurgy in Europe"*, (pp. 221–231). Milano: AIM.

Chiarantini, L., Benvenuti, M., Costagliola, P., Dini, A., Firmati, M., Guideri, S., Villa, I. M., & Corretti, A. (2018). Copper metallurgy in ancient Etruria (southern Tuscany, Italy) at the Bronze-Iron Age transition: a lead isotope provenance study. *Journal of Archaeological Science: Reports*, *19*, 11–23. DOI/URL: https://doi.org/10.1016/j.jasrep.2018.02.005

Chiarantini, L., Benvenuti, M., Costagliola, P., Fedi, M. E., Guideri, S., & Romualdi, A. (2009). Copper production at Baratti (Populonia, southern Tuscany) in the early Etruscan period (9th–8th centuries BC). *Journal of Archaeological Science*, *36*(7), 1626–1636. DOI/URL: https://doi.org/10.1016%2Fj.jas.2009.03.026

Chiarantini, L., Rimondi, V., Bardelli, F., Benvenuti, M., Cosio, C., Costagliola, P., Di Benedetto, F., Lattanzi, P., & Sarret, G. (2017). Mercury speciation in Pinus nigra barks from Monte Amiata (Italy): An X-ray absorption spectroscopy study. *Environmental Pollution*, *227*, 83–88. DOI/URL: https://doi.org/10.1016%2Fj.envpol.2017.04.038

Chirikure, S., Burrett, R., & Heimann, R. B. (2009). Beyond furnaces and slags: a review study of bellows and their role in indigenous African metallurgical processes. *Azania: Archaeological Research in Africa*, *44*(2), 195–215. DOI/URL: https://doi.org/10.1080/00671990903047108

Chiverrell, R. C., Thorndycraft, V. R., & Hoffmann, T. O. (2011a). Cumulative probability functions and their role in evaluating the chronology of geomorphological events during the Holocene. *Journal of Quaternary Science*, *26*(1), 76–85. DOI/URL: https://doi.org/10.1002%2Fjqs.1428

Chiverrell, R. C., Thorndycraft, V. R., & Hoffmann, T. O. (2011b). Reply to comment: Cumulative probability functions and their role in evaluating the chronology of geomorphological events during the Holocene. Richard C. Chiverrell, Varyl, R. Thorndycraft and Thomas, O. Hoffmann, Journal of Quaternary Science 26: 76–85. *Journal of Quaternary Science*, *26*(2), 241–244. DOI/URL: https://doi.org/10.1002%2Fjqs.1485

Cipriani, L., Pranzini, E., Rosas, V., & L., W. (2011). Landuse changes and erosion of pocket beaches in Elba Island (Tuscany, Italy). *Journal of Coastal Research*, (pp. 1774–1778). DOI/URL: https://www.jstor.org/stable/26482481

Clark, N., & Yusoff, K. (2014). Combustion and Society: A Fire-Centred History of Energy Use. *Theory, Culture & Society*, *31*(5), 203–226.
DOI/URL: https://doi.org/10.1177/0263276414536929

Cleere, H. (1976). Some operating parameters for Roman ironworks. *Bulletin of the Institute of Archaeology*, *13*, 233–246.

Cleere, H., & Crossley, D. W. (1995). *The Iron Industry of the Weald*. Cardiff: Merton Priory Press, 2nd ed.

Cleere, H. F. (1981). *The Iron Industry of Roman Britain*. London: University College: PhD thesis.

Clist, B., Bostoen, K., Maret, P. d., Eggert, M. K. H., Höhn, A., Mindzié, C. M., Neumann, K., & Seidensticker, D. (2018). Did human activity really trigger the late Holocene rainforest crisis in Central Africa? *Proceedings of the National Academy of Sciences*, *115*(21), E4733–E4734.
DOI/URL: https://doi.org/10.1073%2Fpnas.1805247115

Cohen, K. M., Finney, S. C., Gibbard, P. L., & Fan, J.-X. (2013). The ICS international chronostratigraphic chart. *Episodes*, *36*(3), 199–204.
DOI/URL: http://www.stratigraphy.org/ICSchart/ChronostratChart2019-05.pdf

Coles, J. (1973). *Archaeology by Experiment*. London: Hutchinson Univ. Library.

Colica, A., Chiarantini, L., Rimondi, V., Benvenuti, M., Costagliola, P., Lattanzi, P., Paolieri, M., & Rinaldi, M. (2016). Toxic metal dispersion in mining areas: from point source to diffusion pollution. The case of the Mt. Amiata Hg mining district (Southern Tuscany - Italy): new results. *Geophysical Research Abstracts*, *18*(EGU2016-9049-4).
DOI/URL: http://adsabs.harvard.edu/abs/2016EGUGA..18.9049C

Colombaroli, D., Marchetto, A., & Tinner, W. (2007). Long-term interactions between Mediterranean climate, vegetation and fire regime at Lago di Massaciuccoli (Tuscany, Italy). *Journal of Ecology*, *95*(4), 755–770.
DOI/URL: https://doi.org/10.1111%2Fj.1365-2745.2007.01240.x

Colombi, C. (2018). Castiglione della Pescaia (Grosseto), Italien. Auf der Suche nach den Häfen der etruskischen Stadt Vetulonia. Die Arbeiten der Jahre 2016 bis 2018. *e-Forschungsberichte*, *2*, 79–85.
DOI/URL: http://nbn-resolving.de/urn:nbn:de:0048-journals.efb-2018-2-p79-85-v6539.6

Colt Hoare, R. (1814). *A Tour Through the Island of Elba*. London: W. Bulmer and Co.

Comitato Tecnico per l'esame dell'utilizzo dei minerali elbani in siderurgia (1980). *Valutazione delle possibilita di utilizzazione dei minerali Elbani in siderurgia*. Rapporto interno Rimin S.p.A., Ex Archivio Rimin. Roma, San Lorenzo in Campo: Aquater S.p.A.
DOI/URL: http://www.neogeo.unisi.it/dbgmnew/ricerca.asp?act=see&id=14798

Contreras, D. A., & Meadows, J. (2014). Summed radiocarbon calibrations as a population proxy: a critical evaluation using a realistic simulation approach. *Journal of Archaeological Science*, *52*, 591–608.
DOI/URL: https://doi.org/10.1016%2Fj.jas.2014.05.030

Cordani, V. (2016). The Development of the Hittite Iron Industry. A Reappraisal of the Written Sources. *Die Welt des Orients*, *46*(2), 162–176.
DOI/URL: https://doi.org/10.13109%2Fwdor.2016.46.2.162

Coresi del Bruno, G. V. (1729). Zibaldone di memorie raccolte dal medesimo [manoscritto inedito Biblioteca Marucelliana Firenze C.29: (trascrizione dattiloscritta di Giacomo Garattoni alla Biblioteca Foresiana in Portoferraio, 1927)].

Corretti, A. (1988). Indagine preliminare sull'attività di riduzione del ferro in età romana all'isola d'Elba. *Geo-Archeologia*, (1), 7–39.
DOI/URL: https://ricerca.sns.it/handle/11384/12974?mode=simple.1#.WWXfo3r-kZ4

Corretti, A. (1991). *Metallurgia Medievale all'Isola d'Elba*. Firenze: All'Insegna del Giglio.

Corretti, A. (1992). Per una carta ragionata degli accumuli delle scorie della lavorazione antica del ferro all'Isola d'Elba. In E. Antonacci Sanpaolo (Ed.) *Archeometallurgia : ricerche e prospettive : atti del colloquio internazionale di archeometallurgia : Bologna, Dozza Imolese, 18-21 ottobre 1988*, Alma mater studiorum. Saecularia nona., (pp. 239–248). Bologna: CLUEB. Cooperativa Libraria Universitaria Editrice.

Corretti, A. (1997). La metallurgia del ferro all'Isola d'Elba nel periodo classico e medievale. In G. Tanelli (Ed.) *L'Ambiente geomineralogico e la Storia mineraria dell'Isola d'Elba, Atti dei Convegini, Rio nell'Elba, 1996*, no. 1 in Quaderni de "I fiori della Terra", (pp. 67–82). Livorno: Belforte Grafica.

Corretti, A. (2004). Per un riesame delle fonti greche e latine sull'isola d'Elba nell'antichità. *Materiali per Populonia*, *3*, 269–289.

Corretti, A. (2009). Siderurgia in ambito elbano e populoniese: Un contributo dalle fonti letterarie. In F. Cambi, F. Cavari, & C. Mascione (Eds.) *Materiali da costruzione e produzione del ferro*, Bibliotheca archaeologica, (pp. 133–139). Bari: Edipuglia.

Corretti, A. (2012). Le fortezze d'altura dell'isola d'Elba: Lo stato della questione. In F. Cambi (Ed.) *Il ruolo degli oppida e la difesa del territorio in Etruria*, Aristonothos. Scritti per il Mediterraneo antico, (pp. 347–370). Trento: Tangram.

Corretti, A. (2016). Scorie di Fucina. In O. Pancrazzi (Ed.) *Castiglione die San Martino – Fortezza di Alture (V–II A. C.), Isola d'Elba*, no. 2 in Studia Erudita, (pp. 215–216). Pisa, Roma: Istituti Editoriali e Poligrafici Internazionali.

Corretti, A. (2017). The mines on the island of Elba. In A. Naso (Ed.) *Etruscology*. Berlin, Boston: De Gruyter.
DOI/URL: https://doi.org/10.1515/9781934078495

Corretti, A., & Benvenuti, M. (2001). The beginning of iron metallurgy in Tuscany, with special reference to "Etruria Mineraria". *Mediterranean Archaeology*, *14*, 127–145.
DOI/URL: http://www.jstor.org/stable/24667998

Corretti, A., Benvenuti, M., Cambi, F., & Chiarantini, L. (2018). "Useful for the whole world": Iron ore from Elba on the routes of the Tyrrhenian Sea [Abstract]. In *XVIIIe congrès monidal d'Union International des Sciences Préhistoriques et Protohistoriques*. Paris.
DOI/URL: https://uispp2018.sciencesconf.org/180176

Corretti, A., Benvenuti, M., Chiarantini, L., & Cambi, F. (2014). The Aithale Project: Men, Earth and Sea in the Tuscan Archipelago (Italy) in Antiquity. Perspectives, aims and first results. In B. Cech, & T. Rehren (Eds.) *Early Iron in Europe*. Montagnac: Editions Monique Mergoil.

Corretti, A., Chiarantini, L., Giuntoli, G., Benvenuti, M., Cambi, F., Firmati, M., Isola, C., & Pagliantini, L. (2012). Un sito di lavorazione del ferro da Monte Strega (Rio nell'Elba, LI). nuovi dati sulle attività dei "fabri pisani" all'Elba nel medioevo. (pp. 650–655). All'Insegna del Giglio.
DOI/URL: https://ricerca.sns.it/handle/11384/12990#.W_K2bcSNy70

Corretti, A., & Firmati, M. (2011). Metallurgia antica e medievale all'isola d'Elba: vecchi dati e nuove acquisizioni. In *Archeometallurgia : dalla conoscenza alla fruizione : atti del Workshop, 22-25 maggio 2006, Cavallino (LE), Convento dei Dominicani*, (pp. 229–241). Bari: Edipuglia.

Corretti, A., & Taddei, N. (2001). Le Antiche Risorse: Ferro e Granito. In R. Rosolani, & M. Ferrari (Eds.) *Elba*, (pp. 248–271). Genova: RS Editore.

Cosci, M. (2001). I domoliti pastorali (caprili) dell'Elba: Evidenze dalla fotografia aerea. In R. Rosolani, & M. Ferrari (Eds.) *Elba*, (pp. 223–229). Genova: RS Editore.

Costagliola, P., Benvenuti, M., Chiarantini, L., Bianchi, S., Benedetto, F. D., Paolieri, M., & Rossato, L. (2008). Impact of ancient metal smelting on arsenic pollution in the Pecora River Valley, Southern Tuscany, Italy. *Applied Geochemistry*, *23*(5), 1241–1259.
DOI/URL: https://doi.org/10.1016/j.apgeochem.2008.01.005

Costagliola, P., Benvenuti, M. M., Benvenuti, M. G., Di Benedetto, F., & Lattanzi, P. (2010). Quaternary sediment geochemistry as a proxy for toxic element source: A case study of arsenic in the Pecora Valley (southern Tuscany, Italy). *Chemical Geology*, *270*(1), 80–89.
DOI/URL: https://doi.org/10.1016%2Fj.chemgeo.2009.11.007

Craigie, N. (2018). *Principles of Elemental Chemostratigraphy: A Practical User Guide*. Advances in Oil and Gas Exploration & Production. Springer International Publishing.
DOI/URL: http://dx.doi.org/10.1007/978-3-319-71216-1

Crema, E. R. (2012). Modelling Temporal Uncertainty in Archaeological Analysis. *Journal of Archaeological Method and Theory*, *19*(3), 440–461.
DOI/URL: https://www.jstor.org/stable/23254638

Cremonesi, G. (2001). *La grotta sepolcrale eneolitica di San Giuseppe all'isola d'Elba*. Pisa: Edizioni ETS.

Crew, P. (1991). The iron and copper slags at Baratti, Populonia, Italy. *Historical metallurgy: journal of the Historical Metallurgy Society*, *25*, 109–115.
DOI/URL: http://hist-met.org/images/Journal_PDFs/25_2_p_109_Crew.pdf

Crew, P., & Mighall, T. (2013). The fuel supply and woodland management at a 14th century bloomery in Snowdonia: a multi-disciplinary approach. In J. Humpries, & T. Rehren (Eds.) *The World of Iron, Proceedings of a Conference at the Natural History Museum 2009*, (pp. 473–482). London: Archetype.

Cuven, S., Francus, P., & Lamoureux, S. F. (2010). Estimation of grain size variability with micro X-ray fluorescence in laminated lacustrine sediments, Cape Bounty, Canadian High Arctic. *Journal of Paleolimnology*, *44*(3), 803–817.
DOI/URL: https://doi.org/10.1007/s10933-010-9453-1

Cyffka, B. (2006). Experiences in the study of land cover transformation on Mediterranean islands caused by change in land tenure. In H. Vogtmann, & N. Dobretsov (Eds.) *Environmental Security and Sustainable Land Use - with special reference to Central Asia*, NATO Security through Science Series, (pp. 85–103). Springer Netherlands.

D'Achiardi, G. (1929). L'Industria metallurgica a Populonia. *Studi etruschi*, *3*, 397–404.

Daems, D., Cleymans, S., Vandam, R., & Broothaerts, N. (2018). Carrying Capacity: A Superseded Concept or a Window of Opportunities. In E. A. o. Archaeologists (Ed.) *Reflecting futures; Abstract Book of the 24th EAA Annual Meeting, Barcelona, 5-8 September 2018*, vol. 2, (p. 877). European Association of Archaeologists.

Dall'Aglio, M., Ferretti, O., Manfredi Frattarelli, F., & Niccolai, I. (2001). The Link between Continental and Marine Geochemistry as shown by Mercury and Arsenic Anomalies in Sediments from Southern Tuscany and Tyrrhenian Sea. In F. M. Faranda, L. Guglielmo, & G. Spezie (Eds.) *Mediterranean Ecosystems: Structures and Processes*, (pp. 427–433). Milano: Springer Milan.
DOI/URL: https://doi.org/10.1007/978-88-470-2105-1_55

David, N., Heimann, R., Killick, D., & Wayman, M. (1989). Between bloomery and blast furnace: Mafa iron-smelting technology in North Cameroon. *African Archaeological Review*, *7*(1), 183–208.
DOI/URL: https://doi.org/10.1007/BF01116843

Davidson, J. (1790). *The Works of Virgil Translated Into English Prose, with the Latin Text and Order of Construction*. Assignment from Joseph Davidson.

Davies, O. (1935). *Roman Mines in Europe*. Oxford: Clarendon Press.

Davis, D. K. (2004). Desert 'wastes' of the Maghreb: desertification narratives in French colonial environmental history of North Africa. *cultural geographies*, *11*(4), 359–387.
DOI/URL: https://doi.org/10.1191/1474474004eu313oa

de Moor, J. J. W., & Verstraeten, G. (2008). Alluvial and colluvial sediment storage in the Geul River catchment (The Netherlands) — Combining field and modelling data to construct a Late Holocene sediment budget. *Geomorphology*, *95*(3–4), 487–503.
DOI/URL: https://doi.org/10.1016%2Fj.geomorph.2007.07.012

Dean, W. E. (1974). Determination of carbonate and organic matter in calcareous sediments and sedimentary rocks by loss on ignition; comparison with other methods. *Journal of Sedimentary Research*, *44*(1), 242–248.
DOI/URL: https://doi.org/10.1306%2F74D729D2-2B21-11D7-8648000102C1865D

Dearing, J. (1999). *Environmental Magnetic Susceptibility: Using the Bartington MS2 System*. Kenilworth: Chi Publishing, 2nd ed.

Del Monte, M. (2017). The Typical Badlands Landscapes Between the Tyrrhenian Sea and the Tiber River. In M. Soldati, & M. Marchetti (Eds.) *Landscapes and Landforms of Italy*, World Geomorphological Landscapes, (pp. 281–291). Cham: Springer International Publishing.
DOI/URL: https://doi.org/10.1007/978-3-319-26194-2_24

Della Seta, M., Del Monte, M., Fredi, P., & Lupia Palmieri, E. (2009). Space–time variability of denudation rates at the catchment and hillslope scales on the Tyrrhenian side of Central Italy. *Geomorphology*, *107*(3), 161–177.
DOI/URL: https://doi.org/10.1016%2Fj.geomorph.2008.12.004

Delpino, F. (1981). Aspetti e problemi della prima età del ferro nell'Etruria settentrionale marittima. In A. Neppi Modona, G. C. Cianferoni, & M. G. M. Costagli (Eds.) *L'etruria mineraria : atti del XII Convegno di Studi Etruschi e Italici, Firenze - Populonia - Piombino, 16-20 giugno 1979*, no. 12 in Atti del Convegno di Studi Etruschi ed Italici, (pp. 265–298). Firenze: Olschki.

Delpino, F. (1989). Siderurgia e protostoria italiana. *Studi etruschi*, *61*, 3–9.

Demeyer, A., Voundi Nkana, J. C., & Verloo, M. G. (2001). Characteristics of wood ash and influence on soil properties and nutrient uptake: an overview. *Bioresource Technology*, *77*(3), 287–295.
DOI/URL: https://doi.org/10.1016%2FS0960-8524(00)00043-2

Demirbaş, A. (2003). Trace Metal Concentrations in Ashes from Various Types of Biomass Species. *Energy Sources*, *25*(7), 743–751.
DOI/URL: https://doi.org/10.1080/00908310390212435

Demirbaş, A. (2005). Heavy Metal Contents of Fly Ashes from Selected Biomass Samples. *Energy Sources*, *27*(13), 1269–1276.
DOI/URL: https://doi.org/10.1080%2F009083190519384

Di Paola, G. (2018). Central place and liminal landscape in the territory of Populonia. *Land*, *7*((3)94), 1–16.
DOI/URL: https://doi.org/10.3390%2Fland7030094

Di Pasquale, G., Buonincontri, M., Allevato, E., & Saracino, A. (2014). Human-derived landscape changes on the northern Etruria coast (western Italy) between Roman times and the late Middle Ages. *Holocene*, *24*(11), 1491–1502.
DOI/URL: https://doi.org/10.1177%2F0959683614544063

Di Rita, F., & Magri, D. (2009). Holocene drought, deforestation and evergreen vegetation development in the central Mediterranean: a 5500 year record from Lago Alimini Piccolo, Apulia, southeast Italy. *The Holocene*, *19*(2), 295–306.
DOI/URL: https://doi.org/10.1177/0959683608100574

Dini, A., Innocenti, F., Rocchi, S., & Westerman, D. S. (2004). The late Miocene Christmas-tree laccolith complex of Elba Island. In G. Pasquare, C. Venturini, & G. Groppelli (Eds.) *Mapping Geology in Italy*, (pp. 248–258). Firenze: S.E.L.C.A.

Dini, A., Westerman, D. S., Innocenti, F., & Rocchi, S. (2008). Magma emplacement in a transfer zone: the Miocene mafic Orano dyke swarm of Elba Island, Tuscany, Italy. *Geological Society, London, Special Publications*, *302*(1), 131–148.
DOI/URL: https://doi.org/10.1144%2FSP302.10

Dinno, A. (2017). *dunn.test: Dunn's Test of Multiple Comparisons Using Rank Sums [R package, v1.3.5]*.
DOI/URL: https://CRAN.R-project.org/package=dunn.test

Dünkel, I. (2002). *The genesis of East Elba iron ore deposits and their interrelation with Messinian tectonics*. Dissertation, Eberhard Karls Universität Tübingen, Mathematisch-Naturwissenschaftliche Fakultät. Tübingen: Universität Tübingen.
DOI/URL: http://hdl.handle.net/10900/48441

Dünkel, I., Kuhlemann, J., & Nohlen, U. (2003). Iron ore formation and neotectonic evolution in Elba (Tuscany, Italy) during Messinian plutonism. *Neues Jahrbuch für Geologie und Paläontologie – Abhandlungen*, (pp. 391–407).
DOI/URL: https://doi.org/10.1127%2Fnjgpa%2F230%2F2003%2F391

Dobler, L. (2001). Vertical gradients of heavy metals in floodplain sediments of the river Selke as indicator of ancient mining activities in the Eastern Harz Mountains. *Hercynia*, *34*(2), 171–186.

Dodson, J., Li, X., Sun, N., Atahan, P., Zhou, X., Liu, H., Zhao, K., Hu, S., & Yang, Z. (2014). Use of coal in the Bronze Age in China. *The Holocene*, *24*(5), 525–530.
DOI/URL: https://doi.org/10.1177/0959683614523155

Donati, A., Protano, G., Riccobono, F., Dallai, L., & Francovich, R. (2004). Influence of ancient mining settlements on Arsenic pollution in the southwest of Tuscany. In A. Donati, C. Rossi, & C. Brebbia (Eds.) *Brownfield Sites II – Assessment, Rehabilitation and Development*, no. 70 in WIT Transactions on Ecology and the Environment.

Donati, A., Pulselli, F. M., Protano, G., Dallai, L., Francovich, R., & Tiezzi, E. (2011). With Arsenic on the Etruscans' Footprints. In C. A. Brebbia (Ed.) *Ecodynamics*, vol. 51 of *WIT Transactions on State of the Art in Science and Engineering*, (pp. 331–333).

Donati, A., Pulselli, F. M., Riccobono, F., Dallai, L., Francovich, R., & Tiezzi, E. (2005). Origin of Arsenic Pollution in Southwest Tuscany: Comparison of Fluvial Sediments. *Annali di Chimica*, *95*(3), 161–166.
DOI/URL: https://doi.org/10.1002%2Fadic.200590018

Donati, L., & Aminti, F. (2006). Una 'carbonaia' e un impianto metallurgico a Poggio Civitella. *Studi etruschi*, *72*, 253–263.

D'Orefice, M., Federici, P., Graciotti, R., Molin, P., & Ribolini, A. (2009). Carta geomorfologica dell'Arcipelago Toscano. No. 86 in Memorie descrittive della Carta Geologico d'Italia. Roma: Istituto Superiore per la Protezione e la Ricerca Ambientale / Servizio Geologico d'Italia.

D'Orefice, M., & Graciotti, R. (2014). *Note illustrative della carta geomorphologica d'italia alla scala 1:50.000 – foglio 316-317-328-329 – Isola d'Elba*. Roma: Istituto Superiore per la Protezione e la Ricerca Ambientale / Servizio Geologico d'Italia.

D'Orefice, M., & Graciotti, R. (2018). *Carta geomorfologica d'Italia alla scala 1:50.000. F. 316-317-328-329. Isola d'Elba*. ISPRA Serv. Geologico d'Italia.

dos Santos Mendes, M. e. A. (2016). *Römische Landnutzung in der Nordeifel - Der Einfluss römischer Siedlungs - und Verhüttungstätigkeit auf die Sedimente im oberen Einzugsgebiet der Urft.*. Dissertation, Rheinisch-Westfälische Technische Hochschule Aachen, Fakultät für Georessourcen und Materialtechnik. Aachen: Publikationsserver der RWTH Aachen University.
DOI/URL: http://nbn-resolving.de/urn/resolver.pl?urn=urn:nbn:de:hbz:82-rwth-2016-088094

Dotterweich, M. (2008). The history of soil erosion and fluvial deposits in small catchments of central Europe: Deciphering the long-term interaction between humans and the environment — A review. *Geomorphology*, *101*(1), 192–208.
DOI/URL: https://doi.org/10.1016%2Fj.geomorph.2008.05.023

Drescher-Schneider, R., Beaulieu, J.-L. d., Magny, M., Walter-Simonnet, A.-V., Bossuet, G., Millet, L., Brugiapaglia, E., & Drescher, A. (2007). Vegetation history, climate and human impact over the last 15,000 years at Lago dell'Accesa (Tuscany, Central Italy). *Vegetation History and Archaeobotany*, *16*(4), 279–299. DOI/URL: https://doi.org/10.1007%2Fs00334-006-0089-z

Duarte, D., Lima, R. P. d., Slatt, R., & Marfurt, K. (2019). Comparison of Clustering Techniques to Define Chemofacies: Case Study for Mississippian Rocks in the STACK Play, Oklahoma [Abstract]. In *2019 AAPG Annual Convention and Exhibition*. DOI/URL: http://www.searchanddiscovery.com/abstracts/html/2019/ace2019/abstracts/115.html

Due Trier, i., Salberg, A.-B., Holger Pilø, L., Tonning, C., Marius Johansen, H., & Aarsten, D. (2016). Semi-automatic mapping of cultural heritage from airborne laser scanning using deep learning. *Geophysical Research Abstracts*, *18*(EPSC2016-5716). DOI/URL: http://adsabs.harvard.edu/abs/2016EGUGA..18.5716D

Dughetti, F., & Tanelli, G. (2013). Preliminary report on arsenic and heavy metals contents in soils and stream bed sediments of Cornia, Bruna and Alma coastal plains (Southern Tuscany). In *E3S Web of Conferences*, vol. 1. EDP Sciences. DOI/URL: http://dx.doi.org/10.1051/e3sconf/20130135005

Dupin, A., Girardclos, O., Fruchart, C., Laplaige, C., Nuninger, L., Dufraisse, A., & Gauthier, E. (2017). Anthracology of charcoal kilns in the forest of Chailluz (France) as a tool to understand Franche-Comte forestry from the mid-15th to the early 20th century AD. *Quaternary International*, *458*, 200–213. DOI/URL: https://doi.org/10.1016%2Fj.quaint.2017.03.008

Durand, A., Duval, S., & Vaschalde, C. (2009). Le charbonnage des Ericacées méditerranéennes : approches croisées archéologiques, anthracologiques et historiques. In D. Cl, T.-P. I, & T. St (Eds.) *Des hommes et des plantes. Exploitation du milieu et gestion des ressources végétales de la Préhistoire à nos jours. XXXe Rencontres internationales d'histoire et d'archéologie d'Antibes*, Rencontres internationales d'histoire et d'archéologie d'Antibes, (pp. 323–331). Antibes. DOI/URL: https://hal.archives-ouvertes.fr/hal-00562670

Dusar, B., Verstraeten, G., D'haen, K., Bakker, J., Kaptijn, E., & Waelkens, M. (2012). Sensitivity of the Eastern Mediterranean geomorphic system towards environmental change during the Late Holocene: a chronological perspective. *Journal of Quaternary Science*, *27*(4), 371–382. DOI/URL: https://doi.org/10.1002%2Fjqs.1555

Duzgoren-Aydin, N. S., Aydin, A., & Malpas, J. (2002). Re-assessment of chemical weathering indices: case study on pyroclastic rocks of Hong Kong. *Engineering Geology*, *63*(1), 99–119. DOI/URL: https://doi.org/10.1016%2FS0013-7952(01)00073-4

Earth Resources Observation and Science Center/U S. Geological Survey/U S. Department of the Interior (1997). USGS 30 ARC-second Global Elevation Data, GTOPO30. DOI/URL: http://dx.doi.org/10.5065/A1Z4-EE71

Edmondson, J. C. (1989). Mining in the Later Roman Empire and beyond: Continuity or Disruption? *The Journal of Roman Studies*, *79*, 84–102. DOI/URL: https://doi.org/10.2307%2F301182

Edwards, R. J. (2007). SEA LEVEL STUDIES \textbar Low Energy Coasts Sedimentary Indicators. In S. A. Elias (Ed.) *Encyclopedia of Quaternary Science*, (pp. 2994–3006). Oxford: Elsevier.
DOI/URL: http://dx.doi.org/10.1016/B0-44-452747-8/00145-9

Egozcue, J. J., Pawlowsky-Glahn, V., Mateu-Figueras, G., & Barceló-Vidal, C. (2003). Isometric Logratio Transformations for Compositional Data Analysis. *Mathematical Geology*, *35*(3), 279–300.
DOI/URL: https://doi.org/10.1023/A:1023818214614

Eichhorn, B., & Robion-Brunner, C. (2017). Wood exploitation in a major pre-colonial West African iron production centre (Bassar, Togo). *Quaternary International*, *458*, 158–177.
DOI/URL: https://doi.org/10.1016/j.quaint.2017.06.02810.1016/j.quaint.2017.08.073

Eichhorn, B., Robion-Brunner, C., Serneels, V., & Perret, S. (2013a). Fuel for Iron: Wood Exploitation for Metallurgy on the Dogon Plateau, Mali. In J. Humphris, & T. Rehren (Eds.) *The World of Iron*, (pp. 435–443). London: Archetype.

Eichhorn, B., Robion-Brunner, C., Serneels, V., & Perret, S. (2013b). Iron Metallurgy in the Dogon Country (Mali, West Africa): "Deforestation" or Sustainable Use? In F. Damblon (Ed.) *Proceedings of the 4th International Meeting of Anthracology, Brussels 8-13 september 2008, Royal Belgian Institute of Natural Sciences*, no. 2486 in British Archaeological Reports. International Series, (pp. 57–70). Oxford: Archaeopress.

Elbaz-Poulichet, F., Dezileau, L., Freydier, R., Cossa, D., & Sabatier, P. (2011). A 3500-year record of Hg and Pb contamination in a mediterranean sedimentary archive (the Pierre Blanche Lagoon, France). *Environmental Science & Technology*, *45*(20), 8642–8647.
DOI/URL: https://doi.org/10.1021%2Fes2004599

Ellis, A. R., Burchett, W. W., Harrar, S. W., & Bathke, A. C. (2017). Nonparametric inference for multivariate data: the R package npmv. *Journal of Statistical Software*, *76*(4), 1–18.

EMODnet Bathymetry Consortium (2018). *EMODnet Digital Bathymetry (DTM 2018)*. EMODnet Bathymetry Consortium.
DOI/URL: http://dx.doi.org/10.12770/18ff0d48-b203-4a65-94a9-5fd8b0ec35f6

Erb, K.-H. (2012). How a socio-ecological metabolism approach can help to advance our understanding of changes in land-use intensity. *Ecological Economics*, *76-341*, 8.
DOI/URL: https://doi.org/10.1016%2Fj.ecolecon.2012.02.005

Eriksson, M. G., Olley, J. M., & Payton, R. W. (2000). Soil erosion history in central Tanzania based on OSL dating of colluvial and alluvial hillslope deposits. *Geomorphology*, *36*(1), 107–128.
DOI/URL: https://doi.org/10.1016%2FS0169-555X(00)00054-4

Eser, R. A., & Becker, F. (submitted). New Insights into an Old Iron Mining Landscape: Elba Island. In *Proceedings of the 19th International Congress of Classical Archaeology*.

Etiégni, L., & Campbell, A. G. (1991). Physical and chemical characteristics of wood ash. *Bioresource Technology*, *37*(2), 173–178.
DOI/URL: https://doi.org/10.1016%2F0960-8524(91)90207-Z

Ettrich, E. (2006). Ökologie. In *Mensch und Landschaft in der Antike: Lexikon der Historischen Geographie*, J.B. Metzler Humanities (German Language), (pp. 378–379). Stuttgart: J.B. Metzler.
DOI/URL: https://doi.org/10.1007/978-3-476-00218-1

F. F. (1814). *Möglichst genaue Beschreibung der merkwürdigen Insel Elba und ihrer Bewohner*. Berlin: Fr. Frankesche Buchhandlung.
DOI/URL: http://mdz-nbn-resolving.de/urn:nbn:de:bvb:12-bsb10717838-2

Fairhead, J., & Leach, M. (1995). False forest history, complicit social analysis: Rethinking some West African environmental narratives. *World Development*, *23*(6), 1023–1035.
DOI/URL: https://doi.org/10.1016%2F0305-750X(95)00026-9

Farina, F. (2008). *Building the Monte Capanne pluton (Elba Island, Italy) by multiple magma batches: emplacement and petrogenetic implications*. Tesi di dottorato di ricerca, Università di Pisa, Pisa.
DOI/URL: https://etd.adm.unipi.it/t/etd-03012008-113728/

Fay, A. H. (1920). *A Glossary of the Mining and Mineral Industry*. No. 95 in Bureau of Mines Bulletin. U.S. Government Printing Office. Google-Books-ID: W1yAKxdeu3oC.

Ferriday, T., & Montenari, M. (2016). Chapter Three - Chemostratigraphy and Chemofacies of Source Rock Analogues: A High-Resolution Analysis of Black Shale Successions from the Lower Silurian Formigoso Formation (Cantabrian Mountains, NW Spain). In M. Montenari (Ed.) *Stratigraphy & Timescales*, vol. 1, (pp. 123–255). Academic Press.
DOI/URL: https://doi.org/10.1016/bs.sats.2016.10.004

Ferruzzi, S. (2010). *Signum: Elba Occidentale: Percorsi storici sulle tracce della toponomastica*. o. O.

Ferruzzi, S., & Carpinacci, F. (2018). *Caprili dell'Elba. Storia della pastorizia nel versante occidentale*. No. 130 in Elba sconosciuta. Capoliveri: Persephone Edizioni.

Figueiral, I., & Mosbrugger, V. (2000). A review of charcoal analysis as a tool for assessing Quaternary and Tertiary environments: achievements and limits. *Palaeogeography, Palaeoclimatology, Palaeoecology*, *164*(1), 397–407.
DOI/URL: https://doi.org/10.1016%2FS0031-0182(00)00195-4

Filzmoser, P., Hron, K., & Reimann, C. (2009). Univariate statistical analysis of environmental (compositional) data: Problems and possibilities. *Science of The Total Environment*, *407*(23), 6100–6108.
DOI/URL: https://doi.org/10.1016%2Fj.scitotenv.2009.08.008

Finch, H., & French, B. (2013). A Monte Carlo Comparison of Robust MANOVA Test Statistics. *Journal of Modern Applied Statistical Methods*, *12*(2).
DOI/URL: https://doi.org/10.22237%2Fjmasm%2F1383278580

Finsinger, W., Colombaroli, D., Beaulieu, J.-L. D., Valsecchi, V., Vannière, B., Vescovi, E., Chapron, E., Lotter, A. F., Magny, M., & Tinner, W. (2010). Early to mid-Holocene climate change at Lago dell'Accesa (central Italy): climate signal or anthropogenic bias? *Journal of Quaternary Science*, *25*(8), 1239–1247.
DOI/URL: https://doi.org/10.1002%2Fjqs.1402

Firmati, M., Principe, C., & Arrighi, S. (2006). L'impianto metallurgico tardorepubblicano di San Bennato all'isola d'Elba. *AGOGE', Atti della Scuola di Specializzazione in Archeologia dell'Università di Pisa*, *3*, 301–313.

Fischer-Kowalski, M., & Erb, K.-H. (2016). Core Concepts and Heuristics. In H. Haberl, M. Fischer-Kowalski, F. Krausmann, & V. Winiwarter (Eds.) *Social Ecology : Society-Nature Relations Across Time and Space*, Human-environment Interactions. Cham: Springer International Publishing.
DOI/URL: https://doi.org/10.1007/978-3-319-33326-7_2

Fischer-Kowalski, M., & Haberl, H. (1997). Tons, joules, and money: Modes of production and their sustainability problems. *Society & Natural Resources*, *10*(1), 61–85.
DOI/URL: https://doi.org/10.1080%2F08941929709381009

Fischer-Kowalski, M., & Weisz, H. (1998). Gesellschaft als Verzahnung materieller und symbolischer Welten. In K.-W. Brand (Ed.) *Soziologie und Natur: Theoretische Perspektiven*, Soziologie und Ökologie, (pp. 145–172). Wiesbaden: VS Verlag für Sozialwissenschaften.
DOI/URL: https://doi.org/10.1007/978-3-663-11442-0_7

Fischer-Kowalski, M., & Weisz, H. (2005). Society as Hybrid Between Material and Symbolic Realms. Toward a Theoretical Framework of Society-Nature Interrelation. In *New Developments in Environmental Sociology. Edward Elgar. Cheltenhem and Northampton. pp. 113 - 149, reprinted from Advances in Human Ecology 8,* (pp. 113–149).

Florsch, N., Llubes, M., Téreygeol, F., Ghorbani, A., & Roblet, P. (2011). Quantification of slag heap volumes and masses through the use of induced polarization: application to the Castel-Minier site. *Journal of Archaeological Science*, *38*(2), 438–451.
DOI/URL: http://www.sciencedirect.com/science/article/pii/S0305440310003535

Foard, G. (2001). Medieval Woodland, Agriculture and Industry in Rockingham Forest, Northamptonshire. *Medieval Archaeology*, *45*(1), 41–95.
DOI/URL: https://doi.org/10.1179/med.2001.45.1.41

Foggi, B., Cartei, L., Pignotti, L., Signorini, M., Viciani, D., Dell'Olmo, L., & Menicagli, E. (2006a). Il paesaggio vegetale dell'Isola d'Elba (Arcipelago Toscano): Studio di fitosociologia e cartografico. *Fitosociologia*, *43*(1 Suppl. 1), 3–95.

Foggi, B., Cartei, L., Pignotti, L., Signorini, M. A., Viciani, D., & Dell'Olmo, L. (2006b). *Carta della vegetazione dell'Isola d'Elba (Arcipelago Toscano). Scala 1:25.000*. Firenze: Dipartimento di Biologia Vegetale, Università di Firenze.

Fontana, A., Mozzi, P., & Bondesan, A. (2008). Alluvial megafans in the Venetian–Friulian Plain (north-eastern Italy): Evidence of sedimentary and erosive phases during Late Pleistocene and Holocene. *Quaternary International*, *189*(1), 71–90.
DOI/URL: https://doi.org/10.1016%2Fj.quaint.2007.08.044

Food and Agriculture Organization of the United Nations (1983). *Simple technologies for charcoal making*. No. 41 in FAO forestry paper. Roma: Food and Agriculture Organization of the United Nations.

Forbes, R. J. (1964). *Metallurgy in Antiquity: A Notebook for Archaeologists and Technologists*. Brill Archive.

Forbiger, A. (1857). *Strabo's Erdbeschreibung übersetzt und durch Anmerkungen erläutert. Buch 3.–5.*, vol. 2. Stuttgart: Hoffmann'sche Verlags-Buchhandlung.
DOI/URL: http://mdz-nbn-resolving.de/urn:nbn:de:bvb:12-bsb10238311-0

Fox, J., & Weisberg, S. (2011). *An R Companion to Applied Regression*. Thousand Oaks, CA: Sage, 2nd ed.
DOI/URL: http://socserv.socsci.mcmaster.ca/jfox/Books/Companion

Freise, F. (1907). Geographische Verbreitung und wirtschaftliche Entwicklung des süd- und mitteleuropäischen Bergbaus im Altertum. *Zeitschrift für das Berg-, Hütten- und Salinenwesen im preussischen Staat*, *55*, 199–268.

Friedrich, I., Cyffka, B., & Zollinger, G. (2000). Rezenter Landnutzungswandel auf der Insel Elba – Auswirkungen und Bedeutung für Mensch und Natur. In *Aktuelle Beiträge zur angewandten Phyischen Geographie der Tropen, Subtropen und Reigio Trirhena. Festschrift zum 60. Geburtstag von Prof. Dr. Rüdiger Mäckel*, no. 60 in Freiburger Geographische Hefte, (pp. 223–240). Freiburg i. Br.: Selbstverlag des Instituts für Physische Geographie der Albert-Ludwigs-Universiät Freiburg i. Br.

Frisch, W., Meschede, M., & Kuhlemann, J. (2008). *Elba: Geologie, Struktur, Exkursionen und Natur*, vol. 98 of *Sammlung geologischer Führer*. Berlin: Borntraeger.

Fryirs, K. (2013). (Dis)Connectivity in catchment sediment cascades: a fresh look at the sediment delivery problem. *Earth Surface Processes and Landforms*, *38*(1), 30–46.
DOI/URL: https://doi.org/10.1002%2Fesp.3242

Fryirs, K. A., Brierley, G. J., Preston, N. J., & Kasai, M. (2007). Buffers, barriers and blankets: The (dis)connectivity of catchment-scale sediment cascades. *CATENA*, *70*(1), 49–67.
DOI/URL: https://doi.org/10.1016%2Fj.catena.2006.07.007

Gagnevin, D., Daly, J. S., & Poli, G. (2008). Insights into granite petrogenesis from quantitative assessment of the field distribution of enclaves, xenoliths and K-feldspar megacrysts in the Monte Capanne pluton, Italy. *Mineralogical Magazine*, *72*(4), 925–940.
DOI/URL: https://doi.org/10.1180%2Fminmag.2008.072.4.925

Galop, D., Carozza, L., Magny, M., & Guilaine, J. (2009). Rhythms and causalities of the anthropisation dynamics in Europe between 8500 and 2500calbp: Sociocultural and/or climatic assumptions. *Quaternary International*, *200*(1), 1–3.
DOI/URL: https://doi.org/10.1016%2Fj.quaint.2009.01.004

Garcin, Y., Deschamps, P., Ménot, G., de Saulieu, G., Schefuß, E., Sebag, D., Dupont, L. M., Oslisly, R., Brademann, B., Mbusnum, K. G., Onana, J.-M., Ako, A. A., Epp, L. S., Tjallingii, R., Strecker, M. R., Brauer, A., & Sachse, D. (2018a). Early anthropogenic impact on Western Central African rainforests 2,600 y ago. *Proceedings of the National Academy of Sciences*, *115*(13), 3261.
DOI/URL: https://doi.org/10.1073%2Fpnas.1715336115

Garcin, Y., Deschamps, P., Ménot, G., de Saulieu, G., Schefuß, E., Sebag, D., Dupont, L. M., Oslisly, R., Brademann, B., Mbusnum, K. G., Onana, J.-M., Ako, A. A., Epp, L. S., Tjallingii, R., Strecker, M. R., Brauer, A., & Sachse, D. (2018b). Reply to Clist et al.: Human activity is the most probable trigger of the late Holocene rainforest crisis in Western Central Africa. *Proceedings of the National*

Academy of Sciences, *115*(21), E4735.
DOI/URL: https://doi.org/10.1073%2Fpnas.1805582115

Garcin, Y., Deschamps, P., Ménot, G., de Saulieu, G., Schefuß, E., Sebag, D., Dupont, L. M., Oslisly, R., Brademann, B., Mbusnum, K. G., Onana, J.-M., Ako, A. A., Epp, L. S., Tjallingii, R., Strecker, M. R., Brauer, A., & Sachse, D. (2018c). Reply to Giresse et al.: No evidence for climate variability during the late Holocene rainforest crisis in Western Central Africa. *Proceedings of the National Academy of Sciences*, *115*(29), E6674.
DOI/URL: https://doi.org/10.1073%2Fpnas.1808481115

Gardner, R. H., & O'Neill, R. V. (1983). Parameter Uncertainty and Model Predictions: A Review of Monte Carlo Results. In M. B. Beck, & G. van Straten (Eds.) *Uncertainty and Forecasting of Water Quality*, (pp. 245–257). Berlin, Heidelberg: Springer Berlin Heidelberg.
DOI/URL: https://doi.org/10.1007/978-3-642-82054-0_11

Garnier, A., Eichhorn, B., & Robion-Brunner, C. (2018). Impact de l'activité métallurgique au cours du dernier millénaire sur un système fluvial soudano-guinéen. Étude multi-proxy des archives sédimentaires de la vallée du Tatré (pays bassar, Togo). *Géomorphologie : relief, processus, environnement*, *24*(3), 257–276.
DOI/URL: https://doi.org/10.4000%2Fgeomorphologie.12446

Gastón, A., Soriano, C., & Gómez-Miguel, V. (2009). Lithologic data improve plant species distribution models based on coarse-grained ocurrence data. *Forest Systems*, *18*(1), 42–49.
DOI/URL: https://doi.org/10.5424%2Ffs%2F2009181-01049

Gäbler, H.-E., & Schneider, J. (2000). Assessment of heavy-metal contamination of floodplain soils due to mining and mineral processing in the Harz Mountains, Germany. *Environmental Geology*, *39*(7), 774–782.
DOI/URL: https://doi.org/10.1007%2Fs002540050493

Gelegdorj, E., Chunag, A., Gordon, R. B., & Park, J.-S. (2007). Transitions in cast iron technology of the nomads in Mongolia. *Journal of Archaeological Science*, *34*(8), 1187–1196.
DOI/URL: https://doi.org/10.1016/j.jas.2006.10.007

Genovese, A., & Mellini, M. (2007). Ferrihydrite flocs, native copper nanocrystals and spontaneous remediation in the Fosso dei Noni stream, Tuscany, Italy. *Applied Geochemistry*, *22*(7), 1439–1450.
DOI/URL: https://doi.org/10.1016%2Fj.apgeochem.2007.01.007

Gentini, U. (2014). La nascita dell'industria siderurgica all'isola d'Elba. *lo scoglio. Elba ieri, oggi, domani*, *102*, 26–32.

Gerngross, E. (1959). *Die Insel Elba, eine landes- und wirtschaftskundliche Übersicht*. München: Steinbauer & Hagemann.

Giardi, A., Pranzini, G., & Serretti, L. (1983). Salt water intrusion in the coastal plains of Versilia and Elba Island (Tuscany). In *Proceddings of the 8th saltwater intrusion meeting, Bari, 25–29 May 1983*, vol. 2, (pp. 335–352). Bari: Istituto di geologia applicata e geotecnica, Università di Bari.

Giardino, C. (2005). Metallurgy in Italy Between the Late Bronze Age and the Early Iron Age. The Coming of Iron. In P. Attema, A. J. Nijboer, & A. Zifferero (Eds.) *Papers in Italian archaeology VI: Proceedings of the 6th Conference of Italian Archaeology*, British Archaeological Reports. International Series, (pp. 491–505). Oxford: Archaeopress.

Gilgen, A., Wilkenskjeld, S., Kaplan, J. O., Kühn, T., & Lohmann, U. (2019). Did the Roman Empire affect European climate? A new look at the effects of land use and anthropogenic aerosol emissions. *Climate of the Past Discussions*, (pp. 1–36). DOI/URL: https://doi.org/10.5194/cp-2019-56

Gill, D., Shomrony, A., & Fligelman, H. (1993). Numerical Zonation of Log Suites and Logfacies Recognition by Multivariate Clustering. *AAPG Bulletin-American Association of Petroleum Geologists*, *77*(10), 1781–1791.

Giménez-Forcada, E., Bencini, A., & Pranzini, G. (2010). Hydrogeochemical considerations about the origin of groundwater salinization in some coastal plains of Elba Island (Tuscany, Italy). *Environmental Geochemistry and Health*, *32*(3), 243–257. DOI/URL: https://doi.org/10.1007/s10653-009-9281-2

Giovannelli, M. (1771). Breve relazione Dell'Isola dell'Elba nel Mediterraneo che l'Autore consacrar vorrebbe al Suo Augusto Sovrano nella seguente forma: Breve relazione Dell'Isola dell'Elba nel Mediterraneo Di un Ufiziale Del R. Servizio Di Toscana: Manoscritto nella Biblioteca Foresiana di Portoferraio.

Giraudi, C. (2005a). Late-Holocene alluvial events in the Central Apennines, Italy. *The Holocene*, *15*(5), 768–773. DOI/URL: https://doi.org/10.1191/0959683605hl850rr

Giraudi, C. (2005b). Middle to Late Holocene glacial variations, periglacial processes and alluvial sedimentation on the higher Apennine massifs (Italy). *Quaternary Research*, *64*(2), 176–184. DOI/URL: https://doi.org/10.1016%2Fj.yqres.2005.06.007

Giraudi, C. (2011). The sediments of the 'Stagno di Maccarese' marsh (Tiber river delta, central Italy): A late-Holocene record of natural and human-induced environmental changes. *The Holocene*, (pp. 1233–1243). DOI/URL: https://doi.org/10.1177%2F0959683611405235

Giraudi, C., Magny, M., Zanchetta, G., & Drysdale, R. (2011). The Holocene climatic evolution of Mediterranean Italy: A review of the continental geological data. *The Holocene*, *21*(1), 105–115. DOI/URL: https://doi.org/10.1177/0959683610377529

Giresse, P., Maley, J., Doumenge, C., Philippon, N., Mahé, G., Chepstow-Lusty, A., Aleman, J., Lokonda, M., & Elenga, H. (2018). Paleoclimatic changes are the most probable causes of the rainforest crises 2,600 y ago in Central Africa. *Proceedings of the National Academy of Sciences*, *115*(29), E6672–E6673. DOI/URL: https://doi.org/10.1073%2Fpnas.1807615115

Giroldini, P. (2012). Between Land and Sea: A GIS Based Settlement Analysis of the Ancient Coastal Lagoon of Piombino (Tuscany, Italy). *eTopoi. Journal for Ancient Studies*, *3*(Landscape Archaeology Conference (LAC 2012)), 383–389. DOI/URL: https://www.topoi.org/publication/20366/

Goldenberg, G. (1993). Frühe Umweltbelastungen durch Bergbau und Hüttenwesen. In H. Steuer (Ed.) *Alter Bergbau in Deutschland*, Archäologie in Deutschland Sonderheft, (pp. 107–113). Stuttgart: Theiss.

Gossellin, P. F. J., Adamantios, K., La Porte du Theil, F. J. G. d., & Letronne, A. J. (1809). *Géographie de Strabon*. Paris: L'Imprimerie royale.
DOI/URL: http://mdz-nbn-resolving.de/urn:nbn:de:bvb:12-bsb10712124-5

Goucher, C. L. (1981). Iron is iron'til it is rust: Trade and ecology in the decline of West African iron-smelting. *The Journal of African History*, *22*(2), 179–189.

Goudie, A. (2013). *Encyclopedia of Geomorphology*. Routledge.

Goudie, A. S., & Viles, H. A. (2016). *Geomorphology in the Anthropocene*. Cambridge University Press.

Graham, B., & Dam, R. V. (2019). Modelling the Supply of Wood Fuel in Ancient Rome. In M. Mulryan, & A. Izdebski (Eds.) *Environment and Society in the Long Late Antiquity*, (pp. 330–341). Leiden: Brill.
DOI/URL: http://dx.doi.org/10.1163/9789004392083_021

Grassi, S., & Netti, R. (2000). Sea water intrusion and mercury pollution of some coastal aquifers in the province of Grosseto (Southern Tuscany — Italy). *Journal of Hydrology*, *237*(3), 198–211.
DOI/URL: https://doi.org/10.1016%2FS0022-1694(00)00307-3

Grattan, J. P., Gilbertson, D. D., & Kent, M. (2013). Sedimentary metal-pollution signatures adjacent to the ancient centre of copper metallurgy at Khirbet Faynan in the desert of southern Jordan. *Journal of Archaeological Science*, *40*(11), 3834–3853.
DOI/URL: https://doi.org/10.1016%2Fj.jas.2012.12.022

Greene, K. (1986). *The archaeology of the Roman economy*. London: B.T. Batsford.

Gregorovius, F. (1864). *Wanderjahre in Italien*. Leipzig: Brockhaus.
DOI/URL: http://mdz-nbn-resolving.de/urn:nbn:de:bvb:12-bsb10080440-0

Grifoni Cremonesi, R. (2004). L'isola d'Elba e L'Arcipelago Toscano nella Preistoria. In S. Bruni, T. Caruso, & M. Massa (Eds.) *Archaeologica pisana*, Terra Italia, (pp. 229–236). Pisa: Giardini.

Grimm, E. C. (1987). CONISS: a FORTRAN 77 program for stratigraphically constrained cluster analysis by the method of incremental sum of squares. *Computers & Geosciences*, *13*(1), 13–35.
DOI/URL: https://doi.org/10.1016%2F0098-3004(87)90022-7

Groskurd, C. G. (1831). *Strabons Erdbeschreibung in siebenzehn Büchern; nach berichtigtem griechischen Texte unter Begleitung kritischer erklärender Anmerkungen verdeutscht*, vol. 1. Berlin, Stettin: Nicolaische Buchandlung.

Grove, A. T., & Rackham, O. (2003). *The Nature of Mediterranean Europe: An Ecological History*. Yale University Press.

Gu, B., Schmitt, J., Chen, Z., Liang, L., & McCarthy, J. F. (1994). Adsorption and desorption of natural organic matter on iron oxide: mechanisms and models. *Environmental Science & Technology*, *28*(1), 38–46.
DOI/URL: https://doi.org/10.1021/es00050a007

Guillon, R., Petit, C., Rajot, J.-L., Bichet, V., Sebag, D., Ide, O. A., & Garba, Z. (2013). Analyse de l'organisation spatiale de deux sites de production du fer dans le Sud-Ouest du Niger. *ArcheoSciences. Revue d'archéométrie*, (37), 123–135.
DOI/URL: https://doi.org/10.4000%2Farcheosciences.4015

Guralnik, D. B. (Ed.) (1986). *Webster's new world dictionary of the American language*. New York: Simon & Schuster, 2nd ed.

Haldon, J., Izdebski, A., Mordechai, L., & Newfield, T. (2019). Can historians work with environmental scientists? New insights for addressing climate change from interdisciplinary research.
DOI/URL: https://atlasofscience.org/can-historians-work-with-environmental-scientists-new-insights

Haldon, J., Mordechai, L., Newfield, T. P., Chase, A. F., Izdebski, A., Guzowski, P., Labuhn, I., & Roberts, N. (2018). History meets palaeoscience: Consilience and collaboration in studying past societal responses to environmental change. *Proceedings of the National Academy of Sciences*, *115*(13), 3210–3218.
DOI/URL: https://doi.org/10.1073%2Fpnas.1716912115

Hall, F. (1837). Notes on a tour in France, Italy, and Elba, with a notice of its mines of iron. *from the American Journal of Science and Arts*, *32*(1).
DOI/URL: http://hdl.handle.net/2027/loc.ark:/13960/t9w09kb46

Hall, G. E. M., Bonham-Carter, G. F., & Buchar, A. (2014). Evaluation of portable X-ray fluorescence (pXRF) in exploration and mining: Phase 1, control reference materials. *Geochemistry: Exploration, Environment, Analysis*, *14*(2), 99–123.
DOI/URL: https://doi.org/10.1144%2Fgeochem2013-241

Hamilton, H. (1903). *The Geography of Strabo*. London: George Bell & Sons.
DOI/URL: http://data.perseus.org/citations/urn:cts:greekLit:tlg0099.tlg001.perseus-eng2:5.2.6

Hammersley, G. (1973). The Charcoal Iron Industry and Its Fuel, 1540-1750. *The Economic History Review*, *26*(4), 593–613.
DOI/URL: https://doi.org/10.2307%2F2593700

Hanesch, M., & Scholger, R. (2005). The influence of soil type on the magnetic susceptibility measured throughout soil profiles. *Geophysical Journal International*, *161*(1), 50–56.
DOI/URL: https://doi.org/10.1111%2Fj.1365-246X.2005.02577.x

Hardy, B., Cornelis, J.-T., Houben, D., Lambert, R., & Dufey, J. E. (2016). The effect of pre-industrial charcoal kilns on chemical properties of forest soil of Wallonia, Belgium. *European Journal of Soil Science*, *67*(2), 206–216.
DOI/URL: https://doi.org/10.1111%2Fejss.12324

Hardy, B., Cornelis, J.-T., Houben, D., Leifeld, J., Lambert, R., & Dufey, J. E. (2017). Evaluation of the long-term effect of biochar on properties of temperate agricultural soil at pre-industrial charcoal kiln sites in Wallonia, Belgium. *European Journal of Soil Science*, *68*(1), 80–89.
DOI/URL: https://doi.org/10.1111%2Fejss.12395

Harris, W. V. (2011). Bois et déboisement dans la Méditerranée antique. *Annales. Histoire, Sciences Sociales*, *66e année*(1), 105–140.
DOI/URL: https://doi.org/10.3917/anna.661.0105

Harris, W. V. (2013). Defining and detecting mediterranean deforestation, 800 BCE to 700 CE. In W. V. Harris (Ed.) *The Ancient Mediterranean Environment between Science and History*, (pp. 173–194). Leiden, Boston: Brill.

Harrison, A. P., Cattani, I., & Turfa, J. M. (2010). Metallurgy, environmental pollution and the decline of Etruscan civilisation. *Environmental Science and Pollution Research*, *17*(1), 165–180.
DOI/URL: http://dx.doi.org/10.1007/s11356-009-0141-5

Harrison, F. A. (1931). Ancient Mining Activities in Portugal. *The Mining Magazine*, *45*(3), 137–145.

Hartmann, N. B. (1982). *Iron-working in Southern Etruria in the Ninth and Eighth Centuries B.C.*. Disseration, University of, Philadelphia.

Hartshorne, R. (1928). Location Factors in the Iron and Steel Industry. *Economic Geography*, *4*(3), 241–252.
DOI/URL: https://doi.org/10.2307%2F140295

Haupt, T. (1888). Der Bergbau der Etrusker, dargestellt nach Erfahrungen, directen geschichtlichen Nachrichten und mittelbaren Folgerungen. *Berg- und Hüttenmännische Zeitung*, *47*.

Healy, J. F. (1978). *Mining and Metallurgy in the Greek and Roman World*. Aspects of Greek and Roman Life. London: Thames & Hudson.

Heiri, O., Lotter, A. F., & Lemcke, G. (2001). Loss on ignition as a method for estimating organic and carbonate content in sediments: reproducibility and comparability of results. *Journal of Paleolimnology*, *25*(1), 101–110.
DOI/URL: https://doi.org/10.1023/A:1008119611481

Hemker, C., & Lentzsch, S. (2012). „Holz ist ein Bedürfniß im Bergbau . . . ". Holzverwendung in den hochmittelalterlichen Silberbergwerken von Dippoldiswalde/Sachsen. *Mitteilungen der Deutschen Gesellschaft für Archäologie des Mittelalters und der Neuzeit*, *24*, 273–282.
DOI/URL: https://doi.org/10.11588%2Fdgamn.2012.1.17171

Herzog, I. (2014). Least-cost Paths – Some Methodological Issues. *Internet Archaeology*, (36).
DOI/URL: https://doi.org/10.11141%2Fia.36.5

Hinz, M., Feeser, I., Sjögren, K.-G., & Müller, J. (2012). Demography and the intensity of cultural activities: an evaluation of Funnel Beaker Societies (4200–2800 cal BC). *Journal of Archaeological Science*, *39*(10), 3331–3340.
DOI/URL: https://doi.org/10.1016%2Fj.jas.2012.05.028

Hirsch, F., Raab, T., Ouimet, W., Dethier, D., Schneider, A., & Raab, A. (2017). Soils on Historic Charcoal Hearths: Terminology and Chemical Properties. *Soil Science Society of America Journal*, *81*(6), 1427–1435.
DOI/URL: https://doi.org/10.2136%2Fsssaj2017.02.0067

Hoelzmann, P., Klein, T., Kutz, F., & Schütt, B. (2017). A new device to mount portable energy-dispersive X-ray fluorescence spectrometers (p-ED-XRF) for semi-continuous analyses of split (sediment) cores and solid samples. *Geoscientific Instrumentation, Methods and Data Systems*, *6*(1), 93–101.
DOI/URL: https://doi.org/10.5194%2Fgi-6-93-2017

Hoffmann, T., Erkens, G., Gerlach, R., Klostermann, J., & Lang, A. (2009). Trends and controls of Holocene floodplain sedimentation in the Rhine catchment. *CATENA*, *77*(2), 96–106.
DOI/URL: https://doi.org/10.1016%2Fj.catena.2008.09.002

Hoffmann, T., Lang, A., & Dikau, R. (2008). Holocene river activity: analysing 14c-dated fluvial and colluvial sediments from Germany. *Quaternary Science Reviews*, *27*(21), 2031–2040.
DOI/URL: https://doi.org/10.1016%2Fj.quascirev.2008.06.014

Hong, S., Candelone, J.-P., Soutif, M., & Boutron, C. F. (1996). A reconstruction of changes in copper production and copper emissions to the atmosphere during the past 7000 years. *Science of The Total Environment*, *188*(2), 183–193.
DOI/URL: https://doi.org/10.1016%2F0048-9697(96)05171-6

Hopper, R. J. (1968). The Laurion Mines: A Reconsideration. *Annual of the British School at Athens*, *63*, 293–326.
DOI/URL: https://doi.org/10.1017%2FS006824540001443X

Horden, P., & Purcell, N. (2000). *The Corrupting Sea: A Study of Mediterranean History*. Oxford, U.K. ; Malden, MS: Blackwell Publishers.

Horne, L. (1982). Fuel for the Metal Worker: The Role of Charcoal and Charcoal Production in Ancient Metallurgy. *Expedition. The Magazine of Archaeology, Anthropology*, *25*(1), 6–13.

Horrocks, M., Baisden, T., Flenley, J., Feek, D., Love, C., Haoa-Cardinali, S., Nualart, L. G., & Gorman, T. E. (2017). Pollen, phytolith and starch analyses of dryland soils from Easter Island (Rapa Nui) show widespread vegetation clearance and Polynesian-introduced crops. *Palynology*, *41*(3), 339–350.
DOI/URL: https://doi.org/10.1080/01916122.2016.1204566

Hürkamp, K., Raab, T., & Völkel, J. (2009). Two and three-dimensional quantification of lead contamination in alluvial soils of a historic mining area using field portable X-ray fluorescence (FPXRF) analysis. *Geomorphology*, *110*(1-2), 28–36.
DOI/URL: https://doi.org/10.1016%2Fj.geomorph.2008.12.021

Héron De Villefosse, A.-M. (1819). *Atlas de la richesse minérale : recueil de faits géognostiques et de faits industriels, constatant l'état actuel de l'art des mines et usines, par des exemples authentiques, tirés de célèbres établissemens, et rendus sensibles à l'œil, au moyen de la représentation géométrique des objets*. s.n.
DOI/URL: http://www.e-rara.ch/zut/doi/10.3931/e-rara-53002

Hudson-Edwards, K., Macklin, M., & Taylor, M. (1997). Historic metal mining inputs to Tees river sediment. *Science of The Total Environment*, *194-195*, 437–445.
DOI/URL: https://doi.org/10.1016%2FS0048-9697(96)05381-8

Hughes, J. D. (1983). How the ancients viewed deforestation. *Journal of Field Archaeology*, *10*(4), 435–445.
DOI/URL: https://doi.org/10.2307%2F529466

Hughes, J. D. (2011). Ancient Deforestation Revisited. *Journal of the History of Biology*, *44*(1), 43–57.
DOI/URL: https://doi.org/10.1007%2Fs10739-010-9247-3

Hughes, J. D. (2014). *Environmental Problems of the Greeks and Romans: Ecology in the Ancient Mediterranean*. JHU Press.

Hughes, J. D., & Thirgood, J. V. (1982). Deforestation, Erosion, and Forest Management in Ancient Greece and Rome. *Journal of Forest History*, *26*(2), 60–75. DOI/URL: https://doi.org/10.2307%2F4004530

Hughes, R. E., Weiberg, E., Bonnier, A., Finné, M., & Kaplan, J. O. (2018). Quantifying Land Use in Past Societies from Cultural Practice and Archaeological Data. *Land*, *7*(1), 9. DOI/URL: https://doi.org/10.3390%2Fland7010009

Humphris, J., & Carey, C. (2016). New Methods for Investigating Slag Heaps: Integrating Geoprospection, Excavation and Quantitative Methods at Meroe, Sudan. *Journal of Archaeological Science*, *70*, 132–144. DOI/URL: https://doi.org/10.1016%2Fj.jas.2016.04.022

Humphris, J., & Eichhorn, B. (2019). Fuel selection during long-term ancient iron production in Sudan. *Azania: Archaeological Research in Africa*, *54*(1), 33–54. DOI/URL: https://doi.org/10.1080/0067270X.2019.1578567

Hunt, A. M. W., & Speakman, R. J. (2015). Portable XRF analysis of archaeological sediments and ceramics. *Journal of Archaeological Science*, *53*, 626–638. DOI/URL: https://doi.org/10.1016%2Fj.jas.2014.11.031

Hunt, C., & Gilbertson, D. (1995). Human activity, landscape change and valley alluviation in the Feccia Valley, Tuscany, Italy. Refereed Proceedings of an International conference University of Cambridge / United Kingdom, 28–29 September 1992. In J. Lewin, M. M. Macklin, & J. C. Woodward (Eds.) *Mediterranean Quaternary River Environments*, (pp. 167–178). Rotterdam, Brookfield: A. A. Balkema.

Iles, L. (2014). The Use of Plants in Iron Production: Insights from Smelting Remains from Buganda. In C. J. Stevens, S. Nixon, M. A. Murray, & D. Q. Fuller (Eds.) *Archaeology of African Plant Use*, Publications of the Institute of Archaeology, University College London, (pp. 267–274). Walnut Creek/CA: Left Coast Press.

Iles, L. (2016). The Role of Metallurgy in Transforming Global Forests. *Journal of Archaeological Method and Theory*, *23*(4), 1219–1241. DOI/URL: https://doi.org/10.1007%2Fs10816-015-9266-7

Iles, L. (2017). African Iron Production and Iron-Working Technologies: Methods. *Oxford Research Encyclopedia of African History*. DOI/URL: https://dx.doi.org/10.1093/acrefore/9780190277734.013.212

Iles, L., Stump, D., Heckmann, M., Lang, C., & Lane, P. J. (2018). Iron Production in North Pare, Tanzania: Archaeometallurgical and Geoarchaeological Perspectives on Landscape Change. *African Archaeological Review*, *35*(4), 507–530. DOI/URL: https://doi.org/10.1007/s10437-018-9312-4

Isard, W. (1948). Some Locational Factors in the Iron and Steel Industry since the Early Nineteenth Century. *Journal of Political Economy*, *56*(3), 203–217. DOI/URL: https://www.jstor.org/stable/1825770

Jackson, J. A. (1997). *Glossary of geology*. Alexandria, Va.: American Geological Inst, 4th ed.

Jackson, N. L., Nordstrom, K. F., Pranzini, E., & Rosas, V. (2013). Dinamica morfologica e sedimentologica della spiaggia di Lacona (Isola d'Elba) e impatto dell'alluvione del 2002. *Studi costieri*, *21*, 55–70.

Jalut, G., Dedoubat, J. J., Fontugne, M., & Otto, T. (2009). Holocene circum-Mediterranean vegetation changes: Climate forcing and human impact. *Quaternary International*, *200*(1), 4–18.
DOI/URL: https://doi.org/10.1016%2Fj.quaint.2008.03.012

Janssen, E., Poblome, J., Claeys, J., Kint, V., Degryse, P., Marinova, E., & Muys, B. (2017). Fuel for debating ancient economies. Calculating wood consumption at urban scale in Roman Imperial times. *Journal of Archaeological Science: Reports*, *11*, 592–599.
DOI/URL: https://doi.org/10.1016%2Fj.jasrep.2016.12.029

Jarmer, T., & Schütt, B. (1998). Analysis of iron contents in carbonate bedrock by spectroradiometric detection based on experimentally designed substrates. In *1st EARSeL Workshop on Imaging Spectroscopy*, (pp. 375–382).

Jasiewicz, J., & Stepinski, T. F. (2013). Geomorphons — a pattern recognition approach to classification and mapping of landforms. *Geomorphology*, *182*, 147–156.
DOI/URL: https://doi.org/10.1016%2Fj.geomorph.2012.11.005

Jervis, W. P. (1860). Metalliferous Minerals; including the History of the Mines of the Tuscan Archipelago, from the earliest period downt to the close of the Lorraine Dynasty, in 1859. *Journal of the Society of Arts*, *8*(406), 723–732.

Jervis, W. P. (1862). *The Mineral Resources of Central Italy: Including a Description of the Mines and Marble Quarries*. London: Stanford.

Jockenhövel, A. (1996). *Bergbau, Verhüttung und Waldnutzung im Mittelalter: Auswirkungen auf Mensch und Umwelt ; Ergebnisse eines internationalen Workshops (Dillenburg, 11.-15. Mai 1994, Wirtschaftshistorisches Museum "Villa Grün")*. No. 121 in Vierteljahrschrift für Sozial- und Wirtschaftsgeschichte. Beihefte. Stuttgart: Franz Steiner Verlag.

Johnson, J. (2014). Accurate Measurements of Low Z Elements in Sediments and Archaeological Ceramics Using Portable X-ray Fluorescence (PXRF). *Journal of Archaeological Method and Theory*, *21*(3), 563–588.
DOI/URL: https://doi.org/10.1007/s10816-012-9162-3

Johnstone, E., Macklin, M. G., & Lewin, J. (2006). The development and application of a database of radiocarbon-dated Holocene fluvial deposits in Great Britain. *CATENA*, *66*(1), 14–23.
DOI/URL: https://doi.org/10.1016%2Fj.catena.2005.07.006

Jones, A. F., Macklin, M. G., & Benito, G. (2015). Meta-analysis of Holocene fluvial sedimentary archives: A methodological primer. *CATENA*, *130*, 3–12.
DOI/URL: https://doi.org/10.1016%2Fj.catena.2014.11.018

Jones, H. L. (1923). *Strabo: Geography, Volume II: Books 3–5. Translated by Horance Leonard Jones*. No. 50 in Loeb Classical Library. Cambridge, MA: Harvard University Press.
DOI/URL: http://dx.doi.org/10.4159/DLCL.strabo-geography.1917

Jones, J. E. (1982). The Laurion Silver Mines: A Review of Recent Researches and Results. *Greece & Rome*, *29*(2), 169–183.
DOI/URL: https://www.jstor.org/stable/642341

Joosten, I., Jansen, J. B. H., & Kars, H. (1998). Geochemistry and the past: estimation of the output of a Germanic iron production site in the Netherlands. *Journal of Geochemical Exploration*, *62*(1–3), 129–137.
DOI/URL: https://doi.org/10.1016%2FS0375-6742(97)00043-5

Jørgensen, B. B. (1977). The sulfur cycle of a coastal marine sediment (Limfjorden, Denmark)1. *Limnology and Oceanography*, *22*(5), 814–832.
DOI/URL: https://doi.org/10.4319%2Flo.1977.22.5.0814

Judson, S. (1963). Erosion and Deposition of Italian Stream Valleys During Historic Time. *Science*, *140*(3569), 898–899.
DOI/URL: https://doi.org/10.1126%2Fscience.140.3569.898

Juggins, S. (2015). *rioja: Analysis of Quaternary Science Data [R package, v0.9-5]*.
DOI/URL: https://CRAN.R-project.org/package=rioja

Juleff, G. (1996). An ancient wind-powered iron smelting technology in Sri Lanka. *Nature*, *379*, 60.
DOI/URL: https://dx.doi.org/10.1038/379060a0

Kaiser, H. F. (1974). An index of factorial simplicity. *Psychometrika*, *39*(1), 31–36.
DOI/URL: https://doi.org/10.1007/BF02291575

Kale, V. S. (2007). Fluvio–sedimentary response of the monsoon-fed Indian rivers to Late Pleistocene–Holocene changes in monsoon strength: reconstruction based on existing 14c dates. *Quaternary Science Reviews*, *26*(11), 1610–1620.
DOI/URL: https://doi.org/10.1016%2Fj.quascirev.2007.03.012

Kalnicky, D. J., & Singhvi, R. (2001). Field portable XRF analysis of environmental samples. *Journal of Hazardous Materials*, *83*(1), 93–122.
DOI/URL: https://doi.org/10.1016%2FS0304-3894(00)00330-7

Kaniewski, D., Marriner, N., Morhange, C., Vacchi, M., Sarti, G., Rossi, V., Bini, M., Pasquinucci, M., Allinne, C., Otto, T., Luce, F., & Campo, E. V. (2018). Holocene evolution of Portus Pisanus , the lost harbour of Pisa. *Scientific Reports*, *8*(1), 11625.
DOI/URL: https://doi.org/10.1038%2Fs41598-018-29890-w

Karlsson, J., Rydberg, J., Segerström, U., Nordström, E.-M., Thöle, P., Biester, H., & Bindler, R. (2016). Tracing a bog-iron bloomery furnace in an adjacent lake-sediment record in Ängersjö, central Sweden, using pollen and geochemical signals. *Vegetation history and archaeobotany*, *25*(6), 569–581.
DOI/URL: https://doi.org/10.1007/s00334-016-0567-x

Kay, P. (2014). *Rome's Economic Revolution*. Oxford Studies on the Roman Economy. Oxford, New York: Oxford University Press.

Kennedy, W. M., Hahn, F., Graßhoff, G., Meyer, M., & Topoi, E. C. (2017). Quantifying Chronological Inconsistencies of Archaeological Sites in the Petra Area.
DOI/URL: http://edocs.fu-berlin.de/docs/receive/FUDOCS_document_000000026268

Kierczak, J., Neel, C., Bril, H., & Puziewicz, J. (2007). Effect of mineralogy and pedoclimatic variations on Ni and Cr distribution in serpentine soils under temperate climate. *Geoderma*, *142*(1), 165–177.
DOI/URL: https://doi.org/10.1016%2Fj.geoderma.2007.08.009

Kierczak, J., Potysz, A., Pietranik, A., Tyszka, R., Modelska, M., Néel, C., Ettler, V., & Mihaljevič, M. (2013). Environmental impact of the historical Cu smelting in the Rudawy Janowickie Mountains (south-western Poland). *Journal of Geochemical Exploration*, *124*, 183–194.
DOI/URL: https://doi.org/10.1016%2Fj.gexplo.2012.09.008

Kilbride, C., Poole, J., & Hutchings, T. R. (2006). A comparison of Cu, Pb, As, Cd, Zn, Fe, Ni and Mn determined by acid extraction/ICP–OES and ex situ field portable X-ray fluorescence analyses. *Environmental Pollution*, *143*(1), 16–23.
DOI/URL: https://doi.org/10.1016%2Fj.envpol.2005.11.013

Kimball, B., Bianchi, F., Walton-Day, K., Runkel, R., Nannucci, M., & Salvadori, A. (2007). Quantification of changes in metal loading from storm runoff, Merse River (Tuscany, Italy). *Mine Water and the Environment*, *26*(4), 8.
DOI/URL: https://doi.org/10.1007%2Fs10230-007-0020-6

Kleßen, R. (1993). Zur Geowissenschaftlichen Aussagemöglichkeit von Hüttenschlacken im rezenten Transportgut der Bode (Harz und Nördliches Vorland). In *Beiträge zur geomorphologischen Entwicklung des norddeutschen Tieflandes und des deutschen Mittelgebirgsraumes im Spätglazial und im Holozän. 18. Tagung des Deutschen Arbeitskreises für Geomorphologie (Gosen bei Berlin, 5.–8.10.1992)*, no. 78 in Berliner geographische Arbeiten, (pp. 193–209). Berlin: Fachbereich Geographie der Humboldt-Universität zu Berlin.

Kleßen, R., & Chrobok, S. M. (1989). Historische Hüttenstandorte im Mittelharz und ihre fluvial transportierbaren technogenen Gesteine. *Zeitschrift für angewandte Geologie*, *35*(1), 24–31.

Klein, J. (2002). Deforestation in the Madagascar Highlands – Established 'truth' and scientific uncertainty. *GeoJournal*, *56*(3), 191–199.
DOI/URL: https://doi.org/10.1023/A:1025187422687

Klein, T., Bebermeier, W., Krause, J., Marzoli, D., & Schütt, B. (2016). Sedimentological evidence of an assumed ancient anchorage in the hinterland of a Phoenician settlement (Guadiana estuary/SW-Spain). *Quaternary International*, *407*, 110–125.
DOI/URL: https://doi.org/10.1016%2Fj.quaint.2015.12.038

Klink, H.-J., Potschin, M., Tress, B., Tress, G., Volk, M., & Steinhardt, U. (2002). Landscape and landscape ecology. In O. Bastian, & U. Steinhardt (Eds.) *Development and Perspectives of Landscape Ecology*, (pp. 1–47). Dordrecht: Springer Netherlands.
DOI/URL: https://doi.org/10.1007/978-94-017-1237-8_1

Knudsen, A. (2011). Logging the 'Frontier': Narratives of Deforestation in the Northern Borderlands of British India, c. 1850–1940. *Forum for Development Studies*, *38*(3), 299–319.
DOI/URL: https://doi.org/10.1080/08039410.2011.577799

Krantz, A. A. (1841). Geognostische Beschreibung der Insel Elba. *Archiv für Mineralogie, Geognosie, Bergbau und Hüttenkunde*, *15*(2), 347–424.

Köstlin, C. H. (1780). *Lettres sur l'histoire naturelle de l'isle d'Elbe: ecrites à son excellence monsieur le Comte de Borch ...*. Wien: Jean Paul Kraus. Google-Books-ID: pps5AAAAcAAJ.
DOI/URL: http://data.onb.ac.at/rec/AC05719232

Kuhlbusch, T. A. J. (1995). Method for Determining Black Carbon in Residues of Vegetation Fires. *Environmental Science & Technology*, *29*(10), 2695–2702.
DOI/URL: https://doi.org/10.1021/es00010a034

Kumar, C. (2004). Narratives on deforestation-Contesting the conventional wisdom. *Social Change*, *34*(4), 86–92.
DOI/URL: https://doi.org/10.1177/004908570403400407

Kurth, V. J., MacKenzie, M. D., & DeLuca, T. H. (2006). Estimating charcoal content in forest mineral soils. *Geoderma*, *137*(1), 135–139.
DOI/URL: https://doi.org/10.1016%2Fj.geoderma.2006.08.003

Kynčlová, P., Hron, K., & Filzmoser, P. (2017). Correlation Between Compositional Parts Based on Symmetric Balances. *Mathematical Geosciences*, *49*(6), 777–796.
DOI/URL: https://doi.org/10.1007%2Fs11004-016-9669-3

Lalonde, K., Mucci, A., Ouellet, A., & Gélinas, Y. (2012). Preservation of organic matter in sediments promoted by iron. *Nature*, *483*(7388), 198–200.
DOI/URL: https://doi.org/10.1038%2Fnature10855

Lambardi, S. (1791). *Memorie antiche, e moderne dell'isola dell'Elba: Ricavate da vari autori e compilate*. Firenze.

Lambeck, K., Antonioli, F., Anzidei, M., Ferranti, L., Leoni, G., Scicchitano, G., & Silenzi, S. (2011). Sea level change along the Italian coast during the Holocene and projections for the future. *Quaternary International*, *232*(1), 250–257.
DOI/URL: https://doi.org/10.1016%2Fj.quaint.2010.04.026

Lambeck, K., & Purcell, A. (2005). Sea-level change in the Mediterranean Sea since the LGM: model predictions for tectonically stable areas. *Quaternary Science Reviews*, *24*(18–19), 1969–1988.
DOI/URL: https://doi.org/10.1016%2Fj.quascirev.2004.06.025

Lamboglia, N. (1955). Sulla cronologia delle anfore romane di età repubblicana (II - I secolo a. C.). *Rivista di studi iguri*, *21*(3-4), 241–270.

Lancelotti, C., Pecci, A., & Zurro, D. (2017). Anthropic Activity Markers: Archaeology and Ethnoarchaeology. *Environmental Archaeology*, *22*(4), 339–342.
DOI/URL: https://doi.org/10.1080/14614103.2017.1364207

Lane, K. F. (2016). *The Economic Definition of Ore: Cut-off Grades in Theory and Practice*. Cleveland, Australia: COMET Strategy.

Lane, P. (2009). Environmental Narratives and the History of Soil Erosion in Kondoa District, Tanzania: An Archaeological Perspective. *The International Journal of African Historical Studies*, *42*(3), 457–483.
DOI/URL: https://www.jstor.org/stable/40646778

Lang, A., & Hönscheidt, S. (1999). Age and source of colluvial sediments at Vaihingen–Enz, Germany. *CATENA*, *38*(2), 89–107.
DOI/URL: https://doi.org/10.1016%2FS0341-8162(99)00068-5

Lang, J. (2017). Roman iron and steel: A review. *Materials and Manufacturing Processes*, *32*(7-8), 857–866.
DOI/URL: https://doi.org/10.1080/10426914.2017.1279326

Lattanzi, P., Rimondi, V., Chiarantini, L., Colica, A., Benvenuti, M., Costagliola, P., & Ruggieri, G. (2017). Mercury Dispersion through Streams Draining The Mt. Amiata District, Southern Tuscany, Italy. *Procedia Earth and Planetary Science*, *17*, 468–471.
DOI/URL: https://doi.org/10.1016%2Fj.proeps.2016.12.118

Lauffer, S. (1979). *Die Bergwerkssklaven von Laureion*, vol. 11 of *Forschungen zur antiken Sklaverei*. Wiesbaden: Steiner, 2., durchges. und erw. aufl. ed.

Leenaers, H. (1989). *The dispersal of metal mining wastes in the catchment of the river Geul (Belgium - The Netherlands)*. No. 102 in Nederlandse Geografische Studies. Amsterdam: Koninklijk Nederlands Aardrijkskundig Genootschap.
DOI/URL: http://dspace.library.uu.nl/handle/1874/13821

Leibundgut, A. (1977). *Die römischen Lampen in der Schweiz: eine kultur- und handelsgeschichtliche Studie*. Handbuch der Schweiz zur Römer- und Merowingerzeit. Bern: Francke.

Leitch, V. (2019). Fuelling roman pottery kilns in britain and north africa: climatic, economic and traditional strategies. In R. Veal, & V. Leitch (Eds.) *Fuel and Fire in the Ancient Roman World – Towards an integrated economic understanding*, McDonald Institute Conversations, (pp. 53–62). McDonald Institute for Archaeological Research, University of Cambridge.

Lemière, B. (2018). A review of pXRF (field portable X-ray fluorescence) applications for applied geochemistry. *Journal of Geochemical Exploration*, *188*, 350–363.
DOI/URL: https://doi.org/10.1016%2Fj.gexplo.2018.02.006

Leoni, L., & Sartori, F. (1997). Heavy metal and arsenic distributions in sediments of the Elba-Argentario basin, southern Tuscany, Italy. *Environmental Geology*, *32*(2), 83–92.
DOI/URL: https://doi.org/10.1007%2Fs002540050196

Leoni, L., Sartori, F., Damiani, V., Ferretti, O., & Viel, M. (1991). Trace element distributions in surficial sediments of the northern Tyrrhenian Sea: Contribution to heavy-metal pollution assessment. *Environmental Geology and Water Sciences*, *17*(2), 103–116.
DOI/URL: https://doi.org/10.1007%2FBF01701566

Lespez, L., Le Drezen, Y., Garnier, A., Rasse, M., Eichhorn, B., Ozainne, S., Ballouche, A., Neumann, K., & Huysecom, E. (2011). High-resolution fluvial records of Holocene environmental changes in the Sahel: the Yamé River at Ounjougou (Mali, West Africa). *Quaternary Science Reviews*, *30*(5), 737–756.
DOI/URL: https://doi.org/10.1016%2Fj.quascirev.2010.12.021

Lewin, J., & Macklin, M. G. (1987). Metal mining and floodplain sedimentation in Britain. In V. Gardiner, & B. G. R. Group (Eds.) *International geomorphology 1986 – Proceedings of the first international conference on Geomorphology*, vol. 1, (pp. 1009–1027). Chichester, New York: John Wiley & Sons.

Lewin, J., & Macklin, M. G. (2003). Preservation potential for Late Quaternary river alluvium. *Journal of Quaternary Science*, *18*(2), 107–120.
DOI/URL: https://doi.org/10.1002%2Fjqs.738

Lohri, C. R., Rajabu, H. M., Sweeney, D. J., & Zurbrügg, C. (2016). Char fuel production in developing countries – A review of urban biowaste carbonization. *Renewable and Sustainable Energy Reviews*, *59*, 1514–1530.
DOI/URL: https://doi.org/10.1016%2Fj.rser.2016.01.088

Loring, D. H. (1991). Normalization of heavy-metal data from estuarine and coastal sediments. *ICES Journal of Marine Science*, *48*(1), 101–115.
DOI/URL: https://doi.org/10.1093%2Ficesjms%2F48.1.101

Lottermoser, B. (2013). *Mine Wastes: Characterization, Treatment and Environmental Impacts*. Springer Science & Business Media.

López-Buendía, A. M., Bastida, J., Querol, X., & Whateley, M. K. G. (1999). Geochemical data as indicators of palaeosalinity in coastal organic-rich sediments. *Chemical Geology*, *157*(3), 235–254.
DOI/URL: https://doi.org/10.1016%2FS0009-2541(98)00207-1

Lätsch, F. (2005). *Insularität und Gesellschaft in der Antike: Untersuchungen zur Auswirkung der Insellage auf die Gesellschaftsentwicklung*. No. Bd. 19 in Geographica historica. Stuttgart: F. Steiner.

Lubos, C., Dreibrodt, S., & Bahr, A. (2016). Analysing spatio-temporal patterns of archaeological soils and sediments by comparing pXRF and different ICP-OES extraction methods. *Journal of Archaeological Science: Reports*, *9*, 44–53.
DOI/URL: https://doi.org/10.1016%2Fj.jasrep.2016.06.037

Lupo, K. D., Schmitt, D. N., Kiahtipes, C. A., Ndanga, J.-P., Young, D. C., & Simiti, B. (2015). On Intensive Late Holocene Iron Mining and Production in the Northern Congo Basin and the Environmental Consequences Associated with Metallurgy in Central Africa. *PLoS ONE*, *10*(7).
DOI/URL: https://doi.org/10.1371%2Fjournal.pone.0132632

Luppi, A., & Salvati, L. (1987). I giacimenti ferriferi della costa orientale dell'Isola d'Elba come alimetatori di placers marini. *Bollettino del Servizio geologico d'Italia*, *105*, 267–278.

Luti, R. (2000). Ricerche sul territorio di Roselle per l'individuazione degli approdi dall'età etrusca a quella moderna. *Ricerche sul territorio di Roselle per l'individuazione degli approdi dall'età etrusca a quella moderna*, (pp. 1000–1051).
DOI/URL: https://doi.org/10.1400%2F19105

Lyaya, E. (2012). Bio-archaeometallurgy, Technology, and Spatial Organization of Ironworking at Mjimwema, Njombe Tanzania. *Papers from the Institute of Archaeology*, *21*(0), 59–79.
DOI/URL: https://doi.org/10.5334%2Fpia.380

Lynch, J. (1990). Provisional Elemental Values for Eight New Geochemical Lake Sediment and Stream Sediment Reference Materials LKSD-1, LKSD-2, LKSD-3, LKSD-4, STSD-1, STSD-2, STSD-3 and STSD-4*. *Geostandards Newsletter*, *14*(1), 153–167.
DOI/URL: https://doi.org/10.1111%2Fj.1751-908X.1990.tb00070.x

Lézine, A.-M., Holl, A. F. C., Lebamba, J., Vincens, A., Assi-Khaudjis, C., Février, L., & Sultan, m. (2013). Temporal relationship between Holocene human occupation and vegetation change along the northwestern margin of the Central African rainforest.

Comptes Rendus Geoscience, *345*(7), 327–335.
DOI/URL: https://doi.org/10.1016%2Fj.crte.2013.03.001

Mackie, K. A., Müller, T., & Kandeler, E. (2012). Remediation of copper in vineyards – A mini review. *Environmental Pollution*, *167*, 16–26.
DOI/URL: https://doi.org/10.1016%2Fj.envpol.2012.03.023

Macklin, M. G., Brewer, P. A., Balteanu, D., Coulthard, T. J., Driga, B., Howard, A. J., & Zaharia, S. (2003). The long term fate and environmental significance of contaminant metals released by the January and March 2000 mining tailings dam failures in Maramureş County, upper Tisa Basin, Romania. *Applied Geochemistry*, *18*(2), 241–257.
DOI/URL: https://doi.org/10.1016%2FS0883-2927(02)00123-3

Macklin, M. G., Brewer, P. A., Hudson-Edwards, K. A., Bird, G., Coulthard, T. J., Dennis, I. A., Lechler, P. J., Miller, J. R., & Turner, J. N. (2006). A geomorphological approach to the management of rivers contaminated by metal mining. *Geomorphology*, *79*(3), 423–447.
DOI/URL: https://doi.org/10.1016%2Fj.geomorph.2006.06.024

Macklin, M. G., Jones, A. F., & Lewin, J. (2010a). River response to rapid Holocene environmental change: evidence and explanation in British catchments. *Quaternary Science Reviews*, *29*(13), 1555–1576.
DOI/URL: https://doi.org/10.1016%2Fj.quascirev.2009.06.010

Macklin, M. G., Jones, A. F., & Lewin, J. (2011). Comment: Cumulative probability functions and their role in evaluating the chronology of geomorphological events during the Holocene. Richard C. Chiverrell, Varyl, R. Thorndycraft And Thomas, O. Hoffmann, Journal of Quaternary Science 26: 76–85. *Journal of Quaternary Science*, *26*(2), 238–240.
DOI/URL: https://doi.org/10.1002%2Fjqs.1478

Macklin, M. G., & Lewin, J. M. (1993). Holocene river alluviation in Britain. *Zeitschrift für Geomorphologie / Supplement*, *88*, 109–122.

Macklin, M. G., Ridgway, J., Passmore, D. G., & Rumsby, B. T. (1994). The use of overbank sediment for geochemical mapping and contamination assessment: results from selected English and Welsh floodplains. *Applied Geochemistry*, *9*(6), 689–700.
DOI/URL: https://doi.org/10.1016%2F0883-2927(94)90028-0

Macklin, M. G., Tooth, S., Brewer, P. A., Noble, P. L., & Duller, G. A. T. (2010b). Holocene flooding and river development in a Mediterranean steepland catchment: The Anapodaris Gorge, south central Crete, Greece. *Global and Planetary Change*, *70*(1), 35–52.
DOI/URL: https://doi.org/10.1016%2Fj.gloplacha.2009.11.006

Macklin, M. G., & Woodward, J. C. (2009). River Systems and Environmental Change. In J. C. Woodward (Ed.) *The Physical Geography of the Mediterranean*, Oxford Regional Environments, (pp. 319–352). Oxford: Oxford University Press.

Maestrini, B., & Miesel, J. R. (2017). Modification of the weak nitric acid digestion method for the quantification of black carbon in organic matrices. *Organic Geochemistry*, *103*, 136–139.
DOI/URL: https://doi.org/10.1016%2Fj.orggeochem.2016.10.010

Maggiani, A. (1981). Nuove evidenze archeologiche all'isola d'Elba: I rinvenimenti di età classica e ellenistica. In A. Neppi Modona, G. C. Cianferoni, & M. G. M. Costagli (Eds.) *L'Etruria mineraria. Atti del XII Convegno di studi etruschi e italici, Firenze - Populonia - Piombino 16-20 giugno 1979*, (pp. 173–192). Firenze: Olschki.

Maggiani, A., & Pancrazzi, O. (1979). *L'Elba preromana: fortezze di altura: Primi risultati di scavo. Monte Castello di Procchio, Castiglione di S. Martino: Catalogo della mostra, Portoferraio, Agosto 1979*. Pisa: Pacini.

Magny, M., de Beaulieu, J.-L., Drescher-Schneider, R., Vannière, B., Walter-Simonnet, A.-V., Miras, Y., Millet, L., Bossuet, G., Peyron, O., Brugiapaglia, E., & Leroux, A. (2007). Holocene climate changes in the central Mediterranean as recorded by lake-level fluctuations at Lake Accesa (Tuscany, Italy). *Quaternary Science Reviews*, *26*(13), 1736–1758. DOI/URL: https://doi.org/10.1016%2Fj.quascirev.2007.04.014

Magny, M., Vannière, B., Zanchetta, G., Fouache, E., Touchais, G., Petrika, L., Coussot, C., Walter-Simonnet, A.-V., & Arnaud, F. (2009). Possible complexity of the climatic event around 4300—3800 cal. BP in the central and western Mediterranean. *The Holocene*, *19*(6), 823–833.
DOI/URL: https://doi.org/10.1177%2F0959683609337360

Maineri, C., Benvenuti, M., Costagliola, P., Dini, A., Lattanzi, P., Ruggieri, G., & Villa, I. M. (2003). Sericitic alteration at the La Crocetta deposit (Elba Island, Italy): interplay between magmatism, tectonics and hydrothermal activity. *Mineralium Deposita*, *38*(1), 67–86.
DOI/URL: https://doi.org/10.1007/s00126-002-0279-2

Maley, J., Giresse, P., Doumenge, C., & Favier, C. (2012). Comment on "Intensifying Weathering and Land Use in Iron Age Central Africa". *Science*, *337*(6098), 1040.
DOI/URL: https://doi.org/10.1126%2Fscience.1221820

Malfatti, J., Principe, C., & Gattiglia, G. (2011). Archaeomagnetic investigation of a metallurgical furnace in Pisa (Italy). *Journal of Cultural Heritage*, *12*(1), 1–10.
DOI/URL: https://doi.org/10.1016%2Fj.culher.2010.03.005

Mameli, P., Mongelli, G., Oggiano, G., & Rovina, D. (2014). First Finding of Early Medieval Iron Slags in Sardinia (Italy): A Geochemical–Mineralogical Approach to Insights into Ore Provenance and Work Activity. *Archaeometry*, *56*(3), 406–430.
DOI/URL: https://doi.org/10.1111%2Farcm.12019

Manca, R., Pagliantini, L., Pecchioni, E., Santo, A. P., Cambi, F., Chiarantini, L., Corretti, A., Costagliola, P., Orlando, A., & Benvenuti, M. (2016). The island of Elba (Tuscany, Italy) at the crossroads of ancient trade routes: an archaeometric investigation of dolia defossa from the archaeological site of San Giovanni. *Mineralogy and Petrology*, *110*(6), 693–711.
DOI/URL: https://doi.org/10.1007%2Fs00710-016-0438-2

Mancuso, A., & Pasquali, A. (2016). St. Giovanni Tower on the Elba Island: survey and analysis for a digital comprehension. In G. Verdiani (Ed.) *Defensive Architecture of the Mediterranean (XV to XVIII Centuries): Proceedings of the International Conference on Modern Age Fortifications of the Mediterranean Coast, FORTMED 2016. Florence, November 10th, 11th, 12ht 2016*, vol. 4, (pp. 257–264). Firenze: DIDAPRESS, Dipartimento di Architettura, Università degli Studi di Firenze.

Marchant, R., Richer, S., Boles, O., Capitani, C., Courtney-Mustaphi, C. J., Lane, P., Prendergast, M. E., Stump, D., De Cort, G., Kaplan, J. O., Phelps, L., Kay, A., Olago, D., Petek, N., Platts, P. J., Punwong, P., Widgren, M., Wynne-Jones, S., Ferro-Vázquez, C., Benard, J., Boivin, N., Crowther, A., Cuní-Sanchez, A., Deere, N. J., Ekblom, A., Farmer, J., Finch, J., Fuller, D., Gaillard-Lemdahl, M.-J., Gillson, L., Githumbi, E., Kabora, T., Kariuki, R., Kinyanjui, R., Kyazike, E., Lang, C., Lejju, J., Morrison, K. D., Muiruri, V., Mumbi, C., Muthoni, R., Muzuka, A., Ndiema, E., Kabonyi Nzabandora, C., Onjala, I., Schrijver, A. P., Rucina, S., Shoemaker, A., Thornton-Barnett, S., van der Plas, G., Watson, E. E., Williamson, D., & Wright, D. (2018). Drivers and trajectories of land cover change in East Africa: Human and environmental interactions from 6000 years ago to present. *Earth-Science Reviews*, *178*, 322–378. DOI/URL: https://doi.org/10.1016%2Fj.earscirev.2017.12.010

Marchegiano, M., Francke, A., Gliozzi, E., Wagner, B., & Ariztegui, D. (2019). High-resolution palaeohydrological reconstruction of central Italy during the Holocene. *The Holocene*, *29*(3), 481–492. DOI/URL: https://doi.org/10.1177/0959683618816465

Mariet, A.-L., Bégeot, C., Gimbert, F., Gauthier, J., Fluck, P., & Walter-Simonnet, A.-V. (2016). Past mining activities in the Vosges Mountains (eastern France): Impact on vegetation and metal contamination over the past millennium. *The Holocene*, *26*(8), 1225–1236. DOI/URL: https://doi.org/10.1177/0959683616638419

Mariotti Lippi, M., Giachi, G., Paci, S., & Di Tommaso, P. L. (2000). Studi sulla vegetazione attuale e passata della Toscana meridionale (Follonica - Italia) e considerazioni sull'impatto ambientale dell'attività metallurgica etrusca nel VI-V secolo a.C. *Webbia*, *55*(2), 279–295. DOI/URL: https://doi.org/10.1080%2F00837792.2000.10670696

Marra, F., Bozzano, F., & Cinti, F. R. (2013). Chronostratigraphic and lithologic features of the Tiber River sediments (Rome, Italy): Implications on the post-glacial sea-level rise and Holocene climate. *Global and Planetary Change*, *107*, 157–176. DOI/URL: https://doi.org/10.1016%2Fj.gloplacha.2013.05.002

Marra, F., Motta, L., Brock, A. L., Macrì, P., Florindo, F., Sadori, L., & Terrenato, N. (2018). Rome in its setting. Post-glacial aggradation history of the Tiber River alluvial deposits and tectonic origin of the Tiber Island. *PLOS ONE*, *13*(3), e0194838. DOI/URL: https://doi.org/10.1371%2Fjournal.pone.0194838

Martin, S. (1994). Trial excavations on Monte Serra, Elba: a medieval iron workshop? *Archeologia medievale*, *21*, 233. DOI/URL: https://doi.org/10.1400%2F245167

Martín-Fernández, J. A., Barceló-Vidal, C., & Pawlowsky-Glahn, V. (2000). Zero Replacement in Compositional Data Sets. In H. A. L. Kiers, J.-P. Rasson, P. J. F. Groenen, & M. Schader (Eds.) *Data Analysis, Classification, and Related Methods*, Studies in Classification, Data Analysis, and Knowledge Organization, (pp. 155–160). Berlin [et al.]: Springer. DOI/URL: https://doi.org/10.1007/978-3-642-59789-3_25

Martín-Fernández, J. A., Barceló-Vidal, C., & Pawlowsky-Glahn, V. (2003). Dealing with Zeros and Missing Values in Compositional Data Sets Using Nonparametric Imputation.

Mathematical Geology, *35*(3), 253–278.
DOI/URL: https://doi.org/10.1023%2FA%3A1023866030544

Martín-Fernández, J.-A., Daunis-i Estadella, J., & Mateu-Figueras, G. (2015). On the interpretation of differences between groups for compositional data. *SORT-Statistics and Operations Research Transactions*, *39*(2), 231–252.
DOI/URL: https://www.raco.cat/index.php/SORT/article/view/302261

Martínez, C. E., & Motto, H. L. (2000). Solubility of lead, zinc and copper added to mineral soils. *Environmental Pollution*, *107*(1), 153–158.
DOI/URL: https://doi.org/10.1016%2FS0269-7491(99)00111-6

Martínez Cortizas, A., López-Merino, L., Bindler, R., Mighall, T., & Kylander, M. (2013). Atmospheric Pb pollution in N Iberia during the late Iron Age/Roman times reconstructed using the high-resolution record of La Molina mire (Asturias, Spain). *Journal of Paleolimnology*, *50*(1), 71–86.
DOI/URL: https://doi.org/10.1007%2Fs10933-013-9705-y

Marwick, B. (2017). Computational Reproducibility in Archaeological Research: Basic Principles and a Case Study of Their Implementation. *Journal of Archaeological Method and Theory*, *24*(2), 424–450.
DOI/URL: https://doi.org/10.1007/s10816-015-9272-9

Marzano, A. (2007). *Roman Villas in Central Italy: A Social and Economic History*. No. 30 in Columbia studies in the classical tradition. Leiden: Brill.

Marzano, A. (2015). The Variety of Villa Production: From Agriculture to Aquaculture. In P. Erdkamp, K. Verboven, & A. Zuiderhoek (Eds.) *Ownership and Exploitation of Land and Natural Resources in the Roman World*, Oxford Studies on the Roman Economy, (pp. 187–206). Oxford: Oxford University Press.

Mascaro, I., Benvenuti, M., Corsini, F., Costagliola, P., Lattanzi, P., Parrini, P., & Tanelli, G. (2001). Mine wastes at the polymetallic deposit of Fenice Capanne (southern Tuscany, Italy). Mineralogy, geochemistry, and environmental impact. *Environmental Geology*, *41*(3), 417–429.
DOI/URL: https://doi.org/10.1007/s002540100408

Mascaro, I., Benvenuti, M., & Tanelli, G. (1995). Mineralogy applied to archaeometallurgy: an investigation of medieval slags from Rocca San Silvestro (Campiglia M.ma, Tuscany). *Science and Technology and Cultural Heritage*, *4*, 87–98.

Mastrolonardo, G., Francioso, O., & Certini, G. (2018). Relic charcoal hearth soils: A neglected carbon reservoir. Case study at Marsiliana forest, Central Italy. *Geoderma*, *315*, 88–95.
DOI/URL: https://doi.org/10.1016%2Fj.geoderma.2017.11.036

Matera, V., Le Hécho, I., Laboudigue, A., Thomas, P., Tellier, S., & Astruc, M. (2003). A methodological approach for the identification of arsenic bearing phases in polluted soils. *Environmental Pollution*, *126*(1), 51–64.
DOI/URL: https://doi.org/10.1016%2FS0269-7491(03)00146-5

Matschullat, J. (2000). Arsenic in the geosphere — a review. *Science of The Total Environment*, *249*(1), 297–312.
DOI/URL: https://doi.org/10.1016%2FS0048-9697(99)00524-0

Mattusch, C. C. (2009). Metalworking and Tools. In J. Oleson (Ed.) *The Oxford Handbook of Engineering and Technology in the Classical World*.
DOI/URL: https://doi.org/10.1093%2Foxfordhb%2F9780199734856.013.0017

Mazzei-Karl, U. (1990). *La carbonaia di Roberto*. Torino: Edizione Azzurra.

Mazzini, I., Anadon, P., Barbieri, M., Castorina, F., Ferreli, L., Gliozzi, E., Mola, M., & Vittori, E. (1999). Late Quaternary sea-level changes along the Tyrrhenian coast near Orbetello (Tuscany, central Italy): palaeoenvironmental reconstruction using ostracods. *Marine Micropaleontology*, *37*(3), 289–311.
DOI/URL: https://doi.org/10.1016%2FS0377-8398(99)00023-7

McCann, J. C. (1997). The Plow and the Forest: Narratives of Deforestation in Ethiopia, 1840-1992. *Environmental History*, *2*(2), 138–159.
DOI/URL: https://www.jstor.org/stable/3985505

McConnell, J. R., & Edwards, R. (2008). Coal burning leaves toxic heavy metal legacy in the Arctic. *Proceedings of the National Academy of Sciences*, *105*(34), 12140.
DOI/URL: https://doi.org/10.1073%2Fpnas.0803564105

McGrail, S. (1989). The Shipment of Traded Goods and of Ballast in Antiquity. *Oxford Journal of Archaeology*, *8*, 353–358.
DOI/URL: https://doi.org/10.1111/j.1468-0092.1989.tb00210.x

McGrail, S. (2009). *Boats of the World from the Stone Age to Medieval Times*. Oxford, New York: Oxford University Press.
DOI/URL: http://hdl.handle.net/2027/heb.31079.0001.001

McKinley, J. M., Hron, K., Grunsky, E. C., Reimann, C., de Caritat, P., Filzmoser, P., van den Boogaart, K. G., & Tolosana-Delgado, R. (2016). The single component geochemical map: Fact or fiction? *Journal of Geochemical Exploration*, *162*, 16–28.
DOI/URL: https://doi.org/10.1016%2Fj.gexplo.2015.12.005

McMahon, L., & Sargent, A. (2019). The Environmental History of the Late Antique Eastern Mediterranean: a Bibliographic Essay. In A. Izdebski, & M. Mulryan (Eds.) *Environment and Society in the Long Late Antiquity*, (pp. 17–30). Leiden: Brill.
DOI/URL: http://dx.doi.org/10.1163/9789004392083_003

Meiggs, R. (1982). *Trees and Timber in the Ancient Mediterranean World*. Oxford: Clarendon Press.

Melamed, D. (2005). Monitoring arsenic in the environment: a review of science and technologies with the potential for field measurements. *Analytica Chimica Acta*, *532*(1), 1–13.
DOI/URL: https://doi.org/10.1016%2Fj.aca.2004.10.047

Mele, M., Servida, D., & Lupis, D. (2013). Characterisation of sulphide-bearing waste-rock dumps using electrical resistivity imaging: the case study of the Rio Marina mining district (Elba Island, Italy). *Environmental Monitoring and Assessment*, *185*(7), 5891–5907.
DOI/URL: https://doi.org/10.1007%2Fs10661-012-2993-2

Mellini, V. (1879). Ricerche sulla I.a età del ferro nell'isola d'Elba. *Bullettino di paletnologia italiana*, *5*, 84–90.

Mensing, S. A., Tunno, I., Sagnotti, L., Florindo, F., Noble, P., Archer, C., Zimmerman, S., Pavon-Carrasco, F. J., Cifani, G., Passigli, S., & Piovesan, G. (2015). 2700 years of Mediterranean environmental change in central Italy: a synthesis of sedimentary and cultural records to interpret past impacts of climate on society. *Quaternary Science Reviews*, *116*, 72–94.
DOI/URL: https://doi.org/10.1016%2Fj.quascirev.2015.03.022

Mercuri, A. M., Bandini Mazzanti, M., Florenzano, A., Montecchi, M. C., & Rattighieri, E. (2013). Olea, Juglans and Castanea: The OJC group as pollen evidence of the development of human-induced environments in the Italian peninsula. *Quaternary International*, *303*, 24–42.
DOI/URL: https://doi.org/10.1016%2Fj.quaint.2013.01.005

Meurer, M. (1986). Effect of Goat Browsing on the Floristic Components of Maquis and Garrigue in North Tunisia. In P. J. Joss, P. W. Lynch, & O. B. Willimas (Eds.) *Rangelands: A Resource Under Siege: Proceedings of the Second Inter Rangeland Congress*, (p. 134). Cambridge, U.K.: Cambridge University Press. Google-Books-ID: uNlBMl46IlUC.

Meyer, M. (2017). Iron and Consequences of the Introduction of its Technologies in Northern Central Europe. In *The Interplay of People and Technologies. Archaeological Case Studies on Innovations*, no. 43 in Berlin Studies of the Ancient World. Berlin: Edition Topoi.
DOI/URL: https://doi.org/10.18452%2F5391

Michczynska, D., & Pazdur, A. (2004). Shape analysis of cumulative probability density function of radiocarbon dates set in the study of climate change in the late glacial and Holocene. *Radiocarbon*, *46*(2), 733–744.
DOI/URL: https://journals.uair.arizona.edu/index.php/radiocarbon/article/view/4206

Michetti, L. M. (2017). Harbors. In A. Naso (Ed.) *Etruscology*, (pp. 391–405). Berlin, Boston: De Gruyter.
DOI/URL: https://doi.org/10.1515/9781934078495-023

Migaszewski, Z., Gałuszka, A., & Dołęgowska, S. (2015). The use of FPXRF in the determinations of selected trace elements in historic mining soils in the Holy Cross Mts., south-central Poland. *Geological Quarterly*, *59*(1), 248–256.
DOI/URL: https://doi.org/10.7306/gq.1216

Mighall, T., Timberlake, S., Martínez-Cortizas, A., Silva-Sánchez, N., & Foster, I. D. L. (2017). Did prehistoric and Roman mining and metallurgy have a significant impact on vegetation? *Journal of Archaeological Science: Reports*, *11*, 613 – 625.
DOI/URL: https://doi.org/10.1016%2Fj.jasrep.2016.12.021

Mighall, T. M., & Chambers, F. M. (1997). Early Ironworking and its Impact on the Environment: Palaeoecological Evidence from Bryn y Castell Hillfort, Snowdonia, North Wales. *Proceedings of the Prehistoric Society*, *63*, 199–219.
DOI/URL: https://doi.org/10.1017%2FS0079497X00002437

Mighall, T. M., Foster, I. D. L., Crew, P., Chapman, A. S., & Finn, A. (2009). Using mineral magnetism to characterise ironworking and to detect its evidence in peat bogs. *Journal of Archaeological Science*, *36*(1), 130–139.
DOI/URL: https://doi.org/10.1016%2Fj.jas.2008.07.015

Mignardi, S., Corami, A., & Ferrini, V. (2012). Evaluation of the effectiveness of phosphate treatment for the remediation of mine waste soils contaminated with Cd, Cu, Pb, and Zn. *Chemosphere*, *86*(4), 354–360.
DOI/URL: https://doi.org/10.1016%2Fj.chemosphere.2011.09.050

Milanesi, C., Scali, M., Vignani, R., Cambi, F., Dugerdil, L., Faleri, C., & Cresti, M. (2016). Archaeobotanical reconstructions of vegetation and report of mummified apple seeds found in the cellar of a first-century Roman villa on Elba Island. *Comptes Rendus Biologies*, *339*(11), 487–497.
DOI/URL: https://doi.org/10.1016%2Fj.crvi.2016.09.003

Millard, S. P. (2013). *EnvStats: An R Package for Environmental Statistics*. New York: Springer.
DOI/URL: https://dx.doi.org/10.1007/978-1-4614-8456-1

Minto, A. (1954). L'antica industria mineraria in Etruria ed il porto di Populonia. *Studi etruschi*, *23*, 291–319.

Misra, M. K., Ragland, K. W., & Baker, A. J. (1993). Wood ash composition as a function of furnace temperature. *Biomass and Bioenergy*, *4*(2), 103–116.
DOI/URL: https://doi.org/10.1016%2F0961-9534(93)90032-Y

Mitchell, P. (2018). *The Donkey in Human History: An Archaeological Perspective*. Oxford: Oxford University Press.

Mohan, D., & Pittman, C. U. (2007). Arsenic removal from water/wastewater using adsorbents—A critical review. *Journal of Hazardous Materials*, *142*(1), 1–53.
DOI/URL: https://doi.org/10.1016%2Fj.jhazmat.2007.01.006

Molina, M. G. d., & Toledo, V. M. (2014). *The Social Metabolism: A Socio-Ecological Theory of Historical Change*. No. 3 in Environmental History. Cham: Springer.
DOI/URL: http://dx.doi.org/10.1007/978-3-319-06358-4_3

Monaco, G., & Mellini, V. (1965). *Memorie storiche dell'isola dell'Elba: Parte archeologica ed artistica: Trascrizione, Commento, Repertorio Archeologico, Note e Indici*, vol. 17 of *Pocket Library of Studies in Art*. Firenze: Olschki.

Monaco, G., & Tabanelli, M. (1976). *Archeologia, storia ed arte all'isola d'Elba: Guida turistica*. Faenza: Fratelli Lega Editori.

Montero-Serrano, J. C., Palarea-Albaladejo, J., Martín-Fernández, J. A., Martínez-Santana, M., & Gutiérrez-Martín, J. V. (2010). Sedimentary chemofacies characterization by means of multivariate analysis. *Sedimentary Geology*, *228*(3), 218–228.
DOI/URL: https://doi.org/10.1016%2Fj.sedgeo.2010.04.013

Morel, J.-P. (1981). Céramique campanienne: Les formes. vol. 244 of *Bibliothèque des Écoles françaises d'Athènes et de Rome*. Rome: École Française de Rome.

Mori, A. (1960). *Studi geografici sull'isola d'Elba*, vol. 7-8 of *Pubblicazioni dell'Istituto di geografia dell'Universita di Pisa*. Pisa: Goliardica.

Murtagh, F., & Legendre, P. (2014). Ward's Hierarchical Agglomerative Clustering Method: Which Algorithms Implement Ward's Criterion? *Journal of Classification*, *31*(3), 274–295.
DOI/URL: https://doi.org/10.1007%2Fs00357-014-9161-z

Myrstener, E., Lidberg, W., Segerström, U., Biester, H., Damell, D., & Bindler, R. (2016). Was Moshyttan the earliest iron blast furnace in Sweden? The sediment record as an archeological toolbox. *Journal of Archaeological Science: Reports*, *5*, 35–44. DOI/URL: https://doi.org/10.1016%2Fj.jasrep.2015.10.040

Napoli, R., Costantini, E. A. C., Castellani, F., & Gardin, L. (2005). New Proposals toward a WRB System for Soil Cartography: The Soil Map at 1: 250000 Scale of the Tuscany Region (Central Italy). *Eurasian Soil Science*, *38*(1), S20–S26.

Nelle, O., Jansen, D., & Overbeck, M. (2013). Charcoals from iron smelting furnaces: fuel supply and environment of a medieval iron smelting site near Peppange/Luxembourg. In F. Damblon (Ed.) *Proceedings of the fourth International Meeting of Anthracology : Brussels, 8-13 September 2008 : Royal Belgian Institute of Natural Sciences*, (pp. 165–172). Oxford: Archaeopress.

Nenninger, M. (2001). *Die Römer und der Wald: Untersuchungen zum Umgang mit einem Naturraum am Beispiel der römischen Nordwestprovinzen*. Franz Steiner Verlag.

Neppi Modona, A., Cianferoni, G. C., & Costagli, M. G. M. (Eds.) (1981). *L'etruria mineraria: atti del XII Convegno di Studi Etruschi e Italici, Firenze - Populonia - Piombino, 16-20 giugno 1979*. No. 12 in Atti del Convegno di Studi Etruschi ed Italici. Firenze: Olschki.

Neumann, K., Eggert, M. K. H., Oslisly, R., Clist, B., Denham, T., Maret, P. d., Ozainne, S., Hildebrand, E., Bostoen, K., Salzmann, U., Schwartz, D., Eichhorn, B., Tchiengué, B., & Höhn, A. (2012). Comment on "Intensifying Weathering and Land Use in Iron Age Central Africa". *Science*, *337*(6098), 1040–1040. DOI/URL: https://doi.org/10.1126%2Fscience.1221747

Nihlén, J. (1958). Fynd av äldre järntillverkning på Elba. Manuskript i Lunds Universitetsbiblioteket Arkiv (John Nihléns efterlämnade papper).

Nihlén, J. (1960). The Prehistoric Iron Industries of Elba: manuskirpt i Tekniska Museet, Teknik- och industrihistoriska arkivet F 51.

Nihlén, J., & Ejlers, C. (1958). *Quaderno Elba 1958: Manuskript i Lunds Universitetsbiblioteket Arkiv (John Nihléns efterlämnade papper)*.

Nikulka, F. (1995). Frühe Eisenerzverhüttung und ihr experimenteller Nachvollzug: Eine Analyse bisheriger Versuche. In M. Fansa (Ed.) *Experimentelle Archäologie: Symposium in Duisburg, August 1993*, Archäologische Mitteilungen aus Nordwestdeutschland Beih., (pp. 255–310). Oldenburg: Isensee.

Ninci, G. (1815). *Storia dell'Isola dell'Elba*. Portoferraio: Broglia.

Norgate, T. E., Jahanshahi, S., & Rankin, W. J. (2007). Assessing the environmental impact of metal production processes. *Journal of Cleaner Production*, *15*(8), 838–848. DOI/URL: https://doi.org/10.1016%2Fj.jclepro.2006.06.018

Nuss, P., & Eckelman, M. J. (2014). Life cycle assessment of metals: a scientific synthesis. *PLoS One*, *9*(7), e101298.

Oksanen, J., Blanchet, F. G., Friendly, M., Kindt, R., Legendre, P., McGlinn, D., Minchin, P. R., O'Hara, R. B., Simpson, G. L., Solymos, P., Stevens, M. H. H., Szoecs, E., & Wagner, H. (2015). *vegan: Community Ecology Package[R package, v2.3-0]*.
DOI/URL: https://CRAN.R-project.org/package=vegan

Olson, S. D. (1991). Firewood and charcoal in Classical Athens. *Hesperia: The Journal of the American School of Classical Studies at Athens*, *60*(3), 411–420.

Olson, S. D. (2012). Charcoal. In *The Encyclopedia of Ancient History*. American Cancer Society.
DOI/URL: https://doi.org/10.1002/9781444338386.wbeah06064

Orton, D., Morris, J., & Pipe, A. (2017). Catch Per Unit Research Effort: Sampling Intensity, Chronological Uncertainty, and the Onset of Marine Fish Consumption in Historic London. *Open Quaternary*, *3*(1), 1.
DOI/URL: https://doi.org/10.5334%2Foq.29

Oxé, A., Comfort, H., & Kenrick, P. M. (2000). *Corpus vasorum Arretinorum: a catalogue of the signatures, shapes, and chronology of Italian Sigillata*. No. 41 in Antiquitas. Bonn: R. Habelt, 2 ed.

Pacchiarini, F. (2016). Le chíese fortificate dell'Isola d'Elba. Documentazione per la conoscenza. In G. Verdiani (Ed.) *Defensive Architecture of the Mediterranean (XV to XVIII Centuries): Proceedings of the International Conference on Modern Age Fortifications of the Mediterranean Coast, FORTMED 2016. Florence, November 10th, 11th, 12ht 2016*, vol. 4, (pp. 273–282). Firenze: DIDAPRESS, Dipartimento di Architettura, Università degli Studi di Firenze.

Pagliantini, L. (2014). *Aithale. L'Isola d'Elba: paesaggi antichi e bacini d'approvvigionamento*. Tesi di dottorato, Università di Foggia, Dipartimento di Studi Umanistici. Foggia: Università di Foggia.
DOI/URL: http://dx.doi.org/10.14274/UNIFG/FAIR/331741

Pagnanelli, F., Moscardini, E., Giuliano, V., & Toro, L. (2004). Sequential extraction of heavy metals in river sediments of an abandoned pyrite mining area: pollution detection and affinity series. *Environmental Pollution*, *132*(2), 189–201.
DOI/URL: https://doi.org/10.1016%2Fj.envpol.2004.05.002

Palarea-Albaladejo, J., & Martín-Fernández, J. A. (2013). Values below detection limit in compositional chemical data. *Analytica Chimica Acta*, *764*, 32 – 43.
DOI/URL: https://doi.org/10.1016%2Fj.aca.2012.12.029

Palarea-Albaladejo, J., & Martín-Fernández, J. A. (2015). zCompositions — R package for multivariate imputation of left-censored data under a compositional approach. *Chemometrics and Intelligent Laboratory Systems*, *143*, 85–96.
DOI/URL: https://doi.org/10.1016/j.chemolab.2015.02.019

Palarea-Albaladejo, J., Martín-Fernández, J. A., & Gómez-García, J. (2007). A Parametric Approach for Dealing with Compositional Rounded Zeros. *Mathematical Geology*, *39*(7), 625–645.
DOI/URL: https://doi.org/10.1007/s11004-007-9100-1

Palmisano, A., Bevan, A., & Shennan, S. (2017). Comparing archaeological proxies for long-term population patterns: An example from central Italy. *Journal of Archaeological Science*, *87*, 59–72.
DOI/URL: https://doi.org/10.1016%2Fj.jas.2017.10.001

Palmisano, A., Bevan, A., & Shennan, S. (2018). Regional Demographic Trends and Settlement Patterns in Central Italy: Archaeological Sites and Radiocarbon Dates. *Journal of Open Archaeology Data*, *6*(1), 2.
DOI/URL: https://doi.org/10.5334%2Fjoad.43

Pancrazzi, O., & Ducci, S. (1996). *Ville e giardini nell'Elba romana*. Firenze: Octavo.

Pandeli, E., Principi, G., Bortolotti, V., Benvenuti, M., Fazzuoli, M., Dini, A., Fanucci, F., Menna, F., & Nirta, G. (2013). The Elba Island: An Intriguing Geological Puzzle in the Northern Tyrrhenian Sea. *Geological Field Trips*, *5*(2,1), 1–114.
DOI/URL: https://doi.org/10.3301%2FGFT.2013.03

Panella, C. (2001). Le anfore di età imperiale del Mediterraneo occidentale. In *Céramiques hellénistiques et romaines*, (pp. 177–275). Paris: Les Belles Lettres.

Panin, A., & Matlakhova, E. (2015). Fluvial chronology in the East European Plain over the last 20ka and its palaeohydrological implications. *CATENA*, *130*, 46–61.
DOI/URL: https://doi.org/10.1016%2Fj.catena.2014.08.016

Paradis-Grenouillet, S. (2012). *Study of metallurgical forests: dendro-anthracologic analyses and geohistoric approaches. The examples of forests on Mount Lozère and in Perigord Limousin — Etudier les forêts métallurgiques : analyses dendro-anthracologiques et approches géohistoriques. L'exemple des forêts du mont Lozère et du Périgord-Limousin*. Thèse, Université de Limoges, Sciences de l'Homme et Société. Université de Limoges.
DOI/URL: https://hal-unilim.archives-ouvertes.fr/tel-01131807

Park, J.-S., Chunag, A., & Gelegdorj, E. (2008). A technological transition in Mongolia evident in microstructure, chemical composition and radiocarbon age of cast iron artifacts. *Journal of Archaeological Science*, *35*(9), 2465–2470.
DOI/URL: https://doi.org/10.1016%2Fj.jas.2008.03.014

Parsons, C., Margui Grabulosa, E., Pili, E., Floor, G. H., Roman-Ross, G., & Charlet, L. (2013). Quantification of trace arsenic in soils by field-portable X-ray fluorescence spectrometry: Considerations for sample preparation and measurement conditions. *Journal of Hazardous Materials*, *262*, 1213–1222.
DOI/URL: https://doi.org/10.1016%2Fj.jhazmat.2012.07.001

Passariello, B., Giuliano, V., Quaresima, S., Barbaro, M., Caroli, S., Forte, G., Carelli, G., & Iavicoli, I. (2002). Evaluation of the environmental contamination at an abandoned mining site. *Microchemical Journal*, *73*(1), 245–250.
DOI/URL: https://doi.org/10.1016%2FS0026-265X(02)00069-3

Pavón-Carrasco, F. J., Osete, M. L., Torta, J. M., & Gaya-Piqué, L. R. (2009). A regional archeomagnetic model for Europe for the last 3000 years, SCHA.DIF.3k: Applications to archeomagnetic dating. *Geochemistry, Geophysics, Geosystems*, *10*(3).
DOI/URL: https://doi.org/10.1029%2F2008GC002244

Paysen, A. (2011). *Nachhaltige Energiewirtschaft? Brenn- und Kohlholznutzung in Schleswig-Holstein in Mittelalter und früher Neuzeit [Dissertation]*. Dissertation, Christian-Albrechts Universität Kiel, Mathematisch-Naturwissenschaftliche Fakultät. Kiel: Multimediale Archiv- und Publikationsserver der Christian-Albrechts-Universität zu Kiel. DOI/URL: https://nbn-resolving.org/urn:nbn:de:gbv:8-diss-68952

Peacock, D. P. S., & Williams, D. F. (1986). *Amphorae and the Roman economy: an introductory guide*. Longman archaeology series. London [et al.]: Longman.

Penna, A. N. (2014). *The Human Footprint: A Global Environmental History*. Hoboken, NJ: John Wiley & Sons.

Perlin, J. (2005). *A Forest Journey: The Story of Wood and Civilization*. Woodstock, VT: The Countryman Press.

Pettersson, G., Karlsson, S., Risberg, J., & Myrdal-Runebjer, E. (2004). Soil chemistry, vegetation history and human impact at the Late Holocene iron production site of Askagsberg, western Sweden. *Journal of Nordic Archaeological Science*, *14*, 101–113.

Peyron, O., Goring, S., Dormoy, I., Kotthoff, U., Pross, J., de Beaulieu, J.-L., Drescher-Schneider, R., Vannière, B., & Magny, M. (2011). Holocene seasonality changes in the central Mediterranean region reconstructed from the pollen sequences of Lake Accesa (Italy) and Tenaghi Philippon (Greece). *The Holocene*, *21*(1), 131–146. DOI/URL: https://doi.org/10.1177/0959683610384162

Peyron, O., Magny, M., Goring, S., Joannin, S., Beaulieu, J.-L. d., Brugiapaglia, E., Sadori, L., Garfi, G., Kouli, K., Ioakim, C., & Combourieu-Nebout, N. (2013). Contrasting patterns of climatic changes during the Holocene across the Italian Peninsula reconstructed from pollen data. *Climate of the Past*, *9*(3), 1233–1252. DOI/URL: https://doi.org/10.5194/cp-9-1233-2013

Pflug, N., & Thalheim, K. (2014). Der historische Eisenerzbergbau des Osterzgebirges und Elbtalschiefergebirges im Spiegel der Archive und Sammlungen. *Geo.Alp*, *11*(11), 215–238.

Phillips, C. P. (1998). The badlands of Italy: a vanishing landscape? *Applied Geography*, *18*(3), 243–257. DOI/URL: https://doi.org/10.1016%2FS0143-6228(98)00005-8

Piatak, N. M., Parsons, M. B., & Seal II, R. R. (2015). Characteristics and environmental aspects of slag: A review. *Applied Geochemistry*, *57*, 236–266. DOI/URL: https://doi.org/10.1016%2Fj.apgeochem.2014.04.009

Piatak, N. M., & Seal II, R. R. (2012). Mineralogy and environmental geochemistry of historical iron slag, Hopewell Furnace National Historic Site, Pennsylvania, USA. *Applied Geochemistry*, *27*(3), 623–643. DOI/URL: https://doi.org/10.1016%2Fj.apgeochem.2011.12.011

Piccarreta, M., Caldara, M., Capolongo, D., & Boenzi, F. (2011). Holocene geomorphic activity related to climatic change and human impact in Basilicata, Southern Italy. *Geomorphology*, *128*(3), 137–147. DOI/URL: https://doi.org/10.1016%2Fj.geomorph.2010.12.029

Piccarreta, M., Capolongo, D., & Miccoli, M. N. (2012). Deep gullies entrenchment in valley fills during the Late Holocene in the Basento basin, Basilicata (southern Italy). *Géomorphologie : relief, processus, environnement*, *18*(2, Alluvial geomorphology in Italy), 239–248.
DOI/URL: https://doi.org/10.4000%2Fgeomorphologie.9856

Piccinini, A. (1938). Il ferro elbano in Italia dall'epoca etrusca alla fine dell'impero romano. In *Miniere e ferro dell'Elba dai tempi Etruschi ai nostri giorni: Giunta dei minerali ferrosi*, (pp. 5–29). Roma: Palombi.

Piercey, S. J., & Devine, M. C. (2014). Analysis of powdered reference materials and known samples with a benchtop, field portable X-ray fluorescence (pXRF) spectrometer: evaluation of performance and potential applications for exploration lithogeochemistry. *Geochemistry: Exploration, Environment, Analysis*, *14*(2), 139–148.
DOI/URL: https://doi.org/10.1144%2Fgeochem2013-199

Pini, E. (1780). *Mineralogische Beobachtungen über die Eisengrube bey Rio und in andern Gegenden der Insel Elba [Osservazioni mineralogiche su la miniera di Ferro di Rio – Aus dem Italiänischen ins Teutsche übersetzt, und mit den neuern Bemerkungen Herrn Köstlin u.a. vermehrt, nebst einer Abhandlung von besondern Kristallgestalten des Feldspats, herausgegeben von Johann Friedrich Gmelin]*. Halle: Johann Jabob Gebauer.
DOI/URL: http://opacplus.bsb-muenchen.de/title/BV001467273/ft/bsb10706523?page=5

Pinna, S. (1992). Sulla probabilità di precipitazioni scarse nell'Isola d'Elba. *Atti Soc. Tosc. Sci. Nat., Mem., Serie A*, *99*, 195–207.

Pistelli, L., D'Angiolillo, F., Morelli, E., Basso, B., Rosellini, I., Posarelli, M., & Barbafieri, M. (2017). Response of spontaneous plants from an ex-mining site of Elba island (Tuscany, Italy) to metal(loid) contamination. *Environmental Science and Pollution Research*, *24*, 7809–7820.
DOI/URL: https://doi.org/10.1007%2Fs11356-017-8488-5

Pistolesi, C. (2013). *Ferro autarchico: L'uso dele antiche scorie ferrifere di Baratti, Poggio Butelli e dell'Isola dell'Elba nella siderurgia del Novecento*. Venturina: Edizioni Archivinform.

Pitman, R. M. (2006). Wood ash use in forestry – a review of the environmental impacts. *Forestry: An International Journal of Forest Research*, *79*(5), 563–588.
DOI/URL: https://doi.org/10.1093%2Fforestry%2Fcpl041

Pleiner, R. (2000). *Iron in Archaeology: The European Bloomery Smelters*. Praha: Archeologický ústav AVČR.

Pococke, R. (1745). *A Description of the East and Some other Countries, Vol. II Part 2 – Observations on the islands of the Archipelago, Asia Minor, Thrace, Greece, and some other parts of Europe.*. London: W. Bowyer.
DOI/URL: http://archive.org/details/ADescriptionOfTheEastAndSomeOtherCountriesVolIiPart2

Poggiali, F., Buonincontri, M. P., D'Auria, A., Volante, N., & Di Pasquale, G. (2017). Wood selection for firesetting: First data from the Neolithic cinnabar mine of Spaccasasso (South Tuscany, Italy). *Quaternary International*, *458*, 134–140.
DOI/URL: https://doi.org/10.1016/j.quaint.2017.06.028

Posamentier, H. W. (2009). *Sequence Stratigraphy and Facies Associations*. John Wiley & Sons.

Pounds, N. J. G. (1957). Historical Geography of the Iron and Steel Industry of France. *Annals of the Association of American Geographers*, *47*(1), 3–14. DOI/URL: https://www.jstor.org/stable/2561556

Powell, A. J., McDonnell, J. G., Batt, C. M., & Vernon, R. W. (2002). An assessment of the magnetic response of an iron-smelting site*. *Archaeometry*, *44*(4), 651–665. DOI/URL: https://doi.org/10.1111%2F1475-4754.t01-1-00091

Pranzini, E. (2001). Updrift river mouth migration on cuspate deltas: two examples from the coast of Tuscany (Italy). *Geomorphology*, *38*(1–2), 125–132. DOI/URL: https://doi.org/10.1016%2FS0169-555X(00)00076-3

Pranzini, E., & Rosas, V. (2007). Pocket beach response to high magnitude–low frequency floods (Elba Island, Italy). *Journal of Coastal Research*, (pp. 969–977). DOI/URL: https://www.jstor.org/stable/26481721

Pranzini, E., Rosas, V., Jackson, N. L., & Nordstrom, K. F. (2013). Beach changes from sediment delivered by streams to pocket beaches during a major flood. *Geomorphology*, *199*, 36–47. DOI/URL: https://doi.org/10.1016%2Fj.geomorph.2013.03.034

Principe, C., Arrighi, S., Malfatti, J., & Brocchini, D. (2011). Datazione archeomagnetica di alcune fornaci dell'Isola d'Elba. In F. Ramacogi (Ed.) *Isola d'Elba: Atlante delle Fornaci*, (pp. 83–97). Viterbo: BetaGamma.

Principi, G., Bortolotti, V., Pandeli, E., Fanucci, F., Moretti, S., Innocenti, F., D'Orefice, M., & Graciotti, R. (2015). *Carta Geologica dell'Isola d'Elba alla scala 1:25,000 (Geological Map of Elba Island)*. CARG - Cartografia geologica e geotematica. Roma: Istituto Superiore per la Protezione e la Ricerca Ambientale / Servizio Geologico d'Italia.

Protano, G., & Riccobono, F. (1997). Environmental levels of antimony, arsenic and mercury in the Tafone mining area (Southern Tuscany, Italy). *Atti Soc Tosc Sci Nat Mem Serie A*, *104*, 75–83.

Pucci, G. (1985). Terra Sigillata Italica. In I. d. E. Italiana (Ed.) *Atlante delle forme ceramiche : 2. Ceramica fine romana nel bacino mediterraneo. (Tardo ellenismo e primo impero)*, Enciclopedia dell'arte antica classica e orientale. Rome: Instituto della Enciclopedia Italiana.

Pyatt, F. B., Gilmore, G., Grattan, J. P., Hunt, C. O., & Mclaren, S. (2000). An Imperial Legacy? An Exploration of the Environmental Impact of Ancient Metal Mining and Smelting in Southern Jordan. *Journal of Archaeological Science*, *27*(9), 771–778. DOI/URL: https://doi.org/10.1006%2Fjasc.1999.0580

Pyatt, F. B., Pyatt, A. J., Walker, C., Sheen, T., & Grattan, J. P. (2005). The heavy metal content of skeletons from an ancient metalliferous polluted area in southern Jordan with particular reference to bioaccumulation and human health. *Ecotoxicology and Environmental Safety*, *60*(3), 295–300. DOI/URL: https://doi.org/10.1016%2Fj.ecoenv.2004.05.002

Pye, K. (1986). Mineralogical and textural controls on the weathering of granitoid rocks. *CATENA*, *13*(1), 47–57.
DOI/URL: https://doi.org/10.1016%2FS0341-8162(86)80004-2

R Core Team (2016). *R: A Language and Environment for Statistical Computing*. Wien: R Foundation for Statistical Computing.
DOI/URL: https://www.R-project.org/

R Core Team (2018). *R: A Language and Environment for Statistical Computing*. Wien: R Foundation for Statistical Computing.
DOI/URL: https://www.R-project.org/

Raab, A., Bonhage, A., Schneider, A., Raab, T., Rösler, H., Heußner, K. U., & Hirsch, F. (2017). Spatial distribution of relict charcoal hearths in the former royal forest district Tauer (SE Brandenburg, Germany). *Quaternary International*.
DOI/URL: https://doi.org/10.1016%2Fj.quaint.2017.07.022

Raab, A., Takla, M., Raab, T., Nicolay, A., Schneider, A., Rösler, H., Heußner, K.-U., & Bönisch, E. (2015). Pre-industrial charcoal production in Lower Lusatia (Brandenburg, Germany): Detection and evaluation of a large charcoal-burning field by combining archaeological studies, GIS-based analyses of shaded-relief maps and dendrochronological age determination. *Quaternary International*, *367*, 111–122.
DOI/URL: https://doi.org/10.1016/j.quaint.2014.09.041

Raab, T., Hürkamp, K., & Völkel, J. (2010). Stratigraphy and chronology of Late Quaternary floodplain sediments in a historic mining area, Vils River Valley, East Bavaria, Germany. *Physical Geography*, *31*(4), 357–384.
DOI/URL: https://doi.org/10.2747%2F0272-3646.31.4.357

Radkau, J. (1986). Zur angeblichen Energiekrise des 18. Jahrhunderts: Revisionistische Betrachtungen über die „Holznot". *VSWG: Vierteljahrschrift für Sozial- und Wirtschaftsgeschichte*, *73*(1), 1–37.
DOI/URL: https://www.jstor.org/stable/20732534

Radkau, J. (2012). *Holz: Wie ein Naturstoff Geschichte schreibt*. No. 3 in Stoffgeschichten. München: oekom verlag, 2nd ed.

Radt, S. (2003). *Strabons Geographika Buch V - VIII: Text und Übersetzung*, vol. 2 of *Strabons Geographika*. Göttingen: Vandenhoeck & Ruprecht.

Radu, T., & Diamond, D. (2009). Comparison of soil pollution concentrations determined using AAS and portable XRF techniques. *Journal of Hazardous Materials*, *171*(1), 1168–1171.
DOI/URL: https://doi.org/10.1016%2Fj.jhazmat.2009.06.062

Ramey, J. A. (2012). *clusteval: Evaluation of Clustering Algorithms [R package, v0.1]*.
DOI/URL: https://CRAN.R-project.org/package=clusteval

Ramrath, A., Sadori, L., & Negendank, J. F. (2000). Sediments from Lago di Mezzano, central Italy: a record of Lateglacial/Holocene climatic variations and anthropogenic impact. *The Holocene*, *10*(1), 87–95.
DOI/URL: https://doi.org/10.1191/095968300669348734

Regione Toscana (2016). *Alluvione all'Isola d'Elba - Interventi straordinari e di emergenza*.
DOI/URL: http://www.regione.toscana.it/-/alluvione-all-isola-d-elba

Rehder, J. E. (2000). *Mastery and Uses of Fire in Antiquity*. McGill-Queen's Press - MQUP.

Reimann, C., Filzmoser, P., Fabian, K., Hron, K., Birke, M., Demetriades, A., Dinelli, E., & Ladenberger, A. (2012). The concept of compositional data analysis in practice — Total major element concentrations in agricultural and grazing land soils of Europe. *Science of The Total Environment*, *426*, 196–210.
DOI/URL: https://doi.org/10.1016%2Fj.scitotenv.2012.02.032

Reimann, C., Filzmoser, P., Hron, K., Kynčlová, P., & Garrett, R. G. (2017). A new method for correlation analysis of compositional (environmental) data – a worked example. *Science of The Total Environment*, *607-608*, 965 – 971.
DOI/URL: https://doi.org/10.1016%2Fj.scitotenv.2017.06.063

Reimer, P. (2013). IntCal13 and Marine13 Radiocarbon Age Calibration Curves 0–50,000 Years cal BP. *Radiocarbon*, *55*(4), 1869–1887.
DOI/URL: https://doi.org/10.2458%2Fazu_js_rc.55.16947

Renberg, I., Bindler, R., & Brännvall, M.-L. (2001). Using the historical atmospheric lead-deposition record as a chronological marker in sediment deposits in Europe. *The Holocene*, *11*(5), 511–516.
DOI/URL: https://doi.org/10.1191/095968301680223468

Renberg, I., Persson, M. W., & Emteryd, O. (1994). Pre-industrial atmospheric lead contamination detected in Swedish lake sediments. *Nature*, *368*(6469), 323–326.
DOI/URL: https://doi.org/10.1038%2F368323a0

Revelle, W. (2018). *psych: Procedures for Psychological, Psychometric, and Personality Research [R package, v1.8.12]*. Evanston, IL: Northwestern University.
DOI/URL: https://CRAN.R-project.org/package=psych

Röhling, H.-G., Teicke, J., & Wellmer, F.-W. (2010). The Upper Harz Water Regale. *Schriftenreihe der Deutschen Gesellschaft für Geowissenschaften*, (pp. 119–121).
DOI/URL: https://doi.org/10.1127%2Fsdgg%2F66%2F2010%2F119

Ridgway, D. (1992). *The First Western Greeks*. Cambridge.

Rinklebe, J., Antić-Mladenović, S., Frohne, T., Stärk, H.-J., Tomić, Z., & Ličina, V. (2016). Nickel in a serpentine-enriched Fluvisol: Redox affected dynamics and binding forms. *Geoderma*, *263*, 203–214.
DOI/URL: https://doi.org/10.1016%2Fj.geoderma.2015.09.004

Roesler, M. (1921). The Iron-Ore Resources of Europe. [Bulletin 706, U.S. Geol. Survey]. Tech. rep., Washington, D. C.

Roller, D. W. (2018). *A Historical and Topographical Guide to the Geography of Strabo*. Cambridge University Press.

Romano, P., Di Vito, M. A., Giampaola, D., Cinque, A., Bartoli, C., Boenzi, G., Detta, F., Di Marco, M., Giglio, M., Iodice, S., Liuzza, V., Ruello, M. R., & Schiano di Cola, C. (2013). Intersection of exogenous, endogenous and anthropogenic factors in the Holocene landscape: A study of the Naples coastline during the last 6000 years. *Quaternary International*, *303*, 107–119.
DOI/URL: https://doi.org/10.1016%2Fj.quaint.2013.03.031

Rondelli, B., Lancelotti, C., Madella, M., Pecci, A., Balbo, A., Pérez, J. R., Inserra, F., Gadekar, C., Ontiveros, M. n. C., & Ajithprasad, P. (2014). Anthropic activity markers and spatial variability: an ethnoarchaeological experiment in a domestic unit of Northern Gujarat (India). *Journal of Archaeological Science*, *41*, 482–492. DOI/URL: https://doi.org/10.1016%2Fj.jas.2013.09.008

Rosas, V., Cipriani, L. E., Pranzini, E., & Wetzel, L. (2011). Landuse Changes and Erosion of Pocket Beaches in Elba Island (Tuscany, Italy). *Journal of Coastal Research*, *64*, 1774–1778.

Rossato, S., Fontana, A., & Mozzi, P. (2015). Meta-analysis of a Holocene 14c database for the detection of paleohydrological crisis in the Venetian–Friulian Plain (NE Italy). *CATENA*, *130*, 34–45. DOI/URL: https://doi.org/10.1016%2Fj.catena.2014.10.033

Rossato, S., & Mozzi, P. (2016). Inferring LGM sedimentary and climatic changes in the southern Eastern Alps foreland through the analysis of a 14c ages database (Brenta megafan, Italy). *Quaternary Science Reviews*, *148*, 115–127. DOI/URL: https://doi.org/10.1016%2Fj.quascirev.2016.07.013

Rossi, V., Amorosi, A., Sarti, G., & Potenza, M. (2011). Influence of inherited topography on the Holocene sedimentary evolution of coastal systems: An example from Arno coastal plain (Tuscany, Italy). *Geomorphology*, *135*(1), 117–128. DOI/URL: https://doi.org/10.1016%2Fj.geomorph.2011.08.009

Rossi, V., Amorosi, A., Sarti, G., & Romagnoli, R. (2012). New stratigraphie evidence for the mid-late holocene fluvial evolution of the arno coastal plain (Tuscany, Italy). *Geomorphologie: Relief, Processus, Environnement*, (2), 201–214.

Rouillon, M., & Taylor, M. P. (2016). Can field portable X-ray fluorescence (pXRF) produce high quality data for application in environmental contamination research? *Environmental Pollution (Barking, Essex: 1987)*, *214*, 255–264. DOI/URL: https://doi.org/10.1016%2Fj.envpol.2016.03.055

Rowe, H., Morrell, A., Nieto, M., Nance, S., Narasimhan, S., Mainali, P., Ganser, N., Garza, J., & Grillo, J. (2017). Inorganic Geochemical Characteristics of Lithofacies and Their Linkages to the Mechanical Stratigraphy of Uppermost Wolfcamp and Lower Bone Spring Formations, Delaware Basin, Texas. Unconventional Resources Technology Conference. DOI/URL: https://doi.org/10.15530%2FURTEC-2017-2689141

Rull, V., Cañellas-Boltà, N., Margalef, O., Sáez, A., Pla-Rabes, S., & Giralt, S. (2015). Late Holocene vegetation dynamics and deforestation in Rano Aroi: Implications for Easter Island's ecological and cultural history. *Quaternary Science Reviews*, *126*, 219–226. DOI/URL: https://doi.org/10.1016%2Fj.quascirev.2015.09.008

Rull, V., Ca\textbackslashtextbackslash\textbackslashtextasciitilde{n}ellas-Bolt\textbackslashtextbackslash‘{a}, N., S\textbackslashtextbackslash’{a}ez, A., Giralt, S., Pla, S., & Margalef, O. (2010). Paleoecology of Easter Island: Evidence and uncertainties. *Earth-Science Reviews*, *99*(1), 50–60. DOI/URL: https://doi.org/10.1016%2Fj.earscirev.2010.02.003

Rutkiewicz, P., Malik, I., Wistuba, M., & Osika, A. (2019). High concentration of charcoal hearth remains as legacy of historical ferrous metallurgy in southern Poland. *Quaternary*

International.
DOI/URL: https://doi.org/10.1016%2Fj.quaint.2019.04.015

Rutkiewicz, P., Malik, I., Wistuba, M., & Sady, A. (2017). Charcoal kilns as a source of data on the past iron industry (an example from the River Czarna valley, Central Poland). *Environmental & Socio-economic Studies*, *5*(3), 12–22.
DOI/URL: https://doi.org/10.1515%2Fenviron-2017-0012

Sabbadini, R. (1919). I nomi locali dell'Elba [von Aithalia bis Gambale]. *Rendiconti. Classe di lettere e scienze morali e storiche, Istituto lombardo, Accademia di scienze e lettere*, *52*, 835–858.

Sadori, L., Mercuri, A. M., & Mariotti Lippi, M. (2010). Reconstructing past cultural landscape and human impact using pollen and plant macroremains. *Plant Biosystems - An International Journal Dealing with all Aspects of Plant Biology*, *144*(4), 940–951.
DOI/URL: http://dx.doi.org/10.1080/11263504.2010.491982

Sallares, R. (2009). Environmental History. In *A Companion to Ancient History*, (pp. 164–174). John Wiley & Sons, Ltd.
DOI/URL: https://doi.org/10.1002/9781444308372.ch16

Sallares, R. F. i. B. S. R., & Sallares, R. (2002). *Malaria and Rome: A History of Malaria in Ancient Italy*. OUP Oxford.

Salminen, R., Batista, M. J., Bidovec, M., Demetriades, A., De Vivo, B., De Vos, W., Duris, M., Gilucis, A., Gregorauskiene, V., Halamic, J., Heitzmann, P., Lima, A., Jordan, G., Klaver, G., Klein, P., Lis, J., Locutura, J., Marsina, K., Mazreku, A., O'Connor, P. J., Olsson, S., Ottesen, R.-T., Petersell, V., Plant, J., Reeder, S., Salpeteur, I., Sandström, H., Siewers, U., Steenfelt, A., & Tarvainen, T. (2005). *Geochemical Atlas of Europe. Part 1: Background Information, Methodology and Maps*. Espoo: Geological Survey of Finland.

Salomon, F., Goiran, J.-P., Noirot, B., Pleuger, E., Bukowiecki, E., Mazzini, I., Carbonel, P., Gadhoum, A., Arnaud, P., Keay, S., Zampini, S., Kay, S., Raddi, M., Ghelli, A., Pellegrino, A., Morelli, C., & Germoni, P. (2018). Geoarchaeology of the Roman port-city of Ostia: Fluvio-coastal mobility, urban development and resilience. *Earth-Science Reviews*, *177*, 265–283.
DOI/URL: https://doi.org/10.1016%2Fj.earscirev.2017.10.003

Sands, R. (2005). *Forestry in a Global Context*. Wallingford: CABI. Google-Books-ID: UO1DAI60IQEC.

Sands, R. (2013). A history of human interaction with forests. In R. Sands (Ed.) *Forestry in a global context*, (pp. 1–36). Wallingford: CABI, 2nd ed.
DOI/URL: http://dx.doi.org/10.1079/9781780641560.0001

Saredo Parodi, N. (2013). *Populonia: Inferno o paradiso? Il polo siderurgico di Populonia nell'antichità, un tentativo di quantificazione. Con CD-ROM*. Roma: Aracne.

Sarti, G., Rossi, V., & Amorosi, A. (2012). Influence of Holocene stratigraphic architecture on ground surface settlements: A case study from the City of Pisa (Tuscany, Italy). *Sedimentary Geology*, *281*, 75–87.
DOI/URL: https://doi.org/10.1016%2Fj.sedgeo.2012.08.008

Schenk, W. (2006). Holznöte im 18. Jahrhundert? – Ein Forschungsbericht zur «Holznotdebatte» der 1990er Jahre [in German; Wood shortage in the 18th century? A report on the wood shortage debate of the 1990s]. *Schweizerische Zeitschrift fur Forstwesen*, *157*(9), 377–383.
DOI/URL: https://doi.org/10.3188%2Fszf.2006.0377

Schillereff, D. N., Chiverrell, R. C., Macdonald, N., & Hooke, J. M. (2014). Flood stratigraphies in lake sediments: A review. *Earth-Science Reviews*, *135*, 17–37.
DOI/URL: https://doi.org/10.1016%2Fj.earscirev.2014.03.011

Schlesinger, W. H., & Bernhardt, E. S. (2013). *Biogeochemistry: an analysis of global change*. Amsterdam, et al.: Elsevier, 3rd ed.

Schmid, E. M., Skjemstad, J. O., Glaser, B., Knicker, H., & Kögel-Knabner, I. (2002). Detection of charred organic matter in soils from a Neolithic settlement in Southern Bavaria, Germany. *Geoderma*, *107*(1), 71–91.
DOI/URL: https://doi.org/10.1016%2FS0016-7061(01)00139-2

Schmidt, M., Leipe, C., Becker, F., Goslar, T., Hoelzmann, P., Mingram, J., Müller, S., Tjallingii, R., Wagner, M., Meyer, H., & Tarasov, P. E. (2018). Methodology, results and calibration of X-ray fluorescence analysis from the sediment core RK12, Lake Kushu, Rebun Island, northern Japan, links to files.

Schmidt, M., Leipe, C., Becker, F., Goslar, T., Hoelzmann, P., Mingram, J., Müller, S., Tjallingii, R., Wagner, M., & Tarasov, P. E. (2019). A multi-proxy palaeolimnological record of the last 16,600 years from coastal Lake Kushu in northern Japan. *514*, 613–626.
DOI/URL: https://doi.org/10.1016%2Fj.palaeo.2018.11.010

Schmidt, M., Mölder, A., Schönfelder, E., Engel, F., & Fortmann-Valtink, W. (2016). Charcoal kiln sites, associated landscape attributes and historic forest conditions: DTM-based investigations in Hesse (Germany). *Forest Ecosystems*, *3*(1), 8.
DOI/URL: https://doi.org/10.1186/s40663-016-0067-6

Schmidt-Wygasch, C. M. (2011). *Neue Untersuchungen zur holozänen Genese des Unterlaufs der Inde. Chronostratigraphische Differenzierung der Auelehme unter besonderer Berücksichtigung der Montangeschichte der Voreifel*. Dissertation, Rheinisch-Westfälische Technische Hochschule Aachen, Fakultät für Georessourcen und Materialtechnik. Aachen: Publikationsserver der RWTH Aachen University.
DOI/URL: http://nbn-resolving.de/urn/resolver.pl?urn=urn:nbn:de:hbz:82-opus-38423

Schneider, A. R., Cancès, B., Breton, C., Ponthieu, M., Morvan, X., Conreux, A., & Marin, B. (2016). Comparison of field portable XRF and aqua regia/ICPAES soil analysis and evaluation of soil moisture influence on FPXRF results. *Journal of Soils and Sediments*, *16*(2), 438–448.
DOI/URL: https://doi.org/10.1007/s11368-015-1252-x

Schneider, H. (1992). *Einführung in die antike Technikgeschichte*. Die Altertumswissenschaft. Darmstadt: Wiss. Buchges.

Schneider, H. (2016). *Geschichte der antiken Technik*. No. 2432 in Beck'sche Reihe. München: C. H. Beck.

Schneider, J. F., Johnson, D., Stoll, N., Thurow, K., Koch, A., & Thurow, K. (2002). Portable X-Ray Fluorescence Analysis of a CW Facility Site for Arsenic Containing Warfare Agents. In R. R. McGuire, & J. C. Compton (Eds.) *Environmental Aspects of Converting CW Facilities to Peaceful Purposes*, NATO Science Series, (pp. 139–147). Springer Netherlands.

Schneider, S., Matthaei, A., Bebermeier, W., & Schütt, B. (2014). Late Holocene human–environmental interactions in the Eastern Mediterranean: Settlement history and paleogeography of an ancient Aegean hill-top settlement. *Quaternary International*, *324*, 84–98.
DOI/URL: https://doi.org/10.1016%2Fj.quaint.2013.05.023

Schroedter, T. M., Dreibrodt, S., Hofmann, R., Lomax, J., Müller, J., & Nelle, O. (2013). Interdisciplinary interpretation of challenging archives: Charcoal assemblages in Drina Valley alluvial and colluvial sediments (Jagnilo, Bosnia and Herzegovina). *Quaternary International*, *289*, 36–45.
DOI/URL: https://doi.org/10.1016%2Fj.quaint.2012.02.030

Schweighardt, E. (1841). *Das Eisen in historischer und national-ökonomischer Beziehung*. Dissertation, Universität Tübingen, Staatswirtschaftliche Facultät. München: Bayerische Staatsbibliothek.
DOI/URL: http://mdz-nbn-resolving.de/urn:nbn:de:bvb:12-bsb10849604-2

Scott, H. (1895). The Mines of Elba. *The Journal of the Iron and Steel Institute*, *47*(1), 141–191.

Seewald, R. (1921). *Reise nach Elba; mit vierundzwanzig Zeichungen*. Augsburg, Köln, Wien: Dr. Benno Filser.

Senn, M., Gfeller, U., Guenette-Beck, B., Lienemann, P., & Ulrich, A. (2010). Tools to Qualify Experiments with Bloomery Furnaces*. *Archaeometry*, *52*(1), 131–145.
DOI/URL: https://doi.org/10.1111%2Fj.1475-4754.2009.00461.x

Serneels, V., & Crew, P. (1997). Ore-slag relationships from experimentally smelted bog-iron ore. *Early Ironworking in Europe: Archaeology and Experiment. Occasional Paper, 3*, 78–82.

Service Hydrographique et Oceanographique de la Marine (2014). *Cote ouest d'Italy – Ile d'Elbe. Échelle (Scale) 1 : 40 000 (42°49")*.

Servida, D. (2009). *Innovative approaches to evaluate geochemical risk related to sulphide-bearing Abandoned Mine Lands*. Doctoral Thesis, Università degli studi di Milano, Dipartimento di Scienze della Terra "Ardito Desio". Milano: Università degli Studi di Milano.
DOI/URL: http://dx.doi.org/10.13130/servida-diego_phd2009

Servida, D., Grieco, G., & De Capitani, L. (2009). Geochemical hazard evaluation of sulphide-rich iron mines: The Rio Marina district (Elba Island, Italy). *Journal of Geochemical Exploration*, *100*(1), 75–89.
DOI/URL: https://doi.org/10.1016%2Fj.gexplo.2008.03.005

Shaw, I. (1998). Exploiting the Desert Frontier: The Logistics and Politics of Ancient Egyptian Mining Expeditions. In A. B. Knapp, V. C. Pigott, & E. W. Herbert (Eds.) *Social Approaches to an Industrial Past*, (pp. 242–258). London, New York: Routledge.

Shepherd, R. (1993). *Ancient Mining*. London: Elsevier Applied Science.

Sherwood, A. N., Nikolic, M., Humphrey, J. W., & Oleson, J. P. (2003). *Greek and Roman Technology: A Sourcebook: Annotated Translations of Greek and Latin Texts and Documents*. Routledge.

Shotyk, W., Weiss, D., Appleby, P. G., Cheburkin, A. K., Frei, R., Gloor, M., Kramers, J. D., Reese, S., & Knaap, W. O. V. D. (1998). History of Atmospheric Lead Deposition Since 12,370 14c yr BP from a Peat Bog, Jura Mountains, Switzerland. *Science*, *281*(5383), 1635–1640. DOI/URL: https://doi.org/10.1126%2Fscience.281.5383.1635

Silva, A. R. d., Malafaia, G., & Menezes, I. P. P. d. (2017). biotools: an R function to predict spatial gene diversity via an individual-based approach. *Genetics and Molecular Research*, *16*, gmr16029655.

Simonin, L. (1858). De l'explotation des mines et de la metallurgie en Toscane pendant l'antiquité et de moyen age. *Annales des mines ou Recueil de mémoires sur l'exploitation des mines et sur les sciences qui s'y rapportent*, *14*, 557–615.

Sivramkrishna, S. (2009). Production Cycles and Decline in Traditional Iron Smelting in the Maidan , Southern India, c. 1750-1950: An Environmental History Perspective. *Environment and History*, *15*(2), 163–197. DOI/URL: www.jstor.org/stable/20723719

Sloto, R. A. (2011). Trace metals related to historical iron smelting at Hopewell Furnace National Historic Site, Berks and Chester Counties, Pennsylvania. USGS Numbered Series 2011-3101, U.S. Geological Survey, Reston, VA. DOI/URL: http://pubs.er.usgs.gov/publication/fs20113101

Sloto, R. A., & Reif, A. G. (2011). Distribution of trace metals at Hopewell Furnace National Historic Site, Berks and Chester Counties, Pennsylvania. USGS Numbered Series 2011-5014, U.S. Geological Survey. DOI/URL: https://doi.org/10.3133/sir20115014

Smith, A. H. V. (1997). Provenance of coals from Roman sites in England and Wales. *Britannia*, *28*, 297–324. DOI/URL: https://doi.org/10.2307/526770

Smith, D. E., Harrison, S., Firth, C. R., & Jordan, J. T. (2011). The early Holocene sea level rise. *Quaternary Science Reviews*, *30*(15), 1846–1860. DOI/URL: https://doi.org/10.1016%2Fj.quascirev.2011.04.019

Snodgrass, A. M. (1980). Iron and Early Metallurgy in the Mediterranean. In T. A. Wertime, & J. D. Muhly (Eds.) *The Coming of the Age of Iron*, (pp. 335–374). New Haven: Yale Univ. Pr.

Sonnabend, H. (2012). *Mensch und Umwelt in der Antike*. Umweltgeschichte in globaler Perspektive: Vorlesungsreihe des Historischen Seminars der Universität Erfurt im Sommersemester 2010. Erfurt: Universität Erfurt, Philosophische Fakultät. DOI/URL: https://nbn-resolving.org/urn:nbn:de:gbv:547-201200053

Sperl, G. (1981). Untersuchungen zur Metallurgie der Etrusker. In A. Neppi Modona, G. C. Cianferoni, & M. G. M. Costagli (Eds.) *L'Etruria mineraria*, (pp. 29–50). Firenze.

Sperl, G. (1993). Eisenschlacken von S. Caterina, Rio nell'Elba. *Quaderni di S. Caterina*, *3*, 73–75.

Spiess, A.-N. (2018). *propage: Propagation of Uncertainty [R package, v1.0-6]*. DOI/URL: https://cran.r-project.org/package=propagate

Stöllner, T. (2003). Mining and Economy: A Discussion of Spatial Organisation and Structures of Early Raw Material Exploitation. In T. Stöllner, G. Körlin, G. Steffens, & J. Cierny (Eds.) *Man and Mining*, Der Anschnitt, Beih. 16 = Veröffentlichungen aus dem Deutschen Bergbau-Museum Bochum, (pp. 415–445). Bochum: Dt. Bergbaumuseum.

Stöllner, T. (2008). Mining Landscapes in Early Societies: Imprinting Processes in Pre- and Protohistoric Economies? In C. Bartels, & C. Küpper-Eichas (Eds.) *Cultural Heritage and Landscapes in Europe = Landschaften. Kulturelles Erbe in Europa: Proceedings of the International Conference*, Veröffentlichungen aus dem Deutschen Bergbau-Museum Bochum, (pp. 65–92). Bochum: Dt. Bergbaumuseum.

Stocchi, P., Vacchi, M., Lorscheid, T., de Boer, B., Simms, A. R., van de Wal, R. S. W., Vermeersen, B. L. A., Pappalardo, M., & Rovere, A. (2018). MIS 5e relative sea-level changes in the Mediterranean Sea: Contribution of isostatic disequilibrium. *Quaternary Science Reviews*, *185*, 122–134.
DOI/URL: https://doi.org/10.1016%2Fj.quascirev.2018.01.004

Stocker, T. F., Dahe, Q., Plattner, G.-K., Alexander, L. V., Allen, S. K., Bindoff, N. L., Bréon, F.-M., Church, J. A., Cubasch, U., Emori, S., Forster, P., Friedlingstein, P., Gillett, N., Gregory, J. M., Hartmann, D. L., Jansen, E., Kirtman, B., Knutti, R., Kanikicharla, K. K., Lemke, P., Marotzke, J., Masson-Delmotte, V., Meehl, G. A., Mokhov, I. I., Piao, S., Ramaswamy, V., Randall, D., Rhein, M., Rojas, M., Sabine, C., Shindell, D., Talley, L. D., Vaughan, D. G., & Xie, S.-P. (2013). Technical Summary. In T. F. Stocker, Q. Dahe, G.-K. Plattner, M. Tigor, S. K. Allen, J. Boschung, A. Nauels, Y. Xia, V. Bex, & P. Midgley (Eds.) *Climate Change 2013: The Physical Science Basis. Contribution of Working Group I to the Fifth Assessment Report of the Intergovernmental Panel on Climate Change*. Cambridge, U.K., New York: Cambridge University Press.

Stoddart, S., Woodbridge, J., Palmisano, A., Mercuri, A. M., Mensing, S. A., Colombaroli, D., Sadori, L., Magri, D., Di Rita, F., Giardini, M., Mariotti Lippi, M., Montanari, C., Bellini, C., Florenzano, A., Torri, P., Bevan, A., Shennan, S., Fyfe, R., & Roberts, C. N. (2019). Tyrrhenian central Italy: Holocene population and landscape ecology. *The Holocene*, *29*(5), 761–775.
DOI/URL: https://doi.org/10.1177/0959683619826696

Stolz, C., Böhnke, S., & Grunert, J. (2012). Reconstructing 2500 years of land use history on the Kemel Heath (Kemeler Heide), southern Rhenish Massif, Germany. *E&G – Quaternary Science Journal*, *61*(2), 169–183.
DOI/URL: https://doi.org/10.23689%2Ffidgeo-1783

Stolz, C., & Grunert, J. (2008). Floodplain sediments of some streams in the Taunus and Westerwald Mts., western Germany, as evidence of historical land use. *Zeitschrift für Geomorphologie*, *52*(3), 349–373.

Stolz, C., Grunert, J., & Fülling, A. (2013). Quantification and dating of floodplain sedimentation in a medium-sized catchment of the German uplands: a case study from

the Aar Valley in the southern Rhenish Massif, Germany. *DIE ERDE–Journal of the Geographical Society of Berlin*, *144*(1), 30–50.

Straka, T. J. (2014). Historic Charcoal Production in the US and Forest Depletion: Development of Production Parameters. *Advances in Historical Studies*, *03*, 104. DOI/URL: https://doi.org/10.4236%2Fahs.2014.32010

Straka, T. J. (2017). Charcoal as a Fuel in the Ironmaking and Smelting Industries. *Advances in Historical Studies*, *06*, 56. DOI/URL: https://doi.org/10.4236%2Fahs.2017.61004

Superson, J., Rodzik, J., & Reder, J. (2014). Natural and human influence on loess gully catchment evolution: A case study from Lublin Upland, E Poland. *Geomorphology*, *212*, 28–40. DOI/URL: https://doi.org/10.1016%2Fj.geomorph.2013.09.011

Surovell, T. A., & Brantingham, P. J. (2007). A note on the use of temporal frequency distributions in studies of prehistoric demography. *Journal of Archaeological Science*, *34*(11), 1868–1877. DOI/URL: https://doi.org/10.1016%2Fj.jas.2007.01.003

Swieder, A. (2014). Landschaftsarchäologie im Ostharz anhand von Laserscan-Daten. *Hallesches Jahrbuch für Geowissenschaften / Beiheft*, *34*(Nutzung von Laserscanhöhendaten für angewandte Umwelt- und Geowissenschaftliche Fragen in Sachsen-Anhalt), 41–52. DOI/URL: http://public.bibliothek.uni-halle.de/index.php/hjgb/article/view/261

Swinburne, H. (1814). Extracts from the portfolio of a man of letters [Swinburne's account of the Island of Elba]. *The Monthly Magazine; or, British Register*, *37*(1), 428–431.

Tanelli, G. (1985). I giacimenti minerari dell'Etruria e le attività estrattive degli etruschi. In G. Camporeale (Ed.) *L'Etruria mineraria*, Progetto Etruschi, (pp. 37–38). Milano: Electa Ed. [u.a.].

Tanelli, G., Benvenuti, M., Costagliola, P., Dini, A., Lattanzi, P., Maineri, C., Mascaro, I., & Ruggieri, G. (2001). The iron mineral deposits of Elba Island: State of the art. *Ofioliti*, *26*(2), 239–248. DOI/URL: https://doi.org/10.4454%2Fofioliti.v26i2a.148

Taylor, G., Eggleton, R. A., & Eggleton, R. A. (2001). *Regolith Geology and Geomorphology*. John Wiley & Sons.

Taylor, M. P. (1996). The variability of heavy metals in floodplain sediments: A case study from mid Wales. *CATENA*, *28*(1), 71–87. DOI/URL: https://doi.org/10.1016%2FS0341-8162(96)00026-4

Tchernia, A. (1983). Italian wine in Gaul at the end of the republic. In P. Garnsey, K. Hopkins, & C. R. Whittaker (Eds.) *Trade in the ancient economy*, (pp. 87–104). London: Chatto & Windus; Hogarth Press.

Täckholm, U. (1937). *Studien über den Bergbau der römischen Kaiserzeit*. Dissertation, Uppsala universitet. Uppsala: Appelbergs Boktryckeriaktiebolag.

Tema, E., Hedley, I., & Lanos, P. (2006). Archaeomagnetism in Italy: a compilation of data including new results and a preliminary Italian secular variation curve. *Geophysical Journal International*, *167*(3), 1160–1171.
DOI/URL: https://doi.org/10.1111/j.1365-246X.2006.03150.x

Templ, M., Filzmoser, P., & Reimann, C. (2008). Cluster analysis applied to regional geochemical data: Problems and possibilities. *Applied Geochemistry*, *23*(8), 2198–2213.
DOI/URL: https://doi.org/10.1016%2Fj.apgeochem.2008.03.004

Templ, M., Hron, K., & Filzmoser, P. (2011). robCompositions: an R-package for robust statistical analysis of compositional data. In V. Pawlowsky-Glahn, K. Hron, & P. Filzmoser (Eds.) *Compositional Data Analysis: Theory and Applications*. John Wiley and Sons.
DOI/URL: https://doi.org/10.1002/9781119976462.ch25

Thelemann, M. (2016). *Human and Environment Interactions in the Environs of Prehistorical Iron Smelting Places in Silesia, Poland*. Doctoral Thesis, Freie Universität Berlin, Department of Earth Sciences, Berlin.
DOI/URL: https://refubium.fu-berlin.de/handle/fub188/3328

Thelemann, M., Bebermeier, W., Hoelzmann, P., & Lehnhardt, E. (2017). Bog iron ore as a resource for prehistoric iron production in Central Europe—A case study of the Widawa catchment area in eastern Silesia, Poland. *CATENA*, *149*, 474–490.
DOI/URL: https://doi.org/10.1016%2Fj.catena.2016.04.002

Thelemann, M., Bebermeier, W., Hoelzmann, P., & Schütt, B. (2018). Landscape history since the Saalian Drenthe stadial in the Widawa Catchment Area in Silesia, Poland: A case study on long-term landscape changes. *Quaternary International*, *463*, 57–73.
DOI/URL: https://doi.org/10.1016%2Fj.quaint.2016.09.015

Thelemann, M., Lehnhardt, E., Bebermeier, W., & Meyer, M. (2015). Iron, Humans and Landscape – Insights from a Micro-Region in the Widawa Catchment Area, Silesia. *eTopoi. Journal for Ancient Studies*, *4*(Bridging the Gap – Integrated Approaches in Landscape Archaeology).
DOI/URL: http://journal.topoi.org/index.php/etopoi/article/view/232

Thiébaut de Berneaud, A. (1814). *A Voyage to the Isle of Elba: with Notices of the Other Islands in the Tyrrhenian Sea*. London: Longman, Hurst, Rees, Orme, and Brown.

Thöne, C., Vögele, H., & Messmer, K. (2004). Die griechischen und römischen Tonlampen. Mainz am Rhein.

Thomas, G. R., & Young, T. P. (1999). The determination of bloomery furnace mass balance and efficiency. *Geological Society, London, Special Publications*, *165*(1), 155–164.
DOI/URL: https://doi.org/10.1144%2FGSL.SP.1999.165.01.12

Thommes, P. (1997). *Eine Methode zur Rekonstruktion der Waldschädigung durch ur-und frühgeschichtliche Meiler- und Verhüttungstechnologie*. Dissertation, Albert-Ludwigs-Universität, Fachbereich Archäologie und Altertumswissenschaften. Freiburg i. Br.: Albert-Ludwigs-Unviersität.

Thompson, G., & Young, R. (1999). Fuels for the Furnace. In M. van der Veen (Ed.) *The Exploitation of Plant Resources in Ancient Africa*, (pp. 221–239). Boston, MA: Springer US.
DOI/URL: https://doi.org/10.1007/978-1-4757-6730-8_18

Thorndycraft, V. R., & Benito, G. (2006). The Holocene fluvial chronology of Spain: evidence from a newly compiled radiocarbon database. *Quaternary Science Reviews*, *25*(3), 223–234.
DOI/URL: https://doi.org/10.1016%2Fj.quascirev.2005.07.003

Toner, J. (2018). *Roman Disasters*. John Wiley & Sons.

Tortora, P., Bellotti, P., & Valeri, P. (2001). Late-Pleistocene and Holocene deposition along the coasts and continental shelves of the Italian peninsula. In G. B. Vai, & I. P. Martini (Eds.) *Anatomy of an Orogen: the Apennines and Adjacent Mediterranean Basins*, (pp. 455–477). Dordrecht: Springer Netherlands.
DOI/URL: https://doi.org/10.1007/978-94-015-9829-3_25

Toti, F., Bertini, A., Vivarelli, M., Costagliola, P., Benvenuti, M., D'Orefice, M., Foresi, L. M., & Fedi, M. E. (2014). Il contributo palinologico alla ricostruzione dei paleoambienti e dell'impatto umano all'Isola d'Elba durante il medio e tardo Olocene: Dati e nuove strategie di ricerca. In M. Marino, A. Girone, R. La Perna, & P. Maiorano (Eds.) *Giornate di Paleontologia XIV edizione*, (pp. 66–67). Bari.

Trambusti, M., Buti, I., Leoni, R., Menci, S., Morini, F., Del Seppia, R., & Del Nista, D. (2014). *Alluvione Isola d'Elba 7 Novembre 2011 – Report*. Livorno.
DOI/URL: http://www.regione.toscana.it/documents/10180/70976/Report+-+Alluvione+Isola+d%27Elba+7+Novembre+2011/450ecc74-7ece-46dc-8f48-9799ea32e781

Turfa, J. M. (2018). The Etruscans. In G. D. Farney, & G. J. Bradley (Eds.) *The Peoples of Ancient Italy*, De Gruyter reference, (pp. 637–671). Boston, Berlin: De Gruyter.

Turner, J. N., Jones, A. F., Brewer, P. A., Macklin, M. G., & Rassner, S. M. (2015). Micro-XRF Applications in Fluvial Sedimentary Environments of Britain and Ireland: Progress and Prospects. In I. W. Croudace, & R. G. Rothwell (Eds.) *Micro-XRF Studies of Sediment Cores: Applications of a non-destructive tool for the environmental sciences*, Developments in Paleoenvironmental Research, (pp. 227–265). Dordrecht: Springer Netherlands.
DOI/URL: https://doi.org/10.1007/978-94-017-9849-5_8

Turner, J. N., Macklin, M. G., Jones, A. F., & Lewis, H. (2010). New perspectives on Holocene flooding in Ireland using meta-analysis of fluvial radiocarbon dates. *CATENA*, *82*(3), 183–190.
DOI/URL: https://doi.org/10.1016%2Fj.catena.2010.06.004

Twidale, C. R., & Romani, J. R. V. (2005). *Landforms and Geology of Granite Terrains*. Leiden: CRC Press.

Tylecote, R. F., Ghaznavi, H. A., & Boydell, P. J. (1977). Partitioning of trace elements between the ores, fluxes, slags and metal during the smelting of copper. *Journal of Archaeological Science*, *4*(4), 305–333.
DOI/URL: https://doi.org/10.1016%2F0305-4403(77)90027-9

United States Bureau of Mines, & Trush, P. W. (Eds.) (1968). *A Dictionary of Mining, Mineral, and Related Terms*. U.S. Bureau of Mines. Special Publication. U.S. Department of the Interior. Google-Books-ID: nTrbAAAAMAAJ.

Vaccaro, E. (2008). An overview of rural settlement in four river basins in the province of Grosseto on the coast of Tuscany (200 B.C.–A.D. 600). *Journal of Roman Archaeology*, *21*, 225–247.
DOI/URL: https://doi.org/10.1017%2FS1047759400004451

Van Andel, T. H., Runnels, C. N., & Pope, K. O. (1986). Five thousands years of land use and abuse in the southern Argolid, Greece. *Hesperia: The Journal of the American School of Classical Studies at Athens*, *55*(1), 103–128.
DOI/URL: https://www.jstor.org/stable/147733

van Andel, T. H., Zangger, E., & Demitrack, A. (1990). Land Use and Soil Erosion in Prehistoric and Historical Greece. *Journal of Field Archaeology*, *17*(4), 379–396.
DOI/URL: https://doi.org/10.1179%2F009346990791548628

Van den Boogaart, K. G., Tolosana, R., & Bren, M. (2014). *compositions: Compositional Data Analysis [R package, v1.40-3]*.
DOI/URL: https://CRAN.R-project.org/package=compositions

Van den Boogaart, K. G., & Tolosana-Delgado, R. (2013). *Analyzing Compositional Data with R*. Use R! Berlin, Heidelberg: Springer-Verlag.
DOI/URL: http://dx.doi.org/10.1007/978-3-642-36809-7

Vanagoli, G. (1971). Elenco site rio marina – cavo – rio nell'elba. *Archivio Storico della ex Soprintendenza Archeologia per la Toscana*, *n.1 pos. 9 Livorno 8*.

Vanagolli, G. (1993). Per una storia della ricerca archeologica all'Isola d'Elba. *Rivista Italiana di Studi Napoleonici*, *30*(1), 127–150.

Vandermersch, C. (1994). *Vins et amphores de Grande Grèce et de Sicile, 4e-3e s: avant J.-C*. Naples: Centre Jean Bérard.

Vanni, E. (2014). Sistemi agro-silvo-pastorali in un contesto dell'Etruria costiera. Aspetti conservativi del paesaggio in una prospettiva di lunga durata.
DOI/URL: https://doi.org/10.14274%2FUNIFG%2FFAIR%2F335328

Vannière, B., Colombaroli, D., Chapron, E., Leroux, A., Tinner, W., & Magny, M. (2008). Climate versus human-driven fire regimes in Mediterranean landscapes: the Holocene record of Lago dell'Accesa (Tuscany, Italy). *Quaternary Science Reviews*, *27*(11), 1181–1196.
DOI/URL: https://doi.org/10.1016%2Fj.quascirev.2008.02.011

Veal, R. (2019). The history and science of fire and fuel in the roman empire. In R. Veal, & V. Leitch (Eds.) *Fuel and Fire in the Ancient Roman World – Towards an integrated economic understanding*, McDonald Institute Conversations, (pp. 11–24). McDonald Institute for Archaeological Research, University of Cambridge.

Veal, R. J. (2012). From Context to Economy: Charcoal as An Archaeological Interpretative Tool: A Case Study from Pompeii, 3rd c. B. C. to A. D. 79. In I. Schrüfer-Kolb (Ed.) *More Than Just Numbers? Ninth Roman Archaeology conference*, International Roman Conference Series = JRA Suppl., (pp. 19–51). Portsmouth, RI: JRA.

Veal, R. J. (2013). Fuelling Ancient Mediterranean Cities: A Framework for Charcoal Research. In W. V. Harris (Ed.) *The Ancient Mediterranean Environment between Science and History*, Columbia Studies in the Classical Tradition, (pp. 37–58). Leiden: Brill.
DOI/URL: https://doi.org/10.1163/9789004254053_004

Veal, R. J. (2017a). The Politics and Economics of Ancient Forests: timber and fuel as levers of Greco-Roman control. Hardt Foundation.
DOI/URL: https://doi.org/10.17863/CAM.13218

Veal, R. J. (2017b). Wood and Charcoal for Rome: Towards an Understanding of Ancient Regional Fuel Economics. In T. de Haas, & G. Tol (Eds.) *The Economic Integration of Roman Italy*, Mnemosyne. A Journal of Classical Studies Supplements, (pp. 388–406). Boston: Brill.
DOI/URL: https://doi.org/10.1163/9789004345027_017

Veldhuijzen, H. A. (2003). 'Slag_fun' - a New Tool for Archaeometallurgy: Development of an Analytical (P)Ed-Xrf Method for Iron-Rich Materials. *Papers from the Institute of Archaeology*, *14*, 102–118.
DOI/URL: http://dx.doi.org/10.5334/pia.199

Verboven, K. (2018). Ancient cliometrics and archaeological proxy-data : between the devil and the deep blue sea. In *Cuantificar las economías antiguas : problemas y métodos : quantifying ancient economies : problems and methodologies*, (pp. 345–371). Universitat de Barcelona. Edicions.
DOI/URL: http://hdl.handle.net/1854/LU-8565379

Vergari, F., Della Seta, M., Del Monte, M., & Barbieri, M. (2013). Badlands denudation "hot spots": The role of parent material properties on geomorphic processes in 20-years monitored sites of Southern Tuscany (Italy). *CATENA*, *106*, 31–41.
DOI/URL: https://doi.org/10.1016%2Fj.catena.2012.02.007

Verola, M. L., & Degl'Innocenti, M. (2016). I reperti faunistici. In O. Pancrazzi (Ed.) *Castiglione di San Martino*, Studia erudita, (pp. 232–247). Pisa: Istituti Editoriali e Poligrafici Internazionali.

Verstraeten, G., Posen, J., Dirk Goossens, Gillijns, K., Bielders, C., Gabriels, D., Ruysschaert, G., Van Den Eeckhaut, M., Vanwalleghem, T., & Govers, G. (2007). Belgium. In J. Boardman, & J. Poesen (Eds.) *Soil Erosion in Europe*, (pp. 385–412). John Wiley & Sons.

Vigliotti, L., Roveri, M., & Capotondi, L. (2003). Etruscan archaeometallurgy record in sediments from the Northern Tyrrhenian Sea. *Journal of Archaeological Science*, *30*(7), 809–815.
DOI/URL: https://doi.org/10.1016%2FS0305-4403(02)00246-7

Vincenzo, S. D., Domdey, C., Hoelzmann, P., Knitter, D., Moede, K., Müller, M., & Obeloer, F. (2013). Zur Archäologie und Landschaftsentwicklung im Turano-Tal (Sabiner Berge), Italien. *eTopoi. Journal for Ancient Studies*, *2*, 45–110.
DOI/URL: https://refubium.fu-berlin.de/handle/fub188/20006

Vinci, A., & Gardin, L. (n.d.a). *Catalogo dei Suoli della Carta dei Suoli della Toscana in Scala 1:250.000*, vol. ea of *Progetto Carta dei suoli d'Italia in scala 1:250 000*.

Vinci, A., & Gardin, L. (n.d.b). *Catalogo delle Unità Cartografiche della Carta dei Souli della Toscana in Scala 1:250,000*. Regione Toscana. Direzione Generale Sviluppo Economico. Settore Foreste e Patrimonio Agro-Forestale.

Visser, R. M. (2010). Growing and felling? Theory and Evidence Related to the Application of Silvicultural Systems in the Roman Period. In A. Moore, G. Taylor, & E. Harris (Eds.) *TRAC 2009*, (pp. 11–22). Oxford: Oxbow Books.

Vita-Finzi, C. (1969). *The Mediterranean Valleys: Geological Changes in Historical Times*. Cambridge, U.K.: Cambridge University Press.

Vogel, S., Märker, M., Rellini, I., Hoelzmann, P., Wulf, S., Robinson, M., Steinhübel, L., Di Maio, G., Imperatore, C., Kastenmeier, P., Liebmann, L., Esposito, D., & Seiler, F. (2016). From a stratigraphic sequence to a landscape evolution model: Late Pleistocene and Holocene volcanism, soil formation and land use in the shade of Mount Vesuvius (Italy). *Quaternary International*, *394*, 155–179.
DOI/URL: https://doi.org/10.1016%2Fj.quaint.2015.02.033

Volk, M., & Steinhardt, U. (2001). Landscape balance. In R. Krönert, U. Steinhardt, & M. Volk (Eds.) *Landscape Balance and Landscape Assessment*, (pp. 163–202). Berlin, Heidelberg: Springer Berlin Heidelberg.
DOI/URL: https://doi.org/10.1007/978-3-662-04532-9_7

von Carlowitz, H. C. (1713). *Sylvicultura oeconomica oder Haußwirthliche Nachricht und Naturmäßige Anweisung zur Wilden Baum-Zucht*, vol. ot. Leipzig: Johann Friedrich Braun.
DOI/URL: https://nbn-resolving.org/urn:nbn:de:bvb:384-uba002974-9

Voss, O. (1988). The Iron Production in Populonia. In G. Sperl (Ed.) *The First Iron in the Mediterranean*, Pact. Revue du Groupe européen d'études pour les techniques physiques, chimiques et mathématiques appliquées à l'archéologie, (pp. 91–100). Rixensart.

Voulgaridis, E. V., & Passialis, C. N. (1995). Characteristics and technological properties of the wood of mediterranean evergreen hardwoods. *Forêt méditerranéenne*.

Wagreich, M., & Draganits, E. (2018). Early mining and smelting lead anomalies in geological archives as potential stratigraphic markers for the base of an early Anthropocene. *The Anthropocene Review*, *5*(2), 177–201.
DOI/URL: https://doi.org/10.1177/2053019618756682

Wallner, M. (2013). Die ‚deserta boiorum' – ein Zentrum der vorrömischen Eisenindustrie. In R. Karl, & J. Leskovar (Eds.) *Interpretierte Eisenzeiten, Tagungsbeitrage der 5. Linzer Gespräche zur interpretativen Eisenzeitarchäologie*, (pp. 209–222). Linz.

Walsh, K., Berger, J.-F., Roberts, C. N., Vanniere, B., Ghilardi, M., Brown, A. G., Woodbridge, J., Lespez, L., Estrany, J., Glais, A., Palmisano, A., Finné, M., & Verstraeten, G. (2019). Holocene demographic fluctuations, climate and erosion in the Mediterranean: A meta data-analysis. *The Holocene*, *29*(5), 864–885.
DOI/URL: https://doi.org/10.1177/0959683619826637

Wang, W., Lai, D., Abid, A., Neogi, S., Xu, X., & Wang, C. (2018). Effects of Steel Slag and Biochar Incorporation on Active Soil Organic Carbon Pools in a Subtropical Paddy Field. *Agronomy*, *8*(8), 135.
DOI/URL: https://doi.org/10.3390%2Fagronomy8080135

Wardenga, U., & Weichhart, P. (2006). Sozialökologische Interaktionsmodelle und Systemtheorien : Ansätze einer theoretischen Begründung integrativer Projekte in der Geographie? *Mitteilungen der Österreichischen Geographischen Gesellschaft*, *148*, 9–31.

Warnes, G. R., Bolker, B., Bonebakker, L., Gentleman, R., Liaw, W. H. A., Lumley, T., Maechler, M., Magnusson, A., Moeller, S., Schwartz, M., & Venables, B. (2016). *gplots: Various R Programming Tools for Plotting Data [R package, v3.0.1.1]*.
DOI/URL: https://CRAN.R-project.org/package=gplots

Warren, G., McDermott, C., O'Donnell, L., & Sands, R. (2012). Recent excavations of charcoal production platforms in the Glendalough valley, Co. Wicklow. *Journal of Irish Archaeology*, *21*, 85–112.

Wedepohl, K. H. (1995). The composition of the continental crust. *Geochimica et Cosmochimica Acta*, *59*(7), 1217–1232.
DOI/URL: https://doi.org/10.1016%2F0016-7037(95)00038-2

Weir, J. (1799). Plan of the Island of Elba. In *Island of Elba with four interesting views of the capital*, no. 1917,1208.4238 in The British Museum – Collection online. London: Thiselton, Printer.

Weisgerber, G., & Willies, L. (2000). The use of fire in prehistoric and ancient miningfiresetting. *Paléorient*, *26*(2), 131–149.
DOI/URL: https://doi.org/10.3406%2Fpaleo.2000.4715

Weltje, G. J., Bloemsma, M. R., Tjallingii, R., Heslop, D., Röhl, U., & Croudace, I. W. (2015). Prediction of Geochemical Composition from XRF Core Scanner Data: A New Multivariate Approach Including Automatic Selection of Calibration Samples and Quantification of Uncertainties. In I. W. Croudace, & R. G. Rothwell (Eds.) *Micro-XRF Studies of Sediment Cores: Applications of a non-destructive tool for the environmental sciences*, Developments in Paleoenvironmental Research, (pp. 507–534). Dordrecht: Springer Netherlands.
DOI/URL: https://doi.org/10.1007/978-94-017-9849-5_21

Weltje, G. J., & Tjallingii, R. (2008). Calibration of XRF core scanners for quantitative geochemical logging of sediment cores: Theory and application. *Earth and Planetary Science Letters*, *274*(3), 423–438.
DOI/URL: https://doi.org/10.1016%2Fj.epsl.2008.07.054

Wertime, T. A. (1983). The furnace versus the goat: The pyrotechnologic industries and Mediterranean deforestation in antiquity. *Journal of Field Archaeology*, *10*(4), 445–452.
DOI/URL: http://www.jstor.org/stable/529467

Westerman, D. S., Dini, A., Innocenti, F., & Rocchi, S. (2004). Rise and fall of a nested Christmas-tree laccolith complex, Elba Island, Italy. *Geological Society, London, Special Publications*, *234*(1), 195.
DOI/URL: https://doi.org/10.1144%2FGSL.SP.2004.234.01.12

Whipkey, C. E., Capo, R. C., Chadwick, O. A., & Stewart, B. W. (2000). The importance of sea spray to the cation budget of a coastal Hawaiian soil: a strontium isotope approach. *Chemical Geology*, *168*(1), 37–48.
DOI/URL: https://doi.org/10.1016%2FS0009-2541(00)00187-X

Wickham, H. (2018). *scales: Scale Functions for Visualization [R package, v1.1.0]*.
DOI/URL: https://CRAN.R-project.org/package=scales

Świetlik, R., Trojanowska, M., & Rabek, P. (2013). Distribution patterns of Cd, Cu, Mn, Pb and Zn in wood fly ash emitted from domestic boilers. *Chemical Speciation & Bioavailability*, *25*(1), 63–70.
DOI/URL: https://doi.org/10.3184/095422912X13497968675047

Wikander, r. (2009). Sources of Energy and Exploitation of Power. In J. P. Oleson (Ed.) *The Oxford Handbook of Engineering and Technology in the Classical World*, Oxford

Handbooks Online, (pp. 1–22). Oxford: Oxford University Press.
DOI/URL: https://doi.org/10.1093/oxfordhb/9780199734856.013.0007

Will, E. L. (1982). Greco-Italic Amphoras. *Hesperia. Journal of the American School of Classical Studies at Athens*, *51*(3), 338–356.

Williams, A. N. (2012). The use of summed radiocarbon probability distributions in archaeology: a review of methods. *Journal of Archaeological Science*, *39*(3), 578–589.
DOI/URL: https://doi.org/10.1016%2Fj.jas.2011.07.014

Williams, C. E. (2005). Iron and stelle: environmental impact. In *The Industrial Revolution in America, Volume 1: Iron and Steel*, (pp. 157–182). New York: ABC-CLIO.

Williams, D., Panella, C., & Keay, S. (2014). Dressel 1. In U. o. Southampton (Ed.) *Roman Amphorae: a digital resource*, vol. 463 of *Archaeological Data Service Collection*. York, U.K.: Department of Archaeology, University of York.

Williams, H. W. (1820). *Travels in Italy, Greece and the Ionian Islands: In a Series of Letters, Description of Manners, Scenery, and the Fine Arts*. A. Constable.

Williams, J. (2009). The environmental effects of Populonia's metallurgical industry: current evidence and future directions. *Etruscan Studies*, *12*(1), 131–152.

Williams, M. (1989). Deforestation: past and present. *Progress in Human Geography*, *13*(2), 176–208.
DOI/URL: https://doi.org/10.1177/030913258901300202

Williams, M. (2000). Dark ages and dark areas: global deforestation in the deep past. *Journal of Historical Geography*, *26*(1), 28–46.
DOI/URL: https://doi.org/10.1006%2Fjhge.1999.0189

Williams, M. (2010). *Deforesting the Earth: From Prehistory to Global Crisis, An Abridgment*. University of Chicago Press.

Williams, S. J., & Meisburger, E. P. (1987). Sand sources for the transgressive barrier coast of Long Island, New York: evidence for landward transport of shelf sediments. In *Coastal Sediments' 87, Proceedings of a Specialty Conference on Advances in Understanding of Coastal Sediment Processes.*, vol. 2, (pp. 1517–1532).

Willis, K. J., Gillson, L., & Brncic, T. M. (2004). How "Virgin" Is Virgin Rainforest? *Science*, *304*(5669), 402–403.
DOI/URL: https://doi.org/10.1126%2Fscience.1093991

Wiman, I. M. B. (2013). Etruscan Environments. In J. M. Turfa (Ed.) *The Etruscan World*, Routledge Worlds, (pp. 11–28). New York: Routledge.

Wing, M. K. C. f. J., Weston, S., Williams, A., Keefer, C., Engelhardt, A., Cooper, T., Mayer, Z., Kenkel, B., Team, t. R. C., Benesty, M., Lescarbeau, R., Ziem, A., Scrucca, L., Tang, Y., Candan, C., & Hunt, T. (2018). *caret: Classification and Regression Training [R package, v6.0-84]*.
DOI/URL: https://CRAN.R-project.org/package=caret

Wolff, H. D. (1855). *The island empire, or, Scenes of the first exile of the Emperor Napoleon I: together with a narrative of his residence on the island of Elba, taken from local information, the papers of the British resident, and other authentic sources*. London: Bosworth.
DOI/URL: https://catalog.hathitrust.org/Record/009039271

Woodbridge, J., Roberts, N., & Fyfe, R. (2018). Pan-Mediterranean Holocene vegetation and land-cover dynamics from synthesized pollen data. *Journal of Biogeography*, *45*(9), 2159–2174.
DOI/URL: https://doi.org/10.1111/jbi.13379

Wrubel, W. (1929). Escavazione e separazione elettromagnetica delle scorie di ferro di fusione etrusca. *Studi etruschi*, *3*, 405–409.

Yu, S.-Y., Berglund, B. E., Sandgren, P., & Lambeck, K. (2007). Evidence for a rapid sea-level rise 7600 yr ago. *Geology*, *35*(10), 891–894.
DOI/URL: https://doi.org/10.1130%2FG23859A.1

Zanchetta, G., Bini, M., Cremaschi, M., Magny, M., & Sadori, L. (2013). The transition from natural to anthropogenic-dominated environmental change in Italy and the surrounding regions since the Neolithic: An introduction. *Quaternary International*, *303*, 1–9.
DOI/URL: https://doi.org/10.1016%2Fj.quaint.2013.05.009

Zanchetta, G., Giraudi, C., Sulpizio, R., Magny, M., Drysdale, R. N., & Sadori, L. (2012). Constraining the onset of the Holocene "Neoglacial" over the central Italy using tephra layers. *Quaternary Research*, *78*(2), 236–247.
DOI/URL: https://doi.org/10.1016%2Fj.yqres.2012.05.010

Zecchini, M. (1978). *Gli Etruschi all'isola d'Elba*. Portoferraio: Ente per la Valorizzazione dell'Isola d'Elba.

Zecchini, M. (1982). *Relitti romani dell'isola d'Elba*. Lucca.

Zecchini, M. (2001). *Isola d'Elba. Le origini*, vol. 65 of *Studi e testi dell'Accademia Lucchese di scienze, lettere ed arti*. Lucca: Accademia Lucchese di scienze, lettere ed arti.

Zecchini, M. (2018). Il granito dell'elba, la 'nave' romana di cavoli e l'iside neoclassico del louvre. *unpublished manuscript*.
DOI/URL: https://www.academia.edu/36316511/IL_GRANITO_DELLELBA_LA_NAVE_DI_CAVOLI_E_LISIDE_DEL_LOUVRE.pdf

Zeileis, A., & Grothendieck, G. (2005). zoo: S3 Infrastructure for Regular and Irregular Time Series. *Journal of Statistical Software*, *14*(1), 1–27.
DOI/URL: http://dx.doi.org/10.18637/jss.v014.i06

Zhornyak, L. V., Zanchetta, G., Drysdale, R. N., Hellstrom, J. C., Isola, I., Regattieri, E., Piccini, L., Baneschi, I., & Couchoud, I. (2011). Stratigraphic evidence for a "pluvial phase" between ca 8200–7100 ka from Renella cave (Central Italy). *Quaternary Science Reviews*, *30*(3), 409–417.
DOI/URL: https://doi.org/10.1016%2Fj.quascirev.2010.12.003

Zielhofer, C., & Faust, D. (2008). Mid- and Late Holocene fluvial chronology of Tunisia. *Quaternary Science Reviews*, *27*(5), 580–588.
DOI/URL: https://doi.org/10.1016%2Fj.quascirev.2007.11.019

Zielhofer, C., Faust, D., & Linstädter, J. (2008). Late Pleistocene and Holocene alluvial archives in the Southwestern Mediterranean: Changes in fluvial dynamics and past human response. *Quaternary International*, *181*(1), 39–54.
DOI/URL: https://doi.org/10.1016%2Fj.quaint.2007.09.016

Zifferero, A. (2017). Mines and Metal Working. In A. Naso (Ed.) *Etruscology*. Berlin, Boston: De Gruyter.
DOI/URL: http://dx.doi.org/10.1515/9781934078495-025

Supplementary material to: Case Study 2, Campo

Please note that this table was originally published as an in-text table (Table 3) in Case Study 2, Becker et al., 2019a, Chapter 7.

Table A.4 Metadata and ages of the radiocarbon-dated organic material from cores F-I, F-III, S-I, and S-II.

Core	Depth [cm]	Material	Lab code	cal-^{14}C-ages	Calibrated age		(Confidence)
F-I	90	Charcoal	Poz-80090	1340 ± 30	1306–1236 cal BP	644–714 CE	(84.1 %)
					1207–1185 cal BP	744–765 CE	(11.3 %)
	331	Charcoal	Poz-80091	5075 ± 35	5910–5741 cal BP	3961–3792 BCE	(95.4 %)
	497	Charcoal	Poz-81133	5950 ± 40	6883–6676 cal BP	4934–4726 BCE	(95.4 %)
	590	Plant remains	Poz-81134	5620 ± 40	6479–6310 cal BP	4530–4361 BCE	(95.4 %)
	694	Plant remains	Poz-77796	5700 ± 40	6628–6585 cal BP	4679–4636 BCE	(7.0 %)
					6569–6405 cal BP	4620–4456 BCE	(88.4 %)
F-III	95	Charcoal	Poz-77791	750 ± 30	728–664 cal BP	1222–1286 CE	(95.4 %)
	165	Charcoal	Poz-77792	1585 ± 30	1544–1406 cal BP	406–544 CE	(95.4 %)
	285	Charcoal	Poz-77793	2035 ± 30	2109–2082 cal BP	160–132 BCE	(4.9 %)
					2066–1921 cal BP	116 BCE–30 CE	(88.3 %)
					1913–1900 cal BP	38–50 CE	(2.2 %)
	446	Charcoal	Poz-77795	2110 ± 30	2153–1995 cal BP	204–46 BCE	(95.4 %)

to be continued . . .

Table A.4 . . . continued.

Core	Depth [cm]	Material	Lab code	cal-^{14}C-ages	Calibrated age		(Confidence)
S-I	70	Charcoal	Poz-81137	535 ± 30	633–598 cal BP	1318–1352 CE	(24.7 %)
					560–512 cal BP	1390–1438 CE	(70.7 %)
	220	Plant remains	Poz-77797	2405 ± 35	2626–1596 cal BP	747–685 BCE	(12.6 %)
					2634–2591 cal BP	666–642 BCE	(3.7 %)
					2535–2533 cal BP	586–584 BCE	(0.2 %)
					2505–2346 cal BP	556–397 BCE	(78.9 %)
	455	Plant remains	Poz-77799	4710 ± 60	5584–5498 cal BP	3634–3549 BCE	(29.9 %)
					5493–5319 cal BP	3544–3370 BCE	(65.5 %)
	1064	Plant remains	Poz-77798	6910 ± 50	7978–5617 cal BP	5968–5956 BCE	(1.0 %)
					7905–7657 cal BP	5906–5708 BCE	(94.4 %)
S-II	80	Charcoal	Poz-81135	1020 ± 30	1042–1038 cal BP	908–912 CE	(0.3 %)
					982–905 cal BP	968–1046 CE	(90.3 %)
					856–830 cal BP	1094–1120 CE	(4.1 %)
					809–803 cal BP	1141–1147 CE	(0.7 %)
	251	Charcoal	Poz-81136	1235 ± 30	1264–1070 cal BP	686–880 CE	(95.4 %)

References to the ‘deforestation narrative’

Table A.5 Deforestation narrative

Reference	Citation	Comment
[1] Pococke, 1745, travel narrative (p. 180–1)	We afterwards passed by the island of Elba . . . They have a vulgar notion that the iron cannot be melted here, which possibly may be owing to what Strabo says of Aethalia, which some have been thought to be Elba ; he affirms they could not melt the iron on the spot, but carried the ore immediately to the continent ; and therefore some think there is a quality in the air which hinders the ore from melting or running ; but it is more probable that they not the conveniency of wood for their foundry in so small an island.	reference to Strabo; size of the island; refers to a translation that says that iron could not be 'melted'
[2] Pini, 1780 (p. 2 and pp. 37–8)	Es gibt viele Waldungen; aber der anhaltende Verkauf des Holzes an Ausländer hat auch dieses Product in dem Land seltener gemacht. . . . Strabo scheibt, man schmelze das Erz auf den Insel Elba nicht; sondern man bringe es in dieser Absicht auf das feste Land an die Küste von Toskana, wo die Oefen darzu errichtet seyen. Das versteht sich aber nur von tenen Zeiten, die nahe an derjenigen sind , zu wechler er schrieb. Dann die grossen Stücke von Eisenschlacken, die ich an verschiedenen Stellen des Gebiets von Portoferrajo antraf, sind mir Bweis genug, daß einmal Oefen entweder zum Schmelzen oder zum Verfeinern des Eisens da gewsen seyn müssen. So viel ist gewiß, daß man gegenwärtig das Erz nicht auf der Insel schmelzt, und auch das rohe Eisen nicht verfeinert, einmal aus Mangel an Holz, und dann, weil das Wasser zu schwach ist, um die zu einer solchen Anstalt nöthige Maschinen in Bewegung zu setzten.	reference to Strabo, but without directly saying that Strabo observed a lack of fuel, Strabo and contemporary lack ('aus Mangel an Holz') only the the passage of the text notices that neither smelting nor refining are possible in the time of his observation, due to a lack of wood

to be continued . . .

Table A.5 . . . continued.

Reference	Citation	Comment
[3] Köstlin, 1780, letters on natural history of Elba (pp. 74–5)	La mine de fer de Rio fournit aujourdhui la Corse, la republique de Genes, environ quatre fourneaux de la Toscane, les trous fourneux du Prince de Piombino qui sont à la Felonica, les fourneaux de Palo et de Nettuno dans l'état ecclésiastique, et les fourneaux d'Amalfi dans le royaume de Naples . . . Les navires approchent assez de terre pour communiquer par un pont, et al amine se charge aux frais de l'acheteur à bras d'hommes. Il y a près de cent famillies qui vivent de ce petit transport, et on assure, que la vente de cette mine rapporte au Prince de Piombino 50000.' seudi par an. It est probable, qu'on a fondu anciennement les mines de fer dans l'isle même, car ils se trouvent encore dans quelques endroits de l'isle de amas de scories de fer, mais qu'on a d°u discontinuer à cause de la disette de bois. [footnote: Strabo 5.2.6 quoted] Et c'est aussi par cette raison qu'on n'y fond pas la mine acutellement.	
[4] Swinburne, 1814 [1776], travel narrative (pp. 429–30)	We descended on the east side of the mountain to Rio, a poor village inhabited by miners. Under it breaks out the only rivulet in Elba, which does not run above a mile before it falls into the sea; but the water gushes out of the rock in such abundance, that it turns seventeen mills in that short course. We followed this pretty stream down a narrow valley, cultivated with great nicety, and planted with orange and other fruit trees, till it brought us to the celebrated iron mine . . . From a scarcity of wood, none of the ore is smelted on the island, but it is sold to the agents of the Tuscan, Roman, Corsican, and Neapolitan furnaces . . . The Corsicans and Tuscans have a right to pick the ore . . . It is a doubt, whether this mine of Rio be the same mentioned, by Aristotle and other ancient authors, to have been open in their time, but it is generally believed to be so . . . The ore of Elba was probably smelted at no other place than from which it derived its name, *Populonium*	no direct relation between contemporary scarcity of wood and notice that ore was not smelted on Elba; only reference to 'other' ancient writers; contemporary transport of ore described similar to ancient ore transport from Elba to the mainland
[5] Weir, 1799, short description of Elba with drawings	It [Elba] produces various fruits, excellent in quality, though not in great plenty;—few places are level enough for corn, consequently it affords but scanty room for cultivation; and Swinburne says, who visited the Island about the year 1780, it then produced little more than six month provision for 7000 people. The trees seldom arrive at any considerable size, owing to the shallowness of the soil; flax, mineral plants, and medical springs (as may be expected on such a tract) are also among the riches.	

to be continued . . .

Table A.5 . . . continued.

Reference	Citation	Comment
[6] Anonymous, 1814	Sie [Elba] ladet ihn [Chateaubriand] zum Genuß der lange entbehrten edlern Menschenfreuden freundlich ein, indem sie ihn Alles darbietet, was der Mensch bedarf. Ihre freie Lage im Meer ist äußert reizend, das Klima im Durchschnitt ungemein lieblich und dem Gedeihen aller organischen geschöpfte sehr zuträglich. Die hohen Berge . . . derselben sind statt der Waldungen mit einer Menge größtentheils wohlriechender Gesträuche umkränzt und mit Gewächsen aller Art bedeckt. In den fruchtbaren Thälern und an den Hügeln baut man viel Wein, der dem spanischen an Güte gleichkommt, dann Oilven, Feigen, Zitronen, Pomeranzen, Mais, Bohnen und etwas Korn. Alle Obstbäume des südlichen Europas — der Apfelbaum allein asugenommen — stehen im üppigen Wuchs	
[7] F. F., 1814	Die ganze Insel hat großen Mangel an Waldungen, Wiesen, Getreide, Baum- und Gartenfrüchten so wie an Vieh. Auf den zwar kleinen aber durchaus felsigen Bergen, wächst meist nur kleines Gesträuch und Kräuter; daher halten die Einwohner an zahmen Vieh nur Schafe, Ziegen, Pferd und Maulesel, in geringer Zahl . . . Einen unerschöpflichen und eigenthümlichen Reichthum hat nun noch die Insel an mancherlei Mineralien, hauptsächlich an sehr gutem Eisenerz, wovon aber gegenwärtig ein Theil, (wegen Holzmangel) ungeschmolzen nach Toskana geführt und dort verarbeitet wird.	

to be continued . . .

Table A.5 . . . continued.

Reference	Citation	Comment
[8] Thiébaut de Berneaud, 1814, travel narrative (p. 6 and p. 23)	The Latin name Ilua, or Ilva, comes from Greek . . . , a forest, of which the people of Latium formed Sylva, by substituting the letter S for the accent, which the Etruscans pronounced without an aspirate. This appellation was bestowed upon Elba, according to my learned colleague Lanzi, from the prodigous quantity of wood which covered its mountainous soil . . . Wood for fuel is still more rare. The island affords nothing beyond a meagre underwood, the chief plantations of which are at Monte-Giove, the valley of Tre-Acque, and Mont de Fonza . . . The oak, though endowed with the hardiest formation, does not arrive at that pitch of peculiar beauty, or at that majestic height which made it the earliest object of the religious worship by which it was consecrated . . . Its branches do not display the stamp of ages ; it is not in Elba, the patriarch of the vegetable world . . . In a word, forest-trees are wanted throughout the island . . . Diodorus (n) speaks of its iron works. It still contained them at the era of the Republic of Pisa ; and in the thirteenth century it was covered with wood. The last of these works was that which, about the year 1589, was still in existence . . . At the present, all the iron works in the island are destroyed ; they have no wood, and they are obligate to transport the ore to Corsica, the coast of Genua, and the shores of Tuscany, in order to have it manufactured.	does not mention scarcity of fuel in antiquity, but reports a lack of fuel in the early 19th; also describes transport from ore to mainland and Corsica
[9] Barker, 1815, travel narrative (p. 4)	The climate is warm and genial . . . notwithstanding these advantages, it supports little to support its population . . . which is supplied with almost every necessary from Leghorn and Piombino; in return they export iron ore, none being manufactured by the Elbese from want of sufficient wood for fuel, also salt and wine, which is of excellent quality. Another article of export is the tunny.	

to be continued . . .

Table A.5 . . . continued.

Reference	Citation	Comment
[10] Brunner, 1828, travel narrative (p. 35–6, p. 46)	. . . Alle Anhöhen [Nordostelbas] sind bis an den Gipfel bewachsen , doch leider nur mit Gesträuche, worunter verschiedene gelbblühende Ginsterarten , der Erdbeerbaum (Arbutus unedo) , der Lentistenstrauch , der strauchartige himmelblaublühende und gelbe Gamander (Teucrium frutescens et flavum) und endlich die Stein- und Korkeiche (Quertus Ilex et Suber) die bemerkenswerthesten sind. Eigentliches Schlag - und Bauholz fehlt in dieser Gegend Elba's ganz , woran ohne Zweifel nicht allein die widerwärtige Natur des Bodens, sondern mehr noch eine verwahrlosete Forst-Oekonomie Schuld ist. . . . Bergmännisches Interesse bietet also die Mine von Rio wenig oder keines dar . Röstofen sind zwar vorhanden aber weniger nothwendig als in manchen andern Eisenbergwerken, indem das Metall hier großentheils gediegen vorkömmt , was übrigens bey dem Mangel an Brennholz auf der Insel ein sehr erwünschter Umstand ist. Es wird meist unmittelbar eingeschifft und seinet Güte wegen weithin in und außerhalb Italiens verführt . . . Mit dem Eintritt in einen dunklen Wald von ehrwürdigen Kastanien ändern sich so ganz alle Umgebungen , nimmt die Physiognomie der Landschaft einen so ganz verschiedenen Charakter an , daß man sich auf einmal in die Lombardie oder doch wenigstens nach der Nordseite des Appennins versetzt glaubt . . . . . Es gilt dieses für den fruchtbarsten Theil der Insel [um Campo], was indessen wenig sagen will , indem auch hier die Getraideäcker erbärmlich mager aussehen , und bedeutende Strecken noch jetzt mit den Wurzelstöcken ausgerotteter Waldungen besetzt stehen.	
[11] Groskurd, 1831; note to translation of Strabo 5.2.6 (fn. 3, pp. 386-7)	Freilich gehört das Giessen und Hämmern des Eisens in Stangen und Platten und Bleche zu seiner Bearbeitung, aber das Ausschmelzen der rohen Erze ist doch das erste und wichtigste Geschäft, ohne welches das andere nicht Statt findet . . . wo das eine geschiht, da geschiht auch das anders, und wo das Giessen nicht möglich ist, da ist auch das Schmelzen nicht möglich. Beides aber war zu Strabons Zeit auf Aithalia nicht mehr möglich, weil es der Insel an Holz fehlte, und noch fehlt, weshalb noch jetzt das rohe Erz aufs Festland gebracht wird. . . . Dass übrigens in älteren Zeiten das Eisen auf Aithalia selbst, weil damals noch Holz da war, ausgeschmolzen und weiter bearbeitet wurde, sehen wir aus Diodor. V., 13.	no evidence, reference to Strabo, reference to Diodor to emphasize the that smelting was possible prior to Strabo, mentions contemporary scarcity of fuel, not only smelting, but also further processing not on the island because of fuel scarcity (see Corretti, 2017 for the hypothesis that smelting was conduct mainly on the mainland because of additional fuel requirements); discussion on translation (smelting or refining to bars; cf. Grove & Rackham, 2003; Radt, 2003).

to be continued . . .

Table A.5 . . . continued.

Reference	Citation	Comment
[12] Schweighardt, 1841, iron and economy (p. 24)	Die Erzmassen in Elba wurden dort geröstet, und nach DIODOR auf das Festland verkauft und dort verarbeitet, auch jetzt werden die Erze wegen Holzmangels nicht auf Elba, sondern auf dem festen Lande verarbeitet.	reference to Elba in the text without direct context.
[13] Blanc, 1846, geographical encyclopedia (p. 572)	Diese durch Napoleons Aufenthalt . . . berühmt gwordene Insel ist durchaus bergig, erreicht im Mte. Capane 3150', ist zwar nicht unfruchtbar, aber doch zum Ackerbau wenig geeignet und leidet an gänzlichem Holzmangel	
[14] Simonin, 1858, on the history of mining in Tuscany	Les Étrusques fondirent quelque temps tout le minerai dans l'île même; de là, selon Diodore de Sicile, le nom d'Athalia que lui donnèrent les Grecs, c'est-à-dire l'île Brûlée, l'île des Feux. On retrouve d'ailleurs encore aujourd'hui des scories ferrugineuses en divers points de l'île, notamment vers Porto Longone. Mais, quand le bois vint à manquer, on transporta tout le minerai à Populonia, cité la plus voisine de l'île sur le continent, et dont la position maritime permettait la facile exportation du métal produit. Le minerai était fondu dans des fours que les Romains laissèrent allumés après la conquête de l'Étrurie. Ces fours marchaient du temps de Strabon, c'est-à-dire sous les règnes d'Auguste et de Tibère, et on les trouve même mentionnés dans le récit d'un voyageur des derniers temps de l'empire romain. C'est donc en tout une durée de plus de quatorze siècles d'un travail non interrompu.	mentions Strabo, but not as direct *evidence* for the shortage of wood

to be continued . . .

Table A.5 . . . continued.

Reference	Citation	Comment
[15] Jervis, 1860, description of mines in Tuscany (p. 724–5)	Varro (born B.C. 116) says that iron ore is indeed abundant in Elba, but in order to be smelted it has to be taken to Populonium, a city of Etruria, not far from the island. About the Christian era, Strabo alludes to the iron mines of Elba as nothing new, and specially mentions that the ores were taken to Populonia to be smelted, since the island did not afford facilities for the requisite metallurgical operations. What the hindrances were he does not inform us, though I conceive the want of forests, which had been previously cut down, quite a sufficient reason . . . In every part of the island ancient slags may be observed, considered to have been produced in the metallurgical operations of the Romans. Little furnaces were evidently established at some remote time wherever abundance of wood and a small stream of water were procurable within easy access of the beach . . . I consider it probable they are exceedingly ancient, dating at least from the Roman kingdom or republic; for my part, I incline to the belief that they may be partly of Etruscan origin, for evidently the island was thickly wooded when the inhabitants smelted their ore so extensively in Elba, and tho reason for tho subsequent abandonment of these localities, and the shipment of ore to Populonia, as was practised in Strato's time, was doubtless because wood and charcoal were there procurable at less cost.	

to be continued . . .

Table A.5 . . . continued.

Reference	Citation	Comment
[16] Colt Hoare, 1814 (p. 5 and p. 15)	The metal is not smelted in the island, but conveyed to the coast of Tuscany, where the Prince of Piombino has two founderies: the one at Fellonica, the other at Cornia, near Sughereto. This seems to have been the practice in the earliest times ; for the geographer Strabo informs us that it was transported to the shores of Tuscany as soon as it was dug from the mine. " Non enim eâ in insulâ fornacibus , liquari potest, sed statim atque effossum est, in continentem perfertur." Strabo, lib. V. Varro also observes that the iron could not be smelted in Elba. . . . few olives are grown near Porto Ferrajo, and there are extensive groves of chestnuts at Poggio and Marciana. At Rio there are many almond, fig, and walnut trees. The very extensive tracts of uncultivated mountains, are depastured by goats, from whose milk cheese is made, but not good ; on the contrary, the curds are the most delicious I ever tasted . . . The ilex, or evergreen oak, predominates among the trees of higher growth, and the declivities of the mountains are frequently feathered with myrtles down to the edges of the sea-shore.	
[17] Hall, 1837, *travel narrative* (p. 9, p. 12)	Some of the high lands are covered with vegetation, but most of the summits of the mountains are naked, and exhibit nothing but rocks, which a hundred centuries have rendered almost as white as Parian marble. The vallies are productive, yielding grapes in vast abundance, and grain of various kinds, the fig, the orange, the watermelon, (which is here called cucumber,) pears, apples, plumbs, &c. &c. . . . There is little wood on the island, and what there is, is a small growth. Jackasses, loaded with faggots, and pieces of wood two or three inches in diameter, are constantly seen coming into Porto Ferrajo from the country. The oak grows here, and the maple, and several other trees, which are common in America : but there is one here that I have not met with before ; it is the cork tree . . . I was a little surprised, on learning that no metallic iron has been obtained in modern times, form this excellent ore, in the island of Elba. The work is done elsewhere, in Sicily, Turkey, and Spain. It is all conveyed to foreign countries in the ore. It was smelted here in old times, but has not been in modern days, nor can it be, for there is no fuel here which can be spared for this purpose, no mineral coal, and next to no wood.	

to be continued . . .

Table A.5 . . . continued.

Reference	Citation	Comment
[18] Krantz, 1841 (p. 350 and p. 422–3)	Oliven werden nur in der Nähe von Porto Ferrajo in grösserer Menge gewonnen, in allen anderen Theilen der Insel lässt man die Oelbäume durch nutzlose Gesträuche verdrängen, ebenso Kastanien, die nur in der Gegend von Marciana einen ansehnlichen Wald dickstämmiger Bäume bilden . . . Doch reicehn auch sie für den Bedarf nicht hin, dennoch ist man nicht bemüht, gleiche Pflanzungen an anderen Orten anzulegen, sondern fällt die vorhandenen Stämme als Schiffsbauholz, ohne sie durch neue zu ersetzten . . . Den grösseren Theil der Insel aber bedecken dichte Gebüsche, oft undurchdringbar verschlungen, wodurch die Bildung nutzbarer Stämme verhindert wird . . . Die Kohlen [für die Hochöfen auf dem Festland] selbs gewinnt man in der Maremma, die noch voller Waldungen ist, in Meilern, die amn aus hartem meist, Eichenholze, von Quercus suber u.a. zusammensetzt; man zahlt für die Somma von 250 bis 300 Pfd. 4 bis 5 Lire. . . . Auf Elba sselbst sind keine Hüttenwerke, da es der Insel theils an Kohlen, die man wohl bequem zuführen könnte, da die Schiffe stets leer einluafen, mehr aber noch an Wasser fehlt, die Maschinen zu bewegen, und an Anlagen mit Dampfkraft noch lange nicht zu denken ist.	
[19] Wolff, 1855, *travel narrative* (p. 95)	During the time of the Emperor [Napoleon] the mine of Rio was the only one worked, and its ore was sent to the Continent to be smelted, there being no fuel in the island.	
[20] Gregorovius, 1864 [1852], travel narrative (p. 42 and p. 49–50)	Der Ort Marciana hat die besten Kastanien. Oliven gibt es wenig und schlechte, wie der Holzmangel der Insel überhaupt groß ist. . . . Seit grauen Zeiten ist der Eisenberg von Rio ausgebeutet worden, ohne seine Unverschöpflichkeit zu verlieren; ein Berg von etwa 500 Fuß Höhe, welcher ganz Eisenmaterial ist. In seiner Nähe gibt es noch andere nicht minder reiche Flötze, die von Terra Nera, von Rio Albano, und den Calamite, einen wahrhaften Magnetberg. Schon die Etrusker beuteten die Werke aus; sie schafften das Material nach Populonium, in dessen Gebiet die Insel gehörte, und dort wurde das Eisen herausgeschmolzen. Der Holzmangel in Elba erl[laubt] hier keine Schmelzwerke, und auch wird das Eisen nicht auf der Insel geschmolzen, sondern drüben in Fabriken in der Nähe des alten Populonium, oder das Material wird nach Neapel, Genau, Marseille, und nach Bastia verladen.	

to be continued . . .

Table A.5 . . . continued.

Reference	Citation	Comment
[21] Campbell & MacLachlan, 1869	Napoleon gave orders to send a vessel with iron ore to the United States of America . . . That renders the the proposition more absurd is, that it is not iron which is exported from Elba, but the ore precisely in its original state. There are no furnaces for extracting and fabricating the iron, on account of the want of fuel	no connection to ancient times
[22] Jones, 1923, translation of Strabo 5.2.6 (p. 355, fn. 3=116)	Literally, "oiled together"; hence not "melted together" merely (the meaning given by the dictionaries and the editors in general), or "reduced to iron bars" (Casaubon and du Theil. Strabo Speaks of "iron," not "iron-ore"; and he does not mean to say that iron-ore was not smelted at all on the island. Indeed, Diodorus Siculus (5. 13) tells us in detail how the people there broke up the masses of "iron-rock," and "burnt" and "melted" the pieces in "ingenious furnaces"; how they divided the resulting mass into lumps of convenient size, in form similar to large sponges; and how they sold the lumps to merchants, who took them over to the various markets on the mainland. Hence Strabo is thinking primarily of the high temperature necessary to bring the iron from a brittle and spongy to a soft and tough texture; but for the lack of wood on the island (see Beckmann on Aristot. Mirab. c. 95) any further working of the iron there was wholly impracticable. On the kinds of iron and how to temper it, see Pliny 34. 41.	
[23] Täckholm, 1937, roman mining (p. 21)	Eine wichtige Rolle hat der Mangel an Brennholtz für den Schmelzbetrieb auf Elba gespielt. Wir wissen durch Strabon V 2.6, dass das Erz direkt aufs Festlande transportiert wurde, ohne noch geschmolzen zu sein . . . Der Grund dafür wird von Strabon nicht angegeben, doch kann er wohl kein anderer als Brennholzmangel gewesen sein. Hier kam kein Fehler in der Qualität oder Quantität des Erzes in Betracht. Noch zu der Zeit, da Diodoros den Betrieb beschreibt, wurde das Erz auf der Insel geschmolzen.	remark in footnote on the controversy of the translation as in Jones (1923)

to be continued . . .

Table A.5 . . . continued.

Reference	Citation	Comment
[24] Piccinini, 1938, iron on Elba in antiquity (p. 12–3)	L'estrazione del ferro per trattamento a fuoco vivo del minerale, richiedeva ili c01I1sumo di fortissime quantità di carbone di legna, caratteristica gravosa che fu anche nei tempi più recenti motivo di spostamenti e di limitazioni di attività della siderurgia fondata sull'uso del combustibile vegetale. E'logico quindi dedurne che in breve il fortissimo incremento dellle lavorazioni etrusche sul suolo elbano deve aver prodotto ila distruzione delle locali foreste, costringendo i fonditori a trasferire le operazioni sul vicino litorale continentale, oye per altro con ogni probabilità già esercitavasi la stessa industria più in piccolo, impiegando come materia prima anche i minerali ferrosi delle non lontane miniere di Monte Valerio presso Campiglia Marittima, nellle quali si possono tuttora osservare ingenti traccie di laboriose escavazioni dell'epoca etrusca. Non è da escludersi però che anche altre ragioni abbiano concorso al detto trasferimento e principalmente quella della scarsa sicurezza dei trasporti per via di mare di grandi quantità di ferro metallico, merce a quei tempi pre21iosa e perciò esposta allle insidie dei naviganti nemici, . . . D'altra parte è indubitato che le immense foreste fin allora esiste;:nti nel promontorio di Populonia e nelle vicine montagne del Campigliese costituissero una riserva di combustibile tale da permettere un facile e grandioso sviluppo delle lavorazioni a fuoco sul litorale di Populonia, mentre la presenza di un porto sicuro come qudlo sottostante alla antica aree Populoniense, assicurava il più agevole e protetto sbarco dei minerali nonchè il più tranquillo svolgimento di ogni specie di traffico. Che il minerale non si potesse più trattare all'isola .è confermato anche da alcuni antichi scrittori. Servio nel suo commento a Virgilio (ad Aen. X-174) riferisce che Varrone, tra l'altro, diceva che il ferro nasce all'Elba ma inon può essere lavorato se non trasportato in Populonia, città della Toscana vicina alla stessa isola : «Varro et aliud dicit, nasci quidem illic ferrum, sed in stricturam non posse cogi, inisi transvectum in Populoniam, Tusciae civitatem, ipsi insulae vicinam ». Strabone pure, riferendo su ciò che vide a Populonia in un suo viaggio dice: (V, 223): «e vedemmo coloro che lavorano il ferro recatovi dall' Aethalia (Elba), perchè nell'isola inon può fondersi in fornaci e perciò subito dopo che è tolto dalle miniere, si porta in terraferma ».	

to be continued . . .

Table A.5 . . . continued.

Reference	Citation	Comment
[25] Nihlén, 1960, field report on archaeometallurgical survey on Elba (pp. 4–6)	The extensive woods in the western part of the island determined the location of these bloomeries in the west . . . The landscape and topography around these smelting sites are also of great interest. Charcoal remains point to the use of chestnut wood and chestnut coals being used as fuel for the smelting. This part of Elba still possesses large traits of chestnut which convey a good impression of the prehistoric landscape. In Valle della Nivera centuries old beech woods now grow on formerly cultivated land. It is still possible to recognize terraces and masonry walls of much greater age than the oldest cestnuts. This area opens up interesting perspectives for a combined archaeological and cultural landscape survey. . . . It was no doubt owing to Etruscan initiative that the mines on Elba and the mainland were opened up. The Romans took over both the mines and smelters and the workings continued, as previously stated, well into Medieval times, Nevertheless, the region lose some of its early importance with the discovery of the rich Spanish mines in the early days of the Empire. Another factor contributing to the gradual decline was no doubt the exhaustion of the timber, which forced the abandonment of both mines and smelters for lack of fuel.	
[26] Forbes, 1964	Still in the neighborhood of mines charcoal burning must have done much damage. On the island of Elba the best iron ore of the Roman world was found, but the local wood and charcoal had apparently already given out before the Empire and the ore had to be transported after roasting to Populonia to be smelted there, were wood and charcoal could be easily obtained from the Ligurian mountains. Pliny complained that "the effect of the shortage of fuel on the roasting operation is particularly noticeable in Gaul, where the second roasting is carried out with charcoal instead of Wood" (Nat. Hist. 34, 96) and he also comments on the shortage of fuel in Campainian metallurgy (Nat. Hist. 34, 67) and therefore the is some truth in the statement of the effect of metallurgy on deforestation.	no ref. to Strabo, but account to Pliny to illustrate the connection between metallurgy and deforestation, n.b.: Ligurian mountains are not close to Populonia (Tuscany)
[27] Healy, 1978, metallurgy in antiquity (p. 148)	Shortages of wood in Gaul and Campania are mentioned by Pliny . . . which led, for example, to iron ore being transported from the mines on Elba to Populonia for smelting [Forbes, Technology VIII, 108].	

to be continued . . .

Table A.5 . . . continued.

Reference	Citation	Comment
[28] Meiggs, 1982, trees and timer in antiquity (p. 31 and p. 379)	[Strabo] also draws attention to the timber resources of other parts of Italy and mentions a visit to Populonia, where the iron-ore from Elba was smelted because the timber supply on the island had been exhausted . . . From the available ancient evidence it is impossible to say how seriously Mediterranean forests were depleted by the end of the Roman Empire. There are indeed a few explicit statements preserved. We learn from Strabo that owing to the exhaustion of fuel on the island, the iron-ore of Elba, the richest source of iron in Italy, had to be taken to Populonia on the Italian coast to be smelted. The ruinous effect of iron production on neighbouring woodlands is amply illustrated in our own history.	
[29] (Camporeale, 1985a), Etruria Mineraria (p. 25)	Viene così confermata l'ipotesi, più volte proposta, che di norma in Etruria l'attività metallurgica si svolgeva nelle adiacenze dei luoghi di estrazione dei minerali. La destinazione di Populonia a luogo di lavorazione del minerale cibano è dovuta a fattori contingenti: scarsezza di acqua, esaurimenlo o insufficienza del legname dell'Elba.	
[30] Corretti, 1988	Le fonti sembrano adombrare una causa di forza maggiore che impediva la riduzione dcl minerale sul suolo cibano. . . Si pensa ragionevolmente alla carenza di combustibile dovuta all'esagerato sfruttamento precedente. anche se questo fenomeno deve a sua volta essere provato e approfondito [footnote: Sembra . . . che i carboni provenissero da lecci o querce, e che quindi la macchia nell'antichità non fosse fondamentalmente diversa da quella attuale. Pochi decenni, a seconda dell'esposizione solare e di altri fattori. sono sufficienti. a detta di moderni carbonai. a far ricrescere una macchia da taglio per il carbone. Più che ad un esaurimento progressivo doHemo quindi pensare ad un impron iso incremento dell'attività metallurgica. nel I sec. a.C.. che non avrebbe lasciato spazio alla ricrescita. oppure anche ad un diverso utilizzo del suolo elbano. forse in connessione con lo sviluppo delle ville.] nella sua dinamica. Una certa preoccupazione di salvaguardare le risorse italiche sembra motivare anche il senatus-consultum riferito, in maniera piuttosto vaga. da Plinio il Vecchio, e definito genericamente vetus . . .	

to be continued . . .

Table A.5 . . . continued.

Reference	Citation	Comment
[31] Corretti, 1992 Archaeology of iron metallurgy on Elba (pp. 241–2)	La fine dell'attività metallurgica all'Elba, che su basi archeologiche e storiche (Varro, apud Serv., Aen., 10, 173; Strabo, 5, 6, 2) possiamo porre intornò alla fine del I sec. a.C:, è dovuta ad un complesso di cause non del tutto chiarite: la concorrenza delle miniere spagnole e poi del Norico; l'esauarirsi delle risorse boschive elbane, parallelo forse ad una diversa utilizzazione del suolo in conseguenza del sorgere sull'isola di alcune ville patrizie; probabilmente anche un senatus consultum di incerta- data, finalizzato, secondo Plinio (Plin., N:H., 3,138; 27, 77; 33; 21), a risparmiare le risorse ell'Italia proibendo lo sfruttamento minerario.	
[32] Schneider, 1992, introduction to the ancient technology (p. 88)	Nicht minder folgenreich als der direkte Eingriff durch die Erzförderung war der hohe Brennstoffbedarf bei der Verhüttung. Es liegen hier Werte aus Experimenten mit verschiedenen Ofentypen vor . . . Es ist signifikant, daß Theophrast in dem Grundriß der Botanik (historia plantarum) mehrmals auf die Verwendung von Holzkohle als Brennstoff beim Verhüttungsprozeß eingeht (5, 9, 1. 9, 3). Negativ für die Wälder wirkte sich dabei aus, daß vor allem das Holz junger Bäume für die Herstellung von Holzkohle für geeignet gehalten wurde (5, 9, 2); die Bäume wurden also verhältnismäßig jung geschlagen; eine systematische Aufforstung erfolgte nicht. Es konnte unter diesen Bedingungen nicht ausbleiben, daß der Waldbestand in den Zentren der Metallgewinnung stark zurückging. Das auf Elba gewonnene Eisenerz wurde wegen Brennstoffmangels auf der Insel in Populonia auf dem Festland verhüttet (Strabo 5, 2, 6), im Fall von Zypern führt Strabo den Rückgang der Bewaldung neben anderen Faktoren wie Schiffbau und Rodung zur Gewinnung von Ackerland auch auf die Metallverarbeitung zurück (14, 6, 5).	

to be continued . . .

Table A.5 . . . continued.

Reference	Citation	Comment
[33] Grove & Rackham, 2003	The iron-mines on Elba were a big fuel-using industry. In the early Empire iron was smelted on the island and sent to the mainland as blooms for further processing. This has sometimes been attributed to 'exhaustion of the forests' on Elba, making it impossible to complete the working on the island. Even Meiggs claimed this as one of the few records of diminution of forests in Italy. But this is not what Strabo and Diodorus Siculus say: they explain that smelting and fining were different industries, run by different groups of people, one on Elba and one on the mainland. We are not told why: it could have been due to lack of fuel on the island, but also to lack of labour or to some quite different cause.	(Meiggs, 1982)
[34] Corretti, 2004, study on text about ancient Elba (p. 284)	Al divieto di lavorare il minerale sull'isola stessa si accompagna poi l'obbligo di trattarlo sulla terraferma, a Populonia (e nel suo territorio). Sono state fornite spiegazioni diverse e non necessariamente in contrasto tra loro di questo paradoxon. L'ipotesi prevalente motiva l'impossibilità di una lavorazione sull'isola con la carenza di combustibile - o quanto meno con la necessità di proteggere le risorse boschive. Di ordine più politico è l'idea che Populonia intendesse controllare in maniera diretta le diverse fasi della produzione.	
[35] Lätsch, 2005, impact of insularity on social development in antiquity (p. 106)	Inseln, die über derartige Heiligtümer oder über Bodenschätze verfügten, entwickelten sich automatisch zu Handelsorten . . . und sei es nur, weil sie, wie im Fall von Elba, das Eisenvorkommen aus Platz- und Holzmangel nicht selbst verhütten konnten und sie zu diesem Zweck das Metall auf das nahe gelegene Festland verschiffen mussten	reference to excavations on Elba and Diodor and Strabo
[36] Perlin, 2005, *wood and civilization* (p. ?)	The Romans mined much of their iron on the island of Elba and most likely smelted the ore by burning pine. So much smoke spewed from the iron furnaces on the island that it was named 'Aethalia', Greek for 'smoky,' suggesting that a perpetual layer of smoke covered Elba. The ore could only be partially smelted on Elba because local wood supplies had become scarce. Strabo saw the iron "brought over . . . to the mainland" at Populonia, which faced Elba on the Etrurian coast. Wood from surrounding mountains supplied the smelters at Populonia with fuel. About 45 million pines had to be felled to produce all the iron smelted at Populonia	'. . .' in the original

to be continued . . .

Table A.5 . . . continued.

Reference	Citation	Comment
[37] Ettrich, 2006, encyclopedia entry on ecology in historical geography	Häufig ist in antiken Quellen von Abholzungen für den Bergbau die Rede (Strab. 5,2,6; Plin. nat. 2,63,158; 33,3 – 4; 33,70 – 76). Der Holzbedarf für den Schmelzprozeß war groß. Die Auswirkungen, die diese Eingriffe in die Natur hatten, beschreibt Strabon (5,2,6): Auf der erzreichen Insel Elba wurde seit frühesten Zeiten Eisen hergestellt. Als die Waldreserven der Insel erschöpft waren, wurde das Erz in das der Insel auf dem Festland genau gegenüberliegende Populonia transportiert und verhütet, weil der benötigte Brennstoff dort beschafft werden konnte. Auf die völlige Zerstörung eines Naturraumes wurde mit Mobilität reagiert. Dies zeigt vor allem, daß Umweltzerstörung in der Antike hauptsächlich ein regionales Problem war, dem man entfliehen konnte.	
[38] Marzano, 2007, roman villas in central Italy (p. 72, fn. 108)	According to Strabo (5.2.6), the metal could no longer be processed on the island for a lack of fuel, and was sent to Populonia.	
[39] Sallares, 2009, environment/ancient history (p. 168)	The question of the causes of soil erosion leads us to the problem of deforestation, the most controversial issue in Mediterranean environmental history. Many historians have believed that extensive deforestation occurred in the Mediterranean in antiquity, leaving a denuded landscape. Undoubtedly by the late republic the city of Rome, for example, had huge requirements for building work, heating houses and baths, industrial activities and many other purposes, which could not be met locally (Meiggs 1982: 218–59). These requirements were mainly met by floating timber down the Tiber to Rome. Wood was also important for metal smelting, for example silver ores in Attica and Spain, copper in Cyprus, iron from Elba near Populonia in Tuscany, and for shipbuilding. Despite the importance of the timber industry in antiquity, the "ruined landscape theory" of Mediterranean deforestation has attracted criticism . . .	

to be continued . . .

Table A.5 . . . continued.

Reference	Citation	Comment
[40] Wikander, 2009, Energy in ancient world (p. 4=139)	Heating, the firing of terracotta and pottery, and the metal industry required increasing amounts of fuel in antiquity, a fact that inspired contemporary comment. For instance, Strabo (14.6.5) attributes deforestation in Cyprus to the production of copper and silver and notes that, during the Empire, iron ore from Elba had to be transported over the sea to Populonia, where there were still large enough forests to supply wood for the smelting (5.2.6). Pliny (HN 34.20.96) comments on the similar situations causing the shortage of fuel in Campania and Gaul. Moreover, since the 1970s, growing interest in the technology of Roman iron-making has pointed out the far-reaching destruction of vegetation that resulted from the production of charcoal . . . Even though this established view of the environmental effect of wood harvesting has been questioned, there is little doubt that both Greece and Italy were subjected to serious deforestation during the last half-millennium B.C.	
[41] Williams, 2010, global historic and present deforestation (p. 78)	on the Italian mainland opposite the Isle of Elba where ore was extracted but could no longer be smelted due to the exhaustion of fuel	
[42] Corretti & Firmati, 2011, archaology of smelting on Elba (p. 234)	Varie ragioni sono state addotte a spiegare la fine di questa attività siderurgica sul suolo elbano, dalla carenza di combustibile, alla volontà di Populonia di esercitare un maggiore controllo sulla produzione e commercializzazione dei semilavorati in ferro, ai mutamenti a livello mediterraneo nella circolazione di beni conseguenti allo sfruttamento delle miniere provinciali; e tutte hanno a che fare con un *senatusconsultum* tanto oscuro quanto citato nei moderni studi, che invitava a *Italiae parci* . . . Anche in questo caso, solo la ripresa dell'indagine in un quadro unitario con la costa antistante potrà fornire una chiara risposta.	
[43] Harris, 2011, forests and deforestation in the ancient mediterranean regions (p. 119)	Il y a aussi d'autres complications possibles qu'il faut prendre en compte comme le type de bois ou le fait, comme F. Braudel le remarque, que ce travail prémoderne du fer était parfois interrompu faute de combustible disponible. Si cela est arrivé dans le monde antique (et je pense que ce fut le cas sur l'île d'Elbe), nous n'en trouverons probablement jamais trace . . .	

to be continued . . .

Table A.5 . . . continued.

Reference	Citation	Comment
[44] Radkau, 2012 history of wood (pp. 24–5)	Was beweisen die antiken Quellen? Für den, der von der Waldgeschichte der Neuzeit herkommt, besteht die große Überraschung darin, dass man jene Klagen über Waldzerstörung und jene Sorgen über den Niedergang der Wälder, von denen die forstlichen Quellen seit dem 16. Jahrhundert wimmeln, in der literarischen Überlieferung der Antike fast gar nicht findet . . . Gewiss waren die Menschen der Antike nicht dümmer als der »Ötzi«, sondern wussten über den vielfältigen Wert des Holzes bestens Bescheid . . . Der Geograph Strabo berichtet, die Erze der Insel Elba (damals Aithalia) müssten, anscheinend wegen Erschöpfung der dortigen Wälder, zur Verhüttung aufs Festland befördert werden – aber er erwähnt das nur kurz als eine Besonderheit der Insel (Strabo V/2 §6).	also in the edition from 2018
[45] Sonnabend, 2012, human–environment interactions in antiquity (p. 6)	Nicht nur in Spanien hatte die Ausbeutung der Metallvorkommen erhebliche Konsequenzen für das ökologische Gefüge. Ein bekanntes und immer wieder angeführtes Beispiel ist die Insel Elba (Strabon 5,2,6). Schon von den Etruskern wurden die dortigen Eisenerzminen ausgebeutet. Bald waren die zur Verhüttung benötigten Waldbestände der Insel erschöpft, und so wurde das Erz nun in das Elba auf dem Festland gegenüberliegende Populonia transportiert und dort verhüttet – mit entsprechenden negativen Folgen für die dortigen Wälder.	Reference to Healy (1978)
[46] Harris, 2013, Mediterranean deforestation in antiquity (p. 177–8)	As far as fuel wood is concerned, most Mediterranean micro-regions probably remained self-sufficient at most periods. There were three exceptions of this patter, possible reducible to two: (1) some areas of intense and prolonged end metal-working . . . Simply to cite one other case, it is reasonably clear that Elba eventually ran short of fuel for processing its iron ore, so that the processing had to be carried out at least in part on the mainland [footnote: Contrast Diodorus Siculus 5.13 with Varro (ap. Servius, Verg. Aen. 10.174) and Strabo 5.223 (cf. Ps.-Aristotle, On Marvellous Things Heard 93). Corretti and Firmati 2011, esp. 229, show that iron production on the island itself had largely ceased by about 50 BCE]	

to be continued . . .

Table A.5 . . . continued.

Reference	Citation	Comment
[47] Sands, 2013, history of human–forest interaction (p. 24)	Shortage of local supplies of fuelwood around smelting operations in southern France and in Britain caused the smelters to relocate to better-forested areas (Perlin, 1989). Copper mining in Cyprus and iron smelting on Elba depleted the islands' forests although there was still significant amounts of forest on Cyprus at the end of the Roman Empire (Meiggs, 1982)	
[48] Wiman, 2013, *Etruscan Environments* (p. 17)	Both the extraction of and the processing of the ores were believed to have taken place near the sources on Elba. It has been shown by recent excavation in the ancient port areas that from the mid-fifth century BC large-scale production was transferred to or concentrated in Populonia. Most scholars believe that this shift took place after the island had become totally deforested. Elba today is still heavily marked by erosion and barren hills.	
[49] Penna, 2014, global environmental history (p. 151)	A fuel crisis created by widespread deforestation curtailed and eventually terminated smelting operations throughout the ancient world. The Romans stopped smelting ore on the 'the smoky island' of Aethaleia in 2100 BP because of declining woodlands. In modern history, the environmental damage done to this same island, now named Elba, is etched in its landscape.	
[50] Hughes, 2014, ancient environmental history (p. 148 and p. 254, note 88)	There were complaints of wood shortage even in Gaul. Coal was uesd only where no wood was available. Pliny reports that coal was burnt in Campania to make bronze because of the wood shortage there; in Britain it was shipped by canal to the treeless fenland . . . Iron used less fuel than copper in smelting, which helps to account for the preference for the black metal over bronze . . . The Roman found other fuel-saving strategies. The depletion of forests on the iron-rich island of Elba explains why only the first stage of smelting was done there; the bloom was shipped to the nearby mainland port of Populonia, where wood and charcaol from the Ligurian Mountains was available. [note: Forbes, Studies in Ancient Technology, 6:18; Robert J. Forbes "Metallurgy," . . . Diod. Sic. 5.13; Strabo 5.2.6, C223.]	idea of fuel from Ligurian Mountains taken from Forbes (1964), see above

to be continued . . .

Table A.5 . . . continued.

Reference	Citation	Comment
[51] Pagliantini, 2014, archaeological landscape on Elba (p. 308)	In particolare Strabone . . . osservava che sull'isola non si poteva ridurre il minerale ferroso se non lo si trasportava sul continente, in particolare a Populonia, ma sono oscure le motivazioni di questo divieto, e se si tratti di una prescrizione sacrale o legale o un'impossibilità di ordine tecnologico L'ipotesi prevalente motiva l'impossibilità di una lavorazione sull'isola con la carenza di combustibile, o quantomeno con la necessità di proteggere le risorse boschive; ma dietro tale notizia potrebbe emergere anche una motivazione politica, per la quale la città di Populonia intendesse avere un controllo diretto sulla produzione e commercializzazione del ferro.	P refers to
[52] Vanni, 2014, agro-silvo-pastoral system in coastal Etruria (p. 21, fn. 94)	Sappiamo bene che alla ripresa ell'attività metallurgica nel golfo di Piombino, in Etruria ettentrionale, furono recuperate le scorie di fusione antiche che ancora possedevano una buona percentuale di minerale ferroso. Questo ci dice molto sulla tecnologia di riduzione del ferro per l'antichità etrusco-romana. È possibile che proprio la mancanza di combustibile sia all'origine dell'interruzione brusca dell'attività metallurgica nell'isola d'Elba. In generale sulla relazione tra mancanza di combustibile ed interruzione delle attività metallurgiche nel Mediterraneao, Braudel 1966: p. 321; Craddock 2008: p. 105. Il paradigma della continuità (temporale) e della contiguità (spaziale) per soddisfare in maniera corretta il fabbisogno di una città di medie dimensioni e di una comunità rurale o di un villaggio, deve aver conosciuto delle eccezioni. Sicuramente, come già accennato, nei pressi delle grandi città antiche. Atene nel corso del terzo quarto del IV secolo a.C., sappiamo che soffriva una penuria di legna per la cantieristica, ma anche per i bisogni primari di riscaldamento. Questo lo sappiamo grazie ad un'iscrizione su piombo in cui un uomo ordina dall'Egitto una grande quantità di legna da ardere117. Sull'isola d'Elba Diodoro Siculo, ci dice che il trattamento del minerale di ferro presente in grandi quantità sull'isola (fusione compresa) si svolgeva sul posto, mentre due generazioni dopo suetonio descrivendo la medesima regione, sembra suggerire che la fusione avvenisse sul continente118.	

to be continued . . .

Table A.5 . . . continued.

Reference	Citation	Comment
[53] Marzano, 2015, Roman resource exploitation (p. 194)	The iron mines on Elba Island haven been exploited since very early times [footnote: Diod. Sic. 5.13.1.1-14.3.1]. The deforestation of the island because of fuel production for the initial smelting of the ore was in such an advanced state that by the early first century AD processing took place on the mainland, near Populonia [footnote: Strabo 5.2.6]	cf. Marzano (2007)
[54] Schneider, 2016, history of ancient technology	Der Brennstoffverbrauch in der Antike war insgesamt beträchtlich und hatte daher nicht geringe Auswirkungen auf die Umwelt. Stärker als der Bedarf nach Bauholz oder an Schiffbauholz hat der Verbrauch von Holz als Brennstoff die Wälder der Antike geschädigt. Versuche mit rekonstruierten Schmelzöfen der Prvinz Britannia erbrachten Ergebnisse, die das Ausmaß des Verbrauchs von Holzkohle bei der Verhüttung von Eisenerzen vedeutlichen: . . . Da der Wald zudem als Viehweide beansprucht wurde, konnte er sich nur schwer oder überhaupt nicht regenerieren. Für die Zeit der Republik ist dieser Fall auf der Insel Elba eingetrefen; hier wurde das geförderte Eisen solage verhüttet, bis dafür schließlich kein geeignetes Holz mehr zu finden war und das Erz zur Verhüttung nach Populonia auf das Festland gebracht werden musste.	
[55] Lang, 2017, material and technology of roman iron production (p. 859)	Diodorus of Sicily (ca. 60–38 BC) described the iron industry on Elba and the nearby coast . . . The demands for charcoal for the furnaces were extensive. It seems that there was a shortage of trees on Elba so that the Etruscans were obliged to transfer their smelting activities to Populonia on the mainland. Calculations by Crew . . . have suggested that 116 tonnes of wood and 1776 kg of ore were required to make 156 kg of iron, while Cleere . . . estimated that between 120 and 140 AD, the six iron production sites in the Weald (United Kingdom) produced 66,000 tons of iron, requiring the felling of 15 km^2 of forest.	Etruscans?

to be continued . . .

Table A.5 . . . continued.

Reference	Citation	Comment
[56] Veal, 2017a, historical/political analysis of ancient timber and fuel supply (p. 321)	Close reading of pollen studies of the Greco-roman period show no real overall large deforestation patterns (until the mediaeval period), however, over-exploitation in a localized sense occurred, especially where the romans were exploiting iron ore for smelting. [footnote: on deforestation generally see Harris (2013a). A well-known example of deforestation is the island of Elba, which was heavily mined for iron ore, starting with the Etruscans. By c. the 3rd century BC, ore was being shipped to the mainland to be smelted in Populonia because woodland on elba was exhausted: Di Pasquale et al. (2014).]	3rd century BCE (?); no reference to Elba in Di Pasquale et al. (2014)
[57] Casevitz & Jacquemin, 2018, comment on translation of Diodor (p. 147)	cf. le commentaire de Servius citant Varron, selon qui le fer natif de l'île était transporté dans la voisine Populonia pour y être travaillé, ce que dit aussi Strabon .... Ce déplacement de la phase de transformation peut s'expliquer par la déforestation de l'île due à une surexploitation des ressources forestières.	reference to Meiggs; 'fer natif' = telluric iron (?)
[58] Roller, 2018, *Historical and Topographical Guide to the Geography of Strabo* (p. 233–4)	Poplonion was already important in the fifth century BC (Diodoros 5.13.1), and served as the mainland port of entry for the iron ore shipped from nearby Aithalia (modern Elba) . . . Aithalia (Ilva in Latin, modern Elba) had long been noted for its iron mines (originally copper, according to the Aristotelian On Marvellous Things Heard 93), but evidently it was impossible to smelt the ore on the island, perhaps because of limited wood supply.	
[59] Toner, 2018, *Roman disasters* (p. 22)	There was also heavy demand for wood as fuel, for use in ship-building and construction, and in mines for the smelting of metal ores. . . . The island of Elba, which had rich deposits of iron ore, had its wood supply exhausted, making it necessary to transport the ore to the mainland for smelting.	
[60] Veal, 2019, *Fuel in the Roman world* (p. 16)	In all of this consumption, however, except for some localized examples, the Romans did not seem to deforest their empire. A pattern of conservative management of woodlands related to fuel or timber use in peninsular Italy appears to have occurred, despite clearance for agriculture . . . Islands were more vulnerable. On the island of Elba, where iron ore was found in such abundance, ore was shipped to the mainland for processing by about the third century bc, as apparently the wood had run out for smelting and working the ore into bars for export elsewhere (Costantini et al. 2013).	lack of fuel in the 3rd century BCE? Why citing Costantini et al. 2013: Costantini, E.A.C., M. Fantappié & G.L'Abate, 2013. Climate and Pedo-Climate of Italy, in The Soils of Italy, eds. E.A. C. Costantini & C. Dazzi. Dordrecht: Springer Science? and Business Media.

to be continued . . .

Table A.5 . . . continued.

Reference	Citation	Comment
[61] Leitch, 2019, *Roman pottery kilns in Britain and North Africa* (p. 57)	However, the dry climatic conditions in North Africa were not favourable for the cultivation of large forests, and wetland deciduous forests were rare (Schmidt 1997). Meiggs indicates that very few tree varieties could in fact be grown there, except in the mountains (Meiggs 1982, 39–41), and states that 'we hear of massive plantings of olive trees but never of forests' (Meiggs 1982, 373–7). Strabo is sometimes also invoked on this issue: he tells us that in Elba the fuel was totally exhausted due to iron production, emphasizing the lack of fuel and potential consequences of over-use of supplies in the dry southern Mediterranean (Meiggs 1982, 379; Strabo 223; Diod 5.13.1–2).	reference to Strabo

Additional figures to support the argumentation in the thesis.

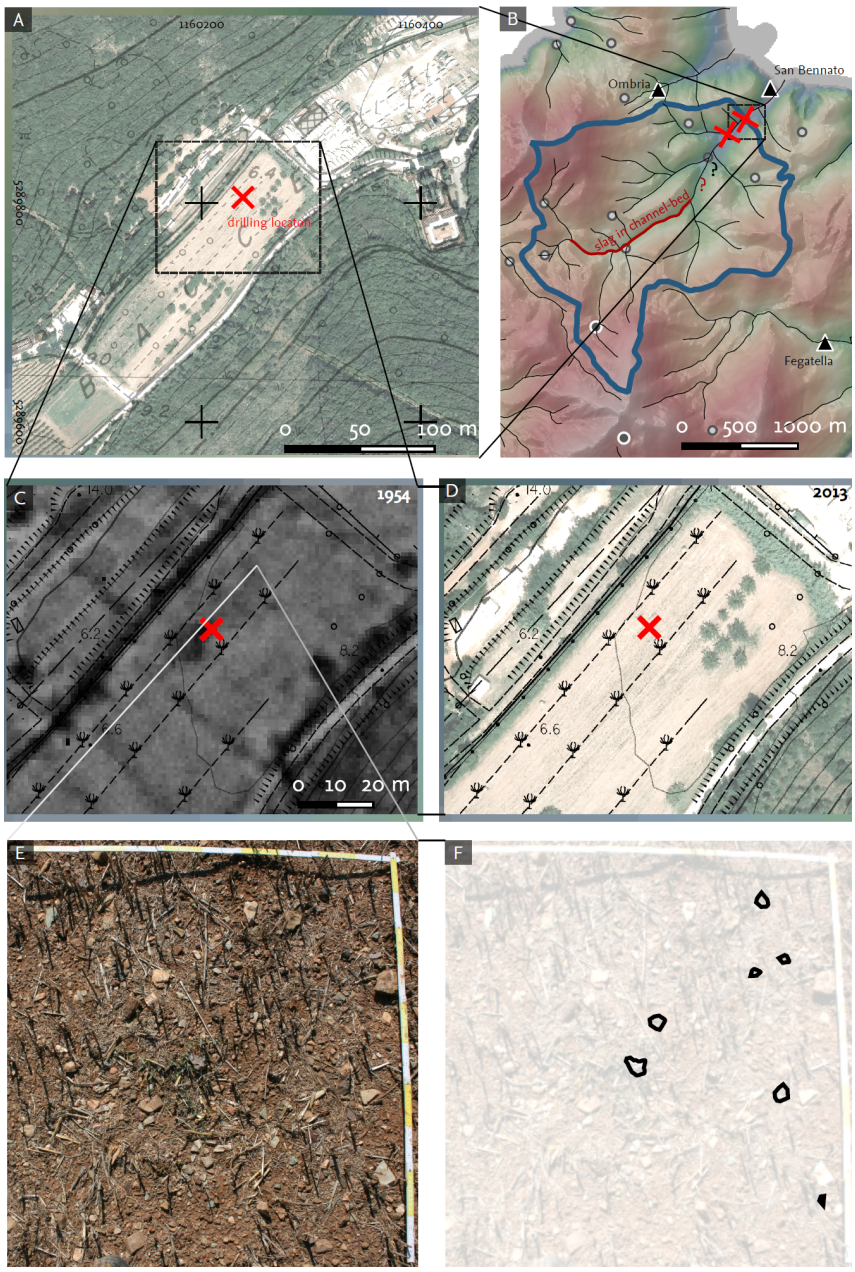

Figure A.9 Location of coring sites and slag finds in the Baccetti valley, northeastern Elba. **(A)** Drilling location B-II on an ortophoto from 2013, contour lines added (10 m); **(B)** catchment of the Baccetti, coring locations B-II and B-III, smelting sites, and location of abundant slag finds in the channel of Fosso Gorgoli; **(C)** coring location B-II, please not the dark spot near the location that possibly indicates a slag accumulation; **(D)** coring location B-II, please note the absence of the spot; **(E)** ground photo taken on the floodplain (location of the photo marked in C); **(F)** Illustration of the slag fragments seen in E. Database: Regione Toscana, 2014 and Corretti, 1988; Corretti & Firmati, 2011; Pagliantini, 2014.

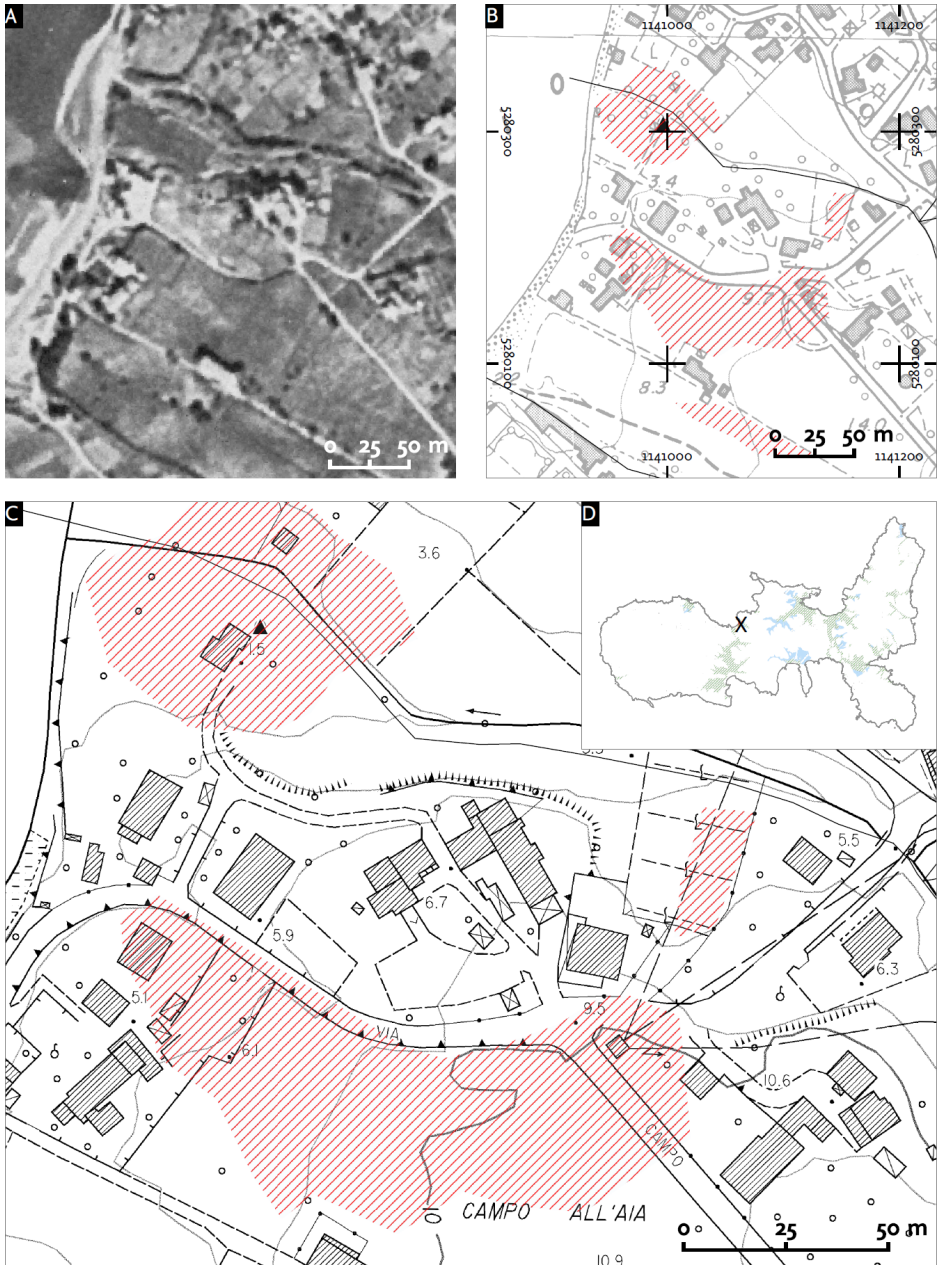

Figure A.10 Detailed view on the ancient iron smelting site at Campo al'Aia. **(A)** Aerial photo of the site (1954); **(B)** Approximated extent of slag finds (southern polygons) and the roasting place mentioned by Nihlén 1958 as mapped by R. A. Eser; **(C)** detailed view of the site; **(D)** location of the view on Elba. Database: *Carta tecnica regionale*, 1:2000, 1:5000 (Regione Toscana, 2014), R. A. Eser, pers. comm., June 20, 2019.

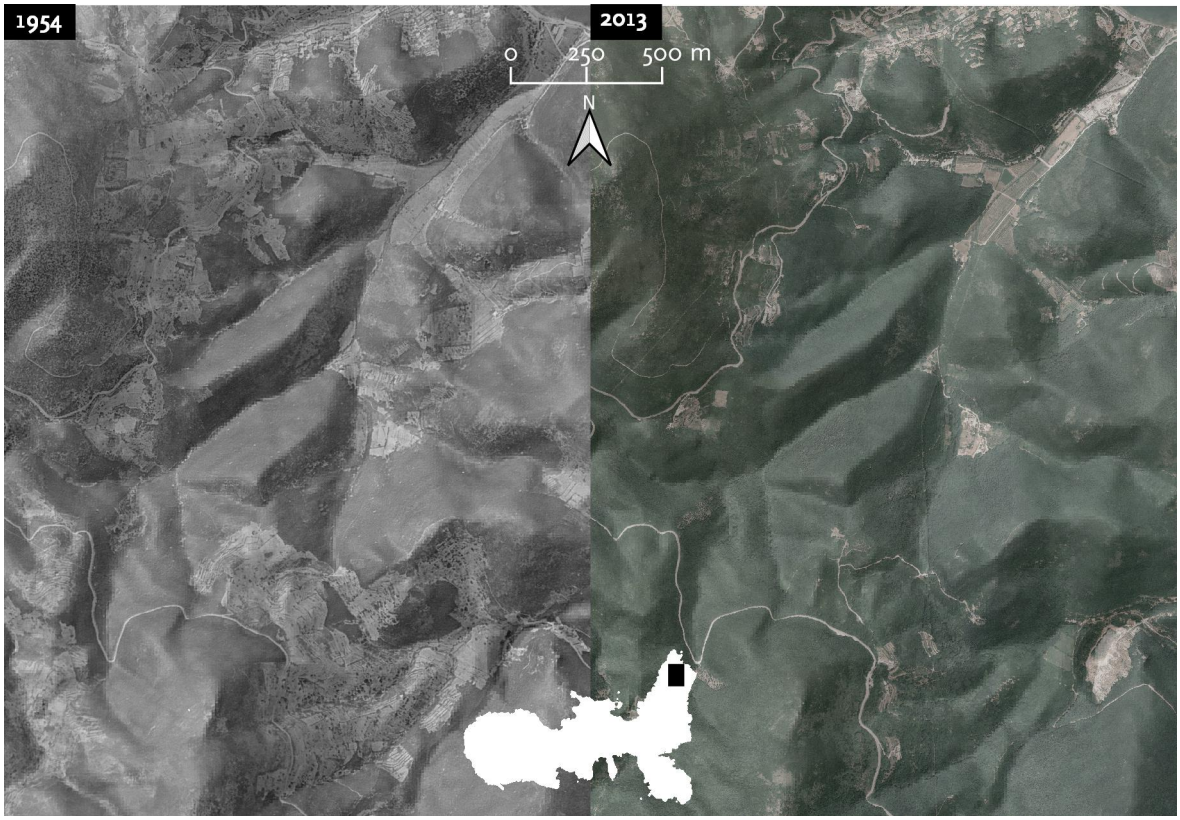

Figure A.11 Land use change around the Baccetti valley in northeastern Elba (1954 and 2013). See also Figure 3.6; and (Carta et al., 2018b) for an quantitative analysis. Database: Regione Toscana, 2014.

Detailed description of the parameters of the woodlot model

S1 Appendix: Description of the model parameters.

Furnace inefficiency

– based on results of smelting experiments summarized in Nikulka (1995)
– we used experimental data for the different furnace types as reported in Nikulka (1995)
– for the definition of the parameter range, we used only experimental data with realistic mass balances
  - Experiments with a very low or high charcoal-to-ore ratio were excluded (a charge of 1:1 ore:charcoal is efficient)
  - a ratio <1:1 may indicate that charcoal consumption for pre-heating was not recorded during the experiment
  - experiments with no reported charcoal consumption for pre-heating were not considered
  - experiments with very high ratio indicates 'wasting' of charcoal and are not included in our data set
– we did not consider unsuccessfull experiments (cf. Paysen (2011); Thommes (1997); experiments with no or nearly no metal output)
– If multiple experiments with similar conditions were conducted by the same operators, we only used the data from the most efficient experiment.
– The uncertainty of the furnace inefficiency parameters were incorporated in our model
  - by using right-skewed *normal* distribution of the *true* furnace inefficiency between the extreme values of our data set
  - The value of the mean is set to account for the assumption that a *true* smelting operation was more efficient than an archaeometallurgical experiment, as the ancient smelters had greater experience in smelting.

Kiln productivity

– We estimated kiln productivity on the basis of on ethnographic records and charcoal burning experiments
– we considered two types of charcoal kilns, viz. pit kilns and mound kilns
  - pit kilns tend to be less productivity than earth mound kilns Thommes (1997)
  - As few ethnographic records of pit kilns are available, we used the data obtained by Horn Horne (1982) in Iran(up to .17 kg/kg—data from Food and Agriculture Organization of the United Nations (1983)
  - For earth mound kiln, we used productivities between .135 kg/kg and .28 kg/kg Paysen (2011); Thommes (1997). With modern (non-traditional) charcoal burning technologies, productivity could even been higher Bailis (2009); Food and Agriculture Organization of the United Nations (1983); Lohri et al. (2016); Straka (2014). indicate even higher efficiencies up to .32 kg/kg).
– We also considered the hypothesis that charcoal production for ancient metallurgy—requiring high quality fuel reaching high temperatures and stable conditions—was less productive (.07 kg/kg)
– to account for variability and uncertainty, we used a normal probability distribution of the *true* kiln productivity K_i between the given extreme values $[K_{min}, K_{max}]$ Janssen et al. (2017)
  - The mean of the normal distribution is here set to half the range of all possible values and the standard deviation is replaced by $1/6$ of the range.
  - Using this approach, there is a small probability that K_i exceeds the given range.
  - We prefer the normal distribution for the productivity parameter over the continuous uniform distribution as high efficiencies from ethnographic records (or even data from archaeological experiments) might be much higher than ancient productivities due to technological development.
  - Low values (from experiments) in contrast might also be less likely, as charcoal burners on Elba Island were most likely experienced specialists (see Olson (1991) for ancient descriptions of charcoal burning)

The labour demand

All labour calculations are based on a 8-hours day and a 300-day year.

Ore extraction

– We estimated the labour requirement for iron mining based on the following parameter:

  - total quantity of slag found on Elba Island, Populonia, and Poggio Butelli
  - chronology of the ancient mining period
  - the quantity of ore that could be extracted by one worker per unit of time
  - a conversion factor from ore to slag from experimental data Nikulka (1995)
- Quantity of slag
  - Scholars estimate that between 2 and 4 Mt of slag were disposed at Baratti beach (Populonia) Saredo Parodi (2013); Voss (1988); Wertime (1983). Estimations from 1920 state that—after small amounts were removed for re-smelting—between 0.4 and 0.6 Mt slag remain in Baratti Pistolesi (2013). From reports of re-smelting contractors, it is known that at least 405,000 t slag were removed in 1921–1932, 1940–1942 and 1960 Pistolesi (2013); this number is in agreement with Crew's assertion Crew (1991) that the common numbers are by one order of magnitude overestimated.
  - For Poggio Butelli it is reported that between 1937 and 1939, 149.000 t of slag were re-smelted Pistolesi (2013). Other authors assume that around 0.5 Mt slag were disposed in the area of Poggio Butelli Costagliola et al. (2008).
  - for data on Elba Island see main text
  - Taking the data from re-smelting contractors as a baseline and assuming that the estimations given above are relatively high, we estimate that between 0.71 and 2.7 Mt slag were disposed.
- Slag-to-ore
  - average ore-to-slag ratio from experimental data (1.35 kg/kg Nikulka (1995))
  - 0.96 and 3.65 Mt ore were at least extracted on Elba Island in antiquity;
  - the most important iron ore deposits in ancient *Etruria Mineraria* (i.e modern Tuscany and northern Latium) were located on Elba Island
  - Sperl (cit. in Saredo Parodi (2013)) estimated that 1.5 Mt ore were processed in Populonia.
  - As for some sites (e.g. Follonica–Rondelli) no data on the amount of slag recovered is available, the estimations can only give a lower basis; ore shipped from Elba Island to remote areas is not included in the calculation.
  - The scale of ore extraction assumed by Haupt Davies (1935); Haupt (1888) in the late 19th c.(11 Mt ore extracted in Rio since the Iron Age) only fits to our estimation if assuming a large scale medieval extraction.
- Chronology and intensity
  - between 600 BCE and 200 CE the intensity of production changed
  - As most of the archaeological record in the mines got lost during later mining operations, it is only possible to give a very rough estimate of the extraction intensities during the centuries

  - Estimations of the annual extraction on Elba Island during the ancient mining period reach up to 10000 t/yr (around 200 BCE Buchwald (2005))
  - we based our estimation on the values given by Saredo ParodiSaredo Parodi (2013) and the assumption that extraction strongly decreased after the mid-1st c. BCE Corretti (2017)
– Per-capita-extraction
  - From the annual extraction in each year x_i we calculated the number of workers necessary for the mining operations by applying a factor of 23 t/capita/yr, as given by Harrison Harrison (1931) for ore extraction in Mouros (including ore preparation and transport)
  - Estimations of labour investment for different extraction operations in antiquity range from 3.5 t/capita/yr in the silver mines of Karthago Nova Kay (2014) over 30 t/capita/yr for limestone removed during the construction of the Corinth canal in the 19th c. Ardaillon (1897); Hopper (1968) to 60–90 t/capita/yr extraction of auriferous material in northwestern Spain during Roman times Andreau (1990) (see Freise (1907): 27 t/capita/yr).
  - for iron ore mining in ancient Elba Island, a relatively low number seems to be appropriate
  - in modern mining period on the island, when explosives were used to aid mining, a productivity of 93 t/capita/yr can be reconstructed Krantz (1841). This value marks a upper bound.

Charcoal burning

– We calculate the number of workers to run one kiln-batch in a given time for a) pit kilns and b) earth mound kilns.
– For pit kilns we assume an average wood load of 3.5 t/batch and 12.5 man-days/batch for operation, which includes the excavation of the pit, the observation of the burning process, and the discharge of charcoal Food and Agriculture Organization of the United Nations (1983).
– Average mound kilns in our model have a wood capacity of 45 t/batch and a work load of 25 man-days/batch. For a large pit kiln, FAO calculated a work load of 22.5 man-days Food and Agriculture Organization of the United Nations (1983); Saredo-Parodi Saredo Parodi (2013) assumes a production of 0.7 t of charcoal (so ca. 3.5 t wood, see above) with the afford of 14 man-days (presumably in a pit kiln); FAO Food and Agriculture Organization of the United Nations (1983) reports for a 69 t earth mound kiln a labour investment of 21 man-days.

Felling

- The labour force necessary for the felling of trees is calculated from the modeled woodlot area as described above.
- We assume that the productivity of woodcutters is 13 ha/capita/yr.
- In a trial clearance of oak trees with flint axes <35 cm in diameter found that 500 m^2 of a forest could be cleared by 3 persons in 4 hours Coles (1973) (i.e. 8.6 ha/capita/year); they additionally report that in Canada in the 18th c., 17.1 ha/capita/year could be cleared using steel axes.
- During Etruscan/Roman times, workload might have been less than the modern values, but felling tools might have been more efficient than the flint axes; our value approximately equals the average of the two values reported in literature.

Smelting

- According to Saredo-Parodi Saredo Parodi (2013), a 18 kg bloom could be produced per batch in 2 days by 3 smelter.
- As labour investment for smelting is calculated based on the amount of slag found on a site, we used a bloom-to-slag ratio of 0.35 kg/kg to get slag output per furnace batch.
- Accordingly, the average productivity of a smelter in our model is 2.5 t/capita/year (slag).

Land transport

- The calculation of the transport capacity of charcoal on Elba Island is based on the transport capacity of mules and donkeys as reported by Mitchell Mitchell (2018) (mule: 150–180 kg load, 20–24 km/d; donkey: 80–100 kg load, 24–30 km/d).
- We assume an average distance of 2 km between kiln sites and smelting sites.
- Thus, a transport animal carrying 100 kg/capita over 25 km/day on a 4 km track (including return) has a capacity of 187.5 t/capita/yr.
- We used the amount of charcoal necessary for each site to calculate the demand on transport animals on Elba Island.
- Approximately 1 driver might have been necessary to guide 5 animals.

Sea transport

- Smelting sites are located in different locations than the mines on Elba Island.
- As outlined by e.g. Nihlén Nihlén (1960), raw ore was mainly transported by ship around Elba Island.

– For our mode, we ignore the transport of ore from a beaching site to the smelting site, as most sites are located directly on the coast; only relatively some small sites (La Pila and Forcioni) are located in the inland.
– we assume that it took 2 days to travel from the mining area to a smelting site by ship in average
– typical ship had a load of ca. 45–65 t McGrail (1989); Saredo Parodi (2013); Zecchini (1982)
– we estimate that a ship had a crew of 6–8 persons Casson (1986); McGrail (2009)
– the same number of persons would have been required for (un)loading the ship Saredo Parodi (2013))
– we determined a transport capacity of 1 t/capita/day (ore) for our model.

Supervision and services

– We used the figures given by Saredo Parodi Saredo Parodi (2013) to account for supervision (+ 30%) and service (+30%).
– Numbers in the same scale are reported for the supervision of ancient Amethyst mines in Wadi el-Hudi (early 2nd millenium BCE), were 1050 worker, 98 administrators, and 362 guards (ca. 24%) were employed Shaw (1998).

Farmland

– We used the data and the spreadsheet provided Hughes et al. Hughes et al. (2018) to calculate the area requirement for the settlement and food supply of ancient people on Elba Island
– some of the parameters we adjusted to local conditions
– The diet of the local population is adjusted based on archaeozoological data from the hilltop settlement Castiglione di San Martino and Populonia Banducci (2013); Verola & Degl'Innocenti (2016)
– Human population dynamics are adjusted to the conditions of mainly industrial area; we did not model age or gender specific caloric requirements as originally proposed by Hughes et al. for a typical village. Caloric requirements were set to
  - 3634 kcal/d for worker with heavy tasks (e.g. mining),
  - 3000 kcal/d for medium task, and
  - 2425 kcal/d for light tasks.
– We obtained productivity values of pastures on Elba Island from the FAO-GAEZ data portal.

– Deviating from Hughes et al., we did not model the requirements for ceramic or bronze production or additional wool sheep keeping because this activities might be insignificant on Elba Island during the smelting period.
– The average requirement for agriculture and horticulture on Elba Island based on the given calculation is 2 ha/capita.

Rangeland

– (modified) calculations given by Hughes et al. (2018) (see also above)
  - estimated area requirement for transport animals is 0.8–1.1 ha/animal
  - he pasture required for meat supply and dairy production is 0.72 ha/capita
  - area required for forest browse is 0.69 ha/capita
– The contribution of fodder from pastures to the diet of the animals varies between 15% (pigs) and 55/60% (sheep/cattle)
– Forest browse is mainly relevant for goats (55%).
– The area required for additional fodder production is included in the total agricultural land area, whereas we assume that feeding with crop residues etc. did not require additional land

Woodland

– We assume that the fuel used in households for heating and cooking was composed of 20% charcoal and 80% firewood Veal (2017b)
– The fuel consumption of an inhabitant of Elba Island is assumed to be between 0.5 and 2 t/capita/year Veal (2017b)
– The production of firewood and charcoal to supply the workforce on Elba Island requires additional afford for charcoal burning and felling and thus increases the total number of worker required, which in turn also increases the necessary fuel production. During a test run of our model, it appeared that the additional number of workers necessary to produce the fuel wood for household purposes is insignificant; so, we did not incorporate it in the final model.

Dating material used for the woodlot model

S2 Table: Dating material

Dating material found on the ancient smelting sites on Elba and the time span of their chronology. IDs correspond to numbers in the main text. Charcoal samples from stratigraphic layers containing slag were dated by the radiocarbon method and calibrated by using Oxcal v4.3.2 (Bronk Ramsey, 2009) and the IntCal13 curve (Reimer, 2013). n = note, f = figure, S = site number; pl = plate; JN = John Nihlén (cf. Nihlén (1958))

ID	Site	Dating material [-BCE/CE]			Reference
		Find	From	To	
1-1	Martella ant.	Greco-It. amph. Will 1A, Will (1982):341–6	-360	-280	Corretti (1991):32
1-2	Martella ant.	As	-211	-154	Sabbadini (1919):855
2-1	Ombria	Camp. bk-glazed, Morel (1981):47	-300	-25	
3-1	San Bennato	Dressel 12	-30	70	Corretti & Firmati (2011):238, Fig. 5
3-2	San Bennato	Morel 2255, Morel (1981):154	-150	-100	Corretti & Firmati (2011):238, Fig. 5
3-3	San Bennato	Morel 2955a 1, Morel (1981):238	-190	-140	Corretti & Firmati (2011):238, Fig. 5
3-4	San Bennato	Morel 2973/4, Morel (1981):242	-150	-100	Corretti & Firmati (2011):238, Fig. 5
3-5	San Bennato	Morel 3121a 2, Morel (1981):248	-170	-120	Corretti & Firmati (2011):238, Fig. 5
3-6	San Bennato	Stratigraphy	-240	-180	Firmati et al. (2006), p. 304
3-7	San Bennato	Terra Sigillata Italica, Pucci (1985)	-60	60	Firmati et al. (2006):30
3-8	San Bennato	Corsican jar	-300	-1	Corretti & Firmati (2011):238, Fig. 5
3-9	San Bennato	Antoninian As	138	139	Sabbadini (1919):842–843
3-10	San Bennato	Claudian Sesterce	54	54	Sabbadini (1919):842
4-1	Fornacelle	Dressel 1 (?); Peacock & Williams (1986):87–8	-140	-10	Sabbadini (1919):855;
4-2	Fornacelle	Vespasian As	73	73	Sabbadini (1919):855
5-1	Capo Pero	Morel 7221b, Morel (1981):405	-300	-201	Corretti (1988):24
5-2	Capo Pero	^{14}C, stratum, 1985±30 BP	-47	74	unpubl.
5-3	Capo Pero	Late Campanian black-glazed ware	-100	-40	Maggiani (1981):176–7/n7
5-4	Capo Pero	Dressel 2/4, Bertoldi (2012):101	-50	100	Maggiani (1981):176–7/n7
5-5	Capo Pero	Morel 2252e 1, Morel (1981)	-200	-101	Monaco & Mellini (1965):91–2
5-6	Capo Pero	Morel 7521a 1, Morel (1981)	-100	-50	Monaco & Mellini (1965):88–9
5-7	Capo Pero	*Warzenlampen*, Thöne et al. (2004):86	-100	15	Maggiani (1981):176–7/n7

Continued on next page . . .

Table A.6 – . . . *continued from previous page*

ID	Site	Dating material [-BCE/CE]			Reference
		Find	From	To	
5-8	Capo Pero	^{14}C-age, inferior stratum	-200	-200	Camporeale (1989):212
5-9	Capo Pero	Corsican jar	-300	-1	Vanagoli (1971)
6-1	Fegatella	Camp. black-glazed, Morel (1981):47	-300	-25	Vanagolli 1974
6-2	Fegatella	Camp. black-glazed ware, Morel (1981):47	-300	-25	Vanagolli 1974
7-1	Valle d. Giove	Camp. black-glazed ware, Morel (1981):47	-300	-25	Pagliantini (2014):S361
7-2	Valle d. Giove	Dressel 1, Peacock & Williams (1986):87–8	-140	-10	Pagliantini (2014):S361
8-1	Vigneria	'Roman ceramics'	-300	-1	Pagliantini (2014):S369
9-1	RM Spiazzi	Morel 1222a 1, , Morel (1981):93	-200	-1	Maggiani (1981):176–7/n6
9-2	RM Spiazzi	Silver denarius L. V. Acisculus (RRC 474/1a)	-45	-45	Monaco & Mellini (1965):83
9-3	RM Spiazzi	*Warzenlampe*, Thöne et al. (2004):86	-30	15	Maggiani (1981):176–177/n6
9-4	RM Spiazzi	Flavian sesterce	71	80	Monaco & Mellini (1965):73
9-5	RM Spiazzi	Several As-coins	-225	-145	Monaco & Mellini (1965):74
9-6	RM Spiazzi	Several As-coins	-114	-82	Monaco & Mellini (1965):74
9-7	RM Spiazzi	Lamp, Leibundgut (1977):nr251	1	50	Monaco & Mellini (1965):87–88/f6
10-1	Barbarossa	Dressel 1 C, Lamboglia (1955):f6	-120	-50	Corretti (1988):11
10-2	Barbarossa	MGS VI, Vandermersch (1994):81–7	-260	-210	Pagliantini (2014):294/S343
11-1	Naregno	MGS VI, Vandermersch (1994):81–7	-260	-210	Corretti (1988):18; Pagliantini (2014):294
12-1	Straccoligno	Lyding Will 1 E, Will (1982)	-200	-120	Corretti (1988):17
12-2	Straccoligno	MGS VI, Vandermersch (1994):81–7	-260	-210	Corretti (1988):17; Pagliantini (2014):294
13-1	Lacona	Dressel 1 (?), Peacock & Williams (1986)	-140	-10	Adamoli & Rigon (2013):69
13-2	Lacona	Dressel 1 (?), Peacock & Williams (1986)	-140	-10	Adamoli & Rigon (2013):69
14-1	Galenzana	Dressel 1 B, Lamboglia (1955):f11	-130	-100	Corretti (1988):23
15-1	Seccheto	Roman ceramics	-280	-25	Corretti (1988)21, Pagliantini (2014):S335
16-1	Sughera	Roman ceramics	-280	-25	Pagliantini (2014):S175

Continued on next page . . .

Table A.6 – . . . *continued from previous page*

ID	Site	Dating material [-BCE/CE]			Reference
		Find	From	To	
17-1	Pomonte	Dressel 1 B, Lamboglia (1955):f10	-130	-100	Corretti (1988):21–22
17-2	Pomonte	Dressel 1 B, Lamboglia (1955):f12	-130	-70	Corretti (1988):21–22
17-3	Pomonte	Dressel 1 B, Lamboglia (1955):f12	-100	-60	Corretti (1988):21–22
17-4	Pomonte	Dressel 1 B, Lamboglia (1955):f13	-100	-60	Corretti (1988):21–22
17-5	Pomonte	Dressel 1 C, Peacock & Williams (1986)	-120	-50	Corretti (1988):21–22
17-6	Pomonte	Dressel 1 C, Peacock & Williams (1986)	-120	-50	Corretti (1988):21–22
18-1	Patresi	Dressel 1, Peacock & Williams (1986)	-140	-10	Corretti (1988):22
18-2	Patresi	^{14}C (2170±30 BP, 2nd peak), lower stratum	-260	-120	unpubl.
18-3	Patresi	Haltern 70, Carreras Monfort (2003)	-80	190	RAE, aug. 2015
18-4	Patresi	Campana A, Morel (1981):47	-220	-40	RAE, sep. 2017
18-5	Patresi	Dressel 1, Peacock & Williams (1986)	-140	-10	RAE, sep. 2017
19-1	S. Andrea	Morel 2614, Morel (1981):191	-200	-101	Corretti (1988):13
19-2	S. Andrea	Beltran 2B,Panella (2001)	50	150	JN's campaign, 1958
19-3	S. Andrea	Dressel 1, Peacock & Williams (1986)	-140	-10	JN's campaign, 1958
19-4	S. Andrea	Dressel 1 C, Lamboglia (1955):f10	-120	-100	JN's campaign, 1958
20-1	Marciana Marina	Dressel 1 A, Lamboglia (1955):f11	-140	-100	Corretti (1988):22
20-2	Marciana Marina	Lyding Will 1 B, Will (1982):345–6	-290	-240	Pagliantini (2014):141/pl.X
20-3	Marciana Marina	MGS VIVandermersch (1994):81–7	-260	-210	Pagliantini (2014):S141/pl.X
20-4	Marciana Marina	Dressel 1 B, Lamboglia (1955):f15	-60	-10	Pagliantini (2014):S141/pl.XI
20-5	Marciana Marina	Morel 1312, Morel (1981):103–4	-200	-101	Pagliantini (2014):S141/pl.XI
20-6	Marciana Marina	Morel 2570, Morel (1981):186–7	-210	-140	Pagliantini (2014):S141/pl.XI
20-7	Marciana Marina	Dressel 1 B, Peacock & Williams (1986)	-130	-10	Zecchini (2001):193
20-8	Marciana Marina	Lyding Will 1 E, Will (1982):353–5	-200	-120	Zecchini (2001):193
21-1	Bagno	Camp. bk-glazed, Morel (1981):47	-220	-40	Pagliantini (2014):S007

Continued on next page . . .

Table A.6 – . . . *continued from previous page*

ID	Site	Dating material [-BCE/CE]			Reference
		Find	From	To	
22-1	Paolina	Morel 2253d 1, Morel (1981):154	-200	-80	Maggiani (1981):176/n5
22-2	Paolina	Morel 2554b 1, Morel (1981):184	-160	-125	Maggiani (1981):176/n5
22-3	Paolina	Terra Sigillata Italica, Pucci (1985)	-60	60	RAE, sep. 2017
22-4	Paolina	Dressel 1 B, Peacock & Williams (1986)	-130	-10	Zecchini (2001):191
22-5	Paolina	Lyding Will 1 E, Will (1982):353–5	-200	-120	Zecchini (2001):191
22-6	Paolina	Marabini Moevs IV, **?**:59–62	-150	-20	Zecchini (2001):191
22-7	Paolina	Morel 1222a 1, Morel (1981):93	-200	-1	Zecchini (2001):191
22-8	Paolina	Morel 2255/7a 1, Morel (1981):154	-200	-135	Zecchini (2001):191
22-9	Paolina	Morel 2286a 1, Morel (1981):162	-185	-115	Zecchini (2001):191
22-10	Paolina	Morel 7541a/b 1, Morel (1981):413	-100	-1	Zecchini (2001):191
22-11	Paolina	*Warzenlampen*, Thöne et al. (2004):86	-100	15	Zecchini (2001):191
23-1	Gnacchera	Camp. ware Morel (1981):47	-300	-25	Pagliantini (2014):S209
24-1	Guardiola	Dressel 1, Peacock & Williams (1986)	-140	-10	Corretti (1988):12
24-2	Guardiola	^{14}C, stratum, 2110±30 BP	-204	-46	unpubl.
24-3	Guardiola	Lyding Will 1 E, Will (1982):353–5	-200	-120	Zecchini (2001):191/n359
25-1	Campo all Aia	Dressel 1 B, Lamboglia (1955):f10	-130	-100	Corretti (1988):12
25-2	Campo all Aia	Dressel 1 B, Lamboglia (1955):f12	-100	-60	Corretti (1988):12
25-3	Campo all Aia	Dressel 1 B Lamboglia (1955):f15	-60	-20	Corretti (1988):12
26-1	La Pila	Dressel 1, Peacock & Williams (1986)	-140	-10	Corretti (1988):18
27-1	Forcioni	Dressel 1, Peacock & Williams (1986)	-140	-10	Pagliantini (2014):20
27-2	Forcioni	Dressel 2/4, Bertoldi (2012):101	-50	100	Pagliantini (2014):20
27-3	Forcioni	Terra Sigillata Italica, Pucci (1985)	-60	60	Pagliantini (2014):S020
28-1	S. Giovanni	Dressel 1 B, Lamboglia (1955):f16	-40	-10	Corretti (1988):15
28-2	S. Giovanni	TSI, C.MA stemp, Oxé et al. (2000):1078	15	100	Corretti (1988):15

Continued on next page . . .

Table A.6 – . . . *continued from previous page*

ID	Site	Dating material [-BCE/CE]			Reference
		Find	From	To	
28-3	S. Giovanni	Dressel 1 C, Lamboglia (1955):f10	-120	-100	Corretti et al. (2014):191/f10
28-4	S. Giovanni	Lyding Will 1 E, Will (1982):353–5	-200	-120	Corretti et al. (2014):191
28-5	S. Giovanni	Py 4 or 4 A, Pagliantini (2014):85/n262	-550	-350	Corretti et al. (2014):191
28-6	S. Giovanni	Morel 2252, Morel (1981):153	-200	-101	RAE, mar. 2017
29-1	Magazzini	Dressel 1, Peacock & Williams (1986)	-140	-10	Corretti (1988):15–16
29-2	Magazzini	Dressel 1 B, Lamboglia (1955):f15	-60	-20	Corretti (1988):15–16
29-3	Magazzini	Dressel 1, Peacock & Williams (1986)	-140	-10	Corretti et al. (2014):187
29-4	Magazzini	TSI, Pucci (1985)	-60	60	Corretti et al. (2014):187
29-5	Magazzini	^{14}C, in-slag charcoal	-260	-165	Becker et al. (2019b)
29-6	Magazzini	Morel 2640, Morel (1981):197–201	-300	-101	Pagliantini (2014):S138/pl.X

Eidesstattliche Erklärung

Hiermit versichere ich, Fabian Becker, dass ich die Dissertation *The impact of ancient iron mining and smelting on the landscape balance on Elba Island, Tuscan Archipelago, Italy* selbstständig angefertigt habe und keine anderen als die von mir angegebenen Quellen und Hilfsmittel verwendet habe.
Ich erkläre hiermit, dass die Dissertation bisher nicht in dieser oder anderer Form in einem anderen Prüfungsverfahren vorgelegen hat.

Fabian Becker
Berlin, January 2020

Colophon: This thesis was typeset with LaTeX (originally developed by Leslie Lamport, based on TeX created by Donald Knuth) in Matthew Carter's *Charter BT* font family. Formatting of chapter headings is based on Ulf A. Lindgrens *Bjornstrup*-theme. I used the *PhD thesis template for Cambridge University Engineering Department* created by Krishna Kumar (https://github.com/kks32/phd-thesis-template). Figures were created in R, QGIs v3.4.5-*Madeira* (and older), and InkScape v0.92.
Upper and middle photo on the title page by the author (San Giovanni, 2017; Ortano valley and Rio, 2015). Lower illustration by courtesy of ©Trustees of the British Museum, 2019. Lines and envelope from Figure 8.4.